FACULTY OF
BIOSCIENCE ENGINEERING

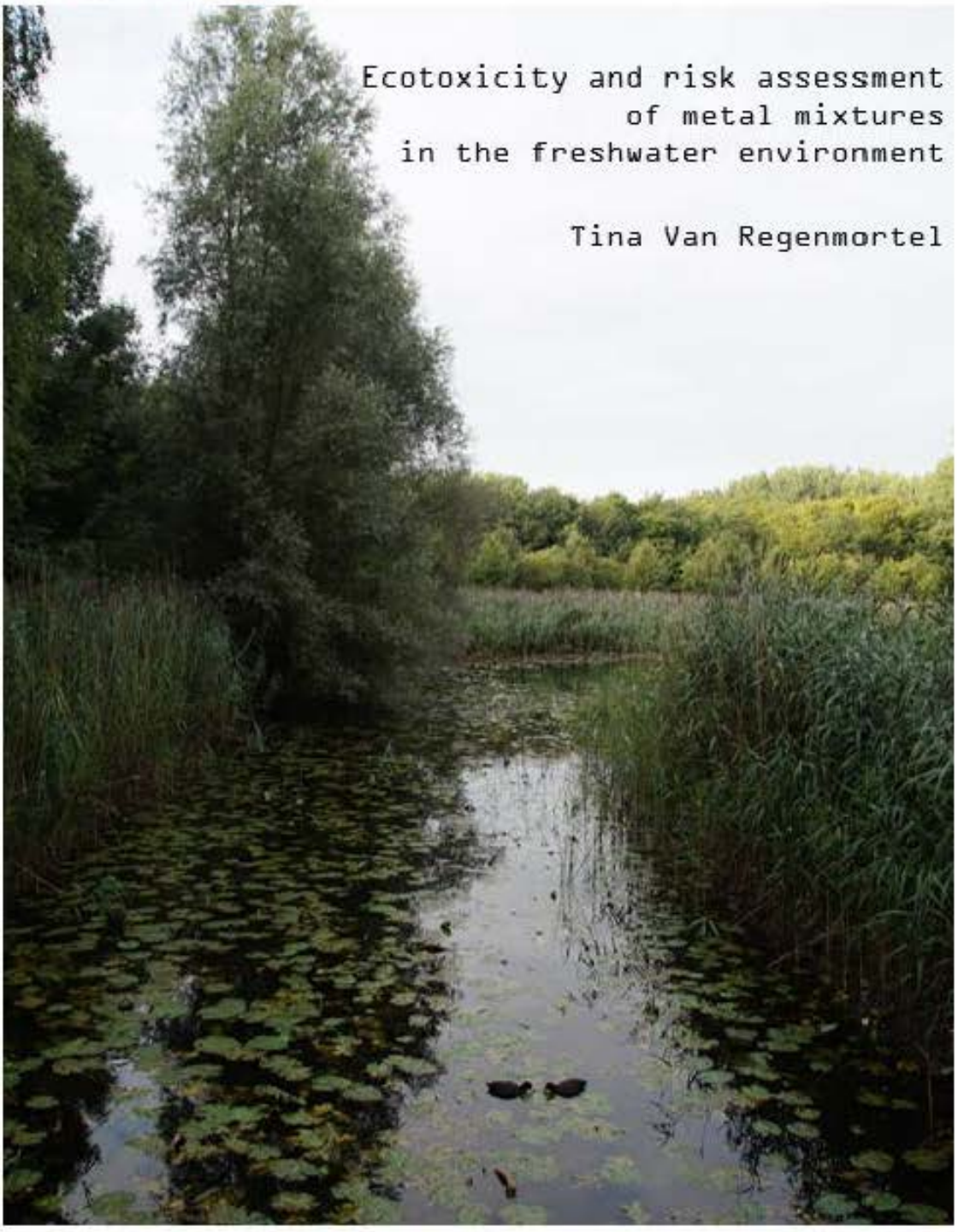

Ecotoxicity and risk assessment of metal mixtures in the freshwater environment

Tina Van Regenmortel

GHENT
UNIVERSITY

“If you want to succeed, you have to work to overcome the obstacles on your path.”

Lailah Gifty Akita

Promotors:

Prof. dr. ir. Karel De Schamphelaere

Prof. dr. Colin Janssen

Environmental Toxicology Unit (GhEnToxLab)

Department of Applied Ecology and Environmental Biology

Ghent University

Dean:

Prof. dr. ir. Marc Van Meirvenne

Rector:

Prof. dr. Rik Van de Walle

TINA VAN REGENMORTEL

Ecotoxicity and risk assessment of metal mixtures in the freshwater environment

Thesis submitted in fulfilment of the requirements for the degree of

Doctor (PhD) in Applied Biological Sciences

Dutch translation of the title:

Ecotoxiciteit en risico-evaluatie van metaalmengsels in het zoetwatermilieu.

Refer to this work as:

Van Regenmortel T. 2017. Ecotoxicity and risk assessment of metal mixtures in the freshwater environment. Thesis submitted in fulfilment of the requirements for the degree of Doctor in Applied Biological Sciences, Ghent University, Ghent, Belgium.

ISBN 978-94-6357-050-3

Dankwoord

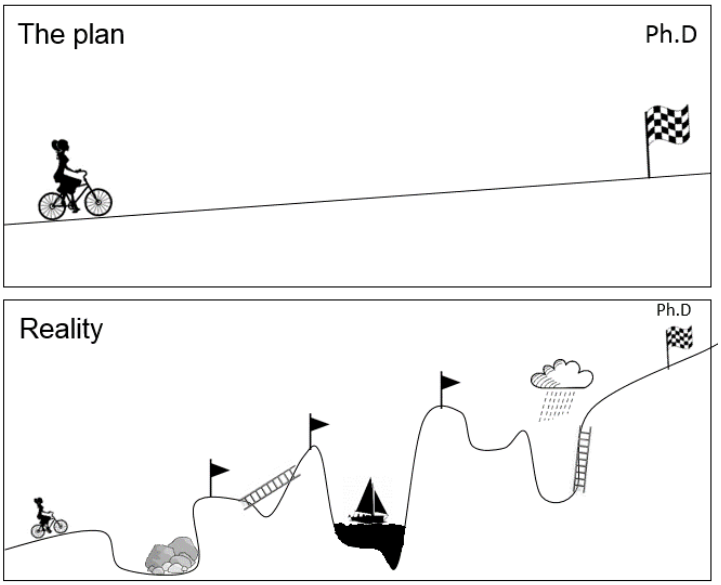

Het heeft wat langer geduurd dan gepland, maar uiteindelijk ligt dit boekje er. Nu rest alleen nog het leuke, om iedereen die er op één of ander manier aan bijdroeg te bedanken.

Karel, bedankt om me de kans te geven om aan dit doctoraat te beginnen en om me tijdens deze vijf jaar op te leiden en te ondersteunen tijdens het uitvoeren van mijn experimenten en in het schrijven van dit werk. Colin, ook jou wil ik bedanken voor de kansen die ik aan het labo gekregen heb.

Collega's, jullie bedank ik graag voor zowel de wetenschappelijke discussies en input als voor de ontspannen momentjes tijdens koffiepauzes, after work drinks, teambuildings en sportdagen. Charlotte, wat was het een plezier om met jouw samen te werken. Hoewel bleek dat we soms allebei chaoten waren, heb ik enorm veel gehad aan jouw kennis, aanwezigheid en steun. "Goe bezig!" Karel, onze 'oase van rust' zorgde ervoor dat ik goed kon werken en de zottere intermezzo's dat ik er plezier aan beleefde. Cecilia, Tara, Jenny, Maarten, David, Jan, Jonathan, Emmanuel, Ilias, Olivier, en nog veel meer collega's, bedankt! Nancy, jij verdient een extra bedanking. Ik liep je meermaals achterna om alweer een lastige vraag te stellen, en je bleef me beantwoorden met een glimlach op het gezicht. Emmy, Jolien, Gisèle en Marc, bedankt voor alle steun in het labo, voor het meten van m'n 1000'en stalen, voor het in goede banen leiden van de staalnames en voor nog veel meer. Marianne en Sigrid, bedankt voor de fijne babbels, de vele snoepjes en al het administratieve werk dat bij een doctoraat komt kijken!

Zonder ontspanning tussen het werken door was ik door deze vijf jaar niet geraakt. Aan de bioloogjes, de BBB, de bende van 12(+4), de mannen (en vrouwen) van de KSA en de Karwendel bende, bedankt om mijn gedachten te verzetten!

Lieve familie, bedankt om er voor me te zijn. Mama, bedankt. Met de jaren is mijn respect voor jou alleen maar gegroeid. Dankjewel voor alle liefde, alle duwtjes in de rug, alle motivational-talks tijdens dipjes, dat je m'n papers wou nalezen en verbeteren, en nog zoveel meer. Trees en Noël, ik kan me geen betere schoonouders wensen. Dankjewel voor alle steun, liefde en tijd die jullie vrijmaakten om bijvoorbeeld onze strijk te doen of om op Elise te passen, zodat ik nog wat kon werken. Opa, je "spinnekop" zal nu écht werk moeten zoeken.

Maarten, al 10 jaar steun je me door dik en dun. De jaren die ik nodig had om aan dit doctoraat te werken zijn jaren geweest met ups en downs. Zonder jouw steun, liefde en de lekkere maaltijden die je voor me kookte was dit schrijfsel er niet geweest. Bedankt bol. En vergeet niet, die drie euro pakken ze niet meer van ons af!
Elise, hoewel je op dit moment nog te klein bent, bestaat er misschien een kleine kans dat je dit boekje later eens van onder het stof haalt en leest. Jouw mama vindt het niet erg als je het alleen bij het dankwoord houdt. Kleine mops, dit laatste jaar en een half van mijn doctoraat was jij mijn motivatie om overdag en 's avonds hard te werken, zodat ik toch nog veel tijd met ons gezinnetje kon spenderen. Dankjewel lieve schat.

Table of Contents

Summary

It is impossible to imagine a world without metals. These substances are part of the earth's crust and are also used for building constructions, the manufacturing of electronic products and batteries, galvanization processes and much more. The extensive use and anthropogenic pollution of metals has led to elevated metal concentrations in aquatic ecosystems worldwide. As a consequence, natural communities around the world are at risk due to metal pollution. This has encouraged authorities worldwide to take action. Environmental Quality Standards (EQS) and European risk assessment frameworks concerning single metals have taken a leap forward since the change of the millennium, by implementing bioavailability based EQS values and bioavailability models. However, European risk assessment frameworks do not account for possible mixture effects due to exposure to metal mixtures. Because there seems to be no clear pattern in the interactions between metals, the development of metal mixture risk assessment frameworks is currently hindered. Recently however, a tiered approach to evaluate mixture risks was presented by Backhaus and Faust (2012). In this approach, the models of Concentration Addition (CA) and Independent Action (IA) are applied directly to species sensitivity distribution (SSD) curves, as explained by De Zwart and Posthuma (2005). Although interest is growing in these methods in the field of mixture risk assessment, they also have an important limitation: the predictions made by the CA and IA models are theoretically only consistent when applied to single species (dose–response curves (DRCs)), and not when applied to communities (SSDs). However, the tiered approach by Backhaus and Faust (2012) also includes a theoretically consistent method that applies CA first to different single species separately and then combines all single-species information to calculate risk estimates for a species assemblage. A similar method, but developed based on the IA method was also proposed by Gregorio et al. (2013).

However, these 2 approaches also have a few limitations. The approach of Backhaus and Faust (2012) only uses the so-called base set of toxicity data for a substance. This base set (i.e., *x*% effect concentration (EC*x*) values for algae, crustaceans, and fish) is the minimum set of data required by REACH for the calculation of a Predicted-No-Effect-Concentration (PNEC). Although their approach can be applied to a broader array of substances (i.e. so-called data-poor substances) and can be extended to a higher number of species, the method applies subjective assessment factors to calculate the risk quotient for a mixture. Gregorio and colleagues (2013) only evaluated their method using sets of species toxicity values that were randomly generated from SSDs of sets of hypothetical substances, and they also assumed a range of possible slope values of dose–response curves for these species, because they argued that implementing the method with existing data was not possible with the typical amount of data available for a substance.

Bearing in mind the limitations found in the research mentioned above, the objective in the present study was to evaluate differences in mixture risk estimates for a number of monitoring databases, using the four approaches listed above but overcoming the limitations mentioned in these approaches.
The present study can be divided into three major sections. In a first section, the toxicity of mixtures of Cu, Ni and Zn was investigated building on the research reported above and bearing in mind their limitations. In the second section, the limitations discovered in Chapter 1 were addressed and adaptations to existing bioavailability models and normalization procured were made (Chapter 3, 4, 5, 7). In a third section, the implications of these adaptations on metal mixture risk evaluation is assessed

(Chapter 6 and 8). Furthermore, the study can be divided into two parts. In a first part (Chapters 2-4), calculations and analyses were done using existing bioavailability models that are also implemented in risk assessments. In a second part (Chapters 5-9), these bioavailability models were improved and these new models were used for calculations and analyses.

Bearing in mind the limitations found in the research mentioned above, in the **second Chapter** in the present study, we aimed to evaluate differences in mixture risk estimates using actual chronic toxicity data for Cu, Ni and Zn for more than the base set of species. Four mixture risk assessment methodologies were compared for risk estimations of mixtures of Cu, Ni and Zn. Across 4 different monitoring datasets and a natural baseline database, between 0% and 52% of the target water samples were estimated to be at risk, but only between 0% and 15% of the target water samples were at risk because of the mixture of metals and not any singe metal individually. Finally, across the 4 monitoring datasets, the following order of conservatism for the 4 methods was shown (from most to least conservative): CASSD > CADRC > IADRC > IASSD. In addition, we developed a general tiered scheme for the risk assessment of metal mixtures in a regulatory context including these 4 methods.

Based on Chapter 2, certain weaknesses/assumptions in our research were encountered. For instance, the underlying assumptions of the four methods should be tested. More specifically, the following research question should be addressed: Is the CA model or the IA model best to predict chronic toxicity of metal-mixtures? Because microalgae, as primary producers, form the base of the food web, it is of utmost importance to understand the effects of metals on these organisms. And although numerous studies have examined the effects of metal mixtures on invertebrates, fish and higher plants, few have conducted on freshwater microalgae. Research that has been conducted with microalgae was conducted in one specific water chemistry, although it has been demonstrated that the interactive effects of metals in mixtures can depend on water chemistry. In **Chapter 3**, we therefore addressed the latter by performing experiments with the freshwater microalgae *Pseudokirchnerialla subcapitata* for the Cu-Ni-(Zn) mixtures in various natural waters that show diverse water-chemistry variables. We showed that the ternary Cu-Ni-Zn mixture acted non-interactively on algal growth, except for in 1 water in which the mixture acted antagonistically. We suggest that a low cationic competition situation in the latter water could be the reason for the antagonistic interaction between the metals. On the other hand, the binary Cu-Ni mixture acted non-interactively on algal growth in all tested waters. We showed that both the CA and IA model can serve as accurate models for toxicity of ternary Cu-Ni-Zn and binary Cu-Ni mixtures to *P. subcapitata* in most cases, and as protective models in all cases.

Another obstacle for applying the four methods described in Chapter 2 is the uncertainty about the degree of conservatism compared to observed community-level metal mixture toxicity effects. To assess this limitation, the metal mixture risk evaluation methods should be validated using multispecies experiments (microcosm/mesocosm studies) and/or field data. To evaluate the conservativeness of our methods, a calculated msPAF, based on measured physico-chemistry, should be compared to community-level effects. Because we did not find the adequate information in literature, we performed a microcosm experiment in which a zooplankton and phytoplankton community were exposed to a mixture of Cu, Ni and Zn (**Chapter 4**). To calculate the msPAF values, we used a SSD that only

contained chronic toxicity data of zooplankton and phytoplankton species. Effects on community composition or diversity were only observed at msPAF values above 0.05. However, effects on community functioning (notably community respiration and phytoplankton metabolism) were observed at msPAF values of 0.05 or lower, i.e. in the Ni-Zn mixture. This indicates that the cut-off msPAF value of 0.05 is not necessarily protective for all community level endpoints against metal mixture exposure. A possible explanation for this result is the mismatch between the species in the SSD and those in our microcosm community. Especially the presence of one single dominant and very Zn and/or Ni sensitive species, i.e. a Cyanobacteria of the genus Oscillatoria, which is not represented in the SSD, might have been the driver of all observed effects at or below an msPAF of 0.05. Overall, our results show that SSDs are not necessarily a good predictor of effects on all types of communities and that the presence of dominant sensitive species may result in significant effects on community functioning endpoints at an msPAF value (0.05) that is generally considered protective.

In a **fifth Chapter**, the bioavailability models that were formerly used to normalize toxicity data in Chapter 2 were evaluated. The main issue that was addressed was the nonlinearity between the H^+ activity and the $EC50_{Me2+}$ activity that was observed for chronic Cu and Zn toxicity to *Daphnia magna* and/or *Oncorhynchus mykiss*. This nonlinearity implies that the effect of pH should not be described by single-site competition between Me^{2+} and H^+. Rather, the effect of pH should be modelled based on an empirical linear relationship between pH and $EC50_{Me2+}$. We will call this type of model a generalized BioAvailability Model (gBAM).The first bioavailability model that we took an in depth look into was the *D. magna* BLM for Cu. Cu BLMs have been applied to derive Water Quality Criteria in the US and PNECs in the EU. Although both frameworks use a similar approach to derive bioavailability-based PNEC or WQC values for copper, the structural formulation and parameterization of the BLMs that is used in both frameworks differ. The purpose was to evaluate the capacity of these two different copper BLMs to predict chronic toxicity of copper for two different D. magna clones.

We found that one BLM performed best with clone K6 data while the other performed best with clone ARO data. We also found that there is an important difference between both BLMs in how they predict bioavailability of copper as a function of pH. Our modelling results suggest that the effect of pH on chronic copper toxicity is different between the two clones considered, which was confirmed with additional chronic toxicity experiments. In addition, we explored the ability of a generalized BioAvailability Model (gBAM) as an alternative for the existing BLMs to predict chronic effect concentrations for copper in two *D. magna* clones.

Secondly, we took an in depth look into the bioavailability models for *D. magna* and *P.subcapitata* for Zn. These models had so far only been validated within a certain range of water chemistry. Yet, around 20% of the European surface waters fall outside this 'validation boundary'. This means that a considerable number of European waters falls outside the applicability range of the bioavailability models. The purpose was therefore to evaluate if the Zn bioavailability models can be extrapolated outside their bioavailability ranges. Results from D. magna experiments suggested that the BLM is not able to reflect the pH effect over a broad pH range (5.5-8.5). In addition, due to calcium deficiency of D. magna in the softwater tests, we can't conclude whether the BLM is applicable below its Ca boundary. Results for P. subcapitata experiments showed that the bioavailability model can accurately predict Zn

toxicity for Ca concentrations down to 0.8mg/L and pH values up to 8.5. Based on the results, we also explored the ability of a generalized BioAvailability Model (gBAM) as an alternative for biotic ligand model to predict chronic effect concentrations for Zn to *D. magna*.
In the two first sections of Chapter 5, gBAMs were developed to predict toxicity of Cu and Zn to *D. magna*. With this, the uniformisation of all bioavailability models (i.e. of Cu, Ni and Zn for invertebrates, fish and algae) to a gBAM-structure was almost complete. The models that did not yet incorporate a pH slope parameter (i.e. had the gBAM-structure) were the bioavailability models for fish for Zn and Cu. Therefore, in a third section of Chapter 5, we developed and validated a gBAM for the metals Zn and Cu for fish. These gBAMs were at least as accurate as the BLM counterparts.

In **Chapter 6**, we evaluated the impact of the implementation of the models developed in Chapter 5 on risk estimations. This was done by repeating the calculations performed in Chapter 2 but implementing the gBAMs developed in Chapter 5 for *D. magna* and fish for the metals Cu and Zn instead of the original BLMs. Implementing these gBAMs only had a small influence on msPAF values and on the % of target water samples that are predicted to be affected by the mixture of Zn, Cu and Ni. However, because the newly developed gBAMs for Cu and Zn for invertebrates and fish more accurately predict single metal toxicity, we recommend the use of the newly developed gBAMs to normalize toxicity data for Cu and Zn prior to metal mixture risk calculations.

A final limitation of the calculations performed in Chapter 2 that was assessed in this work, was that they were based on bioavailability-normalized dissolved metal concentrations. However, when present in a mixture, metals may compete with each other for the binding sites of DOC. Hence, metal mixture risks should ideally be evaluated on the free ion activity level. However, assessing risks based on free ion activities is limited because the chronic bioavailability models for individual metals are currently based on different software to model metal speciation: i.e. WHAM V for Zn and Cu and WHAM VI for Ni. Additionally, some assumptions for chemical speciation calculations differ between these metals. Recently, an updated version of the WHAM software (WHAM/Model VII) was developed. Therefore, in **Chapter 7** we evaluated whether the chronic daphnid, fish and algae metal bioavailability models can all be updated to the WHAM VII speciation software, without loss of predictive capacity. Overall, our results showed that WHAM VII with an assumption of 65% AFA can be used as a speciation model to predict metal toxicity to different species with sufficient accuracy.

In **Chapter 8**, we combined the adaptations made to the bioavailability models (Chapter 5) with the update of the models all WHAM VII (Chapter 7) to evaluate the impact on mixture risk estimations. In this chapter, we performed calculations for all monitoring databases described in Chapter 2, but based on free metal ion activities. For this, the dissolved metal concentrations in the monitoring databases were converted to free ion activities in two ways, one that did not take into account the competition between the metals for DOC binding sites and one that did. Although we had expected that taking into account the competition between metals for DOC binding sites would result in higher free metal activities, we found that, at environmental concentrations, competition between metals for DOC had relatively little effect on free metal ion activity (1.1% - 20%). As a consequence, msPAF values calculated

with both scenarios were similar. We concluded that competition between metals for DOC binding sites has little impact on metal mixture risk estimations.

In a final chapter, **Chapter 9**, we concluded and integrated the research that was conducted in all previous chapters.

The metal (mixture) bioavailability models developed in the present study can be integrated into risk assessment frameworks. The chronic metal (mixture) toxicity data from single species and microcosm experiments increases our overall understanding of chronic metal (mixture) effects on single species and communities. The proposed 4 methods and metal mixture risk evaluation scheme may guide the incorporation of metal mixture toxicity into future risk assessment frameworks.

Samenvatting

Metalen zijn niet weg te denken uit onze samenleving. Deze chemische elementen maken deel uit van de aardkorst en worden gebruikt bij bouwconstructies, de productie van elektronisch materiaal en batterijen, galvanisatieprocessen en nog veel meer. Het uitgebreide gebruik en de antropogene vervuiling van metalen heeft geleid tot verhoogde metaalconcentraties in aquatische ecosystemen wereldwijd. Als gevolg van metaalvervuiling zijn natuurlijke gemeenschappen over de hele wereld in gevaar. Dit heeft de overheden wereldwijd aangezet actie te ondernemen. Europese risico-evaluatieprocedures met betrekking tot individuele metalen hebben sinds de eeuwwisseling vooruitgang geboekt door de implementatie van biobeschikbaarheidsmodellen en door het gebruik van biobeschikbaarheidscorrecties bij de berekening van milieukwaliteitsnormen. Echter, Europese kaderrichtlijnen houden geen rekening met mogelijke mengseleffecten bij blootstelling aan metaalmengsels. Omdat er geen duidelijk patroon in de interacties tussen metalen lijkt te zijn, is de ontwikkeling van risico-evaluatie betreffende metaalmengsels momenteel belemmerd. Onlangs is echter een gecontroleerde aanpak voor het evalueren van mengselrisico's gepresenteerd door Backhaus en Faust (2012). In deze aanpak worden de modellen van Concentratie Additie (CA) en Onafhankelijke Actie (IA) direct toegepast op de soortengevoeligheidscurves (SSDs). Hoewel interesse in deze methoden op het gebied van de risicoanalyse groeit, hebben deze methoden ook een belangrijke beperking: de voorspellingen van de CA- en IA-modellen zijn theoretisch alleen consistent bij toepassing op afzonderlijke soorten (dosis-responscurves) en niet wanneer toegepast op gemeenschappen (SSDs). De aanpak van Backhaus en Faust (2012) bevat echter ook een theoretisch consistente methode die het CA model eerst bij verschillende soorten afzonderlijkbtoepast en vervolgens alle informatie betreffende de individuele soorten combineert om een schatting van het risico voor de gemeenschap van soorten te bepalen. Een soortgelijke methode, maar ontwikkeld op basis van het IA model werd ook voorgesteld door Gregorio et al. (2013).
Deze 2 benaderingen hebben ook een paar beperkingen. De aanpak van Backhaus en Faust (2012) gebruikt alleen de zogenaamde basisset aan toxiciteitsgegevens voor een chemische stof. Deze basisset (x% effectconcentraties (ECx) voor algen, invertebraten en vissen) is het minimum aan data die door REACH vereist is voor de berekening van een PNEC (de voorspelde concentratie waarbij geen effect wordt waargenomen). Hoewel hun aanpak toegepast kan worden op een bredere reeks aan chemische stoffen (de zogenaamde data-arme stoffen) en kan worden uitgebreid naar een groter aantal soorten, past de methode subjectieve beoordelingsfactoren toe om het risicoquotiënt voor een mengsel te berekenen. Gregorio en collega's (2013) hebben hun methode alleen geëvalueerd door gebruik te maken van sets van toxiciteitspunten van soorten die willekeurig gegenereerd werden uit SSDs van hypothetische stoffen. Verder hebben ze een aantal mogelijke hellingswaarden van dosis-responscurves voor deze soorten aangenomen, omdat ze argumenteerden dat de uitvoering van de methode met bestaande gegevens niet mogelijk was met de typische hoeveelheid gegevens die beschikbaar zijn voor een stof.

De huidige studie kan worden onderverdeeld in drie delen. In een eerste deel (hoofdstuk 2) wordt de toxiciteit van mengsels van Cu, Ni en Zn onderzocht op basis van het bovengenoemde onderzoek en rekening houdend met de beperkingen hiervan. In het tweede deel werden de beperkingen die in deel 1 werden ontdekt besproken en werden aanpassingen aan bestaande biobeschikbaarheidsmodellen en

normalisatieprocedures gemaakt (hoofdstuk 3, 4, 5, 7). In een derde deel worden de implicaties van deze aanpassingen op de evaluatie van metaalmengselrisico's beoordeeld (hoofdstukken 6 en 8).

Gebaseerd op de beperkingen die in bovengenoemd onderzoek werden gevonden, was het doel van het **tweede hoofdstuk** van deze studie om de verschillen in risicoschattingen ten gevolge van mengsels te evalueren gebruikmakend van chronische toxiciteitsgegevens voor Cu, Ni en Zn voor meer dan de basisset aan soorten. Er werden vier methodes voor risicoanalyses gebruikt voor de bepaling van risicoschattingen van mengsels van Cu, Ni en Zn. Over 4 verschillende monitoring datasets en een natuurlijke baseline database bleken tussen 0% en 52% van de waters risico te vertonen, maar slechts tussen 0% en 15% van de waters waren in gevaar door het metaalmengsel en niet enkel het individuele metaal. Tenslotte werd over de 4 monitoring datasets heen de volgende volgorde van conservatisme voor de 4 methoden aangetoond (van de meest tot het minst conservatieve): CA_{SSD}> CA_{DRC}> IA_{DRC}> IA_{SSD}. Daarnaast ontwikkelden we in het kader van een risico-evaluatie voor metaalmengsels een algemeen schema dat deze 4 methodes omvat.

Op basis van hoofdstuk 2 werden bepaalde zwakke punten of veronderstellingen in ons onderzoek geconstateerd. Zo moeten de onderliggende assumpties van de vier methoden worden getest. Meer specifiek moet de volgende onderzoeksvraag worden aangepakt: Welk van beide modellen, het CA-model of het IA-model, is het beste om de chronische toxiciteit van metaalmengsels te voorspellen? Omdat microalgen, als primaire producenten, de basis vormen van het voedselweb, is het van groot belang om de effecten van metalen op deze organismen te begrijpen. En hoewel tal van studies de effecten van metaalmengsels op ongewervelde dieren, vissen en hogere planten hebben onderzocht, is er weinig onderzoek gebeurd op zoetwatermicroalgen. Bestaand onderzoek met microalgen is meestal uitgevoerd in één specifiek water, hoewel aangetoond is dat de interactieve effecten van metalen in mengsels afhankelijk kunnen zijn van de waterchemie. In **hoofdstuk 3** behandelden we deze kwestie door experimenten te verrichten met de alg *Pseudokirchnerialla subcapitata* voor mengsels van Cu-Ni- (Zn) in verschillende natuurlijke wateren die een uiteenlopende waterchemie vertoonden. We hebben aangetoond dat het tertiaire Cu-Ni-Zn mengsel non-interactief op de algengroei inwerkte, behalve in 1 water waarin het mengsel antagonistisch optrad. Wij suggereren dat een lage kationische concurrentie in het laatste water de reden zou kunnen zijn voor de antagonistische interactie tussen de metalen. Anderzijds werkte het binaire Cu-Ni-mengsel niet-interactief in op algengroei in alle geteste wateren. We toonden aan dat zowel het CA- als IA-model in de meeste gevallen kunnen dienen als nauwkeurige modellen voor toxiciteit van ternaire Cu-Ni-Zn en binaire Cu-Ni-mengsels bij P. *subcapitata*, en als beschermende modellen in alle gevallen.

Een ander obstakel voor de toepassing van de vier methoden beschreven in hoofdstuk 2 is de onzekerheid over de mate van conservatisme in vergelijking met waargenomen toxiciteitseffecten op het gemeenschapsniveau. Om deze beperking na te gaan, moeten de risico-evaluatiemethoden voor metaalmengsels worden gevalideerd met behulp van multisoortenexperimenten (microkosmos/ mesokosmos studies) en/of veldgegevens. Om het conservatisme van onze methoden te evalueren, moet een voorspelde msPAF, gebaseerd op de gemeten fysico-chemie van het water, worden vergeleken met effecten op gemeenschapsniveau. Omdat we in de literatuur niet voldoende informatie

hebben gevonden, hebben we een microkosmos experiment uitgevoerd waarin een zoöplankton- en fytoplanktongemeenschap blootgesteld werd aan een mengsel van Cu, Ni en Zn (**hoofdstuk 4**). Om de msPAF-waarden te berekenen, gebruikten we een SSD die alleen gegevens over chronische toxiciteit van zoöplankton- en fytoplanktonsoorten bevatte. Effecten op gemeenschapscompositie en diversiteit werden alleen geobserveerd bij msPAF waarden boven 0.05. Effecten op het functioneren van de gemeenschap, meer bepaald op respiratie van de gemeenschap en op phytoplankton metabolisme, werden geobserveerd bij msPAF waarden van 0.05 en lager in het Ni-Zn mengsel. Dit geeft aan dat de drempelwaarde van een msPAF van 0.05 niet noodzakelijk beschermend is tegen metaalmengsel blootstelling voor alle gemeenschaps eindpunten. Een mogelijke reden hiervoor is de mismatch tussen de soorten in de SSD en deze in onze microcosm gemeenschap. Voornamelijk de aanwezigheid van één dominante en erg Zn en/of Ni gevoelige soort, een Cynaobacterie van het genus Oscillatoria, dat niet in de SSD voorkomt, kan de reden zijn voor de geobserveerde effecten beneden de msPAF waarde van 0.05. Onze resultaten tonen dat SSDs niet noodzakelijk een goede voorspelling van effecten geven voor alle gemeenschapstypes en dat de aanwezigheid van een dominante gevoelige soort kan resulteren in significante effecten op het functioneren van de gemeenschap bij msPAF waarden (0.05) die normaal als beschermend worden gezien.

In een **vijfde hoofdstuk** werden de biologische beschikbaarheidsmodellen die in hoofdstuk 2 gebruikt werden om toxiciteitsgegevens te normaliseren geëvalueerd. Het eerste biobeschikbaarheidsmodel dat we bestudeerden, was het *D. magna* BLM voor Cu. Cu BLM's worden toegepast om waterkwaliteitscriteria (WQC) in de Verenigde Staten en PNEC's in de Europese Unie af te leiden. Hoewel beide kaders een vergelijkbare aanpak gebruiken om biologische beschikbaarheid op basis van PNEC- of WQC-waarden voor koper af te leiden, verschillen de structurele formulering en de parametrisering van de BLM's die in beide kaders worden gebruikt. Het doel was de capaciteit van deze twee verschillende koper BLM's in het voorspellen van de chronische toxiciteit van koper voor twee verschillende *D. magna* klonen te evalueren. We toonden aan dat één BLM het beste werkte voor de data van de K6-kloon, terwijl het andere het beste werkte voor de data van de ARO-kloon. We toonden ook aan dat er een belangrijk verschil is tussen beide BLM's in hoe zij biobeschikbaarheid van koper als functie van de pH voorspellen. Onze modelleringsresultaten suggereren dat het effect van de pH op chronische kopertoxiciteit verschilt tussen de twee beschouwde klonen, wat werd bevestigd met aanvullende chronische toxiciteitsexperimenten. Daarnaast onderzochten we de capaciteit van een genormaliseerd biobeschikbaarheismodel (gBAM) als alternatief voor de bestaande BLM's om chronische effectconcentraties voor koper te voorspellen in twee *D. magna* klonen. Ten tweede hebben we de biobeschikbaarheidsmodellen voor *D. magna* en *P.subcapitata* voor Zn bestudeerd. Deze modellen werden tot nu toe alleen gevalideerd binnen een bepaald bereik van waterchemie. Toch valt ongeveer 20% van de Europese oppervlaktewateren buiten deze 'validatiegrens'. Dit betekent dat een aanzienlijk aantal Europese wateren buiten het toepassingsbereik van de biobeschikbaarheidsmodellen valt. Het doel was daarom om te beoordelen of de Zn biobeschikbaarheidsmodellen buiten hun bereik kunnen worden geëxtrapoleerd. Resultaten van *D. magna* experimenten suggereerden dat het BLM het pH-effect niet kan reflecteren over een breder pH-bereik (5.5-8.5). Daarnaast kunnen we, wegens een calciumtekort bij *D. magna*, niet concluderen of het

BLM onder de Ca-grens accuraat is. Resultaten van experimenten met *P. subcapitata* toonden aan dat het biobeschikbaarheidsmodel de Zn toxiciteit bij lage Ca concentraties nauwkeurig kan voorspellen tot 0.8 mg/L en bij pH-waarden tot 8.5. Op basis van de resultaten hebben we ook de capaciteit van een gBAM als alternatief voor het BLM verkend om de chronische toxiciteit van Zn op *D. magna* te voorspellen.
In de eerste twee secties van hoofdstuk 5 werden gBAM's ontwikkeld om toxiciteit van Cu en Zn voor *D. magna* te voorspellen. Hierdoor was de uniformisering van alle biobeschikbaarheidsmodellen (die van Cu, Ni en Zn voor ongewervelde dieren, vissen en algen) naar een gBAM-structuur bijna compleet. De modellen die de gBAM-structuur nog niet hadden waren de biologische beschikbaarheidsmodellen voor vissen voor Zn en Cu. Daarom hebben we in een derde sectie van hoofdstuk 5 een gBAM ontwikkeld en gevalideerd voor de metalen Zn en Cu voor vissen. Deze gBAM's waren minstens even nauwkeurig als hun BLM-tegenhangers.

In **hoofdstuk 6** hebben we de impact van de implementatie van de in hoofdstuk 5 ontwikkelde modellen op de risicoschattingen geëvalueerd. Dit werd gedaan door de berekeningen in hoofdstuk 2 te herhalen, maar in plaats van de oorspronkelijke BLM's de gBAM's te implementeren die in hoofdstuk 5 werden ontwikkeld voor *D. magna* en vissen voor de metalen Cu en Zn. De implementatie van deze gBAM's had slechts een kleine invloed op de msPAF-waarden en op het percentage aan waters dat werd beïnvloed door het mengsel van Cu, Ni en Zn. Aangezien de nieuw ontwikkelde gBAM's voor Cu en Zn voor ongewervelde dieren en vissen nauwkeuriger de toxiciteit van individuele metalen voorspellen, raden we het gebruik van de nieuw ontwikkelde gBAM's aan om de toxiciteitsdata voor Cu en Zn te normaliseren om het risico van metaalmengsels te berekenen.

Een laatste beperking van de berekeningen in hoofdstuk 2 was dat ze gebaseerd waren op biobeschikbaarheid-genormaliseerde opgeloste metaalconcentraties. Bij aanwezigheid in een mengsel kunnen metalen echter concurreren met de bindingsplaatsen van DOC. Daarom zouden de risico's van metaalmengsels idealiter moeten worden beoordeeld op het niveau van de vrije ionactiviteit. Echter, het beoordelen van risico's op basis van vrije ionactiviteiten is beperkt omdat de chronische biobeschikbaarheidsmodellen voor individuele metalen momenteel gebaseerd zijn op verschillende software programma's voor het modelleren van metaalspeciatie: WHAM V voor Zn en Cu en WHAM VI voor Ni. Daarnaast verschillen sommige assumpties voor de chemische speciatieberekeningen tussen deze metalen. Onlangs is een nieuwe versie van de WHAM software (WHAM / Model VII) ontwikkeld. Daarom zijn we in **hoofdstuk 7** nagegaan of de chronische daphnia-, vis- en algen-biobeschikbaarheidsmodellen naar de WHAM VII-speciatiesoftware kunnen worden bijgewerkt, zonder verlies van voorspellingscapaciteit. Over het algemeen tonen onze resultaten aan dat WHAM VII als speciatiemodel met voldoende nauwkeurigheid kan worden gebruikt om metaaltoxiciteit voor verschillende soorten te voorspellen.

In **hoofdstuk 8** combineerden we de aanpassingen aan de biobeschikbaarheidsmodellen (hoofdstuk 5) met de update van de modellen naar WHAM VII (hoofdstuk 7) om de impact op de risico's van het mengsel te evalueren. In dit hoofdstuk hebben we berekeningen uitgevoerd voor alle monitoring databases beschreven in hoofdstuk 2, maar gebaseerd op vrije metaal ion activiteiten. Hiervoor werden

de opgeloste metaalconcentraties in de monitoringdatabases omgezet in ionenactiviteiten en dit op 2 manieren, één waarbij geen rekening gehouden werd met de concurrentie tussen de metalen voor DOC-bindingsplaatsen en één waarbij hiermee wel rekening werd gehouden. Hoewel we hadden verwacht dat wanneer er rekening werd gehouden met de concurrentie tussen metalen voor DOC-bindingsplaatsen dit zou leiden tot hogere vrije metaalactiviteiten, vonden we dat de concurrentie tussen metalen voor DOC relatief weinig effect had op de vrije metaalionactiviteit (1.1%-20%). Als gevolg daarvan waren de msPAF-waarden berekend met beide scenario's vergelijkbaar. We kunnen hieruit concluderen dat de concurrentie tussen metalen voor DOC-bindingsplaatsen weinig impact heeft op de schattingen van de metalenmengselrisico's.

In een laatste hoofdstuk, **hoofdstuk 9**, maken we conclusies en integreren we al het onderzoek dat uitgevoerd werd in deze thesis.

De in de huidige studie ontwikkelde metaal(mengsel)biobeschikbaarheidsmodellen kunnen worden geïntegreerd in risico-evaluatieprocedures. De toxiciteitsgegevens van de chronische metaal(mengsel) experimenten verhogen ons algehele begrip van chronische metalen(mengsel)effecten op individuele soorten en gemeenschappen. De 4 methoden die werden beschreven en het voorgestelde metaalmengsel risico-evaluatie schema kunnen helpen bij het opstellen van toekomstige risico-evaluatieprocessen voor metaalmengsels.

List of Abbreviations

A

%AFA	Percentage of active fulvic acid
AIC	Aikake information criterion

B

BL	Biotic ligand
BLM	Biotic ligand model

C

CA	Concentration Addition
CA_{DRC}	Concentration Addition applied to individual Dose–Response Curves before calculating the msPAF
CA_{SSD}	Concentration Addition applied directly to the Species Sensitivity Distribution
CI	Confidence Interval

D

DIC	Dissolved Inorganic Carbon
DOC	Dissolved Organic Carbon
DOM	Dissolved Organic Matter
DRC	Dose Response Curve

E

EC	European Commission
ECx	X% Effective Concentration
EDTA	Ethylene diamine tetraacetic acid
ERA	Environmental Risk Assessment
EQS	Environmental Quality Standard
EU	European Union

F

FA	Fulvic Acid
FOREGS	Forum of the European geological surveys directors

G

gBAM	generalized BioAvailability Model

H

HA	Humic Acid
HC5	5% hazardous concentration

I

IA	Independent Action
IA_{DRC}	Independent Action applied to individual Dose–Response Curves before calculating the msPAF
IA_{SSD}	Independent Action applied directly to the Species Sensitivity Distribution
ICP-OES	Inductive coupled plasma-optical emission spectroscopy

L

LA50	Lethal accumulation at 50% mortality
LOEC	Lowest observed effect concentration
LOQ	Limit of Quantification
LCx	X% lethal concentration

M

MOPS	3-N-morpholinoproanesulfonic acid
msPAF	multisubstance potentially affected fraction

N

NIST	National Institute of Standards and Technology
NOEC	No Observed Effect Concentration
NOM	Natural Organic Matter

O

OECD	Organisation for Economic Co-operation and Development

O/P	Logarithmic model-measurement deviation; i.e. log Observed ECx – log Predicted ECx
P	
PEC	Predicted Environmental Concentration
PNEC	Predicted No-Effect Concentration
R	
RAR	Risk Assessment Report
RCR	Risk Characterisation Ratio
REACH	Registration Evaluation and Authorisation of Chemicals
RE	Relative Effect
RGR	Relative Growth Rate
RR	Relative Reproduction
RQ	Risk Quotient
S	
SCHER	Scientific Committee on Health and Environmental Risks
SSD	Species Sensitivity Distribution
T	
TU	Toxic Unit
U	
USGS	United States Geological Survey
V	
VMM	Flemish Environmental Agency
W	
WFD	Water Framework Directive
WHAM	Windermere Humic Aqueous Model

One

General Introduction and Research Approach

1. General introduction and research approach

1.1. Copper, nickel and zinc

Copper (Cu), Nickel (Ni) and Zinc (Zn) are three metals that occur in the environment as a result of both natural and anthropogenic sources (Salminen et al. 2005). Therefore, these metals often occur simultaneously in freshwater systems. Because concentrations of these metals can be high and can cause risk to natural communities, the European Union (EU) and member states of the EU are responsible for defining specific environmental quality standards for these substances (e.g. FR 2015) and therefore, the environmental concentration is commonly measured via monitoring efforts (e.g. FEA 2013). In addition, the chronic toxicity of these metals to a variety of organisms (e.g. from algae to fish) has been studied extensively, which makes these metals "data-rich" substances (e.g. De Schamphelaere and Janssen 2002, Heijerick et al. 2002a, Deleebeeck et al. 2008). Furthermore, a lot of effort has been put in the development of bioavailability models and biotic ligand models for these metals, which are also used in risk assessments, to account for the variation in water chemistry variables (i.e. bioavailability of the metals) to predict metal toxicity (e.g. De Schamphelaere and Janssen 2004b, De Schamphelaere and Janssen 2008, Deleebeeck et al. 2007).The availability of monitoring data, chronic toxicity data and bioavailability models make Cu, Ni and Zn good subjects to evaluate risks of mixtures of these metals.

Copper

Since pre-historic times, copper has been an essential material to man. Smelting of Cu dates back as far as 7000 years ago (Radivojevic et al. 2010). Even one of the 'ages' in history, the Bronze age (3200 – 600 BC) is a named after a copper alloy, bronze. It is clear that copper has had a large influence on human history. At the onset of the Industrial Revolution, world Cu production was about 10 000 tonnes per year (Hong et al. 1996). Since then, Cu production has increased strongly up to 18.5 million tonnes in 2014 (USGS 2014a). The global consumption of copper reached 22.9 million tonnes in 2014 and the European Union accounted for 3.2 million tons of this global consumption (USGS 2014a). Currently, Cu is the third most used metal in the world due to its properties of thermal and electrical conductivity, high ductility, and resistance to corrosion (USGS 2014a). In the USA, Cu is mainly used in building construction (Figure 1.1) (USGS 2014a), while in Europe the majority of Cu is used for energy and electricity applications (Figure 1.1) (Sverdrup et al. 2014).

Figure 1.1 Primary uses of copper in the USA and Europe in 2014 (USGS 2014a, Sverdrup et al. 2014)

Because production and consumption of Cu is so high, it is not surprising that copper occurs in the natural environment due to anthropogenic sources. These include the use of pesticides and anti-fouling paints, urban runoff, mining leachates and corrosion (Lifset et al. 2012). However, it is also a naturally occurring element. It is the 26th most abundant element in the earth's crust. Therefore, it is not surprising that the natural sources of copper in the aquatic environment include atmospheric deposition due to windblown dust, volcanic eruptions, forest fires and sea spray as well as natural erosion processes (Davies and Bennet 1985). Dissolved copper concentrations in pristine areas in Europe have been reported to range between 0.1 and 14 µg Cu/L (Salminen 2005; Figure 1.2). However, local concentrations can be much higher due to anthropogenic pollution, such as in the Dommel catchment area in the Netherlands, where Cu concentrations up to 60 µg/L have been reported (Verschoor et al. 2011).

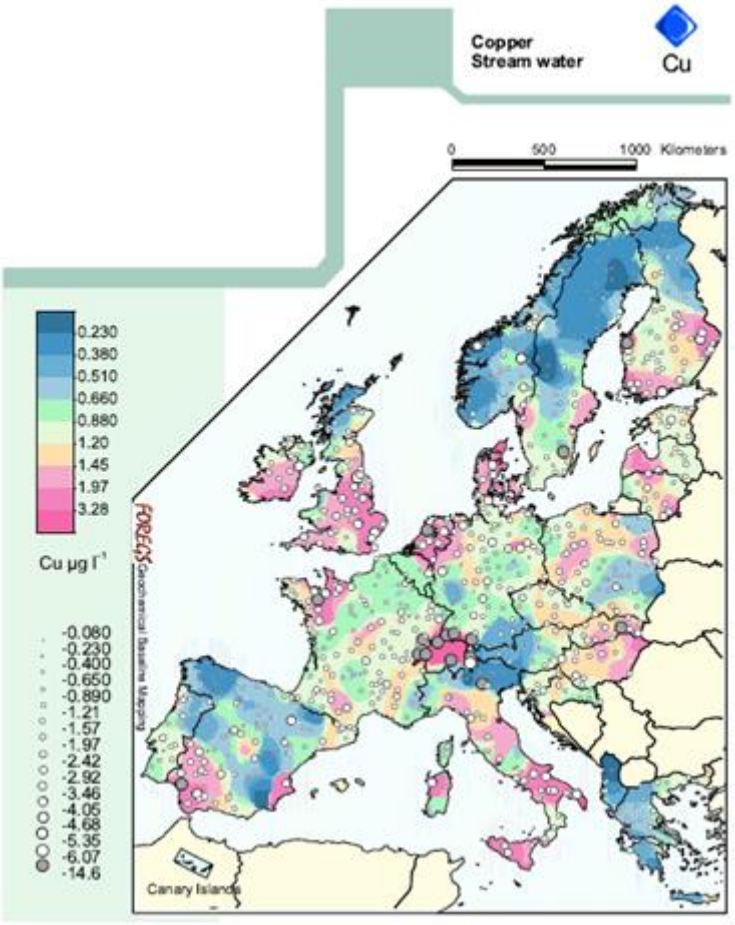

Figure 1.2 Dissolved copper concentrations in pristine areas in Europe in 2006 (Salminen et al. 2005). The dot size scale gives the minimum and maximum of the dataset. The 10% of the lowest Cu concentrations are shown by the smallest symbol size and 2% of the highest concentrations by the big grey symbol. Between these fixed percentiles, the scale is logarithmic. In addition, a colour scale based on the following percentiles: 5, 15, 25, 35, 50, 65, 75, 85 and 95 (Salminen et al. 2005).

Because Cu is present in the aquatic environment, via natural and anthropogenic sources, it can also be present in concentrations that are toxic to organisms. Indeed, when the process of uptake of a metabolically active metal is in imbalance with the detoxification, storage or excretion mechanisms, metal toxicity can occur (Luoma and Rainbow 2008). This metal toxicity can be due to both non-essential and essential metals, and is often a result of the disruption of the ion homeostasis in the organism (Paquin et al. 2002).

Although Cu is an essential micronutrient and is an active component in more than 30 enzymes that catalyse redox reactions and transport oxygen (Wright and Welbourn 2002), an excess of Cu can lead to toxicity. Chronic Cu toxicity has been shown to influence amongst other endpoints, reproduction, survival and growth of fish species (Erickson et al. 1996; Jezierska et al. 2009; Wang et al. 2014), invertebrate species (De Schamphelaere and Janssen 2004a; Schwartz and Vigneault 2007; Arnold et al. 2011) and algal species (Knauer et al. 1997; De Schamphelaere et al. 2003; Wilde et al. 2006).

The mechanisms of uptake of Cu by algae, daphnids and fish is not yet fully understood. Ay et al. (1999) investigated the mechanisms of acute Cu accumulation by the fish *Tilapia zillii*. It was observed by these authors that the activity of the Na/K-ATPase was inhibited significantly by copper. A change in the activity of this enzyme may disturb the ion homeostasis of Na and K. In addition, Cu participates in redox reactions that generate reactive oxygen species (i.e. the hydroxyl radical), which can cause damage to lipids, proteins and DNA (Halliwell and Gutteridge 1984). Furthermore, it was demonstrated that Cu was able to inactivate iron-sulfur dehydratase enzymes (Macomber and Imlay 2009) by replacing the Fe ion. This lead to disturbance of the Fe homeostatis and additional production of reactive oxygen species due to the increase in free Fe ions.

Nickel

The use of nickel also has a long history. In ancient China (1700 – 1400 BC), nickel alloys were used for the manufacturing of weapons (Nriagu 1980). The exploitation of Ni started much later, in the 19th century (Sevin 1980), and due to strong world economic growth until 2007, the rising production of Ni was supported. After the economic crisis, which lead to lower worldwide Ni production, the production recovered in 2010 and has increased ever since (Nickel Institute 2017). The world Ni production in 2014 was estimated at 2.45 million tons, while the demand of primary Ni was estimated at 1.78 million ton in 2014 (USGS 2013). In contrast to Cu, the demand of Ni has not yet exceeded its production. The total Ni consumption in the European Union was 200 000 tons in 2013 (USGS 2013). The main use of Ni on a global scale is for the production of stainless steel (Figure 1.3), because of its valuable properties such as toughness, corrosion resistance, high-temperature stability and ductility (Reck et al. 2008).

Because production and consumption of Ni is ever increasing, it is not surprising that Ni occurs in the natural environment due to anthropogenic sources. These include amongst others, mining, smelting, waste incineration, surface runoff, industrial effluents and waste waters treatment facilities (Chau and Kulikovksy-Cordeiro 1995, Pyle and Couture 2012). However, Ni which is the 22nd most abundant element in the earth crust, also occurs naturally in the aquatic environment due to the same processes as those that were listed for Cu. These include natural erosion processes and atmospheric deposition due to windblown dust, volcanic eruptions, forest fires and sea spray (USGS 1998).

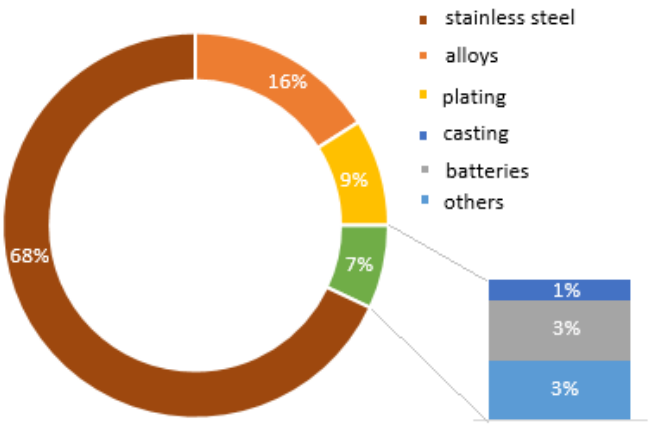

Figure 1.3 Primary global uses of nickel (Nickel institute 2017)

Dissolved nickel concentrations in pristine areas in Europe are usually lower than approximately 6 µg Ni/L (Figure 1.4), but in regions with naturally high Ni concentrations, Ni concentrations of 25 µg/L occur (Salminen 2005). In addition, local concentrations can be much higher due to anthropogenic pollution, such as in the Dommel catchment area in the Netherlands, where Ni concentrations up to 160 µg/L have been reported (Verschoor et al. 2011). In Canada, dissolved Ni concentrations for surface waters near industrial sites of up to 2000 µg Ni/L have been reported (Chau and Kulikovksy-Cordeiro 1995).

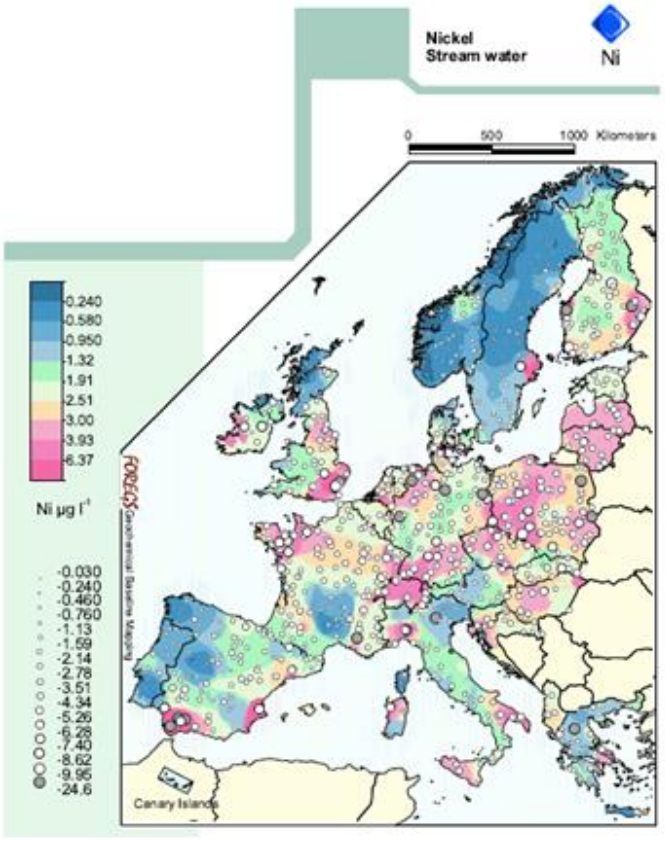

Figure 1.4 Dissolved nickel concentrations in pristine areas in Europe in 2006 (Salminen et al. 2005). The dot size scale gives the minimum and maximum of the dataset. The 10% of the lowest Ni concentrations are shown by the smallest symbol size and 2% of the highest concentrations by the big grey symbol. Between these fixed percentiles, the scale is logarithmic. In addition, a colour scale based on the following percentiles: 5, 15, 25, 35, 50, 65, 75, 85 and 95 (Salminen et al. 2005).

Nickel, an essential micronutrient for plant growth and development (Brown et al. 1987), but only officially labelled essential since 2001 (Lui 2001), can also cause toxicity when present in excess in an organism. Chronic Ni toxicity has been shown to influence amongst other endpoints, reproduction, survival and growth of fish species (Pickering 1974; Hoang et al. 2004; Deleebeeck et al. 2007a), invertebrate species (De Schamphelaere et al. 2006a; Deleebeeck et al. 2007b; Biesinger and Christensen 1972; Muyssen et al. 2006) and algal species (Spencer and Greene 1981; Wong et al. 2000; Deleebeeck et al. 2009).

Chen et al. (2009) demonstrated for plants that Ni toxicity is likely to be caused by indirect mechanisms, as it is not an active or redox metal. One of these routes is the competition between Ni and other essential ions such as Fe and Mg, which leads to less absorption and therefore deficiency of the latter ions. Because Ni has the same oxidation state as Mg, it can be exported into the cell via the Mg^{2+} ion transport system, and can therefore also reduce the Mg^{2+} uptake (Oller et al. 1997). Pane et al. (2003) also observed that Mg^{2+} uptake was reduced during acute and chronic exposure to Ni in *Daphnia magna*. A recent study by Brix et al. (2017), who used an adverse outcome pathway analysis to identify mechanisms of action for Ni, also identified that disruption of Mg^{2+} and $Fe^{2+/3+}$ homesotatis are 2 events by which Ni may exert toxicity to aquatic organisms. This all suggest for plants and daphnids that Ni most probably works as a Mg antagonist. This agrees with the observations of the protective effects of Mg on Ni toxicity to algae and daphnids (Deleebeeck et al. 2009; Deleebeeck et al. 2008). Another indirect route of Ni toxicity is by reducing the activity of antioxidant enzymes such as superoxide dismutase and peroxidase (Baccouch et al. 1998; Chen et al. 2009; Gajewska and Skłodowska 2005; Brix et al. 2017). As such, cells are less well protected against reactive oxygen species that can cause damage to lipids, proteins and DNA.

Zinc

Demands for zinc, which was brought to Europe via India and then China in the 17th century (Weeks 1932), increased rapidly during the industrial revolution (Nriagu 1996). Nowadays, it is the fourth most used non-ferrous metal worldwide, after iron, aluminium and copper (USGS 2014b). It is therefore not surprising that the world Zn production in 2014 was estimated at 13.3 million tons (USGS 2014b). The global demand of primary Zn was estimated at 13.7 million ton in 2014 (USGS 2014b). Similar to Cu, the demand of Zn has exceeded its production. The total Zn consumption in the European Union was approximately 2 million tons in 2013 (USGS 2014b). The main use of Zn on a global scale is for galvanizing (Figure 1.5), because of its most valuable property, corrosion resistance.

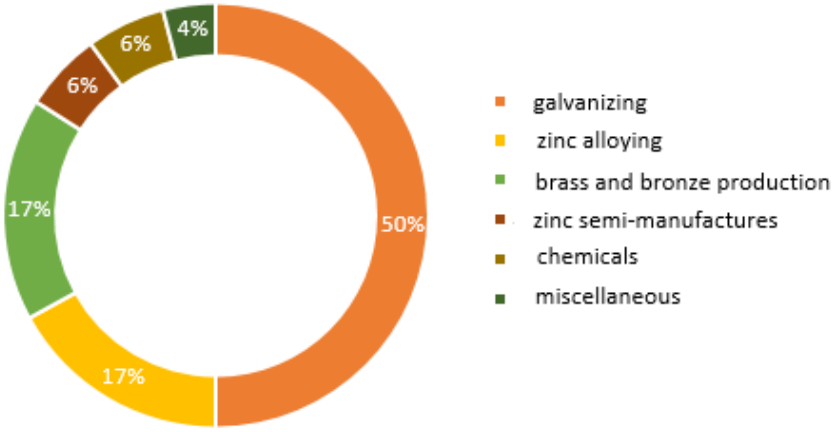

Figure 1.5 Primary global uses of zinc (ILZSG 2017)

Not surprisingly, anthropogenic sources of Zn are significant, arising from corrosion of galvanized products and Zn alloys, atmospheric deposition, wastewater treatment plants, urban runoff and drainage from agricultural soils, mining and metal-related industrial activities (Hogstrand 2012). Additionally, as it is the 25th most abundant element in the earth crust (Luoma and Rainbow 2008), it also enters the aquatic environment via natural sources. These are again similar to those of Cu and Ni: natural erosion processes and atmospheric deposition due to windblown dust, volcanic eruptions, forest fires and sea spray.

Dissolved zinc concentrations in pristine areas in Europe have been reported to range between 0.1 and 31 µg/L (Salminen 2005; Figure 1.6). Van Sprang et al. (2009) reported total Zn values between 5.4 and 42.6 µg/L in European rivers unaffected by historical mining and point sources. However, local Zn concentrations near mining sites (Luoma and Rainbow 2008) and industrial sites (Verschoor et al. 2011) can be much higher.

Zinc, although essential for human, animal and plant life, can cause toxicity when present in excess in an organism. Chronic Zn toxicity has been shown to influence amongst other endpoints, reproduction, survival and growth of fish species (Skidmore 1964; De Schamphelaere and Janssen 2004b; Besser et al. 2007), invertebrate species (Paulauskis and Winner 1988; Heijerick et al. 2005a; De Schamphelaere and Janssen 2010) and algal species (De Schamphelaere et al. 2005; Wilde et al. 2006; Gao et al. 2016).

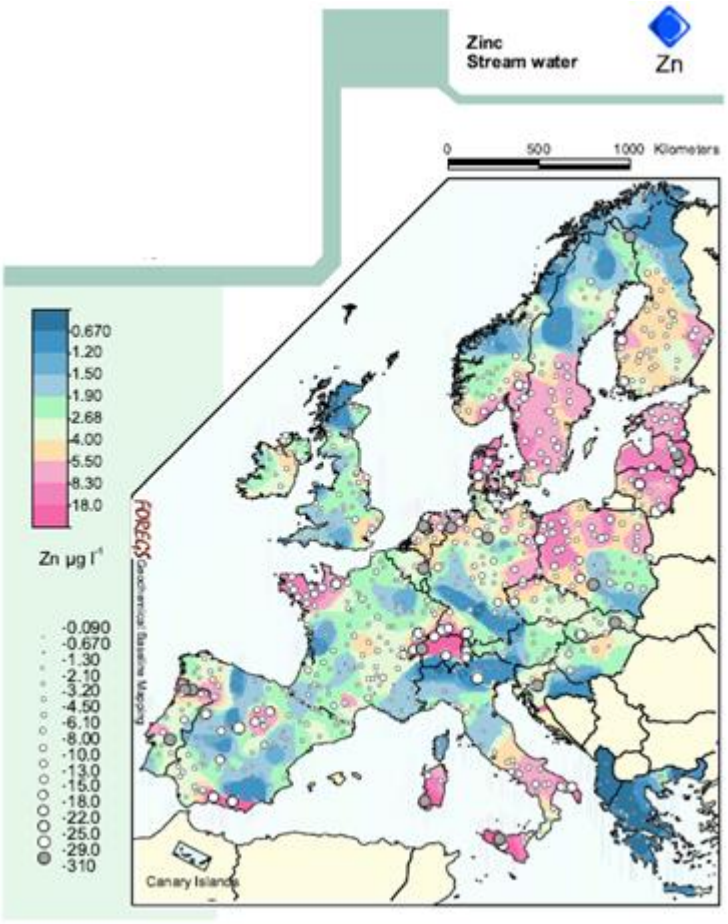

Figure 1.6 Dissolved zinc concentrations in pristine areas in Europe in 2006 (Salminen et al. 2005). The dot size scale gives the minimum and maximum of the dataset. The 10% of the lowest Zn concentrations are shown by the smallest symbol size and 2% of the highest concentrations by the big grey symbol. Between these fixed percentiles, the scale is logarithmic. In addition, a colour scale based on the following percentiles: 5, 15, 25, 35, 50, 65, 75, 85 and 95 (Salminen et al. 2005).

An important mode of action of zinc in fish and daphnids is the inhibition of Ca^{2+} uptake, which can lead to hypocalcaemia (Spry and Wood 1985; Hogstrand et al. 1995; Muyssen et al. 2006). Muyssen et al. (2006) demonstrated that mortality to daphnids was mainly an acute process due to inhibition of the Ca uptake. At sub-lethal reductions of Ca body contents, reduced growth and reproduction is observed due to decreased food intake as a result of inhibited movement and filtration rate. On a chronic timeframe, however, repair processes were observed and Ca body contents were restored (Muyssen et al. 2006). It is therefore not unlogic that Ca provides a protection against acute and chronic Zn toxicity (Heijerick et al. 2003; 2005).

1.2. Metal bioavailability

Metal speciation and its influence on toxicity

As discussed above, metals are present in the aquatic environment due to both natural and anthropogenic sources. However, toxic effects can only occur when the metal is taken up by an organism. Because not all metal species are equally bioavailable to an organism, the speciation of the metal is of critical importance in metal toxicity (Luoma and Rainbow 2008). Metals can be present in two

phases in the water column: the particulate phase and the dissolved phase, although the importance of the former in metal toxicity is less important than the latter (DeForest and Meyer 2015). In the dissolved fraction, the distribution of the metal species is dependent on the water chemistry. For instance, the presence of organic ligands (i.e. dissolved organic matter) and inorganic ligands (e.g. CO_3^{2-}, SO_4^{2-}, OH^-) will result in the complexation and therefore decrease of free metal ions. On the other hand, the competition between protons and metal ions for complexation to these organic ligands will result in an increase of free metal ions (Figure 1.5). In general, the free metal ion is the most bioavailable and therefore most toxic species (Campbell 1995; Paquin et al. 2002; De Schamphelaere and Janssen 2004a).

These chemical speciation processes are embedded in computational models such as the Windermere Humic Aqueous Model VII (WHAM VII; Tipping et al. 2011), which was used in this study. This model incorporates a thermodynamic database containing stability constants for inorganic complexation as well as a model (Humic Ion-Binding Model VII) that describes the interactions of metals and protons at the binding sites of humic and fulvic acids (Tipping et al. 2011). As such, it can be used to calculate chemical speciation of metal ions and inorganic complexes, which has been done successfully in recent studies (Tipping and Lofts 2013; 2015; Iwasaki and Brinkman 2015, Nys et al. 2016).

Competition: how does it influence metal toxicity?

It was already described above that the presence of free metal ions can be influenced by the competition with protons for binding sites of organic ligands, which can increase the toxicity of a metal. However, protons not only affect metal toxicity by their effect on speciation, but also by competitive interactions at the biological surfaces, which decreases metal toxicity (Campbell and Stokes 1985). Hence, the pH of a water is an important factor when the toxicity of a metal is evaluated. In addition, certain other cations such as Ca^{2+}, Mg^{2+} and Na^+ can exert a protective effect against metal toxicity by competitive interactions at the biological surface (Figure 1.7) (Heijerick et al. 2003; De Schamphelaere et al. 2003; Deleebeeck et al. 2008; 2009). However, which cations protect against toxicity and to what extent is dependent on the metal, the organism and the duration of exposure.

For instance, Ca^{2+} and Mg^{2+} ions did not affect toxicity of chronic Cu^{2+} to *Pseudokircherniella subcapitata* (De Schamphelaere et al. 2003), while Mg^{2+} did protect against chronic Ni^{2+} toxicity to the same species (Deleebeeck et al. 2009). The protective effects of Mg^{2+} against Ni^{2+} toxicity, due to competition at the Mg^{2+} uptake sites, were also observed for *D. magna* (Deleebeeck et al. 2008) and *Oncorhynchus mykiss* (Deleebeeck et al. 2007a). The protective effects of Ca^{2+} against Ni^{2+} toxicity on the other hand were attributed to competition at the Ca^{2+} uptake sites in *O. mykiss*, but to secondary effects of Ca in the maintenance of the cell membrane integrity in *D. magna*. Heijerick et al. (2005) demonstrated the protective effects against chronic Zn^{2+} toxicity as a result of competition with Ca^{2+}, Mg^{2+}, Na^+ and H^+ for *D. magna*, whereas the same species is not protected against chronic Cu^{2+} toxicity by competition with Ca^{2+} and Mg^{2+} (De Schamphelaere and Janssen 2004a).

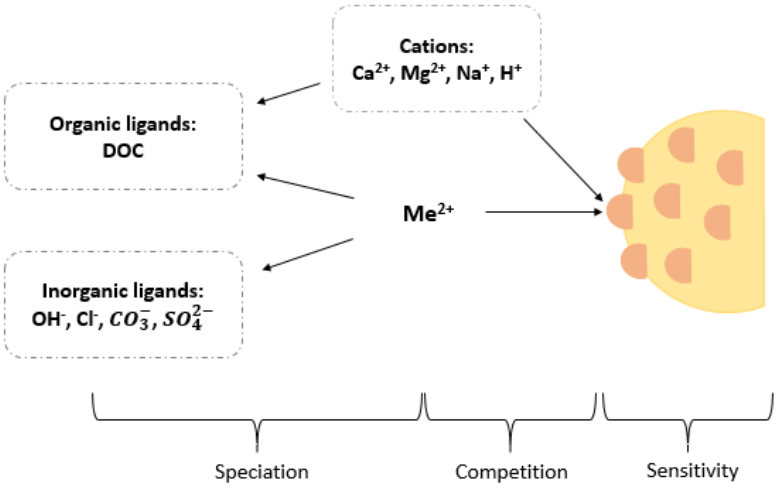

Figure 1.7 General schematic representation of metal bioavailability models

Models incorporating metal bioavailability and toxicity

Metal bioavailability and toxicity have long since been recognized to be determined by water chemistry, which lead to the development of two bioavailability models in the 80s: the free ion activity model (FIAM; Morel 1983) and the gill surface interaction model (GSIM; Pagenkopf 1983). Increased knowledge and understanding of the mechanisms of metal toxicity lead to the formulation of the biotic ligand model (BLM) by Di Toro et al. (2001). The BLM, initially developed to predict acute toxicity, assumes that the metal ions bind to a biotic ligand (Figure 1.5). The biotic ligand represents a discrete receptor or site of action on an organism where accumulation of metal leads to toxicity. The BLM is used to predict the amount of metal accumulation at this site for a variety of chemical conditions and metal concentrations. According to the conceptual framework of the BLM, accumulation of metal at the biotic ligand at or above a critical threshold concentration leads to toxicity. For example, the LA50 is the lethal accumulation of metal at the biotic ligand that results in 50% mortality, and is assumed to be independent of water chemistry (Meyer et al. 1999). In the BLM framework of Di Toro et al. (2001), it is assumed that binding stability constants for both metal ions and competing cations are the same across all species and that the LA50 is species-dependent (Santore et al. 2001).

Soon after Di Toro et al. (2001) introduced the BLM, De Schamphelaere and Janssen (2002) presented an alternative modelling approach, that also received the “BLM” stamp. The main difference between both approaches was that the biotic ligand binding stability constants were calculated directly from observed toxicity data in the approach of De Schamphelaere and Janssen (2002), which allowed for the calculation of species-specific stability constants. These stability constants were derived from the linear relationship between the activity of one cation and the free metal ion toxicity, when other cation activities are kept constant (De Schamphelaere and Janssen 2002). De Schamphelaere and colleagues developed numerous BLMs for the prediction of Zn and Cu to *D. magna* (De Schamphelaere and Janssen 2002; De Schamphelaere et al. 2002; Heijerick et al. 2002a; De Schamphelaere and Janssen 2004b; Heijerick et al. 2005a) and O. mykiss (De Schamphelaere and Janssen 2004b; De Schamphelaere and Janssen 2008).

The relation between free metal ion toxicity and proton activity is not always linear, but can be more curvilinear, which suggests that the effect of pH on free metal toxicity may be a result of other or additional factors besides the competitive effect of H^+. This was observed for chronic Cu toxicity to algae (De Schamphelaere et al. 2003), chronic Zn toxicity to algae (De Schamphelaere et al. 2005) and chronic Ni toxicity to *D. magna*, fish, *C. dubia* and algae (De Schamphelaere et al. 2006a; Deleebeeck et al. 2007a; 2008; 2009). In these models, which are more generally termed 'bioavailability models' due to the difference in model and equation structure compared to the BLMs, the effect of pH (H^+) on metal ion toxicity was expressed as a log-linear effect of pH, represented by a slope parameter, i.e. S_{pH}. When observed, the protective effects of other competitive ions were incorporated as conventional BLM-type competition constants.

1.3. Metal mixture toxicity

Metals are rarely present in the environment as individual substances. More commonly, they occur as mixtures. The effects of individual metals can differ from the effects of the same metals when these metals occur in a mixture. Because testing of every possible mixture of metals that could occur in the aquatic environment is time consuming, costly and unrealistic, predictions of mixture toxicity are made using mathematical models.

Two mixture reference models are generally accepted: the concentration addition (CA) and independent action (IA) model (Jonker et al. 2005; 2011). The CA model assumes that components in a mixture have the same mode of action at the same toxicity site, are non-interactive and work independently (Loewe and Muischneck 1926). The model is described using Equation 1.1.

$$\sum_{i=1}^{n} TU_{i,x} = \sum_{i=1}^{n} \frac{c_i}{ECx_i} = 1 \qquad (1.1)$$

Where *n* is the number of mixture components and TU_i is the toxic unit of component *i* in the mixture. The TU_i, a dimensionless parameter, is defined as the ratio between the concentration of component *i* in the mixture and ECx_i, the x% effective concentration of component *i* in the mixture (Joncker et al. 2005). When the ∑TU equals 1 and the mixture causes x% effect, CA holds true. This model therefore assumes that as long as the $\sum TU_{i,x}$ of the mixture does not change, the components in a mixture are interchangeable without changing the overall mixture toxicity. This implies that toxicity can occur in mixtures wherein the mixture components are present at low concentrations as long as the number of mixture components is high enough, because all mixture components contribute to the overall mixture toxicity proportional to their toxic units.

According to the IA model, the components in a mixture have a dissimilar mode of action, bind to different sites of toxicity and are non-interactive (Bliss 1939). The global mixture effect according to IA is the product of the individual responses to each of the individual components in a mixture and is calculated using Equation 1.2.

$$E_{mix} = 1 - (\prod_{i=1}^{n}(1 - E_i)) \qquad (1.2)$$

Where E_{mix} is the global effect of a mixture that consist of *n* components and E_i is the individual effect of component *i* in the mixture if applied singly. In contrast to the CA model, the IA model assumes that only those components that are present at a concentration that causes an effect (i.e. Ei > 0) will contribute to the overall mixture effect. Therefore, when a mixture contains a lot of components, but these do not cause effect individually, there will also be no mixture effect.

Both CA and IA assume that the components in a mixture are non-interactive. However, interactions between components in a mixture can occur. If the observed effect in a mixture is smaller than those predicted with the CA or IA model, the mixture is said to be antagonistic or “less-than-additive”. In contrast, if the observed effect of the mixture is larger than expected based on CA or IA, the mixture is said to by synergistic or “more-than-additive” (Jonker et al. 2005; 2011).

Both models are commonly used to assess the effects of mixtures, although CA is used more often due to its conservativeness in the context of metal mixture assessment (Vijver et al. 2011). Although countless tests have been conducted to assess metal mixtures, no clear patterns have appeared. Extensive research conducted by Norwood et al. (2003) and Vijver et al. (2011) has shown that mixtures interact (i.e. are synergistic or antagonistic) in more cases than not (i.e. are additive). However, these interactive effects depend on, amongst other things, the species tested, the metal combination tested, the water chemistry and the selected endpoint (Norwood et al. 2003; Vijver et al. 2011; Liu et al. 2015; Sharma et al. 1999; Nys et al. 2017c).

The concepts of both the CA and IA model have been implemented to develop metal mixture bioavailability models (MMBMs). These MMBMs implement the BLM-concept to predict mixture toxicity. When based on the CA-concept, the MMBM assumes that metals bind at a single shared biotic ligand site (Kamo and Nagai 2008; Hatano and Shoji 2008; Jho et al. 2011; Iwasaki et al. 2015; Farley et al. 2015). When based on the IA-concept, the MMBM assumes that multiple biotic ligand sites are present (Versieren et al. 2014; Santore and Ryan 2015; Nys et al. 2017a). Based on the metal mixture modelling evaluation project, in which these models were extensively tested, the IA model is in general the better option to model metal mixture toxicity (Van Genderen et al. 2015; Farley et al. 2015). However, the CA, which is in general more conservative than the IA model (Vijver et al. 2011; Meyer et al. 2015; Nys et al. 2016; Nys et al. 2017b) can be implemented as a default first-tier approach in an assessment of potential mixture toxicity.

1.4. Metal regulations in Europe

Regulations for single metals: the present

Since the start of the 21st century, the Water Framework Directive (WFD) has set out strategies against the pollution of water. A first step was the identification of priority substances that presented a significant risk to the aquatic environment (EC 2001). Amongst these substances, also a number of metals were prioritised, i.e. Ni, Cd, Pb and Hg. For these metals, an Environmental Quality Standard (EQS) was established in the European Union that had to be met by all member states by 2015 (EC 2008). For Ni, this value was originally defined at 20 µg dissolved Ni/L. By 2013, the list of priority substances was

revised and new substances were added to the list, adding up to a total of 33 substances. In addition, the EQS values of the metals present on the list were adapted to a more 'worst-case' generic value. For instance, the EQS for Ni was lowered to 4 µg dissolved Ni/L (EC 2013). In addition, member states were given the authority to take into account the water chemistry and thus evaluating risk based on bioavailability of metals (EC 2013). This bioavailability based EQS may be implemented if it can be determined based on bioavailability models, i.e. BLMs, regression models or speciation models (EC 2011).

Although Ni was selected as a priority substance under the EU WFD (EC 2001), zinc and copper are currently not. Therefore, member states of the EU are responsible for defining member state specific EQS values for these substances. In Flanders, an EQS for dissolved Zn and Cu of 20 µg/L and 7 µg/L is set for surface waters, respectively (VR 2015). However, for all three metals, bioavailability adjusted EQS values can be calculated because BLMs for all metals have been developed (e.g. De Schamphelaere and Janssen 2002; De Schamphelaere et al. 2002; Heijerick et al. 2002a Deleebeeck et al. 2007a).

Next to the WFD that strives against the pollution of water, REACH aims to improve the protection of human health and the environmental by the registration, evaluation and authorisation of chemicals (EC 2006). The REACH regulation requires that industries obtain information on the properties of their chemical products and perform a chemical safety assessment or environmental risk assessment (ERA) in which the risks of the substance are assessed. Typically, this assessment is a three stage process: an exposure assessment, an effect assessment and a risk characterization (Figure 1.8). In the exposure assessment, the concentration of the substance in the environment is predicted (PEC: predicted environmental concentration) or measured (MEC: measured environmental concentration). In the effect assessment, the predicted no effect concentration (PNEC), or the concentration below which no (adverse) effect on the environment is expected, is determined. For metals, a bioavailability based effects assessment is possible (ECHA 2008) (Figure 1.9). For the metals considered in this study, bioavailability based PNECs have been used in European risk assessments, i.e. for Cu (ECI 2008), for Ni (DEPI 2008) and for Zn (Van Sprang et al. 2009). To calculate a bioavailability based PNEC, the effect data (10% effect concentrations (EC10) and no-observed-effect concentrations (NOECs)) in a toxicity database of a metal is normalized to a given river-basin specific physico-chemistry using BLMs. Subsequently a species sensitivity distribution (SSD) is constructed with the lowest geometric mean NOEC or EC10 (i.e. the most sensitive endpoint) per species (Van Sprang et al. 2009). From these SSDs the hazardous concentration affecting 5% of the species in a community (HC5) is calculated. The bioavailability based PNEC is then derived from the HC5 by dividing the HC5 value by an assessment factor between 1 and 5 depending on the uncertainties associated with the method of HC5 derivation (ECI 2008; Van Sprang et al. 2009).

In a final step of the chemical safety assessment, the risk characterisation is performed by comparing the PEC with the PNEC. If the Risk Characterisation Ratio (RCR = PEC/PNEC) is larger than 1, the substance is said to present a risk to the ecosystem of the considered environmental compartment.

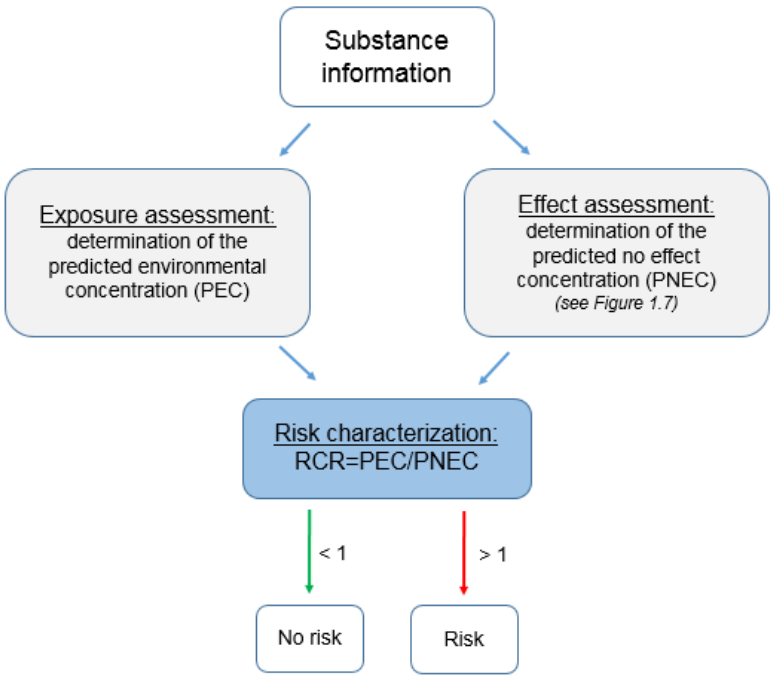

Figure 1.8 General schematic representation of a chemical safety assessment or envrionmetal risk assessment

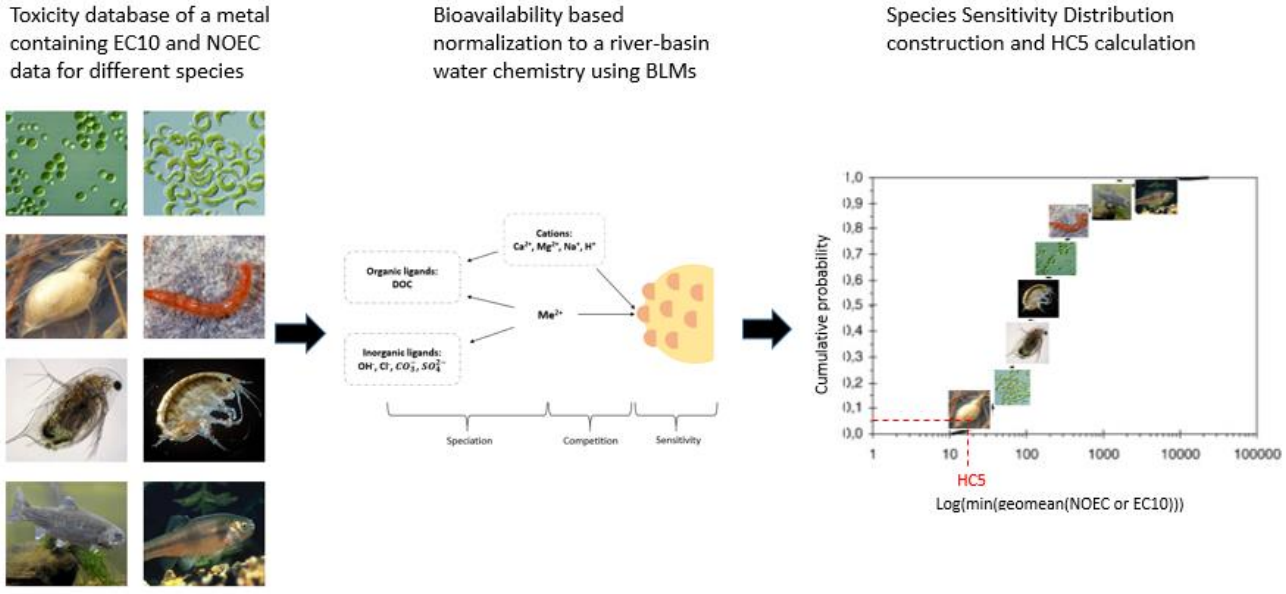

Figure 1.9 General schematic representation of the process in which a bioavailability based HC5 is calculated, from which the bioavailability based PNEC can be derived.

Regulations for metal mixtures: the future

Although the regulation of single metal exposure is nowadays ingrained in the (EU) metal risk assessment frameworks, in the environment, organisms are usually simultaneously exposed to a multitude of metals (EC 2006). However, currently, possible mixture effects of metals are not yet considered in risk assessment frameworks around the world. The only exception is found in Australia and New Zealand, two countries that explicitly incorporate guidelines to calculate metal mixture risk in their regulatory guidelines (A&NZ 2000). In the USA, mixture toxicity of metals is mentioned in guidance documents, but is not yet incorporated into regulations (US EPA 1991; 1994). Possible mixture effects

are also not yet considered in European risk assessment frameworks. This may result in underestimation of the risks to human health and the environment posed by metal exposure. However, a general agreement exists that future risk assessment procedures should require the consideration of mixture toxicity effects (SCHER 2009; CEU 2009). Governments and scientists across the EU have therefore not rested on their laurels, as different initiatives have considered how to regulate chemical mixtures (Kortenkamp et al. 2009; Backhaus et al. 2011; EC 2012). Some examples of approaches that were put forward include calculating a RCRs for mixtures expressed in terms of toxic units ($\sum TU_i=\sum(c_{w,i}/QS_i)$; with $c_{w,i}$ the concentration of substance *i* in the water). In other approaches, each substance in a mixture is treated equally and in turn the EQS of each substance is divided by the total number of substances in the water. In addition, more elaborate methods have been proposed that combine CA and IA models with SSD-approaches to evaluate mixture risks (Traas et al. 2002; De Zwart and Posthuma 2005). Recently, these methods were implemented in a tiered approach to evaluate mixture risks that was presented by Backhaus and Faust (2012) (Figure 1.8). In a first tier of the risk assessment approach, the CA model is first applied on the community level. Here, a risk quotient of the mixture is calculated ($RQ_{PEC/PNEC} = \sum(PEC_i)/(PNEC_i)$). If the RQ is higher than a certain threshold, the CA model is subsequently applied on the toxicity data of the individual species by calculating a RQ_{STU} based on the 'species toxic units'. If the data still suggests mixture effects, the IA model is applied in a second, less conservative tier. Gregorio et al. (2013) also developed a method to evaluate mixture risks starting from information on single species in combination with the IA approach, to calculate risk estimated for species assemblages.

1.5. Objectives

Environmental Quality Standards and European risk assessment frameworks concerning single metals have taken a leap forward since the change of the millennium, by implementing bioavailability based EQS values (EC 2013) and bioavailability models (ECI 2008; DEPA 2008; Van Sprang et al. 2009). However, European risk assessment frameworks do not account for possible mixture effects due to exposure to metal mixtures. Because there seems to be no clear pattern in the interactions between metals, the development of metal mixture risk assessment frameworks is currently hindered (Meyer et al. 2015; Van Genderen et al. 2015). Recently however, a tiered approach to evaluate mixture risks was presented by Backhaus and Faust (2012) (Figure 1.10). In this approach, the models of CA and IA are applied directly to species sensitivity distribution (SSD) curves, as explained by De Zwart and Posthuma (De Zwart and Posthuma 2005). Although interest is growing in these methods in the field of mixture risk assessment, they also have an important limitation: the predictions made by the CA and IA models are theoretically only consistent when applied to single species (dose–response curves (DRCs)), and not when applied to communities (SSDs) (Gregorio et al. 2013). However, the tiered approach by Backhaus and Faust (2012) also includes a theoretically consistent method that applies CA first to different single species separately and then combines all single-species information to calculate risk estimates for a species assemblage. A similar method, but developed based on the IA method was also proposed by Gregorio et al. (2013).

However, these two approaches also have a few limitations. The approach of Backhaus and Faust (2012) only uses the so-called base set of toxicity data for a substance. This base set (i.e., *x*% effect concentration (EC*x*) values for algae, crustaceans, and fish) is the minimum set of data required by REACH for the calculation of a PNEC (ECHA 2008). Although their approach can be applied to a broader array of substances (i.e., so-called data-poor substances) and can be extended to a higher number of species, the method applies subjective assessment factors to calculate the risk quotient for a mixture. Gregorio and colleagues (2013) only evaluated their method using sets of species toxicity values that were randomly generated from SSDs of sets of hypothetical substances, and they also assumed a range of possible slope values of dose–response curves for these species, because they argued that implementing the method with existing data was not possible with the typical amount of data available for a substance.

Bearing in mind the limitations found in the research mentioned above, the objective in the present study was to evaluate differences in mixture risk estimates for a number of monitoring databases, using the four approaches listed above but overcoming the limitations mentioned in these approaches.

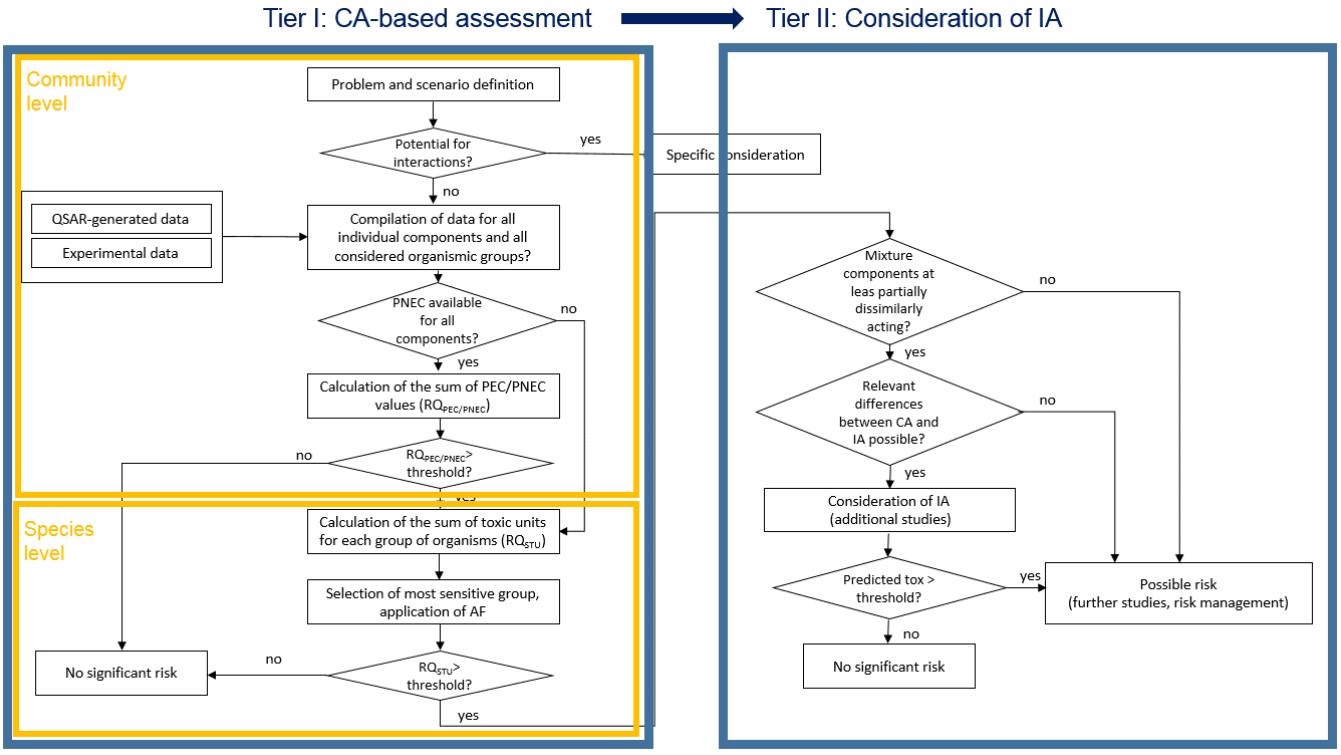

Figure 1.10 Outline for the predictive ecotoxicological risk assessment of chemical mixtures proposed by Backhaus and Faust (2012) (taken from Backhaus and Faust (2012).

1.6. Research approach

The present study can be divided into three major sections. In a first section, the toxicity of mixtures of Cu, Ni and Zn was investigated building on the research reported above and bearing in mind their limitations (Figure 1.11). In the second section, certain limitations discovered in Chapter 1 were addressed and adaptations to existing bioavailability models and normalization procedures were made (Chapter 3, 4, 5, 7). In a third section, the implications of these adaptations on metal mixture risk assessment is evaluated (Chapter 6, 8 and 9).
Furthermore, the study can also be divided into two parts in terms of the bioavailability models that were used. In a first part (Chapters 2-4), all calculations and analyses were done using existing bioavailability models that are already implemented in risk assessments. In a second part (Chapters 5-9), these bioavailability models were improved and these new models were used for calculations and analyses.

Bearing in mind the limitations found in the research mentioned above, in the **second Chapter** in the present study, we aimed to evaluate differences in mixture risk estimates using actual chronic toxicity data for Cu, Ni and Zn for more than the base set of species. In addition, we applied four methods for mixture evaluations on existing environmental monitoring datasets to estimate metal mixture risks. Copper, Ni and Zn were selected because it has been demonstrated for numerous species that toxic effects due to these metals can occur and that these elements are commonly present together in rivers with historic industrial pollution (Verschoor et al. 2001).

Based on Chapter 2, certain weaknesses/assumptions in our research were encountered. For instance, the underlying assumptions of the four methods should be tested. In addition, the uncertainty about the degree of conservatism and accuracy compared to observed community-level metal mixture toxicity effects should be assessed. Furthermore, the bioavailability models used in Chapter 2 should be evaluated and adapted when necessary. In addition, it should be evaluated whether these models can all be updated to the same speciation software, without loss of predictive capacity. These weaknesses/assumptions will be addressed in the following chapters.

In Chapter 2 four methods were used of which the underlying assumptions should be tested. More specifically, the following research question should be addressed: Is the CA model or the IA model best to predict chronic toxicity of metal-mixtures? Because microalgae, as primary producers, form the base of the food web, it is of utmost importance to understand the effects of metals on these organisms. And although numerous studies have examined the effects of metal mixtures on invertebrates, fish and higher plants, few have been conducted on freshwater microalgae. Research that has been conducted so far with microalgae appears not to be suitable to answer our research question. For instance, Franklin et al. (2002) examined the effect of mixtures of Cu, Zn and Cd on *Chlorella sp*. However, these authors only used the CA model and not the IA model as reference model to investigate the mixture effects, which makes it impossible to compare both models. In addition, the toxicity of the mixtures was not investigated simultaneously with those of each of the individual components in the mixture. This was also not the case in the studies on *P.subcapitata* performed by Nagai and Kamo (2014). However, De Laender et al. (2009) demonstrated that when toxicity of single substances and mixtures is not simultaneously assessed erroneous conclusions about the interactive effects can be made.

Furthermore, the above mentioned research was conducted in one specific water chemistry, although it has been demonstrated that the interactive effects of metals in mixtures can depend on water chemistry (Norwood et al. 2003; Vijver et al. 2011). In **Chapter 3**, we therefore addressed the latter by performing experiments with the freshwater microalgae *P.subcapitata* for the ternary mixture Cu-Ni-Zn in various natural waters that show diverse water-chemistry variables. In addition, the toxicity of the individual metals were investigated simultaneously with the mixture.

Another possible obstacle for applying the four methods described in Chapter 2 is the uncertainty about the degree of conservatism and accuracy compared to observed community-level metal mixture toxicity effects. To assess this limitation, the metal mixture risk evaluation methods should be validated using multispecies experiments (microcosm/mesocosm studies) and/or field data. To evaluate the conservativeness of our methods, a calculated msPAF, based on reported or estimated physico-chemistry, should be compared to community-level effects. Several studies have reported data of mixture toxicity (e.g. Richardson and Kiffney 2000; Hickey et al. 2002; Clements 2004; Clements et al. 2013). However, these studies show certain limitations which makes them inadequate for our research. For instance, DOC, an important variable influencing metal toxicity, was not measured. In addition, all mentioned studies deal with short term toxicity, i.e. from 6 days (Richardson and Kiffney 200) to 34 days (Hickey et al. 2002). Furthermore, the organisms that were exposed to the mixture were limited to benthic macroinvertebrates in most studies. Finally, none of the studies investigated the mixture that we are currently examining, i.e. Cu-Ni-Zn. Because we did not find the adequate information in literature, a multispecies microcosm experiment was performed to evaluate the conservativeness and accuracy of our methods (**Chapter 4**). In this experiment, which lasted for 56 days, a naturally occurring zooplankton and phytoplankton community was exposed to a mixture of Cu, Ni and Zn.

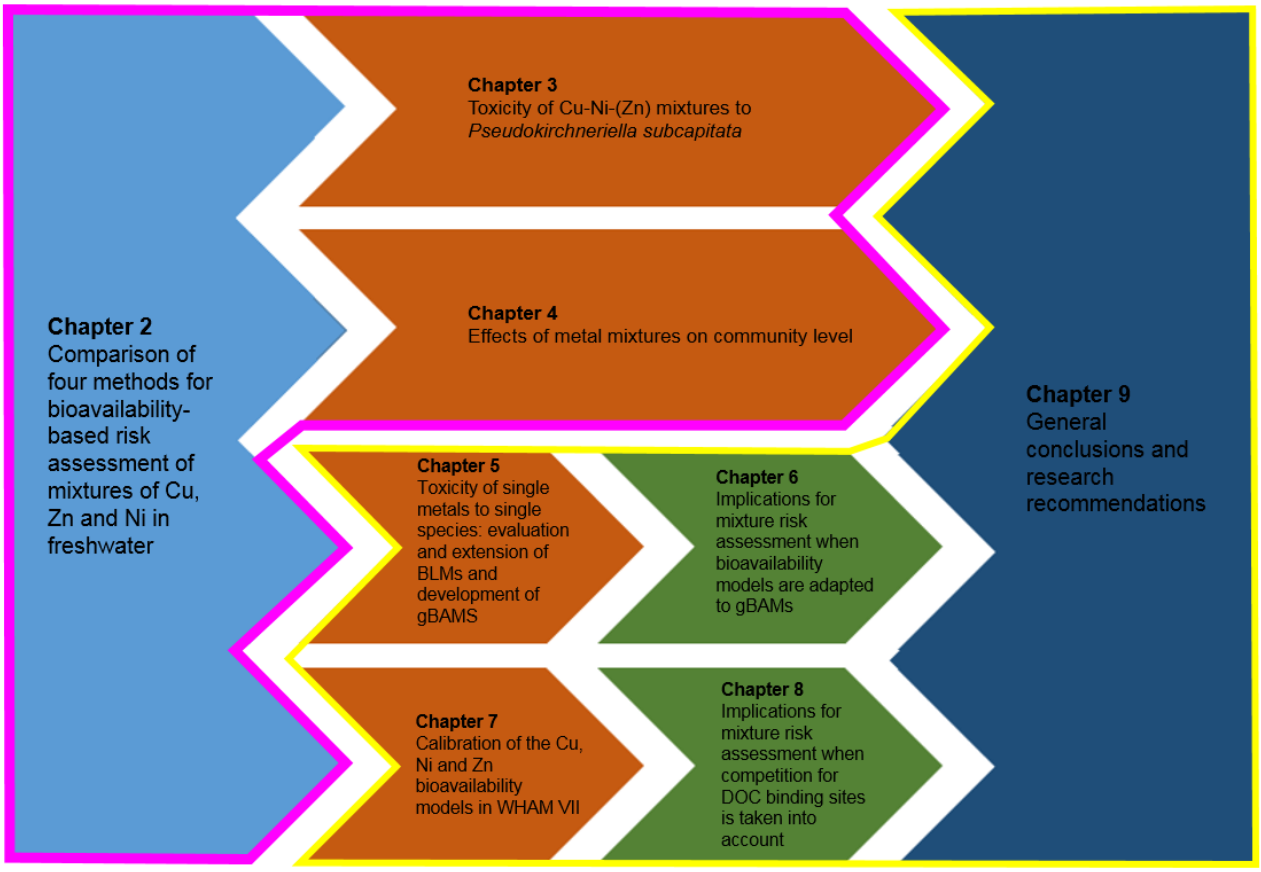

Figure 1.11 General overview of the framework of the study. In Chapter 2 the toxicity of mixtures of Cu, Ni and Zn was investigated (light blue figures). In Chapter 3, 4, 5 and 7 the limitations discovered in Chapter 1 were addressed (orange figures). In Chapter 6 and 8 the implications of these adaptations on metal mixture risk evaluation is assessed (green figures). Chapter 9 gives the general conclusions and research recommendations (dark blue figure). The chapters can also be divided into two parts in terms of the bioavailability models used: in Part I calculations and analyses were done using existing models that have been used in risk assessments (delineated in pink) and in Part II models were improved and implications for risk calculations were assessed (delineated in yellow).

In a **fifth Chapter**, the bioavailability models that were formerly used to normalize toxicity data in Chapter 2 were evaluated and improved when necessary. The main issue that was addressed was the nonlinearity between the H^+ activity and the $EC50_{Me2+}$ activity that was observed for chronic Cu and Zn toxicity to *Daphnia magna* and/or *Oncorhynchus mykiss*. This nonlinearity implies that the effect of pH should not be described by single-site competition between Me^{2+} and H^+. Rather, the effect of pH should be modelled based on an empirical linear relationship between pH and $EC50_{Me2+}$. We will call this type of model a generalized BioAvailability Model (gBAM).

The first bioavailability model that we took an in depth look into was the *D. magna* BLM for Cu. Cu BLMs have been applied to derive Water Quality Criteria in the US and PNECs in the EU. Although both frameworks use a similar approach to derive bioavailability-based PNEC or WQC values for copper, the structural formulation and parameterization of the BLMs that is used in both frameworks differ (US EPA 2007; ECI 2008). The purpose was to evaluate the capacity of these two different copper BLMs to predict chronic toxicity of copper. In addition, we explored the ability of a generalized BioAvailability Model (gBAM) as an alternative for the existing BLMs to predict chronic effect concentrations for copper in two *D. magna* clones. Secondly, we took an in depth look into the bioavailability models for *D. magna* and

P.subcapitata for Zn. These models had so far only been validated within a certain range of water chemistry. Yet, around 20% of the European surface waters fall outside this 'validation boundary' (Salminen et al. 2005). This means that a considerable number of European waters falls outside the applicability range of the bioavailability models. The purpose was therefore to evaluate if the Zn bioavailability models can be extrapolated outside their bioavailability ranges. Based on the results, we also explored the ability of a generalized BioAvailability Model (gBAM) as an alternative for biotic ligand model to predict chronic effect concentrations for Zn to *D. magna*. In the two first sections of Chapter 5, gBAMs were developed to predict toxicity of Cu and Zn to *D. magna*. With this, the uniformisation of all bioavailability models (i.e. of Cu, Ni and Zn for invertebrates, fish and algae) to a gBAM-structure was almost complete. The models that did not yet incorporate a pH slope parameter (i.e. had the gBAM-structure) were the bioavailability models for fish for Zn and Cu. Therefore, in a third section of Chapter 5, we developed and validated a gBAM for the metals Zn and Cu for fish.

In **Chapter 6**, we evaluated the impact of the implementation of the models developed in Chapter 5 on risk estimations. This was done by repeating the calculations performed in Chapter 2 but implementing the gBAMs developed in Chapter 5 for *D. magna* and fish for the metals Cu and Zn instead of the original BLMs.

A final limitation of the calculations performed in Chapter 2 that was evaluated in this work, was that the limitations were based on bioavailability-normalized dissolved metal concentrations. However, when present in a mixture, metals may compete with each other for the binding sites of DOC. Hence, metal mixture risks should ideally be evaluated on the free ion activity level. However, assessing risks based on free ion activities is limited because the chronic bioavailability models for individual metals are currently based on different software to model metal speciation: i.e. WHAM V for Zn (Van Sprang et al. 2009) and Cu (ECI, 2008) and WHAM VI for Ni (DEPA, 2008). Additionally, some assumptions for chemical speciation calculations differ between these metals. Recently, an updated version of the WHAM software (WHAM/Model VII) was developed (Tipping 2011). Therefore, in **Chapter 7** we evaluated whether the chronic daphnid, fish and algae metal bioavailability models can all be updated to the WHAM VII speciation software, without loss of predictive capacity.

In **Chapter 8**, we combined the adaptations made to the bioavailability models (Chapter 5) with the update of the models all WHAM VII (Chapter 7) to evaluate the impact on mixture risk estimations.

In a final chapter, **Chapter 9**, we conclude and integrate the research that was conducted in all previous chapters and propose a possible metal mixture risk evaluation approach.

Part I

In Part I of this work, we first aimed to evaluate differences in mixture risk estimates using four methods for mixture risk evaluations. For this, actual chronic toxicity data for Cu, Ni and Zn for more than the base set of species was used and existing environmental monitoring datasets were used to estimate metal mixture risks (Chapter 2).

In addition, two limitations encountered in Chapter 2 were addressed. First, we tested the underlying assumptions of the four methods. More specifically, the following research question was adressed: Is the CA model or the IA model best to predict chronic toxicity of metal-mixtures? We addressed the latter by performing experiments with the freshwater microalgae *P.subcapitata* for the ternary mixture Cu-Ni-Zn in various natural waters that show diverse water-chemistry variables (Chapter 3). Second, we assessed the uncertainty about the degree of conservatism of the four methods described in Chapter 2 compared to observed community-levels metal mixture toxicity effects. To evaluate the conservativeness of our methods, a calculated msPAF, based on measured physico-chemistry, was compared to community-level effects obtained via a microcosm experiment in which a naturally occurring zooplankton and phytoplankton community was exposed to a mixture of Cu, Ni and Zn (Chapter 4).

For these three chapters in Part I, existing bioavailability models for algae, invertebrates and fish for the metals Cu, Ni and Zn were used that have also been used in risk assessment procedures.

Two

COMPARISON OF FOUR METHODS FOR BIOAVAILABILITY-BASED RISK ASSESSMENT OF MIXTURES OF CU, ZN AND NI IN FRESHWATER

Redrafted from:

Van Regenmortel T, Nys C, Janssen CR, Lofts S, De Schamphelaere. KAC. 2017. Comparison of four methods for bioavailability-based risk assessment of mixtures of Cu, Zn, and Ni in freshwater. Environmental Toxicology and Chemistry 36(8): 2123-2138

2. Comparison of four methods for bioavailability-based risk assessment of mixtures of Cu, Zn and Ni in freshwater

2.1. Introduction

In the environment, organisms are usually simultaneously exposed to a multitude of substances including pesticides, pharmaceuticals, and metals (EU, 2006). Although risk assessment is still mainly performed on a single-substance basis, various approaches toward the risk assessment of mixtures of chemicals have been proposed (Backhaus et al. 2002; De Zwart and Posthuma 2005; Backhaus and Faust 2012; Gregorio et al. 2013; European Commission 2012). These approaches are mainly based on 2 fundamental concepts that predict the joint toxicity of substances in a mixture to a single species based on each substance's individual effects: concentration addition (CA) and independent action (IA). Although these 2 concepts were originally theorized and mathematically developed to predict mixture toxicity to different single species (Backhaus et al. 2003), they have also been applied directly to species assemblages, both real (Balistrieri et al. 2015; Mebane et al. 2016) and mathematical (De Zwart and Posthuma 2005). In the latter case this is done by applying the 2 models directly to species sensitivity distribution (SSD) curves, as explained by De Zwart and Posthuma (De Zwart and Posthuma 2005). These authors estimated the risks of chemical cocktails on species assemblages expressed as a "multisubstance potentially affected fraction of species" (msPAF). Although interest is growing in these methods in the field of mixture risk assessment, they also have an important limitation: the predictions made by the CA and IA models are theoretically only consistent when applied to single species (dose–response curves (DRCs)), and not when applied to communities (SSDs) (Gregorio et al. 2013). More recently, Backhaus and Faust (2012) as well as Gregorio et al. (2013) developed theoretically consistent methods that apply CA or IA first to different single species separately and then combine all single-species information to calculate risk estimates for a species assemblage. However, these 2 approaches also have a few limitations. The approach of Backhaus and Faust (2012) only uses the so-called base set of toxicity data for a substance. This base set (i.e., *x*% effect concentration [EC*x*] values for algae, crustaceans, and fish) is the minimum set of data required by the European Commission's Registration, Evaluation, Authorization, and Restriction of Chemicals (REACH) for the calculation of a predicted no-effect concentration (PNEC) (European Chemicals Agency 2008). Although their approach can be applied to a broader array of substances (i.e., so-called data-poor substances) and can be extended to a higher number of species, the method applies subjective assessment factors to calculate the risk quotient for a mixture. Gregorio and colleagues (2013) only evaluated their method using sets of species toxicity values that were randomly generated from SSDs of sets of hypothetical substances, and they also assumed a range of possible slope values of dose–response curves for these species, because they argued that implementing the method with existing data was not possible with the typical amount of data available for a substance.

Fortunately, limited data availability is not an issue for several metals. Indeed, the effects of the metals copper (Cu), zinc (Zn), and nickel (Ni) on single species have been studied extensively, which makes these metals data-rich substances. More recently, metal mixture toxicity has been receiving increased attention, and study topics are focused both on influences of metal mixtures on single species (Nys et

al. 2015; Nys et a. 2016) and on communities (Balistrieri et al. 2015; Mebane et al. 2016; Iwasaki et al. 2013; Richardson and Kiffney 2000). Because it is not feasible to examine the effects of all possible mixtures of substances on every natural community experimentally, estimations of risks by means of models such as the ones described above are essential.

In the present study, we therefore aimed to evaluate differences in (ternary) mixture risk estimates among 4 methods (Table 2.1) using actual chronic toxicity data for Cu, Zn, and Ni. To this end, available toxicity datasets were first extended with recently published toxicity data as well as with the slope values of the dose-response curves (see *Materials and Methods* section). Then, for the first time, we applied these 4 methods to 4 existing environmental monitoring datasets to estimate metal mixture risks: Dommel (Verschoor et al. 2011), Rhine (ICPR 2013), Austria (ARCHE 2014), and Flanders (or VMM) (FEA 2013). The Dommel dataset represents a local industrial exposure scenario (historic pollution), whereas the Rhine, Austria, and VMM datasets represent a regional mixed exposure scenario (a combination of urban, industrial, and agricultural pollution). In addition to the environmental monitoring datasets, we investigated 1 dataset that contains high-quality environmental geochemical baseline concentrations, that is, natural background metal concentrations of freshwater surfaces across Europe (Forum of European Geological Surveys, FOREGS) (Salminen et al. 2005). By doing so, we aimed to answer 3 questions: 1) How big are the differences in risk estimates among the 4 methods when one is using actual chronic metal toxicity data and real monitoring datasets? 2) Is there a rank-order in risk estimates among the different methods? We expected that the CA_{SSD} method (concentration addition applied directly to the species sensitivity distribution; see Figure 2.1) would always be the most conservative method among the 4, based on findings by Backhaus and Faust (2012), who demonstrated this mathematically for an assemblage of 3 species. 3) If the CA_{SSD} method is the most conservative method, what is the margin of safety (MoS) provided by this method relative to the other 3 methods?

Table 2.1. Four different approaches to calculate the toxic pressure expressed as multisubstance potentially affected fractions (msPAF) of species that are described in the present and other studies[a],

This study	De Zwart and Posthuma (2003)	Backhaus and Faust (2005)	Gregorio et al. (2013)
CA_{SSD}	CA	$RQ_{PEC/PNEC}$	$M2_{ssd,CA}$
CA_{DRC}	NI	RQ_{STU}	$M1_{sp,CA}$
IA_{SSD}	RA or IJA	NI	$M2_{ssd,IA}$
IA_{DRC}	NI	NI	$M1_{sp,IA}$

[a]The terminologies are given of equivalent or analogous approaches used by De Zwart and Posthuma (2003), Backhaus and Faust (2005) and Gregorio et al (2013). The msPAF values reported are on the basis of EC10 values.CA = Concentration Addition; SSD = Species Sensitivity Distribution, RQ = Risk Quotient, PEC = Predicted Environmental Concentration; PNEC = Predicted No Effect Concentration; DRC = Dose-Response Curve, NI = Not Included; RA = Response Addition; IJA = Independent Joint Action; STU = Sum of Toxic Units

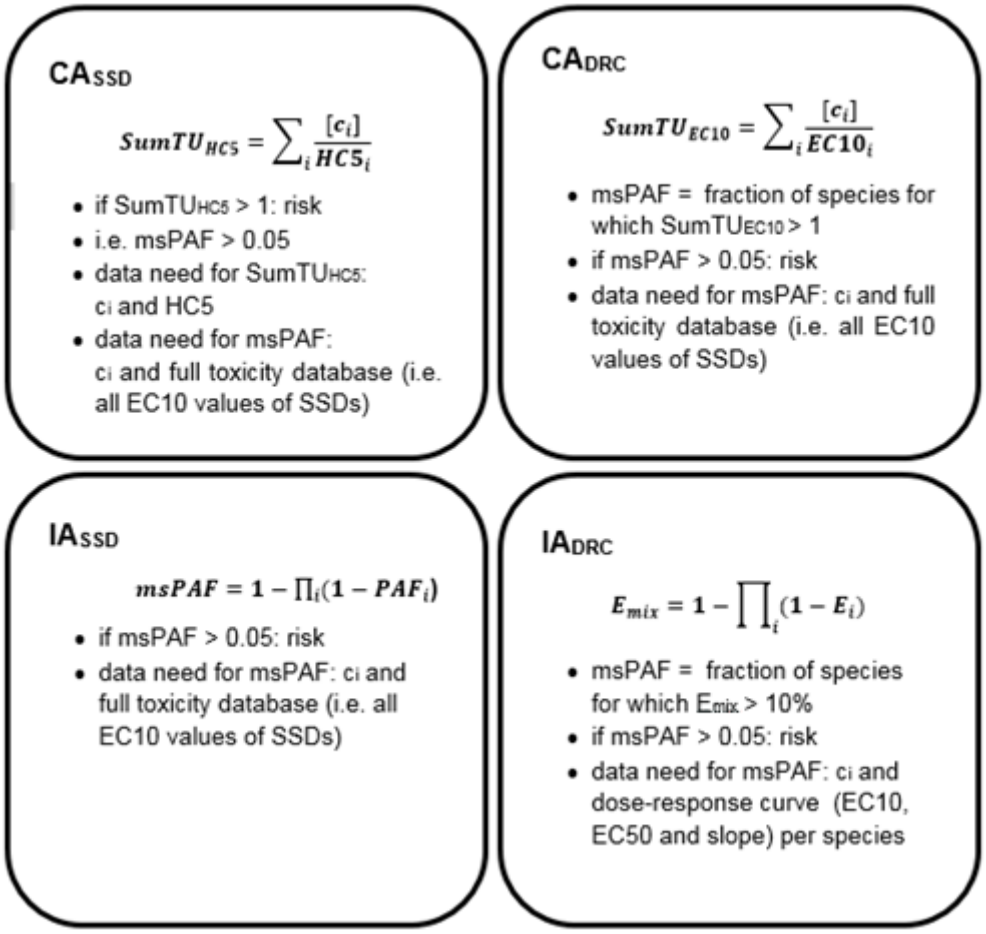

Figure 2.1. Overview of 4 different methods combining 2 mixture toxicity concepts, concentration addition (CA) and independent action (IA) with species sensitivity distribution (SSD) functions to estimate toxic pressure expressed as multisubstance potentially affected fractions (msPAF) of species exposed to metal mixtures. For each method, the general mathematical function is given as well as the data required to calculate the msPAF value. The msPAF values reported are based on 10% effect concentration (EC10) values. TU = toxic unit; HC5 = concentration hazardous to 5% of the species; Σ_i = x; c_i = environmental concentration of a metal *i*; E_{mix} = the mixture effect; DRC = dose-response curves.

2.2. Materials and Methods

A schematic overview of the methodology applied in the present study is given in Figure 2.2 and is explained step by step in the following paragraphs.

Monitoring data gathering

The present study focuses on 4 monitoring datasets, the Dommel (Verschoor et al. 2011), the Rhine (ICPR 2013), the VMM (FEA 2013), and Austria (ARCHE 2014), as well as a dataset with natural baseline concentrations in Europe, the FOREGS database (Salminen et al. 2005). Extensive information on how these datasets were gathered and processed is given in the Appendix A.1. Main results of all datasets are given in the present study.

Data in the monitoring datasets were only retained when information on the major water-chemistry variables was present—dissolved organic carbon (DOC), calcium, pH, and dissolved metal concentrations. When not present in the database, estimations of Na, Mg, K, Cl, and SO_4 were based on reported regression relations with Ca concentrations (Van Sprang et al. 2009). In addition, alkalinity was estimated based on the pH value (Stumm and Morgan 1996). Although we acknowledge that the use of transfer functions (e.g., regressions) to estimate some water characteristics is not ideal, estimation of physicochemical parameters was necessary because otherwise there were too few data. In the different databases, certain metal concentrations in some target water samples were reported as below the detection limit (Appendix A.1 and S.9). Target water samples that included at least 1 metal reported as below the detection limit and for which $\sum_{i=1}^{n} \frac{DL}{HC5}$ was larger than 1 were not retained for data analysis (0.3%, 8–10%, 0%, 16%, and 0% of the target water samples for the Dommel, VMM, Rhine, Austria, and FOREGS database, respectively; Appendix A.1), because such samples would be categorized as at risk whereas 1 or more metals would be below the detection limit, which would not be a meaningful result. For the remaining target water samples (those that were not removed by that filter), concentrations of metals that were reported to be below the detection limit were set equal to the detection limit/2. Although a more detailed investigation of the issue of nondetects is outside the scope of the present study (which was to compare and to rank 4 mixture risk assessment methods), we acknowledge that for many monitoring datasets, the presence of nondetect data is a reality that needs careful consideration. For example, in cases with $\sum_{i=1}^{n} \frac{DL}{HC5}$ >1, water quality managers might be advised to revisit these sampling locations and measure the metal concentrations with more precise equipment.

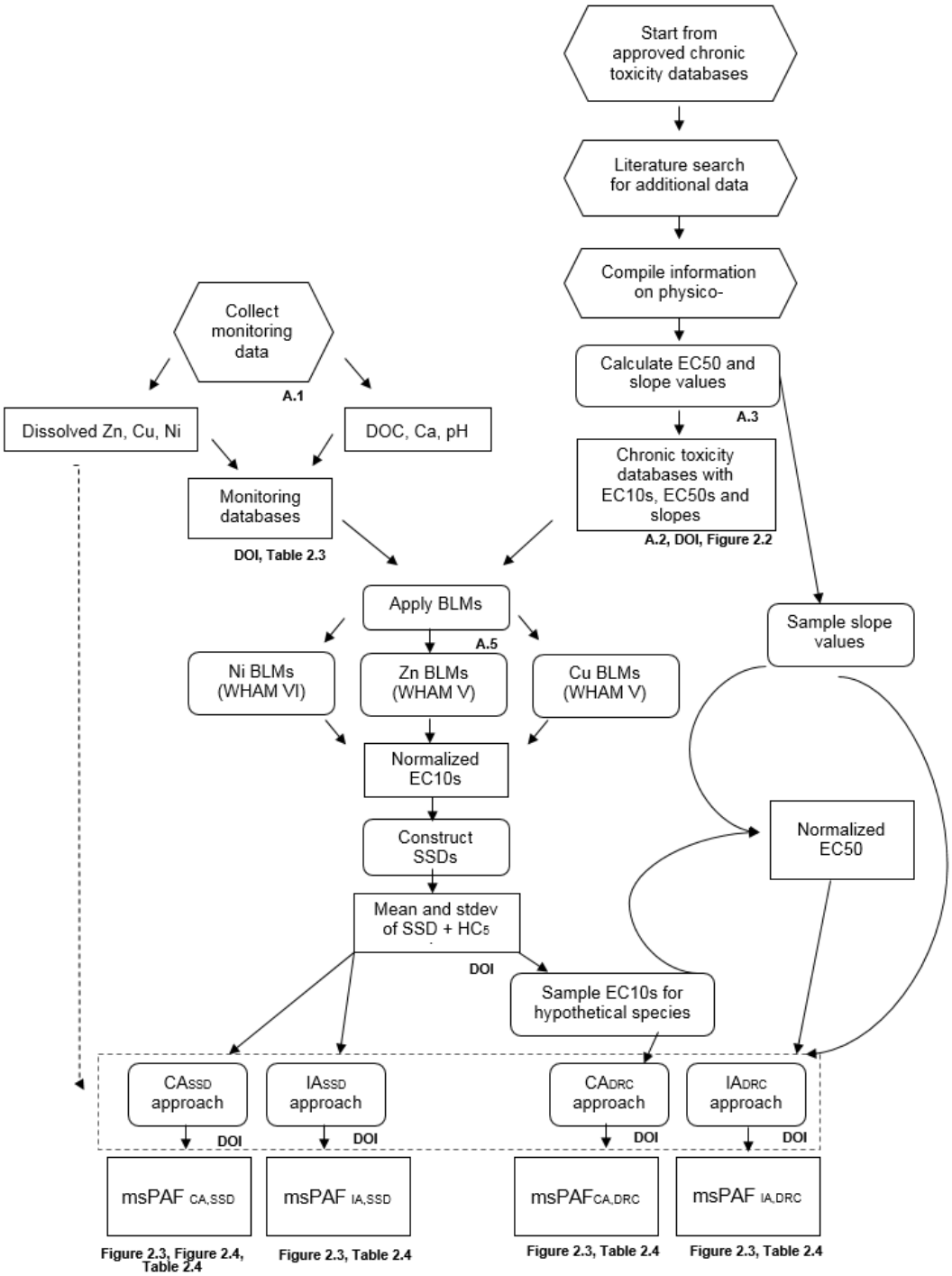

Figure 2.2. Overview of the methodology used for the calculations in the present study. Hexagonal boxes represent different steps of data collection and data handling, rounded boxes represent calculations, and rectangular boxes represent outcomes of calculations. Reference is given to tables, figures, Appendices and the online database at doi:10.1002/etc.3746.. DOC = dissolved organic carbon; ECx = x% effect concentration ; BLM = biotic ligand model; SSD = species sensitivity distribution; HC5 = hazardous concentration affecting 5% of the species within a community; CA= concentration addition; IA = independent action; DRC = dose-response curves; msPAF = multisubstance potentially affected fraction. All msPAF values reported are on the basis of EC10 values.

An overview of the monitoring data is given in Table 2.2. Monitoring data for sampling locations in the Dommel tributary of the river Meuse (The Netherlands) were obtained from Verschoor et al., who had used the data for a previous study (Verschoor et al. 2011). Monitoring data for VMM were gathered from the online database of the Flemish Environmental Agency (FEA 2013). Monitoring data for the Rhine were gathered from the online database of the International Commission for the Protection of the Rhine (ICPR 2013). Monitoring data for Austria was received from Assessing Risks of Chemicals (ARCHE, Ghent, Belgium). The FOREGS–EuroGeoSurveys Geochemical Baseline Database was obtained from the website of the Geological Survey of Finland and can also be found in Salminen et al. (2005). Additional information on the gathering of the monitoring data is given in the Appendix A.1.

Table 2.2. Overview of the monitoring databases used in this study

Database	Exposure scenario	Time period	Number of samples	Number of sampling locations
Dommel	Industrial (historic pollution)	2007-2010	3176	97
VMM	Regional mixed[a]	2012	155	48
Rhine	Regional mixed[a]	2010-2011	209	53
Austria	Regional mixed[a]	2006	2138	249
FOREGS	Natural background	1998-2001	784	784

[a] i.e. a combination of urban, industrial and agricultural pollution

Chronic toxicity databases

Databases containing chronic toxicity information (no-observed-effect concentrations [NOECs] and 10% effect concentrations [EC10s]) for each of the 3 metals (Cu, Zn, and Ni) were used for calculations. For the sake of simplicity as well as for all calculations, from now on EC10 will be used to specify both NOEC and EC10 values. Although there is continuing debate in the literature (Jager 2012; Chapman et al 1996) on the use of NOEC versus EC10, these measures are still being used as equivalents of each other in regulatory single-metal risk assessments (Danish EPA 2008; RIVM 2006; ECI 2008).

The following chronic toxicity databases were used as starting points for further calculations. The chronic Ni database was originally reported in the Nickel European Union Risk Assessment Report (2008) and was recently updated by Nys et al. (2012). The chronic Zn database was reported in 2009 by Van Sprang et al. (2009). The Cu chronic toxicity database was originally reported in the European Union Risk Assessment Report (2008).

The toxicity databases that were used as starting points were updated as follows. For the 3 metals, a literature search was performed to update the databases with new toxicity data published after compilation of the databases. Particular attention was devoted to searching for data for species that were already represented for 1 or 2 metals, but not for all 3, because this was helpful for further calculations. Only data from chronic toxicity studies that reported measured metal concentrations (rather than just nominal) and the physicochemistry of the test media (which is important to account for bioavailability, e.g., pH, Ca, and DOC concentrations) were included. Chronic toxicity data for 3 new species were added to the Zn database,

the great pond snail *Lymnaea stagnalis* (De Schamphelaere and Janssen 2010), the fatmucket clam *Lampsilis siliquoidea* (Wang et al 2010), and a rotifer species *Brachionus calyciflorus* (De Schamphelaere and Janssen 2010). No new species were added to the Cu and Ni chronic toxicity databases.

In addition, the Cu database (ECI 2008) was updated in the present study according to the chemistry found in the original peer-reviewed publications and reports. All adaptations to the Cu database and a description of why EC10 values were not retained can be found in the Appendix A.2. The final toxicity databases for Cu, Ni, and Zn including the physicochemistry of the test media as well as the chronic toxicity data (i.e., EC10 values) can be found in the online database at doi:10.1002/etc.3746. The Cu database contains 133 chronic toxicity test results from 27 species. That of Ni contains 31 species (214 test results) and that of Zn contains 22 species (128 test results). The toxicity databases include 7 species for which data on all 3 metals are present, that is, they have 7 species in common, which include the algae *Pseudokirchneriella subcapitata*, the cladocerans *Daphnia magna* and *Ceriodaphnia dubia*, the amphipod *Hyalella azteca*, the rotifer *Brachionus calyciflorus*, and 2 fish species *Pimephales promelas* and *Oncorhynchus mykiss* (online database at doi:10.1002/etc.3746.). The effect concentrations of these 7 species are evenly distributed within the toxicity databases, that is, this set of 7 comprises species that are both sensitive and less sensitive to the different metals. For example, for an average water sample within the VMM database (pH 7.6, Ca 69.0 mg/L, and DOC 5.9 mg/L), the 7 species reside between potentially affected fraction values ranging from 0.04 to 0.89 for Cu, from 0.06 to 0.97 for Ni, and from 0.05 and 0.82 for Zn.

In addition to the chronic toxicity data that were already present in the toxicity databases (i.e., EC10 values) (online database at doi:10.1002/etc.3746.) , we also needed the slope of the dose–response curves, to be able to apply 1 of the 4 mixture evaluations tools, the IA_{DRC} method. Thus we reviewed all the literature in the toxicity databases for all 3 metals (online database at doi:10.1002/etc.3746.). However, information on the slope of the curves was never reported explicitly in the peer-reviewed papers. Therefore, other methods were used to gather this information. An extensive overview of how slope values were retrieved based on the assumption of a log-logistic dose–response curve (Equation 2.1) is given in the Appendix A.3.

$$y = \frac{100}{1+\left(\frac{x}{EC50}\right)^{\beta}} \tag{2.1}$$

For certain EC10 values within the toxicity databases (online database at doi:10.1002/etc.3746.), no associated information on the slope of the dose–response curve could be retrieved. The percentage of EC10 values for which slope values could be retrieved was 87%, 84%, and 85 % for Cu, Zn, and Ni, respectively. Furthermore, this implies that for certain species within the toxicity databases (online database at doi:10.1002/etc.3746.), no information could be gathered. The percentage of species for which at least 1 slope value could be retrieved was 96%, 82%, and 94% for Cu, Zn, and Ni, respectively. The median slope value was 3.8, 2.5, and 2.1 for Cu, Zn, and Ni, respectively. The 10th and 90th percentile values were 1.9 and 10.9 for Cu, 1.1 and 9.6 for Zn, and 1.4 and 7.1 for Ni, respectively. No correlation was found

between slope values and the sensitivities of the species, that is, species that are sensitive to a certain metal (low EC10) can show both low and high slope values (Appendix A.4). This is also clear from Figure 2.3, which shows the distribution of the slopes for the different metals. Because no correlations were found, slope values for the species generated (see further discussion below in *Generalization of species*) were sampled randomly from the log-logistic distribution fitted to the set of slope values for each metal (best fit distribution based on the Kolmogorov–Smirnov goodness-of-fit statistic (Gan et al. 1991; Stephens 1982)).

Bioavailability models and normalizations

Chronic toxicity of metals to aquatic organisms is influenced by water chemistry variables (e.g., pH, water hardness, and DOC) because of the bioavailability effects of metals. Biotic ligand models (BLMs) were developed to account for this influence of water chemistry variables on metal toxicity (Di Toro et al. 2009). Therefore, all chronic toxicity data from the 3 ecotoxicity databases (Cu, Zn, and Ni) were normalized to the specific physicochemistry of each individual water sample (the target water sample) in each of the 5 monitoring databases before risks for the monitoring sites could be calculated. This was done as explained in Van Sprang et al. (2009) for Zn, in the European Union Risk Assessment Report for Cu (2008), and in Nys et al. (2012) for Ni. An overview of the process of normalization is also given in the Appendix A.5. Normalizations for Zn and Cu were performed using BLM software (HydroQual 2015) that incorporates Windermere Humic Aqueous Model (WHAM) number V (Tipping 1994), and normalizations for Ni were performed using the chronic Ni bioavailability and normalization tool (Nys et al. 2012), which incorporates the WHAM Model VI (Tipping 1998).

SSD construction and HC5 estimation

After normalization of the toxicity data within the 3 databases to the given target water samples, SSD curves were constructed as explained in Van Sprang et al. (2009). The SSDs were fitted in 2 different ways: 1) the log-normal distribution was used to construct the SSD for all target water samples; and 2) 5 different parametric distributions (log-normal, log-gamma, log-logistic, log-exponential, and log-Weibull) were fitted and the best fitting distribution was determined based on the Kolmogorov–Smirnov goodness-of-fit statistic (Gan et al. 1991; Stephens 1982). These 2 different distribution fittings were compared, to examine whether the output based on a single default distribution (i.e., all log-normal) is comparable to the output using the best fit distribution, and whether extensive computational work (i.e., using best-fit distributions) is redundant.

From these SSDs we calculated HC5 values for each of the single metals, that is, hazardous concentrations for these metals that are assumed to protect 95% of the species within a community against adverse effects of exposure beyond their no-effect level (EC10 in the present study). Parameters of the various SSDs can be found in online database at doi:10.1002/etc.3746..

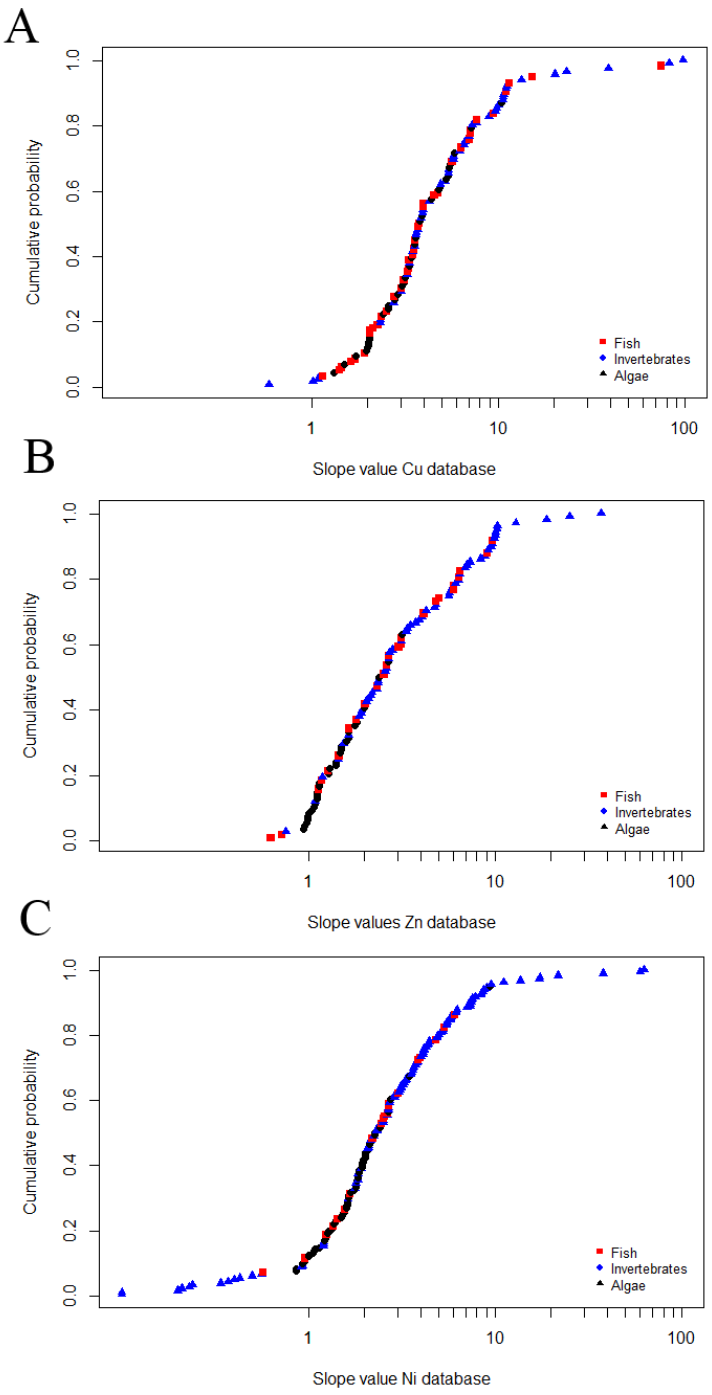

Figure 2.3. Distribution of slope values of dose-response curves for the Zn (A), Cu (B), and Ni (C) chronic ecotoxicity database. Slope values for fish, invertebrates and algae are depicted as squares (red), triangles (blue), and diamonds (black), respectively.

Toxic pressure (msPAF) calculations

All toxic pressures (expressed as msPAF) reported are on the basis of EC10 values and are given as fractions (ranging between 0 and 1), for example, msPAF = 0.5 means that 50% of the species are assumed to experience 10% effect or more by the mixture.

The toxic pressure of the metal mixture for the different target water samples within the monitoring databases was calculated with 4 different methods. The R code used to apply these methods can be found in the online database at doi:10.1002/etc.3746..

A first method, and also the simplest approach (Figure 2.1), was proposed earlier by De Zwart and Posthuma (2005) (their $msPAF_{CA}$ method; Table 2.1). In this approach, the CA model is applied directly to the SSDs. For this, the species are considered the "ecological receptors" in an equivalent way as "toxicological receptors" in individual organisms. Hence, the SSD curve of an individual substance (representing the fraction of species affected as a function of the concentration of a substance) is considered the equivalent of the dose–response curve of a species, that is, it represents the % effect of the considered endpoint as a function of the concentration. Following this approach, a risk quotient (RQ- for a given chemical mixture can be calculated as follows (De Zwart and Posthuma 2005; Equation 2.2)

$$\mathrm{RQ}_{\frac{\mathrm{PEC}}{\mathrm{PNEC}}} = \sum_{i=1}^{\mathrm{n}} \frac{\mathrm{PEC}_i}{\mathrm{PNEC}_\mathrm{i}} \tag{2.2}$$

where PEC_i is the predicted environmental concentration and $PNEC_i$ is the predicted no-effect concentration of substance *i*. However, the PNEC is under the influence of a certain arbitrariness (i.e., choice of the safety factor applied to toxicity data for each individual substance *i* (De Zwart and Posthuma 2005)), and an equivalent, but more general alternative, devoid of arbitrariness, can be formulated based on measured environmental concentrations and the HC5 (Equation 2.3).

$$\mathrm{RQ}_{\frac{\mathrm{c_i}}{\mathrm{HC5}}} = \mathrm{SumTU}_{\mathrm{HC5}} = \sum_i \frac{[\mathrm{c}_i]}{\mathrm{HC5}_i} \tag{2.3}$$

where $[c_i]$ is the environmental concentration of a metal *i* and $HC5_i$ the hazardous concentration of a metal *i* affecting 5% of the species within a community. According to this approach, which we will later call the CA_{SSD} (concentration addition applied directly to the species sensitivity distribution) approach, the community is considered to contain exactly 5% of the species that are potentially affected under the mixture exposure when $\mathrm{RQ}_{\frac{\mathrm{c_i}}{\mathrm{HC5}}} = \mathrm{SumTU}_{\mathrm{HC5}} = 1$, that is, the toxic pressure expressed as the multisubstance potentially affected fraction of species ($msPAF_{CA,SSD}$) = 0.05. When $\mathrm{RQ}_{\frac{\mathrm{c_i}}{\mathrm{HC5}}} = \mathrm{SumTU}_{\mathrm{HC5}} > 1$, more than 5% of the species are potentially affected. To evaluate whether a sample is at risk because of a mixture of metals (in other words, to calculate the $SumTU_{HC5}$), only information on the HC5 of the metals is necessary, which makes this method the simplest of the 4 methods considered (Figure 2.1).

In addition to a risk quotient or $SumTU_{HC5}$ for a given mixture scenario, it is also possible to calculate the exact toxic pressure (expressed as $msPAF_{CA,SSD}$). This is done by solving Equation 2.4 for *x*, that is, searching for *x* such that the $SumTU_{HCx}$ is exactly 1, given the c_i for the 3 metals. This value of *x* is then the $msPAF_{CA,SSD}$ value of the water body. Calculating an exact toxic pressure therefore requires not only information on the HC5 of each metal (as is the case for the $SumTU_{HC5}$ calculations), but also knowledge of the mean and standard deviation (SD) of the SSD distribution.

$$\mathrm{SumTU_{HC}}x = \sum \frac{[c_i]}{\mathrm{HC}x_{\mathrm{i}}} = 1 \tag{2.4}$$

This method of calculating the exact $msPAF_{CA,SSD}$ value is conceptually similar to that of De Zwart and Posthuma (2005). However, with our method we acknowledge that differences between slope values of SSDs may exist among metals, whereas the method of De Zwart and Posthuma assumes that the slopes of the SSDs are equal across chemicals (De Zwart and Posthuma 2005).

A second approach is analogous to what Backhaus and Faust (2012) call the risk quotient expressed relative to the sum of toxic units (RQ_{STU}) approach (Table 2.1), which they applied for demonstrative purposes to a limited toxicity dataset containing 3 acute toxicity values (EC50 values for fish, *Daphnia*, and algae) and which also makes use of a safety factor (the assessment factor; Equation 2.5)

$$\mathrm{RQ_{STU}} = \max\left(\sum_{i=1}^{\mathrm{n}} \frac{\mathrm{PEC_i}}{\mathrm{EC50}_{i,\mathrm{algae}}}, \sum_{\mathrm{i}=1}^{\mathrm{n}} \frac{\mathrm{PEC}_i}{\mathrm{EC50}_{i,\mathrm{daphnids}}}, \sum_{i=1}^{\mathrm{n}} \frac{\mathrm{PEC_i}}{\mathrm{EC50}_{i,\mathrm{fish}}}\right) \times \text{ assessment factor} \tag{2.5}$$

The difference from the approach that we follow in the present study is that we extended their methodology to a method for data-rich substances by using an SSD approach (Backhaus and Faust 2012). In this approach, which we call the CA_{DRC} (concentration addition applied to individual dose–response curves before calculating the msPAF) method, the CA model is first applied to toxicity data (the dose–response data) of the individual species by calculating a $SumTU_{EC10}$ for each species *j* (Equation 2.6)

$$\mathrm{SumTU_{EC10,}}_j = \sum_{i=1}^{\mathrm{n}} \frac{[\mathrm{c}_i]}{\mathrm{EC10_{i,j}}} \tag{2.6}$$

where $[c_i]$ is the environmental concentration of substance *i*, and $EC10_{i,j}$ is the 10% effect affected if the sum of toxic units expressed relative to the EC10 ($SumTU_{EC10,j}$) across *n* substances exceeds 1. The toxic pressure (expressed as $msPAF_{CA,DRC}$) is then estimated as the fraction of species that at a given mixture exposure is predicted to have a $SumTU_{EC10} > 1$, because this implies that the species would experience an effect of >10% compared with a control (according to the CA concept). To calculate the toxic pressure with the CA_{DRC} method therefore requires information on all EC10 values within each SSD, as is the case for calculation of the $msPAF_{CA,SSD}$ value (Figure 2.1). An advantage of this method compared with the CA_{SSD}

method is that we apply the CA concept to individual species, which is consistent with the original theory of CA (De Zwart and Posthuma 2005; Backhaus and Faust 2012).

A third method is grounded in the other important mixture toxicity concept, independent action, and will be called the IA_{SSD} (independent action applied directly to the species sensitivity distribution) method. This method was first proposed by De Zwart and Posthuma (2005) (Table 2.1) and applies the IA model directly to the SSD (Equation 2.7)

$$\mathrm{msPAF_{IA,SSD}} = 1 - \prod_{i=1}^{n}(1 - \mathrm{PAF_i}) \quad (2.7)$$

where PAF_i is the potentially affected fraction of species as a result of substance *i*. Similar to the CA_{SSD} and CA_{DRC} methods, calculation of the toxic pressure with the IA_{SSD} method requires information on the whole SSD of each metal (all EC10 values within each SSD; Figure 2.1).

A final method has been proposed by Gregorio et al. (2013) (Table 2.1) and is the most complex. We term it the IA_{DRC} (independent action applied to individual dose–response curves before calculating the msPAF) approach. For this approach, similar to the CA_{DRC} approach, the IA model is first applied to the dose–response data of the individual species, after which the SSD approach is used to calculate the $msPAF_{IA,DRC}$ value. In a first step, the effect (E) on each individual species *j* because of each substance *i* in a given mixture is calculated following the IA concept (Equation 2.8)

$$\mathrm{E_j} = 1 - \prod_{i=1}^{n}(1 - \mathrm{E}_i) \quad (2.8)$$

To this end it requires the full dose–response curve of each species, that is, not only the EC10 value but also the slope of the dose–response curve. Subsequently, the toxic pressure (expressed as $msPAF_{IA,DRC}$) is estimated as the fraction of species that at a given mixture exposure is predicted to have more than 10% effect ($E_j > 0.1$). This method is the most complex, because it requires not only the EC10 values per species and per substance, but also information on the slopes of the dose–response curves of each substance for each species in the toxicity database (Figure 2.1).

The toxic pressure was calculated using the 4 approaches described above for all target water samples in the monitoring databases and the natural baseline database. A sample was defined to be at risk when the toxic pressure (expressed as msPAF) was higher than 0.05, which is equivalent to the typical protection goal for single substances, that is, a maximum of 5% affected species at the HC5 concentration. The percentage of samples predicted to be at risk was calculated for each database. Furthermore, we determined which individual substances or combinations of substances contributed to the adverse effects.

Generalization of species

Two of the 4 approaches described above (CA_{DRC} and IA_{DRC}) require data on the individual species. If only the data present in the 3 chronic toxicity databases were considered (online database at doi:10.1002/etc.3746.), it would be possible to predict mixture toxicity for only 7 species. This is because only these 7 species are represented in all 3 toxicity databases. Because natural communities are composed of a multitude of species, the set of actual toxicity data was used to generate a set of hypothetical toxicity data for 20 000 hypothetical species (i.e., species sensitivities were sampled from the SSD) by applying methods to extrapolate unknown species sensitivity from known species sensitivity (Verdonck 2003). This was done in 2 ways: 1) by not taking into account intermetal sensitivity correlations when sampling hypothetical species for a given target water sample; and 2) by sampling the species based on the correlations found between the sensitivity of a species for 1 metal and its sensitivity for a second metal for a given target water sample. Because the effects of water chemistry on chronic metal toxicity—as predicted with the bioavailability models used—depend on metal identity and species, intermetal sensitivity correlations can be dependent on the water chemistry of the target water sample. The sampling method that accounted for intermetal sensitivity correlations was executed using the method of Iman and Conover (Iman and Conover 1982). This method is used to generate rank order–correlated input distributions and is often applied in the literature (Verdonck 2003; Cullen and Frey 1999).

The 2 methods described above were performed, and their output (i.e., msPAF values) was compared, to examine whether sampling species randomly (i.e., a less computation time–demanding approach than sampling nonrandomly) has an influence on the outcome of the risk estimates.

For the present study we chose to use the nonrandom sampling technique, and in that way we used full option methods for our toxicity predictions and msPAF estimations. The R codes for both options (random and nonrandom sampling) are given in the online database at doi:10.1002/etc.3746., so that other users can choose which method to use.

Margin of safety

The CA_{SSD} method is the simplest 1 to implement and it is claimed to be conservative. By calculating the MoS provided by the CA_{SSD} approach relative to the other methods, the following question can be answered: By how many fold can the $SumTU_{HC5}$ in a given target water sample be raised until so-called risk (msPAF = 0.05) is just being predicted with each of the methods? For MoS calculations, we start from a situation in which the metals are present at the concentrations and metal–metal ratios reported in the databases. Then the metal concentration of each metal is increased (keeping all metal concentration ratios constant) until the level where toxic pressure according to the different approaches equals 0.05. The $SumTU_{HC5}$ at this new combination of metal concentrations is then calculated, and this value is equal to the MoS provided by the CA_{SSD} approach. Only those target water samples were examined that, according to the 3 different methods (CA_{DRC}; IA_{SSD}, and IA_{DRC}) were not affected by the metal mixture (i.e., msPAF <

0.05), because a MoS calculation does not make sense for target water samples not falling into this category.

2.3. Results and Discussion

Monitoring data

A detailed overview of the 4 monitoring datasets and the geochemical baseline dataset can be found in the online database at doi:10.1002/etc.3746. An overview of the main physicochemical variables and the dissolved metal concentrations is given in Table 2.3 for all datasets. Median Cu concentrations are similar across the monitoring databases and are on average 91% lower than the median bioavailability corrected HC5 values in all 4 monitoring databases (Table 2.3). Median Zn and Ni concentrations differ more between monitoring databases than Cu. Median Zn and Ni concentrations are below the median bioavailability corrected HC5 values in all 4 monitoring databases, and are on average 71% and 84% lower, respectively. For the geochemical baseline dataset (FOREGS), median Cu, Zn, and Ni concentrations are below the median bioavailability corrected HC5 values and are 95%, 93%, and 87% lower, respectively.

SSD construction: log-normal or best-fit?

Probability distributions were fitted to the data using 1) log-normal distributions for all data; and 2) distributions that best fit the data. The log-normal distribution was the best-fit distribution in 29.2%, 1.8%, and 3.9% of the target water samples for Cu, Zn, and Ni, respectively. The highest percentage of data was fitted with the log-logistic distribution, 33.6%, 93.1%, and 73.1% of the target water samples for Cu, Zn, and Ni, respectively. From the fitted distributions, HC5 values (based on dissolved concentrations) per target water sample were estimated, and 10th, 50th (median), and 90th percentiles of the HC5 for each monitoring database are given in Table 2.3.

If the conventional log-normal distribution was fitted to all target water samples, median HC5 values vary between 4.1 µg/L and 46.6 µg/L for Cu, 22.2 µg/L and 52.1 µg/L for Zn, and 7.0 µg/L and 27.3 µg/L for Ni. Fitting the best-fit distribution to all target water samples gives median HC5 values that vary between 4.3 µg/L and 46.6 µg/L for Cu, 22.9 µg/L and 47.9 µg/L for Zn, and 6.9 µg/L and 27.3 µg/L for Ni. On average, the HC5 values generated from log-normal distributions and best-fit distributions are 3.6% higher for Cu, 0.25% higher for Zn, and 0.01% higher for Ni. Thus, using a single default distribution (i.e., all log-normal) for mixture toxic pressure estimations, which is computationally less demanding, seems justified.

Furthermore, because the msPAF values calculated based on log-normal and best-fit SSD distributions were similar (see further discussion below in *Risk calculations*), preference was given to only report data (seen in the figures and tables) and do downstream data analyses based on the log-normal SSDs within the manuscript, and all results are reported based on the best-fitting SSDs in the online database at doi:10.1002/etc.3746..

Table 2.3. Physico-chemical parameters (pH, DOC and Ca concentration) and dissolved metal concentrations (nickel, zinc and copper) of the different monitoring databases. In addition, HC_5 values (hazardous concentration affecting 5% of the species within a community, beyond their no-effect level (here EC10)) for the different monitoring datasets (log-normal SSD and best-fit SSD).

		Dommel	VMM	Rhine	Austria	FOREGS
pH		7.1 (6.5 - 7.6)[a]	7.6 (7.0 - 8.0)	8.0 (7.8 - 8.2)	8.0 (7.6 - 8.3)	7.7 (6.4 - 8.3)
DOC[b] (mg/L)		9.4 (5.5 - 15.0)	7.7 (5.2 – 15.1)	2.4 (1.7 - 3.4)	1.6 (0.7 - 4.5)	5.3 (1.0 - 17.1)
Ca (mg/L)		41.4 (31.0 - 57.0)	84.0 (26.4 - 146.0)	67.0 (50.0 - 110.4)	45.9 (18.8-80.0)	40.3 (2.8 - 118.2)
Ni (µg/L)		8.3 (0.8 - 29.0)	2.5 (2.0 - 11.0)	1.1 (0.5 - 2.0)	0.5 (0.03 - 1.9)	1.9 (0.4 - 4.7)
Zn (µg/L)		28 (3.5 - 98.0)	15.0 (5.0 - 66.0)	2.8 (1.0 - 5.1)	1.9 (0.4 - 7.8)	2.7 (1.0 - 9.8)
Cu (µg/L)		2.1 (0.5 - 4.6)	1.0 (1.0 - 4.0)	1.6 (0.8 - 2.3)	0.5 (0.4 - 1.6)	0.9 (0.3 - 2.3)
Ni HC_5	log-normal	27.3 (18.1-39.4)	20.6 (14.9-32.8)	7.9 (5.3-18.9)	7.0 (3.9-14.4)	14.8 (4.1-39.3)
	best-fit	27.3 (18.2-39.3)	22.1 (16.0-31.3)	7.9 (5.2-17.2)	6.9 (3.8-14.7)	14.6 (3.9-38.1)
Zn HC_5	log-normal	42.8 (27.4-67.9)	52.1 (27.9-92.9)	24.4 (19.1-36.5)	22.2 (13.2-40.4)	36.2 (14.2-100.0)
	best-fit	42.6 (27.3-67.8)	47.9 (27.0-81.9)	25.5 (19.0-40.3)	22.9 (12.9-40.4)	37.8 (14.1-95.3)
Cu HC_5	log-normal	46.6 (19.0-78.8)	39.5 (24.3-82.0)	12.5 (7.3-21.7)	4.1 (1.9-13.3)	19.6 (3.4-74.3)
	best-fit	46.6 (19.0-78.8)	39.4 (24.3-78.5)	13.4 (7.2-23.6)	4.3 (2.2-13.1)	19.7 (3.7-73.9)

[a] Values reported are median values, 10^{th} and 90^{th} percentiles are given in between parentheses.

[b] DOC = Dissolved Organic Carbon

Generalization of species: random or nonrandom?

Hypothetical species were generated in 2 ways: 1) by not taking into account intermetal sensitivity correlations; and 2) by taking into account intermetal sensitivity correlations, which depended on the chemistry of the target water sample. When all monitoring datasets were considered together, correlations between the sensitivity of species to Ni and Zn ranged from $r = –0.36$ to $r = 0.48$. However, none of these correlations were statistically significant ($p > 0.05$). Correlations between Ni and Cu ranged from $r = –0.9$ to $r = 0.22$, and only 6.6% were significant ($p < 0.05$). These significant correlations are strong negative correlations ($r < –0.6$), suggesting that—in these 6.6% of cases—when a species is sensitive to Ni it is more likely to be less sensitive to Cu and vice versa. In addition, these negative correlations between Cu and Ni sensitivity are more likely to occur at low pH, and positive correlations are more likely at high pH (Appendix A.6), meaning that at low pH, a species that is less sensitive to Ni is more likely to be more sensitive to Cu and vice versa. Such a correlation is not apparent with either DOC or Ca concentrations, 2 other variables affecting metal bioavailability. Correlations between Zn and Cu ranged from $r = –0.80$ to $r = 0.47$, and of these only 0.06% were significant correlations ($p < 0.05$). Again, we observed a trend of negative correlations between Zn and Cu sensitivity at low pH and positive correlations at high pH, and again no trend is apparent with either DOC or Ca concentrations (Appendix A.6).

As median correlation coefficients between the sensitivity of species to 1 metal and their sensitivity to a second metal are rather low (Appendix A.6), one would expect that the results (i.e., the msPAF values) when sampling species by not taking into account intermetal sensitivity correlations would be quite similar to results when sampling the species based on the correlations found between the sensitivities. Indeed, we found that differences in msPAF values between these 2 methods were small, on average 0.002 (0.005 SD) difference in toxic pressure for the CA_{DRC} method and on average 0.001 (0.003 SD) difference in toxic pressure for the IA_{DRC} method. Therefore, sampling species randomly appears to be a justifiable option to reduce computational time.

Risk calculations

The results for the simplest method to estimate risks as a result of metal mixtures (CA_{SSD}) are visualized in Figure 2.4. In this figure the (Sum)TU_{HC5} is given for every metal and for every monitoring database. For the Dommel dataset, median TU_{HC5} values are smaller than 1 for all 3 metals. However, 9% of the TU_{HC5} values for Ni, 35% of the TU_{HC5} values for Zn, and 0.3% of the TU_{HC5} values for Cu within the Dommel basin show a $TU_{HC5} > 1$, indicating that there might be a risk from the single metals at these sites. Adding up the TU_{HC5} values gives a $SumTU_{HC5}$ that is indicative for the risk of a mixture of substances. Figure 2.4 shows that the median $SumTU_{HC5}$ for the Dommel lies above 1, indicating a risk from the metal mixture or from single metals in more than half of the cases. Similar results are found for the VMM, Austria, and FOREGS database (Figure 2.4). However, for these waters the median $SumTU_{HC5}$ lies below 1, indicating that less

than half of the cases show a risk because of metal mixtures or single metals. For the Rhine, none of the TU_{HC5} or $SumTU_{HC5}$ values lie above 1, indicating no risk according to the CA_{SSD} method in this waterway. More advanced methods to calculate the toxic pressure include the 4 methods described above in which the exact msPAF value of a sample is calculated. Table 2.4 shows the distribution of toxic pressure (expressed as msPAF values) for all 4 methods for the different monitoring datasets. For the results using the best-fit SSD calculations, Appendix A.7 can be consulted. A toxic pressure > 0.05 indicates that the sample is affected by the metal mixture.

For the Dommel monitoring database, the median toxic pressure is above 0.05 only when the CA_{SSD} method is used (Table 2.4), which suggests that the simplest method is the most conservative. The median toxic pressure is lowest (0.024) using the IA_{SSD} method, suggesting that this method is the most liberal (least conservative) method. The percentage of target water samples affected within the Dommel dataset ranges between 52% and 39% depending on the method used. Similar results were obtained for the best-fit SSD, which shows that using the log-normal distribution by default does not have a large influence on the outcome of the toxic pressure calculations. The results suggest that almost half of the target water samples within the Dommel waterway in The Netherlands are at risk because of metal contamination. However, according to the CA_{SSD} method, 15% of the target water samples from the Dommel are affected by the mixture itself and not by any individual metal, whereas the IA_{SSD} method predicts that only 3% of the target water samples will be affected by the mixture of metals itself (Table 2.4). By going into more detail (Table 2.5), we see that Zn has a large effect individually: in 26.84% of the target water samples a risk is found because of Zn alone. Furthermore, in 8.48% of the samples, a risk is found from both Zn and Ni individually (i.e., the TU_{HC5} of both Zn and Ni is above 1). When the remaining samples that are affected by the mixture and not by any individual metal are examined, 13.01% of the target water samples are found to have an effect from a binary combination of the metals, whereas 2.14% are affected because of a ternary combination of the metals. When the contribution of each metal to the $SumTU_{HC5}$ of these mixture effects is examined, we see that Zn, which has the largest TU_{HC5} in 70.96% of the cases, is the largest contributor to the mixture effect.

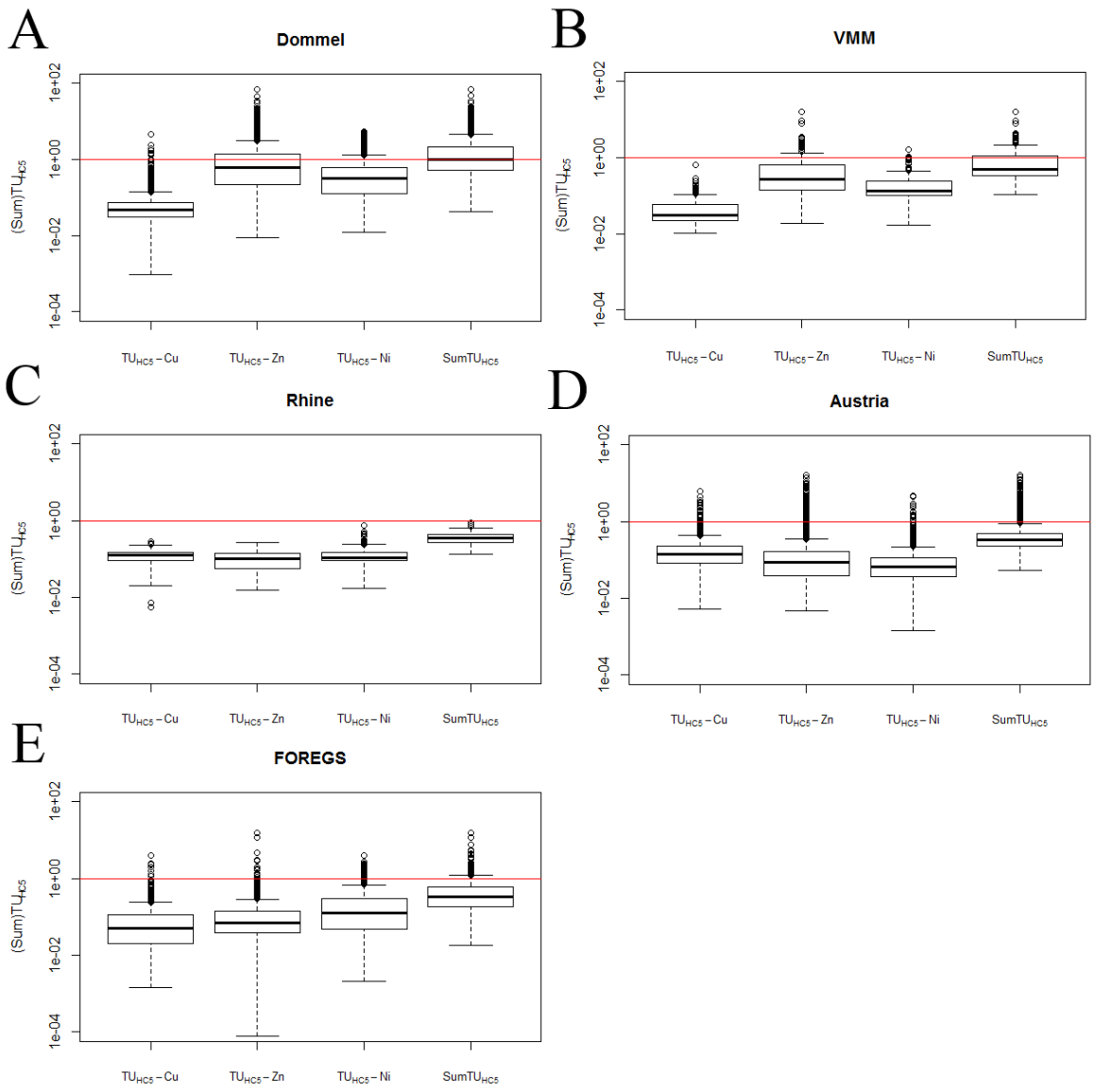

Figure 2.4. Toxic Unit expressed relative to the hazardous concentration affecting 5% of the species within a community (TU_{HC5}) for Ni, Zn and Cu for the different target water samples of the Dommel (A), Flanders (VMM) (B), Rhine (C), Austria (D) and Forum of European Geological Surveys (FOREGS) (E) dataset. $SumTU_{HC5}$ shows the summation of the TU_{HC5}'s according to the CA_{SSD} (concentration addition applied directly to the species sensitivity distribution) method using the log-normal SSD distribution. The horizontal line indicates a TU_{HC5} or $SumTU_{HC5}$ of 1. Results are represented as box plots: median values are given in bold, bottom and top of the box plots give the 25th and 75th percentile. Bottom and top of the error bars represent the 5th and 95th percentile, open circles are outliers.

Table 2.4. Toxic pressure expressed as multisubstance potentially affected fraction of species (msPAF[a]) for the Dommel, VMM, Rhine, Austria and FOREGS database obtained with the different methods (CA_{SSD}; CA_{DRC}; IA_{SSD} and IA_{DRC}) when SSDs are fitted with log-normal distributions [a].

	Dommel				VMM				Rhine			
	CA_{SSD}	CA_{DRC}	IA_{SSD}	IA_{DRC}	CA_{SSD}	CA_{DRC}	IA_{SSD}	IA_{DRC}	CA_{SSD}	CA_{DRC}	IA_{SSD}	IA_{DRC}
median msPAF	0.054	0.038	0.024	0.027	0.009	0.004	0.003	0.003	0.006	0.002	0.002	0.002
10th percentile msPAF	<0.001	<0.001	<0.001	<0.001	<0.001	<0.001	<0.001	<0.001	0.002	<0.001	<0.001	<0.001
90th percentile msPAf	0.423	0.466	0.342	0.364	0.227	0.2201	0.177	0.185	0.012	0.0005	0.003	0.004
% samples affected (msPAF>0.05)	52	46	39	44	27	25	23	23	0	0	0	0
% samples affected by mixture of metals and not by any of the individual metals	15	10	3	5	7	4	2	3	0	0	0	0
MoS provided by the CA_{SSD} approach	NA	1.17	1.48	1.38	NA	1.18	1.57	1.46	NA	1.25	1.72	1.60

	Austria				FOREGS			
	CA_{SSD}	CA_{DRC}	IA_{SSD}	IA_{DRC}	CA_{SSD}	CA_{DRC}	IA_{SSD}	IA_{DRC}
median msPAF	0.004	0.001	0.001	0.001	0.004	0.001	0.001	0.001
10th percentile msPAF	<0.001	<0.001	<0.001	<0.001	<0.001	0	<0.001	<0.001
90th percentile msPAf	0.035	0.023	0.016	0.017	0.052	0.039	0.031	0.033
% samples affected (msPAF>0.05)	8	6	5	5	10	8	7	7
% samples affected by mixture of metals and not by any of the individual metals	3	2	0.2	0.6	4	2	0.4	0.5
MoS provided by the CA_{SSD} approach	NA	1.21	1.52	1.45	NA	1.22	1.52	1.43

[a] The percentage of affected samples is given per method, as well as the median Margin of Safety (MoS) values provided by the CA_{SSD} approach for the other methods. The msPAF values reported are on the basis of EC10 values. CA = Concentration Addition; IA = Independent Action; SSD = Species Sensitivity Distribution; DRC = Dose Response Curve; NA = not applicable; MoS = Margin of Safety

Verschoor and colleagues (2011) also investigated the mixture toxicity from Cu, Zn, and Ni in the Dommel waterways, by calculating the multimetal risk characterization ratio (RCR; Equation 2.9), which is conceptually identical to our CA_{SSD} approach.

$$\sum \mathrm{RCR} = \frac{[Cu]}{HC5_{Cu}} + \frac{[Ni]}{HC5_{Ni}} + \frac{[Zn]}{HC5_{Zn}} \quad (2.9)$$

A similar percentage of affected target water samples was predicted by Verschoor et al. (2011); these authors found that 47% of the target water samples were at risk, whereas we found that 52% of the target water samples were affected (Table 2.4). In addition, when annual mean risk characterization ratio values (calculated by Verschoor et al. (2011)) were compared with TU_{HC5} values (present study), they were found to be equal for Zn (1.36) and Cu (0.075), but not for Ni (1.35 vs 0.47) and therefore also not for the Zn–Cu–Ni mixture (2.79 vs 1.91).

Table 2.5. Percentage of samples that is not affected and percentage that is affected (msPAF value > 0.05) by a mixture of Cu, Zn and/or Ni according to the CA_{SSD} method for the Dommel database.

	Percentage (%)
No effect	48.33
Effect	51.67
Individual metal effects	36.52
Only Zinc[a]	26.84
Only Nickel[a]	0.91
Only Copper[a]	0.09
Both Zinc and Nickel[b]	8.48
Both Zinc and Copper[b]	0.16
Mixture effects	15.15
Binary combinations[c]	13.01
Ternary combination[d]	2.14
Shows the largest TU[e]	
Zn	77.96
Ni	22.04
Cu	0

[a] The Toxic Unit of zinc, nickel or copper is above 1
[b] The Toxic Unit of all mentioned metals is above 1
[c] At least one of the possible binary combinations (i.e.Zn&Ni, Zn&Cu, Ni&Cu) shows an effect
[d] The ternary combination (but none of the 3 possible binary combinations) shows an effect
[e] For each metal the percentages of samples is given in which that metal has the largest Toxic Unit in the sample affected by a binary or ternary combination, i.e.in which that metal is the largest contributor to the toxic effect

The difference between the results of Verschoor et al. (2011) and those from the present study could be because of a number of factors. A first factor could be the different parameterization of the BLMs used for bioavailability normalization. For Cu and Ni, Verschoor et al. (2011) used the stability constants describing the interactions at the biotic ligand from the original BLMs (Danish EPA 2008; De Schamphelaere et al. 2003), whereas we used the updated BLMs (De Schamphelaere and Janssen 2006; Deleebeeck et al. 2007; Deleebeeck et al. 2009; Deleebeeck et al. 2008). Furthermore, the choice of speciation software was different; Verschoor et al. (2011) used WHAM Model VI for all speciation

calculations, and we used WHAM Model V for Cu and Zn speciation calculations because the BLMs for Cu and Zn were originally calibrated and developed with WHAM Model V. Finally, we used updated toxicity databases as well as validated BLMs that have been cross-validated for other species and that are currently used in regulatory environmental risk assessments of the 3 metals. However, despite the considerable differences in methodology, the differences in the % of samples calculated to be at risk as well as the differences in risk characterization ratios are still relatively small.
When the 3 monitoring databases other than the Dommel are considered, the target water samples in the VMM database are found to be most at risk from metals, with 23% to 27% of the target water samples affected (Table 2.4), depending on the method used. The Rhine is the least at risk, with none (0%) of the target water samples at risk from metal contamination. The Austrian target water samples are in between, with 5% to 8% of the waters affected (Table 2.4).

For the FOREGS database, between 7% and 10% of the waters, depending on the method used, are predicted to be affected (Table 2.4). This finding demonstrates that even for waters with assumed natural geochemical baseline concentrations of metals, a substantial number of water bodies are predicted to be at risk. This result is a well-known issue in metals risk assessment in general, which arises when natural background concentrations of metals, which can vary markedly between geologically different areas, are not taken into account in risk assessment procedures. One way to deal with this issue (e.g., in a higher tier of risk assessment) could be to use the added risk approach (Struijs et al. 1997), but this is beyond the scope of the present study.
When we examined those target water samples affected by the metal mixture and not by any single metal individually in the FOREGS database, between 0.3% and 4% of the target water samples were found to be at risk, depending on the method used (Table 2.4). This analysis not only shows that true mixture risks are relatively low for the FOREGS database, but also that the issue of risk at geochemical background levels is higher when CA_{SSD} is used compared with the other methods used. Indeed, 4% of the target water samples are found to be at risk when the CA_{SSD} is used, whereas only 0.3% to 2% of the target water samples are found to be at risk when the other methods are used.

After generalization to all databases, we see that—when the conservative CA_{SSD} method is used—in approximately one-third of the target water samples predicted to be affected, a risk is predicted from an actual mixture of metals (and not from any individual metal; Table 2.4). However, when the theoretically more correct methods are used (CA_{DRC} and IA_{DRC}), 1.5 to 2.0 times fewer target water samples are affected by mixtures according to the CA_{DRC} method and 2.3 to 8.0 times fewer target water samples according to the IA_{DRC} method. The difference between mixtures risk between the 2 latter methods emphasizes the need to establish which model (CA or IA) is the best at predicting chronic metal mixture toxicity to individual aquatic species, such that a well-informed choice can be made between CA_{DRC} or IA_{DRC} in the implementation of metal mixture risk assessment.

Ranking the methods and margin of safety calculations

A larger difference in the percentage of target water samples that are at risk was found among the 4 methods, with a difference of 3% (Austria) to 13% (Dommel) between the methods. At present, it is too early to conclude which method might be the proper approach. Indeed, these approaches arise from 2 major toxicity concepts, CA and IA. It is currently not known which model is the most appropriate. Moreover, the results suggest that the most appropriate model may be dependent on the metal combination, the species tested, the water chemistry of the test medium, and so forth (Nys et al. 2015; Norwood et al. 2003). However, earlier research (Backhaus and Faust 2012) demonstrated mathematically that for an assemblage of 3 species, the $\frac{RQ_{PEC}}{PNEC}$ approach (which is analogous to our CA_{SSD} approach) was always more conservative than the RQ_{TU} approach (which is analogous to our CA_{DRC} method). Nonetheless, we found that at high toxic pressure (above 0.15; expressed as $msPAF_{CA,SSD}$), the CA_{SSD} approach is no longer the most conservative method, with a higher conservatism found for the CA_{DRC} approach (Figures 2.5 and 2.6). Furthermore, for the IA_{DRC} approach, the value at which this shift occurs is higher ($msPAF_{CA,SSD}$ of 0.55; Figures 2.5 and 2.6). However, we see that at toxic pressure values (expressed as $msPAF_{CA,SSD}$) below 0.15, there is 0% chance of finding a $msPAF_{CA,SSD}$ value smaller than $msPAF_{CA,DRC}$ or $msPAF_{IA,DRC}$ (Figure 2.5). Therefore, at toxic pressures of approximately 0.05, the CA_{SSD} method is the most conservative not only for assemblages of 3 species but also at the community level.

This is also clear from our calculations in which the MoS of the CA_{SSD} approach compared with the other methods was determined. Figure 2.7 shows the MoS that the CA_{SSD} method provides relative to the 3 other methods for all monitoring databases. For the Dommel database, using the CA_{DRC} method, variability in the MoS is the lowest and the median MoS is equal to 1.17. The MoS has higher variability and higher median values with the IA_{DRC} and IA_{SSD} methods (1.38 and 1.48, respectively). The CA_{SSD} method is thus more conservative than the other methods by a factor 1.17 to 1.48. This means that, for example, 1.48-fold higher metal concentrations are needed to conclude that risk is present based on the IA_{SSD} approach compared with the CA_{SSD} approach. In addition, if CA (or IA) is a conservative estimator of mixture toxicity across all species, which is demonstrable in toxicity tests, then the simple CA_{SSD} method is on average more conservative by a factor of 1.17 (or 1.48).

Our MoS calculations can be compared with the findings of Gregorio et al. (2013), who based their research on theoretical datasets generated for hypothetical substances. These authors showed that the use of CA directly on SSD (our CA_{SSD} method) may lead to an overestimation or underestimation of the mixture concentration affecting 5% of the species depending on the SD of the SSD of the substances within the mixture. These results were found by calculating the $D_{msPAF=5}$, which is the ratio of the mixture concentration affecting 5% of the species calculated with their $M2_{ssd,CA}$ (method applying CA to the SSD curves) method (our CA_{SSD} method) to the mixture concentration affecting 5% of the species calculated with their $M1_{sp,CA}$ (method applying CA to single species separately) method (our CA_{DRC} method). This $D_{msPAF=5}$ value is therefore the reciprocal of our MoS value (i.e., 1/ MoS). For mixtures of substances with a steep SSD (SD ≤ 0.55), Gregorio et al. (2013) demonstrated a higher likelihood of underestimating the mixture concentration affecting 5% of the species when using CA_{SSD} relative to using CA_{DRC} (i.e.,

$D_{msPAF=5}$ < 1). This is in compliance with our results. The mixtures of metals considered in our analysis also showed steep SSDs (mean SD; Dommel SD = 0.37, VMM SD = 0.39, Rhine SD = 0.47, Austria SD = 0.50), and average margin of safety values for all monitoring databases were larger than 1 (Table 2.4). The results of Gregorio et al. (2013) based on hypothetical data for hypothetical substances are therefore confirmed by our results based on real toxicity data for real substances.

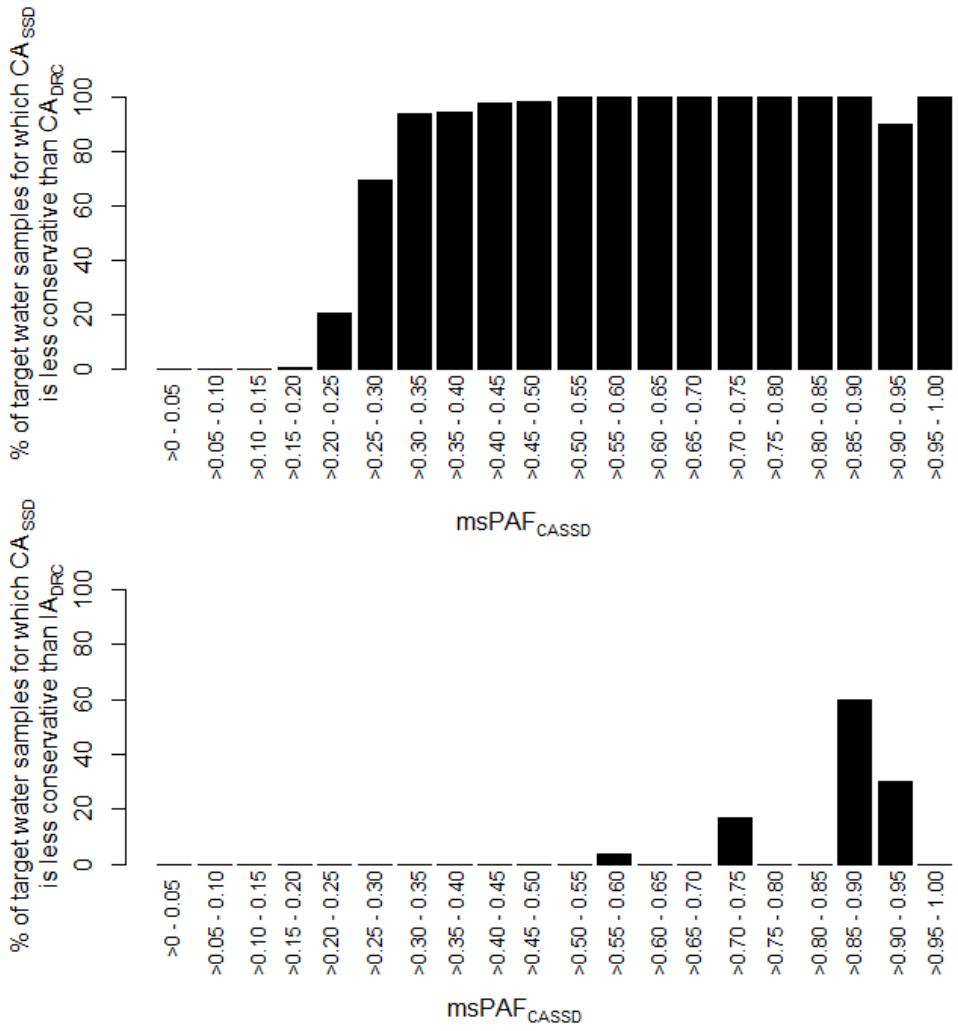

Figure 2.5. Percentage of samples for which the $msPAF_{CA,SSD}$ value (the multisubstance potentially affected fraction of species calculated with the CA_{SSD} method (concentration addition applied directly to the species sensitivity distribution)) is smaller than the $msPAF_{CA,DRC}$ value ($msPAF$ calculated with the CA_{DRC} method (concentration addition applied to individual dose-response curves)) (top) and for which the $msPAF_{CA,SSD}$ value is smaller than the $msPAF_{IA,DRC}$ value ($msPAF$ value calculated with the IA_{DRC} method (independent action applied to individual dose-response curves)) (bottom), for different categories of $msPAF_{CA,SSD}$ values (for the Dommel, Flanders [VMM], Austria, and Forum of European Geological Surveys [FOREGS] databases combined).

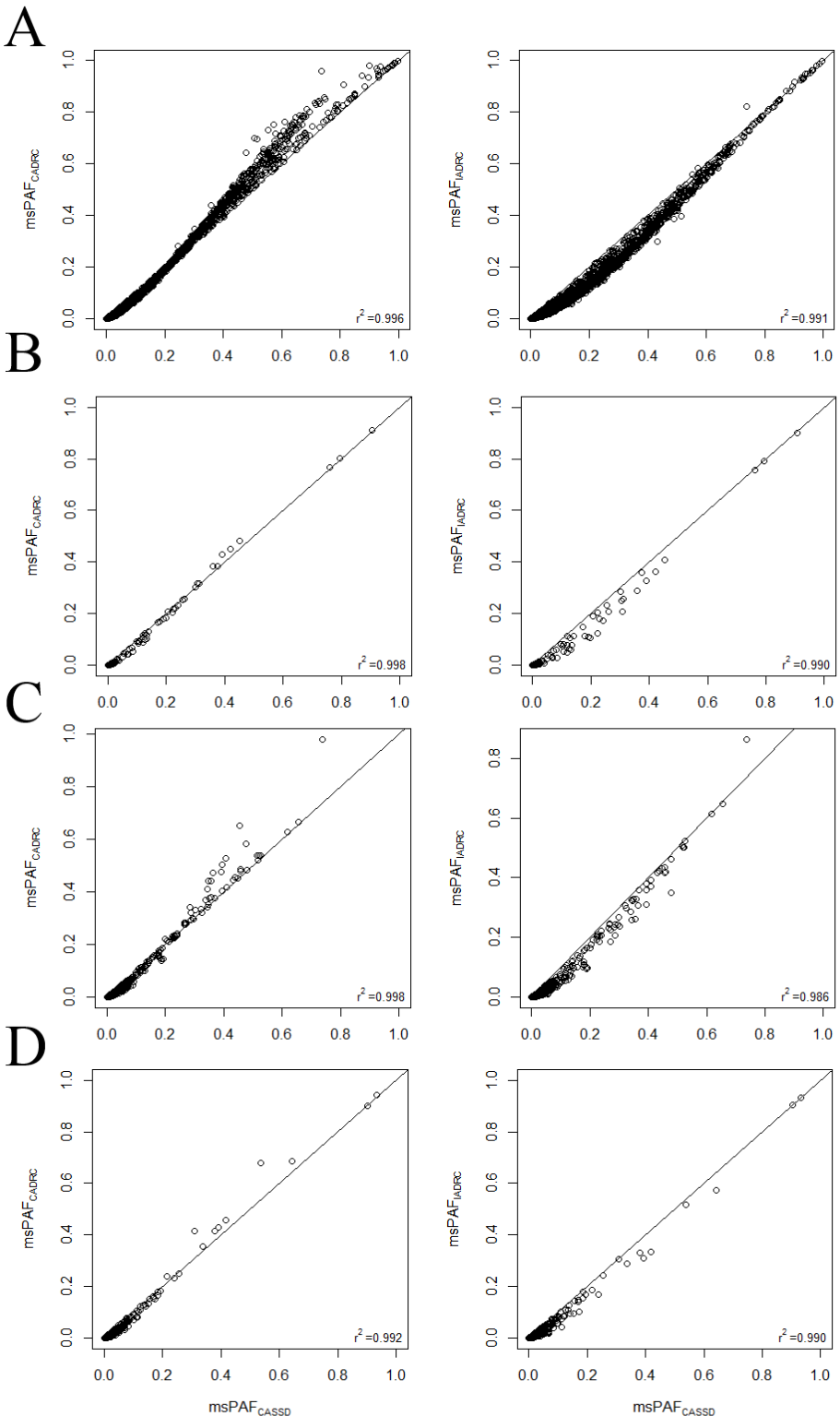

Figure 2.6. Comparison of the toxic pressure (expressed as multisubstance potentially affected fraction [msPAF]) according to the CA_{SSD} method (concentration addition applied directly to the species sensitivity distribution) versus the CA_{DRC} method (concentration addition applied to individual dose-response curves) (left graphs) and according to the CA_{SSD} versus the IA_{DRC} method (independent action applied to the individual dose-response curves) (right graphs) for the Dommel (A), Flanders (VMM) (B), Austria (C), and the Forum of European Geological Surveys (FOREGS) (D) database. The msPAF values reported are on the basis of 10% effect concentration values.

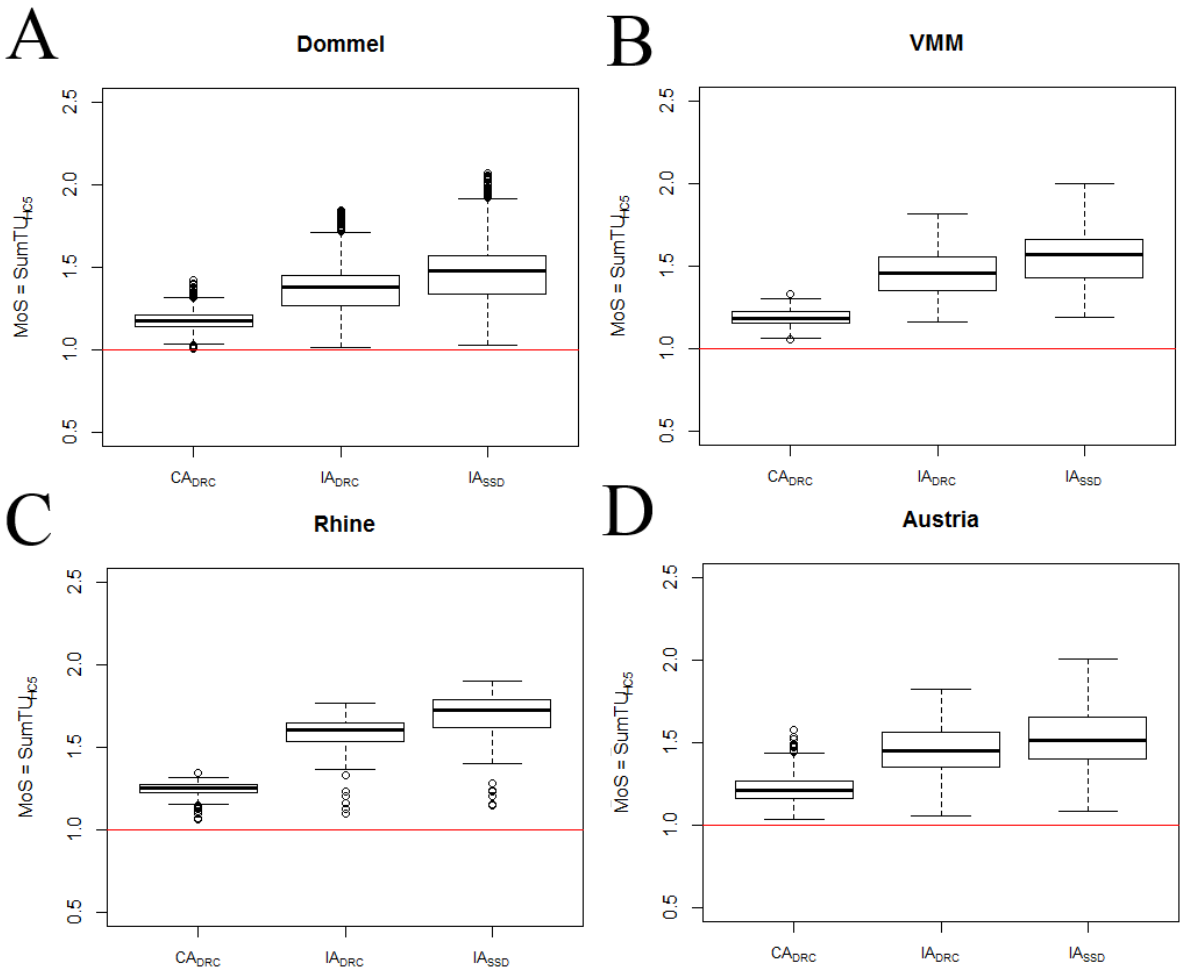

Figure 2.7. Representation of the margin of safety (MoS), which is the sum toxic unit expressed relative to the hazardous concentration affecting 5% of the species within a community ($SumTU_{HC5}$) corresponding to a multisubstance potentially affected fraction (msPAF) of 0.05 for the Dommel (A), Flanders (VMM) (B), Rhine (C), and Austria (D) database, for the different methods: CA_{DRC} (concentration addition applied to individual dose-response curves) , IA_{DRC} (independent action applied to individual dose-response curves), and IA_{SSD} (independent action applied directly to species sensitivity distribution). Results are represented as box plots: median values are given in bold, bottom and top of the box plots give the 25th and 75th percentile. Bottom and top of the error bars represent the 5th and 95th percentile, asterisks are outliers.

In general, our calculations show the following order of conservatism (from most conservative to most liberal)

$CA_{SSD} > CA_{DRC} > IA_{DRC} > IA_{SSD}$

This rank order indicates that these methods could be implemented in a tiered metal-mixtures risk evaluation scheme (Figure 2.8). Because CA gives a more cautious risk estimate (at low msPAF values), the CA_{SSD} method could serve as a first (conservative) tier to identify situations with likely no risk of metal mixtures ($SumTU_{HC5} < 1$). The IA_{SSD} method could be applied in a second tier to identify situations of risk regardless of the method used (msPAF > 0.05). The CA_{DRC} and IA_{DRC} methods could be used in a third tier for more detailed calculations for situations that fall in between ($SumTU_{HC5} > 1$ and $msPAF_{IA,SSD} < 0.05$), for example, as part of a weight-of-evidence approach. For situations in which the outcome depends on the method used (CA_{DRC} or IA_{DRC}), targeted research could be performed in a final tier.

Our MoS calculations also demonstrate the possibility of an intermediate tier between the proposed tiers 1 and 2. When the $SumTU_{HC5}$ is > 2 (Figure 2.7), risk is always predicted, independent of the method used. The intermediate tier could therefore implement a cut-off on the $SumTU_{HC5}$ value, above which risk is always predicted, and thus unneeded time and resource investment in the more complicated calculations could be avoided. However, this case is so far only demonstrated for the 4 monitoring datasets examined in the present study and should first be examined more thoroughly before this intermediate tier can be added to the tiered metal-mixtures risk evaluation scheme (Figure 2.8).

Strengths and weaknesses

The research conducted in the present study shows certain strengths compared with the existing literature. We evaluated the use of 4 mixture risk assessment methodologies simultaneously, using available real toxicity data and monitoring datasets. In addition, we compared the influence of the use of the log-normal and the best-fit SSD on the risk estimations, as well as the influence on the risk estimations of generating hypothetical species randomly versus nonrandomly. However, certain weaknesses in our research also exist. An important obstacle for applying either method is that the underlying assumptions of the different methods need to be tested, and the degree of conservatism compared with community-level metal mixture toxicity effects needs to be investigated (e.g., based on mesocosm or field data). Another limitation of our methods is the fact that calculations of mixture toxicity have been performed based on dissolved metal concentrations, whereas possible interactions between metals at DOC sites have not been accounted for. This is because in the validated bioavailability models, speciation calculations for the different metals are performed with different speciation models in the current BLMs (i.e., WHAM Model V for Cu and Zn vs WHAM Model VI for Ni). Taking into account these interactions at DOC sites could result in higher predicted msPAF values. However, we expect that this would only influence the absolute msPAF values per method, but not the relative ranking of msPAF values among the different methods.

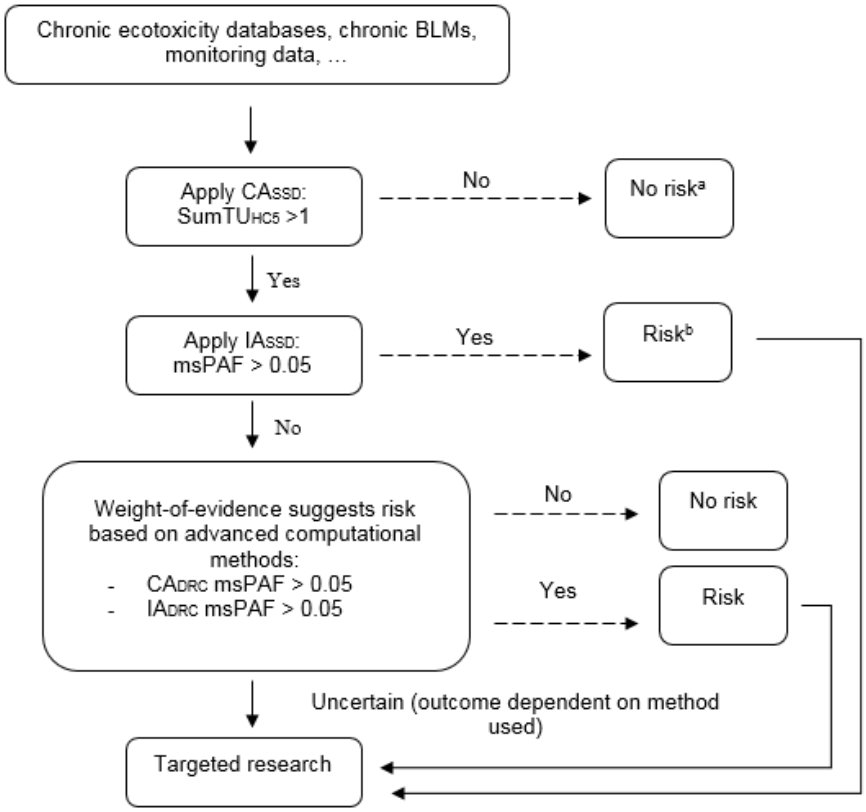

Figure 2.8. Possible tiered metal mixture risk evaluation scheme. A sample is defined to be at risk when the toxic pressure (expressed as multisubstance potentially affected fraction [msPAF]) was higher than 0.05 (or the sum toxic unit expressed relative to the hazardous concentrations affecting 5% of species within a community [$SumTU_{HC5}$] >1), which is equivalent to the typical protection goal for single substances, that is, a maximum of 5% affected species at the HC5 concentration. The msPAF values reported are on the basis of EC10 values. BLMs = biotic ligand models; CA_{SSD} = concentration addition applied directly to the species sensitivity distribution; IA_{SSD} = independent action applied directly to the species sensitivity distribution; CA_{DRC} = concentration addition applied to individual dose-response curves; IA_{DRC} = independent action applied to individual dose-response curves. [a] Unless very strong synergisms at low effect levels. [b] Unless very strong antagonisms at low effect levels.

Research recommendations

Although the CA_{SSD} approach is the most conservative (at $msPAF_{CA,SSD}$ values < 0.15), it is the easiest to implement, and shows a high MoS, more research is needed to conclude whether more complex, liberal methods (CA_{DRC} or IA_{DRC}) might be more accurate in predicting the level of risk posed by mixtures of metals. This could for instance be examined by performing mesocosm experiments. The real ecological meaning of the msPAF has been a topic of research (Smetanova et al. 2014; Posthuma and de Zwart 2006; Posthuma and de Zwart 2012), but uncertainties remain. For instance, although it is assumed that the HC5 value for a single substance is protective for 95% of the species within a community, it is not straightforward to predict what effects may occur in an actual community exposed to a concentration equal to the HC5 of that substance. This uncertainty applies invariantly to mixtures of substances, and thus it is not straightforward to predict what effects on natural communities may be expected after exposure to a metal mixture with a toxic pressure equal to any msPAF. The relation between msPAF and actual effects of metal mixtures on natural communities should be the subject of future research. The calculated toxic pressure (expressed as msPAF values) could possibly be applied in an absolute way if the toxic pressure can be correlated to ecological effects or in a relative way by

ranking contaminated sites. Either way, we propose that a tiered metal mixture risk evaluation scheme in which the 4 methods described in the present study are applied, might be a way forward to evaluate risks implied by mixtures of substances.

In addition, the perception exists that adding more metals to a mixture, even when metals are present at background concentrations, will result in risk predictions for a higher percentage of samples. However, when the results from the FOREGS database are examined, we see that only a limited percentage of samples (up to 4%) is affected by a mixture of 3 metals. In addition, when theoretically more correct models are applied (CA_{DRC} and IA_{DRC}), the issue of mixture toxicity is even lower; 0.5% to 2% of the target water samples are said to be at risk at background concentrations. However, more research is needed to establish whether CA or IA is the best model to implement. Further research is also needed to update existing chronic metal bioavailability models to the same speciation model (e.g., WHAM Model VII) to allow more consistent speciation-based computations of msPAF.

2.4. Conclusions

The present study examined the use of 4 mixture risk assessment methodologies that combine chronic toxicity data, bioavailability modeling, SSDs, and CA or IA for ecological risk assessment by calculating the toxic pressure (expressed as msPAF values) based on measured concentrations of metals in 4 monitoring databases and 1 natural baseline database. The percentage of target water samples predicted to be at risk differed between the methods used and were between 0% (Rhine) and 52% (Dommel) when the simplest approach (CA_{SSD}) was used. When only the target water samples that were at risk from metal mixtures and not from individual metals were examined, the percentage of affected target water samples ranged between 0% (Rhine) and 15% (Dommel). The percentage of target water samples predicted to be affected also differed between the methods used, with a difference of 3% to 13% between methods.

In general, our calculations showed the following order of conservatism for the 4 methods (from most to least conservative): $CA_{SSD} > CA_{DRC} > IA_{DRC} > IA_{SSD}$. Because the CA_{SSD} method, the simplest to implement, was shown to be the most conservative (below certain risk values), MoS values could be calculated. It was demonstrated that the CA_{SSD} method is more conservative by a factor 1.17 to 1.48 than the other methods (based on the Dommel dataset). Finally, we suggest applying these 4 approaches in a general tiered scheme for the risk assessment of chemical mixtures in a regulatory context. The CA_{SSD} method could serve as a first (conservative) tier to identify situations with likely no potential risk at all, regardless of the method used ($SumTU_{HC5} < 1$) and the IA_{SSD} method could be used to identify situations of potential risk, also regardless of the method used ($msPAF_{IA,SSD} > 0.05$). The CA_{DRC} and IA_{DRC} methods could be used for site-specific assessment for situations that fall in between ($SumTU_{HC5} > 1$ and $msPAF_{IA,SSD} < 0.05$).

Three

MIXTURE TOXICITY TO *PSEUDOKIRCHNERIELLA SUBCAPITATA* IN VARIOUS NATURAL WATERS

Redrafted from:

Van Regenmortel T, De Schamphelaere KAC. Mixtures of Cu, Ni and Zn act mostly non-interactively on *Pseudokirchneriella subcapitata* growth in natural waters. Accepted by Environmental Toxicology and Chemistry. DOI 10.002/etc.3999

3. Mixture toxicity to *Pseudokirchneriella subcapitata* in various natural waters

3.1 Introduction

Recent studies (Cooper et al 2009; Shaw et al 2006; Nys et al 2017c, Van Regenmortel et al. 2017a/Chapter 2) have expressed concerns that risk assessment procedures for metals are still mainly based on single metal toxicity, whereas freshwater biota are typically exposed to mixtures of different metals. The effects of metal mixtures have therefore repeatedly been subject of research. Two reference models are commonly used for the prediction of mixture toxicity: the concentration addition (CA) model and the independent action (IA) model. The former model is mostly used to predict the toxicity of mixtures of substances that have a similar mode of action (Loewe & Muischnek 1926), whereas the latter model is mostly used to predict substances that have a dissimilar mode of action (Bliss 1939). Both reference models assume that substances do not interact. However, interactions (i.e. synergistic or antagonistic) can be determined using a more elaborate mixture analysis framework based on CA or IA (Joncker et al 2005). This framework has allowed for the determination of non-interactive, antagonistic and synergistic effects in various metal mixture toxicity studies (Iwasaki et al. 2015; Lynch et al. 2015; Hochmuth et al. 2016; Nys et al. 2015; 2017a). Numerous studies have examined the interactive effects of metal mixtures on invertebrates (Norwood et al. 2007; Naddy et al. 2015; Nys et al. 2015; 2017a) , fish (Spehar and Fiandt 1986; Naddy et al. 2015) and higher plants (Lui et al. 2015; Versieren et al. 2014; 2016; Gapolapillai 2016).

Another group of species, microalgae, have also been subject of research. Because these primary producers are at the base of the food web, it is of utmost to understand the effects of metals on these organisms. Franklin et al (2002) demonstrated for Chlorella sp. that the metal combinations Cu-Zn, Cd-Zn and Cu-Cd-Zn acted antagonistically on cell growth relative to the CA model, whereas the mixture of Cu-Cd acted synergistically. It was hypothesized that this was due to cadmium-enhanced copper uptake. Nagai and Kamo (2014) found that the interactions between Zn, Cd and Cu were antagonistic relative to the CA model for the algae *Pseudokirchneriella subcapitata*. In addition, it was shown that the IA model performed better than the CA model in predicting mixture toxicity. Nagai and De Schamphelaere (2016) demonstrated for *Navicula pelliculosa* that all binary combinations of Zn-Cu-Cd-Ni acted antagonistically relative to the CA model. In addition, here too the IA model performed better than the CA model (for combinations of Cd-Zn and Cd-Cu). However, all of the above mentioned studies with algae show a certain limitation: the interactive effects of the mixtures in the above mentioned algae studies were only tested in one specific water chemistry. However, it has been shown for invertebrates and plants that interactive effects can vary depending on the water chemistry (Naddy et al. 2015; Versieren et al. 2014).

The objective of this study was therefore to test the interactive effects of metal mixtures to *P.subcapitata*, across various natural waters that show diverse water-chemistry characteristics. This was done by performing experiments with ternary Cu-Ni-Zn mixtures in 3 natural waters and binary Cu-Ni mixtures in 5 natural waters. In these experiments, the toxicity of the single metals and mixtures were tested simultaneously. We aimed to answer the following research questions. (1) Does the type of interactive effect between Cu-Ni-Zn and Cu-Ni to *P.subcapitata* growth vary with water chemistry? Our null hypothesis is that the interactive effect is independent of water chemistry. However, based on studies

with *C. dubia* (Naddy et al. 2016; Nys et al. 2017a) and *H. vulgare* (Versieren et al. 2014) that showed different interactive effects in hard and soft waters, interactive effects could be dependent on water chemistry. (2) Do the metals interact or not? Based on research of effects of Cu-Ni mixtures on other algae (Israr et al. 2011; Nagai and Kamo 2014; Flouty and Khalaf 2015) we hypothesized that the Cu-Ni mixture would act antagonistically relative to CA on *P.subcapitata* growth rate. Limited literature was found concerning toxicity of Cu-Ni-Zn mixture to algae (Nys et al. 2016b). Based on this, we hypothesized that the Cu-Ni-Zn mixture would also act antagonistically relative to CA on algal growth. (3) Is the CA or the IA model the best model to predict chronic mixture toxicity to *P.subcapitata*?
In addition, we also aimed to develop a metal mixture bioavailability model by combining single metal bioavailability models, similar to work performed by Nys et al. (2017c, 2017a).

3.2 Materials and methods

Collection of test media

Natural surface waters were sampled in two periods. In 2013, water was sampled for tests on Cu-Ni-Zn mixture toxicity with *P.subcapitata* and in 2014, water was sampled for tests on Cu-Ni mixture toxicity with *P.subcapitata*. Samples of natural surface waters were taken at four locations in France, two locations in Belgium and one location in the Netherlands (Table 3.1). The natural waters were sequentially filtered through 10 µm, 1 µm and 0.2 µm filters (Eurowater, FZ 2001-010, 2021-001, 3005-020) and were collected in acid-washed (1% HNO_3) polyethylene vessels. The water was stored in total darkness until use.

Ecotoxicity testing with *P.subcapitata*

General test design.

The effects of ternary Cu-Ni-Zn and binary Cu-Ni mixtures were investigated using the chronic (48h) *P. subcapitata* growth inhibition test (OECD 2011) using an equitoxic ray design. This entails that each component in a mixture has the same relative toxicity, i.e. is added in equitoxic proportions relative to their toxic units (TU). As it has been shown that metal concentration ratios can influence the metal interactions in a mixture (Nys et al. 2017a), using an equitoxic design ensures that we explicitly tested the effect of differences in water chemistry on the mixture interaction, which is in line with what our hypothesis states, and not the effect of the difference in contribution of each metal on the metal interaction. The latter would have been the case in a design in which a single fixed metal concentration ratio for all waters (for instance based on environmentally realistic concentration ratios) would have been chosen. Mixture combinations were tested at 8 to 10 (ternary mixture) and 5 (binary mixture) mixture treatments. These treatments ranged between 0.2-6.0 and 0.2-4.4 sum of TU ($\sum_{TUMe}$), relative to the median effective concentration ($EC50_{Me}$), for the ternary and binary mixture, respectively. Nominal dissolved $EC50_{Me}$ in the test media were predicted using the existing bioavailability models for Cu (De Schamphelaere & Janssen 2006), Ni (Deleebeeck et al 2009) and Zn (De Schamphelaere & Janssen 2005). For both mixture test series, the individual metals were tested simultaneously with the mixture treatments, to avoid difficulties with data interpretation of mixture interaction analysis due to temporal sensitivity shifts (De Laender et al 2009).

Table 3.1. Overview of the locations and sampling dates of the natural surface waters with which toxicity tests were performed.

Site ID	Coordinates		Location	District or province, country code[a]	Waterbasin	Sampling date (dd-mm-yyyy)
	Latitude	Longitude				
Loire	58° 22' 17.3''	4° 11' 45.5''	Aurec-Sur-Loire	Auvergne, F	Loire	10-04-2013
Dolaizon	45° 0' 53.86''	3° 50' 21.33''	Saint-Christophe-sur-Dolaison	Auvergne, F	Loire	10-04-2013
Moselotte	47° 58' 4.87''	6° 43' 47.32''	Saulxure-sur-Moselotte	Lorraine, F	Rhine	09-04-2013
Bihain (Ruisseau de St. Martin)	50° 8' 52.9''	5° 50' 46''	Bihain	Luxembourg, B	Meuse	28-10-2014
Brisy (l' Ourthe Orientale)	50° 14' 27.3''	5° 48' 30.6''	Brisy	Luxembourg, B	Meuse	28-10-2014
Voyon	50° 6' 4.9''	4° 5' 51.3''	Eppe-Sauvage	Nord-Pas-de-Calais, F	Meuse	28-10-2014
Markermeer	52° 26' 07''	5° 05' 22''	Marken	Flevoland, Nl	Ijssel	10-12-2014

[a] F = France, Nl = the Netherlands, B = Belgium

Preparation of test media.

To investigate the effect of mixtures of Cu-Ni-Zn and Cu-Ni to *P.subcapitata*, tests were conducted in 8 natural waters. A reference water (OECD growth medium) was also prepared according to the standard protocol 201 of the OECD for testing with P.subcapitata (OECD 2011). However, some adjustments were made to the reference water: (1) Stock C was made without addition of Cu and Zn, as background concentrations of these metals were already present in the natural waters. (2) Na-ethylenediamine tetraacetic acid (EDTA) was omitted from Stock B (as has been done previously, e.g. Heijerick et al. 2002a, Deleebeeck et al. 2009) as EDTA is known to be a very strong metal complexing ligand, which complicates speciation calculations and is therefore not appropriate for metal toxicity testing. All OECD stock solutions were subsequently added to the natural waters at the concentrations as indicated in the OECD guideline, to provide extra nutrients during testing. Natural waters were adjusted to the required pH by adding 750 mg/L 3-N-morpholinopropanesulfonic acid (MOPS) (Kandegedara et al 1999; De Schamphelaere et al 2004) (except for the Dolaizon water, as the nominal pH for this water was above the working range of MOPS (pH 6.5-7.9)) and the required amount of NaOH or HCl. The composition of the test media, based on measured water chemistry during the test and after the addition of OECD stock solutions, MOPS and the adjustment of pH, is given in Table 3.2. This water chemistry was used for data analyses.

In the ternary mixture experiment, each treatment received 3 replicates. Next to this 3 control replicates (modified natural medium without extra metals added) and a blank correction per replicate (no algae; used for particle correction, i.e. the average number of particles from all “blank corrections” is subtracted from the particle counts of the metal treatments and controls) were also run. In the binary mixture experiment, each treatment received 3 replicates, the control treatments received 10 replicates and in addition 6 blank corrections were run. All treatments were prepared by adding reagent grade $NiCl_2$, $ZnCl_2$ and $CuCl_2$ purchased from VWR International. To allow equilibration, solutions were spiked with the metals 24 hours prior to testing.

P.subcapitata culturing.

Toxicity tests were performed with a *P.subcapitata* strain (CCAP 278/4) that was obtained from the Culture Collection of Algae and Protozoa (CCAP, at the Scottish Association for Marine Science, Argyll, Scotland, United Kingdom). A culture of the algae was set up 4 days prior to testing in aerated tap water (Gent, Belgium) that was passed sequentially through an activated carbon and a 0.45 µm filter to which the modified Provasoli’s ES enrichment (Bold and Wynne, 1978) at 1/2 strength and, additionally, 1.4 mg/L $FeSO_4.7H_2O$, 15 mg/L $NaH_2PO_4.2H_2O$, 150 mg/L $NaNO_3$ and 2.35 mg/L $MnCl_2.4H_2O$ were added. The flasks containing the algae were placed on a shaking device under continuous light (120 µmol photons.m-2.s-1) at 25°C.

Ecotoxicity testing.

The chronic toxicity tests with *P.subcapitata* were conducted following the OECD Guideline 201 (OECD 2011). Algal tests were performed in 100 mL Erlenmeyer flasks containing 50 mL of test medium. All replicates, except the blank corrections, were inoculated with 104 cells/mL (= cell density N_0 at the start

(t_0) of testing). Next, all Erlenmeyer flasks were incubated at 24 °C on a light table (24 h light, 120 µmol photons m^{-2} s^{-1}) and were manually shaken two times per day. During the test, the pH was adjusted daily by adding NaOH or HCl. Cell densities (N_1, N_2 and N_3) were measured using a particle counter (Coulter Counter Z1, Beckman) after 24 (t_1), 48 (t_2) and 72 (t_3) hours. Growth rate µ (d^{-1}) was determined in each replicate of each treatment as the slope of the linear regression of the natural logarithm of cell density versus time (in days). Test validity was evaluated as described by the OECD guidelines (OECD 2011).

Chemical analyses

During the test period, samples of test media were collected for analysis of total (unfiltered) and dissolved (filtered through 0.45µm; Acrodisc, PALL Life Sciences) metals, major ions, organic carbon (OC) and inorganic carbon (IC). For *P.subcapitata*, total samples of media were taken at test initiation and dissolved samples both at test initiation, and after 48h and 72h. Samples for analysis of DOC (Dissolved Organic Carbon) and TOC (Total Organic Carbon) were taken before addition of MOPS. The pH of fresh and old media were measured daily with a pH glass electrode (Hanna Instruments, Temse, Belgium). Samples for metal analysis were acidified to 0.14 mol/L HNO_3 (Normatom quality, VWR Prolabo). Information concerning the instruments to measure metal concentrations is given in Appendix B.1.

Speciation calculations

The software package WHAM VII (Windermere Humic Aqueuous Model , Tipping et al. 2011) was used to calculate the chemical speciation of Cu, Ni and Zn (using the average measured dissolved metal concentrations between the start and end of the test) in the different test waters. MOPS was added to the default solute database (pKa of 7.2). The default parameters for inorganic ligand-metal complexation of Cu, Ni and Zn in WHAM VII were adapted to those reported by the National Institute for Standards and Technology (Smith et al 2004). The default complexation parameters for the metal - dissolved organic matter (DOM) complexation were used. For the DOM in the test media it was assumed that 65% of the DOM is reactive and behaves as isolated fulvic acid (FA; 65% AFA) while humic acid (HA) was assumed to be 0%. This % was chosen as assumptions of 60% to 70% reactive FA have been shown to work best for predicting metal speciation in natural waters (Tipping 2002) and the assumption of 65% AFA has been used in many recent metal mixture studies (Tipping and Lofts, 2013, 2015; Nys et al. 2016a; 2017a). In addition, it was assumed that DOM contains 50% carbon on a weight basis. Therefore, the measured DOC concentration was multiplied by 1.3 to obtain the FA concentration to be used as the input for speciation calculations. Activities of the metal cation Fe^{3+} were assumed to be controlled by colloidal $Fe(OH)_3$ precipitates using the default equation and solubility product embedded in WHAM VII (Lofts & Tipping 2011).

Data analysis

If the validity criteria of the standard tests for *P.subcapitata* are met after 72h, effect concentration (EC) are calculated based on relative growth rate after 72h. However, if the growth rate of *P.subcapitata* for the control treatments did not pass validity criteria after 72-h, the OECD guideline permits that the tests

may be shortened to 48-h to maintain unlimited, exponential growth during the test as long as the validity criteria are met (OECD 2011), and that ECx values may be based on results of 48h exposure. As not all tests passed the validity criteria after 72h, we used the results of the 48h exposure for all tested waters, in accordance with the OECD test guidelines.

Effect concentrations (EC10 and EC50) were calculated based on average measured dissolved metal concentrations (i.e. the average metal concentration at the start of the test and after 72h for the ternary mixture (as no measurements were taken at 48h) and after 48 hours for the binary mixture) as well as on WHAM VII calculated free ion activities. The relative growth rate (RGR, relative to the mean control reproduction, %) was used as the endpoint.

EC50, EC10 and corresponding confidence intervals were determined for Cu, Ni and Zn using the drc-package in R 1.0.136 (R Development Core Team, Vienna, Austria) with a log-logistic concentration response model with two parameters (Equation 3.1).

$$\mathrm{RGR}_{\mathrm{Me_i}} = \frac{100}{1+\exp^{\left(\mathrm{b}_{\mathrm{Me_i}}\left(\ln\left(\mathrm{x}_{\mathrm{Me_i}}\right)-\ln\left(\mathrm{EC50}_{\mathrm{Me_i}}\right)\right)\right)}} \quad (3.1)$$

Where $\mathrm{RGR}_{\mathrm{Me_i}}$ is the predicted relative growth rate for metal i (%);$\mathrm{b}_{\mathrm{Me_i}}$ is the slope parameter for metal i; $\mathrm{x}_{\mathrm{Me_i}}$ is the dissolved metal concentration (µg/L) or free ion activity of metal i (nmol/L) and $\mathrm{EC50}_{\mathrm{Me_i}}$is the 50% effect concentration of metal i (µg dissolved metal/L or nmol free metal ion/L).

Mixture interactions analysis

For each of the ternary and binary mixtures, the interactive effects were assessed using the mixture analysis framework developed by Jonker et al. (2005) and further extended by Hochmuth et al. (2014), as has been applied elsewhere (Nys et al. 2015; Nys et al. 2016b; Nys et al. 2017a). With this method it is possible to examine whether a mixture deviates from strict non-interaction using the CA and the IA reference models. The analysis of the interactive effects was made based on both the dissolved concentrations and the free ion activities, to identify possible shifts in interactions due to competitive binding of Cu, Ni and Zn onto DOC. The mean RGR for every treatment was used as input for the analysis of the combined effects, which was performed in three subsequent steps. These steps were performed in the software package R-1.0.136 (R development Core Team). A detailed overview of the different steps is given in the Appendix (B.2). In short, a first step entailed the prediction of the RGR for the mixture combinations, which was made with the reference models CA and IA using the parameters of the individual dose response curves of Cu, Ni and Zn ($EC50_{Me_i}$ and b_{Me_i}). In a second step, the RGR were predicted for the mixture combinations with the CA and IA reference models using the parameters fitted to the single metal and mixture data simultaneously. Subsequently, in the third step, the CA and IA reference models were extended with a deviation parameter (a), which is a measure for the deviation of non-interactivity (Joncker et al 2005, Hochmuth et al 2014). To examine whether the deviation from non-interactivity was significant, it was checked whether the addition of the deviation parameter a significantly improved the predictions of the nested models from step 2 and 3 (Hochmuth et al. 2014). This was done by performing an F-test, after checking the validity of the assumptions for this test.

Metal Mixture Bioavailability Model (MMBM) development

Recent meta-analyses (Van Genderen et al. 2015; Nys et al. 2017c) showed that the IA model was the most accurate model in predicting mixture toxicity. Because the IA model was also the most accurate to predict Ni-Zn-Pb toxicity to *C. dubia*, Nys et al. (2017a) developed a MMBM by combining the individual chronic bioavailability models with the IA model. We found that IA was equally as accurate compared to CA for predicting Cu-Ni-Zn toxicity to *P.subcapitata* (see Results section). However, the individual *P.subcapitata* bioavailability models for Cu, Ni and Zn differ in the competing ions that they consider. This suggests that Cu, Ni and Zn have different modes of action and bioavailability relations, which supports the choice of an IA-based MMBM. Hence, we developed a MMBM for *P.subcapitata* as was done by Nys et al. (2017a) by combining the individual chronic bioavailability models for Cu (De Schamphelaere & Janssen 2006), Ni (Deleebeeck et al 2009) and Zn (De Schamphelaere & Janssen 2005) with the IA model (Equation 3.2) on the basis of the free ion activity.

$$\mathrm{RGR_{mix}} = 100 \cdot \prod_{i=1}^{n}\left(\frac{1}{1+\left(\frac{x_{Me_i}}{EC50_{Me_i}}\right)^{b_{Me_i}}}\right) \quad (3.2)$$

Where n is the number of metals in the mixture and RGR_{mix} is the predicted mixture growth rate relative to the control. As was assumed by Nys et al. (2017a) for competition between Ni^{2+}, Zn^{2+} and Pb^{2+}, we also assumed that each metal only binds to its own biotic ligand site and therefore that competition between metals for binding at the biotic ligand site was not allowed. The competitive effects of Mg^{2+} for binding at the Ni biotic ligand site and the effect of pH on the binding of the free metal ion to the biotic ligand sites were integrated in the MMBM using the stability constant ($K_{MgBLMei}$) and pH slopes ($S_{pHMe,i}$) of the individual chronic bioavailability models. Equation 3.3 was used to predict the RGR in the presence of Cu, Ni and/or Zn.

$$\mathrm{RGR_{MMBM,k}} = 100 \cdot \frac{1}{1+\left(\frac{c_{Cu^{2+},k}}{10^{-\left(Q50_{Cu^{2+}}+S_{pH,Cu}\cdot pH_k\right)}}\right)^{b_{Cu^{2+}}}} \cdot \frac{1}{1+\left(\frac{c_{Ni^{2+},k}}{10^{-\left(Q50_{Ni^{2+}}+S_{pH,Ni}\cdot pH_k\right)}(1+K_{MgBL_{Zn}}\{Mg^{2+}\}_k)}\right)^{b_{Ni^{2+}}}} \cdot \frac{1}{1+\left(\frac{c_{Zn^{2+},k}}{10^{-\left(Q50_{Zn^{2+}}+S_{pH,Zn}\cdot pH_k\right)}}\right)^{b_{Zn^{2+}}}} \quad (3.3)$$

In Equation 3.3, $RGR_{MMBM,k}$ is the relative growth rate (%) in water k predicted with the MMBM. $c_{Cu2+,k}$, $c_{Ni2+,k}$ and $c_{Zn2+,k}$ are the WHAM VII predicted free metal activities of Cu^{2+}, Ni^{2+} and Zn^{2+} in test medium k (mol/L), respectively. Q_{50Cu2+}, Q_{50Ni2+} and Q_{50Zn2+} are the intrinsic sensitivities of the chronic Cu, Ni and Zn bioavailability models (log(mol/L)), respectively. b_{Cu2+}, b_{Ni2+} and b_{Zn2+} are the slope parameters of the log-logistic dose response curves of Cu^{2+}, N^{i2+} and Zn^{2+}, which are assumed to be independent of water chemistry. Whether this assumption is valid is not clear, as the factors influencing slope values are not fully understood. In the present study, there is no clear pattern between the observed slopes of the different natural waters and the major physicochemical parameters (i.e. pH, Ca concentration and DOC concentration; Table 4; Pearson's correlation $p > 0.05$). Therefore, until the factors influencing the slopes of dose-response curves are better understood, this assumption is inevitable. In addition, this assumption also avoids making thee MMBM overly complicated.

The $Q50_{Me}$ and b_{Me} values were calibrated on all single metal toxicity data using non-linear least square fitting in R. $S_{pH,Cu}$, $S_{pH,Ni}$ and $S_{pH,Zn}$ are the pH slopes of Cu^{2+}, Ni^{2+} and Zn^{2+} toxicity in the Cu, Ni and Zn bioavailability models, respectively. pH_k is the pH of water k. $K_{MgBL,Ni}$ is the stability constant for the binding of Mg^{2+} to the Ni biotic ligand (L/mol) (Deleebeeck et al. 2009; De Schamphelaere and Janssen 2005; 2006). $S_{pH,Me}$ values and the stability constant for Mg^{2+} were taken from the individual metal BLMs. $\{Mg^{2+}\}$ is the chemical activity of Mg^{2+} in water k predicted with WHAM VII. All MMBM parameters are listed in Table 3.2. The MMBM was used to predict the RGR of Cu, Ni and Zn as a mixture, as well as individually.

Table 3.2 Model parameters of the chronic *Pseudokircherniella subcapitata* metal mixture bioavailability model

		Cu	Ni	Zn
Fixed model parameters	Log $K_{MgBL,Me}$	-	3.3[a]	-
	$S_{pH,Me}$	1.354[b]	0.143[a]	0652[c]
Calibrated model parameters[d]	$Q50_{Me2+}$	-1.98 ± 0.06	4.45 ± 0.04	1.36 ± 0.03
	b_{Me2+}	0.80 ± 0.10	1.97 ± 0.28	1.33 ± 0.14

[a] Model parameters originating from the chronic Ni *P.subcapitata* bioavailability model *(Deleebeeck et al 2009)*
[b] Model parameters originating from the chronic Cu *P.subcapitata* bioavailability model (*De Schamphelaere & Janssen 2006*)
[c] Model parameters originating from the chronic Zn *P.subcapitata* bioavailability model (*De Schamphelaere & Janssen 2005*)
[d] Calibrated MMBM model parameters ± standard error

3.3 Results

Chemical characterisation of natural study waters

An overview of the water chemistry of the natural test media is given in Table 3.3. pH ranged between 6.5 and 8.2, DOC ranged between 2.2 mg/L and 12.7 mg/L and Ca concentrations ranged between 2.6 mg/L and 227.7 mg/L.

Concentration response analysis

The validity criteria of the standard tests for *P.subcapitata* were not met for 2 out of 8 waters after 72h of exposure (Appendix B.3). Therefore, it was decided that the 48-h growth rate, for which all criteria were met in all waters, was used to calculate effect concentrations in each water. The concentration response data of the individual Cu, Ni and Zn exposures based on dissolved metal concentration and free metal ion activity are shown in Appendix B Figure B3.1-2 and Table B3.2-3. Dissolved Ni, Cu and Zn concentrations ranged between 1 µg/L – 2680 µg/L, 1 µg/L – 659 µg/L and 1 µg/L – 450 µg/L in the individual exposures, respectively. Corresponding $EC10_{Me_i}$, $EC50_{Me_i}$ and b_{Me_i} are listed in Table 3.4. A large range in ECx values is observed, e.g. EC10 between 7.2 µg/L Cu_{diss} and 112.0 µg/L Cu_{diss}. This can be linked to the water chemistry of the test medium. For algae, DOC concentration and pH are the main divers of metal toxicity (De Schamphelaere et al. 2003, Deleebeeck et al. 2009, De Schamphelaere et al. 2005) and the reason toxicity is so variable (Table 3.4).

Analysis of interactive mixture effects

Figure 3.1 shows the CA- and IA-predicted and observed relative growth rate of the ternary and binary mixture treatments plotted as a function of the ∑TU based on free ion activities. In addition, the individual log-logistic concentration–response curves of Cu, Ni and Zn (Figure B3.1-2) in the corresponding test waters are plotted in Figure 3.1. A similar figure for dissolved concentrations is given in the Appendix (B.4). The observed type of interactive effect to the two reference models for each mixture for all waters

is given in Table 3.5. The variability between the replicates in some of the binary mixtures was higher than in most ternary mixtures (Figure 3.1), which may have influenced the outcome of the statistical analyses. Despite this, the statistical analysis showed that no significant interactions were observed for the ternary and binary mixture relative to both the CA and the IA model (Appendix B Table B4.3-4), when concentrations were expressed as free ion activities (Figure 3.2, Appendix B Figure B.4.2-3) or as dissolved concentrations (Appendix B Figure B.4.4-5). The only exception was found in the water Moselotte, where the ternary mixture acted antagonistically on *P.subcapitata* growth rate relative to both the CA and IA model, either when concentrations were expressed as free ion activities or as dissolved concentrations.

Table 3.3. Overview of measured test water chemistry of the different experimental series. Mean values ± standard deviations are reported.

	Test series[a]	pH	DOC (mg/L)	DIC (mg/L)	Na (mg/L)	Mg (mg/L)	K (mg/L)	Ca (mg/L)	Cl (mg/L)	SO4 (mg/L)
Loire	1	7.2 ± 0.03	3.7[b]	14.6 ± 0.0	14.8 ± 0.2	6.8 ± 0.1	76.8 ± 11.0	2.6 ± 0.1	65.0 ± 8.5	23.4 ± 2.3
Dolaizon	2	8.2 ± 0.08	4.6 ± 0.5	22.3 ± 1.8	17.7 ± 0.3	14.7 ± 0.1	2.2 ± 0.1	17.9 ± 0.2	37.9 ± 1.0	18.1 ± 2.0
Moselotte	3	7.6 ± 0.02	2.2[b]	9.56 ± 0.0	114.1 ± 0.9	4.2 ± 0.1	1.3 ± 1.3	9.0 ± 0.2	128.8 ± 0.6	14.6 ± 1.3
Bihain	4	6.5 ± 0.01	12.7[b]	2.9 ± 1.1	146 ± 5.7	4.1 ± 0.1	1.8 ± 0.1	9.7 ± 0.7	50.2 ± 3.2	10.4 ± 1.6
Brisy1	4	7.2 ± 0.01	4.4[b]	4.8 ± 2.0	72.5 ± 0.7	6.9 ± 0.4	2.9 ± 0.1	15.5 ± 0.7	51.1 ± 4.6	15.1 ± 2.7
Voyon	4	6.8 ± 0.03	9.0[b]	4.8 ± 2.5	41 ± 4.2	9.4 ± 0.4	2.8 ± 0.1	24.3 ± 1.3	67.0 ± 9.8	19.7 ± 2.7
Brisy2	5	7.2 ± 0.01	7.1[b]	72.5 ± 0.7	6.1 ± 0.3	2.9 ± 0.7	13.5 ± 0.6	54.7 ± 7.0	13.9 ± 0.5	2.5 ± 1.2
Markermeer	5	8.1 ± 0.07	9.9[b]	88.7 ± 0.0	18.8 ± 0.6	4.9 ± 0.0	57.3 ± 2.3	227.7 ± 15.8	89.6 ± 4.2	16 ± 3.6

[a] All natural waters within a test series were tested simultaneously, [b] 750 mg/L MOPS added to the test water, therefore only DOC measurement at the start of the test;
DOC = Dissolved Organic Carbon, DIC = Dissolved Inorganic Carbon

Table 3.4 EC10, EC50 and b of the concentration response curves (± standard error) of the individual Zn, Ni and Cu 48-h exposures

	Parameter	Cu_{diss} (µg/L)	Ni_{diss} (µg/L)	Zn_{diss} (µg/L)	Cu^{2+}_{act} (nmol/L)	Ni^{2+}_{act} (nmol/L)	Zn^{2+}_{act} (nmol/L)
Loire	EC10	29.0 ± 2.2	187.5 ± 19.3	63.8 ± 6.6	2.3 ± 0.4	1736.6 ± 186.3	358.1 ± 42.3
	EC50	99.0 ± 3.4	498.6 ± 22.6	204.2 ± 10.0	26.5 ± 1.9	4784.1 ± 225.3	1336.0 ± 75.3
	b	1.79 ± 0.12	2.25 ± 0.22	1.89 ± 0.17	0.89 ± 0.07	2.17 ± 0.21	1.67 ± 0.15
Dolaizon	EC10	10.0 ± 1.7	224.7 ± 6.6	9.4 ± 1.6	0.03 ± 0.01	1494.1 ± 50.4	24.1 ± 4.5
	EC50	34.5 ± 2.9	484.3 ± 14.8	45.8 ± 3.3	0.4 ± 0.1	3343.8 ± 117.0	140.3 ± 11.4
	b	1.77 ± 0.23	2.86 ± 0.19	1.38 ± 0.13	0.83 ± 0.11	2.73 ± 0.20	1.25 ± 0.12
Moselotte	EC10	7.2 ± 0.9	80.1 ± 3.4	11.5 ± 2.6	0.1 ± 0.03	713.0 ± 31.7	49.9 ± 12.9
	EC50	24.5 ± 1.5	227.9 ± 9.4	52.9 ± 5.0	1.8 ± 0.2	2619.5 ± 92.6	281.3 ± 30.2
	b	1.78 ± 0.18	1.77 ± 0.09	1.44 ± 0.19	0.82 ± 0.07	1.69 ± 0.08	1.27 ± 0.17
Bihain	EC10	112.0 ± 28.5	222.2 ± 22.5	NA	4.3 ± 2.1	1825.9 ± 200.2	NA
	EC50	363.5 ± 33.8	513.0 ± 29.3	NA	80.8 ± 15.9	4542.3 ± 281.7	NA
	b	1.87 ± 0.38	2.63 ± 0.20	NA	0.75 ± 0.12	2.41 ± 0.18	NA
Brisy1	EC10	47.5 ± 8.5	297.1 ± 70.1	NA	3.6 ± 1.5	4678.4 ± 1132.9	NA
	EC50	117.3 ± 6.8	584.3 ± 42.3	NA	49.9 ± 7.6	8657.6 ± 628.1	NA
	b	2.43 ± 0.36	3.25 ± 0.82	NA	0.84 ± 0.10	3.57 ± 1.02	NA
Voyon	EC10	51.0 ± 19.9	552.4 ± 67.5	NA	10.7 ± 5.9	5908.6 ± 737.8	NA
	EC50	284.0 ± 43.6	1102.4 ± 51.1	NA	248.4 ± 51.7	11516.5 ± 530.1	NA
	b	1.28 ± 0.29	3.18 ± 0.48	NA	0.70 ± 0.12	3.29 ± 0.53	NA
Brisy2	EC10	47.5 ± 2.0	207.3 ± 49.9	NA	1.8 ± 0.2	1919.3 ± 492.3	NA
	EC50	120.5 ± 2.3	784.5 ± 67.0	NA	13.2 ± 0.6	7918.9 ± 716	NA
	b	2.36 ± 0.10	1.65 ± 0.25	NA	1.09 ± 0.06	7.55 ± .23	NA
Markermeer	EC10	52.3 ± 1.5	403.89 ± 63.3	NA	0.6 ± 0.2	2769.8 ± 459.8	NA
	EC50	132.2 ± 11.1	1530.3 ± 72.6	NA	4.4 ± .6	11105.0 ± 554.2	NA
	b	2.37 ± 0.45	1.65 ± 0.17	NA	1.12 ± 0.15	1.58 ± .17	NA

EC10 = 10% effective concentration
EC50 = median effective concentration
b = slope of the individual concentration response curves
Me_{diss} = parameters of the individual concentration response curves based on dissolved concentrations (µgL)
Me_{act} = parameters of the individual response curves based on free ion activities (nmol/L)
NA = Not applicable

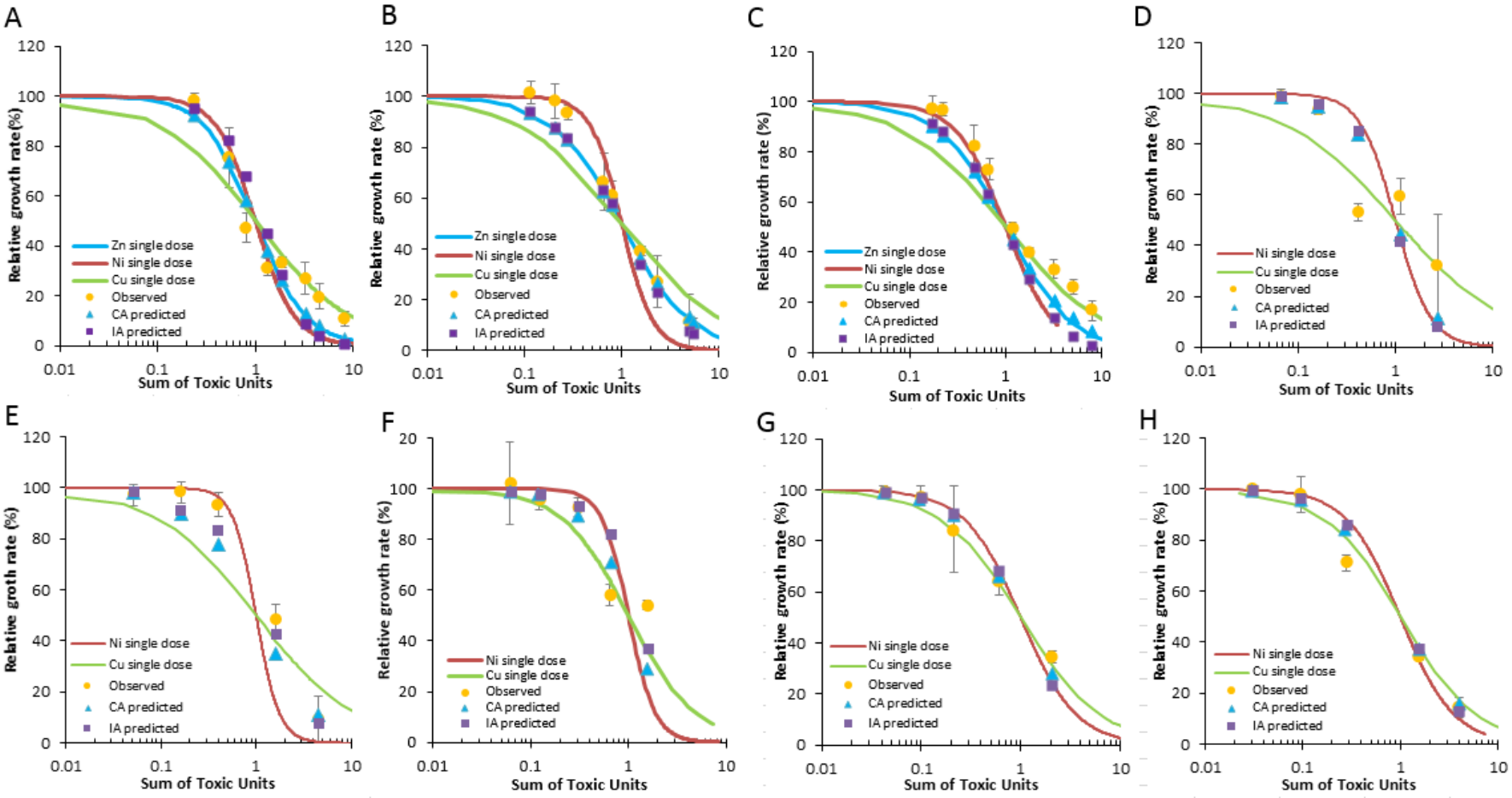

Figure 3.1. Observed and predicted relative growth rate (RGR) as a function of the sum of toxic units (SumTU) based on free ion activities in the ternary Cu-Ni-Zn mixture combinations (A-C) and the binary Cu-Ni mixture combinations (D-H) for *Pseudokirchneriella subcapitata*. Observed RGR (circles), predictions with concentration addition (CA; triangles, Equation B2.1), and predictions with independent action (IA; squares, Equation B2.2 Predictions are based on the 50% effective concentration ($EC50_{Me2+,i}$) and slope ($b_{Me2+,i}$) of the individual concentration–response curves of Cu, Ni and Zn (see Equation 3.1, Table 3.4).

$SumTU = \sum \frac{Me_i^{2+}}{EC50_{Me^{2+},i}}$**. Lines represent the individual log-logistic concentration–response curves of Cu, Ni and Zn in the corresponding test waters. Error bars show standard errors. A=Loire, B=Dolaizon, C=Moselotte, D= Bihain, E=Brisy1, F=Voyon, G=Brisy2, H=Markermeer**

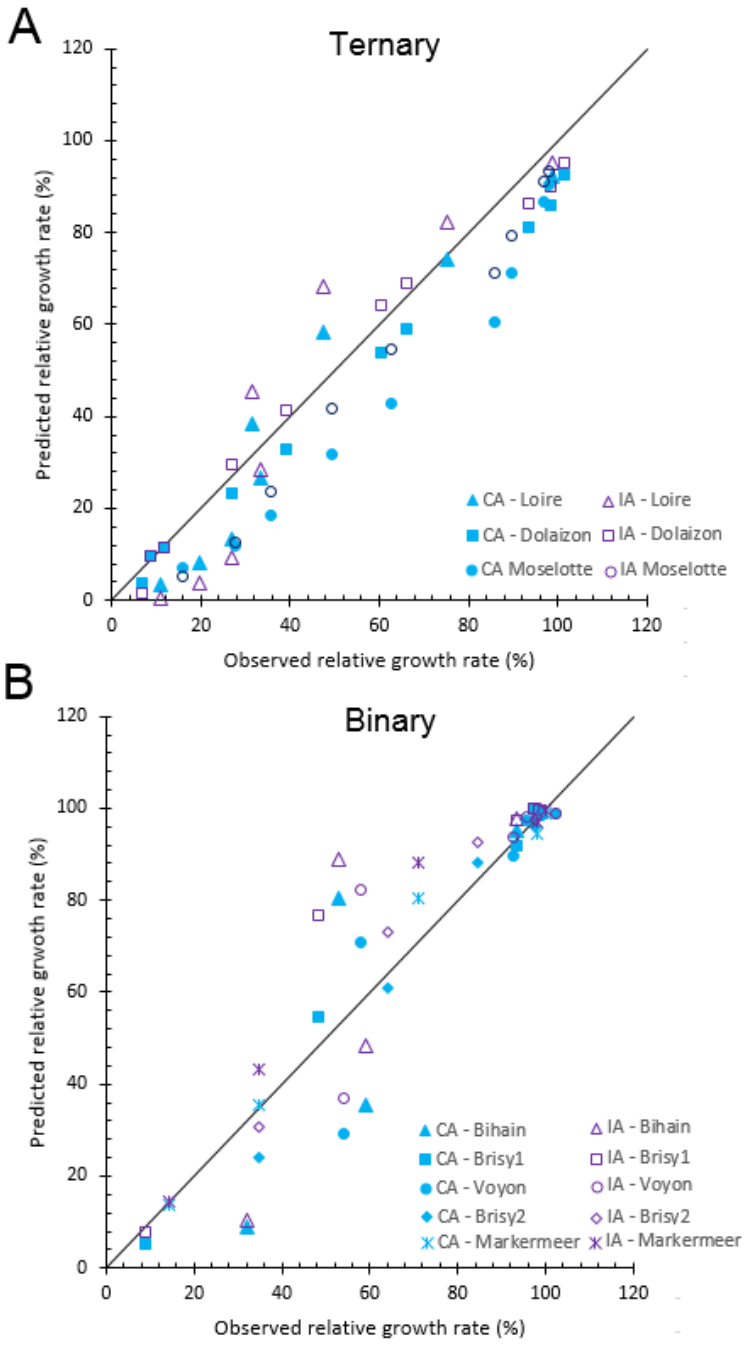

Figure 3.2 Observed relative growth rate versus predicted relative growth rate for the mixture reference models concentration Observed relative growth rate versus predicted relative growth rate for the mixture reference models concentration addition (blue symbols) and independent action (purple symbols) for the *Pseudokircherniella subcapitata* ternary Cu-Ni-Zn (A) and binary Cu-Ni (B) experimental series. Model predictions were based on parameters estimated from single-metal exposures of Cu, Ni and Zn (Table 3.4), with doses expressed as free ion activities.

Table 3.5. Observed type of interactive effect in the Cu-Ni-Zn and Cu-Ni mixtures for *Pseudokirchneriella subcapitata* [a]

	Concentration addition		Independent action	
	Me_{diss}[b]	Me_{2+}[c]	Me_{diss}	Me_{2+}
Ternary				
Loire	NI	NI	NI	NI
Dolaizon	NI	NI	NI	NI
Moselotte	A	A	A	A
Binary				
Bihain	NI	NI	NI	NI
Brisy1	NI	NI	NI	NI
Voyon	NI	NI	NI	NI
Brisy2	NI	NI	NI	NI
Markermeer	NI	NI	NI	NI

[a] All parameters of the fitted models are listed in Table Appendix B3-4
[b] Analysis of mixture interactions based on dissolved concentrations
[c] Analysis of mixture interactions based on free ion activities
A = antagonism; NI = non-interactive

Validation of the MMBM

Figure 3.3 and Figure 3.4 show the MMBA-predicted versus observed relative growth rate of the mixture treatments and individual treatments for the ternary and binary mixture, respectively. For the ternary mixture (Figure 3.3), the MMBM predicted the RGR of 96% of the mixture treatments with less than 20% error. The RGR for the individual Cu, Ni and Zn treatments were predicted within 20% error in 100%, 100% and 100% of the cases. The root mean square errors were 9, 9, 5 and 11 for the mixture, individual Cu, individual Ni and individual Zn treatments, respectively. For the binary mixture (Figure 3.4), the MMBM predicted the RGR of 72% of the mixture treatments with less than 20% error. The RGR for the individual Cu and Ni treatments were predicted within 20% error in 88% and 84% of the cases. The root mean square errors were 19, 15 and 15 for the mixture, individual Cu and individual Ni treatments, respectively.

3.4 Discussion

Analysis of interactive mixture effects

In the present study, we investigated the combined effects of ternary Cu-Ni-Zn and binary Cu-Ni mixtures on *P.subcapitata* growth inhibition. Non-interactivity amongst metals is not an uncommon phenomenon. In a meta-analysis performed by Norwood et al. (2003) which included 77 species and 21 different metals, 27% of the responses showed non-interactivity (although it was not specified against which reference model). A recent meta-analysis performed by Nys et al. (2017c) including 3 species and 5 metals showed non-interactivity in 35% and 29% of the cases relative to the CA and IA model, respectively. One exception to non-interactivity of the Cu-Ni-Zn mixture was found for the Moselotte water. The ternary Cu-Ni-Zn mixture acted non-interactively on algal growth relative to the CA and IA model (Figure 3.1 and Appendix B Table B.3.3), except for in 1 water (Moselotte), in which the mixture acted antagonistically. Mehta et al. (2000) investigated the Ni-adsorption by another freshwater algae, *C. vulgaris*, when Cu and Zn were administered. The simultaneous application of both Cu and Zn appeared to inhibit the adsorption of Ni, possibly by competing with them for binding onto common

functional groups on the cell surface. In a study by Franklin et al. (2002), it was shown that Cu had an inhibitory effect on the uptake of Zn by *Chlorella sp*.. In addition, the binary Cu-Zn mixture acted antagonistically on *Chlorella* sp. growth rate relative to the CA model. This was most likely because of competition for the same transport sites on the cell membrane. Similarly, Cu also had an inhibitory effect on the uptake of Ni by *C. reinhardtii* (Flouty and Khalaf, 2015) which was explained as a competitive binding of Cu with Ni for the transport sites being used for Ni uptake. These studies are therefore consistent with the observed antagonistic effects of Cu-Ni-Zn on algae growth in the Moselotte water. However, in the other 2 waters (Loire and Dolaizon), the Cu-Ni-Zn mixture acted non-interactively on algal growth. Norwood et al. (2003) speculated why deviations from model predictions, for mixtures of the same metals, could be so variable. These authors suggested that difference in test organisms could explain this result. In addition, we observed variable deviations from model predictions, for a mixture of the same metals, for a single species (i.e. *P. subcapitata*). Norwood et al. (2003) suggested that different water chemistry could underlie these variable model predictions.

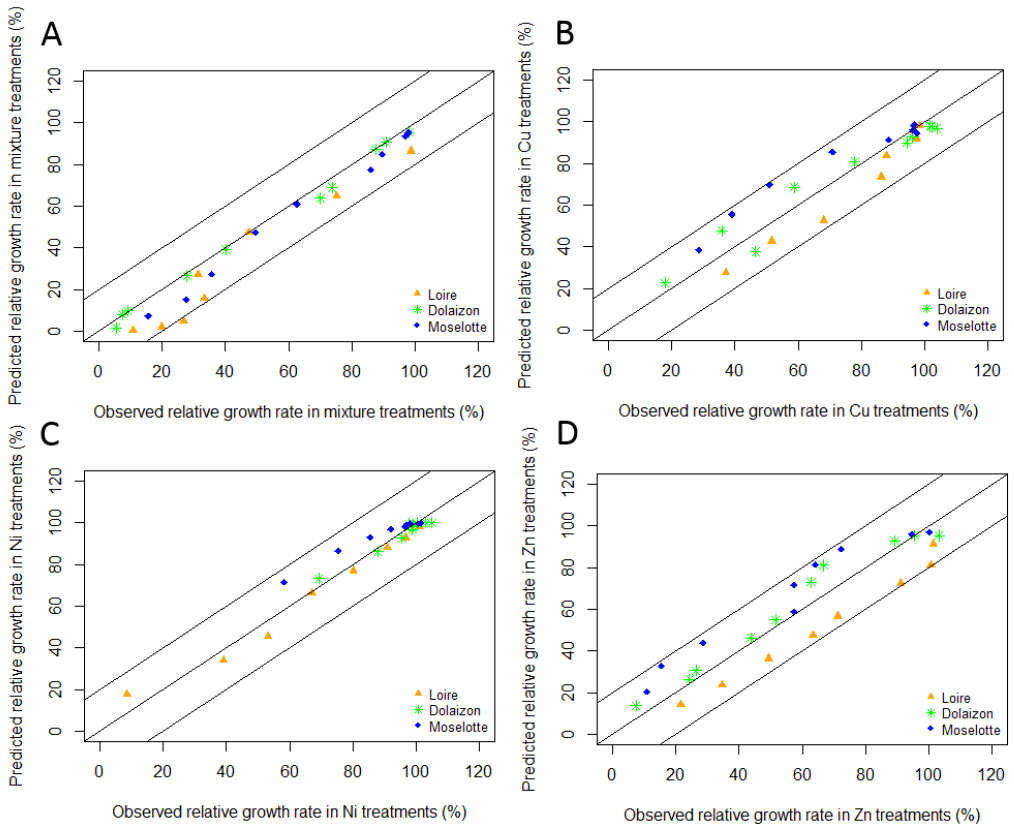

Figure 3.3 Metal mixture bioavailability model predicted versus observed relative growth rate of *Pseudokirchneriella subcapitata* in the Cu-Ni-Zn metal mixture treatments (A), individual Cu treatments (B), individual Ni treatments (C) and individual Zn treatments (D) in the different test waters (Loire (▲), Dolaizon (✳) and Moselotte (◆)). The full line indicates a perfect match between observed and predicted data. The dashed line indicates a difference of 20% between the observed and predicted data.

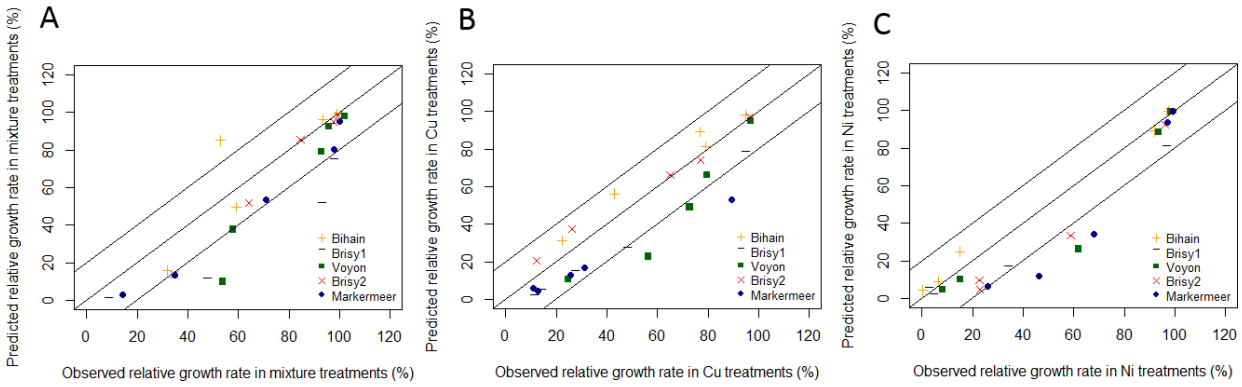

Figure 3.4 Metal mixture bioavailability model predicted versus observed relative growth rate of *Pseudokirchneriella subcapitata* in the Cu-Ni metal mixture treatments (A), individual Cu treatments (B) and individual Ni treatments (C) in the different test waters (Bihain (+), Brisy1 (-), Voyon (■), Brisy2 (X) and Markermeer (●)). The full line indicates a perfect match between observed and predicted data. The dashed line indicates a difference of 20% between the observed and predicted data.

It is well known that the physico-chemistry of a water body influences the bioavailability and thus toxicity of individual metals, which lead to the development of Biotic Ligand Models for numerous individual metals and species (Deleebeeck et al. 2009, De Schamphelaere & Janssen 2005, De Schamphelaere & Janssen 2006). It is therefore apparent that mixture toxicity is also influenced by water chemistry, a factor that has been demonstrated and implemented into mixture models (Tipping & Lofts 2015; Santore & Ryan 2015; Iwasaki et al. 2015; Nys et al. 2017a). Although our results, i.e. that the interactive response of a Cu-Ni-Zn mixture to *P.subcapitata* changes with water chemistry, cannot be confirmed or contradicted by other studies on algae, studies on other species have reported similar results. In these studies (Naddy et al. 2015; Versieren et al. 2014; Nys et al. 2017a) the mixture interaction shifted between soft water and hard water. Nys et al. (2017b) explained this for *H. vulgare* and *C. dubia* by competition reactions at the receptor site. These authors demonstrated that antagonisms among metal ions relative to the CA model decreased as the concentrations of competing ions increased. Hence, in a low cationic competition situations (e.g. a soft water) there is more antagonism between metals than in high cationic competition situations (e.g. a hard water). When examining Table 3. 2, we can observe that the Moselotte water has low concentrations of Mg, Ca and K, and is therefore a low cationic competition situation, which could explain the antagonism observed in this water. However, concentrations of these competitive cations are also low in other waters (e.g. the Loire) in which antagonism was not observed, which shows that a low cationic competition situation can not be the only reason for the observed antagonism in the Moselotte water. Overall, the present study illustrates that the interactive toxic effects of mixtures of Cu-Ni-Zn to *P.subcapitata* may vary under different physico-chemical conditions, although we emphasize that this is due to one exception found for the Moselotte water. However, our first hypothesis, that the type of interaction for the ternary mixture is independent of water chemistry, is therefore rejected. In addition, our second hypothesis, that the ternary mixture would act antagonistically relative to CA on algal growth, independent of water chemistry, is also rejected.

The binary Cu-Ni mixture acted non-interactively on algal growth relative to both the CA and IA reference models (Figure 3.1 and Appendix B Table B4.4). These results are different from results of other studies

on freshwater algae. Nagai et al. (2014) showed for *N. pelliculosa* that the binary Cu-Ni mixture acted antagonistically on algal growth. Flouty and Khalaf (2015) also found an inhibitory effect of Cu on the uptake for Ni by *C. reinhardtii*. Also in the higher plant, *Sesbania drummondii*, Cu uptake in the shoots was decreased in the presence of Ni (Israr et al. 2011) which was possibley explained by the competition between metal transport systems during uptake process. Our results for *P.subcapitata* however, show for 5 different waters, that the mixture of Cu and Ni acts non-interactively on *P.subcapitata* growth. The null hypothesis of our first research question is therefore confirmed, as the type of interactive effect between Cu-Ni to *P.subcapitata* growth is independent of water chemistry. However, the hypothesis of our second research question is not confirmed, as the binary mixture act non-interactively on *P.subcapitata* growth.

For both the ternary and binary mixture, the conclusion about the interactive effect (i.e. no interaction or antagonism) did not change when predictions were based either on dissolved metal concentrations or on free ion activities (Table 3.5). Thus, accounting for competition between the metals for DOC does not change the conclusion about toxicological interactions between the metals in the mixture.

To answer our third research question, whether the CA or IA model is the best model to predict mixture toxicity, the Akaike Information Criterion (AIC) and the lower root-mean-squared-error (RMSE) values can be used as an indicator of model fit. AICs and RMSEs of both reference models were relatively similar between both models in most cases (see Appendix B Table B4.3-5). Therefore, based on these indicators, there is no one “best” model. This can also be observed in Figure 3.1, which shows that the predictions of CA and IA are very close to each other. Our findings also suggest that, although the predictions made by the CA model were in general more conservative than the predictions of the IA model, both models are accurate for estimating the toxicity of ternary Cu-Ni-Zn and binary Cu-Ni mixtures to *P.subcapitata*.

Development and validation of the MMBM

Nys et al (2017a) developed a MMBM that combines the single metal bioavailability models with the IA model because these authors observed that Ni-Zn-Pb mixture toxicity to *C. dubia* showed no interaction relative to the IA model and was most accurately predicted with the IA model. Since we also found no interaction in most waters relative to the IA model and that the IA model was accurate in predicting Cu-Ni-Zn toxicity to *P.subcapitata*, a MMBM was developed in the present study that combines the IA model with the chronic *P.subcapitata* bioavailability models for the individual metals (De Schamphelaere & Janssen 2006, Deleebeeck et al 2009, De Schamphelaere & Janssen 2005). The MMBM model is structured in a way that it predicts toxicity expressed as RGR of *P.subcapitata*. As was highlighted by Nys et al (2017a), this type of model accounts for possible bioavailability effects, as the individual BLMs that form the basis of the MMBM have been validated in waters with different water chemistries (De Schamphelaere & Janssen 2006, Deleebeeck et al 2009, De Schamphelaere & Janssen 2005). This is in contrast to other models that predict metal mixtures (Versieren et al 2014, Tipping and Lofts 2015, Santore and Ryan 2015) and that do not take into account any bioavailability effects.

For the ternary mixture, 96% of the mixture treatments was predicted with less than 20% error. This is at least as accurate as the MMBM developed by Nys et al (2017a) for C. dubia, for which 85% of the

Zn-Ni-Pb mixture treatments were predicted with less than 20% error. In addition, in spite of the significant mixture interaction that was found for the Moselotte water, the MMBM showed a good predictive ability for this test water (Figure 3.3). The root mean square error for the mixture treatments was similar than for the individual metal treatments (i.e. 9 vs 9, 5 and 11), which indicates that the chronic toxicity of the ternary Cu-Ni-Zn mixture predicted with the MMBM calibrated on the single metal toxicities is at least equally as accurate as the toxicity observed in the individual metal treatments. This indicates that the MMBM can be used to predict Cu-Ni-Zn toxicity to *P.subcapitata* under different water characteristics. However, a bias in the model predictions can be observed (Figure 3.3). Indeed, a tendency to overestimate mixture toxicity effects is observed for all waters. This indicates that the MMBM predicted greater toxicity than was actually observed, which implies that the MMBM is a conservative model for ternary Cu-Ni-Zn mixtures. This observation was also seen for a water tested by Nys et al (2017a). A possible explanation for the overestimation of mixture toxicity effects that was given by these authors was that the assumption that free metal ions do not compete for binding at the biotic ligand sites may not be correct. Our results therefore confirm the observations of Nys et al (2017a), that in waters with a low cationic competitions situations, e.g. high pH (our Dolaizon water) or low Ca concentration (our Loire and Moselotte waters), there is theoretically more chance for metal-metal competition which is not incorporated into the MMBM.

For the binary mixture, 72% of the mixture treatments was predicted with less than 20% error (Figure 3.4). The root mean square error for the binary Cu-Ni mixture treatments was approximately the same as for the individual metal treatments (i.e. 19 vs 15 and 15), which indicates that the chronic toxicity of the binary Cu-Ni mixture predicted with the MMBM calibrated on the single metal toxicities is approximately as accurate as the toxicity predicted for the individual metal treatments. This indicates that the MMBM can be used to predict Cu-Ni toxicity to *P.subcapitata* under different water characteristics.

3.5 Conclusion

The present study investigated the effects of ternary Cu-Ni-Zn and binary Cu-Ni mixtures on the growth of the freshwater algae *P.subcapitata* across various natural waters that show diverse water-chemistry characteristics, using equitoxic ray designs. Our modelling analysis showed that the toxicity of the ternary mixture acts non-interactively on algal growth, except in one water in which the mixture acted antagonistically. We suggest that a low cationic competition situation in the latter water could be the reason for the antagonistic interactions between the metals in this water. On the other hand, the binary mixture acted non-interactively on algal growth in 5 waters with different water chemistry. We showed that both the CA and IA model can serve as a protective scenario for toxicity of ternary Cu-Ni-Zn and binary Cu-Ni mixtures to *P.subcapitata*. In addition, although we found that both reference models predict ternary Cu-Ni-Zn and binary Cu-Ni mixture toxicity equally well, we developed a MMBM based on the IA model. We found that the MMBM can be used to accurately predict Cu-Ni-Zn and Cu-Ni toxicity to *P.subcapitata* under different water characteristics. The present study increased the knowledge on chronic metal mixture effects for freshwater microalgae across various waters that show diverse water

chemistry characteristics, which might help advance the integration of metal mixture toxicity into metal risk assessment frameworks (Van Genderen et al 2015).

Four

THE EFFECTS OF A CU-NI-ZN MIXTURE ON THE STRUCTURE, DIVERSITY AND FUNCTIONING OF A FRESHWATER PLANKTONIC COMMUNITY

Redrafted from:

Van Regenmortel T, Van de Perre D, Janssen C, De Schamphelaere KAC. The effects of a Cu-Ni-Zn mixture on the structure, diversity and function of a freshwater planktonic community Submitted to Environmental Toxicology and Chemistry.

4. The effects of a Cu-Ni-Zn mixture on the structure, diversity and functioning of a freshwater planktonic community

4.1. Introduction

It has been recognized that ecological risk assessment should be performed by taking into account the toxic effects of mixtures of substances, as organisms in the aquatic environment are exposed to chemical mixtures rather than isolated substances. Although few countries already consider mixture effects in their risk assessment frameworks (A&NZ 2000), regulatory risk assessment is still primarily performed on a substance-by-substance basis. While considerable research has been performed to assess the influence of mixtures on single species, still little is known on how mixtures influence community structure and functioning. Most data concerning mixture effects on communities are found for pesticides. A review of recent literature concerning exposure of species in aquatic microcosms indicates that most pesticide mixtures act additively on community structure and functioning (Verbruggen and Van den Brink 2010). Synergisms are only found in exceptional cases, but deviations from additivity are small and only found in short-term exposures toxicity (Laetz et al. 2009, Anderson and Lydy 2002). For metals, some field studies and experimental microcosm studies have been performed (e.g. Stockdale et al. 2010, Richardson and Kiffney 2000, Clements et al. 2013, Mebane et al. 2017, Clement 2004). Richardson and Kiffney (2000) did not find significant decreases in benthos densities when exposed to mixtures of Cu, Zn, Mn and Pb in a low-conductivity stream. Clements et al. (2013) and Mebane et al. (2017) on the other hand found in their community level microcosm experiments that effect concentrations for aquatic insects were several orders of magnitude lower than those obtained with single species tests. In addition, Mebane et al. (2017) found that the Cd-Zn mixture acted antagonistically relative to the Independent Action (IA) model. Clements (2004) observed for a macroinvertebrate community that functional community endpoints (e.g. community respiration) were more sensitive to metal mixtures than structural endpoints (e.g. abundance). Although empirical knowledge on community-level effects due to metals is increasing, regulatory risk assessment of metals still mostly relies on methods to extrapolate from single-species to communities, such as the species-sensitivity distribution (SSD) approach (De Zwart and Posthuma 2005, ECI 2008, Van Sprang et al. 2009, Van Sprang et al. 2016). This approach is used to calculate a potentially affected fraction (PAF) of species as a proxy of community-level effect. This is done based on toxicity data derived from single species tests and therefore the approach ignores species interactions (Forbes and Calow 2002, Gregorio et al. 2013). It is generally assumed that as long as the majority of species (i.e. 95%) experiences no adverse effect due to a single substance (i.e. PAF < 5%), no significant long-term structural or functional effects on the community are expected to occur (De Zwart and Posthuma 2005, Gregorio et al. 2013, Van Regenmortel et al. 2017). Single-metal microcosm experiments (Schäfers 2001, Hommen et al. 2016, Van de Perre et al. 2016) support the assumption of protectiveness of this threshold (PAF ≤ 5%). This threshold can also theoretically be applied for exposures to multiple contaminants, i.e. no significant effects on the community level are expected to occur as long as the multisubstance PAF (msPAF) is below 5% (De Zwart and Posthuma 2005). It is, however, not known whether this threshold protects against mixed metal contamination. A recent study by Van Regenmortel et al. (2017) demonstrated that between 0% and 52% of target waters samples from 4 monitoring

databases are predicted to be at risk due to single and mixed metal contamination (i.e. (ms)PAF > 5%) using a simple and conservative approach to calculate an msPAF, i.e. their so-called CA_{SSD} approach. In this approach, which is a classic toxic unit approach, the Concentration Addition method is applied directly to the SSD. One important limitation of this in-silico method, which was already mentioned by Van Regenmortel et al. (2017), is that the indirect effects of the mixture on the community (through ecological interactions between species) are not accounted for. Therefore the degree of conservatism of the CA_{SSD} method compared with community-level metal mixture effects needs to be investigated. A literature search performed prior to the design and execution of this study showed that no studies were appropriate for this investigation (e.g. Stockdale et al. 2010, Richardson and Kiffney 2000, Clements et al. 2013, Clements 2004, Hickey and Golding 2002). One reason is the lack of Dissolved Organic Carbon (DOC) measurements, an important variable influencing metal toxicity and needed to accurately calculate metal bioavailability. Therefore, a multispecies microcosm experiment was performed in the present study. In this experiment, a naturally occurring freshwater planktonic community was exposed to Cu, Ni and Zn, as a mixture, for 8 weeks. We aimed to answer two main research questions. First, what are the direct and indirect effects of the metal mixture on the community? When examining the direct effects of the single metals by inspecting the species sensitivity distributions (SSDs) of Cu, Ni and Zn we can observe that for Ni and Cu zooplankton species are more sensitive than phytoplankton species while for Zn the opposite is observed (ECI 2008, Van Sprang et al. 2009, DEPA 2008). We therefore hypothesize that both organism groups (when present together in a community) will be targeted directly by the Cu-Ni-Zn mixture. Verbruggen and Van den Brink (2010) demonstrated for pesticide mixtures that significant synergisms at the community level are found in cases where different pesticides in the mixture simultaneously target different parts of the foodweb. We can therefore expect, by analogy, that the Cu-Ni-Zn exposure might result in synergistic effects on the community. This might, in contrast to what is expected for single substances, also lead to effects at or below a msPAF value of 0.05.

Second, when using the classic toxic unit approach, i.e. the CA_{SSD} method: as of which msPAF value are effects observed on (A) structural community-level endpoints (species groups abundances, community composition, species diversity and species richness) and on (B) community functioning measured by indirect physico-chemical proxy's (Δ dissolved oxygen (ΔDO) as proxy for community respiration (Van de Perre et al. 2016, Downing and Leibold 2002), ΔpH as proxy for phytoplankton metabolism (Kayambo et al. 2002) and change in DOC as proxy for the microbial loop and pelagic food web interactions (Jumars et al; 1989, Brönmark and Hansson 2005, Wetzel 2003)? Based on microcosm studies on single metals that showed no effects on the community at a PAF value ≤ 0.05 (Schäfers 2001, Hommen et al. 2016, Van de Perre et al. 2016), we expected that no effects due to the mixture would be found at an msPAF value ≤ 0.05. This hypothesis is contrasting to the hypothesis related to our first research question. These two alternative hypotheses are thus the possible outcomes of our experiment.

In addition, we expected that the functional community endpoints would be affected at lower concentrations and earlier in the exposure period compared to the structural community endpoints as has been observed in other cosm studies (Clements 2004, Van de Perre et al. 2016).

4.2. Material and methods

Experimental approach

Community-level effects of Cu, Ni and Zn were investigated by performing a microcosm experiment that lasted 8 weeks. The experimental design included the following treatments: a control treatment (no metals added) and a mixture ray (6 treatments) with metal concentration ratio's based on the average measured dissolved metal concentrations found in a European river basin for which high potential risk due to metal contamination was predicted (i.e. the Dommel; Zn:Ni 2.6 and Zn:Cu 12.6; Van Regenmortel et al. (2017/Chapter 2)). The control treatments received 4 replicates, the mixture treatments received 3 replicates, which gave a total of 22 cosms. Microcosm exposures were performed in plastic aquaria of 10 L (31x18x16 LxWxH; rounded edges; Flamingo) filled with a sediment layer of approximately 2 cm and 5L of water. Both the sediment and the water were collected from an uncontaminated mesotrophic pond (Sinderhoeve Experimental Station, Renkum, The Netherlands) in September 2015. Previous work in which water from this site was use was successful (Van de Perre et al. 2016). Large particulate organic matter and organisms were removed manually from the sediment, after which the sediment was sieved through 5 mm before it was placed in the microcosms. The microcosms were filled with water and were installed randomly in a water bath (16-18°C) for temperature regulation under a 12:12-h light:dark cycle (55 $\mu mol.m^{-2}.s^{-1}$) and were seeded with additional zooplankton that was collected from uncontaminated ditches from the Sinderhoeve experimental site. Prior to zooplankton seeding all macroinvertebrates were removed manually. Three snails smaller than 1 cm (*Lymnaea stagnalis*) were added to every cosm to prevent periphyton growth. A pre-treatment period of 4 weeks was run prior to the actual start of the experiment. During this period (and also during the experiment), nutrients (NH_4NO_3, 1 mg N/L and KH_2P0_4 0.01 mg P/L) were added twice a week to stimulate phytoplankton growth. In addition, in the pre-treatment period, the water from all the microcosms was mixed once a week to guarantee similar start conditions in all test systems (Brock et al. 2014; Van de Perre et al. 2016). This was done by removing the water from all microcosms to just above the sediment layer and mixing it in a central container, after which the water was randomly redistributed over the 40 cosms. Because of the mixing, little variation in the physico-chemistry of the water at the start of the experiment was found (Appendix C1), which ensures that all microcosms started with the same metal bioavailability (ECI 2008, DEPI 2008, Van Sprang et al. 2009). To prevent the development of a bacterial biofilm on the surface of the water, a tubing system was installed above the microcosms that provided each aquarium with a compressed air flow. Macrophytes were manually removed from the microcosms when they became visible. Water loss due to evaporation was supplemented with demineralized water once a week. Water loss due to sampling during the experiment was supplemented with filtered Sinderhoeve water.

To obtain test concentrations, chronic toxicity data for Cu, Ni and Zn were normalized using chronic bioavailability models as was explained in Van Regenmortel et al. (2017a/Chapter 2). Normalization was done based on the average measured water chemistry variables of all 22 microcosms the day before the start of the experiment (Table 4.1). A log-normal SSD was fitted to the BLM-normalized toxicity data for invertebrates, fish and algae, from which the HC5 for every metal were derived. This is in accordance with the European risk assessments for Cu (ECI 2008), Ni (DEPI 2008) and Zn (SCHER 2007), for which the calculation of bioavailability based PNECs also include data for fish, invertebrates and algae.

Table 4.1. Overview of the average measured water chemistry variables of the microcosms the day before the start of the experiment, used for bioavailability normalization.

pH	DOC (mg/L)	Ca (mg/L)	Mg (mg/L)	Na (mg/L)	K (mg/L)	SO4 (mg/L)	Cl (mg/L)	DIC (mg/L)	T (°C)
8.07	13.71	12.03	1.63	4.70	0.31	13.05	12.52	4.16	16.50

For the mixture ray, specific concentrations were chosen (with concentration ratio's for Zn:Ni = 2.6 and Zn:Cu = 12.6) so that the msPAF calculated using the CA_{SSD} method showed a range in values both below and above the 0.05 cut-off value (i.e. nominal msPAF values: 0.01, 0.05, 0.26, 0.48, 0.68, 0.91), to be able to answer our second research question. The CA_{SSD} method was selected for this purpose because it has been shown to be the most simple and conservative method (Van Regenmortel et al. 2017/Chapter 2). An overview of the nominal (ms)PAF values and metal concentrations for all treatments is given in Table 4.2.

Table 4.2. Nominal (multisubstance) potentially affected fraction (msPAF) and copper, nickel and zinc concentrations of the mixture treatments.

Treatment	(ms)PAF	Cu (µg/L)	Ni (µg/L)	Zn (µg/L)
Mixture 1	0.01	2	9	24
Mixture 2	0.05	3	16	41
Mixture 3	0.26	7	34	89
Mixture 4	0.48	11	53	140
Mixture 5	0.68	17	81	212
Mixture 6	0.91	32	154	404

Metal addition and chemical analyses

Metals were applied to every treatment by distributing the correct volume of stock solution (between 0.2 mL and 50 mL) evenly over the water surface of the microcosms. The stock solutions of the individual metals contained 9.7 mg/L Cu, 9.6 mg/L Ni and 4.4 mg/L Zn and were added as solutions of $CuCl_2.6H_2O$, $NiCl_2.6H_2O$ or $ZnCl_2$. The metals were stirred into the water as a result of the compressed air flow above the water column. Metal concentrations were adjusted daily by additional spiking, to compensate for losses from the water column. Metals were added to the concentration 15% above the nominal concentrations in order to maintain an average metal concentration equal to the nominal concentration. Samples for dissolved metals were taken twice a day to monitor the metal concentrations. Samples were taken just before the dosing of the metals and between 15 min and 35 min after the dosing. Sampling consisted of taking a 10-mL filtered sample (filtered through 0.45µm; Acrodisc, PALL Life Sciences; after discarding 5mL of water to clean the filter) per microcosm after gentle stirring of the water using a syringe, approximately 5 cm under the water surface. Total metal concentrations were measured twice a week. Samples for metal analysis were acidified to 0.14 mol/L HNO_3 (Normatom quality, VWR Prolabo). All Zn concentrations and all Cu and Ni concentrations above 10 µg/L were measured using inductively coupled plasma atomic emission spectroscopy (ICP-OES; ICAP 7200 DUO; ThermoFisher Scientific; limit of quantification 2 µg Zn/L, 4 µg Ni/L, 5 µg Cu/L; method detection limit 0.5 µg Zn/L, 1.2 µg Ni/L and 2 µg Cu/L). Cu and Ni concentrations below 10 µg/L were measured using graphite furnace atomic absorption spectrophotometry (GFAAS Furnace Autosampler, Thermo Fisher

Scientific Inc.; reference material TM24.3; limit of quantification, 2.5 µg Cu/L and 1 µg Ni/L; method detection limit, 0.75 µg Cu/L and 0.30 µg Ni/L). Samples for cations and anions were taken twice a week and once every two weeks, respectively. Cations were measured using ICP-OES while anions were measured using ion chromatography (Aquamate, Thermo Electron Corporation; Chloride: Merck, Spectroquant 1.14897.001; Sulphate: Merck, Spectroquant 1.14548.001). Samples for measurements of dissolved and total organic and inorganic carbon were taken once a week and were measured with a Total Organic Carbon analyser following the NPOC method (TOC-5000, Shimadzu, Duisburg, Germany; Limit of Quantification 1.5 mg DOC/L; Method Detection Limit 0.5 mg DOC/L). Samples for the measurements of total and dissolved ammonium, nitrate and nitrite were taken every two weeks and were measured using ion chromatography. The pH, conductivity, temperature and oxygen content of each microcosm was measured before the start and the end of the photoperiod and this twice a week. The pH and conductivity were measured using a pH glass electrode (826 pH mobile, Metrohm) and a conductivity meter (WTW cond 315i), respectively. The temperature and oxygen content were measured using an oximeter (WTW oxi 330i).

Zooplankton and phytoplankton

Samples for zooplankton and phytoplankton identification were taken as explained in Van de Perre et al. (2016). Samples were taken each week from every microcosm, starting the day before the start of the first metal addition. Water was taken randomly from several locations (approximately 7) in the microcosm using a transparent tube (3.3 cm diameter) that was lowered to the sediment surface making sure not to disturb it, until a total volume of 600 mL was collected (Van de Perre et al. 2016). The water was first filtered through a plankton net (mesh width 55 µm) for the collection of zooplankton and subsequently, the water was filtered through another plankton net (mesh width 20 µm) for the collection of phytoplankton. Afterwards, the filtered water was returned to the microcosms. Both zooplankton and phytoplankton samples were preserved with lugol (0.3%). Plankton samples were analysed for week 0, 2, 4, 6 and 8. The identification of zooplankton and phytoplankton was done using an inverted microscope. Macro- and microzooplankton individuals present in the zooplankton samples were identified to the lowest practical taxonomic level and counted. Copepoda were classified as Cyclopoida or Calanoida and counted. The phytoplankton and protozoa species composition in the phytoplankton samples was identified to the lowest practical taxonomic level by counting and identifying at least 300 individual cells of a subsample of 30 mL. The abundances per species were afterwards recalculated to numbers per liter. Colonies of colony forming algae were counted as single individuals.

Data analysis

The following effects were distinguished. (1) individual species abundance effects (univariate analysis), (2) structural community-level effects including (2a) species groups abundance effects (univariate analysis), (2b) community composition effects (multivariate analysis) and (2c) species diversity and richness, and (3) the functional community-level effects measured by indirect physico-chemical proxies including (3a) the $\Delta\mathrm{DO} = DO_{evening\ day\ x}$ - $DO_{morning\ day\ x+1}$ as proxy for the community respiration (Downing and Leibold 2002, Van de Perre et al. 2016), (3b) the $\Delta\mathrm{pH} = pH_{evening\ day\ x} - pH_{morning\ day\ x+1}$, a variable that is influenced by both the increase of pH during the day due to the

uptake of CO_2 via photosynthesis and by the decrease of pH during the night as a result of an increase of CO_2 concentration due to bacteria and algae respiration and decomposition (Kayombo et al. 2002) and is therefore regarded as proxy for the phytoplankton and bacteria abundance (Kayambo et al. 2002) and (3c) the change in DOC concentration, a variable that is regarded as proxy for the microbial loop of the community. In this loop, the dissolved organic matter (DOM) and DOC excreted from organisms (e.g. phytoplankton and zooplankton) is consumed by bacteria and in turn, these bacteria are consumed by protozoa and zooplankton (Jumars et al. 1989).

For the analyses of the individual species abundance effects (1), the species groups abundance effects (2a) and the community composition effects (2b), the zooplankton data were ln(1.2x+1)-transformed and the phytoplankton data were ln(0.001x+1)-transformed (where x is the abundance value) to approximate a log-normal distribution of the data by down-weighting the values of species showing high abundances (see Van Den Brink et al. 2000 for rationale). For the species groups abundance effects, this transformation was done after the summation of the absolute abundances of the taxa within each group. The community composition effects were evaluated by performing multivariate analyses with the principal response curve method (Van den Brink and Ter Braak 1999), using CANOCO 4.5 (Ter Braak & Smilauer 2002). This method is based on redundancy analysis ordinations and shows the changes in community structure in the metal treatments over time, relative to a control treatment. Accompanying the PRC curves are the weights (b_k) of the different species. A positive b_k indicates that the abundance of a species goes in the same direction as that of the graph, a negative bk indicates that the abundance of the species goes in the opposite direction as that of the graph. The statistical significance of the metal application on community composition for each sampling day was tested using Monte Carlo permutation tests in the ordination axis, using the ln-transformed doses as an explanatory variable. The latter was done to fit the intrinsically sigmoid dose-response curves to the linear response model in the RDA as closely as possible (Van den Brink et al. 1996). In addition, the treatments that were significantly different from the controls were determined to derive a community composition no observed effect concentration (NOEC) for that sampling day. This $NOEC_{composisiton}$ was determined by performing univariate analyses with the Williams tests in the Community Analysis computer program, version 4.3.14 (Williams 1972, Hommen et al. 1994), performed on the sample scores resulting from a principal component analysis. This test assumes an increasing effect (either adverse or beneficial) with increasing dose. The individual species abundance effects and species groups abundance effects were also evaluated by performing univariate analyses with the Williams test which resulted in $NOEC_{abundance}$. Lowest observed effect concentrations ($LOEC_{composisiton}$ and $LOEC_{abundance}$) were considered as consistent, when statistically significant deviations in the same direction (increase or decrease) were observed for at least 2 successive sampling days (Van den Brink et al. 2000). Consistent NOECs were defined as the concentration immediately below the consistent LOEC.

The species diversity (2c) in each treatment at each time point was calculated using the Shannon index *H* (Equation 4.1) (Shannon and Weaver 1949) while the species richness was determined as the number of species.

$$H = \sum_{i=1}^{N} p_i \cdot ln\, p_i \qquad \text{(Eq. 4.1)}$$

where p_i is the relative abundance of species *i* and *N* is the total number of species. The treatments for which the diversity index and species richness were significantly different from the controls were determined using Williams tests. In addition, a consistent $LOEC_{diversity}$ and $LOEC_{richness}$ were determined. For the proxies for functional community-level effects (3), the Williams test was applied to determine from which treatment a significant difference was observed and to determine consistent $LOEC_{\Delta DO}$, $LOEC_{\Delta pH}$ and $LOEC_{DOC}$.

Examining from which msPAF value onward an effect occurs

Our second research question was to examine from which msPAF value onward effects on the community structure (species groups abundance, community composition, species diversity and richness) and proxies for community functioning (ΔDO, ΔpH, DOC) are observed. This was done by comparing the "initial msPAF value" to the consistent lowest observed effect concentration (LOEC) values for these endpoints and all treatments and determining at which msPAF value this consistent LOEC occurred. As such, we were also able to examine whether an msPAF value of 0.05 is protective for an aquatic community exposed to a mixture of Cu, Ni and Zn. The initial msPAF values were calculated based on the measured water chemistry (Table 4.1) and measured metal concentrations of every microcosm at the start of the experiment.

4.3. Results

General overview

In the controls, the average dissolved (± standard deviation) Cu, Ni and Zn concentration was 6.1 ± 1.0 µg/L, 3.0 ± 0.6 µg/L and 3.7 ± 1.6 µg/L, respectively. The average metal concentrations in the mixture treatments were within 10% of the target concentrations for Ni and Zn (Table 4.3, Figure S2). For Cu, the three highest environmental ratio treatments were within 10% of the target concentrations. For the three lowest environmental ratio treatments, the measured dissolved Cu concentration was higher than the target concentration. This is due to the fact that the Cu concentration in the control treatment was already higher than that of the two lowest environmental ratio treatments (Table 4.3). This implies that when evaluating effects relative to the control, the two lowest mixture treatments should rather be considered Ni-Zn mixtures than Cu-Ni-Zn mixtures.

Table 4.3. Average (± standard deviation) measured dissolved Cu, Ni and Zn concentration in the different treatments.

Treatment	Dissolved Cu µg/L	Dissolved Ni µg/L	Dissolved Zn µg/L
Control	6.1 ± 1.0	3.0 ± 0.6	3.7 ± 1.6
Mixture 1	5.6 ± 1.0	9.7 ± 1.0	22.5 ± 4.7
Mixture 2	4.8 ± 0.9	16.4 ± 1.7	38.9 ± 7.2
Mixture 3	8.6 ± 1.3	34.5 ± 4.0	80.1 ± 17.7
Mixture 4	12.0 ± 1.9	54.6 ± 6.7	135.0 ± 27.3
Mixture 5	18.0 ± 2.1	82.7 ± 10.9	206.7 ± 38.6
Mixture 6	32.9 ± 4.0	157.4 ± 21.9	397.3 ± 77.7

Average measured water chemistry for the different microcosms is reported in Table 4.4. A full overview of the water chemistry in all microcosm replicates for the different sampling dates can be found in the supplementary material (see the online repository at mda.vliz.be).

Individual species and species groups

Zooplankton community

The zooplankton community consisted of 42 different zooplankton taxa, of which 14 belonged to the macrozooplankton and 28 belonged to the microzooplankton. The most abundant cladocerans in the controls were *Daphnia longispina, Simocephalus vetulus* and *Alonella nana*. The copepods were dominated by *Cyclopoida* and nauplii. Rotifers present in the control treatments were predominantly *Lecane* group *luna*, *Lecane* group *lunaris* and the *Lepadella patella*. The zooplankton species abundances of all microcosms per sampling date can be found in the supplementary material (see the online repository at mda.vliz.be).

Consistent $LOEC_{abundance}$ values could be calculated for 13 out of 42 zooplankton taxa. All other species showed unbounded $LOEC_{abundance}$ values (i.e. $LOEC_{abundance}$ ≥ Mixture 6). All consistent $LOEC_{abundance}$ values are listed in Table 4.5. Figure .4.1 shows the abundance values of the different species groups (e.g. Cladocera, Rotifera) listed in Table 4.5. In general, the abundance of cladocerans as a group was not significantly different from the control (Figure 4.1A). Some cladoceran species (i.e.. *D. longispina* and *A. harpae*) were only significantly affected at the highest mixture treatment Mixture 6) (Table 4.5). Rotifers as a group were already significantly affected at the Mixture 4 treatment (Figure 4.1B). The lowest consistent NOEC (< Mixture 1) was calculated for the rotifers *Trichocerca* group *similis* and *Dissotrocha* sp. Copepods as a group and the nauplli of the copepods were significantly affected by the Mixture 5 and 6 treatments (Figure 4.1C).

Phytoplankton community

In total, 55 phytoplankton taxa were identified, of which 23 belonged to the Chlorophyta and 9 belonged to the Cyanobacteria. The control treatments were dominated by Cyanobacteria (e.g. *Oscillatria* sp. 1, *Pseudoanabaenoideae* sp. and *Anabaena* sp.), Cryptophtya (Flagellate sp. 3) and Chlorophyta (*Chlorococcales* sp., *Scendesmus* sp. 2 and colony sp. 1). The phytoplankton species abundances of all microcosms per sampling date can be found in the supplementary material (see the online repository at mda.vliz.be).

Consistent $LOEC_{abundance}$ values could be calculated for 12 out of 55 phytoplankton taxa. All other species showed unbounded $LOEC_{abundance}$ values (i.e. $LOEC_{abundance}$ ≥ Mixture 6). All consistent $LOEC_{abundance}$ values are listed in Table 4.5. Figure 4.2 shows the abundance values of the different groups (e.g. Cyanobacteria, Chlorophyta) listed in Table 4.5. In general, we can observe that the abundance of the Chlorophyta group was not significantly affected (Figure 4.1E). The abundance of the Cyanobacteria as a group was negatively affected from the first mixture treatment upwards (Figure 4.1D). The abundance of the Chrysophyta, Charophyta, Diatoms and Cryptophyta as groups were all positively affected (Figure 1F-I), those of the Chrysophyta, Cryptophyta and Diatoms from the lowest tested concentration upwards (Table 4.5).

Table 4.4. Measured[a] water chemistry in the microcosms

Treatment	pH	DOC (mg/L)	Ca (mg/L)	Mg (mg/L)	Na (mg/L)	K (mg/L)	SO4 (mg/L)	Cl (mg/L)	DIC (mg/L)	T °C
Control	8.3 ± 0.9	15.7 ± 1.8	13.7 ± 1.7	1.9 ± 0.1	5.3 ± 0.3	0.2 ± 0.1	6 ± 1.2	7.3 ± 1.1	5.9 ± 0.3	16.7 ± 0.5
Mixture 1	7.9 ± 0.7	14.1 ± 1.5	12.2 ± 1.0	1.7 ± 0.2	4.9 ± 0.5	0.3 ± 0.1	5.5 ± 1.2	6.2 ± 0.7	3.4 ± 0.3	16.6 ± 0.2
Mixture 2	7.8 ± 0.5	13.4 ± 1.2	11.7 ± 1.0	1.7 ± 0.4	4.9 ± 0.5	0.3 ± 0.1	5.6 ± 1.1	6.5 ± 1.1	4.1 ± 0.1	16.8 ± 0.1
Mixture 3	7.8 ± 0.5	13.6 ± 1.1	19.9 ± 4.5	2.4 ± 0.4	5.2 ± 0.6	0.4 ± 0.1	6.1 ± 1.3	7.4 ± 0.7	9.1 ± 0.8	16.8 ± 0.1
Mixture 4	7.5 ± 0.3	12.4 ± 1.1	13.6 ± 1.5	2.0 ± 0.3	4.9 ± 0.6	0.4 ± 0.1	6.2 ± 0.9	7.3 ± 0.7	3.6 ± 0.5	16.8 ± 0.2
Mixture 5	7.5 ± 0.2	12.4 ± 1.0	13.3 ± 1.0	2.0 ± 0.2	4.9 ± 0.5	0.4 ± 0.1	6.1 ± 1.4	8.3 ± 1.2	3.1 ± 0.1	16.7 ± 0.2
Mixture 6	7.4 ± 0.3	11.3 ± 0.8	15.9 ± 1.3	2.2 ± 0.3	5.0 ± 0.6	0.4 ± 0.1	6.3 ± 1.3	9.6 ± 1.6	4.0 ± 0.3	16.6 ± 0.2

[a] Average values ± standard deviations are reported
DOC = Dissolved Organic Carbon; DIC = Dissolved Inorganic Carbon

When examining the consistent $NOEC_{abundance}$ values, we can observe that the abundance of two Cyanobacteria (*Pseudanabaenoideae* sp. and *Aphanothece* sp.) were positively affected by the two highest mixture treatments whereas the Cyanobacteria *Oscillatoria* sp. 1 was adversely affected by Mixture 1 and upwards. The abundance of most Chlorophyta were positively affected by the highest mixture treatment (Table 4.5) except for the unknown Chlorophyta colony that was negatively affected at the Mixture 5 and 6 treatments. The Chrysophyta species *Chrysococcus* sp. and the single cell diatoms were both positively affected from the lowest tested mixture concentration (Table 4.5). The only two species that were significantly negatively affected by the mixture treatment (i.e. *Oscillatoria* sp. 1 and the unknown Chlorophyta colony) both belong to the filamentous algae, indicating that this group might be negatively affected by the mixture. Indeed, when dividing the phytoplankton taxa between filamentous algae and non-filamentous, we can observe that the abundance of both groups is significantly affected. That of the former is negatively affected while that of the latter is positively affected by the mixture treatment 1 and upwards (Table 4.5). The lowest consistent $NOEC_{abundance}$ (< Mixture 1) was calculated for the Cyanobacteria species *Oscillatoria* sp. 1, for the Chlorophyta species unknown Flagellate sp. 3, for the Chrysophyta species *Chrysococcus* sp. and for the single cell diatoms.

Community-structure

Zooplankton community

Figure 4.2A shows the PRC graph for the mixture treatments for the zooplankton. Of the variation in zooplankton community composition, 33% was explained by treatment regime, while 38% was explained by exposure time. Table 4.6 shows the results from the $NOEC_{composition}$ analyses. A $NOEC_{composition}$ for the specific mixture of metals was obtained. The deviation in community composition from the control increased with time. In the second week of exposure, a significant difference is found for the Mixture 5 treatment and upwards, while in week 4, 6 and 8, a significant difference is found for the Mixture 6, 3 and 2 treatments and upwards, respectively. The consistent $NOEC_{composition}$ for the mixture treatment was equal to Mixture 2 (Table 4.6).

When investigating Figure 4.2A we can observe that most cladoceran taxa (e.g. *Alonella nana*, *C. sphaericus* and *S. vetulus*) showed a positive weight in the PRC curve, indicating that their abundances decreased in the mixture regime. The abundance of most rotifer taxa (e.g. *Lecane* group *lunaris*, *Lepadella patella* and *Mytina ventralis*) also decreased. An exception is found for the rotifer *Cephalodella gibba,* for which the abundance increased. The adult Copepoda showed a low positive species weight ($b_k < 0.5$), suggesting a small influence of the metals on Copepoda abundance.

Phytoplankton community

Figure 4.2B shows the PRC graph of the mixture treatments for the phytoplankton. Of the variation in phytoplankton community composition, 35% was explained by treatment regime, while 25% was explained by exposure time. Table 4.6 shows the results from the $NOEC_{composition}$ analyses. The effect of the mixture increases with time. In the second week of exposure, a significant difference is found for the Mixture 4 treatment and upwards, while in week 4, 6 and 8, a significant difference is found for the Mixture 3, 1 and 2 treatments and upwards, respectively. The consistent $NOEC_{composition}$ for the mixture

treatments was equal to Mixture 1 (Table 4.5). The species weights (Figure 4.2B) indicated that in general, the abundance of most phytoplankton groups increased (positive b_k). The only species that were adversely affected by most metal treatments include *Oscillatoria* sp. 1, *Mougeotia* sp. and the unknown Chlorophyta colony (Figure 4.2B).

Table 4.5. Lowest-observed effect concentrations (LOEC; Williams test, p <0.05) and consistent no-observed-effect-concentration (NOEC) and LOEC per sampling date for the different plankton endpoints and species[a] for the environmental ratio mixture treatments.

			LOEC[b]					Consistent	Consistent
	As a group	As a taxon	-1[c]	14	28	42	56	NOEC[b,d]	LOEC[b]
Zooplankton									
	Cladocerans		> 6	5↓	> 6	> 6	5↓	≥6	
		Daphnia longispina	> 6	6↓	5↓	6↓	> 6	5	6↓
		Acroperus harpae	> 6	6↓	6↓	6↓	4↓	5	6↓
	Rotifera		> 6	> 6	1 ↓	4 ↓	4 ↓	3	4↓
		Lecane group Lunaris	> 6	> 6	6↓	3↓	1↓	2	3↓
		Lepadella patella	> 6	> 6	6↓	3↓	1↓	2	3↓
		Trichotria pocillum	> 6	> 6	2↓	6↓	1↓	5	6↓
		group Aspancha	6↓	> 6	6↓	6↓	2↓	5	6↓
		Trichocerca group *similis*	> 6	1↓	1↓	> 6	2↓	<1	1↓
		Colurella unicate	> 6	> 6	> 6	2↓	2↓	1	2↓
		Cephalodella gibba	> 6	> 6	5↑	6↑	> 6	5	6↑
		Mytilina ventralis	> 6	> 6	2↓	1↓	4↓	1	2↓
		Dissotrocha sp.	> 6	> 6	> 6	1↓	1↓	<1	1↓
	Copepoda		> 6	6↑	> 6	6↓	6↓	5	6↓
		Nauplii	> 6	5↑	3↑	6↓	6↓	4	5↑
	Ostracoda	*Ostracoda* sp. 2	X	5↓	1↓	X	X	4	5↓
Phytoplankton									
	Cyanobacteria		> 6	6↓	1↓	1↓	2↓	<1	1↓
		Pseudanabaenoideae sp.	> 6	5↓	3↑	5↑	5↑	4	5↑
		Aphanothece sp.	> 6	> 6	4↑	5↑	> 6	4	5↑
		Oscillatoria sp. 1	> 6	4↓	1↓	1↓	2↓	<1	1↓
	Chlorophyta		> 6	> 6	> 6	> 6	> 6	≥6	
		Desmodesmus sp.	X	6↑	3↑	6↑	6↑	5	6↑
		Cryptomonas sp.	> 6	> 6	> 6	5↑	6↑	5	6↑
		Unknown flagellate sp. 3	> 6	6↑	3↑	1↑	1↑	<1	1↑
		Haematococcus sp.	> 6	6↑	6↑	> 6	> 6	5	6↑
		Westella botryoides	> 6	> 6	> 6	5↑	5↑	4	5↑
		Unknown colony	5↓	6↓	6↓	4↓	5↓	4	5↓
	Chrysophyta		> 6	> 6	> 6	1↑	1↑	<1	1↑
		Chrysococcus sp.	> 6	> 6	> 6	1↑	1↑	<1	1↑
	Charophyta		> 6	1↑	> 6	> 6	> 6	≥6	
		Cosmarium sp.	> 6	1↑	4↑	5↑	3↑	4	5↑
	Diatoms		> 6	> 6	1↑	1↑	1↑	<1	1↑
		Single cell diatoms	> 6	6↑	1↑	1↑	1↑	<1	1↑
	Cryptophyta		> 6	> 6	3↑	1↑	1↑	<1	1↑
	Filamentous algae		> 6	6↓	1↓	1↓	1↓	<1	1↓
	Non filamentous algae		> 6	6↑	1↑	1↑	1↑	<1	1↑

[a] Only species that showed a consistent no-observed-effect concentration (NOEC) are shown; b The numbers indicate the following: '<1' denotes an unbounded NOEC that is lower than the lowest tested concentration; '≥6' denotes an unbounded NOEC that is higher or equal to the highest tested concentration, '1', '2', '3', '4', '5' and 6' = Mixture 1, 2, 3, 4, 5 or 6 treatment, respectively; X = no individuals of this taxon were counted in this week.
The direction of the deviation is denoted as follows: ↓ decrease; ↑ increase.; [c] The numbers refer to the day of the experimental period; [d]NOECs were considered as consistent if statistical significant deviations in the same direction were observed for at least 2 consecutive sampling days.

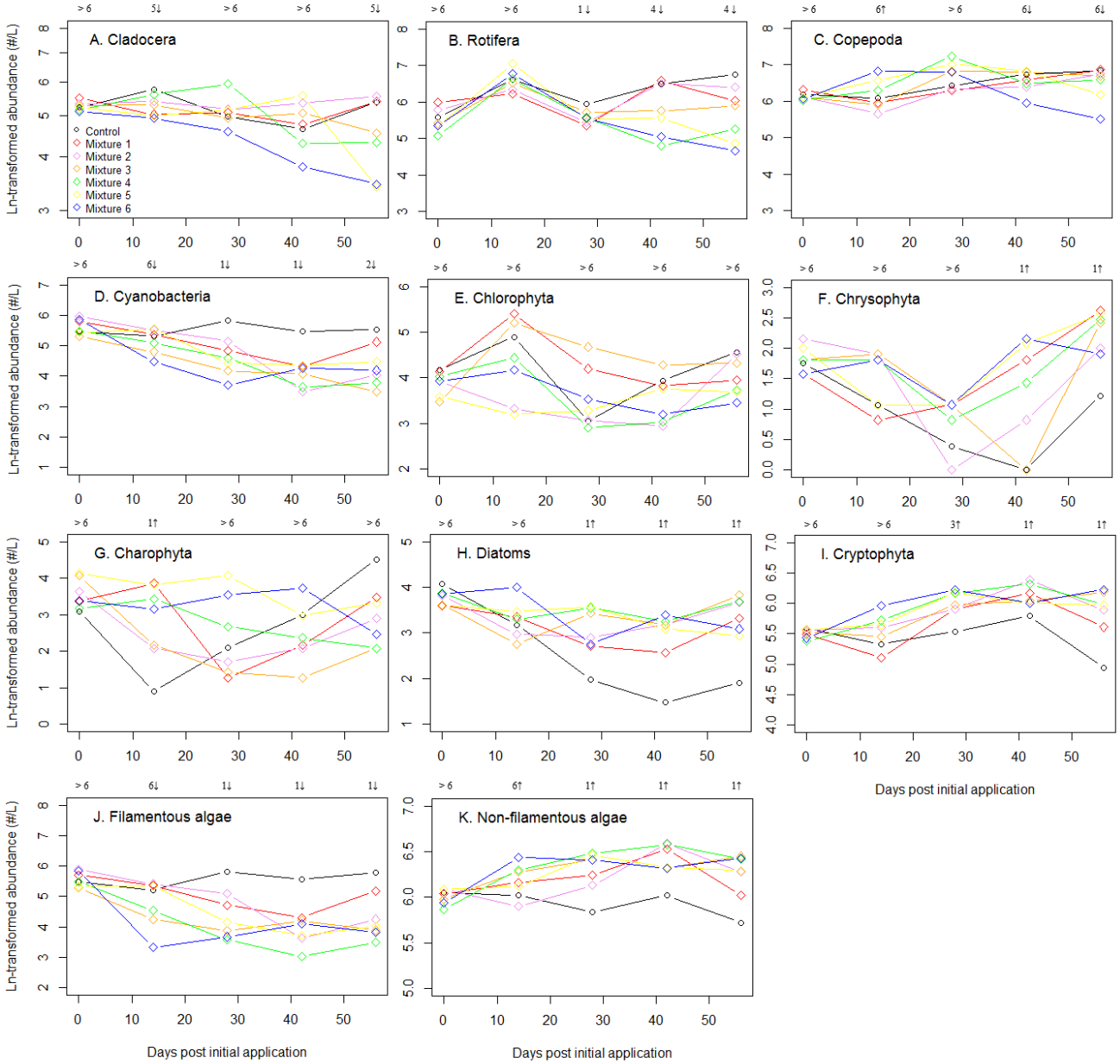

Figure 4.1. Population dynamics of the different zooplankton and phytoplankton groups. The means of the ln-transformed sum of abundances per treatment concentrations are given (*ln(1.2n+1) for zooplankton and ln(0.001n+1) for phytoplankton, see text*) for (A) Cladocera, (B) Rotifera, (C) Copepoda, (D) Cyanobacteria, (E) Chlorophyta, (F) Chrysophyta, (G) Charophyta and (H) Diatoms, (I) Cryptophyta, (J) Filamentous algae and (K) Non-filamentous algae. Calculated lowest-observed-effect concentrations are plotted above the figures (Williams test, p<0.05)

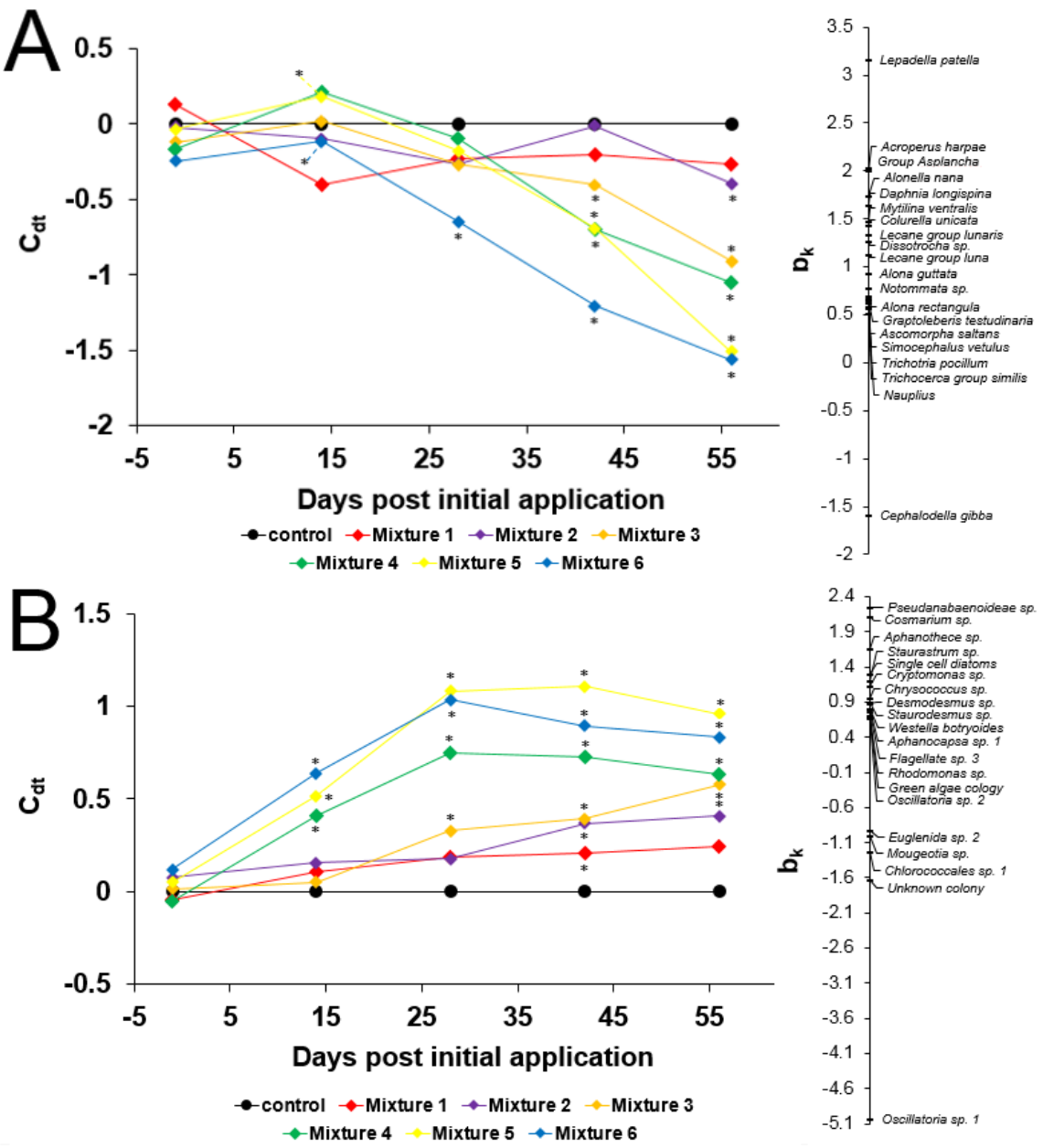

Figure 4.2. Principal response curves (PRC) for the community effects analysis resulting from analysis of the zooplankton data (A) and phytoplankton data (B) for mixture treatments, indicating the effects of the different metal concentrations. The vertical axis represents the difference in community composition of the treatments compared to the control, expressed as the canonical regression coefficients (C_{dt}). The affinity of a taxon in the PRC is expressed as the species weight (b_k; only species for which absolute bk > 0.5 are shown). Asterisks indicate a difference in community structure from the control (Williams test, $p < 0.05$).

Table 4.6. Lowest-observed-effect concentrations ($LOEC_{composition}$) of the zooplankton and phytoplankton community for the different metal treatments and sampling dates.

	$LOEC_{composition}$[a]					Consistent $LOEC_{composition}$[a,b]	Consistent $LOEC_{composition}$[b]
	-1	14	28	42	56		
Zooplankton	>6	**5**	**6**	**3**	**2**	2	3
Phytoplankton	>6	**4**	**3**	**1**	**2**	1	2

[a] The numbers indicate the following: '>6' denotes an unbounded LOEC that is higher than the highest tested concentration, '1', '2', '3', '4', '5' and '6' = Mixture 1, 2, 3, 4, 5 or 6 treatment, respectively
[b] NOECs and LOECs were considered as consistent if statistical significant deviations in the same direction were observed for at least 2 consecutive sampling days.
$LOEC_{composition}$ values indicated in bold are significant (Williams test, p<0.05)

Species diversity and richness

Table 4.7 gives the consistent NOEC values of the zooplankton and phytoplankton species diversity and richness. Figure 4.3 shows the change in species diversity and richness during the exposure period. The zooplankton community diversity and richness is only affected at or above the highest tested concentration. The phytoplankton species richness is affected from Mixture 5 upwards.

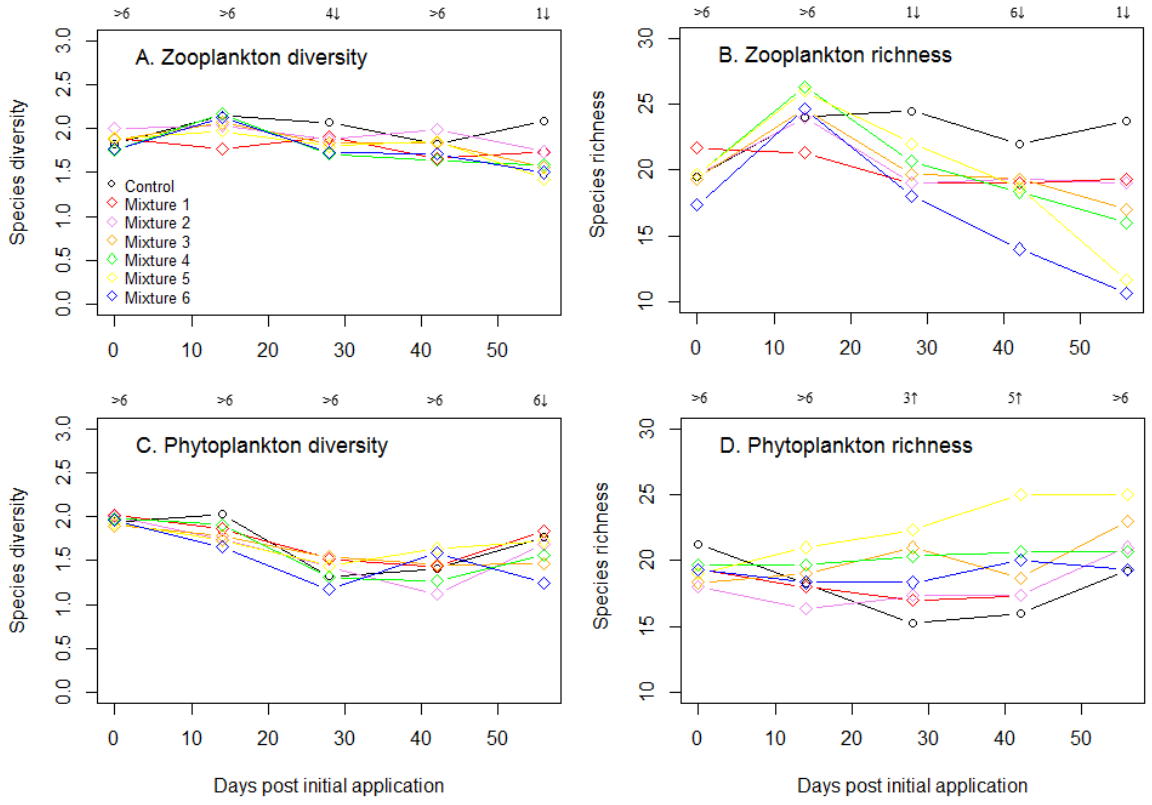

Figure 4.3. Species diversity (Shannon index) and species richness (number of species) for zooplankton (A,B) and phytoplankton (C,D) for the control and mixture treatments. Calculated lowest-observed-effect concentrations (Table 4.5) are plotted above the figures (Williams test, p<0.05)

Indirect physico-chemical proxies for community functioning

Average dissolved oxygen (DO) concentration decreased in the first week of exposure, although less so for the control treatment compared to the metal treatments (Figure 4.4A). After the first week, the DO concentration steadily increased in all treatments, however, the DO concentration in the mixture treatments stayed below that of the controls. The ΔDO as proxy for the community respiration increased in the control treatment during the entire exposure period, but showed an initial decrease followed by an increase at the end of the exposure period for most metal treatments (Figure 4.4B). The consistent LOEC values calculated using the Williams test ($p<0.05$) are given in Table .4.8. A significant effect on the ΔDO was observed from the lowest tested mixture concentration upwards.

In the first week of exposure, the pH in all microcosms showed a decrease (Figure 4.4D). After this, the pH was stable between 7.4 and 8.2 except for the control in which the pH increased to ~8.5 at the end of exposure. The difference in pH between morning and evening (ΔpH), which is here seen as a proxy for phytoplankton and bacteria abundance, is also affected by the metal addition (Figure 4.4E). The ΔpH is affected at the lowest tested mixture concentration (Table 4.8).

Dissolved Organic Carbon concentration, which is regarded as proxy for the microbial loop, decreased during the experimental period for most treatments (Figure 4.4C), except for the control and the Mixture 1 treatment. Based on the consistent LOECs (Table 4.8), the DOC was significantly affected at the Mixture 2 treatment and upwards.

Table 4.7. Lowest-observed-effect concentrations (LOEC) of the species diversity (Shannon index) and species richness (number of species) for the different metal treatments and sampling dates. In addition, consistent no-observed-effect concentration (NOEC) and consistent LOEC for the period day 14-56.

		LOEC[a]					Consistent NOEC[a,b]	Consistent LOEC[b]
		-1	14	28	42	56		
Zooplankton	Species diversity	>6	>6	**4↓**	>6	**1↓**	≥6	
	Species richness	>6	>6	**1↓**	**6↓**	**1↓**	5	6↓
Phytoplankton	Species diversity	>6	>6	>6	>6	**6↓**	≥6	
	Species richness	>6	>6	**3↑**	**5↑**	>6	4	5

[a] The numbers indicate the following: '>6' denotes an unbounded LOEC that is higher than the highest tested concentration, '1', '2', '3', '4', '5' and '6' = Mixture 1, 2, 3, 4, 5 or 6 treatment, respectively

[b] NOECs and LOECs were considered as consistent if statistical significant deviations in the same direction were observed for at least 2 consecutive sampling days.

LOEC values indicated in bold are significant (Williams test, $p<0.05$)

Table 4.8. Lowest-observed-effect concentrations (LOEC) of the ΔDO ΔpH and DOC for the different sampling dates.

	LOEC[a]					Consistent NOEC[b]	Consistent LOEC[b]
	-1	14	28	42	56		
ΔDO	X	**4↓**	**1↓**	**1↓**	**1↓**	<1	1↓
ΔpH	X	**3↓**	**2↓**	**1↓**	**1↓**	<1	1↓
DOC	>6	**6↓**	**2↓**	**1↓**	**2↓**	1	2↓

$\Delta \mathrm{DO} = DO_{evening\ day\ x} - DO_{morning\ day\ x+1}$ as proxy for the community respiration

ΔpH as proxy for the abundance of phytoplankton and bacteria

DOC = dissolved organic carbon as proxy for the microbial loop

[a] The numbers indicate the following: '<1' denotes an unbounded NOEC value lower than the lowest tested concentration; '1', '2', '3', '4', '5' and '6' = Mixture 1, 2, 3, 4, 5 or 6 treatment, respectively

LOEC values indicated in bold are significant (Williams test, $p<0.05$);

[a]NOECs and LOECs were considered as consistent if statistical significant deviations in the same direction were observed for at least 2 consecutive sampling days.

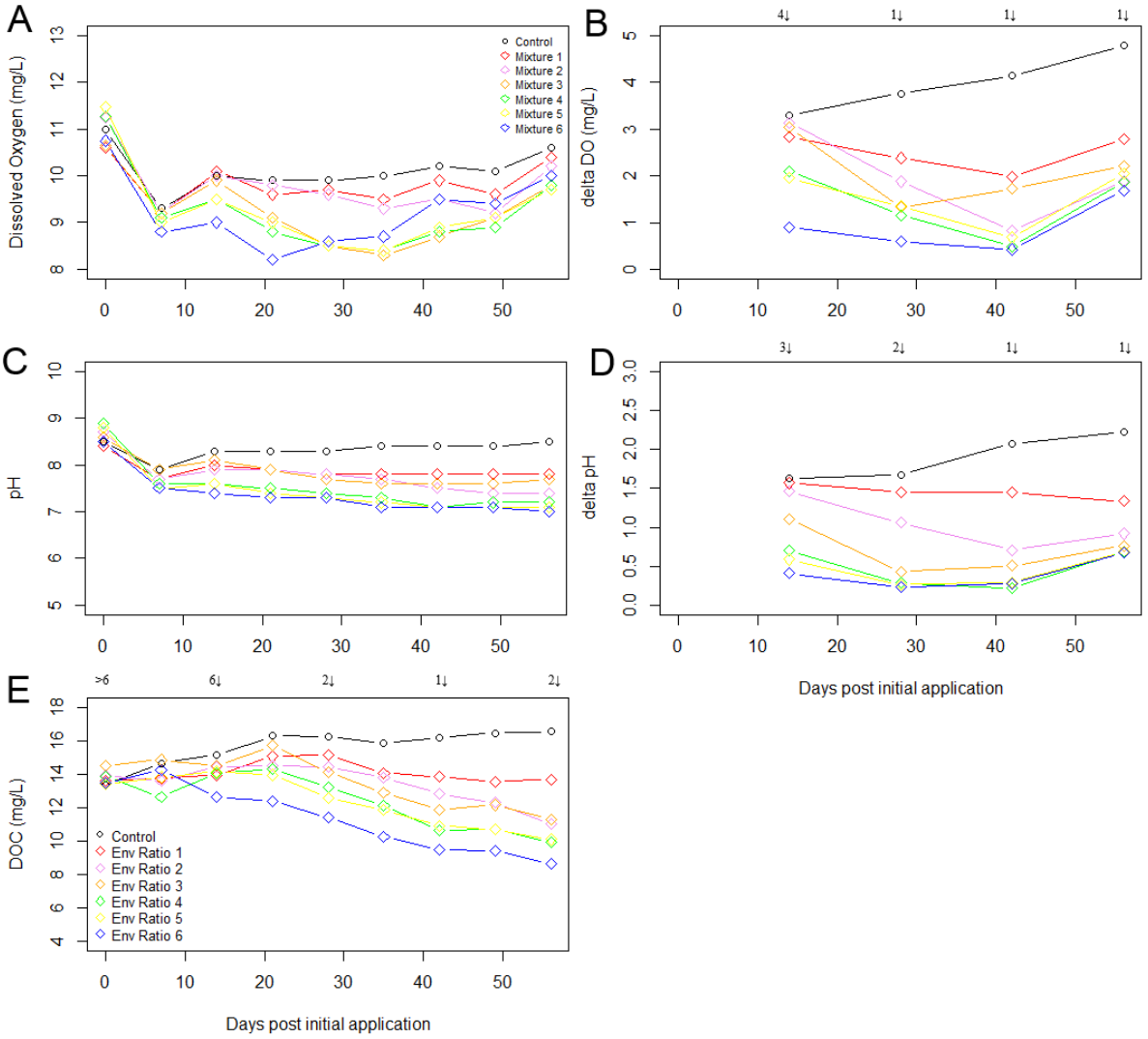

Figure 4.4. Overview of the average dissolved oxygen (DO) (A), ΔDO as proxy for the community respiration (B), pH (C), ΔpH as proxy for the phytoplankton and bacteria abundance and (D) dissolved organic carbon (DOC) as proxy for the microbial loop, per treatment during the 56d exposure period. Calculated lowest-observed-effect concentrations (Table 8) are plotted above the figures (Williams test, p<0.05)

Predicted msPAF versus LOEC values

To examine from which msPAF value effects on the community as a result of exposure to a metal mixture are observed, the "initial msPAF value" are compared to the LOEC values of the different structural endpoints (species groups abundances, community composition, species diversity and species richness) and indirect physico-chemical proxies for community functioning endpoints (ΔDO, ΔpH and DOC). The initial msPAF values are calculated for every replicate of every treatment separately and are based on the measured water chemistry and metal concentrations of every microcosm at the start of the experiment (see Supplementary 5 in the online repository at mda.vliz.be). An overview of the nominal msPAF and the average initial PAF and msPAF values per treatment is given in Table 4.9. A full overview of predicted initial msPAF values for the different replicates per treatment and sampling date can be found in the supplementary material (see Supplementary 6 in the online repository at mda.vliz.be). The initial msPAF values are higher than the nominal msPAF value in some treatments.

This can be attributed to the difference in water chemistry between the average chemistry before the start of the experiment (Table 4.1) that was used to calculate the nominal msPAF values and the water chemistry of the individual microcosms after addition of the metals, as well as the difference between nominal and measured metal concentrations.

The different LOEC values for the tested endpoints can be found in the tables 4.5, 4.6, 4.7 and 4.8. The initial msPAF values corresponding to these LOEC values for the different endpoints are given in Table 4.10. Table 4.10 shows that the functional community endpoints are more sensitive to metal exposure than most of the structural endpoints. When examining the structural community endpoints, the species diversity and richness are in general less sensitive compared to measures of abundance (i.e. most group abundances and the community composition). The lowest msPAF value at which an effect occurs is equal to 0.03 for the structural community endpoints for some phytoplankton species groups (i.e. Cyanobacteria, Chrysophyta, Diatoms and Cryptophyta). However, the overall phytoplankton community composition is only affected from the Mixture 2 treatment, which corresponds to an msPAF value of 0.15 (Table 4.10). The zooplankton species groups abundances and zooplankton community composition are less sensitive than the phytoplankton group abundances and community composition, as effects only occur from an initial msPAF value of 0.61 and 0.38, respectively (Table 4.10). The indirect proxies for the functional community endpoints are affected at lower initial msPAF values. The ΔDO and ΔpH are already affected by the mixture at initial msPAF values of 0.03, while the DOC is affected from an initial msPAF value of 0.15 (Table 4.10).

Table 4.9. Nominal msPAF value and average (± sd) initial msPAF values calculated with the CA_{SSD} method (Van Regenmortel et al. 2017) for the different treatments.

	nominal $msPAF_{CASSD}$ [a]	initial $msPAF_{CASSD,AllSpecies}$ [b]	initial $msPAF_{CASSD,plankton}$ [c]
Control	0.00	<0.01 ± <0.01	<0.01 ± <0.01
Mixture 1	0.01	0.03 ± 0.05	0.05 ± 0.03
Mixture 2	0.05	0.15 ± 0.07	0.20 ± 0.08
Mixture 3	0.26	0.38 ± 0.14	0.48 ± 0.17
Mixture 4	0.50	0.61 ± 0.05	0.72 ± 0.05
Mixture 5	0.68	0.77 ± 0.01	0.86 ± 0.01
Mixture 6	0.91	0.89 ± 0.03	0.94 ± 0.02

$msPAF_{CASSD}$ = multi substance potentially affected fraction of species calculated using the CA_{SSD} method (Van Regenmortel et al. 2017);

[a] msPAF values calculated based on all chronic toxicity data (i.e. fish, invertebrates, algae), using the average water chemistry of the 40 microcosms measured the day before the start of the experiment

[b] msPAF values calculated based on all chronic toxicity data (i.e. fish, invertebrates, algae), using the water chemistry measured in each microcosm separately after spiking the metals on day 1

[c] msPAF values calculated based on chronic toxicity data of planktonic species, using the water chemistry measured in each microcosm separately after spiking the metals on day 1

Table 4.10. Overview of the initial msPAF value corresponding to the consistent Lowest-observed-effect concentration (LOEC) of the structural and functional community endpoints for the mixture treatments

	Effect on	Variable	initial msPAF	
Structural community endpoints	Species groups abundances	Cladocera	>0.89	>0.94
		Rotifera	0.61	0.72
		Copepoda	0.77	0.86
		Cyanobacteria	*0.03*	*0.05*
		Chlorophyta	>0.89	>0.94
		Chrysophyta	*0.03*	*0.05*
		Charophyta	0.77	0.86
		Diatoms	*0.03*	*0.05*
		Cryptophyta	*0.03*	*0.05*
	Community composition	Zooplankton community	0.38	0.48
		Phytoplankton community	0.15	0.20
	Species diversity	Zooplankton	>0.89	>0.94
		Phytoplankton	0.77	0.86
	Species richness	Zooplankton	0.89	0.94
		Phytoplankton	0.77	0.86
Functional community endpoints	*ΔDO (community respiration)*		*0.03*	*0.05*
	ΔpH (phytoplankton + bacteria abundance)		*0.03*	*0.05*
	DOC (microbial loop)		0.15	0.20

msPAF = multisubstance potentially affected fraction of species; DO = dissolved oxygen; DOC = dissolved organic carbon

4.4. Discussion

In this discussion we focus on the two main research questions posed in the Introduction and examine whether our expectations hold true. In addition, we discuss possible explanations when the data did not match with our expectations.

Research question 1: what are the direct and indirect effects on the community?

When examining Table 4.5, the community level interactions seem to differ between the 2 lowest mixture treatments which should rather be considered as Ni-Zn mixtures, and the 3 highest mixture treatments which can be regarded as Cu-Ni-Zn mixtures. Indeed, at the two lowest mixture treatments (Mixture 1 and 2), a consistent LOEC of “1” or “2” (see Table 4.5) is mainly found for the phytoplankton groups, while the zooplankton groups only become affected at the higher mixture treatments (see Table 4.5, consistent LOEC values of “4”,”5” and “6”). Therefore, the direct and indirect effects on the planktonic community in these two groups (Mixture 1-2 vs Mixture 4-5-6) will be discussed separately. As the effect patterns do not seem to change between mixture treatments 2 and 3 (i.e. the addition of Cu above its concentration in the control does not seem to have an effect in treatment 3 but only from treatment 4 onwards), we will not discuss mixture treatment 3 separately.

In Figure 4.5 a schematic overview of the effects of the 2 lowest mixture treatments (Mixture 1 and 2) (Ni-Zn mixture) on the zooplankton and phytoplankton community structure and functioning in the

microcosms is given. At the 2 lowest mixture treatments, the zooplankton groups are not affected (Table 4.5). Most phytoplankton groups and taxa were positively affected by the mixture and showed a significant increase in abundance during the exposure period (Table 4.5). This is not expected because phytoplankton species are usually amongst the most sensitive species according to the SSDs (mainly for Zn; Figure Appendix C2) although only Chlorophyta species are represented in these SSDs. This increase in phytoplankton abundance can possibly be explained by the indirect effects of the decrease in Cyanobacteria abundance. From week 4 onwards Cyanobacteria as a group were directly negatively affected by the Mixture 1 treatment and upwards (Table 4.5). The main driver behind the decrease in Cyanobacteria abundance is possibly the decrease in the abundance of *Oscillatoria* sp. 1, as the relative abundance of this species comprises a large fraction of the total Cyanobacteria abundance (Figure 4.6A). These negative effects could have caused a positive effect on the abundance of the Chrysophyta, Diatoms and Cryptophyta (Table 4.5) which could have been the result of a reduction in nutrient competition. The decrease in Cyanobacteria abundance might also have indirectly influenced the proxies for community functioning (ΔDO, ΔpH and DOC). Although most algae species showed an increase in abundance (Table 4.5) and we would therefore expect an increase in the proxies for community functioning (see *Material and Methods* section), these proxies showed a significant decrease compared to the control treatment from the Mixture 1 or 2 treatment and upwards (Table 4.8). This decrease in ΔDO (as proxy for community respiration) and ΔpH (as proxy for phytoplankton and bacteria abundance) were therefore most likely the result of a decrease in the abundance of a dominant algae species. When examining the relative abundance of *Oscillatoria* sp. 1 compared to all other phytoplankton species (54 in total) we can observe that this species comprises approximately 40% of the total phytoplankton abundance in the control treatment (Figure 4.6B). This species can therefore be regarded as a dominant algae species in terms of biomass, which is even enhanced by the fact that during counting, the filamentous algae were counted as single individuals and the larger biomass of these individuals compared to non-filamentous algae were therefore not accounted for (Figure Appendix C3). The decrease in DOC concentration might also be indirectly linked to the decrease in the abundance of this dominant algae species (i.e. *Oscillatoria* sp. 1). When regarding the microbial loop and pelagic food web interactions, a decrease in DOC concentration is expected when the degradation of DOC is higher than the production of DOC (Kayambo et al. 2002). As the abundance and biomass of the dominant algal species *Oscillatoria* sp. 1 is lower in the mixture treatments compared to the control, the production of DOC by these algae as input for the microbial loop is smaller compared to the degradation of the DOC by bacteria. As such, the decrease in DOC concentration could perhaps be explained by the decrease in Cyanobacteria abundance. Thus, overall, our results suggest that a single highly Ni and/or Zn sensitive Cyanobacteria species, i.e. *Oscillatoria* sp. 1, may have been at the basis of all the community level changes in these Ni-Zn mixture treatments. As this species is not included in the SSDs, this points to a problem with SSDs in general (Forbes and Calow 2002): that SSDs may not necessarily be a good basis for protecting functioning of ecosystems that contain sensitive dominant species, if these are not included in the SSD. Indeed, when this dominant species is lost (or its abundance decreased), this will result in a disproportional effect on ecosystem functioning. It has been shown that this can especially occur in cases when dominant species rank among the most sensitive

species in the system (Pimm 1984, Baert 2017), as is the case in our microcosm system for *Oscillatoria* sp. 1.

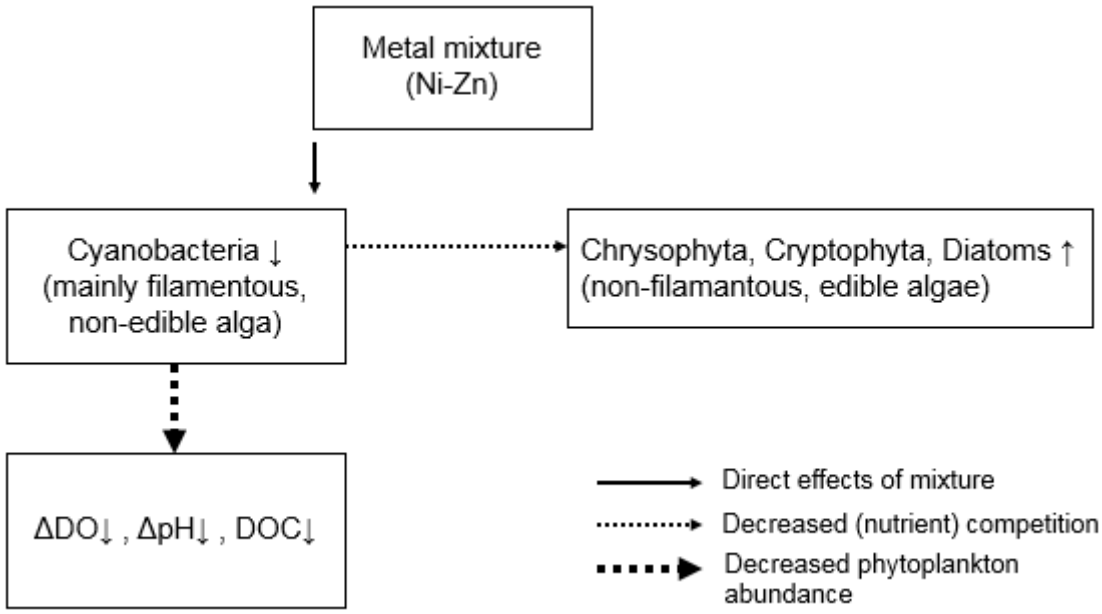

Figure 4.5. Schematic overview of the observed direct and indirect effects of the 2 lowest metal treatments (Mixture 1 and 2) on the zooplankton and phytoplankton community structure and functioning. ↑= increase;↓ = decrease

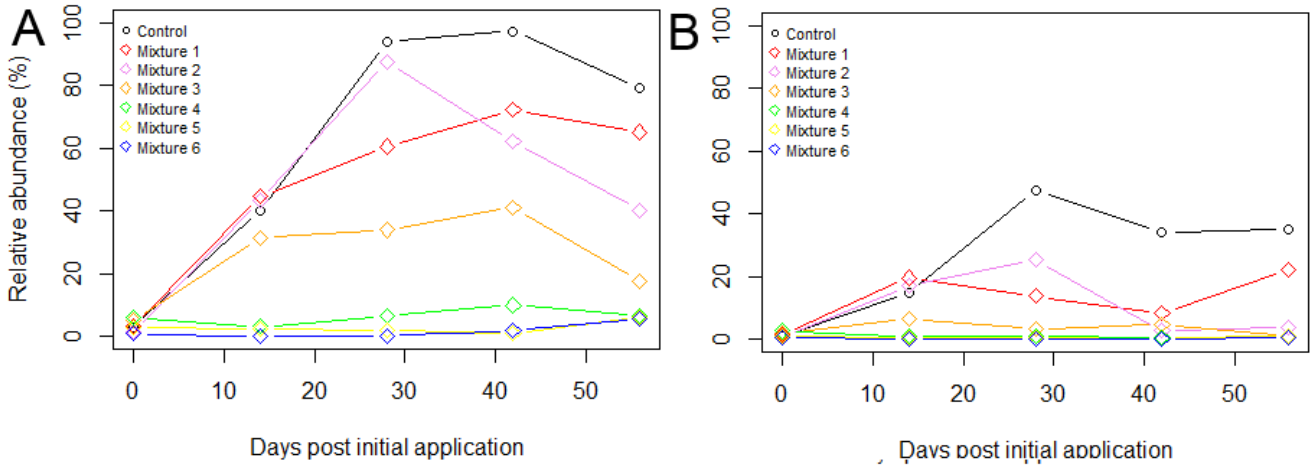

Figure 4.6. Relative abundance of *Oscillatoria* sp. 1 compared to the total abundance of all species within the Cyanobacteria group (A) and compared to the total abundance of all phytoplankton species (B) during the exposure period for the control and mixture treatments.

In Figure 4.7 a schematic overview of the effects of the highest mixture treatments (Mixture 4-6) (Cu-Ni-Zn mixture) on the zooplankton and phytoplankton community composition in the microcosms is given. The same direct effects of the mixture on the Cyanobacteria and the indirect effects of Cyanobacteria on Chrysophyta, Diatoms and Cryptophyta and on the proxies of community functioning are also visible at the highest mixture treatments. In addition, different zooplankton groups now also seem directly and

indirectly affected by the mixture. As a result, the community-level interactions at the highest mixture treatments are more complex than those at the lowest mixture treatments.

From week 2 onwards some cladocerans species were negatively affected by the highest mixture treatment (Table 4.5). These negative effects most likely caused an initial, positive effect on copepod abundances, as these seemed to be initially less sensitive to metal stress, which is mainly reflected in the increase in nauplii abundance (Table 4.5; Figure 4.7). This initial increase in abundance was possibly the result of a reduction in competition for food, which has been reported in numerous other cosm studies (Van de Perre et al. 2016, Fleeger et al. 2003, Van Wijngaarden et al. 2005). In addition, the increase in edible, non-filamentous algae (i.e. Chrysophyta, Diatoms and Cryptophyta) due to the decrease in non-edible, filamentous Cyanobacteria (mainly *Oscillatoria* sp. 1) via reduced nutrient competition (see above) might also have enhanced the food sources for these copepods.

Following this initial increase in copepod abundances, the abundances of copepods, and mainly nauplii, decreased most likely due to the direct effects of the metal mixture exposure. This delay in time of toxic effects on copepods due to the mixture could be attributed to the longer life cycle of copepods compared to rotifers and cladocerans. The latter two groups reproduce parthenogenetically and therefore have short life cycles while the former group reproduces sexually and as a result exhibits longer life cycles and fewer generations (Allan et al. 1976). This direct negative effect on copepod species has been confirmed in single species exposures (e.g. Xu et al. 2014, Wong and Pak 2004). However, this is in contrast to what was observed in microcosm studies exposed to single Zn (Van de Perre et al. 2016) and single Ni (Hommen et al. 2016) in which indirect positive effect of reduced food competition were observed and no negative direct effect of the metal exposure were detected. Schäfers (2001) on the other hand did observe direct negative effects of Cu on the copepod abundances in his microcosm study. As the highest mixture treatments in our study include Cu in the mixture (compared to the absence of Cu in the binary Ni-Zn mixtures of the lowest mixture treatments), these negative effects on copepods are in accordance to what was seen by Schäfers (2001) in his Cu-exposed microcosm experiments. The decrease in copepod abundance might again have enhanced the increase in abundance of the Chrysophyta, Diatoms and Cryptophyta (Figure 4.7). The initial increase in copepod abundances might have caused the decrease in rotifer abundance from week 4 onwards (Table 4.5), possibly due to an increase in competition for food (Figure 4.7). However, this would not explain why the abundance of rotifers does not increase again as a response to the decrease in copepod abundance from week 6 onwards. An alternative explanation might be that at high mixture treatments, the rotifers are directly affected by the mixture due to the addition of Cu in these highest mixture treatments. Rotifers are indeed known to be very sensitive to Cu toxicity (ECI 2008, De Schamphelaere et al. 2006b). In this scenario, the decrease in rotifer abundance might have enhanced the increase in abundance of the Chrysophyta, Diatoms and Cryptophyta via reduced consumption (Figure 4.7). It is clear that the interactions between all species groups at the highest mixture treatments are complex and that it is not possible to mechanistically explain all observed effects (and their sequence) with the available data.

Overall, our study demonstrates that community responses are influenced by both the direct sensitivity of the organisms to the mixture of toxicants and by interspecific interactions (De Schamphelaere et al. 2003, De Schamphelaere et al. 2005, De Laender et al. 2008).

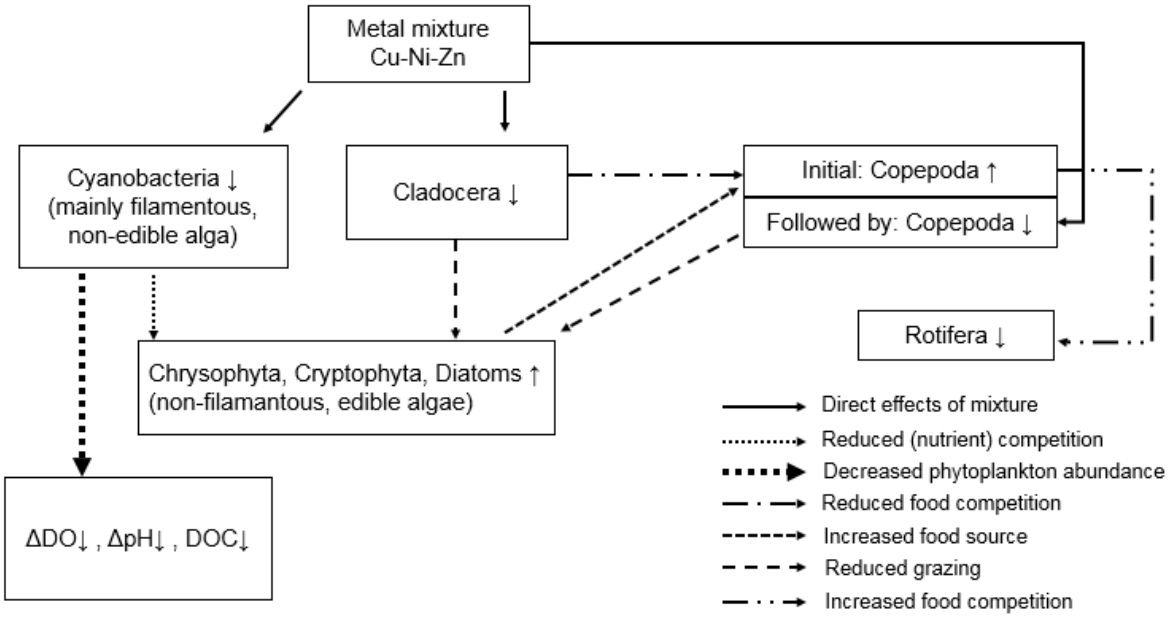

Figure 4.7. Schematic overview of the observed direct and indirect effects of the 3 highest metal treatments (Mixture 4, 5 and 6) on the zooplankton and phytoplankton community structure and functioning. ↑= increase;↓ = decrease

Research question 2: As of which msPAF value do effects on structural and functional endpoints occur, and which of these endpoints are most sensitive?

Table 4.10 shows the initial msPAF value as of which effects on the community occur. When regarding the structural community endpoints, the species diversity and richness are in general less sensitive compared to the other structural community endpoints (i.e. community composition and species groups abundances). This has also been reported previously for experimental streams (Clements 2004, Hickey and Golding 2002, Carlisle and Clements 1999). For the structural community endpoints, the zooplankton community composition is less sensitive than the phytoplankton community composition, as effects only occur from an initial msPAF value of 0.38 for zooplankton while effects observed from an initial msPAF of 0.15 for the phytoplankton (Table 4.10). Although some phytoplankton groups show an initial msPAF value below 0.05 (i.e. 0.03) the overall phytoplankton and zooplankton community composition does thus not seem affected below 0.05. The observation that phytoplankton are more sensitive than zooplankton was also observed for a plankton community exposed to single Cu (Schäfers 2001). In a plankton community exposed to single Ni, the opposite was observed (Hommen et al. 2016), while the phytoplankton and zooplankton were equally sensitive when exposed to single Zn (Van de Perre et al. 2016). Table 4.10 also shows that the functional community endpoints are more sensitive to metal exposure than the structural endpoints. This phenomenon was also observed by Clements (2004) for a macroinvertebrate community exposed to a Zn+Cd mixture, and confirms our expectation. The proxy's for functional community endpoints were affected by the mixture at lower initial msPAF values. The ΔDO and ΔpH were already affected at initial msPAF values of 0.03, while the DOC was affected

from an initial msPAF value of 0.15 (Table 4.10). Based on both structural and functional endpoints, for a community exposed to a mixture of Ni and Zn, the msPAF value from which effects occur is 0.03 (Mixture 1; Table 4.10). Our results show that significant effects on the community already occur at msPAF values below 0.05, which is in regulatory terms regarded as the protective threshold below which no significant long-term effects on the community are expected to occur. Based on these results, the cut-off value of 0.05 does not seem protective for the community structure and functioning when the community is exposed to a mixture of Ni and Zn (i.e. effects at msPAF 0.03). As mentioned in the *Introduction*, we expected effects could occur at or below an msPAF value of 0.05 as a result of different parts of the food web being targeted by the different single mixture components, analogous to what was seen for pesticide mixtures (Verbruggen and Van den Brink 2010). However, this does not seem to be the explanation in our microcosm system, as only one group/species (Cyanobacteria/*Oscillatoria* sp. 1) seems to have been directly affected by the Ni-Zn mixture. Below, we will explore possible explanations for this result.

A first explanation concerns the species sensitivity distribution used for msPAF calculations. First of all, the msPAF values in Table 4.9 are calculated based on species sensitivity distributions for Cu, Ni and Zn containing chronic toxicity data of fish, invertebrates and algae (Van Regenmortel et al. 2017), from now on referred to as "$msPAF_{AllSpecies}$". Because the microcosms in the present study only contained a planktonic community, and not for example fish species, amphibians or benthic invertebrate species, we also calculated msPAF values based on chronic toxicity data of planktonic species alone (see Appendix C4 for details) (from now on referred to as "$msPAF_{plankton}$"). In the study by Van de Perre et al. (2016), the authors also only considered the toxicity data of planktonic species to calculate their HC5 values. Table 4.9 shows the initial predicted $msPAF_{plankton}$ values (full overview in supplementary material S.6 in the online repository at mda.vliz.be). When comparing to the initial $msPAF_{AllSpecies}$ values, we can observe that the $msPAF_{plankton}$ values are higher for all treatments. This is logical, as the planktonic species are on average more sensitive to metal toxicity compared to vertebrates and non-planktonic invertebrates (ECI 2008, Van Sprang et al. 2009, DEPA 2008), and as a result the HC5 values calculated from the SSDs are lower and therefore the $msPAF_{CASSD}$ values are higher. When comparing the LOEC of the different community endpoints to the $msPAF_{plankton}$ values, the lowest $msPAF_{plankton}$ value at which effects occur in the mixture treatments is now equal to 0.05. Calculating the msPAF values based on planktonic toxicity data alone increased the msPAF value from which effects on the community occur. Yet, the effects are still observed at the HC5 threshold value (msPAF 0.05) which is regarded as protective in many regulatory frameworks. Hence, leaving vertebrates and non-planktonic species out of the SSDs does not explain why community-level effects were observed below an msPAF value of 0.05.

A second explanation concerns the mismatch between the planktonic species in the toxicity database and the SSDs and those in our microcosm community. This issue regarding SSDs was also mentioned by Forbes and Calow (2002) who stated that "SSDs usually contain species that are generally not derived from any known community". When examining the planktonic species in the toxicity databases (see Appendix C4) we can see that most zooplankton species belong to the Cladocera and most phytoplankton species belong to the Chlorophyta. Although these species might be the most sensitive

of those in the chronic toxicity databases, they do not necessarily belong to the most sensitive species in our experiment. Indeed, when examining Table 4.5 we can see that the Cladocera as a group and the Chlorophyta as a group are the least sensitive of the zooplankton and phytoplankton groups within the tested community context, respectively. In addition, those groups that are most sensitive, although maybe not via direct effects of the mixtures but more likely via indirect routes, are the Rotifera and Cyanobacteria. The species of these groups are underrepresented in the chronic toxicity databases. This suggests that additional research concerning the sensitivity of these species to metals should be conducted, especially regarding the most dominant species in our system, i.e. *Oscillatoria* sp. 1, which seems to be the most sensitive species. As research has shown that the effects on ecosystem functioning are very large when keystone/dominant species that at the same time rank among the most sensitive species are affected or lost (Pimm 1984, Baert 2017), it is important that the direct toxicity of metals to this organism is examined. Another group of species that is not represented in the SSDs are some of those that take part in the microbial loop. Indeed, chronic toxicity data concerning the sensitivity of bacteria and protozoa to metals is lacking in the SSDs. However, it has been suggested that metals may interfere with the functioning of bacteria and protozoa (Morgan et al. 1958, Larsen and Nilsson 1983) and many studies conducted on heavy metal-polluted waters have revealed changes in the dynamics of protozoan (Cairns et al. 1980, Fernandez-Leborans and Novillo 1993, 1996). The mismatch in sensitive species between the chronic toxicity databases and our microcosms may explain why our community is more sensitive than expected based on the SSD and the calculated msPAF values. This is most clear when examining the effect of the Ni-Zn mixture on the filamentous species *Oscillatoria* sp. 1. This species, which is not represented in the chronic toxicity databases and thus not represented in the SSDs, seems to be the driver and at the basis of all effects in the two lowest (Ni-Zn) mixture treatments. Another issue regarding SSDs that was also mentioned by Forbes and Calow (2002) is that they do not account for interactions between species, and as such the msPAF values based on these SSDs also do not. The effects of these interactions on a community exposed to metal stress, could alter the sensitivity of the community and make it more or less sensitive than expected based on the predicted msPAF values.

A third possible explanation is that our microcosm systems might be more sensitive than other, larger systems, because we tested in aquaria filled with a relatively small volume of water, i.e. 5L. Microcosm experiments that tested the individual effects of Cu (Schäfers 2001), Ni (Hommen et al. 2016) and Zn (Van de Perre et al. 2016) used larger test systems, i.e. 750L, 750L and 14L, respectively. It has been shown that communities with fewer species per functional group, which is more likely to occur in smaller systems, are less stable and more sensitive than those with more species (Van den Brink 2008, Naeem and Li 1997). This is because when the number of species per functional group increases, the probability that compensatory growth will occur by remaining species in the functional group increases (Naeem and Li 1997). As such, effects might occur at lower msPAF values in the present study because our system small is intrinsically more sensitive.

In summary, we showed that our first possible explanation, i.e. to only include phytoplankton and zooplankton species in the SSD, did increase the msPAF values. However, the effects were still observed at the HC5 threshold value (msPAF 0.05). Our second explanation, i.e. the mismatch between

the species in the SSD and in our experiment, and especially regarding species that are at the same time dominant and sensitive (i.e. *Oscillatoria* sp. 1), is most likely the reason why our microcosm system is affected at an msPAF value of 0.05. In addition, our third explanation, i.e. the relatively small systems, could also have contributed as to why our microcosm system is affected at an msPAF value of 0.05. Although we found effects of the Ni-Zn mixture at an msPAF value of 0.05, we do emphasise that this result should only be extrapolated cautiously to other systems because information whether dominant species in other systems are typically also sensitive species is usually lacking. The main reason for the community-level effects found in our study appears to be the presence of a dominant species in the microcosm that appears to be very sensitive to the mixture at an msPAF value of 0.05. This also suggests that the explanation by Verbruggen and Van den Brink (2010) as to why synergistic mixture effects at community-level can occur, is not the only possible explanation as to why effects at or below msPAF=0.05 can occur.

Next to the CA_{SSD} method Van Regenmortel et al. (2017a/Chapter 2) described 3 other methods to calculate msPAF values. These methods are less conservative than the CA_{SSD} method (at msPAF values below 0.15, see Van Regenmortel et al. 2017a/Chapter 2) and some are considered more accurate (i.e. CA_{DRC} and IA_{DRC}) . In the CA_{DRC} and IA_{DRC} methods the CA and IA models are first applied to the dose-response curves of the individual species before calculating the msPAF, respectively. In the IA_{SSD} method the IA model is applied directly to the SSD (Van Regenmortel et al. 2017a/Chapter 2). Table 4.11 gives an overview of the initial $msPAF_{plankton}$ values calculated with the CA_{DRC}, IA_{DRC} and IA_{SSD} methods. Most $msPAF_{plankton}$ values calculated using the CA_{DRC}, IA_{DRC} and IA_{SSD} methods are quite similar to those calculated using the CA_{SSD} method. At high msPAF values (>0.48), the CA_{SSD} method is no longer the most conservative method, as was seen by Van Regenmortel et al. (2017a/Chapter 2). At the Mixture 1 treatment, the lowest treatment at which effects on some functional and structural endpoints were observed, and which showed an initial $msPAF_{CASSD,plankton}$ of 0.05, the 3 other methods give initial $msPAF_{plankton}$ values below 0.05. This implies that based on the other methods, the 0.05 threshold is not protective for some structural and functional long-term effects on the community. However, these methods are protective for community composition, species diversity, species richness and DOC (microbial loop).
In addition, also for these methods, the issue of the more sensitive system (i.e. more sensitive species, more bioavailable metals and small test systems) than expected based on msPAF values implies.

Table 4.11. Average (± sd) initial msPAF values based on toxicity data of planktonic species (Appendix C4) calculated with the CA_{SSD}, CA_{DRC} , IA_{DRC} and IA_{SSD} methods (Van Regenmortel et al. 2017) for the different treatments.

	$msPAFCA_{SSD,plankton}$ [a]	$msPAFCA_{DRC,plankton}$ [a]	$msPAFIA_{DRC,plankton}$ [a]	$msPAFIA_{SSD,plankton}$ [a]
Control	<0.01 ± <0.01	<0.01 ± <0.01	<0.01 ± <0.01	<0.01 ± <0.01
Mixture 1	0.05 ± 0.03	0.03 ± 0.02	0.02 ± 0.02	0.02 ± 0.02
Mixture 2	0.20 ± 0.08	0.19 ± 0.10	0.15 ± 0.08	0.14 ± 0.08
Mixture 3	0.48 ± 0.17	0.52 ± 0.22	0.40 ± 0.23	0.37 ± 0.23
Mixture 4	0.72 ± 0.05	0.84 ± 0.05	0.69 ± 0.07	0.64 ± 0.08
Mixture 5	0.86 ± 0.01	0.97 ± 0.01	0.87 ± 0.01	0.81 ± 0.01
Mixture 6	0.94 ± 0.02	1.00 ± 0.00	0.96 ± 0.02	0.92 ± 0.05

msPAF = multi substance potentially affected fraction of species
$msPAF_{CADRC}$ = msPAF calculated using concentration addition applied to the individual dose response curves (CA_{DRC}) (Van Regenmortel et al. 2017);
$msPAF_{IADRC}$ = msPAF calculated using independent action applied to the individual dose response curves (IA_{DRC}) (Van Regenmortel et al. 2017);
$msPAF_{IASSD}$ = msPAF calculated using independent action applied to the species sensitivity distribution (IA_{SSD}) (Van Regenmortel et al. 2017);
HC5 = concentration hazardous for 5% of the species; HC50 = concentration hazardous for 50% of the species;
Env Ratio = mixture with metal concentration ratio's based on Dommel monitoring dataset;
[a] msPAF values calculated based on chronic toxicity data of planktonic species, using the water chemistry measured in each microcosm separately after spiking the metals on day 1

Metal addition can influence its own bioavailability and therefore its toxicity

The addition of metals to the microcosms most likely changed the metal bioavailability during the exposure period (Figure 5) which could have led to a higher sensitivity of the species than expected based on the SSD and msPAF values. Indeed, when examining Figure 4.4, we can see that the DOC concentration decreased relative to the control treatment during the course of the exposure period. The lower DOC concentration indicates that the mixture treatments had a significant effect on the microbial loop (Jumars et al. 1989, Brönmark and Hansson 2005). A similar effect of metal addition on the DOC concentration was observed in a microcosm experiment with Zn (Van de Perre et al. 2016). In general, when the DOC concentration is lowered, metals become more bioavailable and as a result more toxic for plankton (e.g. De Schamphelaere et al. 2005, De Schamphelaere et al. 2003, Deleebeeck et al. 2007a and 2008, Van Sprang et al. 2009). As such, metals can influence their own toxicity by changing the water chemistry. This can be observed when calculating the HC5 concentrations of the single metals based on the measured physico-chemistry of the water on the different sampling dates (Figure 4.8). The decrease in HC5 values already starts at the beginning of the exposure period for Cu and Zn. For Ni, the HC5 value does not seem to change with time. This might be explained by the low affinity of Ni for DOC compared to Cu and Zn (Tipping et al. 2011), which results in a smaller influence of the decrease in DOC concentration on the Ni HC5 concentration. The decrease in HC5 values is associated with in an increase in the $msPAF_{CASSD}$ values during the course of the experiment (Figure 4.9). The initial decrease of the msPAF values (Figure 4.9) in most treatments is due to the initial increase in DOC concentration in most microcosms (Figure 4.4). This change in $msPAF_{CASSD}$ values is thus the result of the indirect effect of the changing water chemistry due to the addition of metals. This might also partially

explain the higher effects on species abundances towards the end of the exposure period in the present study (e.g. *Colurella unicata*, *Chrysococcus* sp.).

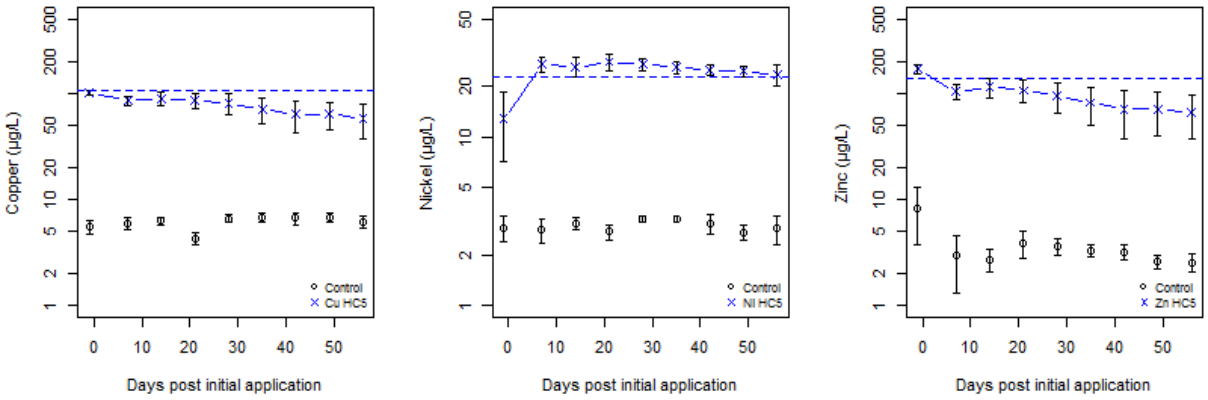

Figure 4.8. Overview of the change in HC5 concentration in time (blue lines) for the mixture treatments. The dashed line indicates the nominal HC5 concentrations in the treatments. The circles indicate the measured metal concentrations in the control treatment. Error bars denote standard deviations.

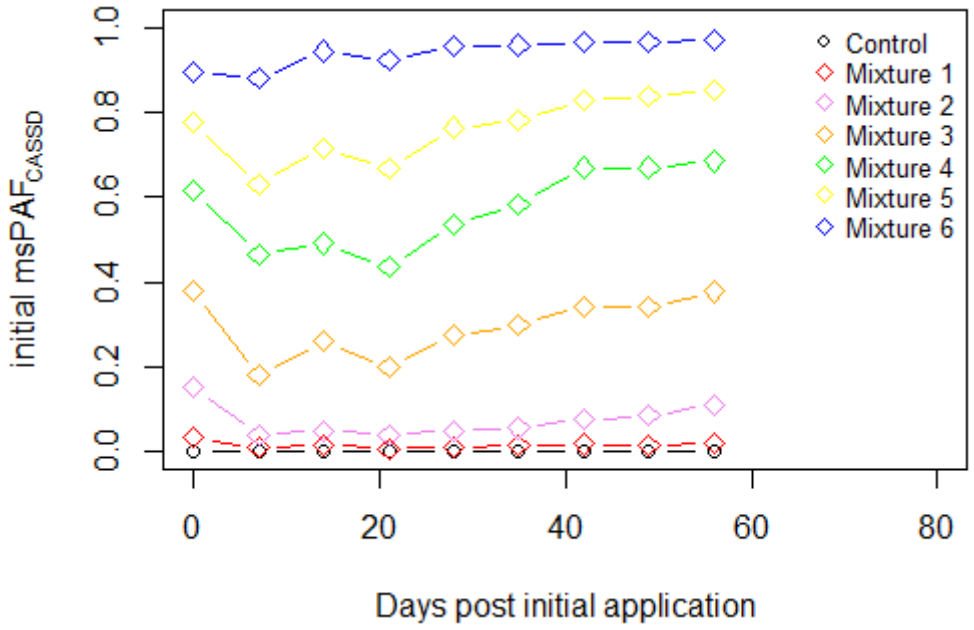

Figure 4.9. Overview of the change in initial msPAF$_{CASSD}$ values during the exposure period.

Conclusion

In the present study, a microcosm experiment was performed in which a freshwater planktonic community was exposed to a mixture of Cu, Ni and Zn with metal concentration ratio's based on the average dissolved metal concentrations found in a European river basin. The pattern of community-level effects of the mixture differed between the low mixture treatments, which should be regarded as Ni-Zn mixtures, and the high mixture treatments, which should be regarded as Cu-Ni-Zn mixtures. In the low mixture treatments (Ni-Zn mixtures), only effects on the phytoplankton community were observed. In these treatments, direct effects of the mixture on Cyanobacteria (mainly *Oscillatoria* sp. 1) were observed and the decrease in Cyanobacteria abundance led to an increase of the abundance of non-filamentous algae. In the high mixture treatments (Cu-Ni-Zn mixtures), more complex effects were

observed. Next to the direct effect on Cyanobacteria, the mixture also negatively affected Cladocera. In addition, although delayed in time, the mixture most likely also directly affected Copepoda and Rotifera abundance. Indirect effects were most likely attributed to reduced food and nutrient competition.

In our microcosm systems many structural community endpoints (e.g. community composition, species diversity, species richness) and one functional community endpoint (i.e. DOC) did not show effects at or below an msPAF value of 0.05 (i.e. these endpoints can be considered protective). For two other functional community endpoints however (i.e. ΔDO and ΔpH), effects at this msPAF value of 0.05, which is regarded as protective in many regulatory frameworks, were observed. For these two functional community endpoints, significant community-level effects were observed at an msPAF value of 0.03 (a Ni-Zn mixture) when the SSDs contained all species (i.e. both planktonic and non-planktonic) and at an msPAF value of 0.05 when the SSDs only contained planktonic species (phytoplankton and zooplankton). A likely explanation for the effects observed at or below this cut-off value of 0.05 is the mismatch between the species in the SSD and those in the microcosm community. Especially the presence of the cyanobacteria species *Oscillatoria* sp. 1 in our community, which is not represented in the SSD, seems to have been the driver for the observed effects on community-function at these low msPAF values. Although the decrease in abundance of *Oscillatoria* sp. 1 due to the direct effects of the Ni-Zn mixture resulted in an increase in abundance of other algae species, a significant decrease in community functioning was observed because the species was very dominant.

Our results show that SSDs are not necessarily a good predictor of effects on all types of communities and that the presence of dominant sensitive species may result in significant effects on community functioning endpoints at an msPAF value (0.05) that is generally considered protective. In addition, our results should only be extrapolated cautiously to other systems because information whether dominant species in other systems are typically also sensitive species is usually lacking and it is often the loss of species that are both dominant and sensitive that can result in a disproportionally large decrease in ecosystem functioning.

Part II

In Part II of this work, two additional limitations encountered in Chapter 2 were addressed. First, the bioavailability models that were used in Chapter 2 to normalize toxicity data were evaluated and improved (Chapter 5). Second, as these bioavailability models were based on different software to model speciation, we evaluated whether the chronic daphnid, fish and algae metal bioavailability models could all be updated to the WHAM VII speciation software, without loss of predictive capacity (Chapter 7).

In addition, we evaluated the impact of the implementation of the models developed in Chapter 5 and the update of all models to WHAM VII on risk estimations (Chapters 6 and 8).

For these four chapters in Part II, improved and newly developed bioavailability models for invertebrates and fish for the metals Cu and Zn in combination with the existing models for algae for Cu, Ni and Zn and for invertebrates and fish for Ni were used that have also been used in risk assessment procedures.

Five

TOXICITY OF SINGLE METALS TO SINGLE SPECIES: EVALUATION AND EXTENSION OF BIOAVAILABILITY MODELS

Section Five.One

CHRONIC CU *DAPHNIA MAGNA* BIOAVAILABILITY MODEL

Redrafted from:

Van Regenmortel T, Janssen CR, De Schamphelaere KAC. 2015. Comparison of the capacity of two biotic ligand models to predict chronic copper toxicity to two *Daphnia magna* clones and formulation of a generalized bioavailability model. Environmental Toxicology and Chemistry 34(7): 1597-1608

5.1. Chronic Cu Daphnia magna bioavailability model

Introduction

Biotic ligand models (BLM) have, during the past years, increasingly been used to account for the influence of water chemistry variables (e.g., pH, water hardness and dissolved organic carbon, DOC) in the evaluation of ecological risks of copper in surface waters. For instance, copper BLMs have been implemented to derive predicted no effect concentrations (PNEC) in the risk assessments performed in the European Union (E.U.) (ECI 2008) and in the derivation of Water Quality Criteria (WQC) in the United States (U.S.), including the Criteria Continuous Concentration (CCC) (US EPA 2007). Although both frameworks use a similar approach to derive bioavailability-based PNEC or WQC values for copper, there are some underlying differences. One of these differences is the structural formulation and parameterization of the BLMs used. The BLM used in the U.S. was originally developed based on gill binding and acute toxicity data for fish and has also been shown applicable to predict acute toxicity data to invertebrates, following calibration of a species-specific lethal accumulation on the biotic ligand (Santore et al. 2001; Di Tore et al. 2001). In addition, U.S. guidelines allow for the derivation of the CCC based on acute BLM output (i.e. acute WQC) by applying a single acute to chronic ratio (ACR), which is assumed constant across all species and water chemistries (U.S. EPA 2007). Thus, the acute BLM is essentially implemented as a chronic BLM. In comparison, the E.U. risk assessment of copper uses three different chronic BLMs depending on the taxonomic affiliation of the (chronic) toxicity test species. It uses a fish BLM to normalize fish toxicity data to site-specific water chemistry (De Schamphelaere and Janssen 2006) and an algae bioavailability model to normalize alga data (De Schamphelaere and Janssen 2008). Furthermore, it uses a specific chronic *Daphnia magna* copper BLM (De Schamphelaere and Janssen 2004), which was developed based on chronic toxicity data with *D. magna* and which was successfully cross-validated with other invertebrates (De Schamphelaere et al. 2006b; Van Sprang et al. 2008), to normalize chronic toxicity data for other invertebrates. These normalized toxicity data are then used concurrently with chronic toxicity data for algae and fish, also normalized with chronic bioavailability models for these specific groups (De Schamphelaere and Janssen 2006; De Schamphelaere and Janssen 2008), to calculate the PNEC (ECI 2008). Thus, in the E.U. risk assessment, specific chronic BLMs developed based on chronic toxicity are implemented.

The purpose of the present study was to evaluate the capacity of these two different copper BLMs (i.e. the ones used in the E.U. and U.S) to predict chronic toxicity of copper. For this purpose, a dataset of chronic copper toxicity to *D. magna* was compiled that contained 21-day 50% effective concentrations as dissolved copper (21-day EC50) and corresponding water chemistry of the test media for each of these. Subsequently, both the acute BLM (Santore et al. 2001; Di Toro et al. 2001) and the chronic *D. magna* BLM (De Schamphelaere and Janssen 2004) were evaluated using this dataset. It was hypothesized that the chronic *D. magna* BLM has a better predictive capacity than the acute BLM, since it was specifically developed based on chronic toxicity data with *D. magna* (De Schamphelaere and Janssen 2004).

Based on initial model comparisons it appeared that additional experiments were needed to directly compare the effect of pH on the chronic Cu toxicity to the two different *D. magna* clones represented in the dataset. The results of these experiments are also reported in the present paper. Finally, through a combination of all studies on both *D. magna* clones, we explored the ability of a generalized BioAvailability Model (gBAM) as an alternative for the existing BLMs to predict chronic effect concentrations for copper in both *D. magna* clones.

Materials and Methods

Comparison of BLM predictive capacity

Data selection.

To ensure that the data used for modeling was of high quality, different quality criteria were set to which the data was met. When measured metal concentrations were not reported or when important bioavailability influencing characteristics, such as DOC, were not measured, the data were not considered for use.

Chronic toxicity data were collected from the following 5 datasets. De Schamphelaere and Janssen (De Schamphelaere and Janssen 2004c) investigated the effect of organic carbon concentrations and source (3 types of natural organic matter, NOM), pH and water hardness on the chronic toxicity of copper to *D. magna* (K6 clone). A total of 35 test media were investigated. The water chemistry and corresponding 21-day EC50 values were taken from their Table 4. De Schamphelaere and Janssen (2004c) also reported on the 21-day toxicity of copper to *D. magna* (K6 clone) in 3 exposure media containing Aldrich humic acid at 3 different sodium concentrations. Chemical composition of the test media and corresponding 21-day EC50 values were taken from their Table 3. Rodriguez et al. (Rodriguez and Arbildua 2012) investigated the effect of hardness on the toxicity of copper to *D. magna* (ARO clone). In total, 3 test media, each with a different hardness level, were investigated. The water chemistry and corresponding 21-day EC50 values were taken from their Tables 5 and 1, respectively. Villavicencio et al. (2011) reported on the 21-day toxicity of copper to *D. magna* (ARO clone) in 20 spiked natural and 19 reconstituted waters. The chemical composition of these tested waters and the corresponding 21-day EC50 values were taken from their Table 3 and 4. Heijerick et al. (2002) reported on the chronic toxicity of copper to *D. magna* (K6 clone) in 10 spiked natural waters. Water chemistry was taken from their supplementary info and 21-day EC50 data were taken from their Tables 8, 10, 16, 18, 20, 22 and 26. All details on the chemical composition of the different test media used for modeling can be found in the online database (DOI: 10.1002/etc.2952; Supplementary 1). For the comparison of the predictive performances of the two BLMs, the data that were used to develop the UGent BLM, i.e. the chronic toxicity data with the 17 test media that contained “Ankeveen” Natural Organic Matter (NOM) reported by De Schamphelaere and Janssen (2004b) and the toxicity data obtained at 3 different sodium concentrations reported by De Schamphelaere and Janssen (2004c), were excluded from the dataset. As such, the comparison between both BLMs is done on the basis of model performance evaluations with a dataset that is independent from the development of both BLMs.

BLM modeling

To predict effect concentrations (21-day EC50s), we used the software BLM Version 2.1.2. (HydroQual 2005; incorporating WHAM 5 speciation software). In all cases, we maintained all stability constants for cation binding to the biotic ligand at their original values and only adjusted the critical accumulation of copper to the biotic ligand. Stability constants were taken from the parameter sets for the chronic Cu-BLM specifically developed for *D. magna* (K6 clone) (De Schamphelaere and Janssen 2004a; i.e. "Cu-BLM-3") or the acute Cu-BLM that was described by Santore et al. (2001), with addition of Mg^{2+} and $CuOH^{+}$ constants as described in the software (Malmberg and Maryott 1956). For simplicity, these two BLMs will be referred to as the "UGent BLM" and the "HydroQual BLM", respectively (Table 5.1). The critical accumulation value resulting in 50% reproductive inhibition, i.e. the intrinsic sensitivity or the EA50, was calibrated for all available *D. magna* EC50 data by using the input dataset constructed from the measured water chemistry (De Schamphelaere and Janssen 2004c; De Schamphelaere and Janssen 2004a; Rodriguez and Arbildua 2012; Villavicencio et al. 2011; Heijerick et al. 2002b) and subsequently calculating an 'average' EA50. How this was done is explained in detail in Appendix D (D1.1). The EA50 represents the amount of Cu bound to the biotic ligand that results in 50% effect and is expressed in nanomoles Cu per gram wet weight of the biotic ligand. After this calibration, the BLM was run using the calibrated EA50 value and the same input water chemistry dataset to make predictions of EC50s. When necessary, alkalinity was calculated based on pH, temperature and inorganic carbon (IC) (Stumm and Morgan 1996). Dissolved Organic Matter (DOM) was always assumed to consist of 50% carbon (on a weight basis). For the HydroQual BLM, the amount of natural DOM was assumed to be composed of 100 % active humic substances. Of these humic substances, 10% was assumed to be humic acid (HA) and 90% fulvic acid (FA) (default model inputs for HydroQual BLM, according to (Santore et al. 2001) and the BLM software (HydroQaul 2005)). For the UGent BLM, 50% of natural DOM was assumed to be composed of humic substances and of the latter 0% was assumed to be HA and 100 % FA (default model inputs for UGent BLM, according to De Schamphelaere et al. 2004c).
For example, for running the 2 BLMs with the BLM software (HydroQual 2005) for a medium in which 3.6 mg DOC/L was measured in test medium, 3.6 mg DOC/L and 10% HA were set as model inputs for the HydroQual BLM while 1.8 mg DOC/L and 0% HA were set as inputs for the UGent BLM. Additions of DOC to media in the form of Aldrich humic acid (AHA, Sigma Aldrich Chemie, Steinheim, Germany) were assumed to be 100% humic acid for both BLMs, in accordance with De Schamphelaere and Janssen 2004a. Inorganic binding constants used by both BLMs are also slightly different. These differences can be found in the online database (DOI: 10.1002/etc.2952; Supplementary 3).
The predicted effect concentrations were first compared with observed effect concentrations based on free ion concentrations. Subsequently, the relations between pH, Ca^{2+}, Mg^{2+} , Na^{+} activities and observed effect concentrations expressed as free ion activities were examined. Since free ion activities are not provided as BLM output, Cu^{2+}, Ca^{2+}, Mg^{2+} and Na^{+} activities were calculated with the Davies Equation (Stumm and Morgan 1996; Malmberg and Maryott 1956) as explained in Appendix D (D1.2).
Finally, predicted chronic 21-day EC50 values were compared with observed 21-day EC50 values to evaluate the predictive capacity of both BLMs.

Table 5.1. Biotic ligand model (BLM) copper constants, competition constants, thermodynamic parameters, and humic material assumptions of the UGent BLM (De Schamphelaere and Janssen 2006) and HydroQual BLM (Santore et al. 2001; Di Toro et al. 2001) that were used for modeling, as well as parameter values for all generalized bioavailability models (gBAM) used

Parameter	UGent BLM *Daphnia magna* (chronic)	HydroQual BLM All organisms (acute)	gBAM-A			gBAM-B			gBAM-C		
			gBAM-A_{K6}	gBAM-A_{ARO}	gBAM-A_{uni}	gBAM-B_{K6}	gBAM-B_{ARO}	gBAM-B_{uni}	gBAM-C_{K6}	gBAM-C_{ARO}	gBAM-C_{uni}
Biotic ligand (BL) species											
Log K_{CuBL}	8.02[a]	7.4 [a]	NA	NA	NA	NA	NA	NA	NA	NA	NA
Log K_{CuHBL}	8.02[b] (–0.5)	6.22 [b, c] (–1.3)	NA	NA	NA	NA	NA	NA	NA	NA	NA
Log K_{CuCO_3BL}	7.44[d] (–14.21)	NA	NA	NA	NA	NA	NA	NA	NA	NA	NA
Log K_{CaBL}	NA	3.6	NA	NA	NA	NA	NA	NA	3.53	3.53	3.53
Log K_{MgBL}	NA	3.6[c]	NA	NA	NA	NA	NA	NA	3.53	3.53	3.53
Log K_{HBL}	6.67	5.4	NA	NA	NA	NA	NA	NA	NA	NA	NA
Log K_{NaBL}	2.91	3	NA	NA	NA	2.67	2.67	2.67	2.67	2.67	2.67
S_{pH}	NA	NA	0.77	0.53	0.65	0.77	0.53	0.65	0.77	0.53	0.65
Q_{50}, K6 clone	NA	NA	2.73	NA	3.59	3.24	NA	4.04	3.46	NA	4.38
Q_{50}, ARO clone	NA	NA	NA	5.08	4.12	NA	5.21	4.24	NA	5.52	4.55
Bioavailable species that can bind to the biotic ligand	Cu^{2+}, $CuOH^+$, $CuCO_3^0$	Cu^{2+}, $CuOH^+$	NA	NA	NA	NA	NA	NA	NA	NA	NA
Thermodynamic database											
pK_{MHA} Cu-HA	1.9	1.5	1.9	1.9	1.9	1.9	1.9	1.9	1.9	1.9	1.9
pK_{MHA} CuOH-HA	1.9	1.5	1.9	1.9	1.9	1.9	1.9	1.9	1.9	1.9	1.9
log K for $CuCO_3^0$ (aq)	6.77	6.75	6.77	6.77	6.77	6.77	6.77	6.77	6.77	6.77	6.77
log K for $Cu(CO_3)_2^{-2}$ (aq)	10.2	9.92	10.2	10.2	10.2	10.2	10.2	10.2	10.2	10.2	10.2
log K for $CuHCO_3^+$ (aq)	12.13	14.62	12.13	12.13	12.13	12.13	12.13	12.13	12.13	12.13	12.13
Humic material assumptions											
% of natural DOM composed of humic substances[e]	50%	100%	50%	50%	50%	50%	50%	50%	50%	50%	50%
% of the humic substances that is HA (rest is FA)[f]	0%	10%	0%	0%	0%	0%	0%	0%	0%	0%	0%

[a] Reaction: BL-Cu = Cu^{2+} + BL; [b] First constant refers to the reaction: BL-CuOH = $CuOH^+$ + BL. The constant in parentheses refers to the reaction BL-CuOH + H^+ = Cu^{2+} + H_2O + BL; [c] These constants were not reported in Santore et al. (2001) but are described in the BLM software (HydroQaul 2005); [d] First constant refers to the reaction: BL-$CuCO_3$ = $CuCO_3^0$ + BL. The constant in parentheses refers to the reaction BL-$CuCO_3$ = Cu^{2+} + CO_3^{2-} + BL; [e] Exception: When humic acid is added to the medium, all models assume 100% of the DOM to be composed of humic substances; [f] Exception: When humic acid is added to the medium, all models assume 100% of the humic substances to be composed of humic acid; NA = not applicable as constant in the UGent BLM, HydroQual BLM, or gBAM; DOM = dissolved organic matter; HA = humic acid; FA = fulvic acid.

Experimental testing of two D. magna *clones*

Preparation of test media.

To investigate the individual effect of pH on chronic copper toxicity to two *D. magna* clones, tests were conducted in synthetic test solutions, based on the M4 medium (Muyssen and Janssen 2001). All test solutions were prepared using deionized water and reagent-grade chemicals purchased from VWR International. The M4 medium was modified compared to its original composition (Muyssen and Janssen 2001) as follows: the background Zn concentration was increased to 13 µg/L as the original concentration (6 µg/L) causes Zn deficiency (Elendt and Bias 1990), hardness was reduced to 180 mg $CaCO_3$/L (keeping the Ca:Mg ratio at its original value), EDTA was omitted and replaced with Bihain River NOM (Ruisseau de Saint Martin, Belgium) at a nominal concentration of approximately 5 mg DOC/L. Tests were conducted at pH 6.5 and pH 8.3. Test solutions were adjusted to the required pH of 6.5 by adding 3-N-morpholinopropanesulfonic acid (MOPS) and the required amount of NaOH or HCl. MOPS has the property not to affect metal speciation (Kandegedara and Rorabacher 1999), nor is it toxic or does it affect Cu toxicity to freshwater organisms (De Schamphelaere et al 2004). Because the buffering capacity of MOPS is restricted to a pH range of 6.5 – 7.9 (pK_a = 7.2), test solutions for pH 8.3 were adjusted to the required pH by adding $NaHCO_3$ (3 mmol/L) and the required amount of NaOH or HCl. For each test, a copper concentration series was prepared by adding $CuCl_2$. Each test series consisted of a control treatment and 7 or 8 copper treatments. For the test at pH 6.5 the following nominal Cu concentrations were used: 20, 28, 40, 57, 80, 113 and 160 µg/L for the K6 clone and 13, 20, 28, 40, 57, 80, 113 and 160 µg/L for the ARO clone. For the test at pH 8.3 the following nominal Cu concentrations were used: 40, 57, 80, 113, 160, 226 and 320 µg/L for both clones. To allow equilibration, solutions were spiked with copper 48 hours prior to testing.

Daphnia magna chronic toxicity testing.

Toxicity tests were performed with 2 *D. magna* clones. The K6 clone was originally collected from a pond in Kiel (Antwerp, Belgium) and has been cultured at the Laboratory for Environmental Toxicology and Aquatic Ecology (University of Ghent, Belgium) for the past 20 years under standardized conditions. The culture medium consisted of aerated and filtered Ghent (Belgium) city tap water to which a selenium (0.1 µg/L) and vitamin solution (7.5 mg/L thiamine, 100 µg/L cyanocobalamin and 75 µg/L biotin) was added (pH 7.7, DOC 2.1-3.3 mg/L, hardness 127-136 mg/L as CaCO3). The ARO clone was obtained from the Chilean Mining and Metallurgy Research Center (CIMM) who purchases the clone from Aquatic Research Organisms (Hampton, New Hampshire, USA). At the moment we received the ARO clone, it had been cultured at CIMM for one-and-a-half years. For both clones, cultures were kept at 20 ± 1 °C, with a 12:12 light:dark photoperiod. Daphnids were maintained in 5 L culture glass vessels with 4 L medium, each containing 200 individuals. The medium was changed 3 times a week. The daphnids were fed with a mixture

of *Pseudokirchneriella subcapitata* and *Chlamydomonas reinhardtii* in a 3:1 ratio based on cell number (3.75×10^6 cells/daphnid from day 0 to day 8 and 7.5×10^6 cells/daphnid from day 9 onward).

Prior to testing, all organisms from both clones were acclimated to the test media (i.e. pH 6.5 or pH 8.3) without extra copper for 1 generation. In that way individuals used in the actual tests were offspring from mothers that had been held in the test medium since their birth. Nominal concentrations of major cations and anions in the medium were 57.7 mg Ca/L, 8.8 mg Mg/L, 17.9 mg Na/L, 3.2 mg K/L, 35 mg SO_4/L and 91.7 mg Cl/L.

Chronic *D. magna* tests were performed according to the Organization of Economic Cooperation and Development test guideline 211 (OECD 2012). For each treatment, 10 juvenile animals (< 24h old) were held individually in polyethylene cups containing 50 mL of test medium. Animals were fed daily with an algal mixture of *P.subcapitata* and *C. reinhardtii* in a 3:1 ratio (based on cell number). Each cup received 250, 500 or 750 µg dry weight of food per day in the first, second and third week of exposure, respectively. The total duration of the test was 21 days. Tests were started on Tuesday and the medium was renewed and parent mortality and number of produced juveniles was counted on Friday of the first week and every Monday, Wednesday and Friday during the subsequent weeks.

Chemical analysis.

From the toxicity test vessels, samples of fresh (sample of new medium just before transfer of daphnids to the cup) and old (sample taken of medium just after transfer of daphnids to a new cup) test medium were collected regularly for analysis of Cu, IC and organic carbon (OC). Total and dissolved Cu (0.45 µm, Gelman Sciences, Ann Arbor, MI, USA) samples of fresh medium were taken on day 0, 7, 14 and 19. Dissolved Cu samples of old medium were taken on day 2, 9, 16 and 21. The copper samples were acidified to 0.14 mol/L HNO_3 (Normaton quality, VWR International) immediately after sampling. Copper concentrations were measured using flame atomic absorption spectrophotometry (SpectrAA800; Varian; reference material TMDA-70; for nominal concentrations > 50 µg Cu/L; Limit of Quantification 60 µg Cu/L; Method Detection Limit 20 µg Cu/L) or graphite furnace atomic absorption spectrophotometry (GFAAS Furnace Autosampler, Thermo Fisher Scientific; reference material TM-24.3; for nominal concentrations < 50 µg Cu/L; Limit of Quantification 1 µg Cu/L; Method Detection Limit 0.3 µg Cu/L). Calibration standards and a reagent blank were analyzed with every 25 samples. Inorganic carbon and dissolved organic carbon (DOC) samples were taken on day 0, 3, 7, 9, 14, 16 and 21. These samples were analyzed with a Total Organic Carbon analyzer following the NPOC method (TOC-5000, Shimadzu; Limit of Quantification 1.5 mg DOC/L; Method Detection Limit 0.5 mg DOC/L). The NPOC method (Non-Purgeable Organic Carbon) entails that after purging the sample with air (to remove inorganic carbon), the remaining organic carbon is measured. The pH of fresh medium was measured on day 0, 7, 14 and 21 and that of old medium on day 2, 9, 16 and 23. Measurements of pH were performed with a pH glass electrode (P407, Consort).

Data treatment and analysis.

Effect concentrations (21-day EC10, EC20 and EC50) were calculated based on average dissolved Cu concentrations in fresh and old test media. The dissolved copper concentrations in old test medium was 33% lower than in fresh medium at pH 6.5 and 35% lower at pH 8.3. The total reproduction (i.e. number of offspring per female) was used as endpoint. The mean number of offspring in the control treatment was always greater than 60, as is prescribed by OECD guideline 211 (2012). Effect concentrations and corresponding confidence intervals were determined with the drc-package in R 2.15.2 (R Development Core Team) with a Weibull concentration response model with three parameters (Equation 5.1), as this best fitted our concentration-response data (i.e. highest log likelihood).

$$y = d \times \exp(-\frac{x}{k})^b \quad (5.1)$$

Where y = predicted reproduction (number of offspring per female), d = the value of the maximal response (i.e. in the control), b = a slope parameter, k = a scale parameter and x = the dissolved Cu concentration (µg/L). The function *drm* in R 2.15.2 was used to calculate the ECx values.

Results and Discussion

Comparison of BLM predictive capacity

Across the entire *D. magna* chronic toxicity dataset, measured 21-day EC50 values ranged from 7.4 to 367 µg/L. First, a single EA50 value was calibrated to this entire dataset for both BLMs. For the UGent and HydroQual BLM this value was 7.01 nmol/g and 0.046 nmol/g, respectively. All parameter files for running the models in the BLM software (HydroQual 2005) are available in the online database (DOI: 10.1002/etc.2952; Supplementary 3).

Predictions of copper toxicity to *D. magna* with both BLMs were compared with observed 21-day EC50 values. The UGent BLM predictions for chronic toxicity are plotted in Figure 5.1A. The UGent BLM was able to predict 79% of the toxicity data within twofold error and showed a mean prediction error of 1.7-fold. In comparison, the HydroQual BLM predictions for chronic toxicity are plotted in Figure 5.1B. The model was able to predict 63% of the toxicity data within twofold error and showed a mean prediction error of 2.4-fold. These results suggest that the UGent BLM is able to predict chronic toxicity somewhat more accurately than the HydroQual BLM. However, when examining Figure 5.1 in more detail, a bias is noted in the relation between observed and predicted 21-day EC50 values for both models. The UGent BLM predicts the higher 21-day EC50 values more accurately, while the HydroQual BLM predicts lower 21-day EC50 values better. Furthermore, regardless of the BLM that is used for making predictions, the data points appear to cluster in two groups, with each group corresponding to one of the two clones used in the datasets. The ARO and the K6 clone data cluster at lower and higher observed EC50 values, respectively. Rodriguez et al. (2012) and Villavicencio et al. (2011) used the *D. magna* ARO clone in all their toxicity tests while De Schamphelaere and Janssen (2004b) and Heijerick et al. (2002) always used the *D. magna* K6 clone.

Without doing a more in-depth analysis, one could attribute this clustering to two factors. First, one could attribute it to differences in bioavailability conditions between the toxicity tests done with the K6 clone and the ARO clone. Indeed, in most tests with the ARO clone copper could have been generally more bioavailable (e.g., due to lower DOC concentrations), relative to the conditions in which the K6 clone was tested. Second, one could also attribute this clustering could also be due to the fact that these two *D. magna* clones exhibit differences in their intrinsic sensitivity to copper (due to genetic differences), as has been shown extensively in several other metal toxicity studies (Baird et al. 1991; Barata et al. 1998; Muyssen et al. 2002; Bossuyt and Janssen 2005; Messiaen et al. 2013). To be able to discriminate between those two factors, we repeated our calculations, but now by calibrating a separate intrinsic sensitivity for both clones, followed by BLM toxicity predictions.

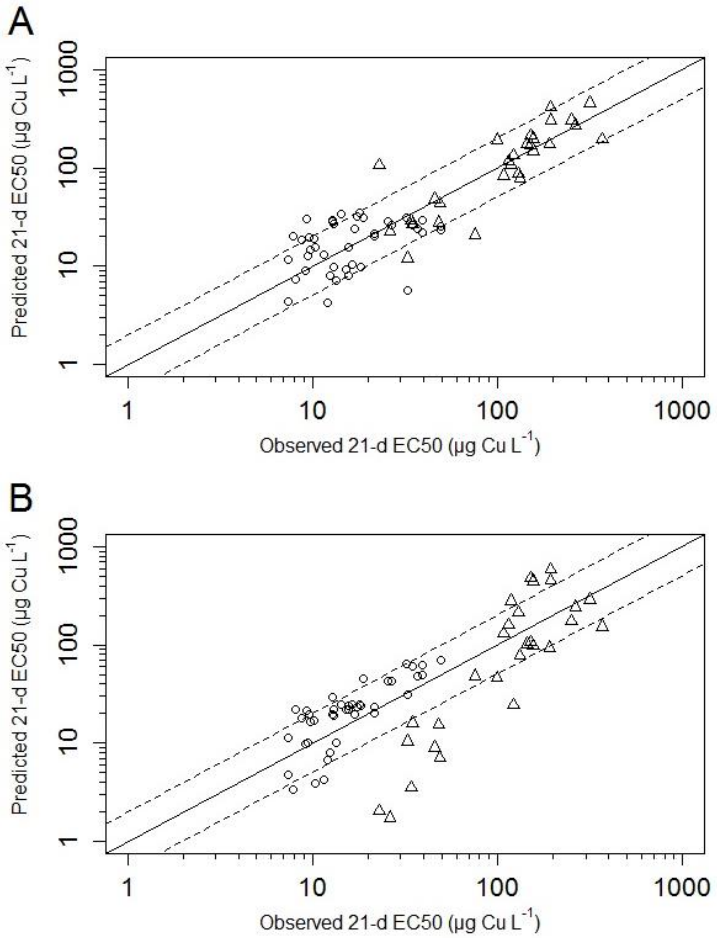

Figure 5.1. Predictive capacity of the UGent (A) and HydroQual (B) biotic ligand models (BLMs) as shown by observed versus predicted 21-d 50% effective concentrations (EC50s) of copper to *Daphnia magna* (K6 clone [triangles] and ARO clone [circles]). The solid line is the 1:1 reference line indicating a perfect match between observed and predicted values; the dashed lines indicate an error of a factor of 2 between observed and predicted values. UGent BLM = the chronic *D. magna* BLM (De Schamphelaere and Janssen 2006); HydroQual BLM = the acute BLM (Santore et al. 2001; Di Toro et al. 2001).

The obtained intrinsic sensitivities for each clone separately are given in Appendix D (D1.3) and are 7.70 nmol/g (K6 clone) and 6.57 nmol/g (ARO clone) for the UGent BLM and 0.089 nmol/g (K6 clone) and 0.031

nmol/g (ARO clone) for the HydroQual BLM. Again, the predictions of copper toxicity to the two *D. magna* clones by both BLMs were compared with measured 21-day EC50 values. The UGent BLM predictions are plotted in Figure 5.2A. The UGent BLM was now able to predict 77% of all data within twofold prediction error (mean prediction error = 1.7-fold). However, when the data with the K6 and ARO clone were considered separately, it was clear that the model more accurately predicted the K6 clone data than the ARO clone data (82% and 74% within twofold error, respectively and 1.6-fold and 1.8-fold mean prediction error, respectively). The HydroQual predictions can be found in Figure 5.2B. The HydroQual BLM now predicted 70% within twofold prediction error (mean prediction error = 2.0-fold). However, considering the data with both clones separately shows that this model more accurately predicted the ARO clone data than the K6 clone data (83% and 50% within twofold error, respectively and 1.6-fold and 2.6-fold mean prediction error, respectively).

In addition to possible differences in intrinsic sensitivity between *D. magna* clones, it is recognized that metal sensitivities of *D. magna* laboratory populations may change with time (i.e. between two or more studies performed in the same laboratory, but separated in time (e.g. Deleebeeck et al. 2008; Baird and Barrate 1997)) which could be due to differences in culture environment (e.g. temperature, food). Therefore, it is recognized that this should also be accounted for. To explore the influence of this on the predictive capacity of both BLMs, we also calculated intrinsic sensitivities per clone and per study (for the UGent BLM these are 5.76 nmol/g for the study by De Schamphelaere and Janssen (2004b), 3.98 nmol/g for Rodriguez and Arbildua (2012), 6.81 nmol/g for Villavicencio et a. (2011) and 12.10 nmol/g for Heijerick et al. (2002); for the HydroQual BLM these are equal to 0.058 nmol/g for the study by De Schamphelaere and Janssen (2004b), 0.15 nmol/g for Rodriguez et al. (2012), 0.027 nmol/g for Villavicencio et al. (2011) and 0.16 nmol/g for Heijerick et al. (2002)). The obtained intrinsic sensitivities can also be found in Appendix D (D1.3). The UGent BLM was now able to predict 81% of all data within twofold prediction error (mean prediction error = 1.7-fold) (Appendix D1.4). However, when the data with the K6 and ARO clone were considered separately, 93% of the K6 clone and 74% of the ARO clone data were predicted within twofold error (mean prediction error = 1.6-fold and 1.8-fold, respectively). The HydroQual BLM predicted 76% within twofold prediction error (mean prediction error = 1.6-fold). However, considering the data with both clones separately showed 91% of the ARO clone data and 54% of the K6 clone data were predicted within twofold error (mean prediction error = 1.3-fold and 2.5-fold, respectively). Based on all these comparisons, it is clear that the predictive capacity of both BLMs is considerably influenced by the clone considered. The UGent BLM, which was developed based on a K6 clone chronic toxicity dataset, performs best for this clone. The HydroQual BLM on the other hand, which has the same stability constants as the acute fish BLM, performs best for the ARO clone. This strongly suggests that both BLMs not only differ in how they take into account the influence of water chemistry for predicting chronic copper toxicity, but also that the two clones differ in how copper bioavailability to them is influenced by water chemistry.

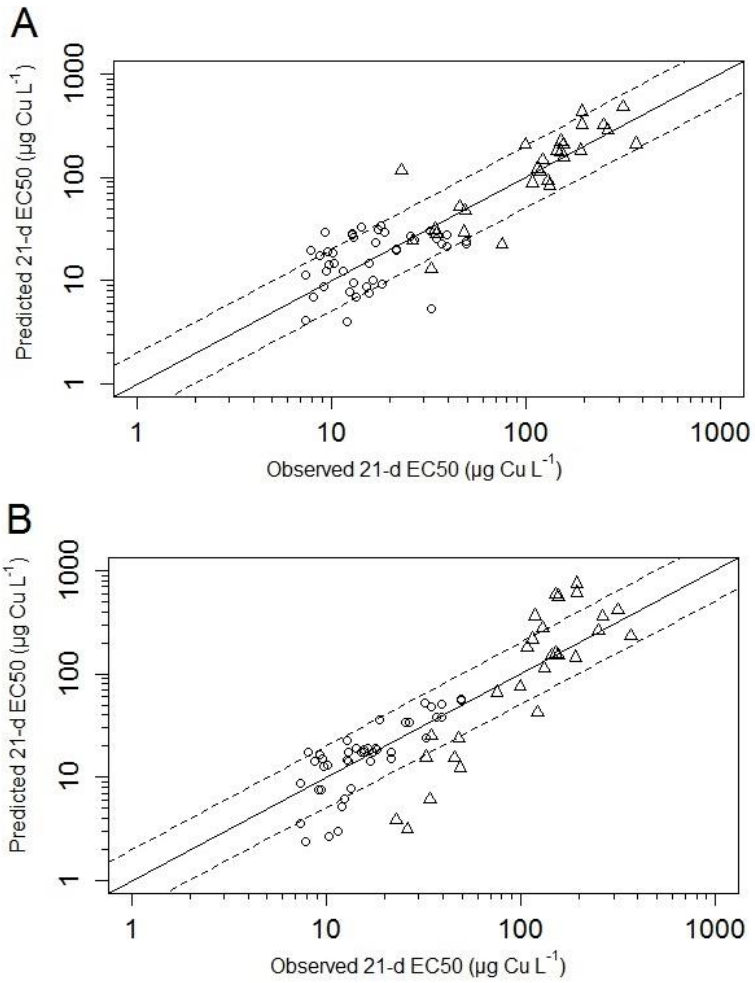

Figure 5.2. Predictive capacity of the UGent (A) and HydroQual (B) biotic ligand models (BLMs) as shown by observed versus predicted 21-d 50% effective concentrations (EC50s) of copper to *Daphnia magna*. Intrinsic sensitivities of the BLMs were calculated from data grouped by *D. magna* clone (K6 clone [triangles] and ARO clone [circles]). The solid line is the 1:1 reference line indicating a perfect match between observed and predicted values; the dashed lines indicate an error of a factor of 2 between observed and predicted values. UGent BLM (De Schamphelaere and Janssen 2006); HydroQual BLM = the acute BLM (Santore et al. 2001; Di Toro et al. 2001).

To investigate these differences in more detail, we examined the relation between logarithmic model-measurement deviations (i.e. log observed EC50 – log predicted EC50; further denoted O/P) and the chemistry of the test media for the two BLMs and two clones. To this end, the correlation (r^2) was determined between O/P and pH, Na^+ activity, Ca^{2+} activity and Mg^{2+} activity. Figure 5.3 shows that there is a clear difference in how both BLMs account for copper bioavailability with increasing pH. According to the UGent BLM O/P data, the influence of pH on the Cu toxicity to the K6 clone is appropriately accounted for by the UGent BLM, whereas the toxicity to the ARO clone is underestimated at pH < 8 and overestimated at pH > 8. The opposite is seen for the HydroQual BLM O/P data. Here the influence of pH on the Cu toxicity to the ARO clone data is appropriately accounted for by the HydroQual BLM whereas toxicity to the K6 clone is underestimated at pH < 7 and overestimated at pH > 7. The influence of the other physico-chemical parameters on the responses of the two clones is not as clear as for pH (smaller r^2 or non-significant

correlation). These results indicate that there is a fundamental difference between both BLMs in how they predict the change of bioavailability of Cu with increasing pH. To illustrate this further we performed simulations with both BLMs using the original intrinsic sensitivity values of these BLMs (i.e. 11.78 nmol/g for the UGent BLM and 0.069 nmol/g for the HydroQual BLM). For the BLM input file, the average water chemistry of all the toxicity data (De Schamphelaere and Janssen 2004c; De Schamphelaere and Janssen 2004a; Rodriguez and Arbildua 2012; Villavicentio et al. 2001; Heijerick et al. 2002b) was used, i.e. 5.8 mg DOC/L, 49.6 mg Ca/L, 11.2 mg Mg/L, 80.0 mg Na/L, 2.4 mg K/L, 67.9 mg SO_4/L and 148,7 mg Cl/L. However, the pH was varied between 5.5 and 8.5 and the alkalinity was calculated based on this pH value (Stumm and Morgan 1996). Results from these simulations can be seen in Figure 5.4, from which it is again clear that both BLMs differ in how they predict changes of bioavailability of Cu with increasing pH.

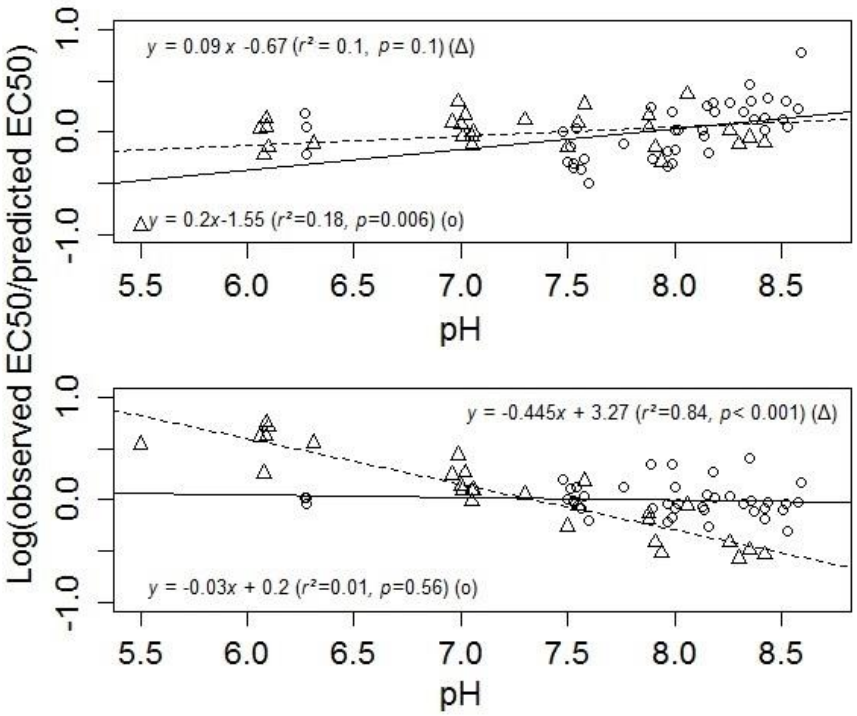

Figure 5.3. Logarithmic differences of the observed and predicted 21-d 50% effective concentrations (EC50) of copper to *Daphnia magna* [i.e., log(observed EC50) – log(predicted EC50)] against pH for the UGent biotic ligand model (BLM; top) and HydroQual BLM (bottom) for the 2 clones (K6 clone [triangles] and ARO clone [circles]). Predicted EC50s were calculated with intrinsic sensitivities calculated per clone and per study. See Appendix D.4 for the plot of the corresponding observed 21-d EC50s versus predicted 21-d EC50s.

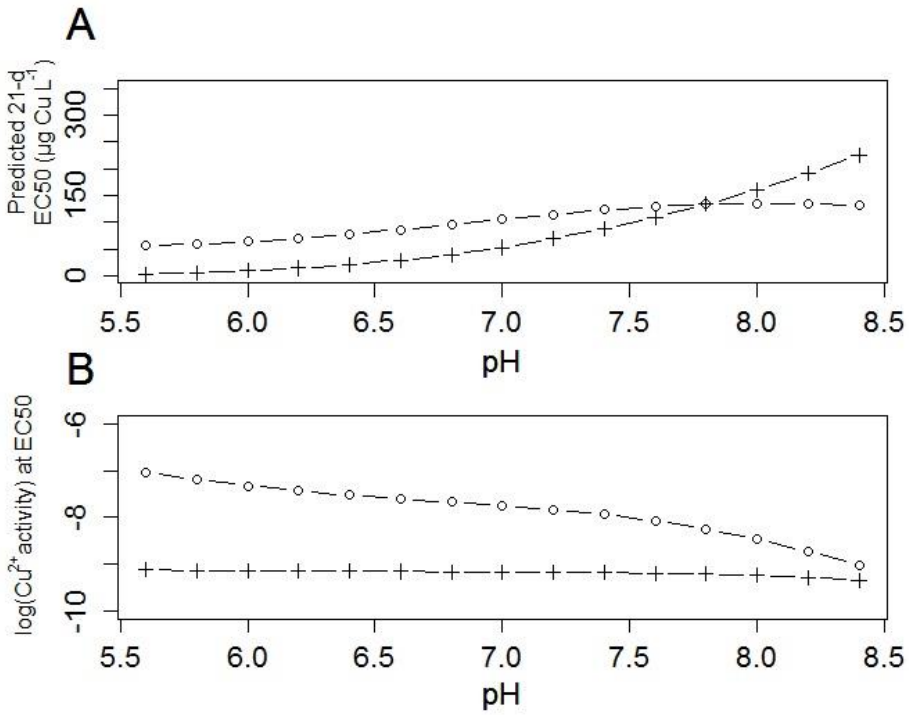

Figure 5.4. Influence of pH on the predictive capacity of the UGent (circles) and HydroQual (plus signs) biotic ligand models (BLMs) as shown by (A) the predicted 21-d 50% effective concentrations (EC50s) of copper to *Daphnia magna* and (B) the free Cu^{2+} ion activity at the predicted 21-d EC50s of copper to *Daphnia magna*. Water chemistry input for the BLMs was held constant at the average water chemistry of all the toxicity data (De Schamphelaere and Janssen 2004c; De Schamphelaere and Janssen 2004a; Rodriguez and Arbildua 2012; Villavicencio et al. 2011), with the exception of pH, which was varied between 5.5 and 8.5. UGent BLM (De Schamphelaere and Janssen 2006); HydroQual BLM = the acute BLM (Santore et al. 2001; Di Toro et al. 2001).

To investigate this difference even further, we examined the linear relations between $\log_{10}$(21-day $\mathrm{EC50}_{Cu^{2+}}$) versus pH for both *D. magna* clones (Figure 5.5A). However, a correlation between pH and Na^+ activity in certain datasets was observed. This correlation could influence the analysis of the relation between the copper toxicity and pH of the water, and thus the interpretation of the effect of pH on copper toxicity to both clones. Therefore, the Cu^{2+} activity was "corrected" for the sodium effect (Figure 5.5B) (Equation 5.2).

$$EC50^{*}_{Cu^{2+}} = \frac{EC50_{Cu^{2+}}}{1 + K_{NaBL} \times (Na^{+})} \quad (5.2)$$

Where $\mathrm{EC50}_{\mathrm{Cu^{2+}}}$ = the observed 21-day EC50 as Cu^{2+} activity $(\mathrm{mol \cdot L^{-1}})$, $(\mathrm{Na^{+}})$ the sodium activity $(\mathrm{mol \cdot L^{-1}})$ and $\mathrm{K_{NaBL}}$ = the competition constants for sodium of 471 $(\mathrm{L \cdot mol^{-1}})$ (Log K_{NaBL} = 2.67), taken from a study by De Schamphelaere and Janssen (2004a).

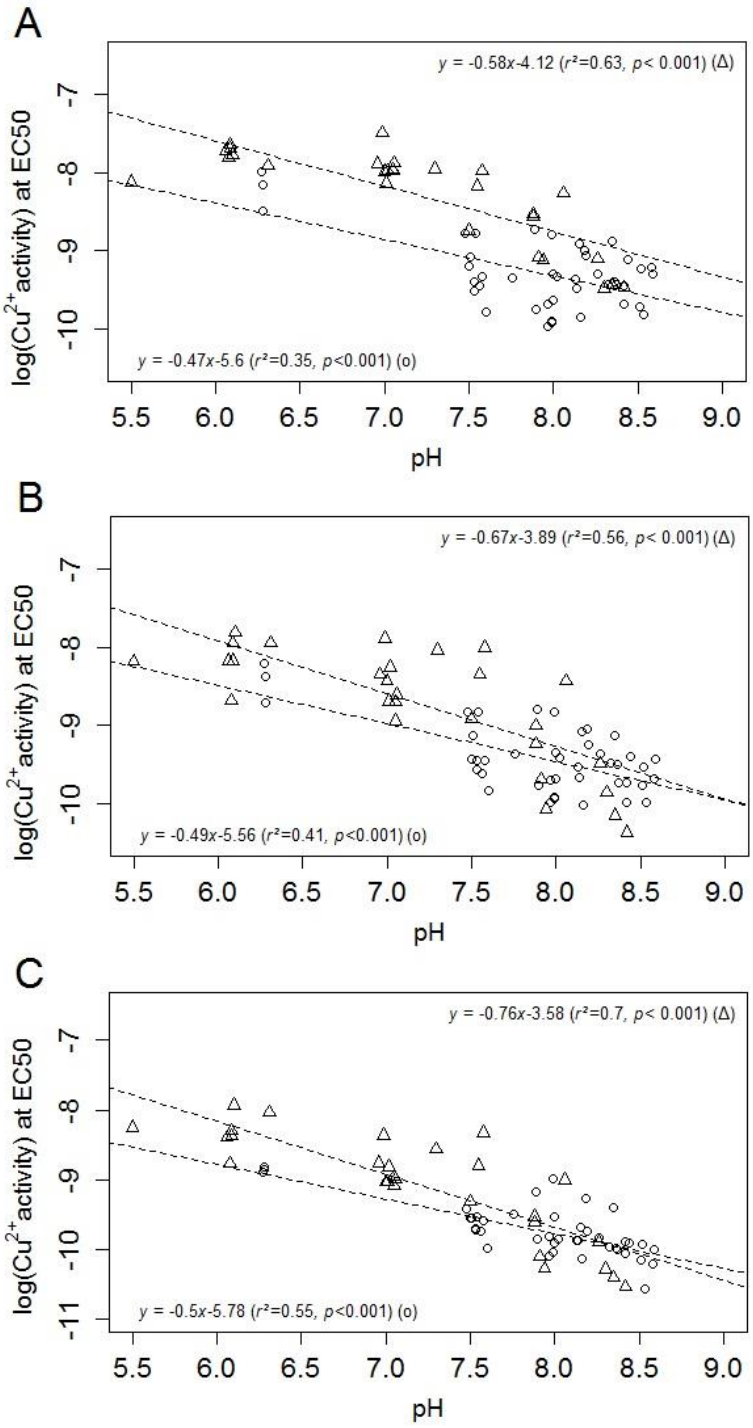

Figure 5.5. Free Cu^{2+} ion activity at the 21-d 50% effective concentration (EC50) as a function of pH for the K6 (triangles) and ARO (circles) *Daphnia magna* clone. (A) Chronic toxicity data from the studies used to compare the UGent and HydroQual BLM (De Schamphelaere and Janssen 2004c; De Schamphelaere and Janssen 2004a; Rodriguez and Arbildua 2012; Villavicencio et al. 2011), with exclusion of the data used to develop the UGent BLM; (B) same data as panel (A) with correction of the Cu^{2+} activity for the sodium effect (Equation 5.2) and (C) same data as panel (A) with correction of the Cu^{2+} activity for the sodium, calcium, and magnesium effects (Equation 5.3).

Further examination of the data showed us a correlation between pH and Mg^{2+} and Ca^{2+} activity. This correlation could also influence the analysis of the relation between the copper toxicity and pH of the water, and thus the interpretation of the effect of pH on copper toxicity to both clones. The Cu^{2+} activity was therefore corrected for the sodium, calcium and magnesium effects (Figure 5.5C) (Equation 5.3).

$$EC50^{**}_{Cu^{2+}} = \frac{EC50_{Cu^{2+}}}{1+(K_{NaBL}\times(Na^{+})+K_{CaBL}\times(Ca^{2+})+K_{MgBL}\times(Mg^{2+}))} \quad (5.3)$$

Where $EC50_{Cu^{2+}}$ = the observed 21-day EC50 as Cu^{2+} activity (mol x L^{-1}), (Na^{+}), (Ca^{2+}) and (Mg^{2+}) are the sodium, calcium and magnesium activities (mol x L^{-1}), K_{NaBL}= the competition constant for sodium (mol x L^{-1}) and K_{CaBL} and K_{MgBL} are the competition constants for calcium and magnesium of 3409 (mol x L^{-1}) (Rodriguez and Arbildua 2012), respectively. The latter two were calculated based on data by Rodriguez and Arbildua (2012). These authors have demonstrated a significant effect of hardness on chronic copper toxicity in a univariate experiment with the ARO clone, although the effect is considerably smaller than its effect on acute toxicity. The competition by Ca and Mg ions may be of a specific chemical nature (De Schamphelaere and Janssen 2004a), but may also take place at specific membrane transporter uptake routes (e.g. Divalent Metal Transporters (DMI)) (Deleebeeck et al. 2007a). These constants were calculated according to De Schamphelaere and Janssen (Grosell 2011) by performing a linear regression between the 21-day $EC50_{Cu^{2+}}$ and the sum of the Mg^{2+} and Ca^{2+} activities. Both Mg^{2+} and Ca^{2+} were evaluated together because their activities in this experiment were correlated as a consequence of the experimental test design. The values of both constants were assumed the same as no data was available to determine separate values.

The results shown in Figure 5.5 suggest a different effect of pH on chronic Cu toxicity for the two *D. magna* clones that should be further investigated. As mentioned earlier, this different effect of pH could be attributed to one of the following: (1) there are true inter-clonal differences due to genetic factors or (2) the observed differences are due to differences in experimental design, i.e. the clones could respond differently to pH because the clone K6 was tested in other experimental conditions (e.g., most media were pH buffered with a strong pH buffer) than the ARO clone (most test media were not strongly pH buffered). Indeed, the latter has recently been examined by Esbaugh and colleagues (Esbaugh et al. 2013) who tested the effect of three pH buffer methods on the acute toxicity of Pb to *P. promelas*. They found that a strong pH buffer (MOPS, also used in our experiments) had a large impact on the acute Pb toxicity. However, we believe that their results do not necessarily apply to our study because of the following reasons: (a) tests were performed on lead, (b) their three buffer methods were not tested simultaneously and with different batches of fish test populations and (c) the ion concentrations (e.g. Ca concentrations) in the test water of the MOPS-tests were lower than those of the other two buffers which could have influenced the LC50. Furthermore, De Schamphelaere et al. (OECD 2012) demonstrated that when evaluating the effect of using MOPS and $NaHCO_3$ pH buffering on acute Cu (and Zn) toxicity to *D.magna*, there was no significant difference observed between MOPS or $NaHCO_3$ buffered test media. Since acute to chronic ratios are low for copper for *D. magna* (ECI 2008), it is reasonable to believe that the use of 750 mg/L MOPS in chronic experiments (as was done for all K6 clone tests) does not influence the chronic copper toxicity to *D. magna*. However,

in order to exclude this explanation further and to be conclusive on the above, we performed an additional experiment to test if the difference in effects of pH on chronic Cu toxicity among both clones suggested by this modeling effort could be attributed to true inter-clonal differences (i.e. genetic factors) by excluding the experimental differences. This was done by testing both clones simultaneously and in exactly the same conditions in a single laboratory (UGent).

Experimental testing of two D. magna clones

Physico-chemical composition of the test media and 21-day EC10, EC20 and EC50 are given in Table 5.2. The control reproduction in all chronic toxicity assays was > 60 offspring per parent animal surviving after 21 days and parental mortality was less than 20%, as is required by the OECD guideline (OECD 2012). At a pH of 6.5, the K6 clone had a significantly higher 21-day ECx than the ARO clone ($p < 0.05$, Wheeler test, Wheeler et al. 2006), indicating clonal differences in sensitivity to copper of approximately 2-fold. However, this difference is not observed at a pH of 8.3, which emphasizes the importance of examining interclonal sensitivity differences at different physico-chemical compositions. As mentioned before, clonal differences in sensitivity have been studied extensively. However, most studies have focused on clonal differences at a single physico-chemical test medium composition (Baird et al. 1991; Barata et a. 1998; Muyssen et al. 2002; Bossuyt and Janssen 2005; Messiaen et al. 2013), whereas few studies have examined sensitivity shifts at different compositions. One exception is Barrata et al. (1998) who observed differences in the effect of hardness (soft, moderate-hard and hard waters) on acute Cu toxicity between different *D. magna* clones. When examining the ratio $\frac{UGent\ EC_x}{CIMM\ EC_x}$, we see that this value decreases with increasing pH. This indicates that the copper bioavailability relations with pH between both clones are different. This is confirmed in Figure 5.6, which shows the 21-day EC50 as Cu^{2+} activity (Eqn. D1.7) against the pH. Here, the slope of the regression in the K6 clone is steeper, which corresponds to a stronger pH effect in the K6 clone (Sokal and Rohlf 1995). The effect of pH on Cu^{2+} ion toxicity is larger for the K6 clone compared to the ARO clone. Thus, our results confirm the hypothesis generated by the above-reported modeling efforts and the trends observed in Figure 5.3, i.e. that it is unlikely that the differences in experimental design (i.e. pH buffering method) caused the different effects of pH on chronic copper toxicity, but that true inter-clonal differences between both *D. magna* clones exist in how pH influences the chronic copper toxicity. One could therefore raise the question as to how adequate the *D. magna* BLMs are to predict chronic Cu toxicity to all invertebrates, after recalibrating for intrinsic sensitivity differences, as is done in the EU Risk Assessment (ECI 2008). However, all cross-species validations that have so far been conducted with the UGent BLM (De Schamphelaere et al. 2006b Van Sprang et al. 2008) show that extrapolation of the Daphnia BLM to other invertebrates give predictions of chronic copper toxicity that fall within a factor 2 of the observed toxicity. Therefore, we believe that the extrapolation from Daphnia to all invertebrates is an assumption that has no dramatically erroneous implications.

Table 5.2. pH of the test media and 21-day 50%, 20% and 10% effective concentrations (EC50, EC20 and EC10) for chronic copper toxicity tests with two *Daphnia magna* clones[a]

Clone	pH	EC50 (µg Cu/L)[a]	EC20 (µg Cu/L)[a]	EC10 (µg Cu/L)[a]
K6	6.4	41.7 (37.8-45.6)	36.1 (26.6-45.6)	32.9 (20.1-45.6)
K6	8.4	83.9 (68.2-99.5)	79.6 (43.7-115.6)	76.9 (28.7-125.1)
ARO	6.4	14.4 (13.3-15.5)	12.0 (10.3-13.7)	10.7 (8.7-12.6)
ARO	8.5	73.6 (69.3-77.9)	62.1 (55.8-68.4)	55.4 (47.9-62.9)

[b] For EC50s, EC20s and EC10s, 95% confidence intervals are reported in parentheses.

However, in addition, this log-linear pH effects suggests that the Biotic Ligand within the BLM concept is not adequately represented by a chemical parameter alone, i.e. binding constants for Cu and H^+ for a single monodentate binding site (De Schamphelaere and Janssen 2004a), as a single-site competitive effect would yield a linear relationship between H^+ and Cu. It suggests that there are interactions between thermodynamic principles and physiological processes. Some possible processes that may explain this non-linearity have been suggested by others (e.g. Deleebeeck et al. 2007). For example, the differences in pH may result in a change of membrane permeability and ion transport or the possible existence of a Mg^{2+}/HCO_3^- transporter (found in *Yoshida ascites* tumor cells (Günther et al. 1986)) which could transport Zn^{2+} as Mg analogue, could increase uptake and toxicity of Zn^{2+} at increased HCO_3^- concentrations, which occur at increased pH. There are a few papers that express similar thoughts, in particular for algae. For zinc (De Schamphelaere et al. 2005), the effect of pH could not be fully explained by H^+ competition for a single zinc-binding site. In addition, it was suggested that the cell wall of algae consists of different types of metal-binding sites. Furthermore, similar results were found for copper (De Schamphelaere et al. 2003) and nickel (Deleebeeck et al. 2009).

A generalized BioAvailability Model (gBAM)

In the previous sections, we have demonstrated that the UGent and HydroQual BLMs differ in their predictive capacity depending on the clone (K6 or ARO) for which chronic Cu toxicity predictions are made. However, as risk assessment typically aims to protect natural populations (consisting of various clones) instead of a single clone, it would be beneficial to have a single bioavailability model that predicts copper toxicity to genetically variable populations. In what follows, we take a first step towards such a model, by constructing and calibrating an 'average' model that can predict chronic toxicity to both clones investigated here with reasonable accuracy.

Unfortunately, unifying the UGent and HydroQual BLMs (i.e. creating an 'average' model of both to be able to predict both clones accurately) by simply averaging model parameter values is not possible, since the UGent and HydroQual BLM are structurally different (Santore et al. 2001; De Schamphelaere and Janssen 2006). Indeed, the HydroQual model does not have a log K_{CuCO_3-BL}(while the UGent BLM does), and the UGent BLM does not have a log K_{CaBL} or a log K_{MgBL} (while the HydroQual BLM) does.

Therefore, in this section we develop a model with a different structure which we call the generalized BioAvailability Model (gBAM), with the aim of accurately predicting chronic effects of copper in both *D. magna* clones. This will be done by first developing two separate models, 1 for each clone, and then unifying these to create an 'average' model to predict chronic Cu toxicity to both clones with a single set of parameter values. In summary, 3 types of gBAM models were created: (1) one only including a pH parameter: gBAM-A, (2) one including a pH and a sodium parameter: gBAM-B and (3) one including a pH, a sodium, a calcium and a magnesium parameter: gBAM-C. For all 3 models the assumptions of the UGent BLM concerning the HA and FA composition of the DOM were applied.

The first type of model only incorporated a pH constant and is structurally similar to bioavailability models developed with algae for Cu (De Schamphelaere et al. 2003), Zn (De Schamphelaere et al. 2005) and Ni (Deleebeeck et al. 2009) (Equation 5.4). This model will be referred to as gBAM-A.

$$\log_{10}(EC50_{Cu^{2+}}) = Q_{50} - S_{pH} \times pH \quad (5.4)$$

With $EC50_{Cu^{2+}}$ the 21-day EC50 expressed as Cu^{2+} activity (mol x L^{-1}), Q_{50} = the intrinsic sensitivity of the *D. magna* clone and S_{pH} = the pH slope parameter. To obtain this S_{pH} parameter, we investigated the experimental data generated in the present study as the Ca, Mg, Na and DOC concentrations were kept constant and only the pH was varied. The linear relations ($p < 0.05$) between $\log_{10}$(21-day $EC50_{Cu^{2+}}$) versus pH generated the S_{pH} values for both *D. magna* clones (Figure 5.6), resulting in S_{pH} values of 0.77 for K6 and 0.53 for ARO.

The S_{pH} values specified above were used to develop the models that will be referred to as gBAM-A_{K6} and gBAM-A_{ARO}. To be able to compare the predictive performances of the gBAMs with that of the two BLMs, the data that were used to develop the UGent BLM (De Schamphelaere and Janssen 2004c, De Schamphelaere and Janssen 2004a) and the data that were used to develop all gBAM models (data from this study and Rodriguez and Arbildua 2012) were excluded from the dataset. As such, the comparison between both BLMs and the gBAMs is done on the basis of model performance evaluations with an independent dataset. All parameter files with calibrated values for running the model in the BLM software (HydroQual 2005) are available in the online database (DOI: 10.1002/etc.2952; Supplementary 3) and an overview of all parameters is given in Table 5.1. Figure 5.7A shows the performance of both toxicity models in predicting Cu toxicity for the clone that they were developed for.

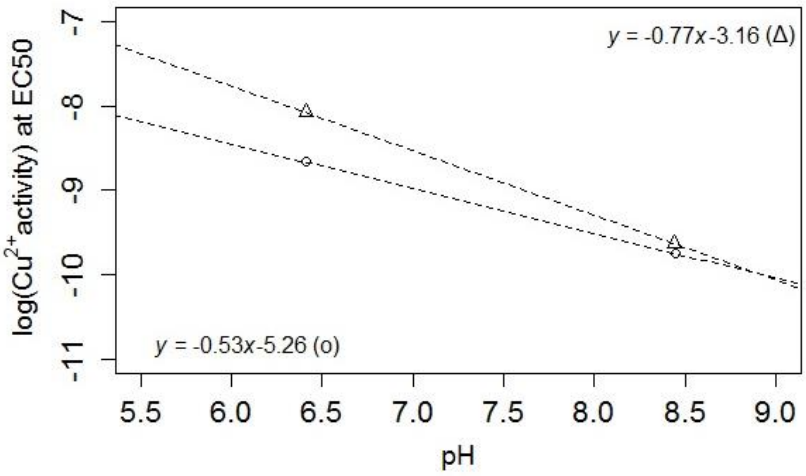

Figure 5.6 Free Cu^{2+} ion activity at the 21-d 50% effective concentration (EC50) as a function of pH for the K6 (triangles) and ARO (circles) *Daphnia magna* clone for the data generated in the present study (Table 5.13).

The gBAM-A_{K6} model predicts 96% of the K6 clone data within twofold prediction error (mean prediction error = 1.5-fold; Table 5.3), which is 14% higher than the UGent BLM and 46% higher than the HydroQual BLM (compare with Figure 5.1). The gBAM-A_{ARO} model predicts 92% of the ARO clone data within twofold prediction error (mean prediction error = 1.5-fold; Table 5.3), which is 18% higher than predictions with the UGent BLM and 9% higher than those of the HydroQual BLM.

These first results suggest that the gBAM-A, which only incorporates a pH slope parameter is, in general, more accurate than BLMs that have many more parameters for interactions at the biotic ligand (i.e. 5 for the UGent BLM and 6 for the HydroQual BLM).

Yet it is recognized that factors other than the pH may be important for predicting chronic copper toxicity to *D. magna*. For instance, gBAM-A does not account for some of the bioavailability effects that have been observed in studies where individual effects of some water quality variables were studied, notably Ca (Rodriguez and Arbildua 2012), Mg (Rodriguez and Arbildua 2012) and Na (De Schamphelaere and Janssen 2004a). De Schamphelaere and Janssen (2004a) performed a test in 3 test media with different sodium concentrations, but otherwise identical water chemistry (with the exception of the Cl^- concentration). These authors found a protective effect of sodium on chronic copper toxicity with the K6 clone. The same authors were able to derive a sodium stability constant (log K_{NaBL}) from these data. We used this value to extend gBAM-A into gBAM-B.

Although we acknowledge that the sodium constant may, just like the pH effect, also be clone-specific, we here assume that the constant derived for the K6 clone is the same for the ARO clone. Thus, gBAM-B includes not only a pH slope parameter but also a sodium parameter and the assumption was made that there is no interactive effect between pH and sodium on chronic copper toxicity. The Na effect is incorporated as a conventional BLM-type competition constant (i.e. as in both the UGent BLM (De Schamphelaere and Janssen 2004c) and HydroQual BLM (Santore et al. 2001)). This model is structurally

similar to the chronic Ni bioavailability model for Daphnia (Deleebeeck et al. 2008) and fish (De Schamphelaere and Janssen 2002) (Equation 5.5).

$$\log_{10}(EC50_{Cu^{2+}}) = \left(Q_{50} - S_{pH} \times pH\right) + log_{10}\left(1 + K_{NaBL} \times (Na^{+})\right) \quad (5.5a)$$

Or, formulated alternatively, but equivalently

$$EC50_{Cu^{2+}} = 10^{(Q_{50} - S_{pH} \times pH)} \times [1 + K_{NaBL} \times (Na^{+})] \quad (5.5b)$$

With K_{NaBL} the competition constant for sodium of 471 ($\mathrm{L \cdot mol^{-1}}$) (log K_{NaBL} = 2.67) (De Schamphelaere and Janssen 2004a) and (Na^{+}) the sodium activity ($\mathrm{mol \cdot L^{-1}}$), Q_{50} = the intrinsic sensitivity of the *D. magna* clone and S_{pH} = the pH slope parameter.

Table 5.3. Prediction statistics (% of data predicted within twofold prediction error and mean fold prediction error) of the UGent BLM, HydroQual BLM and gBAMs for *Daphnia magna* chronic copper toxicity data.

Intrinsic sensitivity calculated based on:	Data considered in calculation of predictive capacity	UGent BLM	HydroQual BLM	gBAM-A	gBAM-B	gBAM-C	gBAM-A_{uni}	gBAM-B_{uni}	gBAM-C_{uni}
All data	all data	79 (1.7)[a]	63 (2.4)	NA	NA	NA	NA	NA	NA
Data per clone	all data	77 (1.7)	70 (2.0)	NA	NA	NA	93 (1.5)	85 (1.5)	91 (1.4)
	K6 clone	82 (1.6)	50 (2.6)	96 (1.6)	79 (1.7)	89 (1.5)	96 (1.6)	75 (1.6)	89 (1.5)
	ARO clone	74 (1.8)	83 (1.6)	92 (1.5)	92 (1.5)	92 (1.3)	90 (1.5)	92 (1.5)	92 (1.3)
Data per clone and per study	all data	81 (1.7)	76 (1.6)	NA	NA	NA	NA	NA	NA
	K6 clone	93 (1.6)	54 (2.5)	NA	NA	NA	NA	NA	NA
	ARO clone	74 (1.8)	90 (1.3)	NA	NA	NA	NA	NA	NA

[a] Percentage of data predicted within twofold prediction error; mean fold prediction error is reported in parentheses
NA = Not Applicable; BLM = Biotic Ligand Model; gBAM = generic BioAvailability Model

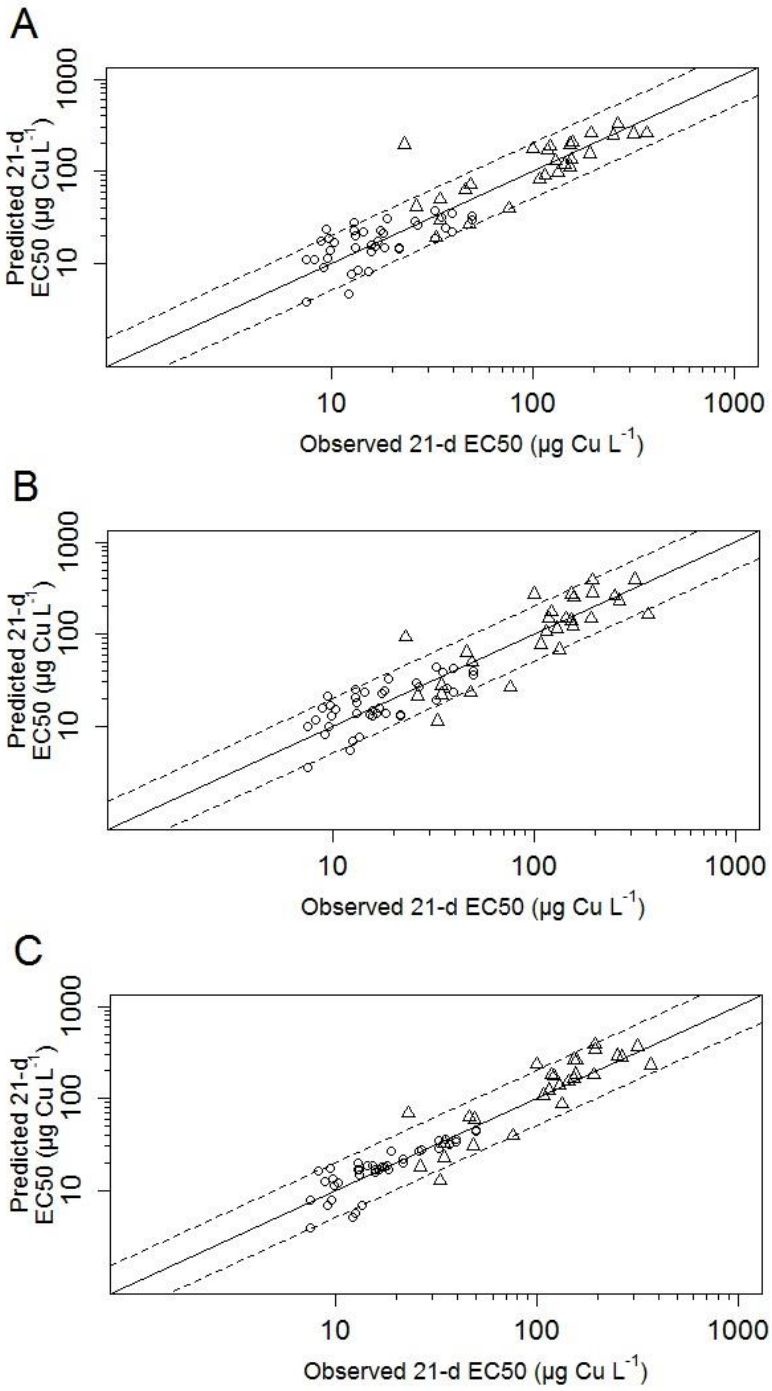

Figure 5.7. Predictive capacity of the models gBAM-X_{K6} and gBAM-X_{ARO} as shown by observed versus predicted 21-d 50% effective concentrations (EC50s) of copper to *Daphnia magna*. The K6 clone data (triangles) were predicted with the gBAM-A_{K6} (A), gBAM-B_{K6} (B), and gBAM-C_{K6} (C) models; the ARO clone data (circles) were predicted with the gBAM-A_{ARO} (A), gBAM-B_{ARO} (B), and gBAM-C_{ARO} (C) models. The solid line is the 1:1 reference line indicating a perfect match between observed and predicted values; the dashed lines indicate an error of a factor of 2 between observed and predicted values. gBAM = generalized bioavailability model.

The developed models will be referred to as gBAM-B_{K6} and gBAM-B_{ARO} (Appendix D1.3, Table D1.1). Figure 5.7B shows the performance of the toxicity models in predicting Cu toxicity for the *D. magna* clones. The gBAM-B_{K6} model now predicts 79% of the K6 clone data within twofold prediction error

(mean prediction error = 1.7-fold; Table 5.3) while the gBAM-B_{ARO} model predicts 92% of the ARO clone data within twofold error (mean prediction error = 1.5-fold; Table 5.3). Incorporating the sodium constant did not further improve model predictions for the K6 clone or the ARO clone.

Next to the effect of Na demonstrated by De Schamphelaere and Janssen (2008), Rodriguez and Arbildua (2012) have demonstrated a significant effect of hardness on chronic copper toxicity in a univariate experiment with the ARO clone. A calcium and a magnesium competition constant (K_{CaBL} and K_{MgBL}) were calculated based on their data, as was explained previously. These calcium and magnesium constants were included in a third type of gBAM, i.e. gBAM-C (Equation 5.6a). It should be noted, however, that these constants may be ARO clone-specific. Here we assume that these constant are the same for the K6 clone.

$$\log_{10}(EC50_{Cu^{2+}}) = \left(Q_{50} - S_{pH} \times pH\right) log_{10}\left(1 + K_{NaBL} \times (Na^{+}) + K_{CaBL} \times (Ca^{2+}) + K_{MgBL} \times (Mg^{2+})\right) \quad (5.6a)$$

Or, formulated alternatively, but equivalently

$$EC50_{Cu^{2+}} = 10^{(Q_{50} - S_{pH} \times pH)} \cdot [1 + K_{NaBL} \times (Na^{+}) + K_{CaBL} \times (Ca^{2+}) + K_{MgBL} \times (Mg^{2+})] \quad (5.6b)$$

With K_{CaBL} = the calcium competition constant and K_{MgBL} = the magnesium competition constant both of 3409 ($\mathrm{L \cdot mol^{-1}}$) (log K_{CaBL} = log K_{MgBL} = 3.53) and (Ca^{2+}) and (Mg^{2+}) the calcium and magnesium activities ($\mathrm{mol \cdot L^{-1}}$), respectively. Q_{50} = the intrinsic sensitivity of the *D. magna* clone and S_{pH} = the pH slope parameter. The developed models will be referred to as gBAM-C_{K6} and gBAM-C_{ARO} (Appendix D1.3, Table D1.1). Figure 5.7C shows the performance of the toxicity models in predicting Cu toxicity for the *D. magna* clones. The gBAM-C_{K6} model now predicts 89% of the K6 clone data within twofold prediction error (mean prediction error = 1.5-fold; Table 5.3) while the gBAM-C_{ARO} model predicts 92% of the ARO clone data within twofold error (mean prediction error = 1.3-fold; Table 5.3). Incorporating a sodium, a calcium and a magnesium constant gives a similar model output as the gBAM-A model for the ARO clone, but shows a lower predictive capacity for the K6 clone.

Finally, our aim was to develop a model that could accurately predict toxicity for both clones. Therefore, an 'average' model was created based on the gBAM-X_{K6} and gBAM-X_{ARO} models, i.e. the gBAM-X_{uni} model (where 'X' stand for A, B or C). This average model incorporated a S_{pH} value that was the average of the S_{pH} values from the gBAM-X_{K6} and gBAM-X_{ARO} models, i.e. 0.65, but with an intrinsic sensitivity value that was kept separate for each clone. These intrinsic sensitivity values were kept separate as we acknowledge that both clones originated from possibly different environmental conditions and showed a different genotype, which could imply a different sensitivity to metal exposure. The output of the gBAM-A_{uni} is given in Figure 5.8A. The generalized model was able to predict most of the 21-day EC50s within a factor of 2 from the observed values (93% of all data; mean prediction error = 1.5-fold; Table 5.3). For one surface water the model yielded a large underprediction of toxicity, i.e. the predicted 21-day EC50 was 5 times higher than the observed value. This was also observed in De Schamphelaere and Janssen (2004a), who attributed the phenomenon to the large amount of iron and aluminum in the sample, which could reduce copper complexation to DOM (Gable and Schnitzer 1973).

The predictive capacity of the gBAM-A_{uni} (93 %) is a clear improvement compared to the UGent BLM (77%) and the HydroQual BLM (70%).

The gBAM-B_{uni} model (Figure 5.8B) lost some predictive capacity compared to the gBAM-A_{uni} model (i.e. 85% within twofold prediction error; mean prediction error = 1.5-fold; Table 5.3). The gBAM-C_{uni} model (Figure 5.8C) predicts 91% within twofold prediction error (mean prediction error = 1.4-fold; Table 5.3) and has thus overall similar predictive capacity as that of gBAM-A_{uni}, but is more accurate than the UGent and HydroQual BLMs. Furthermore, the 21-day EC50 of the surface water that was overestimated by a factor 5 in the gBAM-A_{uni} model and a factor of up to 8 by the UGent BLM (De Schamphelaere and Janssen 2004a), was now also predicted within twofold prediction error. Therefore, it is possible that not only the large amount of iron and aluminum in this sample had an influence on the predictive capacity of gBAM-A_{uni} and the UGent BLM (De Schamphelaere and Janssen 2004a), but that hardness, which is included in the gBAM-C_{uni} as a calcium and a magnesium constant, may also have an influence on the predictive capacity of the models. Indeed, the hardness in this test medium was very low, i.e. 2.4 mg/L Ca and 0.5 mg/L Mg, compared to all other toxicity tests, which could explain the lower 21-day EC50 value due to low competition between Ca, Mg and Cu for the biotic ligand.

The gBAM-X_{uni} models could be considered as a first step toward a relatively simple alternative model to predict copper toxicity to different clones or even true populations of *D. magna* (so far only 2 clones, however). In addition, based on all model calculations evaluated above, we recommend the gBAM-C_{uni} model as a valuable (and improved) alternative model for the BLMs. This suggestion is made based on 2 qualities of the model. (1) The predictive capacity of this model is at least as good or better than the BLMs and at least as good as the most simple gBAM (i.e. gBAM-A_{uni}); (2) furthermore, it incorporates demonstrated effects of Na, Ca and Mg that have been shown in univariate experiments (De Schamphelaere and Janssen 2006; Rodriguez and Arbildua 2012) (although only with 1 clone and for a single water chemistry). Due to the latter, further research should therefore aim to investigate individual effects of these ions (and pH) in other clones and for other water chemistry variables. Furthermore, the assumption of non-interactive effects between pH and these ions (an assumption made in the model structure formation of the gBAM) should also be tested.

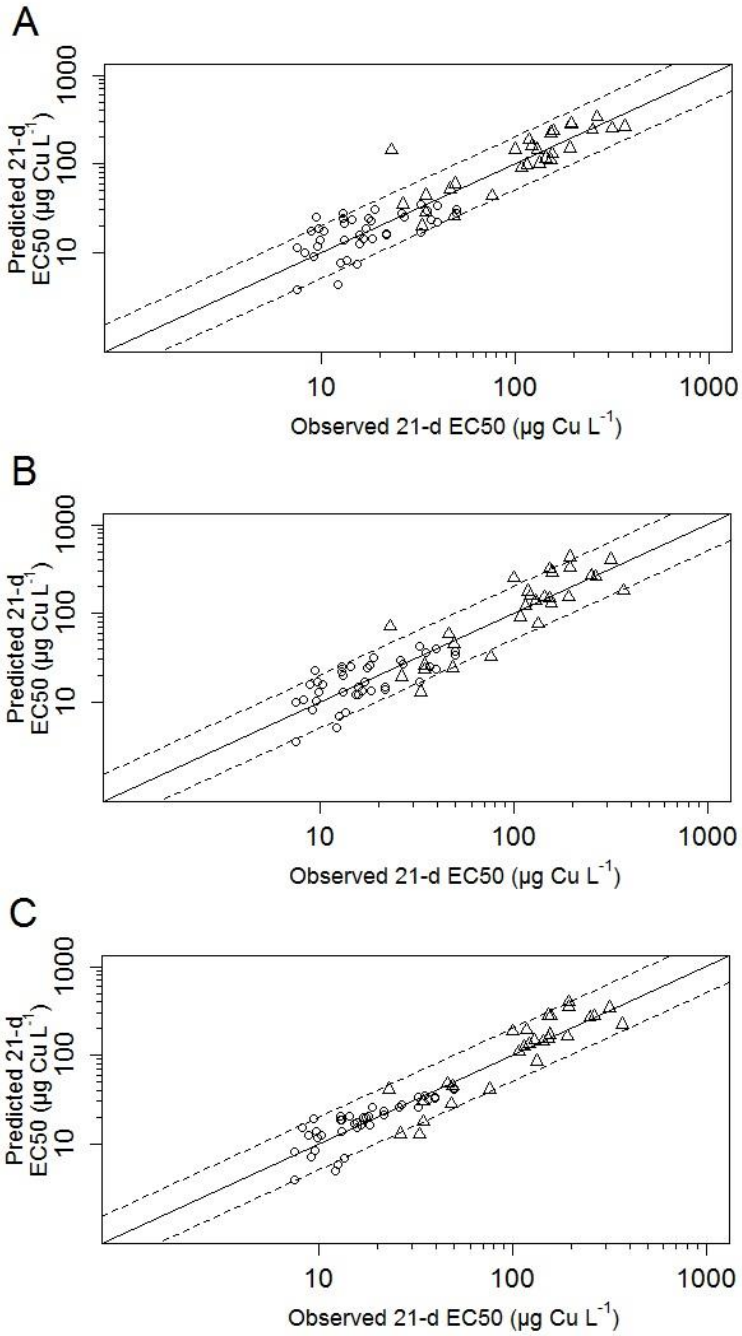

Figure 5.8. Predictive capacity of the models gBAM-X_{uni} as shown by observed versus predicted 21-d 50% effective concentrations (EC50s) of copper to 2 *Daphnia magna* clones (K6 clone [triangles] and ARO clone [circles]). Both clone data were predicted with the gBAM-A_{uni} (A), gBAM-B_{uni} (B), and gBAM-C_{uni} (C) models. The solid line is the 1:1 reference line indicating a perfect match between observed and predicted values; the dashed lines indicate an error of a factor of 2 between observed and predicted values. gBAM = generalized bioavailability model.

Conclusion

Our modeling analysis of chronic toxicity of copper to *D. magna* suggests that there is an important difference between the UGent BLM and HydroQual BLM in how they predict the change of chronic bioavailability of copper with increasing pH. Furthermore, it suggests the existence of a different effect of pH on chronic Cu toxicity between two *D. magna* clones. The latter was confirmed with a chronic copper toxicity experiment with these clones, K6 and ARO, conducted at two pH levels.

On the basis of all these results 3 new models, which we call generalized BioAvailability Models, were developed. The predictive capacity of these models, i.e. gBAM-A_{uni}, gBAM-B_{uni} and gBAM-C_{uni} was quite similar and all models were more accurate than the UGent BLM and HydroQual BLM. Furthermore, they could be considered a first step in predicting toxicity to different clones or even natural populations of *D. magna*. Although more research is needed to (i) further optimize the competition constants, (ii) to test the underlying assumption that there is no interactive effect between pH and competitive ions, (iii) to test the effect of pH on copper toxicity at intermediate pH levels and (iv) to expand to more clones than just the two investigated here, we recommend gBAM-C_{uni} as a valuable alternative model for the current BLMs for further improving methods for criteria derivation and for use in regulatory applications. This because the gBAM-C_{uni} is even more accurate than those already robust current BLMs and since it also incorporates demonstrated effects of competing ions whereas the two other gBAMs do not. Furthermore, the use of this model would be analogous to the use of similarly structured Nickel bioavailability models that are being used to derive EQS values and risk assessments in Europe (DEPI 2008).

Section Five.Two

CHRONIC ZN *DAPHNIA MAGNA* AND *PSEUDOKIRCHNERIELLA SUBCAPITATA* BIOAVAILABILITY MODEL

Redrafted from:

Van Regenmortel T, Berteloot O, Janssen CR, De Schamphelaere KAC. 2017. Analyzing the capacity of the *Daphnia magna* and *Pseudokirchneriella subcapitata* bioavailability models to predict chronic zinc toxicity at high pH and low Ca concentrations and formulation of a generalized BioAvailability Model (gBAM) for D. magna. Environmental Toxicology and Chemistry. Accepted. DOI: 10.1002/etc.3840

5.2. Chronic Zn Daphnia magna bioavailability model

Introduction

Different chronic Zn bioavailability models have been developed and validated for several aquatic organisms: *Daphnia magna* (invertebrate) (Heijerick et al. 2005b), *Onchorhynchus mykiss* (fish) (De Schamphelaere and Janssen 2004b) and *Pseudokirchneriella subcapitata* (algae) (De Schamphelaere et al. 2005). These bioavailability models account for the influence of water chemistry variables of surface waters on chronic toxicity of Zn. In general Ca, Mg and Na are protective against chronic Zn toxicity to aquatic organisms, whereas an increase in pH increases the chronic Zn toxicity (Heijerick et al. 2005b; De Schamphelaere and Janssen 2004b; De Schamphelaere et al. 2005). It has been shown that chronic Zn bioavailability models can be extrapolated to several other species, including *Lymnaea stagnalis* (snail) (De Schamphelaere and Janssen 2010), *Brachionus calyciflorus* (rotifer) (De Schamphelaere and Janssen 2010) and *Chlorella* sp. (algae) (Wilde et al. 2006). This makes so-called 'read-across' during normalization of toxicity data possible to any given target water chemistry (Van Sprang et al. 2009).

Bioavailability models have, during the past years, increasingly been used in the evaluation of ecological risks of Zn in surface waters. For instance, Zn bioavailability models have been implemented to derive bioavailability-normalized predicted no effect concentrations (PNEC) in the risk assessments performed in the European Union (Van Sprang et al. 2009; RAR Zn 2006). However, the bioavailability models used in risk assessments have only been validated within certain ranges of water chemistry. For instance, the *D. magna* and *P.subcapitata* models are both validated for a pH up to 8.0 and Ca concentrations between 5 and 160 mg/L (Heijerick et al. 2005b; De Schamphelaere et al. 2005). Yet, 28% and 20% of the European surface waters have a pH above or a Ca concentration below this 'validation boundary', respectively (Salminen et al. 2005). This means that a considerable number of European waters falls outside the applicability range of the bioavailability models. Therefore, the use of the bioavailability normalization in regulatory frameworks for Zn involves uncertainty for these waters.

The purpose of the present study was therefore to evaluate if the Zn bioavailability models, i.e. that for *D. magna* and *P.subcapitata*, can be extrapolated to pH above 8 and a Ca concentration below 5 mg/L or if modifications of the current chronic bioavailability models are needed. For this purpose, chronic toxicity experiments were conducted with natural surface waters representative for high pH and low Ca concentration waters.

Based on the results, we also explored the ability of a generalized BioAvailability Model (gBAM) as an alternative for biotic ligand model to predict chronic effect concentrations for Zn to *D. magna*. In addition, the cross-validation of the gBAM to species other than *D. magna* was also evaluated.

Materials and Methods

Collection of test media

Test media were sampled in two time periods. In April 2013 (from now referred to as 'first time period'), water was sampled for tests with *D. magna* and *P.subcapitata* and in October 2014 (from now referred to as 'second time period'), water was sampled for additional tests with *P.subcapitata*. Samples of natural surface waters were taken at nine locations in France and two locations in Belgium (Table 5.4), of which was known that yearly average pH values were above 8 and/or yearly average Ca concentrations were below 5 mg/L. The natural waters were sequentially filtered on site through 10 µm, 1 µm and 0.2 µm filters (Eurowater, FZ 2001-010, 2021-001, 3005-020) and were collected in acid-washed (1% HNO_3) polyethylene vessels. The water was stored in total darkness until use.

Ecotoxicity testing with D. magna

Preparation of test media.

To investigate the individual effect of pH and Ca on chronic zinc toxicity to *D. magna*, tests were conducted in 7 natural waters as well as two synthetic test solutions based on the EEG medium (Elendt and Bias 1990). Both synthetic test solutions were prepared using deionized water and reagent-grade chemicals purchased from VWR International. Tests with synthetic test media were conducted at pH 8.4 and pH 7.2 (reference EEG medium). The latter test solution was adjusted to the required pH of 7.2 by adding 750 mg/L of 3-N-morpholinopropanesulfonic acid (MOPS) and the required amount of NaOH or HCl. MOPS has the property not to affect metal speciation (Kandegedara and Rorabacher 1999), nor is it toxic or does it affect Zn toxicity to freshwater organisms (De Schamphelaere et al. 2004). All test solutions were adjusted to the target pH by adding dilute HCl or NaOH.
For each test, a zinc concentration series was prepared by adding $ZnCl_2$. Each test series consisted of a control treatment and 7 zinc treatments. To allow equilibration, solutions were spiked with zinc 48 hours prior to testing.

D. magna culturing.

Toxicity tests were performed with the *D. magna* K6 clone which was originally collected from a pond in Kiel (Antwerp, Belgium) and has been cultured at the Laboratory for Environmental Toxicology and Aquatic Ecology (University of Ghent, Belgium) for more than 20 years under standardized conditions. The culture medium consisted of aerated and filtered Ghent (Belgium) city tap water to which selenium (1 µg/L) and vitamins (75 µg/L thiamine, 1 µg/L cyanocobalamin and 0.75 µg/L biotin) was added (pH 7.7, DOC 2.1-3.3 mg/L, hardness 127-136 mg/L as $CaCO_3$, 5-7 µg/L zinc dissolved (Muyssen et al. 2006)). Cultures were kept at 20 ± 1 °C, with a 12:12 light:dark photoperiod. Daphnids were maintained in 5 L culture glass vessels with 4 L medium, each containing 200 individuals. The medium was changed 3 times a week. The daphnids were fed with a mixture of *P.subcapitata* and *Chlamydomonas reinhardtii* in a 3:1 ratio based on cell number (3.75×10^6 cells/daphnid from day 0 to day 8 and 7.5×10^6 cells/daphnid from day 9 onward).

Table 5.4. Overview of the locations and sampling dates of the natural surface waters with which toxicity tests were performed.

Site ID	Coordinates		Location	District, country code[a]	Waterbasin	Sampling date (dd-mm-yyyy)
	Latitude	Longitude				
La Voyon	50° 6' 4.9"	4° 5' 51.3"	Eppe-Sauvage	Nord-Pas-de-Calais, F	Meuse	28-10-2014
La Brisy	50° 14' 27.3"	5° 48' 30.6"	Brisy	Luxembourg, B	Meuse	28-10-2014
Le Bihain	50° 8' 52.9"	5° 50' 46"	Bihain	Luxembourg, B	Meuse	28-10-2014
La Seille	48° 56' 30.93"	6° 7' 30.10"	Tomblaine	Lorraine, F	Rhine	8/04/2013 and 29-10-2014
Le Madon	48° 34' 33.78"	6° 6' 29.63"	Xeuilley	Lorraine, F	Rhine	8/04/2013 and 29-10-2014
Le Loire	58° 22' 17.3"	4° 11' 45.5"	Aurec-Sur-Loire	Auvergne, F	Loire	29-10-2014
La Moselotte	47° 58' 4.87"	6° 43' 47.32"	Saulxure-sur-Moselotte	Lorraine, F	Rhine	9/04/2013
La Dolaizon	45° 0' 53.86"	3° 50' 21.33"	Saint-Christophe-sur-Dolaison	Auvergne, F	Loire	10/04/2013 and 30-10-2014
Le Taurion	45° 47' 27.95"	2° 1' 59.13"	Gentioux-Pigerolles	Limousin, F	Loire	11/04/2013 and 30-10-2014
La Maulde	45° 50' 55.79"	1° 48' 16.23"	Saint-Martin-Chateau	Limousin, F	Loire	11/04/2013 and 30-10-2014
La Gartempe	46° 4' 18.96"	1° 55' 21.50"	Lépinas	Limousin, F	Loire	11/04/2013

[a] F = France, B = Belgium

Ecotoxicity testing.

Chronic *D. magna* tests were performed according to the Organization of Economic Cooperation and Development (OECD) test guideline 211 (2012). For each treatment, 10 juvenile animals (< 24h old) were held individually in polyethylene cups containing 50 mL of test medium. Animals were fed daily with an algal mixture of *P.subcapitata* and *C. reinhardtii* in a 3:1 ratio (based on cell number). Each cup received 250, 500 or 750 µg dry weight of food per day in the first, second and third week of exposure, respectively. The total duration of the test was 21 days. The medium was renewed three times a week during the experimental period (i.e. day 3, 6, 8, 10, 13, 15, 17 and 19). Parent mortality and number of produced juveniles was recorded daily. Total reproduction per daphnid was measured by counting the juveniles in each daphnid test unit. Test validity was evaluated as described by the OECD guidelines (2012).

Ecotoxicity testing with P.subcapitata

Preparation of test media.

To investigate the individual effect of pH and Ca on chronic zinc toxicity to *P.subcapitata*, tests were conducted in 15 natural waters showing high pH or low Ca concentrations. In addition, three waters were tested that showed pH and Ca concentrations that fell inside the bioavailability model 'validity ranges'

A reference water (OECD growth medium) was prepared according to the standard protocol 201 of the OECD for testing with *P.subcapitata* (OECD 2011). However, some adjustments were made. (1) Stock C was made without addition of Zn and (2) Na-EDTA was omitted from Stock B as EDTA is known to be a very strong metal complexing ligand and is therefore not appropriate for metal toxicity testing. All OECD stock solutions were subsequently added to the natural waters at the concentrations as indicated in the OECD guideline, to provide extra nutrients during testing.

Natural waters that fell within BLM boundaries (pH 5.7 – 8, Ca 5 – 160 mg/L) as well as those with low Ca concentrations (Ca < 5 mg/L) were adjusted to the required pH by adding MOPS (Kandegedara and Rorabacher 1999; De Schamphelaere et al. 2004) and the required amount of NaOH or HCl. High pH waters (pH > 8) were not MOPS-buffered and were adjusted to the required pH by adding NaOH or HCl only.

For each test, a zinc concentration series was prepared by adding $ZnCl_2$. Each test series consisted of a control treatment and 6 zinc treatments. To allow equilibration, solutions were spiked with zinc 24 hours prior to testing.

P.subcapitata culturing.

Toxicity tests were performed with a *P.subcapitata* strain (CCAP 278/4) that was obtained from the Culture Collection of Algae and Protozoa (CCAP, at the Scottish Association for Marine Science, Argyll, Scotland, United Kingdom). A culture of the algae was set up 4 days prior to testing in aerated tap water (Gent, Belgium) that was passed sequentially through an activated carbon and a 0.45 µm filter to which the modified Provasoli's ES enrichment (Bold and Wynne, 1978) at 1/2 strength and, additionally, 1.4 mg/L $FeSO_4.7H_2O$, 15 mg/L $NaH_2PO_4.2H_2O$, 150 mg/L $NaNO_3$ and 2.35 mg/L $MnCl_2.4H_2O$ were added.

The flasks containing the algae were placed on a shaking device under continuous light (120 µmol photons.m^{-2}.s^{-1}) at 25°C.

Ecotoxicity testing.

The chronic toxicity tests with *P.subcapitata* were conducted following the OECD Guideline 201 (2011). Algal tests were performed in 100 mL Erlenmeyer flasks containing 50 mL of test medium. Each concentration had three replicates. In addition, 5 replicates with a blank correction (no algae) were tested. All replicates, except the blank corrections, were inoculated with 10^4 cells/mL (= cell density N_0 at the start (t_0) of testing). Afterwards, all Erlenmeyer flasks were incubated at 24 °C on a light table (24 h light, 120 µmol photons.m^{-2}.s^{-1}) and were manually shaken two times per day. During the test, the pH was adjusted daily by adding NaOH or HCl. Cell densities (N_1, N_2 and N_3) were measured using a particle counter (Coulter Counter Z1, Beckman) after 24 (t_1), 48 (t_2) and 72 (t_3) hours. Growth rate µ (d^{-1}) was determined in each replicate of each treatment as the slope of the linear regression of the natural logarithm of cell density versus time (in days). Test validity was evaluated as described by the OECD guidelines (2011).

Chemical analysis

During the test period, samples of fresh (sample of new medium just before transfer of daphnids to the cup or inoculating the algae to the Erlenmeyer flask) and old (sample taken of medium just after transfer of daphnids to a new cup or at the end of the experimental period for *P.subcapitata*) test media were collected regularly for analysis of total (unfiltered) and dissolved (filtered through 0.45 µm; Acrodisc, PALL Life Sciences) metals, major ions, organic carbon (OC) and inorganic carbon (IC). For *P.subcapitata,* total samples of media were taken at test initiation and dissolved samples both at test initiation, and after 48h and 72h. However, for tests in natural waters with addition of MOPS, samples for analysis of DOC (Dissolved Organic Carbon) and TOC (Total Organic Carbon) were taken before addition of MOPS. For *D. magna*, total and dissolved samples of fresh media were taken during the first renewal of each week. Dissolved samples of old media were taken during the second renewal of each week.

Samples for metal analysis were acidified to 0.14 mol/L HNO_3 (Normatom quality, VWR Prolabo). All Zn concentrations above 20 µg/L were measured using flame atomic absorption spectrophotometry (SpectrAA100, Varian, Mulgrave, Australia). Zinc concentrations below 20 µg/L were measured with inductively coupled plasma mass spectrometry (ICP-MS; Agilent 7700x, in the He mode using ^{72}Ge as internal standard). OC and IC were measured with a Total Organic Carbon analyser following the NPOC method (TOC-5000, Shimadzu, Duisburg, Germany; Limit of Quantification 1.5 mg DOC/L; Method Detection Limit 0.5 mg DOC/L). The NPOC method (Non-Purgeable Organic Carbon) entails that after purging the sample with air (to remove inorganic carbon), the remaining organic carbon is measured. Samples for calcium and magnesium were taken at the start and at the end of the test, and were measured with flame atomic absorption spectrophotometry. for sodium and potassium were also taken at the start and at the end of the test, and were measured with inductively coupled plasma mass spectrometry (ICP-MS; Agilent 7700x, in the He mode using ^{72}Ge as internal standard). Chloride and sulphate samples were taken at the start and at the end of the test, and were measured with

spectrophotometry (Aquamate, Thermo Electron Corporation; Chloride: Merck, Spectroquant 1.14897.001; Sulphate: Merck, Spectroquant 1.14548.001). The pH of fresh and old media were measured daily with a pH glass electrode (Hanna Instruments, Temse, Belgium).

Data analysis

Effect concentrations (EC10 and EC50) were calculated based on average measured dissolved metal concentrations. For *D. magna* this is the average zinc concentration of new and old medium, for *P.subcapitata* this is the average zinc concentration at the start of the test and after 72 or 48 hours. Total number of juveniles per female was used as the endpoint for the *D. magna* experiments. Relative growth rate (relative to the mean control reproduction, %) was used as the endpoint for the *P.subcapitata* experiments.

EC50, EC10 and corresponding confidence intervals were determined for Zn using the drc-package in R 2.14.1 (R Development Core Team, Vienna, Austria) with a log-logistic concentration response model with two parameters (Equation 5.7).

$$y = \frac{100}{1+exp^{(b(\ln(x)-\ln(EC50)))}} \quad (5.7)$$

Where y is the total number of juveniles (*D. magna*) or the predicted relative growth rate (%) (*P.subcapitata*); b is a slope parameter; x is the dissolved metal concentration (µg/L) and EC50 is the 50% effect concentration (µg dissolved metal/L).

Bioavailability modeling

To investigate whether the chronic Zn bioavailability models can be reliably extrapolated to pH above 8 and Ca concentrations below 5 mg/L, predictions of Zn toxicity were made using the existing chronic Zn Biotic Ligand Model (BLM) for *D. magna* (Heijerick et al. 2005b) and the existing chronic bioavailability model for *P.subcapitata* (De Schamphelaere et al. 2005). In all cases, we maintained all stability constants for cation binding to the biotic ligand as well as the critical accumulation of zinc to the biotic ligand at their original values.

For *D. magna*, chronic EC50 values were estimated using Equation 5.8.

$$EC_{50(Zn^{2+})} = \frac{f_{ZnBL}^{50\%}}{(1-f_{ZnBL}^{50\%})\cdot K_{ZnBL}} \cdot \{1 + K_{CaBL} \cdot (Ca^{2+}) + K_{MgBL} \cdot (Mg^{2+}) + K_{NaBL} \cdot (Na^{+}) + K_{HBL} \cdot (H^{+})\} \quad (5.8)$$

Where $f_{ZnBL}^{50\%}$ is the fraction of the total number of zinc binding sites of the BLM occupied by zinc resulting in a 50% effect, and K_{XBL} is the stability constant of cation X (i.e., Ca^{2+}, Mg^{2+}, Na^{+} or H^{+}) reacting with the BL sites. Stability constants and $f_{ZnBL}^{50\%}$ values that were used in this equation were taken from Heijerick et al. (2005) and are given in Table 5.5. We would like to remark however, that in the paper by Heijerick et al. (2005), a slightly wrong constant for $f_{ZnBL}^{50\%}$ was reported, likely due to a typographic error, i.e. 0.127 was reported while the correct value of 0.117 has always been used in the BLM parameter files for modeling in our previous bioavailability studies with *D. magna* (Heijerick et al. 2005b; De Schamphelaere et al. 2005). In the present study too, the correct value of 0.117 was used. All computations were executed with the available BLM software (HydroQual 2005), for which the parameter files can be found in the online database (DOI 10.1002/etc.3840, Supplementary 1).

Table 5.5. Bioavailability model constants for chronic Zn exposure of *Daphnia magna* and *Pseudokirchneriella subcapitata*

	Daphnia magna BLM[a]		*Pseudokirchneriella subcapitata* Bioavailability model[b]	
	EC10[c]	EC50[d]	EC10	EC50
Log K_{ZnBL}[e]	5.31	5.31	NI[f]	NI
Log K_{CaBL}	3.22	3.22	NI	NI
Log K_{MgBL}	2.69	2.69	NI	NI
Log K_{NaBL}	1.9	1.9	NI	NI
Log K_{HBL}	5.77	5.77	NI	NI
$f_{ZnBL}^{x\%}$	0.0979 [g]	0.117 [h]	NI	NI
S_{pH}[i]	NI	NI	-0.754	-0.652
Q[j]	NI	NI	1.294	1.197

[a] Endpoint: 21-d reproduction, Heijerick *et al.* [3]
[b] Endpoint = 72-h growth rate, De Schamphelaere *et al.* [5]
[c] EC10 = the 10% effective concentration
[d] EC50 = the 50% effective concentration
[e] Log K_{XBL} = stability constant of cation X (Zn^{2+}, Ca^{2+}, Mg^{2+}, Na^{+} or H^{+}) to the biotic ligand.
[f] NI = Not Included in the model
[g] faction of biotic ligand sites occupied by Zn at 10% effect, calculated from data reported in De Schamphelaere *et al*. [5]
[h] fraction of biotic ligand sites occupied by Zn at 50% effect.
[i] The slope of the linear regression between the $\log(ECx)_{Zn^{2+}}$ and pH, for the EC10 and EC50, respectively.
[j] Intrinsic sensitivity of *P.subcapitata* at the EC10 and EC50, respectively.

To predict the EC10s of the natural waters, the observed EC10 of the synthetic water in De Schamphelaere et al. (2005) was used to generate a $f_{ZnBL}^{10\%}$. This was done by using the BLM software in speciation mode, with the physico-chemistry of the synthetic water and the observed EC10 as input. The $f_{ZnBL}^{10\%}$ is given in Table 5.5.

For *P.subcapitata*, chronic effect concentrations resulting in x% effect (ECx) were estimated using Equation 5.9.

$$\log(EC_{x(Zn^{2+})}) = S_{pH} \cdot pH - Q_x \quad (5.9)$$

Where S_{pH} is the slope of the pH-regression and Q_x is a measure for the intrinsic sensitivity that corresponds with x% growth inhibition. The interpretation of the Qx value is analogous to that of the critical accumulation on the biotic ligand in the BLM (where it is, for instance, called the LA50 at 50% effect). Likewise, the Qx value is also (just like the LA50) assumed to be independent of water chemistry and hence an intrinsic property of the organism. Slopes and intrinsic sensitivities that were used in this equation can be found in De Schamphelaere et al. (2005) and are given in Table 5.7. Computations were executed with available BLM software (HydroQual 2005), for which the parameter files can be found in the online database (DOI: 10.1002/etc.3840 , Supplementary 1).

The predicted chronic ECx values were compared with the observed ECx values to evaluate the predictive capacity of both bioavailabity models. In addition, the relations between pH, Ca^{2+}, Mg^{2+} , Na^{+} activities and observed effect concentrations expressed as free ion activities were examined. Since free ion activities are not provided as BLM output, Zn^{2+}, Ca^{2+}, Mg^{2+} and Na^{+} activities were calculated from the BLM software output with the Davies Equation (Stumm and Morgan 1996; Malmberg and Maryott 1956) as explained in Appendix D (D1.2).

Results and Discussion

Evaluation of D. magna BLM predictive capacity

The validity criteria of the standard tests for *D. magna* were met for all waters with high pH, but only in 1 out of 4 waters with low Ca concentrations. The latter is most likely due to calcium deficiency of *D. magna* in the softwater test waters (Alstad et al. 1999; Hessen et al. 2000; Hooper et al. 2008; Muyssen et al. 2009). Therefore, to assess the effect of low calcium concentrations on chronic Zn toxicity, experiments should in the future be conducted with a species such as *Daphnia pulex*, which is a native to Europe (Colbourne et al. 1998). This species has previously been successfully tested in our lab (De Coninck et al. 2014) and originates from a softwater environment (Edwards et al. 2015). Results from the experiments with *D. magna* in low Ca concentration waters will therefore not be investigated or discussed in further detail in this manuscript.

Concentration response data and fitted concentration response curves for *D. magna* based on dissolved Zn concentrations are shown in Appendix D (D2.1). EC10 and EC50, expressed as dissolved Zn, as well as the water chemistry data are summarized in Table 5.6. DOC levels for the synthetic waters are given as a range of DOC values between the approximate background DOC concentration in deionized water used for preparing the synthetic test waters (0.3 mg/L DOC) [24] and the Limit of Quantification (LOQ) of the TOC analyzer (2.1 mg/L DOC). This was done because all DOC measurements were below the LOQ, but DOC concentrations can increase during the test due to DOC excretion by *D. magna* and *P.subcapitata* (as food organism). All calculations were executed with this range of DOC values.

Predictions of Zn toxicity to *D. magna* were compared with observed 21-day EC50 and EC10 values. The ECx data on *D. magna* reported in Heijerick et al. (2005) and De Schamphelaere et al. (2005) were also included in the comparison. The BLM predictions for chronic toxicity are plotted in Figure 5.9. A bioavailability model is in general accepted to be sufficiently accurate and applicable in risk assessment when the majority of ECx_{Mediss} is predicted within twofold error (RAR Zn 2006; ECI 2008; DEPI 2008). The BLM was able to predict 91% of the EC50 toxicity data within twofold error and showed a mean prediction error of 1.39-fold (Table 5.7). Futhermore, the BLM was able to predict 36% of the EC10 toxicity data within twofold error and showed a mean prediction error of 2.44-fold (Table 5.7). A range of predictions for the reference EEG and the synthetic water are given due to the DOC assumptions made earlier. It is clear that for *D. magna*, the influence of this DOC range on the toxicity predictions is limited (i.e. 1.13 fold for the EC50 of the reference EEG medium and 1.23 fold for the EC50 of the synthetic water).

A trend of underestimation of toxicity (overestimation of EC50) at higher pH levels can be observed in the data generated in this study, which confirms previous results by De Schamphelaere et al. (2005), who also found the same trend in their toxicity data.

Table 5.6. Physico-chemistry and effect concentrations of zinc (µg/L as dissolved) obtained for the toxicity tests in 7 natural and 2 synthetic waters with *Daphnia magna* (numbers between parentheses are 95% confidence limits) [a]

Test water	Boundaries[b]	pH[c]	DOC[c] (mg/L)	Ca[c] (mg/L)	Mg[c] (mg/L)	Na[c] (mg/L)	K[c] (mg/L)	SO_4[c] (mg/L)	Cl[c] (mg/L)	DIC[c] (mg/L)	21-d EC10	21-d EC50	Slope β
La Seille	High pH	8.2	3.93	155.89	53.03	245.40	4.96	195.75	366.13	48.90	165 (73-257)	340 (261-420)	3.03
Le Madon	High pH	8.07	3.13	131.50	40.27	33.13	2.83	182.78	38.04	48.62	203 (165-242)	311 (283-339)	5.17
La Dolaizon	High pH	8.07	4.26	15.03	13.00	11.22	1.81	5.14	10.39	16.84	109 (71-146)	173 (150-197)	4.71
Synthetic water	High pH	8.4	0.3-2.1[d]	68.02	11.67	59.57	3.21	46.22	154.85	29.97	NC[e]	126 (58-194)	1.45
La Moselotte	Low Ca	7.15	5.13	4.75	1.31	7.78	0.81	5.56	10.7	2.89	58 (49-67)	64 (33-95)	22.44
Le Taurion[f]	Low Ca	6.48	6.26	1.88	0.59	4.61	0.69	4.64	5.65	1.26	< 58.2	< 58.2	ND[g]
La Maulde[f]	Low Ca	6.51	6.37	1.87	0.5	3.76	0.8	4.57	7.30	1.49	< 66.2	< 66.2	ND[g]
La Gartempe[f]	Low Ca	7.02	10.14	2.81	0.94	6.11	1.19	5.72	6.05	2.77	< 96.5	< 96.5	ND[g]
EEG reference	Within	7.21	0.3-2.1[d]	92.08	14.11	85.03	3.51	57.95	161.65	9.41	312 (234 -390)	376 (333-419)	11.87

[a] EC10 and EC50 = the 10% and 50% effective concentration, respectively.

[b] Does the water fall within the BLM boundaries, or does is represent a water with high pH or low Ca concentrations

[c] pH, Dissolved Organic Carbon, cations, anions and Dissolved Ionrganic Carbon, given as the mean value between the start and the end of the test.

[d] DOC concentration between the approximate background DOC concentration in deionized water used for preparing this synthetic test water [20] and the LOQ (Limit of Quantification) of the TOC (Total Organic Carbon) analyzer.

[e] NC = could not be calculated due **to** high mortality or only partial effects observed in the toxicity tests.

[f] Toxicity tests performed in these waters did not pass validity criteria, as the mean reproduction of the control treatment did not exceed the required 60 offspring.

[g] ND = value could not be determined because the toxicity tests did not pass validity criteria

To assess the effects of physico-chemical parameters in more detail, we examined the relation between logarithmic model-measurement deviations (i.e. log Observed $EC50_{Zn^{2+}}$ – log Predicted $EC50_{Zn^{2+}}$; further denoted O/P) and the chemistry of the test media. To this end, the correlation (r^2) was determined between O/P and pH, H^+ activity, DOC, Na^+ activity, Ca^{2+} activity and Mg^{2+} activity. Figure 5.10 shows that there is a high and significant correlation between O/P and pH ($r^2 = 0.58$, $p < 0.001$). According to the BLM O/P data, the BLM tends to overestimate the EC50 (as Zn^{2+} activity) at high pH and therefore underestimates toxicity, which again confirms results from De Schamphelaere et al. (2005). The influence of the other physico-chemical parameters on the responses of *D. magna* is not as clear as for pH (much smaller r^2 or non-significant correlation).

The trend of underestimation of toxicity at higher pH levels is also observed in the significant correlation between the observed Zn^{2+} activities and pH ($r^2= 0.4$, $p<0.001$) (Figure 5.11). Data generated in the present study fall within the range of observed data points from previous studies, suggesting that there is no shift in sensitivity between studies. Predictions made by the BLM are also indicated on Figure 5.11 (for a water with high Ca concentration (160.3 mg/L) and low Ca concentration (1.87 mg/L); orange dashed lines). It is clear from this figure, that the BLM predicts almost no change of the $EC50_{Zn^{2+}}$ as a function of pH, once pH gets above a value of about 6.5. Indeed the BLM only predicts an important effect of pH on $EC50_{Zn^{2+}}$ below pH 6.5, due to the H^+ competition included in the BLM (2005). Yet, this contrasts with the data (dots and dashed linear regression in Figure 5.3), that indicate a more or less continuous decrease of $EC50_{Zn^{2+}}$ with increasing pH over the entire pH range (0.17 log units per pH unit), and certainly above pH>6.5. This suggests that the current chronic Zn BLM for *D. magna* is not able to reflect the observed pH effect over such a broad pH range (5.5-8.5) and that a refinement of this model is justified.

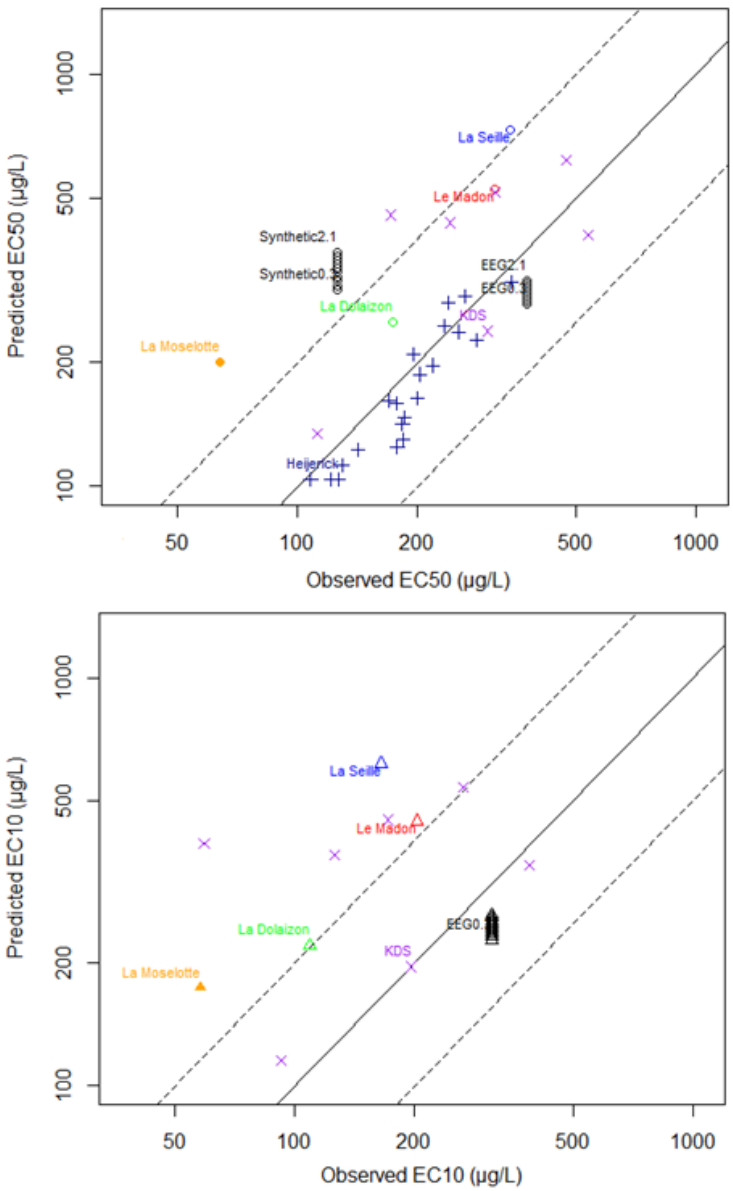

Figure 5.9. Observed versus predicted effect concentrations (EC) of zinc (as dissolved Zn) for four natural and two synthetic waters, and for four natural and one synthetic water, for the 21-d EC50 (○) (top) and the 21 d EC10 (∆) (bottom) for *Daphnia magna*, respectively. Full symbols indicate data for which the tests did not pass validity criteria. ECx values reported in De Schamphelaere et al. (2005) (X) and Heijerick et al. (2005) (+) are also included in the figure. The full line and dashed lines indicate a perfect match and a factor two difference between the observed and predicted EC. EC50 = the 50% effective concentration, EC10 = the 10% effective concentration. A range of predicted EC50 values is given for the synthetic waters (those marked with "synthetic" or "EEG") as a consequence of the range of DOC values of these waters, which lied between the approximate background DOC concentration in deionized water used for preparing the synthetic test waters (0.3 mg/L DOC) [20] and the Limit of Quantification (LOQ) of the TOC analyzer (2.1 mg/L DOC). As all DOC measurements were below the LOQ, but DOC concentrations can increase during the test due to DOC excretion by *D. magna* and *P.subcapitata* (as food organism), all calculations were executed with this range of DOC values.

Table 5.7. Prediction statistics (fold prediction error) of the BLM for *Daphnia magna* (Heijerick et al. 2005b) and the bioavailability model for *Pseudokirchneriella subcapitata* (De Schamphelaere et al. 2005)

	Daphnia magna[a]			
	EC50[e]		EC10[e]	
	All[f] (n = 33)	New[g] (n=5)	All (n=11)	New (n=4)
Mean prediction error	1.39	1.82	2.44	2.31
Median prediction error	1.23	1.7	2.04	2.11
75th percentile error	1.41	2.15	2.77	2.58
90th percentile error	1.78	2.4	3.74	3.28
Predicted within 2-fold error (%)	91	60	36	25

	Pseudokirchneriella subcapitata[b] Existing model				*Pseudokirchneriella subcapitata*[c] Model with new intrinsic sensitivity				*Pseudokirchneriella subcapitata*[d] Model with new intrinsic sensitivity and slope value			
	EC50		EC10		EC50		EC10		EC50		EC10	
S_{pH}[e]	-0.752		-0.652		-0.752		-0.652		-0.727		-0.816	
Q[f]	1.294		1.197		2.231, 1.816[g]		2.144, 1.646[g]		1.720, 1.260, 0.796[h]		1.769, 1.186, 0.943[h]	
	All[i] (n = 30)	New[j] (n=23)	All[i] (n = 27)	New[j] (n = 20)	All[i] (n = 30)	New[j] (n=23)	All[i] (n = 27)	New[j] (n = 20)	All[i] (n = 30)	New[j] (n=23)	All[i] (n = 27)	New[j] (n = 20)
Mean prediction error	3.55	4.18	2.54	2.99	1.54	1.56	1.60	1.72	1.50	1.53	1.55	1.65
Median prediction error	2.80	3.32	1.62	2.46	1.49	1.52	1.44	1.65	1.41	1.42	1.48	1.56
75th percentile error	3.91	4.08	3.11	3.48	1.70	1.77	1.85	1.96	1.65	1.64	1.65	1.84
90th percentile error	6.16	9.16	4.63	5.63	2.18	2.15	2.12	2.23	1.86	1.87	1.93	2.08
Predicted within 2-fold error (%)	30	13	56	40	87	87	81	75	93	91	89	85

[a] Prediction statistics for the existing *D. magna* BLM [1] (see Table 5.2); [b] Prediction statistics for the existing *P.subcapitata* bioavailability model (De Schamphelaere et al. 2005) (see Table 5.2); [c] Prediction statistics for the existing *P.subcapitata* bioavailability model (De Schamphelaere et al. 2005) with recalibrated intrinsic sensitivity (Q); [d] Prediction statistics for the existing *P.subcapitata* bioavailability model (De Schamphelaere et al. 2005) with recalibrated intrinsic sensitivity (Q) and S_{pH} value; [e] The slope of the linear regression between the $\log(ECx)_{Zn^{2+}}$ and pH, for the EC0 and EC10, for the different bioavailability models; [j] Intrinsic sensitivity of *P.subcapitata* at the EC50 and EC0, for the different bioavailability models; [g] Intrinsic sensitivity for the first time period and the second time period, respectively; [h] Intrinsic sensitivity for the first time period, the second time period, and the data reported in De Schamphelaere et al (2005), respectively; [i] All data reported in De Schamphelaere et al (2005), Heijerick et al (2005) and this study (data that passed validity criteria); [j]All data that passed validity criteria generated in this study; EC50 = 50% effective concentration, EC10 = 10% effective concentration

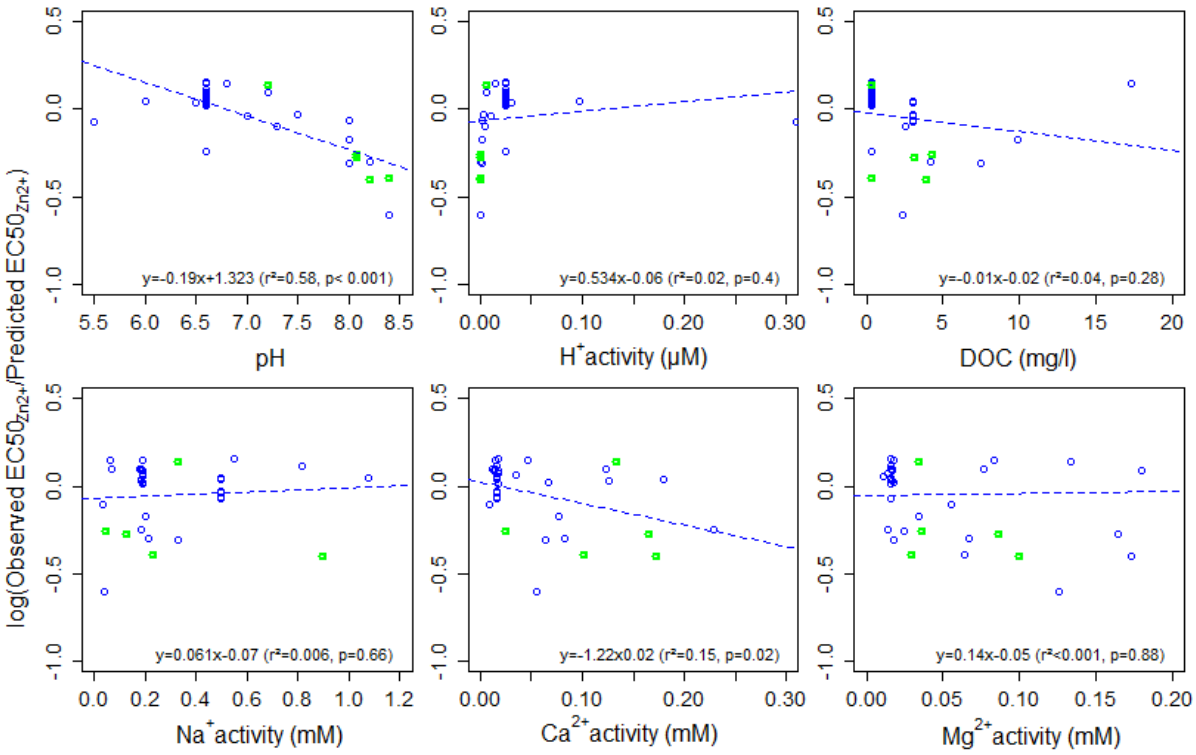

Figure 5.10. Logarithmic differences (i.e. log Observed Zn^{2+} activity – log Predicted Zn^{2+} activity) against different chemical parameters (pH, H^+ activity, DOC (mg/L), Na^+ activity, Ca^{2+} activity and Mg^{2+} activity). Blue symbols indicate data from De Schamphelaere et al. (2005) and Heijerick et al. (2005), green symbols indicate data from this study for *D. magna* that passed the validity criteria.

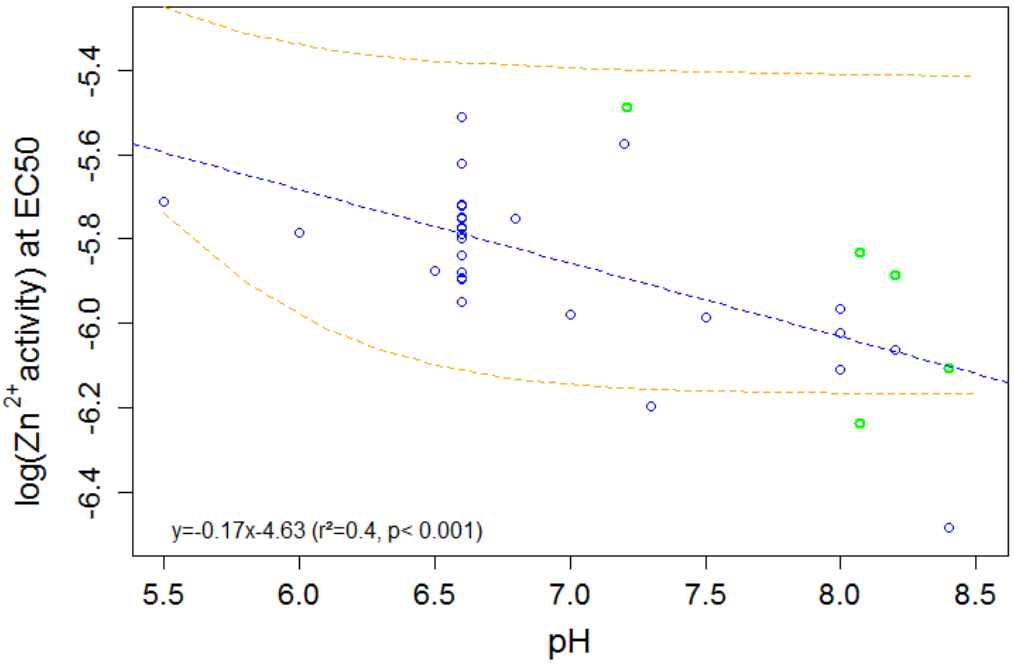

Figure 5.11. Zinc activity at the 72-h 50% effective concentration (EC50) as a function of pH for three natural and two synthetic waters (green symbols). Data reported in De Schamphelaere et al. (2005) and Heijerick et al. (2005) are indicated with blue symbols. Orange dashed lines give the range of predictions made by the BLM for a water with low Ca concentration (1.87 mg/L) and high Ca concentration (160.3 mg/L).

Evaluation of P.subcapitata BLM predictive capacity

The validity criteria of the standard tests for *P.subcapitata* were not met for some waters (D2.2). However, if the growth rate of *P.subcapitata* for the control treatments did not pass validity criteria after 72-h, the OECD guideline permits that the tests may be shortened to 48-h to maintain unlimited, exponential growth during the test as long as the validity criteria are met. Therefore, the 48-h growth rate, for which all criteria were met, was used to calculate effect concentrations. Concentration response data and fitted concentration response curves for *P.subcapitata* based on dissolved Zn concentrations are shown in Appendix D (D2.1). EC10 and EC50, expressed as dissolved Zn, as well as the water chemistry data are summarized in Table 5.8.

Predictions of Zn toxicity to *P.subcapitata* were compared with observed 48-h or 72-h EC50 and EC10 values. The ECx data on *P.subcapitata* reported in De Schamphelaere et al. (2005) were also included in the comparison. The bioavailability model predictions for chronic toxicity are plotted in Figure 5.12. The bioavailability model was able to predict 30% of the EC50 toxicity data within twofold error and showed a mean prediction error of 3.6-fold (Table 5.7). Furthermore, the bioavailability model was able to predict 56% of the EC10 toxicity data within twofold error and showed a mean prediction error of 2.5-fold (Table 5.7).

It is clear from Figure 5.12 that the predicted toxicity data for waters that have a water chemistry (pH and calcium) that fall within the bioavailability model boundaries (green color) do generally not fall within a factor 2 prediction error. This suggests that the sensitivity of the algae have shifted compared to the tests performed by De Schamphelaere et al. (2005), as has been observed previously (Deleebeeck et al. 2009). Therefore, bioavailability model predictions were repeated after recalibration of the intrinsic sensitivity of the algae for the toxicity data generated in the present study. As the intrinsic sensitivity for those waters that fell within bioavailability model boundaries was similar to that for waters that fell outside bioavailability model boundaries, an intrinsic sensitivity value was calculated based on all data. Furthermore, as the intrinsic sensitivity for the 48-h and 72-h tests were similar, we chose to calculate one average value for both test durations. A separate intrinsic sensitivity value was calculated for the 2 time periods in which experiments were conducted, because metal sensitivities of *P.subcapitata* laboratory populations may change with time (i.e. between two or more studies performed in the same laboratory, but separated in time).

Table 5.8. Physico-chemistry and effect concentrations of zinc (µg/L as dissolved) obtained for the toxicity tests in nine natural *Pseudokirchneriella subcapitata* (numbers between parentheses are 95% confidence limits) [a]

Time period[b]	Test water	Boundaries[c]	Validity[d]	T °C	pH[e]	DOC[e] mg/L	Ca[e] mg/L	Mg[e] mg/L	Na[e] mg/L	K[e] mg/L	SO4[e] mg/L	Cl[e] mg/L	DIC[e] mg/L	EC10[a] µg/L	EC50[a] µg/L	Slope b
First	Madon	high pH	72-h	25	8.31	3	135.7	46.2	134.4	5.6	210.6	53.7	38.9	NC[f]	25 (4-41)	0.67
First	Dolaizon	high pH	72-h	25	8.4	4.3	13.8	12.8	14.0	2.3	10.3	18.1	19.8	NC[f]	22 (19-25)	1.44
First	Moselotte	low Ca	48-h	25	5.85	2.9	5.1	1.6	7.7	11.1	6.7	32.5	0.4	62 (36-89)[g]	169 (143-194)	2.20
First	Taurion	low Ca	72-h	25	6.08	4.5	2.8	0.4	15.4	1.3	<5	19.5	0.5	22 (18-27)[g]	72 (66-77)	1.88
First	Maulde	low Ca	72-h	25	6.01	4.4	2.9	0.4	12.6	1.1	<5	17	0.4	32 (12-51)[g]	90 (73-106)	2.11
First	Gartempe	low Ca	48-h	25	5.83	8.6	2.9	0.8	7.6	1.7	<5	14.5	0.8	NC[f]	124 (81-167)	1.44
Second	Voyon	within	48-h	25	6.98	9.5	17.1	7.9	44.3	2.7	19.9	47.3	8.7	89 (74-104)	231 (211-250)	2.29
Second	Brisy	within	48-h	25	7.26	12	8.8	5.6	72.5	2.8	5.2	34.8	1.5	36 (30-42)	100 (89-112)	2.15
Second	Bihain	low Ca	48-h	25	6.26	4.1	3	3.4	151.2	1.7	13.5	34.4	7	116 (98-134)	395 (356-433)	1.80
Second	Voyon	high pH	48-h	25	8.54	9	15.2	7.9	37.8	2.8	21.3	25	13.3	17 (15-18)[g]	62 (59-65)	1.66
Second	Voyon	high pH	72-h	25	8.54	9	15.2	7.9	39	2.8	21.3	25	13.3	14 (10-17)[g]	54 (49-59)	1.61
Second	Bihain	low Ca	48-h	25	6.16	11.3	3	3.7	140.3	1.8	7.2	26.2	0.4	89 (54-123)[g]	398 (331-466)	1.46
Second	Brisy	within	48-h	25	7.13	9.9	8.9	6.2	72.8	2.9	15.1	25.8	2.3	51 (44-58)	110 (103-117)	2.89
Second	Brisy	within	72-h	25	7.15	9.9	8.9	6.2	73.8	2.9	15.1	25.8	2.3	55 (50-60)	138 (132-143)	2.41
Second	Loire	high pH	48-h	25	8.27	4.5	8.3	6.3	40.8	3.8	14.1	32.8	9	6 (4-9)[g]	49 (40-58)	1.06
Second	Loire	high pH	72-h	25	8.32	4.5	8.3	6.3	41.4	3.8	14.1	32.8	9	10 (8-12)	45 (41-50)	1.42
Second	Loire	high pH	48-h	25	8.51	4.8	8.1	6.3	39.2	3.8	14.8	27	9.4	16 (13-18)[g]	38 (33-44)	2.42
Second	Loire	high pH	72-h	25	8.53	4.8	8.1	6.3	39.9	3.8	14.8	27	9.4	16 (15-17)	33 (32-35)	2.97
Second	Bihain	low Ca	48-h	25	6.23	9.3	2.2	3.3	147.1	1.8	4.7	24.6	0.6	80 (58-101)[g]	284 (254-314)	1.73
Second	Bihain	low Ca	72-h	25	6.23	9.3	2.2	3.3	148.4	1.8	4.7	24.6	0.6	131 (116-146)	310 (294-326)	2.55
Second	Madon	high pH	48-h	25	8.32	7	159.1	28.2	55.7	6.8	172.3	76.1	39.2	34 (29-39)	123 (115-130)	1.72
Second	Taurion	low Ca	48-h	25	6.67	2.3	0.8	3	42	1.3	7.8	35.9	1.1	65 (44-86)	161 (141-180)	2.41
Second	Maulde	low Ca	48-h	25	6.72	3.7	0.9	2.8	45.7	1.3	7.7	23.9	1.7	68 (60-76)	154 (143-164)	2.70

[a] EC10 and EC50 = the 10% and 50% effective concentration, respectively; [b] Time period in which the tests were conducted: first time period = 2013, second time period = 2014; [c] Does the water fall within the BLM boundaries, or does is represent a water with high pH or low Ca concentrations; [d] Did the toxicity test pass validity criteria after 72-hours and/or 48-hours; [e] pH, Dissolved Organic Carbon, cations, anions and Dissolved Inorganic Carbon, given as the mean value between the start and the end of the test; [f] NC = could not be calculated due to insufficient number of tested Zn concentrations with a low effect (cf. high confidence limits); [g] EC10 value is below the concentration of the first treatment, i.e. it is an extrapolated effect concentration

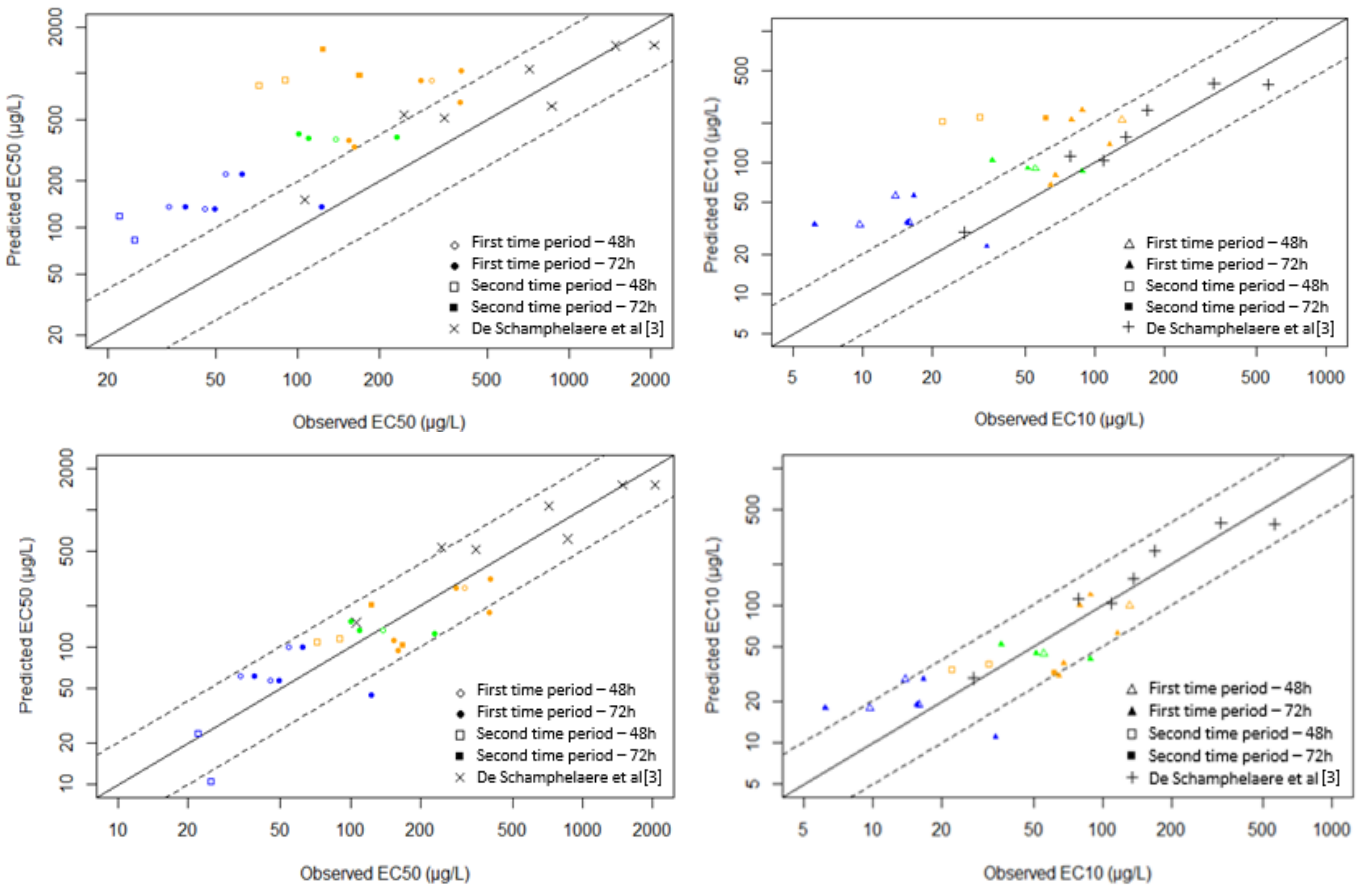

Figure 5.12. Observed versus predicted 50% effect concentrations (EC50) (top left) and 10% effect concentrations (EC10) (top right) of zinc (as dissolved Zn) for data generated in this study and De Schamphelaere et al. [3], for predictions made with the existing bioavailability model [3]. In addition, observed versus predicted 50% effect concentrations (EC50) (bottom left) and 10% effect concentrations (EC10) (bottom right) of zinc (as dissolved Zn) for data generated in this study and De Schamphelaere et al. [3], for predictions made with the recalibrated BLM. Filled symbols indicate 72-h ECx for *Pseudokirchneriella subcapitata*, open symbols indicate 48-h ECx for *Pseudokirchneriella subcapitata.* Symbols in green indicate waters with water chemistry that fall within the BLM boundaries (pH and calcium), blue symbols indicate waters with high pH values, orange symbols indicate waters with low calcium concentrations. The full line and dashed lines indicate a perfect match and a factor two difference between the observed and predicted EC50.

New intrinsic sensitivity values were equal to 2.144 for Q_{EC10} and 2.231 for Q_{EC50} for the first time period and equal to 1.646 for Q_{EC10} and 1.816 for Q_{EC50} for the second time period (see online database DOI 10.1002/etc.3840 Supplementary 1).

Figure 5.12 shows the performance of the recalibrated bioavailability model in predicting Zn toxicity for *P.subcapitata* for EC50 and EC10 data. Now, for all EC50 data, the bioavailability model predicts 87% within twofold error and a mean prediction error of 1.6-fold (Table 5.8). For all EC10 data, the bioavailability model predicts 81% within twofold error and a mean prediction error of 1.6-fold (Table 5.8). Now, data points within the bioavailability model boundaries (green points) and data points with Ca concentrations below the Ca boundary (orange points) are predicted more evenly around the 1:1 line (Figure 5.12), whereas zinc toxicity for waters with pH values above the pH boundary (blue points) is in general again underpredicted. These results suggest that the bioavailability model in its current form is capable to predict toxicity for waters outside its bioavailability model boundaries. However, a bias in toxicity predictions does exist and therefore it should be evaluated whether the bioavailability model should be refined to cover the wider chemistry range.

This was done by examining whether deviations in predictive capacity are influenced by parameters that are not incorporated in the model. To assess these effects of physico-chemical parameters, we examined the relation between logarithmic model-measurement deviations (O/P) and the chemistry of the test media. To this end, the correlation (r^2) was determined between O/P and pH, DOC, Na^+ activity, Ca^{2+} activity and Mg^{2+} activity (Figure 5.13). Figure 5.13 shows no significant correlation between O/P and pH (r^2=0.02, p=0.42). A significant correlation was found between O/P and Na^{2+} activity (r^2=0.14, p=0.043), Ca^{2+} activity (r^2=0.22, p=0.01) and Mg^{2+} activity (r^2=0.15, p=0.036), although r^2 values were small. No significant correlation was found between O/P and DOC (r^2=0.004, p=0.73). When the observed Zn^{2+} activities were used to perform a correlation analysis with pH, the relation between $\log(EC50)_{Zn^{2+}}$ and pH was significant (r^2=0.8, p<0.001) (Figure 5.14). Correlations between $(EC50)_{Zn^{2+}}$ and Ca and Na were not significant (p > 0.05), with r^2=0.05 and r^2 < 0.001, respectively. Correlations between $(EC50)_{Zn^{2+}}$ and Mg were significant (p < 0.05), but r^2 was small, i.e. 0.17. This confirms, as in previous studies (De Schamphelaere et al. 2005; Heijerick et al. 2002a), that pH is much more important than Ca, Mg and Na for determining Zn^{2+} ion toxicity to *P.subcapitata.*

Figure 5.14 shows that at lower pH, the data points generated in the second time period nicely fit within the existing data, whereas those of the first time period do not. Those at higher pH also do so less, especially at pH above 8. Therefore, the bioavailability model should be recalibrated with a new S_{pH} value calculated based on all this data. This slope could be obtained from Figure 5.14, i.e. S_{pH} = -0.75 (the average slope value). However, we prefer to calculate a S_{pH} value based on the weighted mean of the slopes of the different datasets, because smaller datasets (e.g. that of time period 1) behave differently from the other datasets and might have a large influence on the slope value. Equation 5.10 shows the calculations for the weighted mean slope:

$$S_{pH} = \frac{(n_a * S_{pH-a}) + (n_b * S_{pH-b}) + (n_c * S_{pH-c})}{n_a + n_b + n_c} \quad (5.10)$$

Where a, b and c are the different datasets, i.e. data from the first time period, the second time period and De Schamphelaere et al. (2005), respectively; S_{pH-x} is the slope value calculated for each dataset x

separately, with $S_{pH\text{-}a}$ = -0.55, $S_{pH\text{-}b}$ = -0.81 and $S_{pH\text{-}c}$ = -0.66; n_x is the number of data points within the dataset x, i.e. n_a = 6, n_b = 17 and n_c = 6. The new S_{pH} value is equal to -0.727 and was implemented into the bioavailability model to predict zinc toxicity. Intrinsic sensitivities were recalibrated based on this S_{pH} value and were equal to 1.720 for the data from the first time period, 1.260 for the data from the second time period and 0.796 for the data from De Schamphelaere et al. (2005) (see online database DOI 10.1002/etc.3840 Supplementary 1).

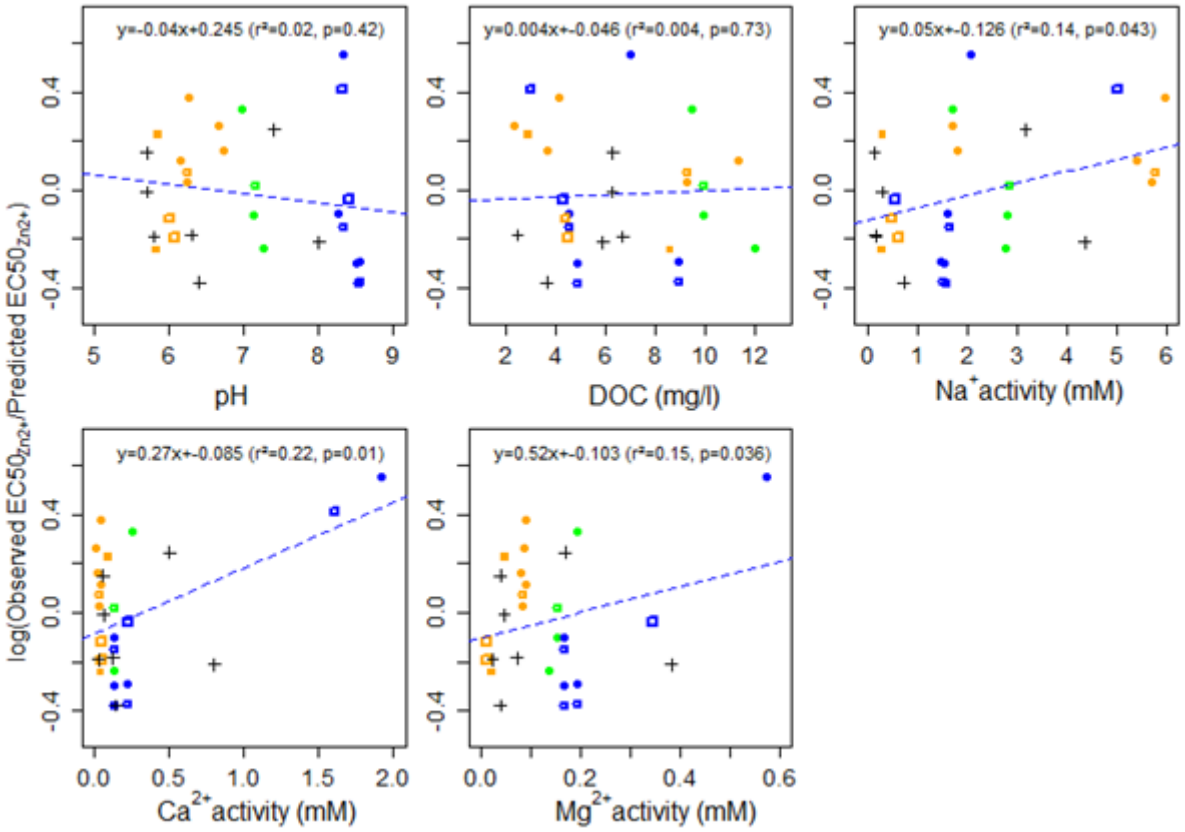

Figure 5.13. Logarithmic differences (i.e. log Observed Zn^{2+} activity – log Predicted Zn2+ activity) against different chemical parameters (pH, DOC (mg/L), Na^+ activity (mM), Ca^{2+} activity (mM) and Mg^{2+} activity (mM)). Squares indicate toxicity data generated in the first time period, circles indicate data generated in the second time period, crosses indicate toxicity data generated in De Schamphelaere et al. (2005). Filled symbols indicate 72-h EC50 for *Pseudokirchneriella subcapitata*, open symbols indicate 48-h EC50 for *Pseudokirchneriella subcapitata.* Symbols in green indicate waters with water chemistry that fall within the BLM boundaries (pH and calcium), blue symbols indicate waters with high pH values, orange symbols indicate waters with low calcium concentrations.

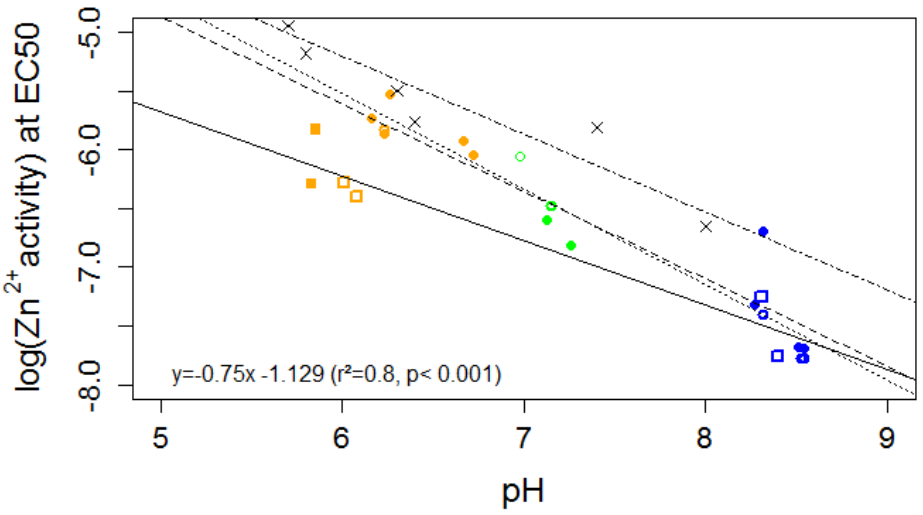

Figure 5.14. Free Zn^{2+} ion activity at the 72-h and 48-h 50% effective concentration (EC50) as a function of pH. Squares indicate toxicity data generated in the first time period, circles indicate data generated in the second time period, crosses indicate toxicity data generated in De Schamphelaere et al. (2005). Filled symbols indicate 72-h EC50 for *Pseudokirchneriella subcapitata*, open symbols indicate 48-h EC50 for *Pseudokirchneriella subcapitata.* Symbols in green indicate waters with water chemistry that fall within the BLM boundaries (pH and calcium), blue symbols indicate waters with high pH values, orange symbols indicate waters with low calcium concentrations. Regressions are fitted for every dataset separately and for all data together, i.e. solid line = first time period, dotted line = second time period , dotted dashed line (=top line) is De Schamphelaere et al. (2005) and dashed line = all data.

Figure 5.15, corresponding to the toxicity predictions made with the bioavailability model with new pH slope parameter and new intrinsic sensitivities, shows the performance of the bioavailability model in predicting Zn toxicity for EC50 data. Now, 93% of all data are predicted within a factor two prediction error (mean prediction error of 1.50-fold) (Table 5.7), which is 6% better than the original bioavailability model (De Schamphelaere et al. 2005) (Figure 5.13), and which indicates that the new slope used in the log-linear bioavailability model is able to make a slightly more optimal prediction of toxicity when a wide range of chemistry is considered. However, when examining Figure 5.15 more closely we see that two data points are not predicted well. This could already be observed in Figure 5.13 which showed that the toxicity for two data points, both performed with water from the Madon, is overpredicted. Indeed, the EC50 is underestimated by a factor of 3.0 (Madon time period 1) and 3.1 (Madon time period 2), respectively. When examining the water chemistry of the Madon tests, we see that the calcium concentrations, i.e. 159.1 mg/L and 135.7 mg/L, are much higher than that of the other waters (0.8-17.1 mg/L). Furthermore, the magnesium concentrations, i.e. 28.2 mg/L and 46.2 mg/L, also lie higher than that of the other waters (0.4-12.8 mg/L). A possible explanation could be that at very high calcium and/or magnesium concentrations, the calcium and/or magnesium ions provide a protective effect from zinc, which is not incorporated in the current algae bioavailability model.

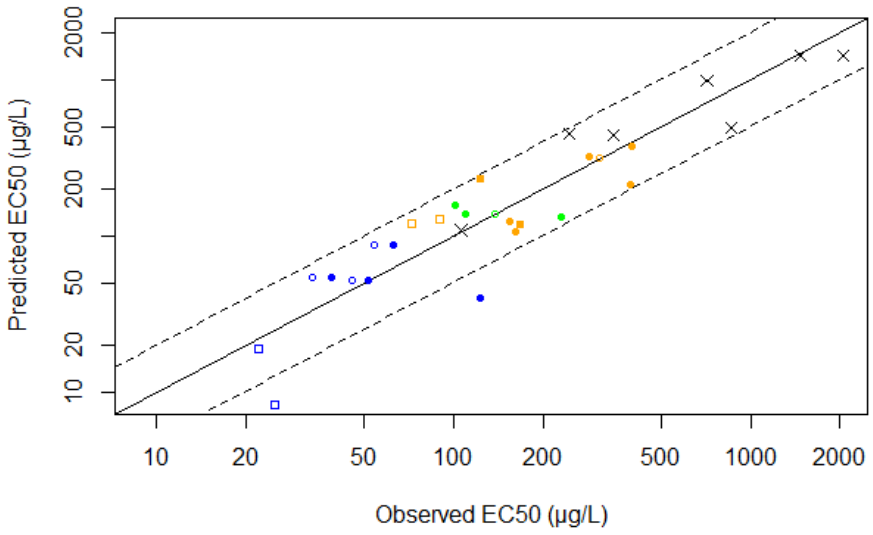

Figure 5.15. Observed versus predicted 50% effect concentrations (EC50) of zinc (as dissolved Zn). Predictions were made with the recalibrated BLM with new S_{pH} value and intrinsic sensitivities. Squares indicate toxicity data generated in the first time period, circles indicate data generated in the second time period, crosses indicate toxicity data generated in De Schamphelaere et al. (2005). Filled symbols indicate 72-h EC50 for *Pseudokirchneriella subcapitata*, open symbols indicate 48-h EC50 for *Pseudokirchneriella subcapitata.* Symbols in green indicate waters with water chemistry that fall within the BLM boundaries (pH and calcium), blue symbols indicate waters with high pH values, orange symbols indicate waters with low calcium concentrations. The full line and dashed lines indicate a perfect match and a factor two difference between the observed and predicted EC50.

To further examine the influence of calcium and magnesium, we determined the intrinsic sensitivity (i.e. $Q_{50,i}$) of the algae and plotted this against the Ca^{2+} and Mg^{2+} activity (Figure 5.16). To calculate the bioavailability corrected $Q_{50,i}$, we used the pH-slope in combination with Equation 5.11.

$$Q_{50,i} = S_{pH} \cdot pH_i + \log(EC_{50(Zn^{2+}),i}) \quad (5.11)$$

Where $Q_{50,i}$ is the sensitivity of the algae for water body *i*; S_{pH} is the slope of -0.727; pH_i is the pH value of water body *i* and $EC_{50(Zn^{2+}),i}$ is the observed EC50 as Zn^{2+} activity for water body *i*. Figure 5.16 shows that the $Q_{50,i}$ of the algae during the test with Madon water was very different from the intrinsic sensitivities of the algae for the other natural waters within the same experiment. This suggests that at very high calcium and/or magnesium concentrations, the calcium and/or magnesium ions provide a protective effect from zinc. However, as calcium and magnesium activities are correlated amongst each other in this dataset ($r^2 = 0.8$), it is not clear now which parameter might be most important. Incorporating a calcium and/or magnesium competition constant into the bioavailability model is for the time being not considered. However, the influence of calcium and magnesium on chronic zinc toxicity to *P.subcapitata* should be further investigated in the future. Possibly, the influence of calcium and/or magnesium might be important at high pH values. However, for now we only have two data points, tested with the same water, to support this. Therefore, whether or not a competition constant for either of these two parameters should be included, should be subject for further research.

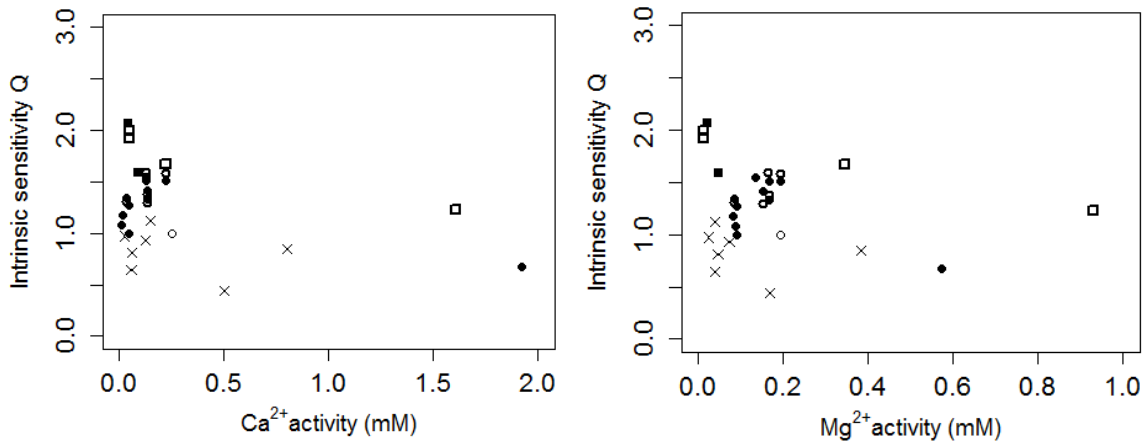

Figure 5.16. Intrinsic sensitivity Q of the algae as a function of Ca^{2+} activity (mM) and Mg^{2+} activity (mM). Filled symbols indicate 72-h EC50 for *Pseudokirchneriella subcapitata*, open symbols indicate 48-h EC50 for *Pseudokirchneriella subcapitata.* Squares indicate toxicity data generated in the first time period, circles indicate data generated in the second time period, crosses indicate toxicity data generated in De Schamphelaere et al. (2005).

Similar calculations as above were performed for the EC10 data (Appendix D.2.2). No significant correlation between O/P and pH, DOC, Na^+ activity, Ca^{2+} activity and Mg^{2+} activity ($p > 0.05$) were observed. When the observed Zn^{2+} activities were used to perform a correlation analysis with pH, the relation between $\log(EC10)_{Zn^{2+}}$ and pH was significant (r^2=0.87, $p<0.001$). The slope value was used as new S_{pH} value (-0.816) for recalibration of the bioavailability model. Intrinsic sensitivities were recalibrated based on this S_{pH} value and were equal to 1.769 for the data from the first time period, 1.186 for the data from the second time period and 0.943 for the data from De Schamphelaere et al. (2005).

For all EC10 data, the bioavailability model now predicts 89% within twofold error (mean prediction error of 1.6-fold) which is only 8% better than the original bioavailability model (De Schamphelaere et al. 2005) (Table 5.7). Here too, the chronic zinc toxicity for the data point from the Madon water is overpredicted.

As the refined bioavailability model performs only slightly better than the existing bioavailability model (i.e. 6% and 8% more EC50 and EC10 data predicted within twofold prediction error, respectively, and a difference in average x-fold prediction error of 0.1 and 0 for EC50 and EC10 data, respectively), the existing algae bioavailability model (i.e. with S_{pH} values of -0.754 for EC50 data and -0.652 for EC10 data (De Schamphelaere et al. 2005) can be continued to be used for the wider range of water chemistry variables, i.e. low calcium concentrations (down to 0.8 mg/L) and high pH values (pH up to 8.54).

A generalized BioAvailability Model (gBAM)

Evaluation of the predictive capacity of the chronic *D. magna* Zn BLM suggested that the current BLM is not able to reflect the observed pH effect over a broad pH range (5.5-8.5) and that a refinement of this model may be warranted. To do this, all available data from the previous BLM development and validation work (Heijerick et al. 2005b; De Schamphelaere et al. 2005) and from this study was compiled to evaluate if an adapted BLM structure would perform better than the current BLM. A model consisting of a log-linear pH effect, combined with competitive Ca, Mg and/or Na effects, as is the case for the Ni

D. magna BLM (DEPI 2008) and was recently developed for the Cu *D. magna* BLM (Van Regenmortel et al. 2015/Chapter 5.1; Section 5.1), might work better over a wider range of chemistry (i.e. outside the pH boundaries). Therefore, the predictive capacity of this type of model, referred to as a generalized BioAvailability Model (gBAM) (Van Regenmortel et al. 2015/Chapter 5.1; Section 5.1), will be compared to the predictive capacity of the chronic *D. magna* BLM in the following sections. To be able to compare the predictive performances of the gBAMs with that of the BLM, the data that were used to develop the BLM and the data that were used to develop all gBAM models (i.e. data from Heijerick et al. 2005b) were excluded from the dataset. As such, the comparison between the BLM and the gBAMs is done on the basis of model performance evaluations with an independent dataset.

Predictive capacity of the chronic D. magna BLM.

To start off, the predictive capacity of the chronic *D. magna* BLM was tested, so comparison with the predictive capacity of the gBAMs is possible. To predict effect concentrations (21-day EC50s), we maintained all stability constants for cation binding to the biotic ligand at their original values (Heijerick et al. 2005b) and only adjusted the critical accumulation of zinc to the biotic ligand. The BLM was recalibrated based on the data by De Schamphelaere et al. (2005) and the data generated in this study. The intrinsic sensitivity $\int_{ZnBL}^{50\%}$ was equal to 0.085. Figure 5.17 shows the performance of the BLM in predicting Zn toxicity for *D. magna.* The model predicts 91% of all data within twofold prediction error (mean prediction error = 1.5-fold).

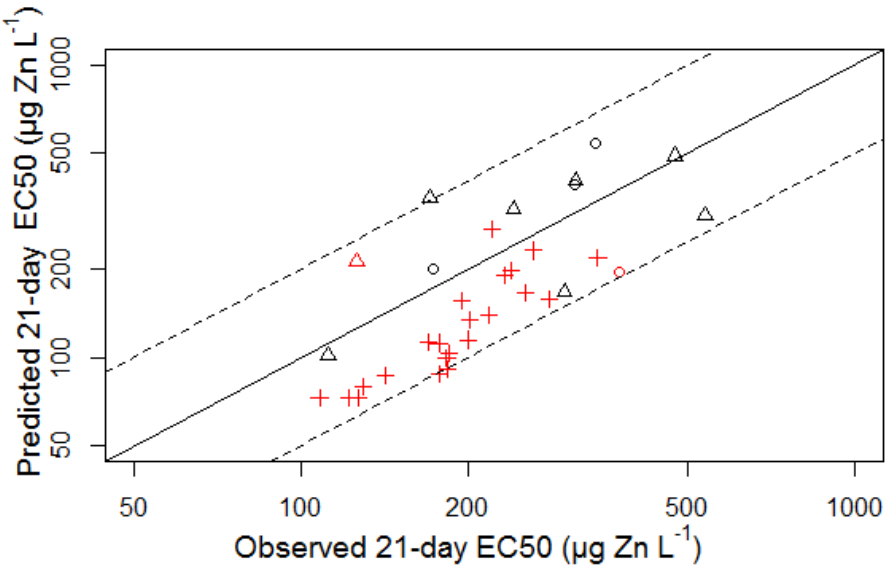

Figure 5.17. Predictive capacity of the BLM as shown by observed versus predicted 21-day 50% effective concentrations (EC50s) of zinc to *Daphnia magna*. The intrinsic sensitivity of *D. magna* was calculated based on data by De Schamphelaere et al (2005) (Δ) and data from this study (○). Data by Heijerick et al (2005) (+) is also plotted. Red data points indicate toxicity tests performed in synthetic water, black data points indicate toxicity tests performed in natural water. The solid line is the 1:1 reference line indicating a perfect match between observed and predicted values; the dashed lines indicate an error of a factor of two between observed and predicted values. BLM = Biotic Ligand Model.

Development of a gBAM.

The development of the gBAM was done in a same way as is described in Section 5.1 (Van Regenmortel et al. 2015). The first type of model (gBAM-A) only incorporates a pH constant and is structurally similar to bioavailability models developed with algae for Zn (Heijerick et al. 2005b), Cu (De Schamphelaere et al. 2003) and Ni (Deleebeeck et al. 2009) and recently with *D. magna* for Cu (Van Regenmortel et al. 2015; Section 5.1) (Equation 5.12).

$$\log_{10}(EC50_{Zn^{2+}}) = Q_{50} - S_{pH} \times pH \quad (5.12)$$

Where $EC50_{Zn^{2+}}$ is the 21-day EC50 expressed as Zn^{2+} activity (mol x L^{-1}); Q_{50} is the intrinsic sensitivity of *D. magna* and S_{pH} is the pH slope parameter. To obtain this S_{pH} parameter, we used the data from the pH-series reported by Heijerick et al. (2005) as the Ca, Mg, Na and DOC concentrations were kept constant and only the pH was varied. The linear relations ($p < 0.05$) between $\log_{10}$(21-day $EC50_{Zn^{2+}}$) versus pH generated the S_{pH} value for *D. magna* of 0.13 (Figure 5.18A), that was incorporated into the gBAM-A. All parameter files with calibrated values for running the model in the BLM software (HydroQual 2005) are available in the online database (DOI: 10.1002/etc.3840; Supplementary 5) and an overview of all parameters is given in Table 5.9. Figure 5.19 shows the performance of the toxicity model in predicting Zn toxicity for *D. magna*.

Table 5.9. Biotic ligand model (BLM) zinc constants, competition constants, thermodynamic parameters and humic material assumptions of the chronic *Daphnia magna* BLM (De Schamphelaere et al. 2005) that were used for modelling, as well as parameter values for all generalized BioAvailability Models (gBAM) used

Parameter	*Daphnia magna* (chronic) BLM	gBAM-A	gBAM-B1	gBAM-B2	gBAM-B3	gBAM-C	gBAM-D
Biotic Ligand (BL) Species							
Log K_{ZnBL}	5.31[a]	NA	NA	NA	NA	NA	NA
Log K_{CaBL}	3.22	NA	NA	3.22	NA	3.22	3.22
Log K_{MgBL}	2.69	NA	NA	NA	2.69	2.69	2.69
Log K_{HBL}	5.77	NA	NA	NA	NA	NA	NA
Log K_{NaBL}	1.90	NA	1.90	NA	NA	NA	1.90
S_{pH}	NA	0.13	0.13	0.11	0.12	0.12	0.13
Q_{50}	NA	4.963	5.00	5.45	5.07	5.45	5.38
$f_{ZnBL}^{50\%}$	0.085	NA	NA	NA	NA	NA	NA
Bioavailable species that can bind to the biotic ligand	Zn^{2+}	NA	NA	NA	NA	NA	NA
Thermodynamic Database							
pK_{MHA} Zn-HA	2.3	2.3	2.3	2.3	2.3	2.3	2.3
Humic Material Assumptions							
% of natural DOM composed of humic substances [b]	50%	50%	50%	50%	50%	50%	50%
% of the humic substances that is HA (rest is FA) [c]	0%	0%	0%	0%	0%	0%	0%

[a] Reaction: BL-Zn = Zn^{2+} + BL; [b] Exception: when humic acid is added to the medium, all models assume 100% of the DOM to be composed of humic substances; [c] Exception: when humic acid is added to the medium, all models assume 100% of the humic substances to be composed of humic acid ; NA = Not Applicable as constant in the Chronic BLM or gBAM; DOM = Dissolved Organic Matter; HA = Humic Acid; FA = Fulvic Acid

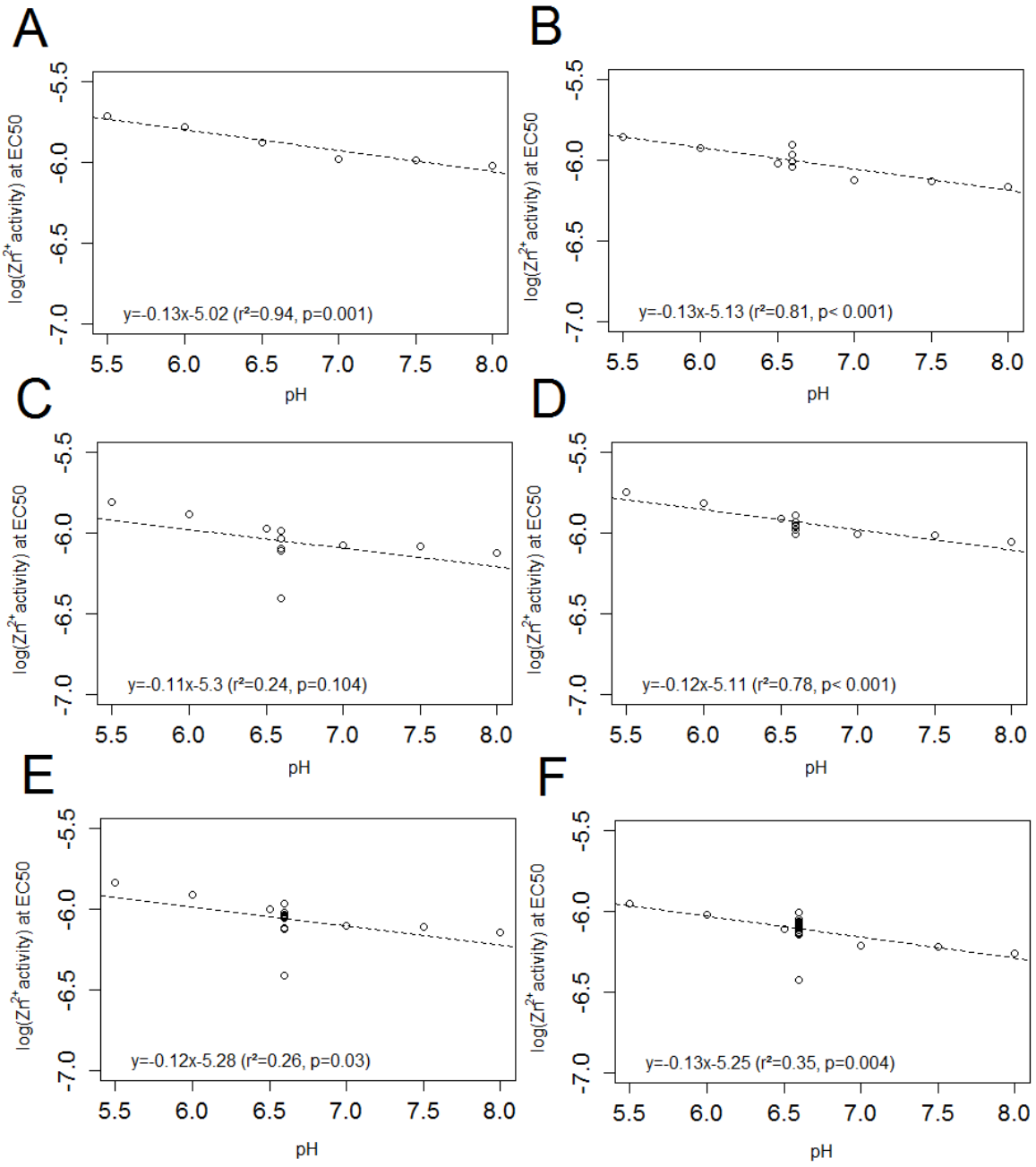

Figure 5.18. Free Zn^{2+} ion activity at the 21-day 50% effective concentration (EC50) as a function of pH for *Daphnia magna* for the data from the pH-series (A), the pH-series and Na-series (B), the pH-series and Ca-series (C), the pH-series and Mg-series (D), the pH-series, Ca-series and Mg-series (E) and the pH-series, Na-series, Ca-series and Mg-series (F) by Heijerick et al. (2005).

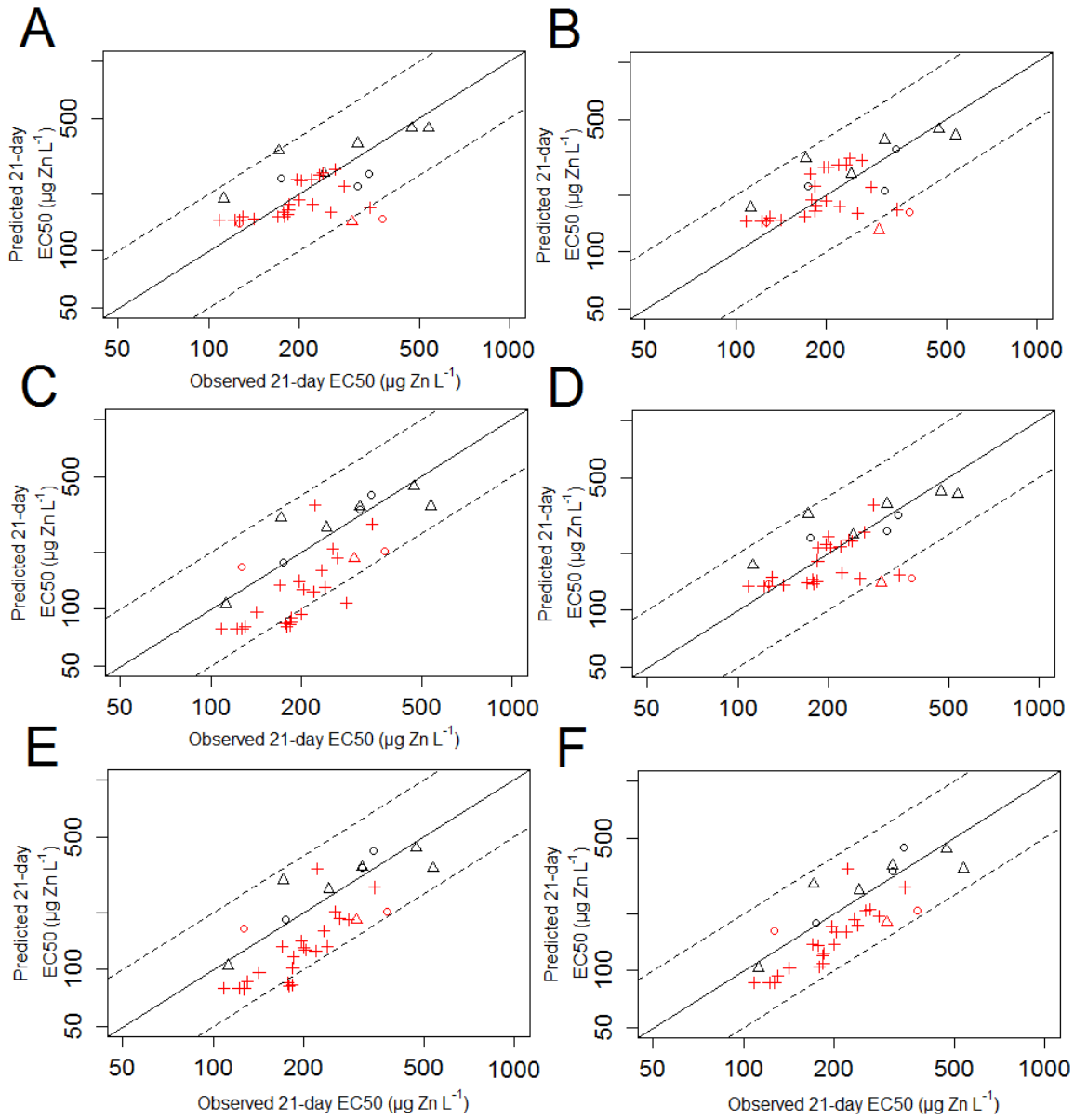

Figure 5.19 Predictive capacity of the gBAM-A (A), gBAM-B1 (B), gBAM-B2 (C), gBAM-B3 (D), gBAM-C (E) and gBAM-D (F) models as shown by observed versus predicted 21-day 50% effective concentrations (EC50s) of zinc to *Daphnia magna*. The intrinsic sensitivity of *D. magna* was calculated based on data by De Schamphelaere et al. (2005) (Δ) and data from this study (2005) (○). Data by Heijerick et al. (2005) (+) is also plotted. Red data points indicate toxicity tests performed in synthetic water, black data points indicate toxicity tests performed in natural water. The solid line is the 1:1 reference line indicating a perfect match between observed and predicted values; the dashed lines indicate an error of a factor of two between observed and predicted values. gBAM = generalized BioAvailability Model.

The gBAM-A model predicts 83% of the data from De Schamphelaere et al. (2005) and this study within twofold prediction error (mean prediction error = 1.5-fold). The model predicts 91% of all data (Heijerick et al. 2005b; De Schamphelaere et al. 2005 and the present study) within twofold prediction error (mean prediction error = 1.3-fold), which is as accurate as the chronic BLM (Figure 5.17).

These results suggest that the gBAM-A, which only incorporates a pH slope parameter is, in general, as accurate as the BLM that has many more parameters for interactions at the biotic ligand (i.e. 5 for the chronic *D. magna* BLM).

However, factors other than the pH may be important for predicting chronic zinc toxicity to *D. magna*. Indeed, Heijerick et al. (2005) demonstrated the individual effects of Na, Ca and Mg on Zn toxicity to *D. magna*. These authors were able to derive a sodium (log K_{NaBL}), calcium (log K_{CaBL}) and magnesium (log K_{MgBL}) stability constant from their data. In the following steps of the gBAM development, we will add these constants individually, and thereby create gBAM-B1, gBAM-B2 and gBAM-B3.

Heijerick et al. (2005) performed a test in 4 test media with different sodium concentrations, but otherwise identical water chemistry. A protective effect of sodium on chronic zinc toxicity was observed, although less pronounced than the protective effect of calcium and magnesium. The same authors were able to derive a sodium stability constant (log K_{NaBL}) from these data.

We used this value to extend gBAM-A into gBAM-B1. The latter model now includes a pH slope parameter and a sodium parameter and the assumption was made that there is no interactive effect between pH and sodium on chronic zinc toxicity. The Na effect is incorporated as a conventional BLM-type competition constant (i.e. as in the chronic BLM (Heijerick et al. 2005b)). This model is structurally similar to the chronic Ni bioavailability model for Daphnia (ECI 2008) and fish (Heijerick et al. 2002a) (Equation 5.13).

$$EC50_{Zn^{2+}} = 10^{(Q_{50} - S_{pH} \times pH)} \times [1 + K_{NaBL} \times (Na^{+})] \quad (5.13)$$

Where K_{NaBL} is the competition constant for sodium of 79 ($\mathrm{L \cdot mol^{-1}}$; log K_{NaBL} = 1.9) (Heijerick et al. 2005b) and (Na^{+}) is the sodium activity ($\mathrm{mol \cdot L^{-1}}$); Q_{50} is the intrinsic sensitivity of *D. magna* and S_{pH} is the pH slope parameter. The latter was recalculated based on EC50 data (as Zn^{2+} activity) that has been corrected for the sodium effect (Equation 5.14).

$$EC50^{*}_{Zn^{2+}} = \frac{EC50_{Zn^{2+}}}{1 + K_{NaBL} \cdot (Na^{+})} \quad (5.14)$$

Where $EC50_{Zn^{2+}}$ is the observed EC50 as Zn^{2+} activity ($mol \cdot L^{-1}$); (Na^{+}) is the sodium, activity ($mol \cdot L^{-1}$) and K_{NaBL} is the competition constant for sodium ($\mathrm{L \cdot mol^{-1}}$). The new correlation between pH and the EC50 as Zn^{2+} activity is given in Figure 5.18B. The S_{pH} and intrinsic sensitivity that are obtained from this log linear relation (i.e. S_{pH} = 0.13 and Q_x = 5.00) are used in the gBAM-B1 (Table 5.9). Figure 5.19B shows the performance of the toxicity model in predicting Zn toxicity for *D. magna.* The gBAM-B1 model predicts 83% of the data from De Schamphelaere et al. (2005) and from this study within twofold prediction error (mean prediction error = 1.5-fold). The model predicts 91% of all data (Heijerick et al. 2005b; De Schamphelaere et al. 2005 and the present study) within twofold prediction error (mean prediction error = 1.3-fold). Incorporating the sodium constant did not further improve model predictions for *D. magna*.

Next to the effect of Na, Heijerick et al. (2005) also demonstrated a significant effect of calcium on chronic zinc toxicity in a univariate experiment with *D. magna*. These authors were able to derive a calcium stability constant (log K_{CaBL}) from these data. We used this value to extend gBAM-A into gBAM-

B2. The latter model now includes a pH slope parameter and a calcium parameter and the assumption was made that there is no interactive effect between pH and calcium on chronic zinc toxicity. The Ca effect is also incorporated as a conventional BLM-type competition constant (i.e. as in the chronic BLM (Heijerick et al. 2005b)).

$$EC50_{Zn^{2+}} = 10^{(Q_{50} - S_{pH} \times pH)} \times [1 + K_{CaBL} \times (Ca^{2+})] \quad (5.15)$$

Where K_{CaBL} is the competition constant for calcium of 1660 ($\mathrm{L \cdot mol^{-1}}$; log K_{CaBL} = 3.22) (Heijerick et al. 2005b) and (Ca^{2+}) is the calcium activity ($\mathrm{mol \cdot L^{-1}}$); Q_{50} is the intrinsic sensitivity of *D. magna* and S_{pH} is the pH slope parameter. The latter was recalculated based on EC50 data (as Zn^{2+} activity) that has been corrected for the calcium effect (Equation 5.16).

$$EC50^{*}_{Zn^{2+}} = \frac{EC50_{Zn^{2+}}}{1 + K_{CaBL} \cdot (Ca^{2+})} \quad (5.16)$$

Where $EC50_{Zn^{2+}}$ is the observed EC50 as Zn^{2+} activity ($mol \cdot L^{-1}$); (Ca^{2+}) is the calcium, activity ($mol \cdot L^{-1}$) and K_{CaBL} is the competition constant for calcium ($\mathrm{L \cdot mol^{-1}}$). The new correlation between pH and the EC50 as Zn^{2+} activity is given in Figure 5.18C. The S_{pH} and intrinsic sensitivity that are obtained from this log linear relation (i.e. S_{pH} = 0.11 and Q_x = 5.45) are used in the gBAM-B2 (Table 5.9). Figure 5.19C shows the performance of the toxicity model in predicting Zn toxicity for *D. magna.* The gBAM-B2 model predicts 100% of the data from De Schamphelaere et al. (2005) and from this study within twofold prediction error (mean prediction error = 1.3-fold). However, the model predicts only 79% of all data (Heijerick et al. 2005b; De Schamphelaere et al. 2005 and the present study) within twofold prediction error (mean prediction error = 1.6-fold). Incorporating the calcium constant improved model predictions for *D. magna* for the data by De Schamphelaere et al. (2005) and this study but not for the data from the study by Heijerick et al. (2005).

Next to the effect of Na and Ca, Heijerick et al. (2005) were also able to derive a magnesium stability constant (log K_{MgBL}) from their data. We used this value to extend gBAM-A into gBAM-B3. The latter model now includes a pH slope parameter and a magnesium parameter and the assumption was made that there is no interactive effect between pH and magnesium on chronic zinc toxicity. The Mg effect is again incorporated as a conventional BLM-type competition constant (i.e. as in the chronic BLM (Heijerick et al. 2005b)).

$$EC50_{Zn^{2+}} = 10^{(Q_{50} - S_{pH} \times pH)} \times [1 + K_{MgBL} \times (Mg^{2+})] \quad (5.17)$$

Where K_{MgBL} is the competition constant for calcium of 490 ($\mathrm{L \cdot mol^{-1}}$; log K_{MgBL} = 2.69) (Heijerick et al. 2005b) and (Mg^{2+}) is the magnesium activity ($\mathrm{mol \cdot L^{-1}}$); Q_{50} is the intrinsic sensitivity of *D. magna* and S_{pH} is the pH slope parameter. The latter was again recalculated based on EC50 data (as Zn^{2+} activity) that has been corrected for the magnesium effect (Equation 5.18).

$$EC50^{*}_{Zn^{2+}} = \frac{EC50_{Zn^{2+}}}{1 + K_{MgBL} \cdot (Mg^{2+})} \quad (5.18)$$

Where $EC50_{Zn^{2+}}$ is the observed EC50 as Zn^{2+} activity ($mol \cdot L^{-1}$); (Mg^{2+}) is the magnesium, activity ($mol \cdot L^{-1}$) and K_{MgBL} is the competition constant for magnesium ($\mathrm{L \cdot mol^{-1}}$). The new correlation between pH and the EC50 as Zn^{2+} activity is given in Figure 5.18D. The S_{pH} and intrinsic sensitivity that

are obtained from this log linear relation (i.e. S_{pH} = 0.12 and Q_x = 5.07) are used in the gBAM-B3 (Table 5.9). Figure 5.19D shows the performance of the toxicity model in predicting Zn toxicity for *D. magna.* The gBAM-B3 model predicts 83% of the data from De Schamphelaere et al. (2005) and from this study within twofold prediction error (mean prediction error = 1.5-fold). The model predicts 91% of all data (Heijerick et al. 2005b; De Schamphelaere et al. 2005 and the present study) within twofold prediction error (mean prediction error = 1.3-fold). Incorporating the magnesium constant did not further improve model predictions for *D. magna*.

Incorporating the protective effect of Na and Mg individually into the gBAM did not further improve model predictions for *D. magna*. Incorporating the protective effect of Ca into the gBAM did improve model predictions for the data by De Schamphelaere et al. (2005) and this study, but not for the data generated by Heijerick et al. (2005). Heijerick et al. (2005) showed that the protective effect of calcium and magnesium was more pronounced than that of sodium. Therefore, we will include the calcium and magnesium constants in a third type of gBAM, i.e. gBAM-C (Equation 5.19).

$$EC50_{Zn^{2+}} = 10^{(Q_{50} - S_{pH} \times pH)} \cdot [1 + K_{CaBL} \times (Ca^{2+}) + K_{MgBL} \times (Mg^{2+})] \quad (5.19)$$

Where K_{CaBL} is the competition constant for calcium of 1660 ($\mathrm{L \cdot mol^{-1}}$; log K_{CaBL} = 3.22); K_{MgBL} is the magnesium competition constant of 490 ($\mathrm{L \cdot mol^{-1}}$; log KMg_{BL} = 2.69) and (Ca^{2+}) and (Mg^{2+}) are the calcium and magnesium activities ($\mathrm{mol \cdot L^{-1}}$), respectively; Q_{50} is the intrinsic sensitivity of *D. magna* and S_{pH} is the pH slope parameter.

Also here, the latter was recalculated based on EC50 data (as Zn^{2+} activity) that has been corrected for the calcium and magnesium effect (Equation 5.20).

$$EC50^{*}_{Zn^{2+}} = \frac{EC50_{Zn^{2+}}}{1 + K_{CaBL} \cdot (Ca^{2+}) + K_{MgBL} \cdot (Mg^{2+})} \quad (5.20)$$

Where $EC50_{Zn^{2+}}$ is the observed EC50 as Zn^{2+} activity ($\mathrm{mol \cdot L^{-1}}$), ($Ca^{2+}$) and ($Mg^{2+}$) are the calcium and magnesium activities ($\mathrm{mol \cdot L^{-1}}$), respectively and K_{CaBL} and K_{MgBL} are the competition constants for calcium ($\mathrm{L \cdot mol^{-1}}$) and magnesium ($\mathrm{L \cdot mol^{-1}}$), respectively. The new correlation between pH and the EC50 as Zn^{2+} activity is given in Figure 5.18E. The S_{pH} and intrinsic sensitivity that are obtained from this log linear relation (i.e. S_{pH} = 0.12 and Q_x = 5.45) are used in the gBAM-C (Table 5.9). Figure 5.19E shows the performance of the toxicity model in predicting Zn toxicity for *D. magna.* The gBAM-C model now predicts 100% of the data from De Schamphelaere et al. (2005) and from this study within twofold prediction error (mean prediction error = 1.3-fold). The model predicts 91% of all data (Heijerick et al. 2005b; De Schamphelaere et al. 2005 and the present study) within twofold prediction error (mean prediction error = 1.5-fold). Incorporating the calcium and magnesium constant improved model predictions for *D. magna* for the data from De Schamphelaere et al. (2005) and from this study. However, when investigating all data (Heijerick et al. 2005b; De Schamphelaere et al. 2005 and the present study), the gBAM-C performance is still as accurate as that of the gBAM-A and that of the chronic *D. magna* BLM (Figure 5.17).

Although the effect of Na on Zn toxicity was less pronounced than the effect of Ca and Mg (Heijerick et al. 2005b), it was still shown that it had a protective effect. Therefore, in a final step, the effect of Na on

chronic zinc toxicity Heijerick et al. 2005b) should also be incorporated into the gBAM. Including the sodium gives us a fourth type of gBAM, i.e. gBAM-D (Equation 5.21).

$$EC50_{Zn^{2+}} = 10^{(Q_{50} - S_{pH} \times pH)} \cdot [1 + K_{NaBL} \times (Na^{+}) + K_{CaBL} \times (Ca^{2+}) + K_{MgBL} \times (Mg^{2+})] \quad (5.21)$$

Where K_{NaBL} is the competition constant for sodium of 79 ($\mathrm{L \cdot mol^{-1}}$; log K_{NaBL} = 1.9); K_{CaBL} is the calcium competition constant of 1660 ($\mathrm{L \cdot mol^{-1}}$; log K_{CaBL} = 3.22); K_{MgBL} is the magnesium competition constant of 490 ($\mathrm{L \cdot mol^{-1}}$; log K_{MgBL} = 2.69) and (Na^{+}), (Ca^{2+}) and (Mg^{2+}) are the sodium, calcium and magnesium activities ($\mathrm{mol \cdot L^{-1}}$), respectively; Q_{50} is the intrinsic sensitivity of *D. magna* and S_{pH} is the pH slope parameter.

Again, the latter was recalculated based on EC50 data (as Zn^{2+} activity) that has been corrected for the sodium, calcium and magnesium effect (Equation 5.22).

$$EC50^{*}_{Zn^{2+}} = \frac{EC50_{Zn^{2+}}}{1 + K_{NaBL} \cdot (Na^{+}) + K_{CaBL} \cdot (Ca^{2+}) + K_{MgBL} \cdot (Mg^{2+})} \quad (5.22)$$

Where $EC50_{Zn^{2+}}$ is the observed EC50 as Zn^{2+} activity ($mol \cdot L^{-1}$), (Na^{+}), (Ca^{2+}) and (Mg^{2+}) are the sodium, calcium and magnesium activities ($\mathrm{mol \cdot L^{-1}}$), respectively; K_{NaBL}, K_{CaBL} and K_{MgBL} are the competition constant ($\mathrm{L \cdot mol^{-1}}$) for sodium, calcium and magnesium, respectively. The new correlation between pH and the EC50 as Zn^{2+} activity is given in Figure 5.18F. The S_{pH} and intrinsic sensitivity that are obtained from this log linear relation (i.e. S_{pH} = 0.13 and Q_x = 5.38) are used in the gBAM-D (Table 5.9). Figure 5.19F shows the performance of the toxicity model in predicting Zn toxicity for *D. magna.* The gBAM-D model now predicts 100% of the data from De Schamphelaere et al. (2005) and from this study within twofold prediction error (mean prediction error = 1.3-fold). The model predicts 100% of all data (Heijerick et al; 2005; De Schamphelaere et al. 2005 and the present study) within twofold prediction error (mean prediction error = 1.4-fold). Incorporating the sodium, calcium and magnesium constant improved model predictions for *D. magna*. The predictive capacity of the gBAM-D model is now 19% better than that of the chronic *D. magna* BLM (Figure 5.17).

Based on the above, the gBAM models could be considered as a first step toward an alternative model to predict zinc toxicity to *D. magna*. In addition, based on all model calculations evaluated above, we recommend the gBAM-D model as a valuable (and improved) alternative model for the BLM. However, prior to implementing the gBAM-D, a read-across of the model to other invertebrate species should preferably be evaluated. Read-across of the existing *D. magna* chronic Zn BLM (Heijerick et al. 2005b) to *Lymnaea stagnalis* and *Brachionus calyciflorus* was successful (De Schamphelaere and Janssen 2010). The latter should preferably also be examined for the gBAM-D.

Read across of the gBAM-D

In this section, we investigated if the chronic zinc gBAM-D developed for *D. magna* could be extrapolated to predict chronic toxicity of zinc as a function of water chemistry to two species from other phyla, i.e. the mollusc *L. stagnalis* and the rotifer *B. calyciflorus*.

Toxicity data for these two species was taken from De Schamphelaere and Janssen (2010). These authors reported on the chronic, 28-day toxicity of Zn to *L. stagnalis* in 6 natural surface waters and the chronic, 2-day toxicity of Zn to *B. calyciflorus* in 5 natural surface waters.

The cross-species predictive capacity of the developed gBAM-D was compared to that of the chronic *D. magna* BLM by comparing with the results found in De Schamphelaere and Janssen (2010). The constants and intrinsic sensitivities that were used for modelling with gBAM-D can be found in Appendix D (D2.3), the parameter files used for modelling can be found in the online database (DOI 10.1002/etc.3840, Supplementary 5). Although the S_{pH} parameter was calibrated on EC_{50} data, we additionally investigated whether this value could also be used to predict EC_{10} values for both *L. stagnalis* as well as *B. calyciflorus*. The gBAM-D was calibrated to reflect the intrinsic sensitivities (i.e. Q_x values) of *L. stagnalis* and *B.* calyciflorus. These Q_x values were calculated based on observed Zn^{2+} activities and Equation 5.17.

All predictions of EC_{10}s and EC_{50}s were within 1.5-fold difference from observations for *L. stagnalis*. Average prediction errors for EC_{10} and EC_{50} values were 1.24 and 1.16-fold, respectively (Appendix D2.3). These predictions are slightly better than the predictions made with the chronic *D. magna* BLM (Appendix D2.3), which showed an average prediction error of 1.31 and 1.19-fold for EC_{10} and EC_{50} values, respectively (De Schamphelaere and Janssen 2010). All predictions for *B. calyciflorus* were also within 1.3-fold prediction error Appendix D2.3. Average prediction error for EC_{10} and EC_{50} values were 1.22 and 1.18-fold, respectively (Appendix D2.3). These predictions are also slightly better than the predictions made with the chronic *D. magna* BLM (Appendix D2.3), i.e. average prediction error of 1.29 and 1.33-fold for EC_{10} and EC_{50} values, respectively (De Schamphelaere and Janssen 2010).

The above results show that the gBAM-D model was able to predict all EC_x values within less than a 1.5-fold error, which is slightly better than the chronic BLM for *D. magna* and which demonstrates that the gBAM-D can be extrapolated to other invertebrate phyla. Furthermore, it demonstrates that the S_{pH} parameter value that was calculated based on EC_{50} data can be used to calculate EC_{10} values for both *L. stagnalis* and *B. calyciflorus*.

Conclusion

Chronic zinc toxicity to *D. magna* was underestimated by the BLM for waters with high pH. This is a confirmation of previous work done by De Schamphelaere et al. (2005) who also found overestimation of the EC50 at higher pH levels in their dataset. This suggests that the current chronic Zn BLM for *D. magna* is not able to reflect the observed pH effect over such a broad pH range (5.5-8.5) and that a refinement of this model is justified.

Low calcium tests on *D. magna* were not successful due to calcium deficiency at such low Ca concentrations. We propose to conduct tests with a species that does occur in softwater environments (e.g. *D. pulex*).

The chronic zinc bioavailability model for algae with recalibrated intrinsic sensitivities was able to predict almost all chronic toxicity data for *P.subcapitata* within twofold prediction error. Examination of the model deviations revealed significant deviations with increasing $Ca^{2+,}$ Mg^{2+} and Na^{+} activity. Yet, a significant correlation between the observed Zn^{2+} activity and pH showed that pH is much more important than Ca, Mg and Na for determination of Zn^{2+} ion toxicity to *P.subcapitata*. A recalibrated bioavailability model, with new slope value based on all previous and newly generated data, was capable of predicting Zn toxicity to *P.subcapitata* slightly more accurate than the original bioavailability model. However, the

improvement of predictive capacity was rather limited. In addition, an overprediction of toxicity was observed for two data points that were tested with the same natural water. This could be attributed to the high calcium and/or magnesium concentrations that were observed in this water. To be able to conclude on the above, future research should focus on examining the influence of calcium and magnesium on chronic zinc toxicity to *P.subcapitata*. As the refined bioavailability model performs only slightly better than the existing bioavailability model, we recommend to continue the use of the existing algae bioavailability model (i.e. S_{pH} = -0.754 for EC50 data and -0.652 for EC10 data (De Schamphelaere et al. 2010)) for the wider range of water chemistry variables, i.e. low calcium concentrations (< 5 mg/L) and high pH values (pH up to 8.54). Furthermore, it should be kept in mind that conservative predictions of toxicity are made for hard waters.

Our modeling analysis of chronic toxicity of zinc to *D. magna* suggested that a refinement of this model is warranted. On the basis of data by Heijerick et al. (2005), 4 new models, generalized BioAvailability Models, were developed. The predictive capacity of these models, i.e. gBAM-A, gBAM-B, gBAM-C and gBAM-D was quite similar or more accurate than the existing BLM. Therefore, the gBAM models could be considered as a first step toward an alternative model to predict zinc toxicity to *D. magna*. In addition, based on all model calculations evaluated, we recommend the gBAM-D model as a valuable (and improved) alternative model for the BLM for Zn toxicity predictions for waters with pH values up to 8.4. This suggestion is made based on 4 qualities of the model. (1) The predictive capacity of this model is better than the BLM and the most simple gBAM (i.e. gBAM-A); (2) the model incorporates demonstrated effects of Na, Ca and Mg that have been shown in univariate experiments [1]. (3) Furthermore, the model can be extrapolated to other invertebrate phyla, as was demonstrated in a read-across evaluation. (4) In addition, the use of this model would be analogous to the use of similarly structured Nickel bioavailability models that are being used to derive EQS values and risk assessments in Europe (DEPI 2008; Bio-met 2017).

Section Five.Three

CHRONIC ZN AND CU FISH BIOAVAILABILITY MODELS

5.3 Chronic Zn and Cu Fish bioavailability models

Introduction

In the previous sections in this chapter we developed a gBAM for *Daphnia magna* for the metals Zn and Cu. This type of model incorporates a pH slope parameter in addition to competition constants for ions such as Ca and Mg. We showed that these gBAMs were more accurate in predicting toxicity to *D. magna* than their BLM-counterparts. By adapting the BLM for *D. magna* for Zn and Cu to a gBAM, we made the models structurally similar to the bioavailability models for algae for Zn (De Schamphelaere et al. 2005), Ni (Deleebeeck et al. 2009) and Cu (De Schamphelaere et al. 2003), for *D. magna* for Ni (Deleebeeck et al. 2008) and for fish for Ni (Deleebeeck et al. 2003). The uniformisation of the bioavailability models to a gBAM-like structure is therefore almost complete. The models that as yet do not incorporate a pH slope parameter are the bioavailability models for fish for Zn and Cu. Because we previously showed for *D. magna* that the predictive capacity of a gBAM is higher compared to a BLM, we hypothesize that this will also be the case for fish. In addition, the development of a gBAM will contribute to the uniformisation of all bioavailability models for the metals Zn, Cu and Ni. Therefore, in this section, the aim is to develop and validate a gBAM for the metals Zn and Cu for fish.

Material and Methods

Fish gBAM development for Zn

For the development of the Zn gBAM for fish (i.e. *Oncorhynchus mykiss*), all available data from the previous BLM development and validation work (De Schamphelaere and Janssen 2004b; De Schamphelaere et al. 2005; most sensitive endpoint mortality) was compiled to evaluate if an adapted BLM structure would perform better than the current BLM. The BLM incorporated biotic ligand constants for the competitive Ca, Mg and Na effects. Therefore, for the gBAM, we developed a model consisting of a log-linear pH effect, combined with competitive Ca, Mg and Na effects (Equation 5.23).

$$LCx_{Zn^{2+}} = 10^{(Q_x - S_{pH} \times pH)} \cdot [1 + K_{NaBL} \times (Na^{+}) + K_{CaBL} \times (Ca^{2+}) + K_{MgBL} \times (Mg^{2+})] \quad (5.23)$$

Where K_{NaBL} is the competition constant for sodium of 251 ($\mathrm{L \cdot mol^{-1}}$; log K_{NaBL} = 2.4); K_{CaBL} is the calcium competition constant of 3981 ($\mathrm{L \cdot mol^{-1}}$; log K_{CaBL} = 3.6); K_{MgBL} is the magnesium competition constant of 1259 ($\mathrm{L \cdot mol^{-1}}$; log K_{MgBL} = 3.1) (De Schamphelaere and Janssen 2004b) and (Na^{+}), (Ca^{2+}) and (Mg^{2+}) are the sodium, calcium and magnesium activities ($\mathrm{mol \cdot L^{-1}}$), respectively; Q_x is the intrinsic sensitivity of *O. mykiss* for the *x*% lethal concentration and S_{pH} is the pH slope parameter.

To obtain this S_{pH} parameter, we used the LC50 and LC10 data from the pH test-series reported by De Schamphelaere and Janssen (2004b) as the Ca, Mg, Na and DOC concentrations were kept constant in this series and only the pH was varied. The linear relations between $\log_{10}$(21-day $\mathrm{LCx}_{Zn^{2+}}$) versus pH generated the S_{pH} value for *O. mykiss*.

Predictions of Zn toxicity expressed as LCx values were made using the chronic Zn fish gBAM linked to WHAM V. The predictive capacity of the gBAM was compared to the predictive capacity of the original chronic fish BLM (De Schamphelaere and Janssen 2004b).

Fish gBAM development for Cu

In the Cu Risk Assessment Report (Cu RAR, 2008), it was shown that chronic toxicity of Cu to fish is best predicted with the acute Cu BLM developed for *D. magna* calibrated to account for the different sensitivity for fish (De Schamphelaere et al. 2002). The data for which this was investigated was taken from an experiment with *Pimephales promelas* performed by Erickson et al (1996), in which Cu^{2+} activities were measured.

The fish BLM (i.e. acute *D. magna* BLM) incorporated biotic ligand constants for the competitive Ca, Mg and Na effects. Therefore, for the gBAM, we developed a model consisting of a log-linear pH effect, combined with competitive Ca, Mg and Na effects (Equation 5.24).

$$EC60_{Cu^{2+}} = 10^{(Q_{60} - S_{pH} \times pH)} \cdot [1 + K_{NaBL} \times (Na^{+}) + K_{CaBL} \times (Ca^{2+}) + K_{MgBL} \times (Mg^{2+})] \quad (5.24)$$

Where K_{NaBL} is the competition constant for sodium of 1549 ($\mathrm{L \cdot mol^{-1}}$; log K_{NaBL} = 3.19); K_{CaBL} is the calcium competition constant of 2951 ($\mathrm{L \cdot mol^{-1}}$; log K_{CaBL} = 3.47); K_{MgBL} is the magnesium competition constant of 3802 ($\mathrm{L \cdot mol^{-1}}$; log K_{MgBL} = 3.58) (De Schamphelaere and Janssen 2002) and (Na^{+}), (Ca^{2+}) and (Mg^{2+}) are the sodium, calcium and magnesium activities ($\mathrm{mol \cdot L^{-1}}$), respectively; Q_{60} is the intrinsic sensitivity of *P. promelas* for the 60% effect concentration and S_{pH} is the pH slope parameter.
To obtain this S_{pH} parameter, we used the EC60 data from the pH-series reported by Erickson et al (1996) as the Ca, Mg, Na and DOC concentrations were kept constant and only the pH was varied. The linear relation between $\log_{10}$(7-day $\mathrm{EC60}_{Cu^{2+}}$) versus pH generated the S_{pH} value for *P. promelas.*
Predictions of Cu toxicity expressed as EC50 values were made using the chronic Cu fish gBAM in combination with the measured Cu^{2+} activities. The predictive capacity of the gBAM was compared to the predictive capacity of the original chronic fish BLM (De Schamphelaere et al. 2002).

Results and Discussion

gBAM for Zn

Figure 5.20 shows the linear relation between $\log_{10}$(21-day $\mathrm{LCx}_{Zn^{2+}}$) versus pH for *O. mykiss*. The S_{pH} value for *O. mykiss* is equal to 0.22 and 0.37 for LC50 and LC10 data, respectively. These values were incorporated into the gBAM.

A separate intrinsic sensitivity (Qx) was calculated for the natural and synthetic waters. The Q50 was equal to -4.35 and -4.11 for synthetic and natural waters, respectively. The Q10 was equal to -3.76 and -3.44 for natural and synthetic waters, respectively. Figure 5.21 shows the performance of the toxicity model in predicting Zn toxicity for *O. mykiss*. The model performance is compared to the performance of the BLM in Table 5.10. For the synthetic media, the gBAM model predicts 90% and 93% of the LC50 and LC10 data within twofold prediction error, respectively (mean prediction error = 1.37 and 1.40 for LC50 and LC10 data, respectively). This is approximately 10% less accurate than the fish BLM, that was able to predict 100% of the LC50 and LC10 data for synthetic media within twofold prediction error. The ultimate aim of the developed model, however, is to accurately predict Zn toxicity in natural surface water samples. For natural media, the gBAM model predicts 100% of the LC50 and LC10 data within twofold prediction error (mean prediction error = 1.32 and 1.30 for LC50 and LC10 data, respectively).

For the LC50 data, this is as accurate as the original fish BLM. However, for the LC10 data, the gBAM is 20% more accurate than the BLM in predicting Zn toxicity to *O. mykiss*.

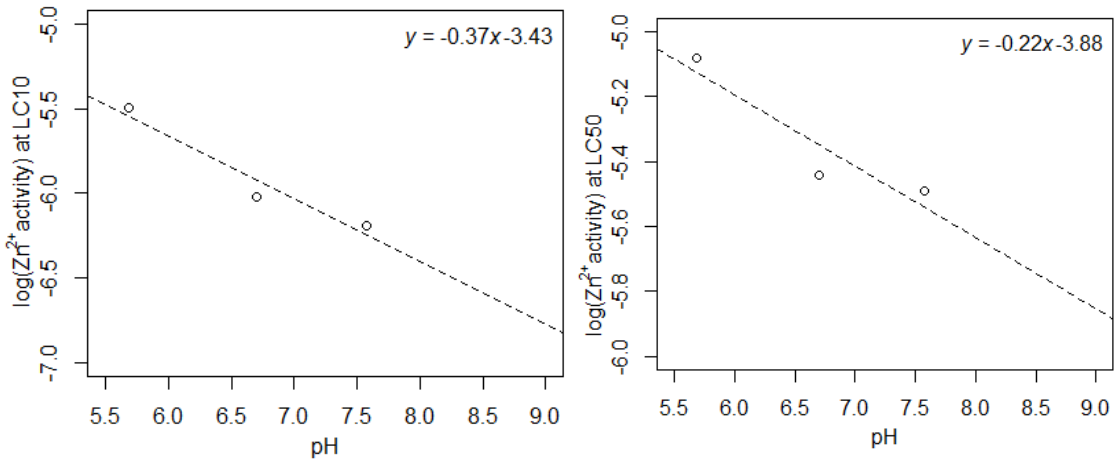

Figure 5.20. Free Zn^{2+} ion activity at the 21-day 50% and 10% lethal concentration (LC50 and LC10) as a function of pH for *Oncorhynchus mykiss* for the data from the pH-series by De Schamphelaere and Janssen (2004b).

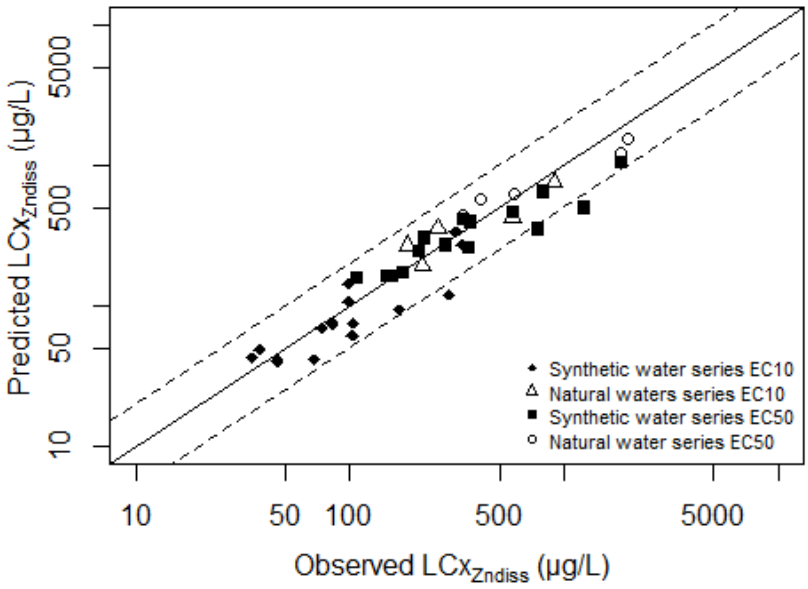

Figure 5.21. Predictive capacity of the generalized BioAvailability Model as shown by observed versus predicted 21-day x% lethal concentrations (LCxs) of zinc to *Oncorhynchus mykiss*. The intrinsic sensitivity of *O. mykiss* was calculated based on data of the natural water series and the synthetic water series separately. Predictions were made using the chronic Zn fish gBAM linked to WHAM V. The solid line is the 1:1 reference line indicating a perfect match between observed and predicted values; the dashed lines indicate an error of a factor of two between observed and predicted values.

Table 5.10. Prediction statistics of the LCx_{Zndiss} data[a] predicted with the chronic Zn fish BLM and gBAM in WHAM V

	Fish BLM				Fish gBAM			
	Synthetic waters		Natural waters		Synthetic waters		Natural waters	
	LC50 data	LC10 data	LC50 data	LC10 data	LC50 data	LC10 data	LC50 data	LC10 data
Mean prediction error	1.41	1.31	1.43	1.61	1.37	1.40	1.32	1.30
Median prediction error	1.40	1.27	1.42	1.52	1.28	1.26	1.32	1.35
% predicted within twofold error	100	100	100	80	90	93	100	100

[a] Data from De Schamphelaere and Janssen (2004b) and from De Schamphelaere et al. 2005

gBAM for Cu

Figure 5.22 shows the the linear relation between $\log_{10}$(7-day $EC60_{Zn^{2+}}$) versus pH for *P. promelas*. The S_{pH} value for *P. promelas* is equal to 0.38. This value were incorporated into the gBAM.

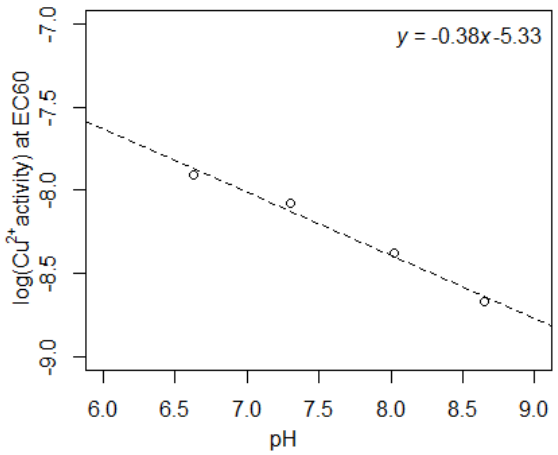

Figure 5.22 Free Cu^{2+} ion activity at the 7-day 60% effective concentration (EC60) as a function of pH for *Pimephales promelas* for the data from the pH-series by Erickson et al (1996).

The intrinsic sensitivity (Q60) was equal to -5.65. Figure 5.23 shows the performance of the toxicity model in predicting Cu toxicity for *P. promelas*. The model performance is compared to the performance of the BLM in Table 5.11. The gBAM predicts 78% of the EC60 data within twofold prediction error, which is 11% more accurate than the original fish BLM, which is able to predict 68% of the data within twofold prediction error.

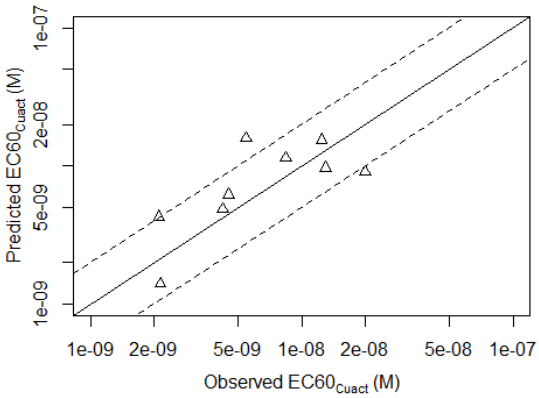

Figure 5.23. Predictive capacity of the generalized BioAvailability Model as shown by observed versus predicted 7-day 60% effective concentrations (EC60) of Cu as Cu^{2+} activity to *Pimephales promelas*. Predictions were made using the chronic Cu fish gBAM linked to WHAM V. The solid line is the 1:1 reference line indicating a perfect match between observed and predicted values; the dashed lines indicate an error of a factor of two between observed and predicted values.

Table 5.11. Prediction statistics of the $EC60_{CuAct}$ data[a] predicted with the chronic Cu fish BLM and in WHAM V

	Fish BLM (=acute *D. magna* BLM)	Fish gBAM
Mean prediction error	1.68	1.70
Median prediction error	1.38	1.16
% predicted within twofold error	67	78

Comparison of the fish BLM and gBAM is not possible based on dissolved concentrations but only based on free metal ion activities, which were measured in the study by Erickson et al (1996). This is because of the very low reaction time allowed between Cu and DOC (i.e. a hydraulic residence time of approximately 45 minutes) during the test. This resulted in the fact that the Cu spiked in the test media was not able to attain equilibrium with the DOC present in the test media. Therefore, equilibrium speciation calculations conducted with speciation software (i.e. WHAM V) cannot be used to accurately estimate the complexation of Cu with the organic matter present in the water (due to the non-equilibrium situation). More recently however, new datasets concerning Cu toxicity to fish have become available. This data includes chronic toxicity data on additional life stages and endpoints than the one investigated here. As such, the gBAM developed in the present study should in the future be validated using this data.

Conclusion

In this section, we developed a gBAM for fish for the metals Zn and Cu. Although the Zn gBAM was slightly less accurate than the Zn BLM in predicting Zn toxicity within synthetic media, it was more accurate for natural media. As predicting toxicity accurately within natural media is the ultimate aim of the developed model, the Zn gBAM for fish is a worthy and at least equally good alternative compared to the Zn BLM. The Cu gBAM was also more accurate than the Cu BLM for predicting Cu toxicity to fish. By developing these two gBAMs for Zn and Cu for fish, we have completed the uniformisation of the bioavailability models for Ni, Zn and Cu for algae, daphnids and fish to the gBAM structure. These models are structurally identical to the use of similarly structured Ni bioavailability models that are being used to derive EQS values and perform risk assessments in Europe (EU RAR Ni, 2008; De Schamphelaere and Janssen, 2010).

OVERALL CONCLUSION CHAPTER 5

In Chapter 5, four gBAMs were developed that showed improvements compared to the original BLMs to predict single metal toxicity of Zn and Cu to invertebrates and fish. Table 5.12 gives an overview of the main characteristics and differences between the BLM and gBAM. First, in the BLM the relation between H^+ activity and Me^{2+} activity is linear, assuming single-site competition, whereas in the gBAM this relation is non-linear and thus the assumption of multiple binding sites is made. On the other hand, both models assume single-site competition for other constants such as Ca and Mg.

In addition, some improvements were made to the model constants in the gBAMs which can be seen as advantages for the gBAM compared to the BLM. First, instead of a K_{HBL} parameter calculated based on data for one *D. magna* clone, the Cu *D. magna* gBAM incorporates a S_{pH} parameter that was calibrated on data for two different *D. magna* clones. Second, because recent research unambiguously showed the influence of hardness on Cu toxicity to *D. magna* (Rodriguez and Arbildua 2012), the Cu *D. magna* gBAM rightfully contains Ca and Mg competition parameters (Van Regenmortel et al. 2015/Chapter 5.1), whereas the original Cu *D. magna* BLM does not (De Schamphelaere and Janssen 2004a). Third, in contrast to the Cu fish BLM, for which the pH effect was calibrated on acute *D. magna* data, the pH effect of the Cu fish gBAM was specifically calibrated on chronic fish toxicity data. Fourth, the Zn *D. magna* gBAM is applicable to a broader range of water chemistry compared to the original BLM. Finally, for all four newly developed gBAMs we showed that they were equally or more accurate than the original BLMs in predicting metal toxicity.

Table 5.12. Overview of some characteristics and differences between the original *Daphnia magna* and *Oncorhynchus mykiss* BLMs for Cu and Zn and the newly developed gBAMs

	Cu & Zn Daphnia and Fish BLM	Cu and Zn Daphnia and Fish gBAM
Relation between Me^{2+} and H^+?	Linear relationship (single-site competition) ➔ H^+ biotic ligand constant	Relation seen as non-linear (relation between Me^{2+} and pH linear) ➔ SpH slope value
Other constants	Single-site competition (linear relationship) ➔ "BLM-type" constants	Single-site competition (linear relationship) "BLM-type" constants
Mathematical formula		
Intrinsic sensitivity	$f^{50\%}$ Gill metal concentration; "median lethal concentration"	Q50 Intrinsic sensitivity
Some advantages of the gBAM compared to the BLM	• SpH value in Cu *D. magna* gBAM calculated on data of two clones • Additional constants based on new research • Cu fish gBAM based on fish data instead of acute *D. magna* data • Usually more accurate than BLM in predicting single metal toxicity	

Six

IMPLICATIONS FOR RISK ASSESSMENT WHEN BIOAVAILABILITY MODELS ARE ADAPTED TO GBAMS

6. IMPLICATIONS FOR RISK ASSESSMENT WHEN BIOAVAILABILITY MODELS ARE ADAPTED TO GBAMS

6.1. Introduction

In Chapter 2, 4 mixture risk assessment methodologies were compared for risk estimations of mixtures of copper, zinc and nickel across 4 different monitoring datasets and a natural baseline database. We estimated that between 0% and 52% of the target water samples were at risk because of single metals or their mixtures; when the most conservative method was used (i.e., CA_{SSD}).

In Chapter 5, 4 generalized BioAvailability models (gBAMs) were developed. It was shown that these gBAMs for *D. magna* and for fish, for the individual metals Cu and Zn, showed a higher accuracy in predicting metal toxicity than their BLM-counterparts. In addition, the development of these models contributed to the uniformisation of all bioavailability models for Ni, Zn and Cu to the gBAM-structure. The use of these newly developed models in risk assessments would be analogous to the use of similarly structured Nickel bioavailability models that are being used to derive EQS values and perform risk assessments in Europe (DEPA 2008; Bio-met 2017).

To understand the impact of the implementation of these models on risk estimations, the calculations performed in Chapter 2 were repeated. The purpose of the present study was therefore to evaluate how the msPAF values changed when implementing the gBAMs for *D. magna* and fish for the metals Cu and Zn. These gBAMs differ from the original BLMs in certain aspects. First of all, all BLMs and gBAMs differ in how the effect of pH on free metal ion toxicity is described. In the BLM, the relationship between free metal ion toxicity and proton (H^+) activity is linear. However, the relationship between metal ion toxicity and proton activity is not always linear, but can also be curvilinear, which suggests that also other factors besides the competitive effect of H^+ may be important in determining the effect of pH on free metal ion toxicity. Therefore, in the gBAM, the effect of H^+ on the free metal ion is expressed as a log-linear effect of pH (S_{pH}). The Cu *D. magna* BLM and gBAM also differ in the presence of a competition parameter for Ca and Mg in the gBAM and not in the BLM. Because of these differences between the BLM and gBAM models, we hypothesized that a correlation would be found between the difference in msPAF between both models and pH and/or Ca and Mg.

6.2. Materials and Methods

Small adaptation for Chapter 2 results

In Chapter 2, all chronic toxicity data where normalized to the specific physico-chemistry of each individual water sample (the target water sample) in each of the 5 monitoring databases before risks for the monitoring sites could be calculated. For Ni, this was done using the Ni normalization tool developed by Nys et al. (2014). However, a refined tool was recently published (Nys et al. 2016), in which the S_{pH} slope values that are used to calculate Ni toxicity for pH > 8.2 were optimized compared to those reported in Nys et al. (2014). In line with this adaptation, the calculations performed in Chapter 2 were first redone using this adapted tool for Ni, before the comparison with the gBAM-adaptations for this chapter was made. These calculations, in which all originally published bioavailability models were used, will be referred to as "Scenario A".

Adaptation of parameter files

In risk assessments, toxicity data of *D. magna*, *C. dubia*, *O. mykiss*, *P. promelas* and *P.subcapitata* are normalized with the BLMs developed for these specific species, respectively. However, the chronic toxicity databases contain several species other than the ones listed above. As it is infeasible to develop specific BLMs for each separate species, the assumption is made that the intrinsic sensitivity (i.e. $f_{MeBL,i,x}$ or $Q_{i,x}$) between related species is different but that the interactions between the metals and other cations (e.g. Ca^{2+}, Mg^{2+}, Na^{+}, H^{+}) at the biotic ligand are equal among related species (i.e. invertebrates, fish and algae) (Van Sprang et al. 2009). The cross-validation of the specific BLMs to related species has shown to be successful (De Schamphelaere and Janssen 2010; De Schamphelaere et al. 2006b; Schlekat et al. 2010). Therefore, all invertebrate EC10 values are normalized with the *D. magna* or *C. dubia* bioavailability models, all vertebrate (fish) EC10 values with the *O. mykiss* or *P. promelas* bioavailability models and all algae EC10 values with the *P.subcapitata* bioavailability models. Before the gBAMs are implemented, it should therefore be checked whether the cross-validation of these models to related species is successful. For the Zn *D. magna* gBAM, this was confirmed in Chapter 5 (Van Regenmortel et al. 2017b). For the Cu *D. magna* gBAM, the cross-validation was also successful (Appendix E.1).

For Cu and Zn, the bioavailability model parameter files for invertebrates and fish were modified to reflect the adaptations that were made to the models, i.e. adaptation to the gBAMs. The WHAM-Model V speciation software (Tipping 1994) was used.

The calculations, in which the originally published bioavailability models for invertebrates and fish for the metals Zn and Cu were replaced by gBAMs developed in Chapter 5, will be referred to as "Scenario B".

Ecoregions

To examine the influence of the possible implementation of the gBAMs on the HC5 values, we calculated HC5 values for the different European Union (EU) ecoregions (Table 6.1). This procedure, in which a model is tested in different EU ecoregions, was also followed in the Cu and Ni Risk Assessment Reports (ECI 2008, DEPA 2008). These seven surface waters show a diverse physico-chemistry and are representative for waters found in the EU.

Table 6.1. Summary of the physico-chemistry characteristic of the different surface waters selected for HC5 calculations.

Type	Name	Country	pH	DOC (mg/L)	Na (mg/L)	Mg (mg/L)	K (mg/L)	Ca (mg/L)	Cl (mg/L)	SO_4 (mg/L)	CO_3 (mg/L)
Lake (oligotrophic)	Lake Monate	Italy	7.7	2.5	2.3	3.5	0.8	13.6	3.2	18.8	63.8
River (Large)	River Rhine	the Netherlands	7.8	2.8	36.8	10.9	5.7	68.9	81.5	51.9	147.8
River (medium)	River Otter	United Kingdom	8.1	3.2	14.2	11.6	5.4	46.9	23.5	34.0	141.1
River (medium)	River Teme	United Kingdom	7.6	8.0	12.9	8.4	3.7	49.9	22.3	22.7	149.9
Lake (acidic)	/	Sweden	6.7	3.8	7.7	1.5	0.9	8.7	11.6	10.7	24.2
River (Mediterranean)	River Ebro	Spain	8.2	3.7	5.3	22.1	1.1	72.9	5.6	6.6	43.2
River (ditches)	/	the Netherlands	6.9	12.0	59.8	31.6	8.4	88.2	113.4	76.0	413.8

In a first step, all the original bioavailability models were used to calculate the HC5 values for Cu and Zn. Subsequently, the newly developed gBAMs (i.e. those for *D. magna* and fish, for Cu and Zn) were used one by one, to examine the individual effect of the gBAM on the HC5 values. In addition, the newly developed gBAMs were both used simultaneously, to examine the effect of both gBAMs on the HC5 values

Toxic pressure (msPAF) calculations

As was done in Chapter 2, the toxic pressure of the metal mixture for the different target water samples within the monitoring databases was calculated with 4 different methods. The R code used to apply these methods was the same as was applied in Chapter 2. The only difference was the implementation of the gBAMs for *D. magna* and fish for the normalization of the chronic toxicity data for the metals Cu and Zn (i.e. Scenario B) (Figure 6.1).

The results of Chapter 2 showed that use of the log-normal species sensitivity distribution (SSD) instead of the best-fit distribution had little impact on risk estimates. Therefore, for this chapter, we will only use the log-normal SSD to calculate HC5 values.

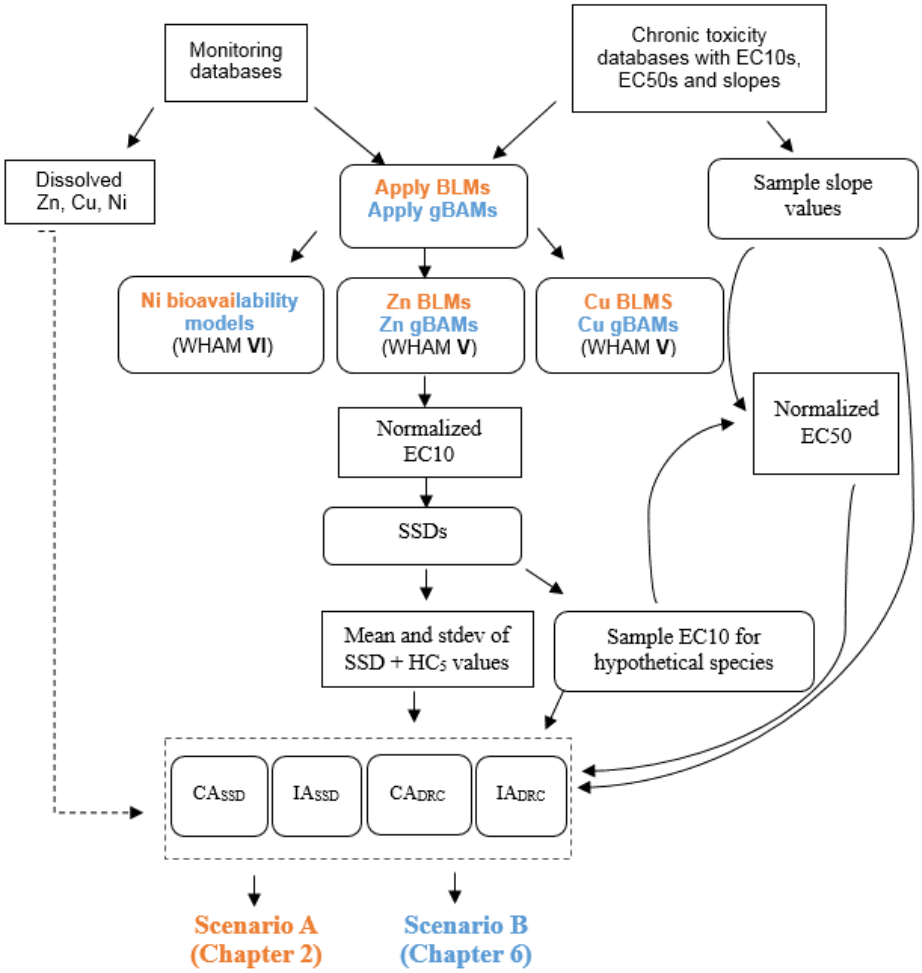

Figure 6.1 Overview of the methodology used for the calculations in Scenario A for which all original bioavailability models are used to normalize toxicity data (orange) and Scenario B for which the gBAMs for *D. magna* and fish for the metals Cu and Zn developed in Chapter 5 are implemented together with all original bioavailability models for Ni and the original bioavailability models for algae for Cu and Zn for (blue) (these original bioavailability models for Ni and Cu already had the gBAM-structure).

6.3. Results and Discussion

Small adaptation for Chapter 2 results

The use of the refined Ni normalization tool only brought about small changes in absolute msPAF values (Appendix E.2). In addition, the main conclusions of Chapter 2, related to the comparison of the four methods, were not affected. For example, the order of conservatism of our four methods, the tiered metal-mixtures risk evaluation scheme and the MoS provided by the CA_{SSD} method were not affected. The results obtained when using the refined Ni normalization tool, and not the results from Chapter 2 in which the former Ni normalization tool was implemented, will be used for the comparison with the calculations made with the adapted bioavailability models (i.e. gBAMs; Scenario B).

Ecoregions

Application of the Cu gBAMs

Table 6.2 shows the HC5 values for Cu when all original bioavailability models were used to calculate the HC5 values. Furthermore, it also shows the HC5 values when the Cu gBAM was implemented for *D. magna*, together with the original algae and fish bioavailability models, when the Cu gBAM was implemented for fish, together with the original *D. magna* and algae bioavailability models and when the Cu gBAM was implemented for *D. magna* and for fish, together with the original algae bioavailability models.

Implementing the gBAM for invertebrates has considerable influence on the average HC5 values (i.e. average difference of 47.5%). When investigating the correlation between (1) the factor difference between the gBAM and BLM HC5 results and (2) the pH, Ca concentration and Mg concentration (Figure 6.2; blue lines; circles), it is clear that Ca has a significant influence on the difference between both models. At the highest Ca concentration (i.e. for the ditch in the Netherlands) the gBAM predicts a 60% higher HC5 value compared to the BLM, while at the lowest Ca concentration (i.e. the Swedish lake) a decrease in HC5 concentration of 40% is observed. The influence of Ca on the difference between the BLM and gBAM results is in line with expectations, as the BLM does not incorporate a Ca competition constant (De Schamphelaere et al. 2004) while the gBAM does (Chapter 5, Van Regenmortel et al. 2015).

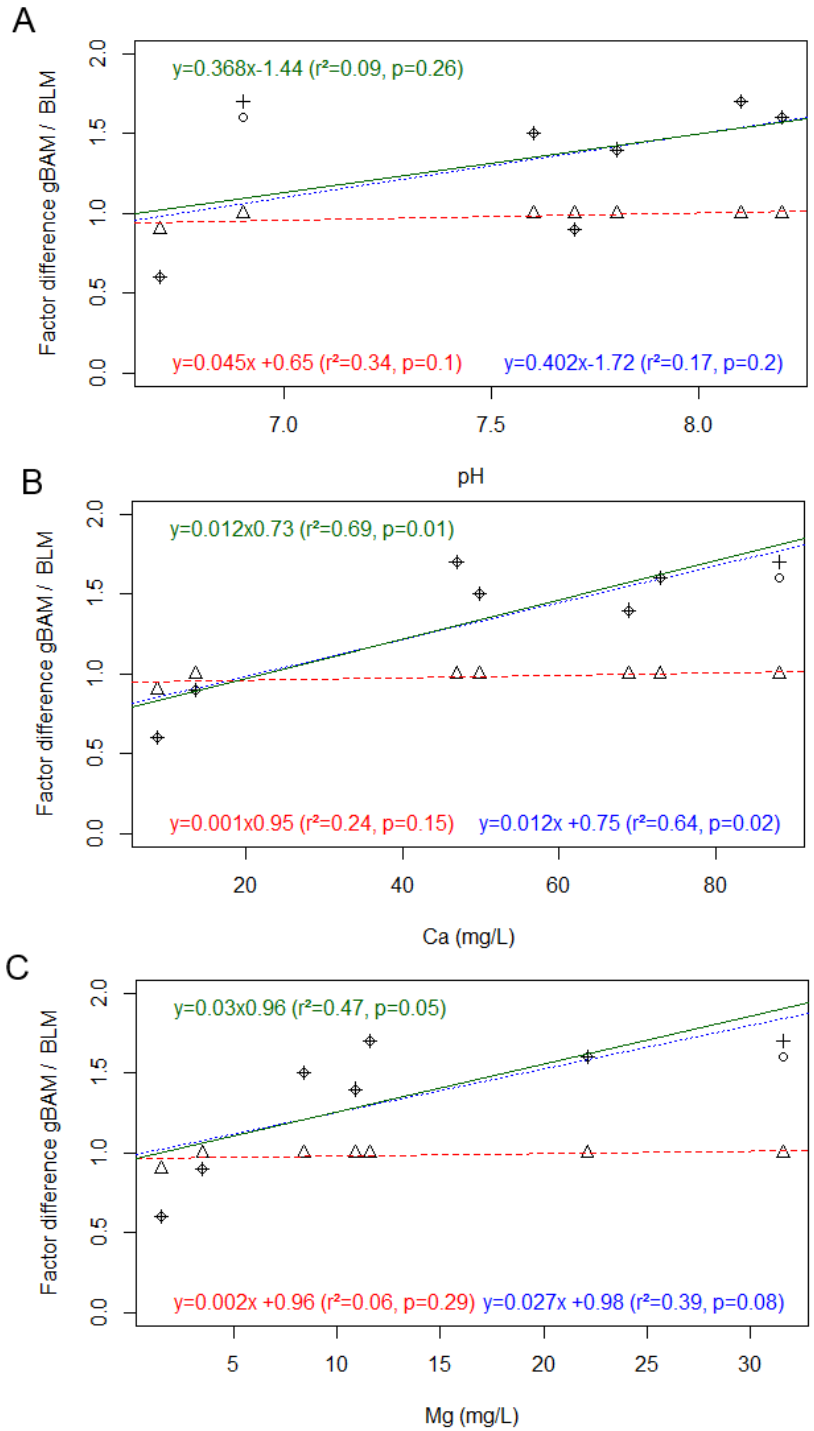

Figure 6.2 Factor differences (i.e. HC5 calculated with gBAM / HC5 calculated with BLM) against different chemical parameters (pH, Ca concentration (mg/L) and Mg concentration (mg/L)). Circles (blue), triangles (red) and crosses (green) indicate the factor differences when HC5 values are calculated with (1) a combination of the Cu gBAM for invertebrates and the original Cu bioavailability models for algae and fish (blue), (2) a combination of the Cu gBAM for fish and the original Cu bioavailability models for invertebrates and algae (red) and (3) a combination of the Cu gBAM for invertebrates and fish and the original Cu bioavailability model for algae (green).

Table 6.2. Overview of the HC5 values for copper for the different EU ecoregions calculated with (1)[a] a combination of all original bioavailability models for copper, (2)[b] a combination of the gBAM for invertebrates and the original bioavailability models for algae and fish, (3)[c] a combination of the gBAM for fish and the original bioavailability models for invertebrates and algae and (4)[d] a combination of the gBAM for invertebrates and fish and the original bioavailability model for algae. The percentage difference and the factor differences between combination (1) and (2), between combination (1) and (3) and between combination (1) and (4) are given.

Type	Name	Country	original bioavailability models[a] HC5 (µg/L)	gBAM Daphnia[b] HC5 (µg/L)	% difference	Factor difference	gBAM Fish[c] HC5 (µg/L)	% difference	Factor difference	gBAM Daphnia and Fish[d] HC5 (µg/L)	% difference	Factor difference
Lake (oligotrophic)	Lake Monate	Italy	10.32	9.24	-10.48	0.9	10.02	-2.90	1.0	9.00	-12.84	0.9
River (Large)	River Rhine	The Netherlands	8.46	11.87	40.30	1.4	8.39	-0.77	1.0	12.04	42.41	1.4
River (medium)	River Otter	United Kingdom	8.29	13.96	68.37	1.7	8.14	-1.77	1.0	14.46	74.48	1.7
River (medium)	River Teme	United Kingdom	22.06	33.40	51.38	1.5	22.15	0.40	1.0	33.73	52.91	1.5
Lake (acidic)	/	Sweden	11.25	6.77	-39.80	0.6	10.58	-5.92	0.9	6.50	-42.22	0.6
River (Mediterranean)	River Ebro	Spain	12.52	20.30	62.21	1.6	12.52	-0.01	1.0	20.17	61.13	1.6
River (ditches)	/	The Netherlands	25.99	41.55	59.85	1.6	26.46	1.81	1.0	43.11	65.86	1.7
					Mean: 47.5			Mean 1.9			Mean: 50.3	

Implementing the gBAM for fish does not have a large influence on the average HC5 values (i.e. average difference of 1.9%; Table 6.2). In addition, no significant correlation between the factor differences and the physico-chemical parameters is observed (Figure 6.2; red line; triangles). This can be explained by the less sensitive nature of fish to Cu compared to invertebrates. The majority fish species that are present in the chronic Cu toxicity database are situated in the middle of the SSD curve. This implies that a change in the EC10 value of these fish between the calculations with the BLM and the gBAM, has a small influence on the HC5 value. Therefore, implementing the gBAM for fish does not have a large influence on the HC5 values.

As was expected from the above results, implementing both the Cu *D. magna* and fish BLM has an even larger influence on the HC5 values (Table 6.2) than when implementing the gBAMs separately (i.e. up to 75% difference). However, the largest influence on the HC5 values in due to the *D. magna* gBAM. Again, a significant correlation between the factor difference of both models and the Ca concentration is observed (Figure 6.2; green line; crosses). In addition, a significant correlation with Mg concentration is found (Figure 6.2). Implementing both gBAMs has the largest influence on waters with high hardness. In those waters, the HC5 is higher when estimated using the gBAM than with the BLM. In waters with low hardness however, the HC5 is lower when estimated with the gBAM than with the BLM.

Application of the Zn gBAMs

Table 6.3 shows the HC5 values for Zn when all original bioavailability models were used to calculate the HC5 values. Furthermore, it also shows the HC5 values when the Zn gBAM was implemented for *D. magna*, together with the original algae and fish bioavailability models, when the Zn gBAM was implemented for fish, together with the original *D. magna* and algae bioavailability models and when the Zn gBAM was implemented for *D. magna* and for fish, together with the original algae bioavailability models.

Implementing the Zn gBAM for invertebrates has a smaller influence on the HC5 values than implementing the Cu gBAM for invertebrates. However, an average difference of 6.9% is still observed when implementing the Zn gBAM for invertebrates. When investigating the correlation between (1) the factor difference between the gBAM and BLM HC5 results and (2) the pH, Ca concentration and Mg concentration (Figure 6.3; blue lines; circles), it is clear that pH has a significant influence on the difference between both models. At the lowest pH (i.e. the Swedish lake) the gBAM predicts a 17% higher HC5 value compared to the BLM, while at the highest pH (i.e. the river Ebro) a decrease in HC5 concentration of 6.5% is observed. This was somewhat expected, as Heijerick et al. (2005) calculated a stability constant for H^+ based on a linear regression between the EC50 as Zn^{2+} activity and the H^+ activity (Figure 6.4), whereas it seemed that a non-linear relationship may have better fitted the data. The relation between Zn toxicity and pH is therefore better explained by a log-linear relationship implemented in the gBAM.

As was observed for Cu, implementing the Zn gBAM for fish does not have a large influence on the average HC5 values (i.e. average difference of 3.1%; Table 6.3). Again, this can be explained by the fact that fish are less sensitive to Zn toxicity than invertebrates and algae. This implies that the a change

in the normalized EC10 value of these fish between the calculations with the BLM and the gBAM, has a small influence on the HC5 value.

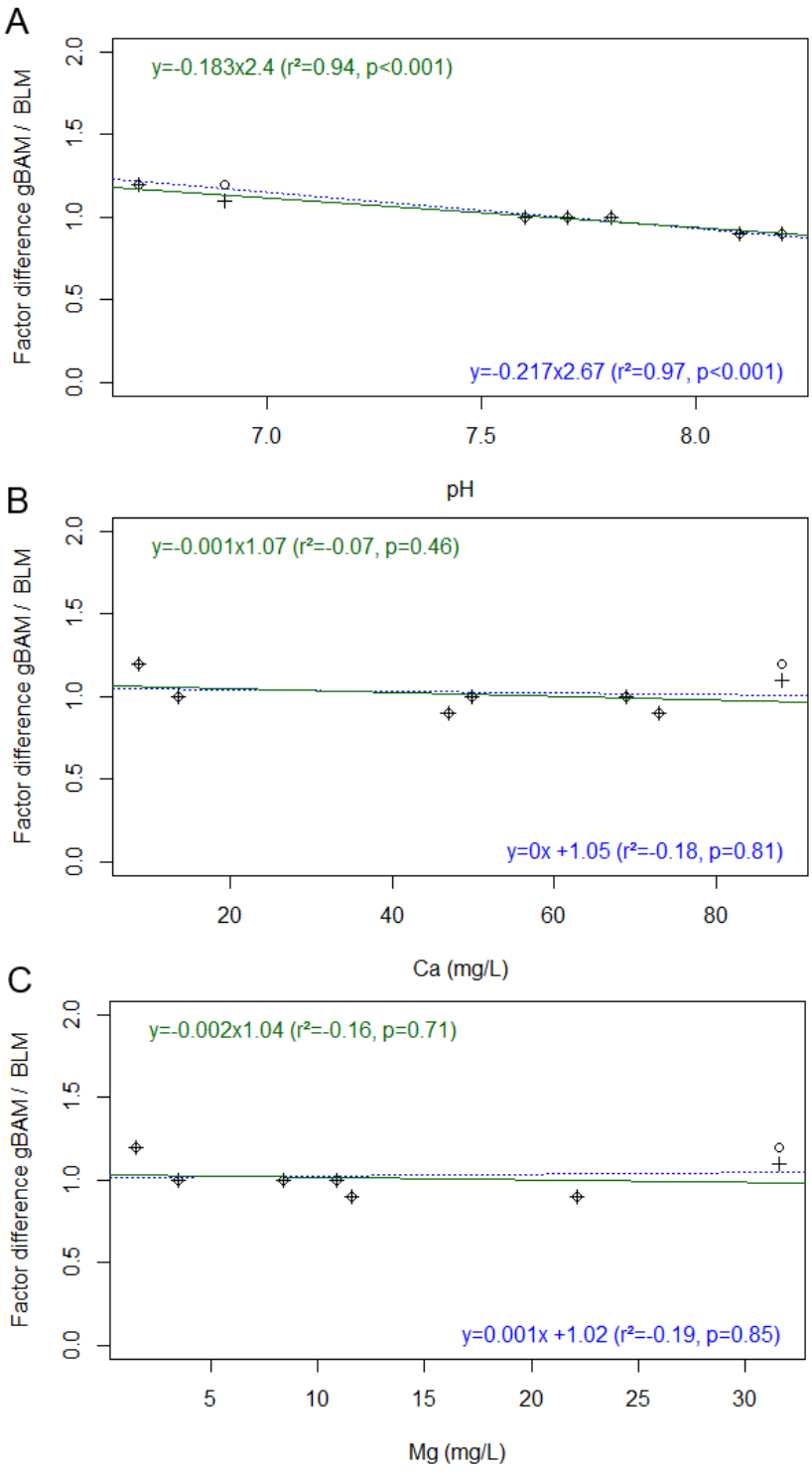

Figure 6.3. Factor differences (i.e. HC5 calculated with gBAM / HC5 calculated with BLM) against different chemical parameters (pH, Ca concentration (mg/L) and Mg concentration (mg/L)). Circles (blue) and crosses (green) indicate the factor differences when HC5 values are (1) calculated with a combination of the Zn gBAM for invertebrates and the original Zn bioavailability models for algae and fish and (2) calculated with a combination of the Zn gBAM for invertebrates and fish and the original Zn bioavailability model for algae, respectively.

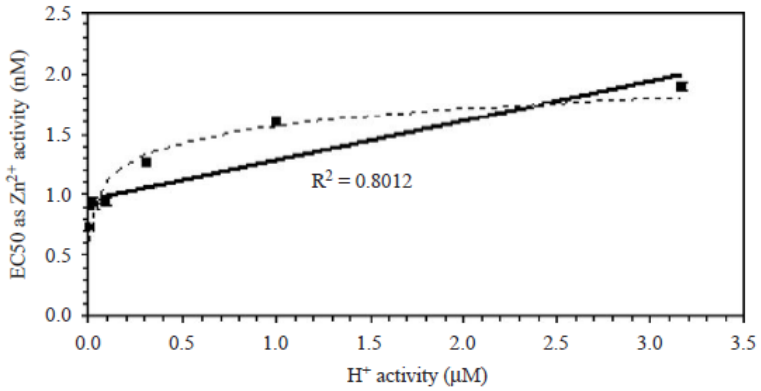

Figure 6.4. Relationship between the 21-day EC50 (µM Zn2+ activity) and the proton concentrations (as free ion activity) in the test medium (H^+ in µM). Full line = linear function; dotted line = logarithmic function (taken from Heijerick et al. 2005).

As was expected from the above results, implementing both the Zn *D. magna* and fish BLM has an even larger influence on the HC5 values (Table 6.3) than when implementing the gBAMs separately (up to 22% difference). However, the influence is smaller than compared to implementation of the Cu gBAMs. Again, a significant correlation between the factor difference of both models and the pH is observed (Figure 6.3; green line; crosses). Implementing both gBAMs has the largest influence on waters with low pH. In those waters, the HC5 is overestimated using the BLM. In waters with high pH however, the HC5 is underestimated with the BLM. Therefore, in these waters, the HC5 calculated with the BLM is not protective for 5% of the species within the communities.

Application of the gBAMs for the Ecoregions

Implementing the newly developed gBAMs to calculate HC5 values for the Ecoregions is a procedure that is applied in risk assessments (ECI 2008, DEPI 2008). However, it only gives a first impression of the implications of these gBAMs for risk estimations because only 7 waters are considered. For more robust results, monitoring datasets including data for numerous waters should be assessed. In the following section, this was done for the monitoring databases described in Chapter 2.

Table 6.3. Overview of the HC5 values for zinc for the different EU ecoregions calculated with (1)[a] a combination of all original bioavailability models for copper, (2)[b] a combination of the gBAM for invertebrates and the original bioavailability models for algae and fish, (3)[c] a combination of the gBAM for fish and the original bioavailability models for invertebrates and algae and (4)[d] a combination of the gBAM for invertebrates and fish and the original bioavailability model for algae. The percentage difference and the factor differences between combination (1) and (2), between combination (1) and (3) and between combination (1) and (4) are given.

Type	Name	Country	original bioavailability models [a] HC5 (µg/L)	gBAM Daphnia [b] HC5 (µg/L)	% difference	Factor difference	gBAM Fish [c] HC5 (µg/L)	% difference	Factor difference	gBAM Daphnia and Fish[d] HC5 (µg/L)	% difference	Factor difference
Lake (oligotrophic)	Lake Monate	Italy	18.31	18.40	0.47	1.0	17.66	-3.57	1.0	17.76	-2.99	1.0
River (Large)	River Rhine	the Netherlands	25.09	24.67	-1.69	1.0	24.47	-2.47	1.0	24.17	-3.70	1.0
River (medium)	River Otter	United Kingdom	27.05	25.53	-5.62	0.9	25.80	-4.63	1.0	24.78	-8.39	0.9
River (medium)	River Teme	United Kingdom	44.32	44.95	1.43	1.0	43.60	-1.62	1.0	44.23	-0.19	1.0
Lake (acidic)	/	Sweden	14.69	17.17	16.86	1.2	15.08	2.60	1.0	17.95	22.13	1.2
River (Mediterranean)	River Ebro	Spain	28.35	26.50	-6.54	0.9	27.21	-4.01	1.0	25.99	-8.32	0.9
River (ditches)	/	the Netherlands	46.78	54.07	15.58	1.2	45.50	-2.75	1.0	53.34	14.02	1.1
					Mean: 6.9			Mean: 3.1			Mean: 8.5	

Toxic pressure (msPAF) calculations

Figure 6.5 shows the differences in HC5 values when calculations were performed with Scenario A and B for Cu, in relation to the Ca concentration. As was observed for the Ecoregions (see above), the factor difference is influenced by the Ca concentration, which was explained by the presence of a competition parameter for Ca in the *D. magna* gBAM and not in the *D. magna* BLM. However, for 2 monitoring databases (i.e. the Rhine and the Dommel database) no clear pattern can be observed. In Figure 6.6 the differences in HC5 values when calculations were performed with Scenario A and B for Cu, in relation to the pH is plotted. For all monitoring databases, including the Rhine and Dommel, the influence of pH on the factor difference can be observed. From Figure 6.5 and 6.6 it can be deducted that a combination of Ca concentration and pH determines the difference between the results using Scenario A and B, although for most monitoring databases these differences are mostly within 2-fold error. For Cu, Scenario B predicts a higher HC5 value at high Ca concentration and high pH and a lower HC5 value at low Ca concentration and low pH compared to Scenario A. In Chapter 5, we showed that the predictive accuracy of the gBAMs for *D. magna* and fish is higher than that of the BLMs. Therefore, in current risk assessment procedures for Cu in which Scenario A is implemented, risk estimates of Cu might be somewhat over-conservative for high Ca concentration and high pH waters, but somewhat under-conservative for low Ca and low pH waters.

Figure 6.7 shows the differences in HC5 values when calculations were performed with Scenario A and B for Zn, in relation to the pH. The difference between both scenarios is smaller for Zn than for Cu. For Zn these differences are within 2-fold error for all monitoring databases. As was observed and explained above for the Ecoregions, the difference in HC5 values is influenced by pH. For Zn, Scenario B predicts a lower HC5 value at low pH and high pH and a higher HC5 value at intermediate pH compared to Scenario A. Here too, this implies that risk estimates for Zn in which Scenario A is implemented, could somewhat underestimate risk due to Zn in waters with low and high pH and somewhat overestimate risk in waters with intermediate pH. However, the over or underestimations will in any case be less pronounced for zinc than for copper.

Table 6.4 shows the distribution of toxic pressure (expressed as msPAF values) for all 4 methods for the different monitoring datasets, when calculations were performed with Scenario B. Table 4 also shows the absolute difference in median msPAF, % target water samples affected and MoS between Scenario B and Scenario A. A positive difference implies that the value calculated with Scenario B is higher than when calculated with Scenario A. A negative value implies the opposite. It can be deducted from Table 4 that the influence of adapting the bioavailability models to gBAMs for invertebrates and fish for the metals Cu and Zn on the risk estimation is small. This can be explained by the individual toxic unit contribution ($TU= c_i/HC5_i$) of the three metals to the mixture. Averaged over all 5 monitoring databases, the toxic unit contribution (TU_{HC5}) of Zn, Cu and Ni is equal to 45% ± 26%, 22% ± 22% and 32%± 21% (average ± sd), respectively. Therefore, although the influence of the implementation of the Cu *D. magna* and fish gBAM on the HC5 values is considerable (mostly 2-fold, but up to 4-fold for some monitoring databases), the influence on the calculated risk estimations is low because the contribution of Cu to the mixtures in these monitoring datasets is the lowest of all three metals.

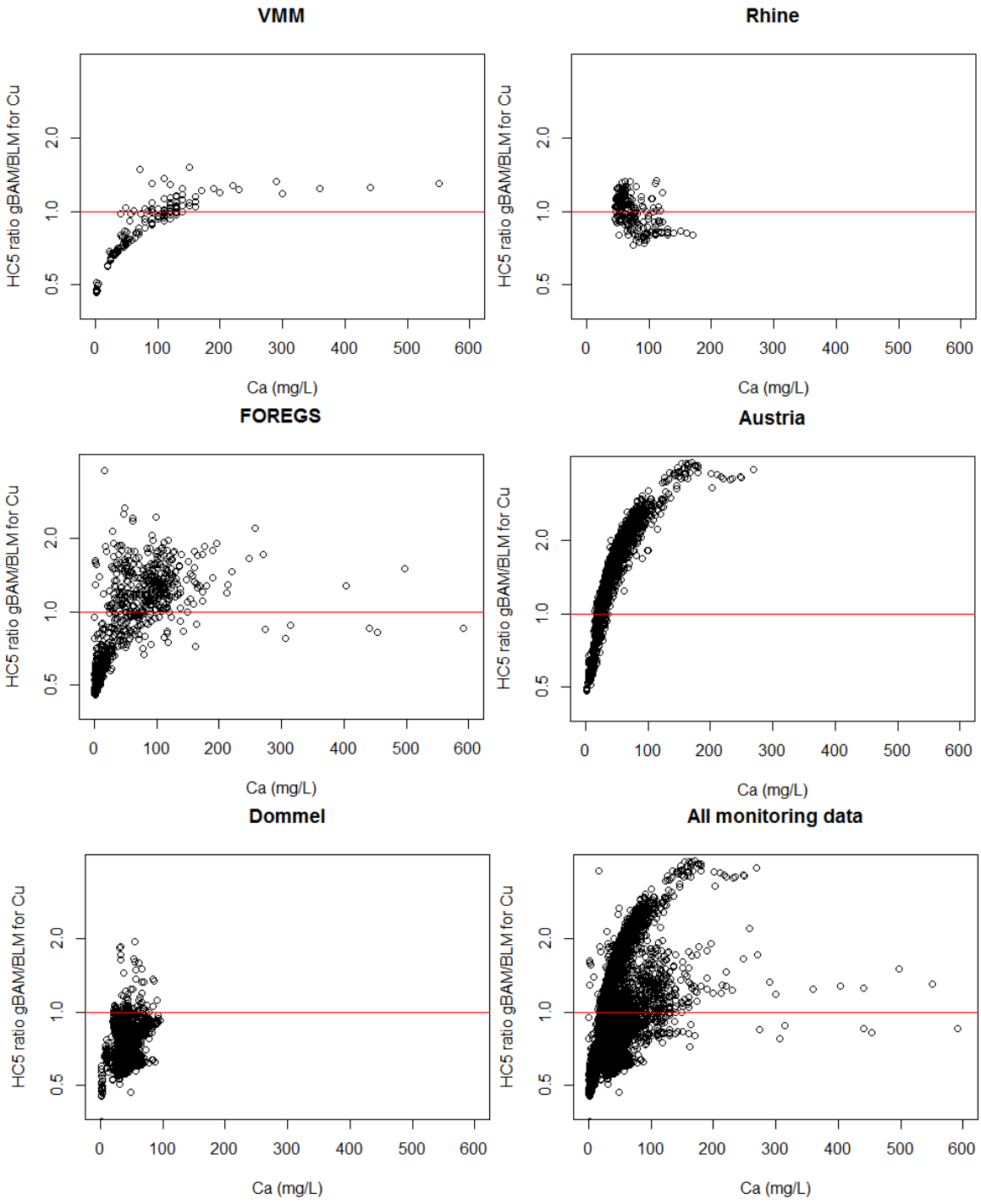

Figure 6.5 Difference in HC5 value (µg/L) for Cu when HC5 values are calculated with Scenario B (i.e. toxicity data for invertebrates and fish normalized with the gBAMs developed in Chapter 5 and the toxicity data for algae were normalized with the original algae bioavailability model) and Scenario A (i.e. toxicity data normalized with all original bioavailability models) (Scenario B/Scenario A), in relation to Ca concentration, for the different monitoring databases.

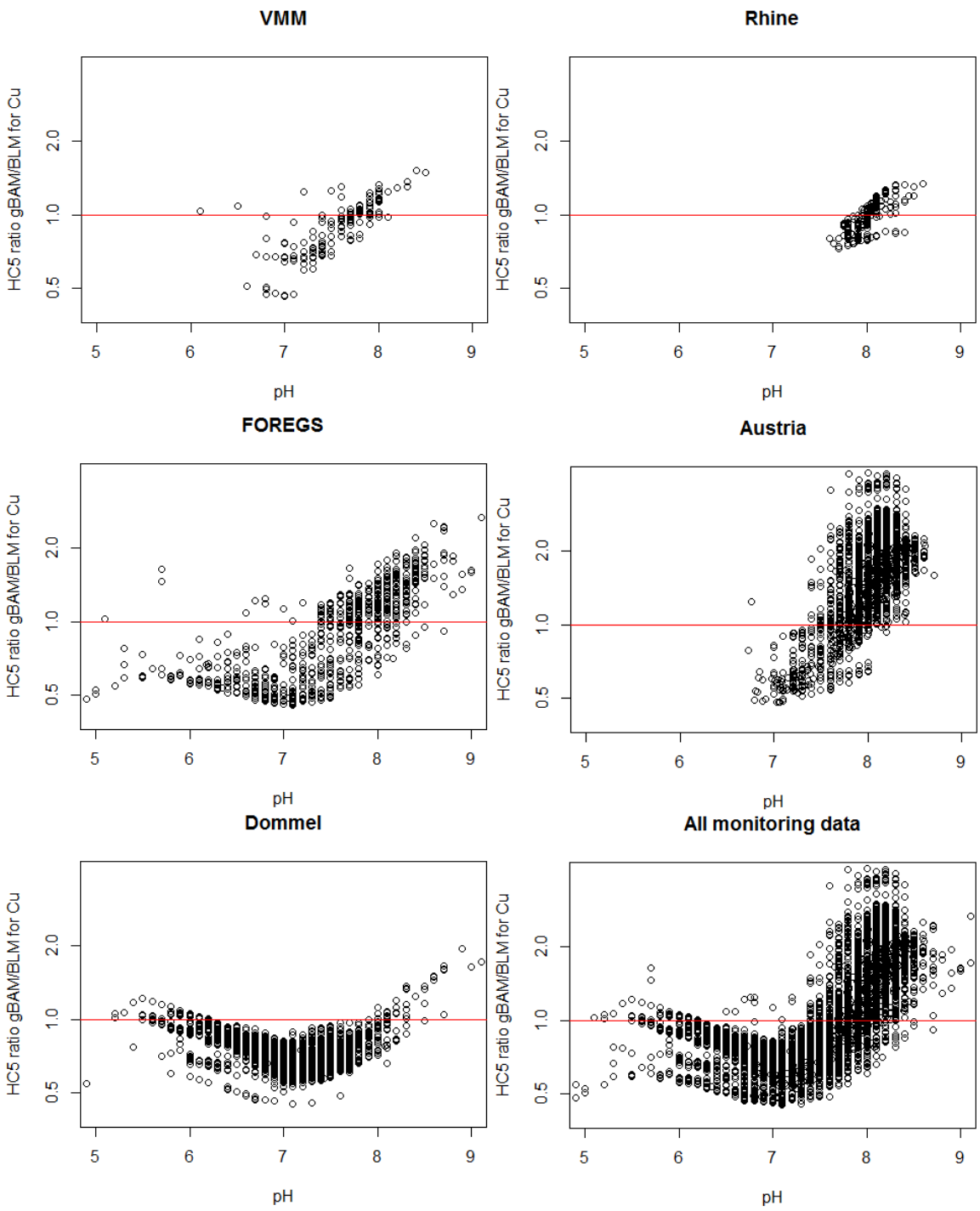

Figure 6.6 Difference in HC5 value (µg/L) for Cu when HC5 values are calculated with Scenario B (i.e. toxicity data for invertebrates and fish normalized with the gBAMs developed in Chapter 5 and the toxicity data for algae were normalized with the original algae bioavailability model) and Scenario A (i.e. toxicity data normalized with all original bioavailability models) (Scenario B/Scenario A), in relation to pH, for the different monitoring databases.

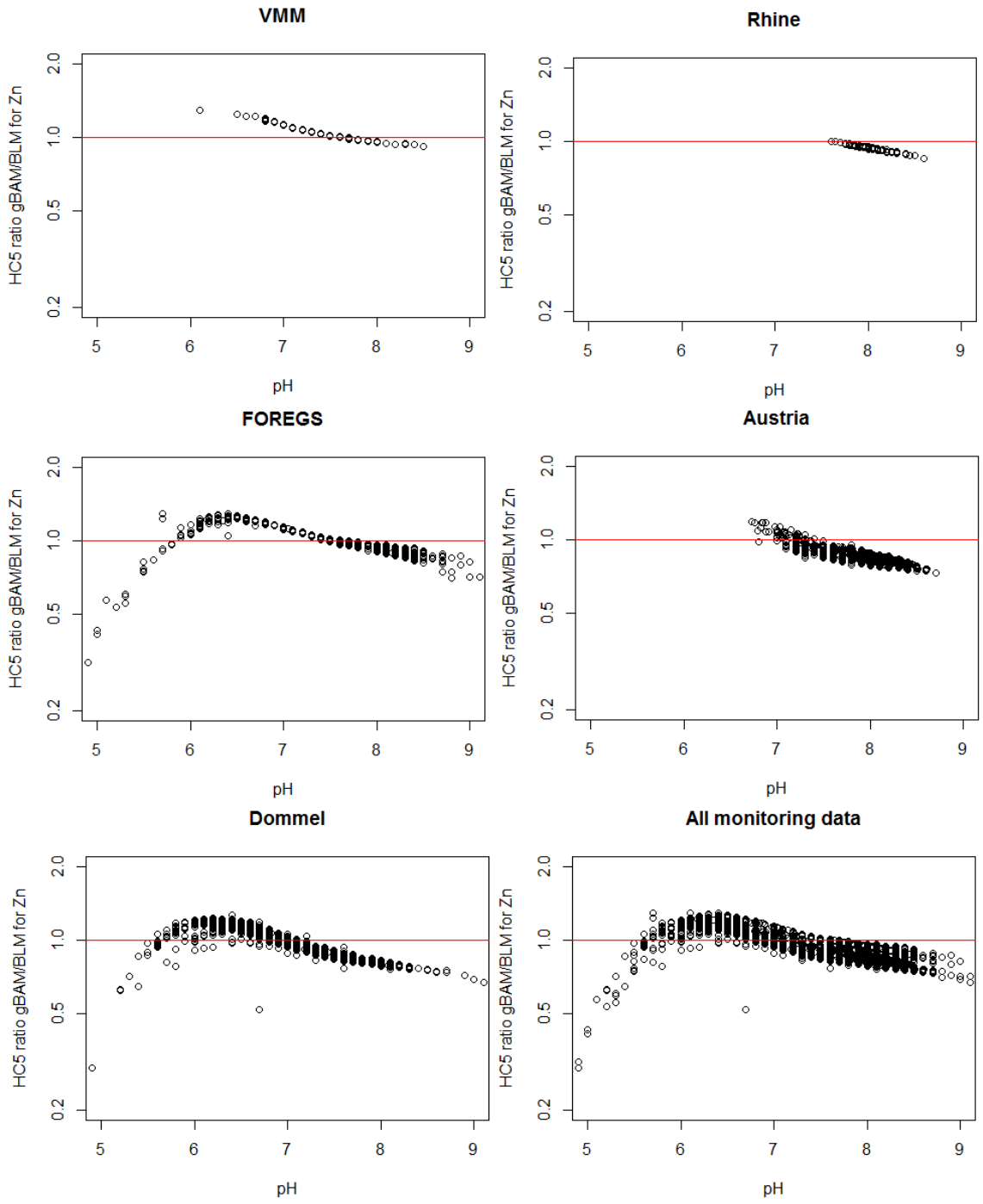

Figure 6.7 Difference in HC5 value (µg/L) for Zn when HC5 values are calculated with Scenario B (i.e. toxicity data for invertebrates and fish normalized with the gBAMs developed in Chapter 5 and the toxicity data for algae were normalized with the original algae bioavailability model) and Scenario A (i.e. toxicity data normalized with all original bioavailability models) (Scenario B/Scenario A), in relation to pH, for the different monitoring databases.

Table 6.4 Toxic pressure expressed as multisubstance potentially affected fraction of species (msPAF) for the Dommel, Flanders (VMM), Rhine, Austria, and FOREGS database obtained with the different methods. Normalisation of the toxicity data was performed with Scenario B, i.e. the Cu and Zn toxicity data for invertebrates and fish were normalized with the gBAMs developed in Chapter 5 and the Cu and Zn toxicity data for algae were normalized with the original algae bioavailability models. The Ni toxicity data was normalized with the original bioavailability models in both scenarios. The values between parentheses indicate the absolute difference in results between Scenario B and Scenario A (B-A). in the latter method, the toxicity data were normalized with all original bioavailability models. A positive difference implies that the msPAF value calculated with Scenario B is higher than when calculated with Scenario A.

	Dommel				VMM				Rhine			
	CA_{SSD}	CA_{DRC}	IA_{SSD}	IA_{DRC}	CA_{SSD}	CA_{DRC}	IA_{SSD}	IA_{DRC}	CA_{SSD}	CA_{DRC}	IA_{SSD}	IA_{DRC}
median msPAF	0.063 (0.009)	0.042 (0.007)	0.028 (0.0045)	0.031 (0.005)	0.008 (-0.001)	0.004 (0.000)	0.002 (0.000)	0.003 (0.000)	0.004 (0.000)	0.001 (0.000)	0.001 (0.000)	0.001 (0.000)
% Samples affected (msPAF > 0.05)	55 (3.4)	47 (2.6)	41 (1.7)	42 (1.6)	27 (0.0)	25 (0.7)	21 (-1.9)	23 (-1.3)	0 (0.0)	0 (0.0)	0 (0.0)	0 (0.0)
% Samples affected by mixture of metals and not by any individual metals	17 (2.1)	10 (1.2)	3 (0.5)	4 (0.4)	8 (1.3)	6 (2.6)	2 (-0.7)	4 (1.3)	0 (0.0)	0 (0.0)	0 (0.0)	0 (0.0)
MoS provided by the CA_{SSD} approach	NA	1.23 (0.021)	1.53 (0.045)	1.45 (0.039)	NA	1.16 (-0.019)	1.59 (0.013)	1.46 (0.004)	NA	1.22 (-0.032)	1.76 (0.043)	1.64 (0.031)

	Austria				FOREGS			
	CA_{SSD}	CA_{DRC}	IA_{SSD}	IA_{DRC}	CA_{SSD}	CA_{DRC}	IA_{SSD}	IA_{DRC}
median msPAF	0.003 (-0.001)	0.001 (-0.001)	0.001 (0.000)	0.001 (0.000)	0.003 (0.000)	0.001 (0.000)	0.001 (0.000)	0.001 (0.000)
% Samples affected (msPAF > 0.05)	7 (-0.4)	6 (-0.1)	5 (-0.1)	5 (-0.1)	9 (0.4)	6 (-0.1)	4 (0.1)	4 (0.0)
% Samples affected by mixture of metals and not by any individual metals	3 (-0.4)	1 (-0.1)	0.2 (-0.1)	0.4 (-0.0)	5 (0.3)	2 (-0.3)	0.3 (0.0)	0.4 (-0.1)
MoS provided by the CA_{SSD} approach	NA	1.20 (-0.014)	1.55 (0.099)	1.48 (-0.036)	NA	1.21 (-0.025)	1.56 (0.004)	1.46 (-0.004)

CA = Concentration Addition, IA = Independent Action, SSD = Species Sensitivity Distribution, DRC = Dose-Response Curve, msPAF = multisubstance Potentially Affected Fraction of species, MoS = Margin of Safety, NA = Not Applicable

6.4. Conclusion

In the present chapter, Scenario B, in which the toxicity data for Cu and Zn for invertebrates and fish in the chronic toxicity databases were normalized with the gBAMs developed in Chapter 5, was implemented for bioavailability-based risk calculations. Implementing Scenario B generally showed a less than 2-fold difference of HC5 values compared to Scenario A, in which all original bioavailability models were implemented. The largest differences were found for Cu (up to 4-fold in some monitoring databases), which was related to the experimental evidence-based incorporation of a Ca competition parameter in the *Daphnia* gBAM. Yet, despite these differences, implementing Scenario B only had a small influence on median msPAF values and on the % of target water samples that are predicted to be affected by the mixture of Zn, Cu and Ni. The latter is a result of the relatively low contribution of Cu to the mixture effects in the investigated monitoring databases.

Because the newly developed gBAMs for Cu and Zn for invertebrates and fish more accurately predict single metal toxicity, we recommend Scenario B (with the gBAMs) instead of Scenario A (with the original BLMs) to normalize toxicity data for Cu and Zn prior to metal mixture risk calculations.

Seven

CALIBRATION OF THE CU, NI AND ZN BIOAVAILABILITY MODELS IN WHAM VII

7. Calibration of the Cu, Ni and Zn bioavailability models in WHAM VII

7.1. Introduction

Our calculations of msPAFs have so far been based on bioavailability-normalized dissolved metal concentrations (Van Regenmortel et al. 2017/Chapter 2). However, an important aspect to consider is that in a mixture of metals, metals may compete with each other for the binding sites of Dissolved Organic Carbon (DOC). As a consequence, a risk assessment based on dissolved concentrations might lead to some underestimation of metal mixture risks. Hence, metal mixture risks should ideally be evaluated on the free ion activity level. However, an evaluation based on free ion activities is currently limited due to the use of different speciation programs in the chronic biotic ligand models (BLMs) for the individual metals, i.e. WHAM V for Zn (Van Sprang et al. 2009) and Cu (ECI, 2008) and WHAM VI for Ni (DEPA, 2008). In addition, the use of different speciation assumptions regarding DOC 'activity' for the different individual metals also limits an evaluation based on free ion activities. Indeed, for Ni, it was shown that a % active fulvic acid (%AFA) of 40% resulted in the best fit between measured and WHAM VI calculated Ni^{2+} activities (De Schamphelaere et al. 2006a), whereas for Zn it is assumed that 61% of the FA in natural water is reactive (De Schamphelaere et al. 2005) and for Cu, even another %AFA is used, i.e. 50% (De Schamphelaere and Janssen, 2004b).

Only a uniformisation of the speciation calculations performed for the individual metals will enable to account for the competing effects between metals at the binding sites of DOC. This uniformisation should include both the uniform use of a single speciation program for all metals as well as the uniform use of a single %AFA assumption. Nys (2016) showed that recalibrating the daphnid bioavailability models of Ni, Zn and Pb in WHAM VII (the most recent version of the Windermere Humic Aqueous model) using the same speciation assumptions for each metal resulted in similar predictive capacities as the original bioavailability models. Nys (2016) used the assumption of 65% active fulvic acid (AFA). Indeed, assumptions of 60% to 70% AFA have been shown to work best for predicting metal toxicity in natural waters (Tipping, 2002) and the assumption of 65% AFA has been used in most recent metal mixture studies (Tipping and Lofts, 2013, 2015; Nys, 2016). In addition, Nys (2016) compared the predictive capacity of WHAM VII using default inorganic complexing stability constants and NIST updated inorganic binding stability constants for Ni, Zn and Pb.

Confirmation of the observations by Nys (2016) for other bioavailability models (i.e. for other species and metals) used in the risk assessment approaches for metals (e.g. Van Regenmortel et al. 2017/Chapter 2) would allow a metal mixture risk assessment that accounts for metal-metal competitive interactions at the DOC binding sites (i.e. "simultaneous speciation calculations"). Therefore, we evaluated if metal toxicity can be predicted using a single speciation software (i.e. WHAM VII) and a single set of speciation assumptions regarding the DOC 'activity' (i.e. 65% AFA) for all bioavailability models (Table 7.1), without significantly decreasing the predictive capacity of each of the individual bioavailability models. WHAM VII is the most recent version of the Windermere Humic Aqueous Model (Tipping et al. 2011) and it was shown that it can be used to accurately calculate free metal ion activity in natural waters (Lofts and Tipping, 2011).

Nys (2016) evaluated the performance of WHAM VII using EC50 data only. However, as the risk assessment that was performed in Chapter 2 (Van Regenmortel et al. 2017) uses EC10 values reported in toxicity databases to eventually calculate msPAF values, we considered it important to also evaluate the performance of WHAM VII using EC10 (or NOEC) data. In addition, as was done in Nys (2016), to assess the importance of inorganic complexation stability constants we evaluated the impact of two speciation scenarios on the prediction capacity of the bioavailability models: (1) using the default WHAM VII thermodynamic database for inorganic complexation and (2) using the stability constants for inorganic complexation reported by NIST (Smith et al. 2004).

In the present study, the predictive performance of the bioavailability models coupled with WHAM VII was compared to the predictive performances reported in the original publications.

7.2. Methodology

Data selection

Data to test the validity of the bioavailability models in WHAM VII was taken from the original publications in which the bioavailability models were developed and validated (Table 7.1). For the Cu and Zn *D. magna* BLM, in addition to the data that is specified in Table 7.1, the data that was used to validate the Cu and Zn *D. magna* gBAM (Table 7.1) was also used to validate the Cu and Zn *D. magna* BLM. This was done to make the comparison in predictive capacity between the *D. magna* BLM and gBAM possible. For the Cu fish BLM (De Schamphelaere & Janssen, 2008), as was mentioned in Chapter 5, equilibrium speciation calculations conducted with speciation software (e.g. WHAM V or WHAM VII) can't be used to accurately estimate the complexation of Cu with the organic matter present in the water. This is because of the very low reaction time (i.e. a hydraulic residence time of approximately 45 minutes) during the test which resulted in the fact that the Cu spiked in the test media was not able to attain equilibrium with the DOC present in the test media. Therefore, in this Chapter, it is not possible to validate whether the fish BLM can be used in combination with WHAM VII to accurately predict Cu toxicity. However, we do know from Chapter 5 that the BLM predictions for the fish BLM are accurate. Therefore, we will assume that the model can be used in combination with WHAM VII when the Cu bioavailability models for species other than fish (i.e. Daphnia and algae) are accurate in predicting Cu toxicity when coupled to WHAM VII.

Speciation calculations

Speciation calculations were performed as is explained in Nys 2016. WHAM VII (Tipping et al. 2011) was used to calculate the chemical metal speciation in the different test waters. MOPS was added to the default solute database (pKa of 7.2). The default complexation parameters for the metal - dissolved organic matter (DOM) complexation were used. For DOM from natural origin it was assumed that 65% of the DOM is reactive and behaves as isolated fulvic acid (FA; 65% AFA). This % was chosen as assumptions of 60% to 70% reactive FA have been shown to work best for predicting metal toxicity in natural waters (Tipping 2002). In addition, it was assumed that DOM contains 50% carbon on a weight basis. Therefore, the measured DOC concentration was multiplied by 1.3 to obtain the FA concentration to be used as the input for speciation calculations. Activities of the metal cation Fe^{3+} were assumed to

be controlled by colloidal $Fe(OH)_3$ precipitates using the default equation and solubility product embedded in WHAM VII; i.e. Fe^{3+} activity is a function of pH only (Lofts & Tipping 2011) (Equation 7.1).

$$Fe(OH)_n + nH^+ \rightarrow Fe^{3+} + nH_2O \text{ with } n = 2.49 \text{ and } \log K = -0.52 = \frac{\{Fe^{3+}\}}{\{H^+\}^n} \quad (7.1)$$

As was done in Nys 2016, two speciation scenarios were evaluated in the present study. A first scenario ("Speciation Scenario I") used the WHAM VII default parameters for inorganic ligand-metal complexation (Table 7.2). A second scenario ("Speciation Scenario II") used stability constants for inorganic-metal complexation that were adapted to those reported by the National Institute for Standards and Technology (Table 7.2).

Both scenarios were used to recalibrate the pH slope parameter to WHAM VII for all models containing this type of value. For Cu and Zn, this includes the bioavailability models for algae and the gBAMs for Daphnia and fish. For Ni, this includes the bioavailability models for algae, Daphnia, Ceriodaphnia and Fish. To recalibrate the SpH value to WHAM VII, all data that was used in the original papers to calibrate the SpH value were used. All biotic ligand constants other than the SpH value were kept as in the original publications.

Both scenarios were used to calculate metal speciation and predict chronic Cu, Ni and Zn toxicity to daphnids, algae, fish, rotifers, snails and midges using the metal-specific bioavailability models. Comparing bioavailability-model predicted ECx_{Mediss} using both speciation scenarios with observed ECx_{Mediss} made it possible to evaluate the predictive performance of the models.

Table 7.1. Overview of the data for the different individual chronic bioavailability models that were calibrated in WHAM VII for the metals Cu, Ni and Zn in the present study.

Metal	Bioavailability model	Reference	Location in reference [a]	Species [b]	Effect concentration [c]	Total number of waters [d]	natural waters [e]	synthetic waters [f]
Cu	*Daphnia magna* BLM	De Schamphelaere and Janssen (2004b)	Table 4	*Daphnia magna*	EC50; NOEC	45; 45[g]	0; 0	35; 35
		Heijerick et al (2002)	Tables 8, 10, 16, 18, 20, 22, 26	*D. magna*	EC50; NOEC	10; 10	10; 10	0; 0
	Algae bioavailability model	De Schamphelaere and Janssen (2006b)	Supplementary information	*Pseudokircherniella subcapitata - Chlorella vulgaris - Chlamydomonas reinhardtii*	EC50; EC10	35-17-3; 35-17-3 [h]	0-0-0; 0-0-0	37-17-3; 37-17-3
		Heijerick et al (2005a)	Table 1	*P. subcapitata*	NOEC	10	10	0
	D. magna gBAM	Van Regenmortel et al (2015)	Supplementary information	*D. magna*	EC50	67	30	37
		Van Regenmortel et al (2015), De Schamphelaere and Janssen (2004a), Heijerick et al (2002), Rodriguez and Arbildua (2012)	Table 2, Table 4, Tables 8-10-16-18-20-22-26, Table 1	*D. magna*	NOEC; EC10	10; 18	10; 0	0; 18
	Read across of the *D. magna* BLM and gBAM	De Schamphelaere et al (2006c)	Table 1	*Brachionus calyciflorus*	NOEC; LOEC	4; 4	0; 0	4; 4
Ni	*D. magna* bioavailability model	Deleebeeck et al (2008)	Table 3	*D. magna*	EC10 [i]	21	6	15
	Algae bioavailability model	Deleebeeck et al (2009)	Table 3	*P. subcapitata*	EC50; EC10	43; 43	13; 13	30; 30
	Fish bioavailability model	Deleebeeck et al (2007)	Table 3	*Oncorhynchus mykiss*	LC50; NOEC	17; 18	5; 5	12; 13
	Ceriodaphnia dubia bioavailability model	De Schamphelaere et al (2006a)	Table 3.7	*C. dubia*	EC50	6	6	0
	Read across of the *D. magna* and *C. dubia* bioavailability models	Schlekat et al (2010)	Table 3 and 4	*Chironumus tentans - Lymnaea stagnalis -B. calyciflorus - Lemna minor*	EC50; EC20	0-4-0-5; 4-0-7-0	0-4-0-4; 4-0-4-0	0-0-0-1; 0-0-3-0
Zn	*D. magna* BLM	Heijerick et al (2005b)	Table 1	*D. magna*	NOEC [i]	22	0	22
		De Schamphelaere et al (2005)	Table 5	*D. magna*	NOEC	8	7	1
	Algae bioavailability model	De Schamphelaere et al (2005)	Table 4	*P. subcapitata*	EC50; EC10	7; 7	7; 7	0; 0
	Fish BLM	De Schamphelaere and Janssen (2004c)	Table 2, Table 4, Tables 8-10-16-18-20-22-26, Table 1	*O. mykiss*	LC50; LC10	15; 14	0; 0	15; 14
		De Schamphelaere et al (2005)	Table 6	*O. mykiss*	LC50; LC10	5; 5	5; 5	0; 0
	D. magna gBAM	Van Regenmortel et al (2017)	Supplementary information	*D. magna*	EC50; EC10; NOEC	34; 11; 22	16; 1; 16	18; 10; 6
	Fish gBAM	De Schamphelaere and Janssen (2004c)	Table 2, Table 4, Tables 8-10-16-18-20-22-26, Table 1	*O. mykiss*	LC50; LC10	15; 14	0; 0	15; 14
		De Schamphelaere et al (2005)	Table 6	*O. mykiss*	LC50; LC10	5; 5	5; 5	0; 0
	Read across of the *D. magna* BLM and gBAM	De Schamphelaere and Janssen (2010)	Table 2	*L. stagnalis - B. calyciflorus*	EC50; EC10	6-5; 6-5	6-5; 6-5	0-0; 0-0

[a] Information on the location (e.g. Table number) where the effect concentrations can be found in the respective reference
[b] The species for which the bioavailability mode was calibrated in WHAM VII
[c] The effect concentrations for which the bioavailability model was calibrated in WHAM VII
[d] The total number of waters (natural and synthetic) for which the bioavailability mode was calibrated in WHAM VII
[e] The number of natural waters out of the total number of waters
[f] The number of synthetic waters out of the total number of waters
[g] when numbers are separated by a " ; " this refers to the respective effect concentrations that are considered
[h] numbers are separated by a " - " when more than one species is considered
[i] calibration of EC50 data to WHAM VII for this species and bioavailability model was performed by Nys et al (2016)

Table 7.2 Default and adapted stability constants for Cu, Ni and Zn for inorganic complexes used for speciation calculations in WHAM VII

Element	Parameter	Default stability constant in WHAM VII (log K)	Adapted stability constant (log K)[a]
Cu	$K = [CuCO_3]/\{[Cu^{2+}].[CO_3^{2-}]\}$	6.75	6.77
	$K = [CuHCO_3^{+}]/\{[Cu^{2+}].[H+].[CO_3^{2-}]\}$	14.62	12.13
Ni	$K = [NiCO_3]/\{[Ni^{2+}].[CO_3^{2-}]\}$	5.78	4.57
	$K = [NiHCO_3^{+}]/\{[Ni^{2+}].[H^{+}].[CO_3^{2-}]\}$	13.41	12.42
Zn	$K = [ZnCO_3]/\{[Zn^{2+}].[CO_3^{2-}]\}$	4.76	4.76
	$K = [ZnHCO_3^{+}]/\{[Zn^{2+}].[H^{+}].[CO_3^{2-}]\}$	13.12	11.83
	$K = [Zn(OH)_2]/\{[Zn^{2+}].[OH^{-}].[OH^{-}]\}$	11.1	10.2

[a] As proposed by the National Institute of Standards and Technology (Smith et al. 2004)

Bioavailability modelling

Cu bioavailability modelling

Cu^{2+} toxicity to *D. magna* was predicted using the BLM reported by De Schamphelaere and Janssen (2004b) (Equation 7.2).

$$ECx_{Cu^{2+},i} = ECx^{*}_{Cu^{2+}} \cdot \left\{ \frac{1+K_{CaBL}(Ca^{2+})_i+K_{MgBL}(Mg^{2+})_i+K_{NaBL}(Na^{+})_i+K_{HBL}(H^{+})_i}{1+K_{CuBL}+K_{CuOHBL}\,K_{CuOH}\,(OH^{-})_i+K_{CuCO_3BL}\,K_{CuCO_3}\,(CO_3^{2-})_i} \right\} \quad (7.2)$$

In Equation 7.2, $ECx_{Cu^{2+},i}$ is the x% effective concentration of Cu^{2+} in test solution *i*. K_{CaBL}, K_{MgBL}, K_{NaBL}, K_{HBL} K_{CuOHBL} and $K_{CuCO3BL}$ are the stability constants for binding of Ca^{2+}, Mg^{2+}, Na^{+}, H^{+}, $CuOH^{+}$ and $CuCO_3$ to the Cu biotic ligand, respectively (L/mol) (Table 7.3). K_{CuOH} and K_{CuCO3} are stability constants for the formation of the $CuOH^{+}$ and $CuCO_3$ complex, respectively (L/mol). (Ca^{2+}), (Mg^{2+}), (Na^{+}) and (H^{+}) are the chemical activities of Ca^{2+}, Mg^{2+}, Na^{+} and H^{+} in test solution *i* (mol/L). $ECx^{*}_{Cu^{2+}}$ is a measure of the intrinsic sensitivity of a species in the Cu BLM, which can be regarded as the $ECx_{cu^{2+}}$ value expressed as Cu^{2+} in the hypothetical situation without cation competition and in the absence of $CuOH^{+}$ and $CuCO_3$ in the solution. The intrinsic sensitivity $ECx^{*}_{Cu^{2+}}$ was calibrated from a number of observed ECx across various test waters using Equation 7.3:

$$ECx^{*}_{Cu^{2+}} = \prod_i^n \left(\frac{ECx_{Cu^{2+},i,observed}}{\left\{ \frac{1+K_{CaBL}(Ca^{2+})_i+K_{MgBL}(Mg^{2+})_i+K_{NaBL}(Na^{+})_i+K_{HBL}(H^{+})_i}{1+R_{CuOH}\,K_{CuOH}\,(OH^{-})+R_{CuCO_3}\,K_{CuCO_3}\,(CO_3^{2-})} \right\}} \right)^{\frac{1}{n}} \quad (7.3)$$

In Equation 7.3, *n* is the number of test solutions considered. $ECx_{Cu^{2+},i,observed}$ is the observed Cu^{2+} activity in test solution *i* (mol/L).

For the *D. magna* dataset, the EC50 value for the "Ankeveen 12" medium was not included in the modelling efforts, as the EC50 value was extrapolated. The intrinsic sensitivity was calculated based on the "Ankeveen" synthetic media reported in De Schamphelaere et al (2004a). All synthetic media reported in De Schamphelaere et al (2004a) and the natural media reported in De Schamphelaere et al (2004b) were predicted using this intrinsic sensitivity value. The predicted $EC50_{Cu^{2+},i}$ and $NOEC_{Cu^{2+},i}$ values were transformed to $EC50_{Cudiss,i,pred}$ and $NOEC_{Cudiss,i,pred}$ values using WHAM VII and compared to the $EC50_{Cudiss,i,observed}$ and $NOEC_{Cudiss,i,observed}$. In addition to the above, we also wanted to be able to compare the results of the Cu *D. magna* BLM to those of the Cu *D. magna* gBAM. Therefore, in a separate validation series, the *D. magna* dataset that was used for the validation of the Cu gBAM

was also used for validation of the Cu BLM (see 6.2.1.3 for more information on the intrinsic sensitivity calculations).

Table 7.3. Model parameters of the chronic Cu BLM for *Daphnia magna*[a], the chronic Cu bioavailability model for algae[b], the chronic Cu gBAM for *D. magna*[c]

	Cu *D. magna* BLM[a]	Cu Algae Model[b]	Cu *D. magna* gBAM[c]
Log K_{MgBL}	-	-	3.53
Log K_{CaBL}	-	-	3.53
Log K_{NaBL}	2.91	-	2.67
Log K_{HBL}	6.67	-	-
S_{pH}	-	0.985/0.998[d]	0.14/0.22 [d]
$R_{CuOH} = \frac{K_{CuOHBL}}{K_{CuBL}}$	1	-	-
$R_{CuCO_3} = \frac{K_{CuCO_3BL}}{K_{CuBL}}$	0.26	-	-
K_{CuOHBL}	8.02	-	-
K_{CuCO_3BL}	7.44	-	-

[a] De Schamphelaere & Janssen (2004a); Equation 7.2
[b] De Schamphelaere et al. (2008); Equation 7.3
[c] Van Regenmortel et al (2015); Chapter 5; Equation 7.4
[d] the SpH parameter recalibrated in WHAM VII using Speciation Scenario I/ Speciation Scenario II

Cu^{2+} toxicity to *P.subcapitata, C. vulgaris* and *C. reinhartii* was predicted using the bioavailability model reported by De Schamphelaere & Janssen (2006b) (Equation 7.4).

$$ECx_{Cu^{2+},i} = 10^{-(S_{pH\,Cu} \cdot pH_i + Qx_{Cu})} \quad (7.4)$$

In Equation 7.4, $ECx_{Cu^{2+},i}$ is the predicted x% effective concentration of Cu^{2+} in test solution *i*. Qx_{Cu} is the intrinsic sensitivity of the chronic Cu bioavailability model. The intrinsic sensitivity of the Cu bioavailability model is the intercept of the linear relationship between the log ECx_{Cu2+} and pH (De Schamphelaere and Janssen, 2005). SpH_{Cu} is the pH slope of Cu toxicity in the Cu bioavailability model (Table 7.3) and pH is the pH of test solution *i*.

The intrinsic sensitivity, Qx_{cu2+}, was calibrated from the observed ECx_{Cu2+}, from all test solutions using Equation 7.5.

$$Qx_{Cu} = \frac{\sum_i^n (-\log(ECx_{Cu^{2+},i,observed}) - S_{pH\,cu} \cdot pH_i)}{n} \quad (7.5)$$

In this equation, $ECx_{Cu^{2+},i,observed}$ is the observed Cu^{2+} activity in test solution *i* at the x% effective concentration (mol/L). The intrinsic sensitivity, $Qx_{Cu2+,}$ for *P.subcapitata* (growth rate endpoint) was calculated based on the observed ECx values of all synthetic waters reported in De Schamphelaere and Janssen (2006b), except for the EC50 value of the "Ankeveen 11" medium, as no reliable EC50 could be calculated because the highest test concentration resulted in less than 30% reduction of growth rate (De Schamphelaere and Janssen, 2006). The intrinsic sensitivity, $Qx_{Cu2+,}$ for *C. vulgaris* was calculated based on the observed ECx values of all synthetic waters reported in De Schamphelaere and Janssen

(2006). The intrinsic sensitivity, $Qx_{Cu2+,}$ for *C. reinhardtii* was calculated based on the observed ECx values of all synthetic waters reported in De Schamphelaere and Janssen (2006b). The intrinsic sensitivity, $Qx_{Cu2+,}$ for *P.subcapitata* (biomass yield endpoint) was calculated based on the observed ECx values of all natural waters reported in Heijerick et al. (2005), except for the data from the test waters Bihain and Somerain for which the pH shifted more than 0.5 pH units during the exposure, in addition to the data from the test water Skarsjön because of the suspected influence of high Fe and/or Al concentrations on the test results (De Schamphelaere and Janssen, 2006b).

Cu^{2+} toxicity to *D. magna* was also predicted using the chronic Cu *D. magna* gBAM developed in Chapter 5.1 (Van Regenmortel et al. 2015) (Equation 7.6).

$$ECx_{Cu^{2+},i} = 10^{-(S_{pH\,Cu}\cdot pH_i + Qx_{Cu})}\left\{1 + K_{CaBL}(Ca^{2+})_i + K_{MgBL}(Mg^{2+})_i + K_{NaBL}(Na^{+})_i\right\} \quad (7.6)$$

In Equation 7.6, $ECx_{Cu^{2+},i}$ is the predicted x% effective concentration of Cu^{2+} in test solution *i*. Qx_{Cu} is the intrinsic sensitivity of the chronic Cu gBAM. The intrinsic sensitivity of the Cu gBAM is the intercept of the linear relationship between the log ECx_{Cu2+} and pH (Van Regenmortel et al. 2015/Chapter 5.1), after correction for Ca^{2+}, Mg^{2+} and Na^{+} competition. K_{CaBL}, K_{MgBL} and K_{NaBL} are the stability constants for binding of Ca^{2+}, Mg^{2+} and Na^{+} to the Cu gBAM, respectively (L/mol) (Table 7.3). $(Ca^{2+})_i$, $(Mg^{2+})_i$ and $(Na^{+})_i$ are the chemical activities of Ca^{2+}, Mg^{2+} and Na^{+} in test solution *i* (mol/L), respectively. SpH_{Cu} is the pH slope of Cu toxicity in the Cu gBAM (Table 7.3) and pH is the pH of test solution *i*.

The intrinsic sensitivity, Qx_{Cu2+}, was calibrated from the observed ECx_{Cu2+} using Equation 7.7.

$$Qx_{Cu} = \frac{\sum_i^n(-\log\left(\frac{ECx_{Cu^{2+},i,observed}}{1+K_{CaBL}(Ca^{2+})_i+K_{MgBL}(Mg^{2+})_i+K_{NaBL}(Na^{+})_i}\right)-S_{pH\,Cu}\cdot pH_i)}{n} \quad (7.7)$$

In this equation, $ECx_{Cu^{2+},i,observed}$ is the observed Cu^{2+} activity in test solution *i* at the x% effective concentration (mol/L). One intrinsic sensitivity, $Qx_{Cu2+,}$ for *D. magna* was calculated based on the data reported for the K6 *D. magna* clone and one Qx_{Cu2+} was calculated based on the data reported for the ARO *D. magna* clone.

In addition to validating the chronic Cu *D. magna* gBAM with EC50 values, we also attempted to validate the gBAM with EC10 values. However, the gBAM was developed based on EC50 values (i.e. SpH value based on EC50 values; Van Regenmortel et al. 2015/Chapter 5). Therefore, we also used this SpH value for EC10 values. For the EC10 dataset, intrinsic sensitivities were calibrated for the same data subsets as was done for the EC50 dataset.

The predicted $ECx_{Cu^{2+},i}$ were transformed to $ECx_{Cudiss,i,pred}$ using WHAM VII and compared to the $ECx_{Cudiss,i,observed}$.

Cu^{2+} toxicity to *B. calyciflorus* was predicted using the Cu *D. magna* BLM and gBAM (Equations 7.2 and 7.6). The intrinsic sensitivities were calculated using Equations 7.3 and 7.7. The intrinsic sensitivity of *B. calyciflorus* was calculated based on the observed NOEC and LOEC values of all synthetic waters reported By De Schamphelaere et al (2006c). The predicted $N(L)OEC_{Cu^{2+},i}$ were transformed to $N(L)OEC_{Cudiss,i,pred}$ using WHAM VII and compared to the $N(L)OEC_{Cudiss,i,observed}$.

Ni bioavailability modelling

Ni^{2+} toxicity to *D. magna*, *P.subcapitata*, *O. mykiss* and *C. dubia* was predicted using the bioavailability models reported by Deleebeeck et al (2008, 2009, 2007) and De Schamphelaere et al (2006a). All BLMs have the same model structure (Equation 7.8), but differ in the magnitude of the slope of the effect of pH on Ni^{2+} toxicity (S_{pH}) and the magnitude of the effect of the cations on Ni^{2+} toxicity (K_{CaBL}, K_{MgBL}, K_{NaBL} and K_{HBL}).

$$ECx_{Ni^{2+},i} = 10^{-(S_{pH_{Ni}} \cdot pH_i + Qx_{Ni})}\left\{1 + K_{CaBL}(Ca^{2+})_i + K_{MgBL}(Mg^{2+})_i\right\} \quad (7.8)$$

In Equation 7.8 $ECx_{Ni^{2+},i}$ is the predicted x% effective concentration of Ni^{2+} in test solution *i*. Qx_{Ni} is the intrinsic sensitivity of the chronic Ni bioavailability model. The intrinsic sensitivity of the Ni bioavailability model is the intercept of the linear relationship between the log ECx_{Ni2+} and pH, after correction for Ca^{2+} and Mg^{2+} competition. K_{CaBL} and K_{MgBL} are the stability constants for binding of Ca^{2+} and Mg^{2+} to the Ni bioavailability model (L/mol), respectively. $(Ca^{2+})_i$ and $(Mg^{2+})_i$ are the chemical activities of Ca^{2+} and Mg^{2+} in test solution *i* (mol/L), respectively. SpH_{Ni} is the pH slope of Ni toxicity in the the Ni bioavailability model and pH is the pH of test solution *i*. All model parameters can be found in Table 7.4.

The intrinsic sensitivity, Qx_{Ni2+}, was calibrated from a number of the observed ECx_{Ni2+} across various test waters from using Equation 7.9.

$$Qx_{Ni} = \frac{\sum_i^n(-\log\left(\frac{ECx_{Ni^{2+},i,observed}}{1+K_{CaBL}(Ca^{2+})_i+K_{MgBL}(Mg^{2+})_i}\right)-S_{pH_{Ni}} \cdot pH_i)}{n} \quad (7.9)$$

In this equation, $ECx_{Ni^{2+},i,observed}$ is the observed Ni^{2+} activity in test solution *i* at the x% effective concentration (mol/L).

For *D. magna,* as was done in Deleebeeck et al (2008), a separate intrinsic sensitivity was calculated for the synthetic media and the natural media. This was done by these authors because they suspected that the sensitivity of the *D. magna* clone could have temporally shifted between the two types of test media, as the tests in the natural surface waters were conducted approximately a year earlier that those in the artificial waters. For the calculation of the intrinsic sensitivities the data for the tests conducted at the highest Ca and Mg concentrations as well as the test conducted at pH 5.87 was not included in the modelling efforts (Deleebeeck et al 2008). In addition, the test conducted in the Bihain medium was not included in modelling efforts, as it had a pH below the lower boundary of the model (Deleebeeck et al 2008). A first intrinsic sensitivity was calculated based on the synthetic media reported by Deleebeeck et al (2008) in combination with the SpH value of 0.1987 (Table 7.4). Subsequently, $EC10_{Ni2+}$ values were predicted for all synthetic waters using this intrinsic sensitivity. A second intrinsic sensitivity was calculated based on the natural media reported by Deleebeeck et al (2008) in combination with the SpH value of 0.3335 (Table 7.4). Subsequently, $EC10_{Ni2+}$ values were predicted for the natural waters using this intrinsic sensitivity. The predicted $EC10_{Ni^{2+},i}$ values were transformed to $EC10_{Nidiss,i,pred}$ using WHAM VII and compared to the $EC10_{Nidiss,i,observed}$.

For *P.subcapitata*, as was done in Deleebeeck et al (2009), two different intrinsic sensitivities were calculated. One intrinsic sensitivity was calculated based on data points used for model development (i.e. all data points obtained in the univariate Mg and pH test series). This intrinsic sensitivity was used

to predict $ECx_{Ni^{2+}}$ values for the synthetic test media. A second intrinsic sensitivity was calculated based on test results obtained in OECD test media. This intrinsic sensitivity was used to predict $ECx_{Ni^{2+}}$ values in the natural test media. The predicted $ECx_{Ni^{2+}}$ values were transformed to $ECx_{Nidiss,i,pred}$ using WHAM VII and compared to the $ECx_{Nidiss,i,observed}$.

For *O. mykiss*, data for the test media "Mg 0.5 mM", "Mg 1.0 mM" and "Mg 3.0 mM" were not included in the calculation of the $Q50_{Ni}$, as LC50s could not be calculated due to no or limited mortality at the highest exposure concentration (Deleebeeck et al 2007). Data for the test media "Mg 1.0 mM" and "Mg 3.0 mM" were not included in the calculation of the $QNOEC_{Ni}$, as NOECs could not be calculated because no significant mortality was observed (Deleebeeck et al 2007). As was done by Deleebeeck et al (2007), the intrinsic sensitivities (Q50 and QNOEC) were based on the synthetic media. These intrinsic sensitivities were used to predict LC50 and NOEC values in the synthetic and natural test media. The predicted $LC50_{Ni^{2+}}$ values and $NOEC_{Ni^{2+}}$ values were transformed to $LC50_{Nidiss,i,pred}$ and $NOEC_{Nidiss,i,pred}$ using WHAM VII and compared to the $LC50_{Nidiss,i,observed}$ $NOEC_{Nidiss,i,observed}$.

For *C. dubia*, data for the test media Eppe and Markermeer were not included in modelling efforts as ECx values were extrapolated below the lowest test concentration. (De Schamphelaere et al. 2006). The intrinsic sensitivities were calculated based on the observed ECx values of all remaining field waters reported by De Schamphelaere et al (2006a). The predicted $ECx_{Ni^{2+}}$ values were transformed to $ECx_{Nidiss,i,pred}$ using WHAM VII and compared to the $ECx_{Nidiss,i,observed}$.

Ni^{2+} toxicity to *C. tentans* was predicted using the *D. magna* and *C. dubia* bioavailability models (Equation 7.8 , Table 7.4). Ni^{2+} toxicity to *L. stagnalis* was predicted using the *C. dubia* bioavailability model (Equation 7.8 , Table 7.4). Ni^{2+} toxicity to *B. calyciflorus and L. minor* was predicted using the *D. magna* bioavailability model (Equation 7.8 , Table 7.4). Data from the pH-adjusted S. Platte River were not included in modelling efforts as it was suggested that high toxicity in this water was caused by pH-sensitive contaminants in the river (Schlekat et al 2010). The intrinsic sensitivities were calculated using Equations 7.9. The intrinsic sensitivities of *C. tentans*, *L. stagnalis*, *B. calyciflorus and* L. minor were calculated based on the observed ECx values of all remaining field and synthetic waters reported by Schlekat et al. (2010). The predicted $ECx_{Ni^{2+}}$ values were transformed to $ECx_{Nidiss,i,pred}$ using WHAM VII and compared to the $ECx_{Nidiss,i,observed}$.

Table 7.4 Model parameters of the chronic Ni bioavailability model for *Daphnia magna*[a], *Pseudokirchneriella subcapitata*[b], *Oncorhynchus* mykiss and *Pimephales promelas*[c] and *Ceriodaphnia dubia*[d].

	Ni *D. magna* model[a]	Ni Algae model[b]	Ni Fish model[c]	Ni *C. dubia* model[d]
Log K_{MgBL}	3.57	3.30	3.60	3.57
Log K_{CaBL}	3.53	-	3.60	3.53
S_{pH}	0.1987[e];0.617/0.305[f]	0.1430[f]	0.3240[f]	1.046/0.662[f]

[a] Deleebeeck et al (2008); Equation 7.8; [b] Deleebeeck et al (2009); Equation 7.8; [c] Deleebeeck et al (2007); Equation 7.8 [d]; De Schamphelaere et al (2006a); Equation 7.8; [e] Slope reported by Deleebeeck et al (2008) for synthetic waters. The slope value was not adapted as the value was calibrated for synthetic media, without the addition of natural DOC; [f] the SpH parameter recalibrated in WHAM VII using Speciation Scenario I/ Speciation Scenario II

Zn bioavailability modelling

Zn^{2+} toxicity to *D. magna* and O. *mykiss* was predicted using the BLMs reported by Heijerick et al (2005b) and De Schamphelaere & Janssen (2004). Both BLMs have the same model structure (Equation 7.10), but differ in the magnitude of the effect of the cations on Zn^{2+} toxicity (K_{CaBL}, K_{MgBL}, K_{NaBL} and K_{HBL}).

$$NOEC_{Zn^{2+},i} or\ LCx_{Zn^{2+},i} = NOEC^{*}_{Zn^{2+}}\ or\ LCx^{*}_{Zn^{2+}} \cdot \{1 + K_{CaBL}(Ca^{2+})_i + K_{MgBL}(Mg^{2+})_i + K_{NaBL}(Na^{+})_i + K_{HBL}(H^{+})_i\} \quad (7.10)$$

In Equation 7.10, $NOEC_{Zn^{2+},i}$ and $LCx_{Zn^{2+},i}$ are the predicted No Observed Effect Concentration and the x% Lethal Concentration of Zn^{2+} in test solution *i,* respectively. K_{CaBL}, K_{MgBL}, K_{NaBL} and K_{HBL} are the stability constants (L/mol) for binding of Ca^{2+}, Mg^{2+}, Na^{+} and H^{+} to the Zn biotic ligand, respectively (Table 7.5). (Ca^{2+}), (Mg^{2+}), (Na^{+}) and (H^{+}) are the chemical activities of Ca^{2+}, Mg^{2+}, Na^{+} and H^{+} in test solution *i* (mol/L). $NOEC^{*}_{Zn^{2+}} or\ LCx^{*}_{Zn^{2+}}$ are the intrinsic sensitivities of the Zn BLM, which can be regarded as the $NOEC_{Zn^{2+}} or\ LCx_{Zn^{2+}}$ of the organism in a solution where all cationic competition effects are absent (Heijerick et al. 2005). The intrinsic sensitivity $NOEC^{*}_{Zn^{2+}} or\ LCx^{*}_{Zn^{2+}}$ was calibrated from a number of the observed NOEC or LCx values using Equation 7.11:

$$NOEC^{*}_{Zn^{2+}} or\ LCx^{*}_{Zn^{2+}} = \prod_{i}^{n} \left(\frac{NOEC_{Zn^{2+},i,observed}\ or\ LCx_{Zn^{2+},i,observed}}{1 + K_{CaBL}(Ca^{2+})_i + K_{MgBL}(Mg^{2+})_i + K_{NaBL}(Na^{+})_i + K_{HBL}(H^{+})_i}\right)^{\frac{1}{n}} \quad (7.11)$$

In Equation 7.11, *n* is the number of test solutions considered. $NOEC_{Zn^{2+},i,observed}$ or $LCx_{Zn^{2+},i,observed}$ is the observed Zn^{2+} activity in test solution *i* (mol/L).

For the calculation of the intrinsic sensitivity for *D. magna*, data from the "Ca-series" reported in Heijerick et al (2005b) for the highest Ca concentration tested was not included in the modelling efforts due to high Ca toxicity. In addition, the test conducted in the Rhine and Voyon media (De Schamphelaere et al 2005) were not included in modelling efforts, as they have a pH above the upper boundary of the model. For *D. magna* two separate intrinsic sensitivities were calculated. One intrinsic sensitivity was calculated for the Heijerick et al. (2005) dataset. A second intrinsic sensitivity was calculated for the De Schamphelaere et al. (2005) dataset. The predicted $NOEC_{Zn^{2+},i}$ and $LCx_{Zn^{2+},i}$ were transformed to $NOEC_{Zndiss,i,pred}$ and $LCx_{Zndiss,i,pred}$ using WHAM VII and compared to the $NOEC_{Zndiss,i,observed}$ and $LCx_{Zndiss,i,observed}$. In addition to the above, we also wanted to be able to compare the results of the Zn *D. magna* BLM to those of the Zn *D. magna* gBAM. Therefore, in a separate validation series, the *D. magna* dataset that was used for the validation of the Zn gBAM was also used for validation of the Zn BLM.

For *O. mykiss*, a data-specific intrinsic sensitivity was calculated for the data of De Schamphelaere and Janssen (2004c) and De Schamphelaere and Janssen (2005) separately. The predicted $LCx_{Zn^{2+},i}$ were transformed to $LCx_{Zndiss,i,pred}$ using WHAM VII and compared to the $LCx_{Zndiss,i,observed}$.

Table 7.5 Model parameters of the chronic Zn BLM for *Daphnia magna*[a], the chronic Zn bioavailability model for algae[b], the chronic Zn BLM for fish[c] , the chronic Zn gBAM for *D. magna*[d] and the chronic Zn gBAM for fish[e]

	Zn *D. magna* BLM	Zn Algae BLM	Zn Fish BLM	Zn *D. magna* gBAM	Zn Fish gBAM
Log K_{MgBL}	2.69	-	3.10	2.69	3.10
Log K_{CaBL}	3.22	-	3.60	3.22	3.60
Log K_{NaBL}	1.90	-	2.40	1.90	2.40
Log K_{HBL}	5.77	-	6.30	-	-
$S_{pH\text{-}EC50}$; $S_{pH\text{-}EC10}$	-	0.598; 0.626[f]/ 0.541; 0.581[g]	-	0.1165; 0.1518/ -	0.25;0.41/ 0.21;0.36

[a] Heijerick et al. (2005b); Equation 7.10
[b] De Schamphelaere et al. (2005); Equation 7.12
[c] De Schamphelaere & Janssen (2004c); Equation 7.10
[d] Van Regenmortel et al (2017b); Equation 7.14
[e] Chapter 5
[f] when seperated by a ";" the SpH is given for EC50 and EC10 data, respectively
[g] when seperated by a "/" the SpH parameters were recalibrated in WHAM VII using Speciation Scenario I/Speciation Scenario II

Zn^{2+} toxicity to *P.subcapitata* was predicted using the bioavailability model reported by De Schamphelaere & Janssen (2005) (Equation 7.12).

$$ECx_{Zn^{2+},i} = 10^{-(S_{pH\,Zn}\cdot pH_i + Qx_{Zn})} \quad (7.12)$$

In Equation 7.12, $ECx_{Zn^{2+},i}$ is the predicted x% effective concentration of Zn^{2+} in test solution *i*. Qx_{Zn} is the intrinsic sensitivity of the chronic Zn bioavailability model. The intrinsic sensitivity of the Zn bioavailability model is the intercept of the linear relationship between the log ECx_{Zn2+} and pH (De Schamphelaere and Janssen, 2005). SpH_{Zn} is the pH slope of Zn toxicity in the Zn bioavailability model (Table 7.5) and pH is the pH of test solution *i*.

The intrinsic sensitivity, Qx_{Zn2+}, was calibrated from a number of the observed ECx_{Zn2+} using Equation 7.13.

$$Qx_{Zn^{2+}} = \frac{\sum_i^n (-\log(ECx_{Zn^{2+},i,observed}) - S_{pH\,Zn}\cdot pH_i)}{n} \quad (7.13)$$

In this equation, $ECx_{Zn^{2+},i,observed}$ is the observed Zn^{2+} activity in test solution *i* at the x% effective concentration (mol/L). The intrinsic sensitivity, $Qx_{Zn2+,}$ for *P.subcapitata* was calculated based on the observed ECx values of all field waters reported in De Schamphelaere and Janssen (2005), except for the Brisy medium (also excluded by De Schamphelaere and Janssen (2005) for model development). The predicted $ECx_{Zn^{2+},i}$ were transformed to $ECx_{Zndiss,i,pred}$ using WHAM VII and compared to the $ECx_{Zndiss,i,observed}$.

Zn^{2+} toxicity to *D. magna* and O. mykiss was also predicted using the chronic Zn *D. magna* and fish gBAM developed in Chapter 5 (Equation 7.14).

$$ECx_{Zn^{2+},i} = 10^{-(S_{pH\,Zn}\cdot pH_i + Qx_{Zn})}\left\{1 + K_{CaBL}(Ca^{2+})_i + K_{MgBL}(Mg^{2+})_i + K_{NaBL}(Na^{+})_i\right\} \quad (7.14)$$

In Equation 7.14, $ECx_{Zn^{2+},i}$ is the predicted x% effective concentration of Zn^{2+} in test solution *i*. Qx_{Zn} is the intrinsic sensitivity of the chronic Zn gBAM. The intrinsic sensitivity of the Zn gBAM is the intercept of the linear relationship between the log ECx_{Zn2+} and pH (Van Regenmortel et al. 2017b/Chapter 5.2), after correction for Ca^{2+}, Mg^{2+} and Na^{+} competition. K_{CaBL}, K_{MgBL} and K_{NaBL} are the stability constants (L/mol) for binding of Ca^{2+}, Mg^{2+} and Na^{+} to the Zn gBAM, respectively (Table 7.5). $(Ca^{2+})_i$, $(Mg^{2+})_i$ and $(Na^{+})_i$ are the chemical activities of Ca^{2+}, Mg^{2+} and Na^{+} in test solution *i* (mol/L), respectively. SpH_{Zn} is the pH slope of Zn toxicity in the Zn gBAM (Table 7.5) and pH is the pH of test solution *i*.

The intrinsic sensitivity, Qx_{Zn2+}, was calibrated from a number of the observed ECx_{Zn2+} using Equation 7.15.

$$Qx_{Zn^{2+}} = \frac{\sum_i^n (-\log\left(\frac{ECx_{Zn^{2+},i,observed}}{1+K_{CaBL}(Ca^{2+})_i+K_{MgBL}(Mg^{2+})_i+K_{NaBL}(Na^{+})_i}\right)-S_{pH_{Zn}}\cdot pH_i)}{n} \quad (7.15)$$

In this equation, $ECx_{Zn^{2+},i,observed}$ is the observed Zn^{2+} activity in test solution *i* at the x% effective concentration (mol/L).

For *D. magna*, one intrinsic sensitivity, $Q50_{Zn2+,}$ was calculated based on the combined dataset of the observed EC50 values of all field waters reported in De Schamphelaere and Janssen (2005) and of the field and synthetic waters reported in Chapter 5 (Van Regenmortel et al. 2017b). Subsequently, this $Q50_{Zn2+}$ was used to predict the EC50 data for this combined dataset as well as the waters reported in De Schamphelaere et al (2003).

In addition to validating the chronic Zn *D. magna* gBAM with EC50 values, we also attempted to validate the gBAM with EC10 values. However, the gBAM was developed based on EC50 values (i.e. SpH value based on EC50 values; Chapter 5). Therefore, we also used this SpH value for EC10 values. For the EC10 dataset, one intrinsic sensitivity, $Q10_{Zn2+,}$ for *D. magna* was calculated based on the combined dataset of the observed EC10 values of all field waters reported in De Schamphelaere and Janssen (2005) and of the field and synthetic waters reported in Chapter 5 (Van Regenmortel et al. 2017b). Subsequently, this $Q10_{Zn2+}$ was used to predict the EC10 data for this combined dataset as well as the waters reported in De Schamphelaere et al (2003).

In addition, a separate intrinsic sensitivity was calculated based on the data reported in De Schamphelaere et al (2003). This $Q10_{Zn2+}$ was used to predict the EC10 data for the waters reported in De Schamphelaere et al (2003). The predicted $ECx_{Zn^{2+},i}$ were transformed to $ECx_{Zndiss,i,pred}$ using WHAM VII and compared to the $ECx_{Zndiss,i,observed}$.

For *O. mykiss*, a data-specific intrinsic sensitivity was calculated for the data of De Schamphelaere and Janssen (2004c) and De Schamphelaere and Janssen (2005) separately.

Zn^{2+} toxicity to *L. stagnalis* and *B. calyciflorus* was predicted using the *D. magna* BLM and gBAM (Equations 7.10 and 7.12). The intrinsic sensitivities were calculated using Equations 7.11 and 7.13. The intrinsic sensitivities of *L. stagnalis* and *B. calyciflorus* were calculated based on the observed ECx values of all field waters reported By De Schamphelaere and Janssen (2010). The predicted $ECx_{Zn^{2+},i}$ were transformed to $ECx_{Zndiss,i,pred}$ using WHAM VII and compared to the $ECx_{Zndiss,i,observed}$.

7.3. Results

Calibration of the Cu bioavailability models in WHAM VII

Validation of the chronic Cu D. magna BLM in WHAM VII

The intrinsic sensitivities ($Q10_{Cu2+}$) for the Speciation Scenario I and II are reported in Table 7.6. For the synthetic waters, both speciation scenarios predicted chronic Cu toxicity to *D. magna* less accurately compared to WHAM V for the Ankeveen water, but more accurately for the Bihain and Ossenkolk water (Figure 7.1; Table 7.7). For natural waters, both speciation scenarios predicted chronic Cu toxicity to *D. magna* inaccurately (i.e. maximum 20% and 30% of the data is predicted within twofold error for Speciation Scenario I and II, respectively).

Overall, the Cu *D. magna* BLM coupled with WHAM VII (Speciation Scenario II) was comparable in predictive capacity to the original Cu *D. magna* BLM coupled with WHAM V (Table 7.7) for synthetic waters but predicted Cu toxicity less well than the WHAM V calculations for natural waters.

Table 7.6 Average calibrated intrinsic Cu^{2+} sensitivities for *Daphnia magna* ($EC50^{*}_{Cu2+}$ and $NOEC^{*}_{Cu2+}$ (nmol/L); calculated using Equation 7.3) under Speciation Scenario I and II

	Synthetic waters[a]	
	$EC50^{*}_{Cu2+}$	$NOEC^{*}_{Cu2+}$
Speciation Scenario I[b]	74	48
Speciation Scenario II[c]	87	55

[a] Data from De Schamphelaere and Janssen (2004a); [c] Speciation Scenario I: default WHAM VII stability constants for inorganic complexation; [d] Speciation Scenario II: stability constants for inorganic complexation reported by NIST

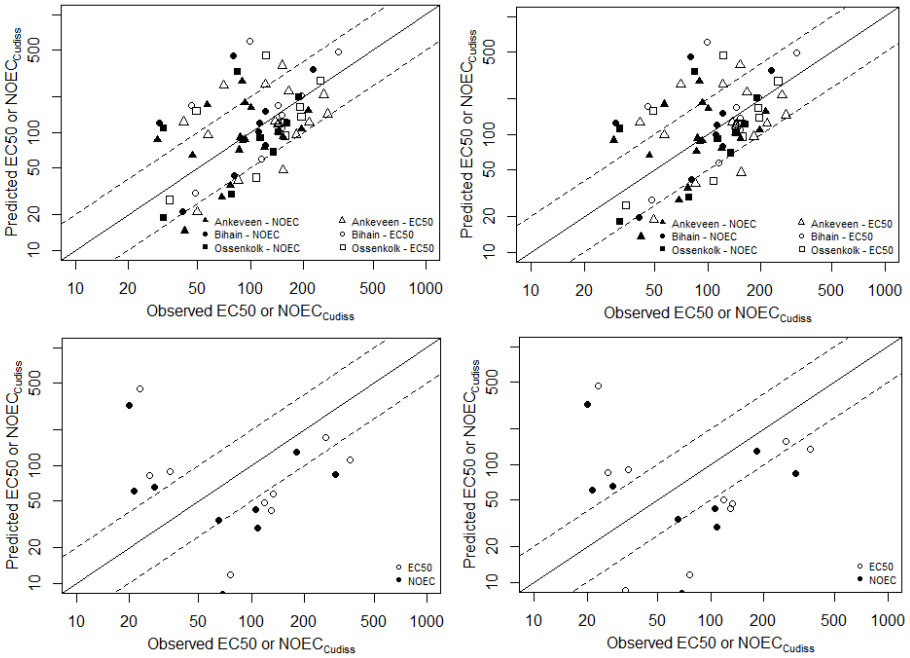

Figure 7.1. Predicted versus observed 50% effective concentration ($EC50_{Cudiss}$) and no observed effect concentration ($NOEC_{Cudiss}$) for *Daphnia magna* using Speciation Scenario I (i.e. using the default WHAM VII stability constants for inorganic complexation; left graph) and Speciation Scenario II (i.e. using stability constants for inorganic complexation reported by NIST; right graph). Predictions were made using the chronic Cu *D. magna* BLM linked to WHAM VII (Equation 7.8). The solid line represents a perfect fit between the observed and predicted data, the dashed lines represent a difference of a factor 2 between the observed and predicted data.

Table 7.7 Prediction statistics of the $EC50_{Cudiss}$ and $NOEC_{Cudiss}$ predicted with the chronic Cu *D. magna* BLM (Equation 7.2) in WHAM V[a] and in WHAM VII using Speciation Scenario I[b] and Speciation Scenario II[c]

	WHAM V							
	Ankeveen		Bihain		Ossenkolk		Natural waters	
	NOEC data	EC50 data	NOEC data	EC50 data	NOEC data	EC50 data	NOEC data	EC50 data
Mean prediction error	1.35	1.23	2.50	2.26	1.89	1.86	2.09	2.13
Median prediction error	1.30	1.12	2.23	2.09	1.92	1.81	1.51	1.36
% predicted within twofold error	94	100	22	44	67	56	70	80

	WHAM VII Speciation Scenario I							
	Ankeveen		Bihain		Ossenkolk		Natural waters	
	NOEC data	EC50 data	NOEC data	EC50 data	NOEC data	EC50 data	NOEC data	EC50 data
Mean prediction error	1.90	1.97	2.21	2.15	2.08	1.93	7.49	6.23
Median prediction error	1.68	1.89	1.55	1.53	1.69	1.43	3.19	3.15
% predicted within twofold error	65	59	78	78	67	67	20	10

	WHAM VII Speciation Scenario II							
	Ankeveen		Bihain		Ossenkolk		Natural waters	
	NOEC data	EC50 data	NOEC data	EC50 data	NOEC data	EC50 data	NOEC data	EC50 data
Mean prediction error	1.94	2.02	2.26	222	2.11	1.97	4.86	7.36
Median prediction error	1.65	1.89	1.54	1.56	1.76	1.41	3.02	2.54
% predicted within twofold error	65	59	67	78	67	67	20	30

[a] Data from De Schamphelaere and Janssen (2004a) and Heijerick et al (2002) (see Table 7.1)
[b] Speciation Scenario I: default WHAM VII stability constants for inorganic complexation
[c] Speciation Scenario II: stability constants for inorganic complexation reported by NIST

To be able to compare the accuracy of the *D. magna* BLM and gBAM coupled with WHAM VII, a separate validation was performed, as was explained in the *Material and Methods* section. For this validation, the data that was used to validate the gBAM was used. The intrinsic sensitivities (Qx_{Cu2+}) for the Speciation Scenario I and II are reported in Table 7.8.

Table 7.8 Average calibrated intrinsic Cu^{2+} sensitivities for *Daphnia magna*[a] (Qx_{Cu2+} calculated using Equation 7.3) under Speciation Scenario I and II.

	K6 clone		ARO clone	
	$Q50_{Cu2+}$[b]	$Q10_{Cu2+}$[c]	$Q50_{Cu2+}$[b]	$Q10_{Cu2+}$[c]
Speciation Scenario I[b]	46	27	82	-
Speciation Scenario II[c]	52	31	93	-

[a] Data from Van Regenmortel et al (2015; Chapter 5)
[b] Speciation Scenario I: default WHAM VII stability constants for inorganic complexation
[c] Speciation Scenario II: stability constants for inorganic complexation reported by NIST

The prediction statistics for the chronic Cu *D. magna* BLM for both speciation scenarios are given in Table 7.9. For the EC50 data, the Cu toxicity to the K6 and ARO *D. magna* clones is not accurately predicted using the BLM coupled to WHAM VII, i.e. only 50% of the data predicted within twofold prediction error (Table 7.9). Cu toxicity is predicted a little more accurate for the NOEC data compared to the EC50 data. These results will make it possible to compare the predictive capacity of the Cu Daphnia BLM to that of the gBAM. This comparison will be done in a next section (7.*3 Discussion*).

Table 7.9 Prediction statistics of the $EC50_{Cudiss}$ and $NOEC_{Cudiss}$ predicted with the chronic Cu *Daphnia magna* BLM[a] (Equation 7.2) in WHAM V and in WHAM VII using Speciation Scenario I[b] and Speciation Scenario II[c]

	WHAM VII Speciation Scenario I				
	K6 clone			ARO clone	
	EC50 data	NOEC data		EC50 data	NOEC data
	All data	Bihain	Ossenkolk	All data	
Mean prediction error	4.15	2.29	2.07	3.80	-
Median prediction error	2.10	1.67	1.52	1.98	-
% predicted within twofold error	50	78	67	51	-

	WHAM VII Speciation Scenario II				
	K6 clone			ARO clone	
	EC50 data	NOEC data		EC50 data	NOEC data
	All data	Bihain	Ossenkolk	All data	
Mean prediction error	5.29	2.36	2.11	5.31	-
Median prediction error	2.10	1.72	1.58	2.01	-
% predicted within twofold error	50	78	67	49	-

[a] Data from Van Regenmortel et al (2015 Chapter 5) (see Table 7.1)
[b] Speciation Scenario I: default WHAM VII stability constants for inorganic complexation
[c] Speciation Scenario II: stability constants for inorganic complexation reported by NIST;

Validation of the Cu bioavailability model for freshwater green microalgae in WHAM VII

The intrinsic sensitivities ($Q10Cu_{2+}$) for the Speciation Scenario I and II are reported in Table 7.10. Both speciation scenarios predicted chronic Cu toxicity to *P. subcapitata, C. vulgaris and C. reinhardtti* with reasonable accuracy (Figure 7.2; Table 7.11). The Speciation Scenario I and II, predicted the ECx_{Cudiss} values with comparable accuracy. When comparing with the predictions made by WHAM V, we see that for *P.subcapitata* and *C. vulgaris*, the prediction errors of WHAM VII are a little less accurate. However, for *C. reinhardtti*, the prediction errors made by WHAM VII are similar to those of WHAM V.
Overall, the Cu bioavailability model coupled with WHAM VII (Speciation Scenario II) predicted Cu toxicity to *P. subcapitata, C. vulgaris and C. reinhardtti* with comparable accuracy as the original Cu bioavailability model coupled with WHAM V (Table 7.11).

Table 7.10 Average calibrated intrinsic Cu^{2+} sensitivities for *Pseudokirchneriella subcapitata, Chlorella vulgaris and Chlamydomonas reinhardtti* (Qx_{Cu2+}; calculated using Equation 7.5) under Speciation Scenario I and II

	P.subcapitata[a]		*C. vulgaris*[a]		*C. reinhardtii*[a]		*P.subcapitata*[b]
	$Q10Cu_{2+}$	$Q50Cu_{2+}$	$Q10Cu_{2+}$	$Q50Cu_{2+}$	$Q10Cu_{2+}$	$Q50Cu_{2+}$	$QNOEC_{Cu2+}$
Speciation Scenario I[c]	-1.17	-0.40	-0.67	-0.03	-0.76	-0.11	-1.12
Speciation Scenario II[d]	-1.24	-0.44	-0.73	-0.05	-0.82	0.15	-1.18

[a] Data from De Schamphelaere and Janssen (2006b); *P.subcapitata* growth rate endpoint
[b] Data from Heijerick et al (2005a); *P.subcapitata* biomass yield endpoint
[c] Speciation Scenario I: default WHAM VII stability constants for inorganic complexation
[d] Speciation Scenario II: stability constants for inorganic complexation reported by NIST

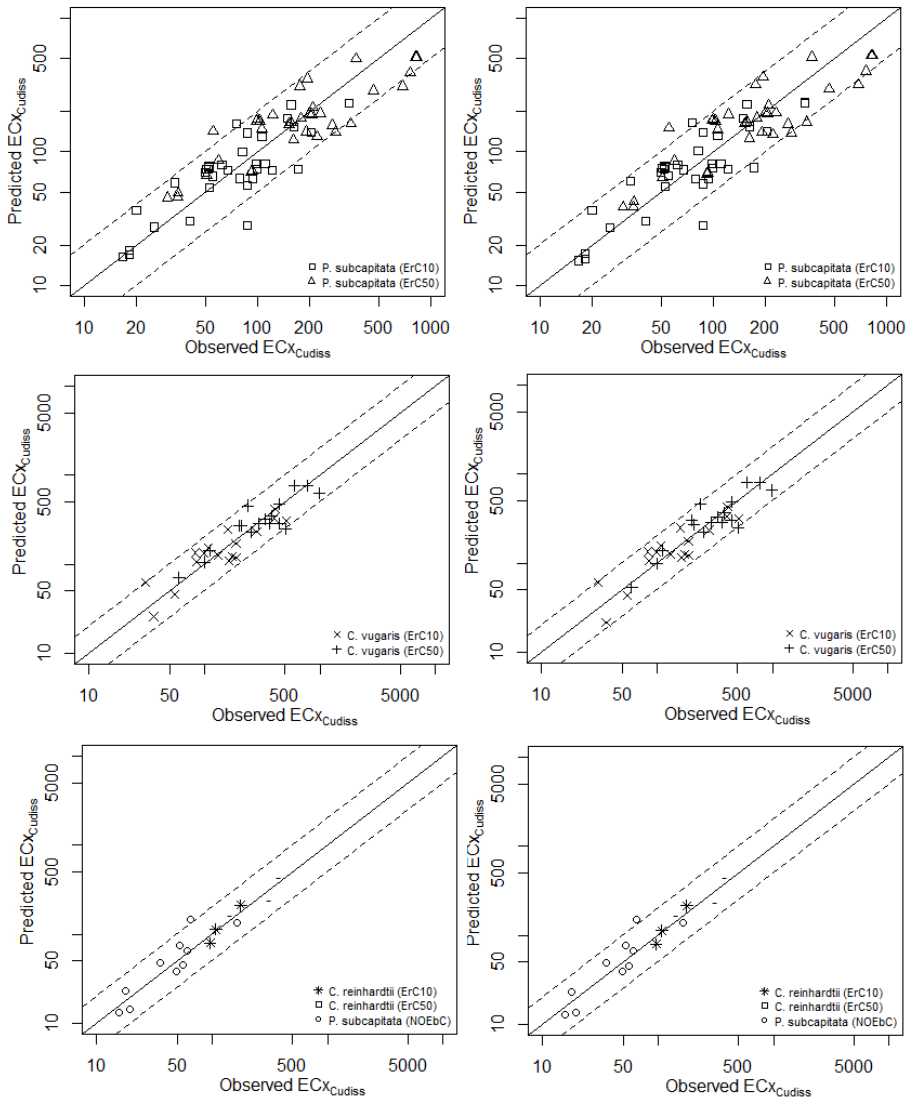

Figure 7.2 Predicted versus observed x% effective concentration (ECx_{Cudiss}) and no observed effect concentration ($NOEC_{Cudiss}$) for *Pseudokirchneriella subcapitata, Chlorella vulgaris and Chlamydomonas reinhardtti* using Speciation Scenario I (i.e. using the default WHAM VII stability constants for inorganic complexation; left graph) and Speciation Scenario II (i.e. using stability constants for inorganic complexation reported by NIST; right graph). Predictions were made using the chronic Cu freshwater green migroalgae bioavailablilty model linked to WHAM VII (Equation 7.2). The solid line represents a perfect fit between the observed and predicted data, the dashed lines represent a difference of a factor 2 between the observed and predicted data.

Table 7.11 Prediction statistics of the ECx_{Cudiss} and $NOEC_{Cudiss}$ values predicted with the chronic Cu freshwater green microalgae bioavailability model (Equation 7.4) in WHAM V[a] and in WHAM VII using Speciation Scenario I[b] and Speciation Scenario II[c]

	WHAM V						
	P.subcapitata		*C. vulgaris*		*C. reinhardtii*		*P.subcapitata*
	EC10 data	EC50 data	EC10 data	EC50 data	EC10 data	EC50 data	NOEC data
Mean prediction error	1.32	1.30	1.36	1.28	1.09	1.32	1.39
% predicted within one-and-a-half fold error	86	82	71	88	100	100	70
% predicted within twofold error	97	94	94	94	100	100	90

	WHAM VII Speciation Scenario I						
	P.subcapitata		*C. vulgaris*		*C. reinhardtii*		*P.subcapitata*
	EC10 data	EC50 data	EC10 data	EC50 data	EC10 data	EC50 data	NOEC data
Mean prediction error	1.44	1.52	1.39	1.30	1.15	1.20	1.37
Median prediction error	1.41	1.47	1.41	1.27	1.19	1.15	1.28
% predicted within one-and-a-half fold error	74	53	71	76	100	100	90
% predicted within twofold error	91	88	100	94	100	100	90

	WHAM VII Speciation Scenario II						
	P.subcapitata		*C. vulgaris*		*C. reinhardtii*		*P.subcapitata*
	EC10 data	EC50 data	EC10 data	EC50 data	EC10 data	EC50 data	NOEC data
Mean prediction error	1.45	1.50	1.40	1.30	1.15	1.22	1.38
Median prediction error	1.41	1.42	1.38	1.24	1.20	1.18	1.27
% predicted within one-and-a-half fold error	74	53	65	76	100	100	90
% predicted within twofold error	91	88	100	94	100	100	90

[a] Data from De Schamphelaere and Janssen (2006b) for the growth rate endpoint and Heijerick et al (2005a) for the biomass endpoint (see Table 7.1)
[b] Speciation Scenario I: default WHAM VII stability constants for inorganic complexation
[c] Speciation Scenario II: stability constants for inorganic complexation reported by NIST

Validation of the chronic Cu D. magna gBAM in WHAM VII

The intrinsic sensitivities (Qx_{Cu2+}) for the Speciation Scenario I and II are reported in Table 7.12. The prediction statistics for the chronic Cu *D. magna* gBAM for both speciation scenarios are given in Table 7.13. For the EC50 and NOEC data, the Cu toxicity to the K6 and ARO *D. magna* clones is almost as accurately predicted using the gBAM coupled to WHAM VII using Speciation Scenario II compared to Speciation Scenario I (Figure 7.3; Table 7.13). When comparing with results from the gBAM coupled to WHAM V, we see that the WHAM VII predictions are less accurate but still comparable.
Overall, the Cu *D. magna* gBAM coupled with WHAM VII predicted Cu toxicity almost as accurate as the original Cu *D. magna* gBAM coupled with WHAM V for EC50 data.

Table 7.12 Average calibrated intrinsic Cu^{2+} sensitivities for *Daphnia magna*[a] (QX_{Cu2+} calculated using Equation 7.7) under Speciation Scenario I and II.

	K6 clone		ARO clone	
	$Q50_{Cu2+}$[b]	$Q10_{Cu2+}$[c]	$Q50_{Cu2+}$[b]	$Q10_{Cu2+}$[c]
Speciation Scenario I[b]	-7.69	-7.91	-8.27	-
Speciation Scenario II[c]	-7.06	-7.29	-7.58	-

[a] Data from Van Regenmortel et al (2015; Chapter 5)
[b] Speciation Scenario I: default WHAM VII stability constants for inorganic complexation
[c] Speciation Scenario II: stability constants for inorganic complexation reported by NIST

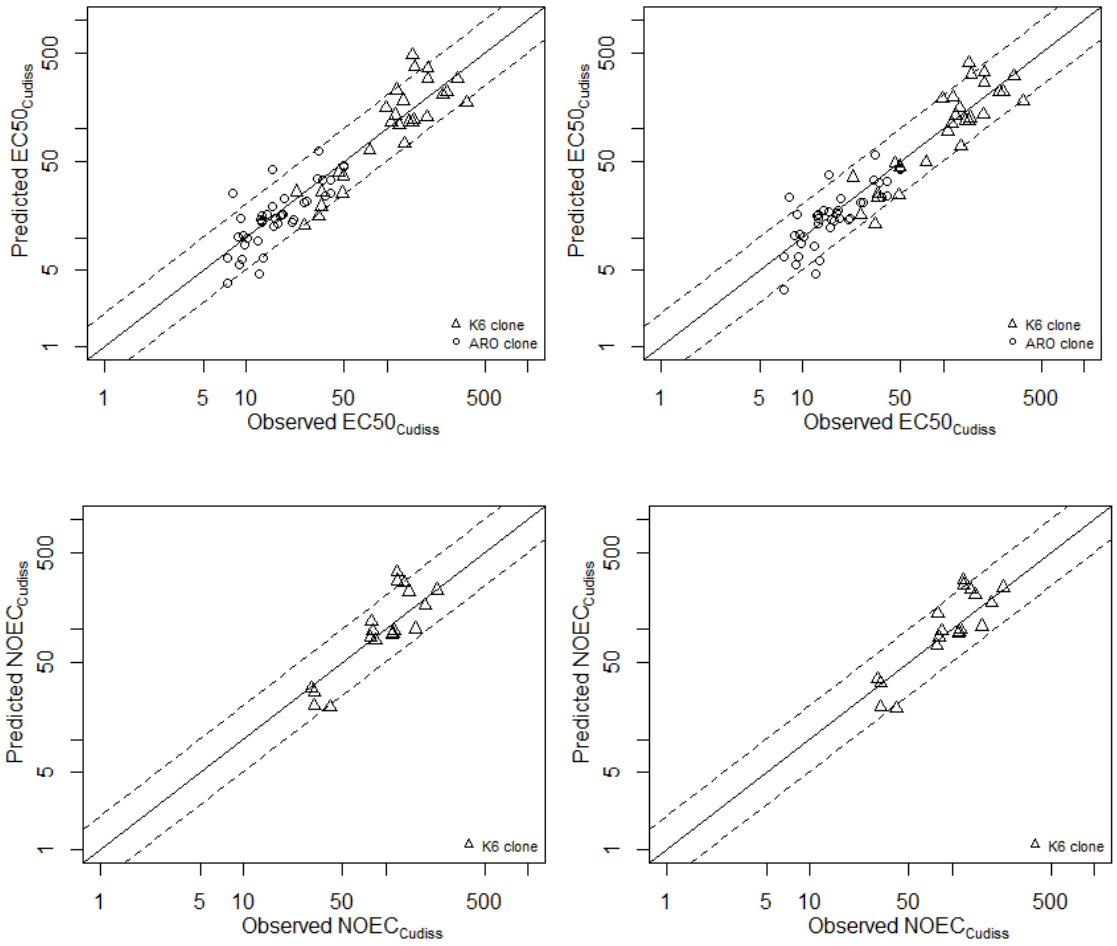

Figure 7.3. Predicted versus observed 50% effect concentration ($EC50_{Cudiss}$) and no observed effect concentration ($NOEC_{Cudiss}$) for *Daphnia magna* using the gBAM coupled to WHAM V (left graphs); Speciation Scenario I (i.e. using the default WHAM VII stability constants for inorganic complexation; middle graphs) and Speciation Scenario II (i.e. using stability constants for inorganic complexation reported by NIST; right graphs). Predictions were made using the chronic Cu gBAM linked to WHAM VII (Equation 7.4). The solid line represents a perfect fit between the observed and predicted data, the dashed lines represent a difference of a factor 2 between the observed and predicted data.

Table 7.13 Prediction statistics of the $EC50_{Cudiss}$ and $NOEC_{Cudiss}$ predicted with the chronic Cu *Daphnia magna* gBAM[a] (Equation 7.6) in WHAM V and in WHAM VII using Speciation Scenario I[b] and Speciation Scenario II[c]

WHAM V

	K6 clone			ARO clone	
	EC50 data	NOEC data[d]		EC50 data	NOEC data
	All data	Bihain	Ossenkolk	All data	
Mean prediction error	1.5	1.47	1.31	1.3	-
Median prediction error	-	1.15	1.29	-	-
% predicted within twofold error	89	78	100	92	-

WHAM VII
Speciation Scenario I

	K6 clone			ARO clone	
	EC50 data	NOEC data		EC50 data	NOEC data
	All data	Bihain	Ossenkolk	All data	
Mean prediction error	1.57	1.59	1.37	1.41	-
Median prediction error	1.37	1.23	1.19	1.21	-
% predicted within twofold error	82	67	100	90	-

WHAM VII
Speciation Scenario II

	K6 clone			ARO clone	
	EC50 data	NOEC data		EC50 data	NOEC data
	All data	Bihain	Ossenkolk	All data	
Mean prediction error	1.52	1.55	1.31	1.42	-
Median prediction error	1.40	1.20	1.14	1.22	-
% predicted within twofold error	86	67	100	87	-

[a] Data from Van Regenmortel et al (2015; Chapter 5) (see Table 7.1)
[b] Speciation Scenario I: default WHAM VII stability constants for inorganic complexation
[c] Speciation Scenario II: stability constants for inorganic complexation reported by NIST;
[d] prediction statistics not given in Van Regenmortel et al (2015; Chapter 5) but calculated for this Chapter

Validation of the read-across to B. calyciflorus using the D. magna BLM and gBAM in WHAM VII

For the validation of the read-across of the *D. magna* BLM, the intrinsic sensitivities ($N(L)OEC^{*}_{Cu2+}$) for the Speciation Scenario I and II are reported in Table 7.14. Both speciation scenarios were not accurate in predicting chronic Cu toxicity to *B. calyciflorus* (Figure 7.4; Table 7.15), i.e. only 25% of the NOEC and LOEC values were predicted within twofold prediction error for *B.*

For the validation of the *D. magna* gBAM, the intrinsic sensitivities ($QN(L)OEC_{Cu2+}$ for the Speciation Scenario I and II are reported in Table 7.15. The chronic Cu toxicity to *B. calyciflorus* was predicted with comparable accuracy using Speciation Scenario I and II compared to predictions using WHAM V. When comparing the predictions from the *D. magna* BLM and gBAM for *B. calyciflorus*, we see that the Cu *D. magna* gBAM is more accurate.

Table 7.14 Average calibrated intrinsic Cu^{2+} sensitivities for *Brachionus calyciflorus* ($N(L)OEC^{*}_{Cu2+}$ and $QN(L)OEC_{Cu2+}$; calculated using Equations 7.3 and 7.7) under Speciation Scenario I and II

	B. calyciflorus[a]			
	D. magna BLM (nmol/L)		*D. magna* gBAM	
	$NOEC^{*}_{Cu2+}$	$LOEC^{*}_{Cu2+}$	$QNOEC_{Cu2+}$	$QLOEC_{Cu2+}$
Speciation Scenario I[b]	3.70	7.91	-8.45	-8.12
Speciation Scenario II[c]	3.76	8.10	-7.89	-7.56

[a] Data from De Schamphelaere & Janssen (2010)

[b] Speciation Scenario I: default WHAM VII stability constants for inorganic complexation

[c] Speciation Scenario II: stability constants for inorganic complexation reported by NIST

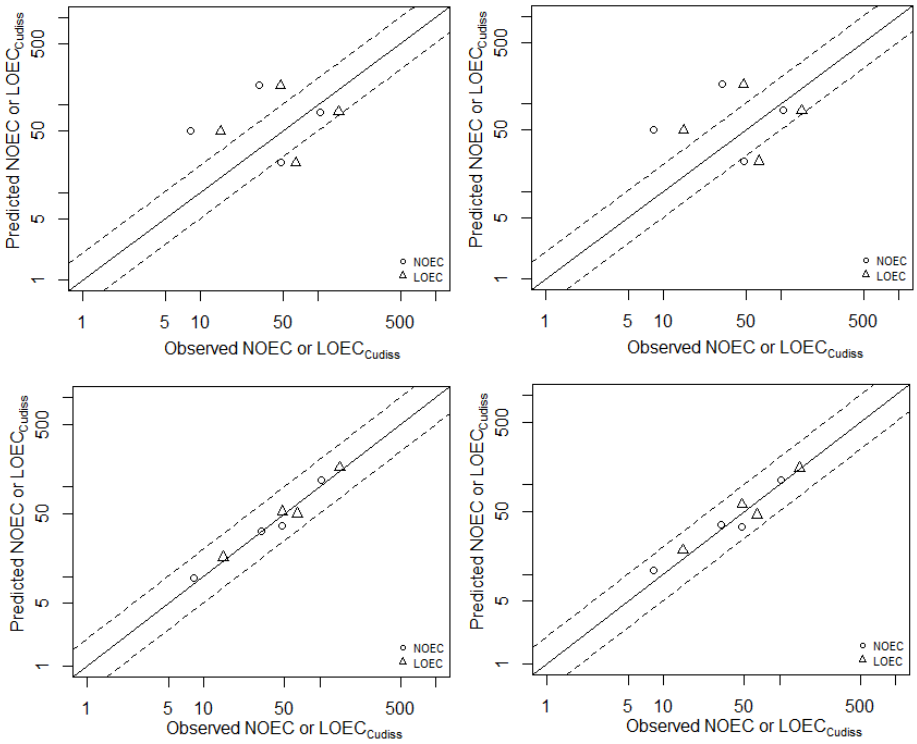

Figure 7.4. Predicted versus observed no (lowest) observed effect concentration ($N(L)OEC_{Cudiss}$) for *Brachionus calyciflorus* using Speciation Scenario I (i.e. using the default WHAM VII stability constants for inorganic complexation; left graph) and Speciation Scenario II (i.e. using stability constants for inorganic complexation reported by NIST; right graph). Predictions were made using the chronic Cu *D. magna* BLM (upper graphs) and gBAM (lower graphs) linked to WHAM VII (Equations 7.1 and 7.4). The solid line represents a perfect fit between the observed and predicted data, the dashed lines represent a difference of a factor 2 between the observed and predicted data.

Table 7.15 Prediction statistics of the N(L)OEC$_{Cudiss}$ predicted with the chronic Cu *D. magna* BLM and gBAM [a] (Equations 7.2 and 7.6) in WHAM V and in WHAM VII using Speciation Scenario I[b] and Speciation Scenario II[c]

	WHAM V				WHAM VII Speciation Scenario I				WHAM VII Speciation Scenario II			
	D. magna BLM		*D. magna* gBAM		*D. magna* BLM		*D. magna* gBAM		*D. magna* BLM		*D. magna* gBAM	
	NOEC data	LOEC data	NOEC data	LOEC data	NOEC data	LOEC data	NOEC data	LOEC data	NOEC data	LOEC data	NOEC data	LOEC data
Mean prediction error	1.18	1.14	1.16	1.12	3.72	2.90	1.17	1.15	3.72	2.90	1.25	1.23
Median prediction error	-	-	1.15	1.09	3.77	3.17	1.18	1.11	2.78	3.16	1.24	1.25
Minimum prediction error	1.03	1.02	1.05	1.04	1.24	1.79	1.02	1.11	1.23	1.78	1.10	1.04
% predicted within twofold error	100	100	100	100	25	25	100	100	25	25	100	100

[a] Speciation Scenario I: default WHAM VII stability constants for inorganic complexation

[b] Speciation Scenario II: stability constants for inorganic complexation reported by NIST

[c] Data from De Schamphelaere et al (2006c) and Van Regenmortel et al (2017b) (see Table 7.1)

Calibration of the Ni bioavailability models in WHAM VII

Validation of the chronic Ni D. magna bioavailability model in WHAM VII

The intrinsic sensitivities ($Q10_{Ni2+}$) for the Speciation Scenario I and II are reported in Table 7.16. Both speciation scenarios predicted chronic Ni toxicity to *D. magna* with reasonable accuracy (Figure 7.5; Table 7.17). The Speciation Scenario II, using the NIST stability constants for inorganic ligand complexation predicted the $EC10_{Nidiss}$ values more accurate than the Speciation Scenario I, certainly for the synthetic water dataset. When comparing with the predictions made by WHAM VI, we see that the mean prediction errors of WHAM VI and WHAM VII using Speciation Scenario II are quite similar.

Overall, the Ni *D. magna* bioavailability model coupled with WHAM VII (Speciation Scenario II) predicted Ni toxicity in natural and synthetic waters almost as accurate as the original Ni *D. magna* bioavailability model coupled with WHAM VI (Table 7.17).

Table 7.16 Average calibrated intrinsic Ni^{2+} sensitivities for *Daphnia magna* ($Q10_{Ni2+}$; calculated using Equation 7.9) under Speciation Scenario I and II

	Synthetic waters [a]	Natural waters [a]
	$Q10_{Ni2+}$ [b]	$Q10_{Ni2+}$ [c]
Speciation Scenario I[d]	5.72	4.63
Speciation Scenario II[e]	5.64	4.24

[a] Data from Deleebeeck et al (2008)

[b] $Q10_{Ni2+}$ for synthetic waters calculated based on data for synthetic waters and an S_{pH} of 0.1987 (Table 7.4)

[c] $Q10_{Ni2+}$ for natural waters calculated based on data for natural waters and an S_{pH} of 0.3335 (Table 7.4)

[d] Speciation Scenario I: default WHAM VII stability constants for inorganic complexation

[e] Speciation Scenario II: stability constants for inorganic complexation reported by NIST

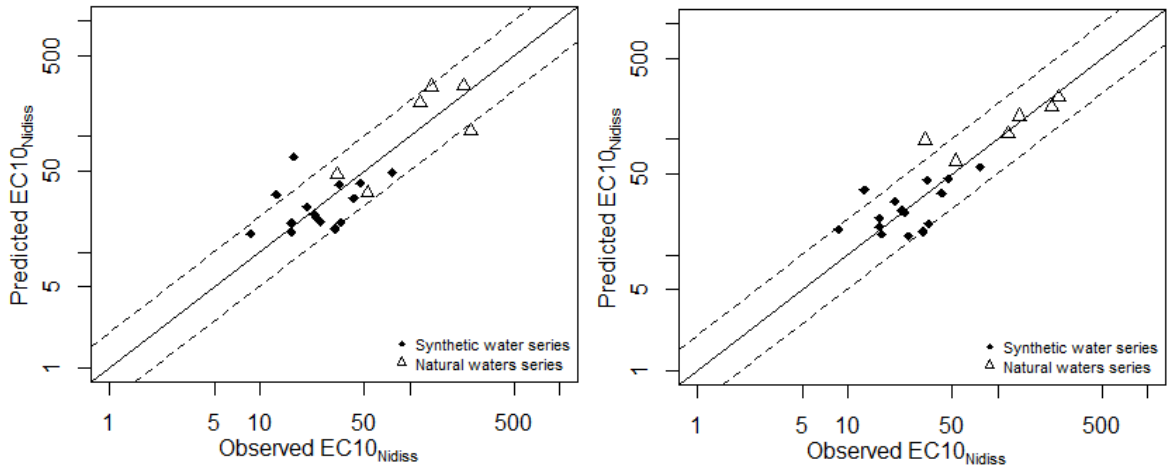

Figure 7.5. Predicted versus observed 10% effective concentration ($EC10_{Nidiss}$) for *Daphnia magna* using Speciation Scenario I (i.e. using the default WHAM VII stability constants for inorganic complexation; left graph) and Speciation Scenario II (i.e. using stability constants for inorganic complexation reported by NIST; right graph). Predictions were made using the chronic Ni *D. magna* bioavailability model linked to WHAM VII (Equation 7.8). The solid line represents a perfect fit between the observed and predicted data, the dashed lines represent a difference of a factor 2 between the observed and predicted data.

Table 7.17 Prediction statistics of the $EC10_{Nidiss}$ predicted with the chronic Ni *Daphnia magna* bioavailability model (Equation 7.8) in WHAM VI[a] and in WHAM VII using Speciation Scenario I[b] and Speciation Scenario II[c]

	WHAM VI		WHAM VII Speciation Scenario I		WHAM VII Speciation Scenario II	
	Synthetic waters	Natural waters	Synthetic waters	Natural waters	Synthetic waters	Natural waters
Mean prediction error	1.4	1.4	1.63	1.69	1.48	1.46
Median prediction error	-	-	1.42	1.64	1.31	1.17
Minimum prediction error	1.0	1.1	1.08	1.19	1.03	1.06
% predicted within twofold error	-	-	80	83	87	83

[a] Data from Deleebeeck et al (2008) (see Table 7.1)
[b] Speciation Scenario I: default WHAM VII stability constants for inorganic complexation
[c] Speciation Scenario II: stability constants for inorganic complexation reported by NIST

Validation of the Ni bioavailability model for P.subcapitata in WHAM VII

The intrinsic sensitivities (Qx_{Ni2+}) for the Speciation Scenario I and II are reported in Table 7.18. Both speciation scenarios predicted chronic Ni toxicity to *P.subcapitata* with reasonable accuracy (Figure 7.6; Table 7.19). For the univariate Mg, pH and Ca test series, both speciation scenarios showed comparable accuracy or more accuracy compared to the WHAM VI results. For the bivariate pH-Mg test series Speciation Scenario II was more accurate than the results with WHAM VI. For the validation waters, Speciation Scenario I was less accurate than WHAM VI, while Speciation Scenario II showed comparable and less accuracy compared to WHAM VI for EC50 and EC10 data, respectively.
Overall, the prediction performance of the Ni *P.subcapitata* bioavailability model coupled with WHAM VII under Speciation Scenario II was relatively comparable with the performance of the original model. (Table 7.19).

Table 7.18 Average calibrated intrinsic Ni^{2+} sensitivities for *Daphnia magna* (Qx_{Ni2+}; calculated using Equation 7.9) under Speciation Scenario I and II

	Synthetic waters [a]		Validation waters [b]	
	$Q50_{Ni2+}$[c]	$Q10_{Ni2+}$[c]	$Q50_{Ni2+}$[d]	$Q10_{Ni2+}$[d]
Speciation Scenario I[e]	5.03	5.51	4.48	5.39
Speciation Scenario II[f]	4.82	5.29	4.33	5.14

[a] Data from Deleebeeck et al (2009): univariate Ca, Mg and pH test series and the bivariate pH-Mg test series
[b] Data from Deleebeeck et al (2009): the OECD waters and natural waters used in the validation test series
[c] Qx_{Ni2+} for synthetic waters was calculated based on data for the univariate Mg and pH test series (Deleebeeck et al (2009)
[d] Qx_{Ni2+} for natural waters was calculated based on the OECD waters used in the validation test series (Deleebeeck et al (2009)
[e] Speciation Scenario I: default WHAM VII stability constants for inorganic complexation
[f] Speciation Scenario II: stability constants for inorganic complexation reported by NIST

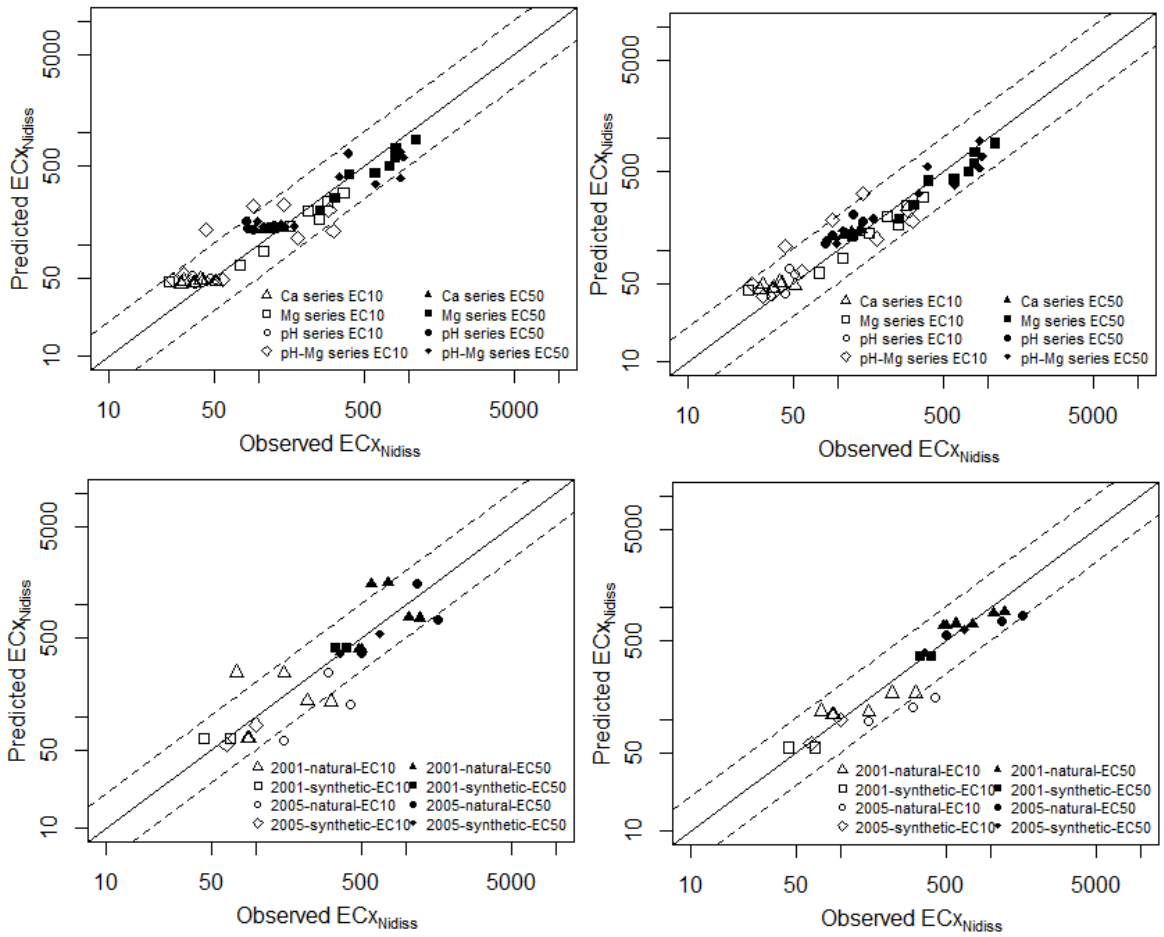

Figure 7.6. Predicted versus observed x% effective concentration (ECx$_{Nidiss}$s) for *Pseudokircherniella subcapitata* using Speciation Scenario I (i.e. using the default WHAM VII stability constants for inorganic complexation; left graph) and Speciation Scenario II (i.e. using stability constants for inorganic complexation reported by NIST; right graph). Predictions were made using the chronic Ni *P.subcapitata* bioavailability model linked to WHAM VII (Equation 7.8). Top graphs: model performance for the synthetic waters used in the univariate Ca, Mg and pH test series and the bivariate pH-Mg test series. Lower graphs: model performance for the OECD waters and natural waters used in the validation test series. The solid line represents a perfect fit between the observed and predicted data, the dashed lines represent a difference of a factor 2 between the observed and predicted data.

Table 7.19 Prediction statistics of the ECx_{Nidiss} predicted with the chronic Ni *Pseudokirchneriella subcapitata* bioavailability model (Equation 7.8) in WHAM VI[a] and in WHAM VII using Speciation Scenario I[b] and Speciation Scenario II[c]

	WHAM VI							
	Synthetic waters						Validation waters	
	Mg and pH series		Ca series		pH-Mg series			
	EC50 data	EC10 data	EC50 data	EC10 data	EC50 data	EC10 data	EC50 data	EC10 data
Mean prediction error	1.3	1.2	1.2	1.3	1.3	1.7	1.2	1.3
Median prediction error	-	-	-	-	-	-	-	-
Minimum prediction error	1.0	1.1	1.0	1.1	1.1	1.1	1.0	1.0
% predicted within twofold error	100	100	100	100	100	-	100	100

	WHAM VII Speciation Scenario I							
	Synthetic waters						Validation waters	
	Mg and pH series		Ca series		pH-Mg series			
	EC50 data	EC10 data	EC50 data	EC10 data	EC50 data	EC10 data	EC50 data	EC10 data
Mean prediction error	1.33	1.24	1.15	1.26	1.53	1.90	1.50	1.81
Median prediction error	1.30	1.15	1.15	1.22	1.50	1.71	1.30	1.42
Minimum prediction error	1.01	1.04	1.01	1.12	1.17	1.18	1.00	1.07
% predicted within twofold error	100	100	100	100	89	67	77	69

	WHAM VII Speciation Scenario II							
	Synthetic waters						Validation waters	
	Mg and pH series		Ca series		pH-Mg series			
	EC50 data	EC10 data	EC50 data	EC10 data	EC50 data	EC10 data	EC50 data	EC10 data
Mean prediction error	1.33	1.24	1.17	1.29	1.31	1.70	1.27	1.51
Median prediction error	1.36	1.18	1.19	1.22	1.33	1.72	1.17	1.29
Minimum prediction error	1.01	1.07	1.04	1.09	1.07	1.11	1.05	1.01
% predicted within twofold error	100	100	100	100	100	67	100	85

[a] Data from Deleebeeck et al (2008 and 2009) (see Table 7.1)
[b] Speciation Scenario I: default WHAM VII stability constants for inorganic complexation
[c] Speciation Scenario II: stability constants for inorganic complexation reported by NIST

Validation of the Ni fish bioavailability model in WHAM VII

The intrinsic sensitivities (Qx_{Ni2+}) for the Speciation Scenario I and II are reported in Table 7.20. Both speciation scenarios predicted chronic Ni toxicity to *O. mykiss* with reasonable accuracy (Figure 7.7; Table 7.21). For the LC50 data, Speciation Scenario II was as accurate compared to the WHAM VI results, for both synthetic and natural waters. For the NOEC data, no information was given on the prediction statistics in Deleebeeck et al (2007). However, Speciation Scenario II showed high accuracy, i.e. all waters within twofold prediction error, for the synthetic waters. For the natural waters, Speciation Scenario II showed little less accuracy (i.e. 80% within twofold error), which is still better than the prediction statistics of the LC50 data for the natural waters using WHAM VI.

Overall, the prediction performance of the Ni fish bioavailability model coupled with WHAM VII under Speciation Scenario II was relatively comparable with the performance of the original model. (Table 7.21).

Table 7.20 Average calibrated intrinsic Ni^{2+} sensitivities for *Oncorhynchus mykiss* (QX_{Ni2+}; calculated using Equation 7.9) under Speciation Scenario I and II

	$Q50_{Ni2+}$[a]	$QNOEC_{Ni2+}$[a]
Speciation Scenario I[b]	3.15	3.63
Speciation Scenario II[c]	2.93	3.40

[a] Data from Deleebeeck et al (2007): QX_{Ni2+} calculated based on synthetic test media
[b] Speciation Scenario I: default WHAM VII stability constants for inorganic complexation
[c] Speciation Scenario II: stability constants for inorganic complexation reported by NIST

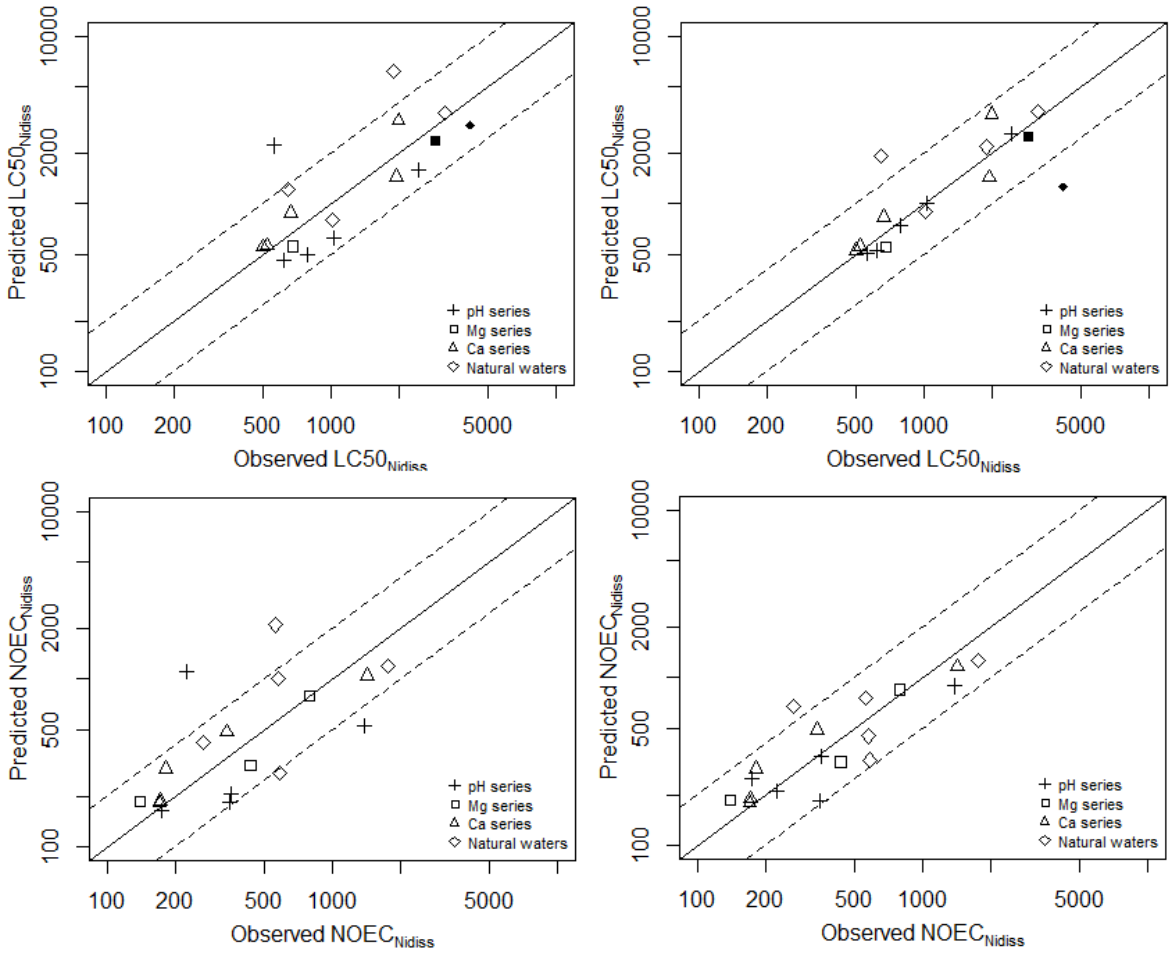

Figure 7.7. Predicted versus observed 50% lethal concentration ($LC50_{Nidiss}$) and no observed effect concentration ($NOEC_{Nidiss}$) for *Oncorhynchus mykiss* using Speciation Scenario I (i.e. using the default WHAM VII stability constants for inorganic complexation; left graph) and Speciation Scenario II (i.e. using stability constants for inorganic complexation reported by NIST; right graph). Predictions were made using the chronic Ni fish bioavailability model linked to WHAM VII (Equation 7.8). The solid line represents a perfect fit between the observed and predicted data, the dashed lines represent a difference of a factor 2 between the observed and predicted data.

Table 7.21 Prediction statistics of the $LC50_{Nidiss}$ and $NOEC_{Nidiss}$ predicted with the chronic Ni fish bioavailability model (Equation 7.8) in WHAM VI[a] and in WHAM VII using Speciation Scenario I[b] and Speciation Scenario II[c]

	WHAM VI				WHAM VII Speciation Scenario I				WHAM VII Speciation Scenario II			
	Synthetic waters		Natural waters		Synthetic waters		Natural waters		Synthetic waters		Natural waters	
	LC50 data	NOEC data	LC50 data	NOEC data	LC50 data	NOEC data	LC50 data	NOEC data	LC50 data	NOEC data	LC50 data	NOEC data
Mean prediction error	1.20	-	1.55	-	1.58	1.73	1.95	2.13	1.19	1.32	1.64	1.68
Median prediction error	-	-	1.10	-	1.34	1.41	1.60	1.74	1.14	1.33	1.18	1.40
Minimum prediction error	-	-	1.10	-	1.09	1.00	1.14	1.47	1.02	1.03	1.08	1.29
% predicted within twofold error	100	-	75	-	92	85	75	60	100	100	75	80

[a] Data from Deleebeeck et al (2007) (see Table 7.1)

[b] Speciation Scenario I: default WHAM VII stability constants for inorganic complexation

[c] Speciation Scenario II: stability constants for inorganic complexation reported by NIST

Validation of the chronic Ni C. dubia bioavailability model in WHAM VII

The intrinsic sensitivities ($Q50_{Ni2+}$) for the Speciation Scenario I and II are reported in Table 7.22. In general, Speciation Scenario I and II predicted Ni toxicity to *C. dubia* with the same accuracy (Figure 7.8; Table 7.23). Overall, Ni toxicity to *C. dubia* for EC50 values was less well predicted when the Ni *C. dubia* bioavailability model was coupled to WHAM VII (Speciation Scenario II) than when it was coupled to WHAM VI.

Table 7.22 Average calibrated intrinsic Ni^{2+} sensitivities for *Ceriodaphnia dubia* ($Q50_{Ni2+}$; calculated using Equation 7.9) under Speciation Scenario I and II

	$Q50_{Ni2+}$[a]
Speciation Scenario I[b]	-0.0077
Speciation Scenario II[c]	2.49

[a] Data from De Schamphelaere et al (2006a)
[b] Speciation Scenario I: default WHAM VII stability constants for inorganic complexation
[c] Speciation Scenario II: stability constants for inorganic complexation reported by NIST

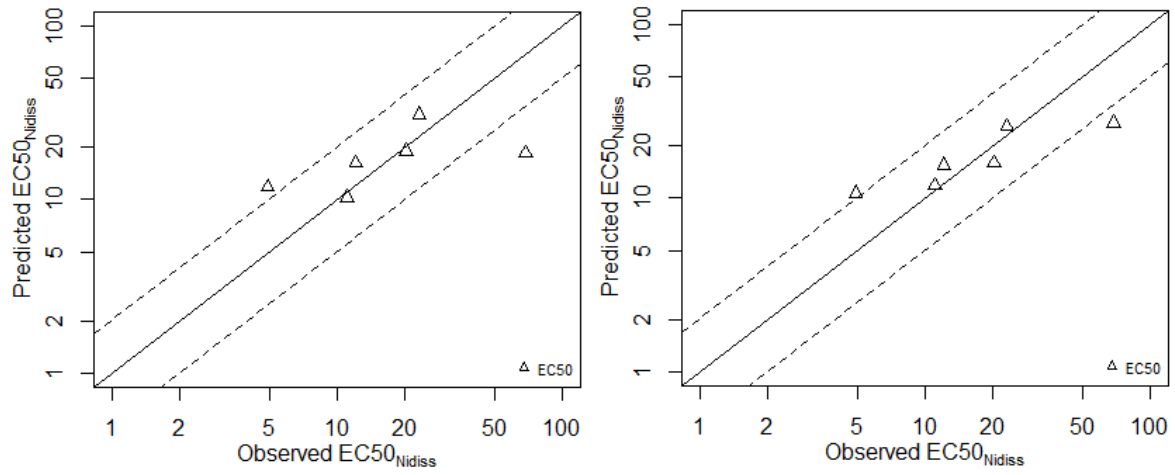

Figure 7.8. Predicted versus observed 50% effective concentration ($EC50_{Nidiss}$)) for *Ceriodaphnia dubia* using Speciation Scenario I (i.e. using the default WHAM VII stability constants for inorganic complexation; left graph) and Speciation Scenario II (i.e. using stability constants for inorganic complexation reported by NIST; right graph). Predictions were made using the chronic Ni *C. dubia* bioavailability model linked to WHAM VII (Equation 7.3). The solid line represents a perfect fit between the observed and predicted data, the dashed lines represent a difference of a factor 2 between the observed and predicted data.

Table 7.23 Prediction statistics of the $EC50_{Nidiss}$ predicted with the chronic Ni *Ceriodubia daphnia* bioavailability model (Equation 7.8) in WHAM VI[a] and in WHAM VII using Speciation Scenario I[b] and Speciation Scenario II[c]

	WHAM VI	WHAM VII Speciation Scenario I	WHAM VII Speciation Scenario II
	EC50 data	EC50 data	EC50 data
Mean prediction error	1.37	1.82	1.57
Median prediction error	1.19	1.34	1.27
Minimum prediction error	-	1.06	1.07
% predicted within twofold error	100	67	67

[a] Data from De Schamphelaere et al (2006a) (see Table 7.1)
[b] Speciation Scenario I: default WHAM VII stability constants for inorganic complexation
[c] Speciation Scenario II: stability constants for inorganic complexation reported by NIST

Validation of the read-across to C. tentans, L. stagnalis, B. calyciflorus and L. minor using the D. magna and C. dubia bioavailability models in WHAM VII

For the cross-species extrapolation of the chronic Ni *D. magna* and *C. dubia* bioavailability models in WHAM VII , the intrinsic sensitivities (ECx^{*}_{Zn2+}) for the Speciation Scenario I and II are reported in Table 7.24. For *C. tentans, B. calyciflorus* and *L. minor,* Speciation Scenario II, using the NIST stability constants for inorganic ligand complexation, predicted chronic Ni toxicity more accurately than WHAM VI (Figure 7.9, Table 7.25). For *L. stagnalis*, Speciation Scenario II predicted chronic Ni toxicity with comparable accurately than WHAM VI.

Overall, the prediction performance of the Ni *D. magna* and *C. dubia* bioavailability models coupled with WHAM VII under Speciation Scenario II was relatively comparable with the performance of the original models for the EC20 and EC50 data (Table 7.25).

Table 7.24 Average calibrated intrinsic Ni^{2+} sensitivities for *Chironomus tentans*, *Brachionus calyciflorus, Lemna minor and Lymnaea stagnalis* (Qx_{Ni2+}; calculated using Equation 7.9) under Speciation Scenario I and II

	C. tentans[a]		*B. calyciflorus*[a]
	D. magna BLM	*C. dubia BLM*	*D. magna* BLM
	$Q20_{Ni2+}$	$Q20_{Ni2+}$	$Q20_{Ni2+}$
Speciation Scenario I[b]	1.67	-1.57	1.56
Speciation Scenario II[c]	3.57	0.88	3.52

	L. minor[a]	*L. stagnalis*[a]
	D. magna BLM	*C. dubia BLM*
	$Q50_{Ni2+}$	$Q50_{Ni2+}$
Speciation Scenario I[b]	2.10	-0.027
Speciation Scenario II[c]	4.01	2.44

[a] Data from Schlekat et al (2010) (see Table 7.1)
[b] Speciation Scenario I: default WHAM VII stability constants for inorganic complexation
[c] Speciation Scenario II: stability constants for inorganic complexation reported by NIST

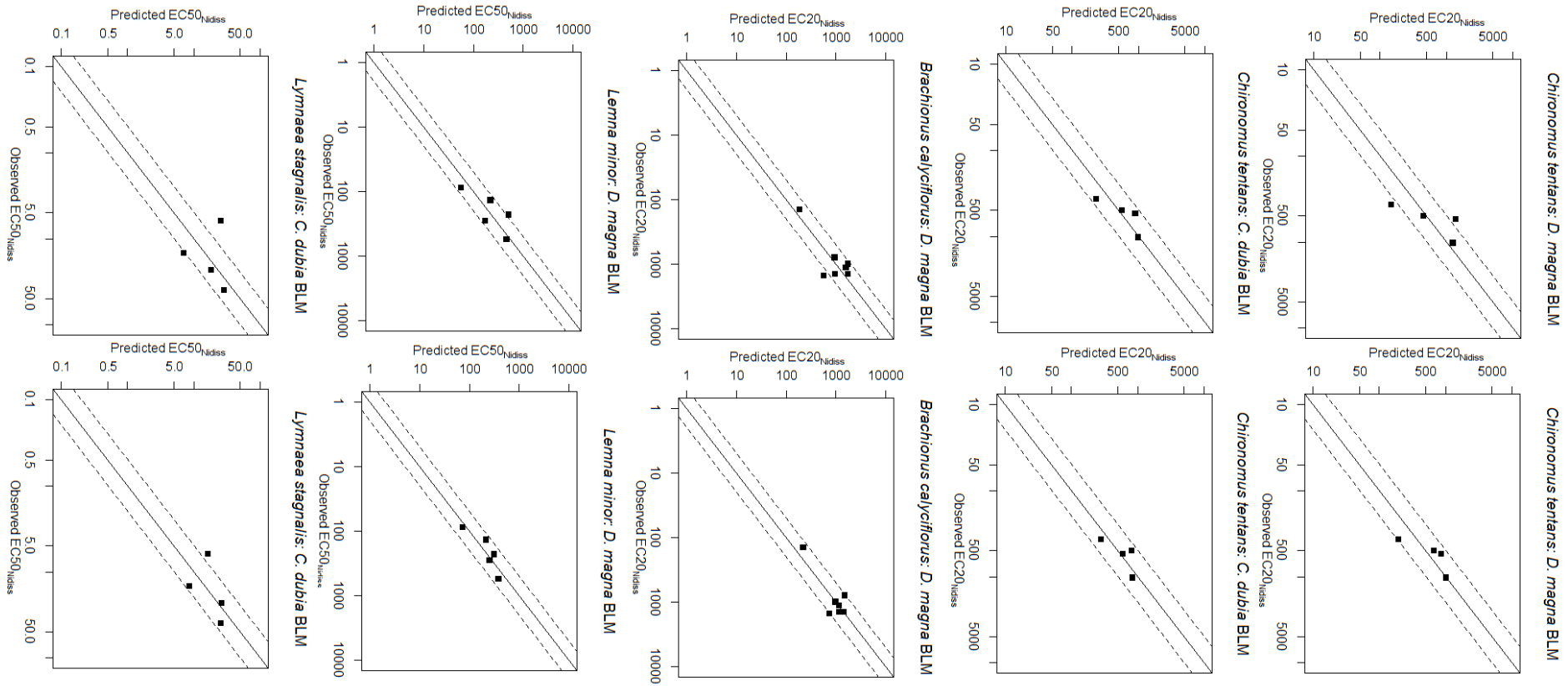

Figure 7.9. Predicted versus observed x% effective concentration ($EC_{x_{Nidiss}}$) for *Chironomus tentans*, *Brachionus calyciflorus, Lemna minor and Lymnaea stagnalis* using Speciation Scenario I (i.e. using the default WHAM VII stability constants for inorganic complexation; left graph) and Speciation Scenario II (i.e. using stability constants for inorganic complexation reported by NIST; right graph). Predictions were made using the chronic Ni *D. magna* and *C. dubia* bioavailability models linked to WHAM VII (Equation 7.8). The solid line represents a perfect fit between the observed and predicted data, the dashed lines represent a difference of a factor 2 between the observed and predicted data.

Table 7.25 Prediction statistics of the ECx_{Nidiss} predicted with the chronic Ni *D. magna* and *C. dubia* bioavailability models (Equation 7.8) in WHAM V[a] and in WHAM VII using Speciation Scenario I[b] and Speciation Scenario II[c]

	WHAM V				
	C. tentans		*B. calyciflorus*	*L. minor*	*L. stagnalis*
	D. magna BLM	*C. dubia BLM*	*D. magna* BLM	*D. magna* BLM	*C. dubia BLM*
	EC20 data	EC20 data	EC20 data	EC20 data	EC50 data
Mean prediction error	1.6	1.6	1.8	1.3	1.5
Median prediction error	-	-	-	-	-
Maximum prediction error	<2 .0	<2 .0	<2 .2	< 1.6	<1.8

	WHAM VII Speciation Scenario I				
	C. tentans		*B. calyciflorus*	*L. minor*	*L. stagnalis*
	D. magna BLM	*C. dubia BLM*	*D. magna* BLM	*D. magna* BLM	*C. dubia BLM*
	EC20 data	EC20 data	EC20 data	EC20 data	EC50 data
Mean prediction error	1.85	1.36	1.57	1.65	2.22
Median prediction error	1.85	1.36	1.36	1.59	1.77
% predicted within twofold error	50	100	86	80	50

	WHAM VII Speciation Scenario II				
	C. tentans		*B. calyciflorus*	*L. minor*	*L. stagnalis*
	D. magna BLM	*C. dubia BLM*	*D. magna* BLM	*D. magna* BLM	*C. dubia BLM*
	EC20 data	EC20 data	EC20 data	EC20 data	EC50 data
Mean prediction error	1.45	1.31	1.39	1.34	1.76
Median prediction error	1.42	1.30	1.27	1.35	1.67
% predicted within twofold error	100	100	86	100	75

[a] Data from Schlekat et al (2010) (see Table 7.1); [b] Speciation Scenario I: default WHAM VII stability constants for inorganic complexation;
[b] Speciation Scenario II: stability constants for inorganic complexation reported by NIST;

Calibration of the Zn bioavailability models in WHAM VII

Validation of the chronic Zn D. magna BLM in WHAM VII

The intrinsic sensitivities ($NOEC^*_{Zn2+}$) for the Speciation Scenario I and II are reported in Table 7.26. Both speciation scenarios predicted chronic Zn toxicity to *D. magna* with better accuracy than predictions using WHAM V (Figure 7.10; Table 7.27). Between 62% and 100% of the $NOEC_{Zndiss}$ values were predicted within 2-fold error. The Speciation Scenario II, using the NIST stability constants for inorganic ligand complexation predicted the $NOEC_{Zndiss}$ values more accurate than the Speciation Scenario I and the predictions using WHAM V, certainly for the natural water dataset. In De Schamphelaere et al (2005), Zn toxicity in the high pH field waters Voyon and Rhine was underestimated, i.e. prediction errors of factors of 3.8 and 2.3 were observed. Using WHAM VII, the underestimation of toxicity in these waters is much lower; i.e. prediction errors using Speciation Scenario I of factors of 2.1 and 2.1 for Voyon and Rhine, respectively, and prediction errors using Speciation Scenario II of factors of 2.1 and 1.7 for Voyon and Rhine, respectively.

Overall, the Zn *D. magna* BLM coupled with WHAM VII predicted Zn toxicity in natural and synthetic waters more accurate than the original Zn *D. magna* BLM coupled with WHAM V (Table 7.27).

Table 7.26 Average intrinsic Zn^{2+} sensitivities for Daphnia magna (21d-$NOEC^*_{Zn2+}$; calculated using Equation 7.11) under Speciation Scenario I and II

	Synthetic waters (nmol/L)[a]	Natural waters (nmol/L)[b]
Speciation Scenario I[c]	412	352
Speciation Scenario II[d]	426	421

[a] Data from Heijerick et al (2005b)
[b] Data from De Schamphelaere et al (2005)
[c] Speciation Scenario I: default WHAM VII stability constants for inorganic complexation
[d] Speciation Scenario II: stability constants for inorganic complexation reported by NIST

Table 7.27 Prediction statistics of the 21d-$NOEC_{Zndiss}$ predicted with the chronic Zn *Daphnia magna* BLM (Equation 7.10) in WHAM V[a] and in WHAM VII using Speciation Scenario I[b] and Speciation Scenario II[c]

	WHAM V			WHAM VII Speciation Scenario I			WHAM VII Speciation Scenario II		
	All data	Synthetic waters	Natural waters	All data	Synthetic waters	Natural waters	All data	Synthetic waters	Natural waters
Mean prediction error	1.62	1.51	1.93	1.53	1.48	1.66	1.47	1.46	1.50
Median prediction error	1.63	1.51	1.79	1.48	1.48	1.48	1.49	1.49	1.45
% predicted within twofold error	83	90	62	90	100	62	93	100	75

[a] Data from Heijerick et al (2005b) and De Schamphelaere et al (2005) (see Table 7.1)
b Speciation Scenario I: default WHAM VII stability constants for inorganic complexation
[d] Speciation Scenario II: stability constants for inorganic complexation reported by NIST

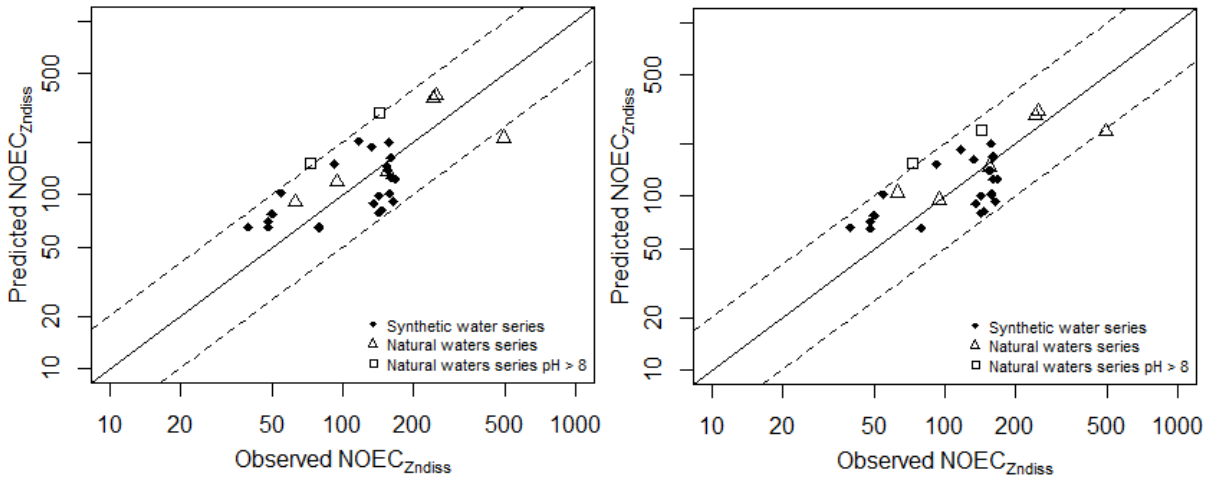

Figure 7.10. Predicted versus observed no observed effect concentration (NOEC$_{Zndis}$S) for *Daphnia magna* using Speciation Scenraio I (i.e. using the default WHAM VII stability constatns for inorganic complexation; left graph) and Speciation Scenario II (i.e. using stability constants for ionrganic complexation reported by NIST; right graph). Predictions were made using the chronic Zn *D. magna* BLM linked to WHAM VII (Equation 7.9). The solid line represents a perfect fit between the observed and predicted data, the dashed lines represent a difference of a factor 2 btween the observed and predicted data.

To be able to compare the accuracy of the *D. magna* BLM and gBAM coupled with WHAM VII, a separate validation was performed, as was explained in the *Material and Methods* section. For this validation, the data that was used to validate the gBAM was used. The intrinsic sensitivities (Qx$_{Cu2+}$) for the Speciation Scenario I and II are reported in Table 7.28. Prediction statistics are given in Table 7.29.

Table 7.28 Average intrinsic Zn^{2+} sensitivities for Daphnia magna ($EC x^{*}_{Zn2+}$ (nmol/L); calculated using Equation 7.11) under Speciation Scenario I and II

	$EC50^{*}_{Zn2+}$	$EC10^{*}_{Zn2+}$	$EC10^{*}_{Zn2+}$	
	KDS+TVR	KDS+TVR	KDS+TVR	Heijerick
Speciation Scenario I[e]	423	292	437	2292
Speciation Scenario II[f]	539	361	449	361

[a f] Data from Heijerick et al (200b5); De Schamphelaere et al (2005) and Van Regenmortel et al (2017b; Chapter 5)
[c] Q50 was calculated based on the "KDS+TVR" data
[d] Q10 was calculated based on the "KDS + TVR" data
[e] Two separate Q10 values were calculated, one based on the "KDS+TVR" data, and one based on the "Heijerick" data
[e] Speciation Scenario I: default WHAM VII stability constants for inorganic complexation
[f] Speciation Scenario II: stability constants for inorganic complexation reported by NIST

Table 7.29 Prediction statistics of the $EC50_{Zndiss}$ and $EC10_{Zndiss}$ predicted with the chronic Zn *Daphnia magna* BLM (Equation 7.10) in WHAM V[a] and in WHAM VII using Speciation Scenario I[b] and Speciation Scenario II[c]

	WHAM VII Speciation Scenario I					
	EC50 data[d]		EC10 data[e]		EC10 data[f]	
	Heijerick	KDS + TVR	Heijerick	KDS + TVR	Heijerick	KDS + TVR
Mean prediction error	1.71	1.83	1.64	2.15	1.53	2.15
Median prediction error	1.73	1.69	1.54	2.06	1.46	2.06
% predicted within twofold error	91	58	73	45	95	45

	WHAM VII Speciation Scenario II					
	EC50 data[d]		EC10 data[e]		EC10 data[f]	
	Heijerick	KDS + TVR	Heijerick	KDS + TVR	Heijerick	KDS + TVR
Mean prediction error	1.76	1.59	1.65	1.79	1.51	1.79
Median prediction error	1.75	1.48	1.58	1.45	1.49	1.45
% predicted within twofold error	77	75	73	64	95	64

[a] Data from Heijerick et al (2005b), De Schamphelaere et al (2005) and Van Regenmortel et al (2017b; Chapter 5) (see Table 7.1); [b] Speciation Scenario I: default WHAM VII stability constants for inorganic complexation ; [c] Speciation Scenario II: stability constants for inorganic complexation reported by NIST; [d] Q50 was calculated based on the "KDS+TVR" data ; [e] Q10 was calculated based on the "KDS + TVR" data; [f] Two separate Q10 values were calculated, one based on the "KDS+TVR" data, and one based on the "Heijerick" data

Validation of the Zn bioavailability model for P.subcapitata in WHAM VII

The intrinsic sensitivities (Qx_{Zn2+}) for the Speciation Scenario I and II are reported in Table 7.30. The prediction statistics for the chronic Zn *P.subcapitata* bioavailability model for both speciation scenarios are given in Table 7.31. For the EC50 data, the Zn toxicity to *P.subcapitata* is better predicted with the bioavailability model coupled to WHAM V, i.e. 100% of the data is predicted within twofold prediction error using WHAM V while only 86% and of the data is predicted within twofold prediction error using Speciation Scenario I and II coupled to WHAM VII (Figure 7.11). For the EC10 data, both speciation scenarios predicted chronic Zn toxicity to *P.subcapitata* as accurate as the bioavailability model coupled to WHAM V (Table 7.31).

Overall, the Zn *P.subcapitata* bioavailability model coupled with WHAM VII predicted Zn toxicity in natural waters less accurate than the original Zn *P.subcapitata* bioavailability model coupled with WHAM V for EC50 data, but as accurate for EC10 data (Table 7.31).

Table 7.30 Average intrinsic Zn2+ sensitivities for *Pseudokircheriella subcapitata* (Qx_{Zn2+}; calculated using Equation 7.13) under Speciation Scenario I and II.

	Natural waters (nmol/L)[a]	
	$Q50_{Zn2+}$	$Q10_{Zn2+}$
Speciation Scenario I[b]	1.54	2.06
Speciation Scenario II[c]	1.86	2.31

[a] Data from De Schamphelaere et al (2005)

[c] Speciation Scenario I: default WHAM VII stability constants for inorganic complexation

[d] Speciation Scenario II: stability constants for inorganic complexation reported by NIST

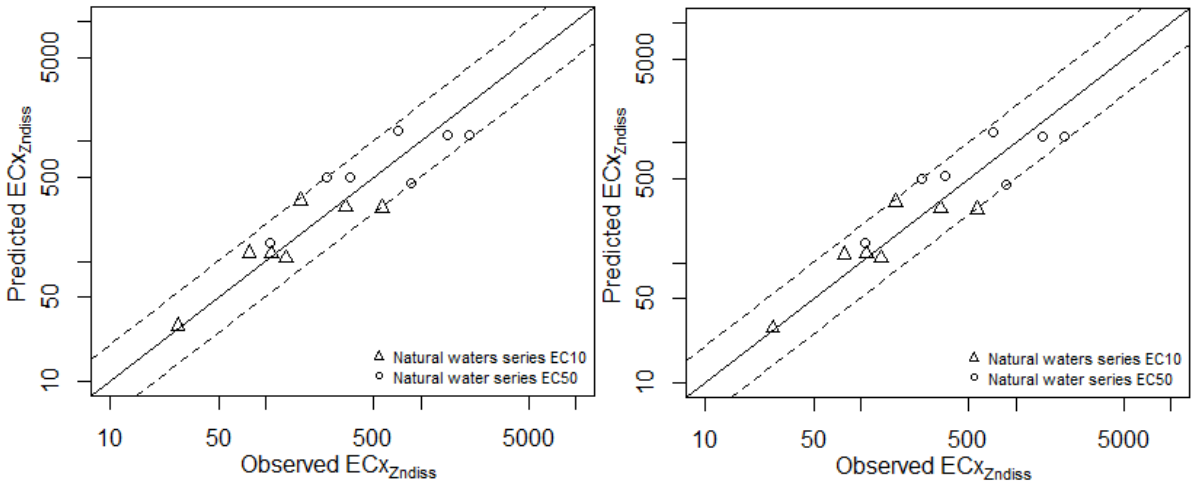

Figure 7.11. Predicted versus observed 50% and 10% effect concentration (ECx_{Zndiss}) for *Pseudokircherniella subcapitata* using Speciation Scenario I (i.e. using the default WHAM VII stability constants for inorganic complexation; left graph) and Speciation Scenario II (i.e. using stability constants for inorganic complexation reported by NIST; right graph). Predictions were made using the chronic Zn Algae bioavailability model linked to WHAM VII (Equation 7.11). The solid line represents a perfect fit between the observed and predicted data, the dashed lines represent a difference of a factor 2 between the observed and predicted data.

Table 7.31 Prediction statistics of the 21d-NOEC$_{Zndiss}$ predicted with the chronic Zn *Daphnia magna* BLM (Equation 7.12) in WHAM V[a] and in WHAM VII using Speciation Scenario I[b] and Speciation Scenario II[c]

	WHAM V		WHAM VII Speciation Scenario I		WHAM VII Speciation Scenario II	
	EC50 data	EC10 data	EC50 data	EC10 data	EC50 data	EC10 data
Mean prediction error	1.59	1.36	1.65	1.42	1.42	1.61
Median prediction error	1.65	1.15	1.71	1.28	1.26	1.53
% predicted within twofold error	100	86	86	86	86	86

[a] Data from De Schamphelaere et al (2005) (see Table 7.1)
[b] Speciation Scenario I: default WHAM VII stability constants for inorganic complexation
[c] Speciation Scenario II: stability constants for inorganic complexation reported by NIST

Validation of the Zn fish BLM in WHAM VII

The intrinsic sensitivities (ECx^*_{Zn2+}) for the Speciation Scenario I and II are reported in Table 7.32. Both speciation scenarios predicted chronic Zn toxicity to *O. mykiss* with better accuracy than predictions using WHAM V (Figure 7.12; Table 7.33). The Speciation Scenario II, using the NIST stability constants for inorganic ligand complexation predicted the ECx$_{Zndiss}$ values more accurate than the Speciation Scenario I and the predictions using WHAM V, certainly for the natural water dataset.

Overall, the Zn fish BLM coupled with WHAM VII predicted Zn toxicity in natural and synthetic waters more accurate than the original Zn fish BLM coupled with WHAM V (Table 7.33).

Table 7.32 Average intrinsic Zn^{2+} sensitivities for Oncorhynchus mykiss (ECx^*_{Zn2+}; calculated using Equation 7.11) under Speciation Scenario I and II

	Synthetic waters (nmol/L)[a]		Natural waters (nmol/L)[b]	
	$EC50^*_{Zn2+}$	$EC10^*_{Zn2+}$	$EC50^*_{Zn2+}$	$EC10^*_{Zn2+}$
Speciation Scenario I[c]	791	234	1557	662
Speciation Scenario II[d]	987	291	1752	689

[a] Data from De Schamphelaere et al (2003); [b] Data from De Schamphelaere et al (2005)
[c] Speciation Scenario I: default WHAM VII stability constants for inorganic complexation
[d] Speciation Scenario II: stability constants for inorganic complexation reported by NIST

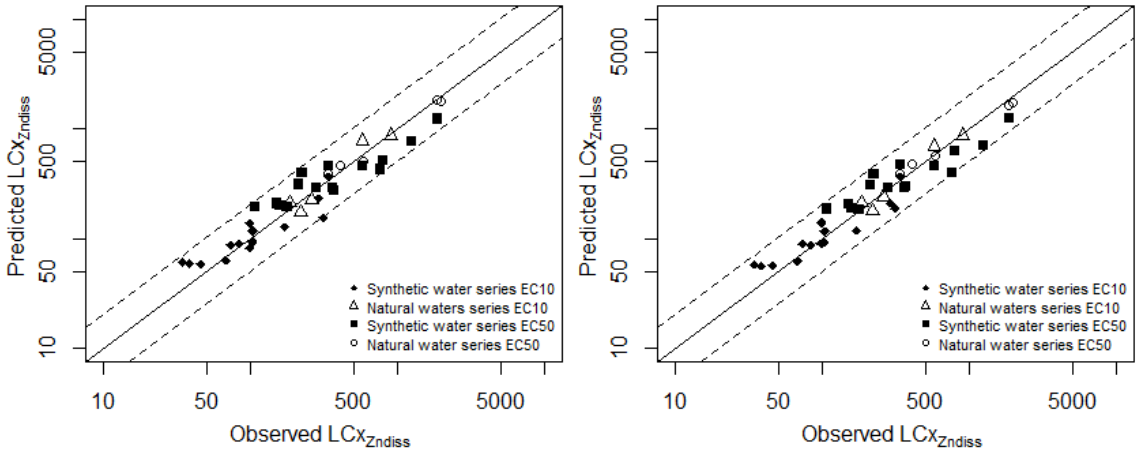

Figure 7.12. Predicted versus observed x% effective concentration (ECx$_{Zndiss}$) for *Oncorhynchus mykiss* using Speciation Scenario I (i.e. using the default WHAM VII stability constants for inorganic complexation; left graph) and Speciation Scenario II (i.e. using stability constants for inorganic complexation reported by NIST; right graph). Predictions were made using the chronic Zn fish BLM linked to WHAM VII (Equation 7.9). The solid line represents a perfect fit between the observed and predicted data, the dashed lines represent a difference of a factor 2 between the observed and predicted data.

Table 7.33 Prediction statistics of the ECx_{Zndiss} predicted with the chronic Zn fish BLM (Equation 7.10) in WHAM V[a,b] and in WHAM VII using Speciation Scenario I[c] and Speciation Scenario II[d]

	WHAM V				WHAM VII Speciation Scenario I				WHAM VII Speciation Scenario II			
	Synthetic waters[a]		Natural waters[b]		Synthetic waters		Natural waters		Synthetic waters		Natural waters	
	LC50 data	LC10 data	LC50 data	LC10 data	LC50 data	LC10 data	LC50 data	LC10 data	LC50 data	LC10 data	LC50 data	LC10 data
Mean prediction error	1.41	1.31	1.43	1.61	1.43	1.32	1.12	1.19	1.40	1.29	1.13	1.14
Median prediction error	1.40	1.27	1.42	1.52	1.38	1.24	1.14	1.16	1.35	1.22	1.14	1.15
% predicted within twofold error	100	100	100	80	100	93	100	100	100	100	100	100

[a] Data from De Schamphelaere et al (2004c and 2005) (see Table 7.1)
[b] Speciation Scenario I: default WHAM VII stability constants for inorganic complexation
[c] Speciation Scenario II: stability constants for inorganic complexation reported by NIST

Validation of the chronic Zn D. magna gBAM in WHAM VII

The intrinsic sensitivities (Qx_{Zn2+}) for the Speciation Scenario I and II are reported in Table 7.34. The prediction statistics for the chronic Zn *D. magna* gBAM for both speciation scenarios are given in Table 7.35. For the EC50 and EC10 data, the Zn toxicity to *D. magna* is as accurately predicted using the gBAM coupled to WHAM VII with Speciation Scenario II compared to the gBAM coupled to WHAM V (Figure 7.13).

Overall, the Zn *D. magna* gBAM coupled with WHAM VII predicted Zn toxicity in natural and synthetic media as accurate as the original Zn *D. magna* gBAM coupled with WHAM V for EC50 data and EC10 data (Table 7.35).

Table 7.34 Average intrinsic Zn^{2+} sensitivities for *Daphnia magna*[a] (Qx_{Zn2+} calculated using Equation 7.15) under Speciation Scenario I and II.

	$Q50_{Zn2+}$[b] KDS+TVR	$Q10_{Zn2+}$[c] KDS+TVR	$Q10_{Zn2+}$[d] KDS+TVR	Heijerick
Speciation Scenario I[e]	-5.55	-5.75	-5.75	-5.59
Speciation Scenario II[f]	-5.13	-5.35	-5.35	-5.34

[a f] Data from Heijerick et al (200b5); De Schamphelaere et al (2005) and Van Regenmortel et al (2017b; Chapter 5)
[c] Q50 was calculated based on the "KDS+TVR" data; [d] Q10 was calculated based on the "KDS + TVR" data
[e] Two separate Q10 values were calculated, one based on the "KDS+TVR" data, and one based on the "Heijerick" data; [e] Speciation Scenario I: default WHAM VII stability constants for inorganic complexation; Speciation Scenario II: stability constants for inorganic complexation reported by NIST

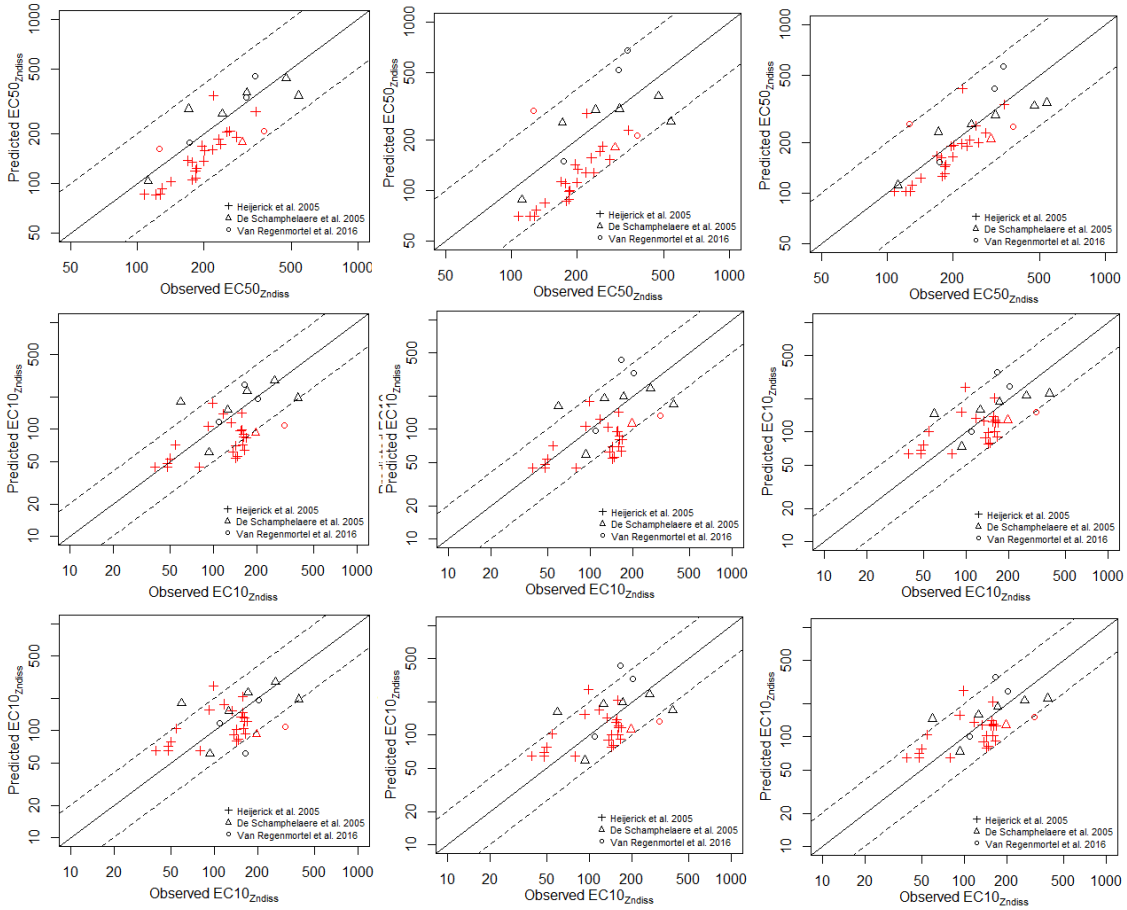

Figure 7.13. Predicted versus observed 50% and 10% effect concentration (ECx_{Zndiss}) for *Daphnia magna* using the gBAM coupled to WHAM V (left graphs); Speciation Scenario I (i.e. using the default WHAM VII stability constants for inorganic complexation; middle graphs) and Speciation Scenario II (i.e. using stability constants for inorganic complexation reported by NIST; right graphs). Predictions were made using the chronic Zn gBAM linked to WHAM V and WHAM VII (Equation 7.13). For the top graphs, the $Q50_{Zn2+}$ was calculated based on the data reported by De Schamphelaere et al (2005) and Van Regenmortel et al (2017b). For the central graphs, the $Q10_{Zn2+}$ was calculated based on the data reported by De Schamphelaere et al (2005) and Van Regenmortel et al (2017b). For the bottom graphs, two $Q10_{Zn2+}$ values were calculated, one based on the data reported by De Schamphelaere et al (2005) and Van Regenmortel et al (2017b) and one based on the data reported by Herijerick et al (2005). The solid line represents a perfect fit between the observed and predicted data, the dashed lines represent a difference of a factor 2 between the observed and predicted data.

Table 7.35 Prediction statistics of the $EC50_{Zndiss}$ and $EC10_{Zndiss}$ predicted with the chronic Zn *Daphnia magna* gBAM (Equation 7.14) in WHAM V[a] and in WHAM VII using Speciation Scenario I[b] and Speciation Scenario II[c]

	WHAM V					
	EC50 data		EC10 data		EC10 data	
	Heijerick	KDS + TVR	Heijerick	KDS + TVR	Heijerick	KDS + TVR
Mean prediction error	1.39	1.32	1.68	1.72	1.52	1.72
Median prediction error	1.38	1.22	1.69	1.52	1.49	1.52
% predicted within twofold error	100	100	68	73	95	73

	WHAM VII Speciation Scenario I					
	EC50 data[d]		EC10 data[e]		EC10 data[f]	
	Heijerick	KDS + TVR	Heijerick	KDS + TVR	Heijerick	KDS + TVR
Mean prediction error	1.67	1.59	1.70	1.81	1.53	1.81
Median prediction error	1.69	1.57	1.71	1.62	1.45	1.62
% predicted within twofold error	91	83	64	64	95	64

	WHAM VII Speciation Scenario II					
	EC50 data[d]		EC10 data[e]		EC10 data[f]	
	Heijerick	KDS + TVR	Heijerick	KDS + TVR	Heijerick	KDS + TVR
Mean prediction error	1.21	1.38	1.51	1.56	1.51	1.56
Median prediction error	1.18	1.39	1.44	1.28	1.44	1.28
% predicted within twofold error	100	92	95	73	95	73

[a] Data from Heijerick et al (2005b), De Schamphelaere et al (2005) and Van Regenmortel et al (2017b; Chapter 5) (see Table 7.1); [b] Speciation Scenario I: default WHAM VII stability constants for inorganic complexation ; [c] Speciation Scenario II: stability constants for inorganic complexation reported by NIST; [d] Q50 was calculated based on the "KDS+TVR" data ; [e] Q10 was calculated based on the "KDS + TVR" data; [f] Two separate Q10 values were calculated, one based on the "KDS+TVR" data, and one based on the "Heijerick" data

Validation of the Zn fish gBAM in WHAM VII

The intrinsic sensitivities (ECx^*_{Zn2+}) for the Speciation Scenario I and II are reported in Table 7.36. Both speciation scenarios predicted chronic Zn toxicity to *O. mykiss* with better accuracy than predictions using WHAM V (Figure 7.14; Table 7.37), especially for synthetic waters. The Zn fish gBAM showed a comparable accuracy compared to the Zn fish BLM (Table 7.37)

Overall, the Zn fish gBAM coupled with WHAM VII predicted Zn toxicity in natural and synthetic waters more accurate than the original Zn fish BLM coupled with WHAM V (Table 7.37).

Table 7.36 Average intrinsic Zn^{2+} sensitivities for Oncorhynchus mykiss (ECx^*_{Zn2+}; calculated using Equation 7.15) under Speciation Scenario I and II

	Synthetic waters (nmol/L)[a]		Natural waters (nmol/L)[b]	
	$LC50^*_{Zn2+}$	$LC10^*_{Zn2+}$	$LC50^*_{Zn2+}$	$LC10^*_{Zn2+}$
Speciation Scenario I[c]	-4.179	-3.554	-3.928	-3.200
Speciation Scenario II[d]	-4.412	-3.777	-4.184	-3.463

[a] Data from De Schamphelaere et al (2003)
[b] Data from De Schamphelaere et al (2005)
[c] Speciation Scenario I: default WHAM VII stability constants for inorganic complexation
[d] Speciation Scenario II: stability constants for inorganic complexation reported by NIST

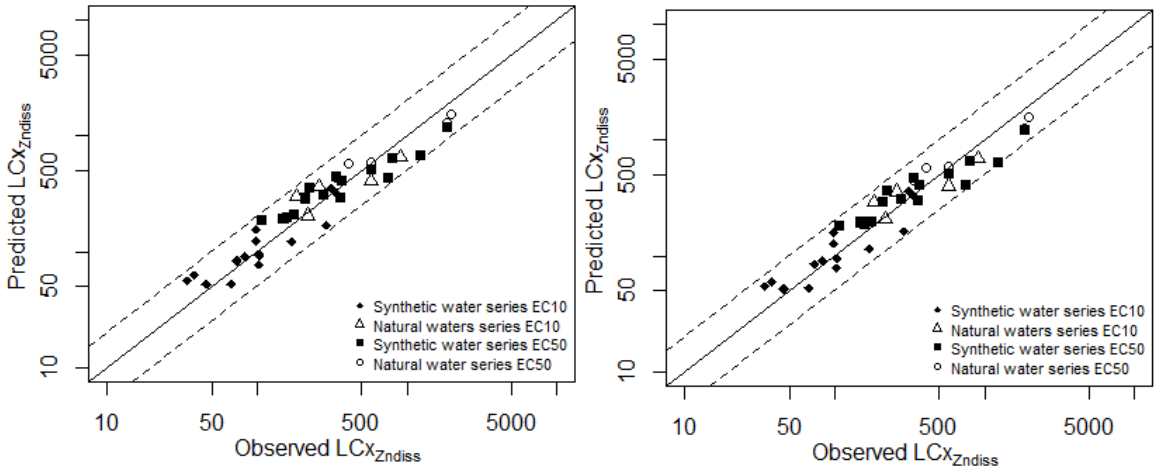

Figure 7.14. Predicted versus observed x% effective concentration (ECx_{Zndiss}) for *Oncorhynchus mykiss* using Speciation Scenario I (i.e. using the default WHAM VII stability constants for inorganic complexation; left graph) and Speciation Scenario II (i.e. using stability constants for inorganic complexation reported by NIST; right graph). Predictions were made using the chronic Zn fish BLM linked to WHAM VII (Equation 7.9). The solid line represents a perfect fit between the observed and predicted data, the dashed lines represent a difference of a factor 2 between the observed and predicted data.

Table 7.37 Prediction statistics of the ECx_{Zndiss} predicted with the chronic Zn fish gBAM (Equation 7.14) in WHAM V[a,b] and in WHAM VII using Speciation Scenario I[c] and Speciation Scenario II[d]

	WHAM V				WHAM VII Speciation Scenario I				WHAM VII Speciation Scenario II			
	Synthetic waters[a]		Natural waters[b]		Synthetic waters		Natural waters		Synthetic waters		Natural waters	
	LC50 data	LC10 data	LC50 data	LC10 data	LC50 data	LC10 data	LC50 data	LC10 data	LC50 data	LC10 data	LC50 data	LC10 data
Mean prediction error	1.37	1.40	1.32	1.30	1.38	1.32	1.29	1.38	1.39	1.32	1.26	1.35
Median prediction error	1.28	1.26	1.32	1.35	1.27	1.27	1.31	1.41	1.34	1.29	1.29	1.39
% predicted within twofold error	90	93	100	100	100	100	100	100	100	100	100	100

[a] Data from De Schamphelaere et al (2004c and 2005) (see Table 7.1)
[b] Speciation Scenario I: default WHAM VII stability constants for inorganic complexation
[c] Speciation Scenario II: stability constants for inorganic complexation reported by NIST

Validation of the read-across to L. stagnalis and B. calyciflorus using the D. magna BLM and gBAM in WHAM VII

For the validation of the read-across of the *D. magna* BLM, the intrinsic sensitivities (ECx^{*}_{Zn2+}) for the Speciation Scenario I and II are reported in Table 7.38 . Both speciation scenarios predicted chronic Zn toxicity to *L. stagnalis* and *B. calyciflorus* with good accuracy (Figure 7.15; Table 7.39), i.e. all ECx_{Zndiss} were predicted within twofold prediction error for *L. stagnalis* and *B. calyciflorus* (with the exception of the EC10 data for B*. calyciflorus* using Speciation Scenario II). The Speciation Scenario II, using the NIST stability constants for inorganic ligand complexation predicted the ECx_{Zndiss} values more accurate than the Speciation Scenario I

For the validation of the *D. magna* gBAM, the intrinsic sensitivities ($Qx^{Zn2+)}$ for the Speciation Scenario I and II are reported in Table 7.38. Both speciation scenarios predicted chronic Zn toxicity to *L. stagnalis* and *B. calyciflorus* with good accuracy (Figure 7.16; Table 7.40), i.e. all ECx_{Zndiss} were predicted within twofold prediction error for *L. stagnalis* and *B. calyciflorus*. Also here, the Speciation Scenario II predicted the ECx_{Zndiss} values more accurate than the Speciation Scenario I

Overall, the prediction performance of the Zn *D. magna* BLM and gBAM coupled with WHAM VII under Speciation Scenario II was relatively comparable with the performance of the original models (Table 7.37).

Table 7.38 Average intrinsic Zn^{2+} sensitivities for *Lymnaea stagnalis* and *Brachionus calyciflorus* (ECx^{*}_{Zn2+} and Qx_{Zn2+}; calculated using Equation 7.11 and 7.15) under Speciation Scenario I and II

	L. stagnalis[a]				*B. calyciflorus*[a]			
	D. magna BLM (nmol/L)		*D. magna* gBAM		*D. magna* BLM (nmol/L)		*D. magna* gBAM	
	$EC50^{*}_{Zn2+}$	$EC10^{*}_{Zn2+}$	$Q50_{Zn2+}$	$Q10_{Zn2+}$	$EC50^{*}_{Zn2+}$	$EC10^{*}_{Zn2+}$	$Q50_{Zn2+}$	$Q10_{Zn2+}$
Speciation Scenario I[b]	1596	979	-4.89	-5.10	720	373	-5.24	-5.53
Speciation Scenario II[c]	2183	1328	-4.48	-4.70	1065	543	-4.80	-5.10

[a] Data from De Schamphelaere & Janssen (2010)
[b] Speciation Scenario I: default WHAM VII stability constants for inorganic complexation
[c] Speciation Scenario II: stability constants for inorganic complexation reported by NIST

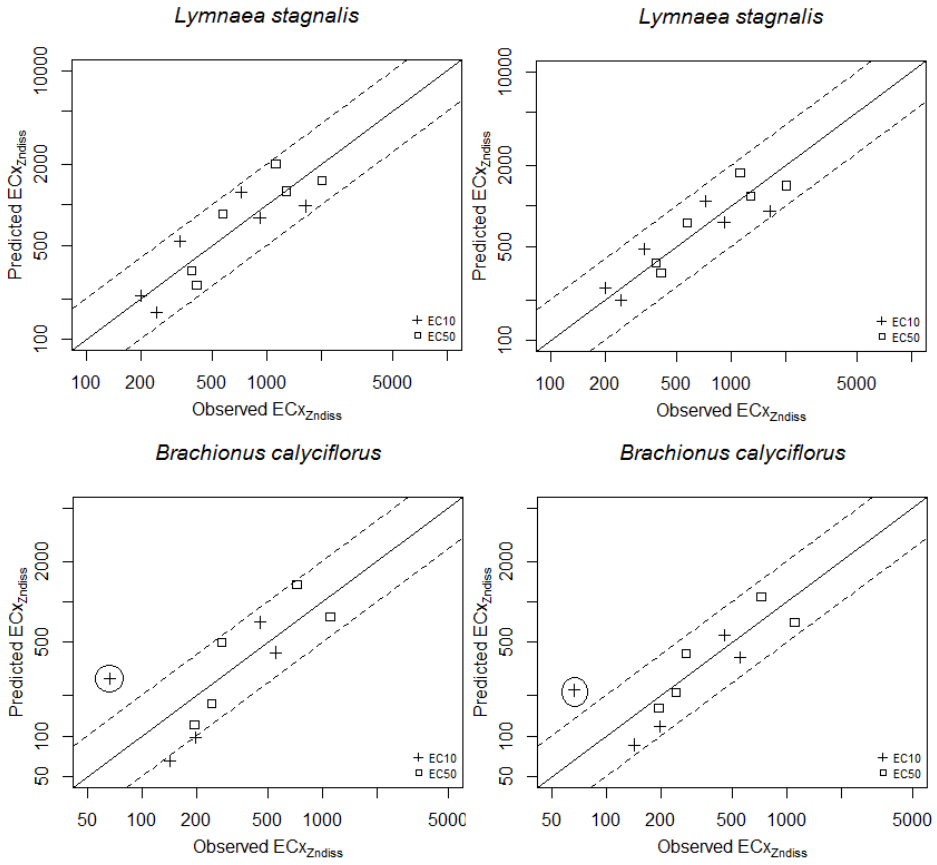

Figure 7.15. Predicted versus observed x% effective concentration (ECx_{Zndiss}) for *Lymnaea stagnalis* and *Brachionus calyciflorus* using Speciation Scenario I (i.e. using the default WHAM VII stability constants for inorganic complexation; left graph) and Speciation Scenario II (i.e. using stability constants for inorganic complexation reported by NIST; right graph). Predictions were made using the chronic Zn *D. magna* BLM linked to WHAM VII (Equations 7.9 and 7.13). The solid line represents a perfect fit between the observed and predicted data, the dashed lines represent a difference of a factor 2 between the observed and predicted data. For *B. calyciflorus*, the encircled EC10 is considered unreliable (see De Schamphelaere & Janssen, 2010).

Table 7.39 Prediction statistics of the ECx_{Zndiss} predicted with the chronic Zn *D. magna* BLM (Equation 7.10) in WHAM V and in WHAM VII using Speciation Scenario I[a] and Speciation Scenario II[b]

	WHAM V				WHAM VII Speciation Scenario I[a]				WHAM VII Speciation Scenario II[b]			
	L. stagnalis[c]		*B. calyciflorus*[c]		*L. stagnalis*		*B. calyciflorus*		*L. stagnalis*		*B. calyciflorus*	
	EC50 data	EC10 data	EC50 data	EC10 data	EC50 data	EC10 data	EC50 data	EC10 data	EC50 data	EC10 data	EC50 data	EC10 data
Mean prediction error	1.25	1.34	1.33	1.29	1.41	1.46	1.62	1.77	1.29	1.40	1.39	1.77
Median prediction error	1.30	1.37	1.38	1.23	1.42	1.58	1.59	1.80	1.30	1.34	1.49	1.88
% predicted within twofold error	100	100	100	100	100	100	100	50	100	100	100	100

[a] Speciation Scenario I: default WHAM VII stability constants for inorganic complexation; [b] Speciation Scenario II: stability constants for inorganic complexation reported by NIST; [c] Data from De Schamphelaere and Janssen (2010) (see Table 7.1)

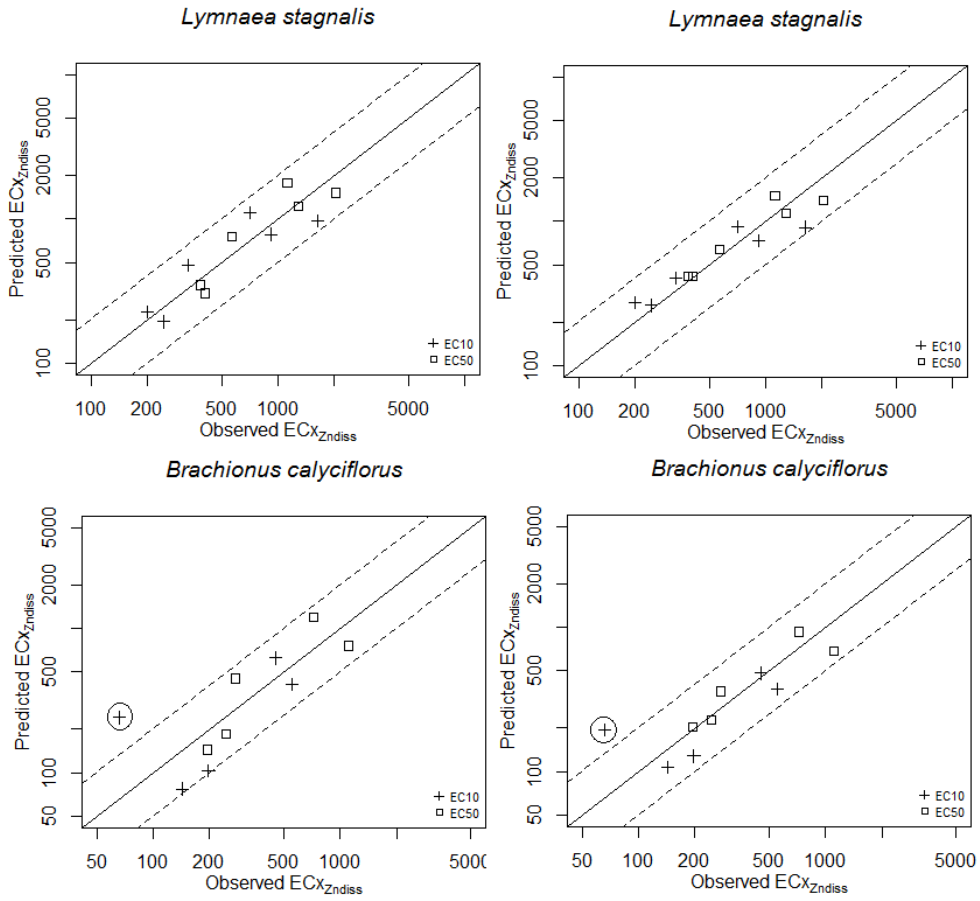

Figure 7.16. Predicted versus observed x% effective concentration (ECx_{Zndiss}) for *Lymnaea stagnalis* and *Brachionus calyciflorus* using Speciation Scenario I (i.e. using the default WHAM VII stability constants for inorganic complexation; left graph) and Speciation Scenario II (i.e. using stability constants for inorganic complexation reported by NIST; right graph). Predictions were made using the chronic Zn *D. magna* gBAM linked to WHAM VII (Equation 7.14). The solid line represents a perfect fit between the observed and predicted data, the dashed lines represent a difference of a factor 2 between the observed and predicted data. For *B. calyciflorus*, the encircled EC10 is considered unreliable (see De Schamphelaere & Janssen, 2010).

Table 7.40 Prediction statistics of the ECx_{Zndiss} predicted with the chronic Zn *D. magna* gBAM (7.14) in WHAM V and in WHAM VII using Speciation Scenario I[a] and Speciation Scenario II[b]

	WHAM V				WHAM VII Speciation Scenario I[a]				WHAM VII Speciation Scenario II[b]			
	L. stagnalis[c]		*B. calyciflorus*[c]		*L. stagnalis*		*B. calyciflorus*		*L. stagnalis*		*B. calyciflorus*	
	EC50 data	EC10 data	EC50 data	EC10 data	EC50 data	EC10 data	EC50 data	EC10 data	EC50 data	EC10 data	EC50 data	EC10 data
Mean prediction error	1.16	1.24	1.18	1.22	1.29	1.37	1.49	1.62	1.19	1.33	1.26	1.35
Median prediction error	1.13	1.14	1.16	1.22	1.33	1.35	1.45	1.61	1.12	1.27	1.30	1.40
% predicted within twofold error	100	100	100	100	100	100	100	100	100	100	100	100

[a] Speciation Scenario I: default WHAM VII stability constants for inorganic complexation; [b] Speciation Scenario II: stability constants for inorganic complexation reported by NIST; [c] Data from De Schamphelaere and Janssen (2010) (see Table 7.1)

7.4. Discussion

A bioavailability model is in general accepted to be sufficiently accurate and applicable in risk assessment when the majority of $EC50_{Mediss}$ is predicted within twofold error (Di Toro et al. 2001; Santore et al. 2001; De Schamphelaere and Janssen, 2004b; De Schamphelaere and Janssen, 2008; De Schamphelaere and Janssen, 2005). Often, the predictive capacity of these models is only examined based on high % effect concentrations (e.g. 50%) (Di Toro et al. 2001; Santore et al. 2001; Van Regenmortel et al. 2015; De Schamphelaere and Janssen, 2008; Deleebeeck et al. 2007) to conclude whether a model is applicable. This can be attributed to the fact that EC50 data are usually calculated with higher precision (i.e. smaller % confidence interval) than for example EC10 data. However, these bioavailability models are in risk assessment not only applied for EC50 data but also for EC10 data (see Van Regenmortel et al. 2015; Chapter). Therefore, in this Chapter, we not only examined whether the bioavailability models calibrated on metal speciation with WHAM VII were accurate for predicting EC50 data but also for predicting EC10 (or NOEC) data.

For Cu, most bioavailability models performed well when the models were calibrated on metal speciation with WHAM VII. An exception was the performance of the *D. magna* BLM. For natural waters, only 10% and 30% of the EC50 data and 20% of the NOEC data was predicted within twofold prediction error using the Cu *D. magna* BLM with Speciation Scenario I and II, respectively (Table 7.7). In comparison, 80% of the EC50 data and 70% of the NOEC data for the natural waters was predicted within twofold error using WHAM V. When comparing the Cu^{2+} activity from WHAM V and WHAM VII, we see a bias toward higher calculated Cu^{2+} activity by WHAM VII for a high number of test waters (Figure 7.17), while a lower number of test waters do show similar Cu^{2+} activities when calculated with WHAM V and WHAM VII. When examining the differences in physico-chemistry between these two groups of test waters, we see a significant difference in pH, while there is no significant difference in DOC concentration or Ca concentration (Figure 7.18). Apparently, for test waters with a pH > 7, Cu^{2+} activity calculated using WHAM VII is higher compared to WHAM V, while for waters with pH < 7 Cu^{2+} activity calculated using WHAM VII and WHAM V are similar. Certain differences between the two speciation software's, such

as differences in organic complexation constants, are most likely the reason for the large difference in predictive capacity between WHAM V and VII. However, more research should be conducted by comparing both speciation software's to pinpoint the differences that lead to the differences in calculated Cu^{2+} activities.

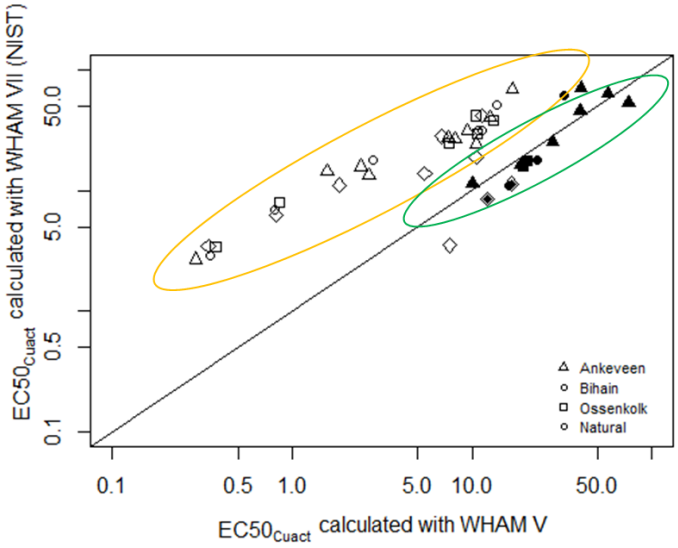

Figure 7.17. Observed 50% effective concentration expressed as Cu^{2+} activity ($EC50_{Cuact}$) for *Daphnia magna* calculated using the speciation software WHAM V and WHAM VII. The solid line represents a perfect correspondence between the calculated Cu2+ activities for both models. The orange oval groups data for which Cu2+ activity calculated using WHAM VII is higher compared to WHAM V, the green oval groups data for which Cu2+ activity calculated using WHAM VII and WHAM V is comparable. Empty symbols = test waters with pH > 7, filled symbols = test waters with pH < 7.

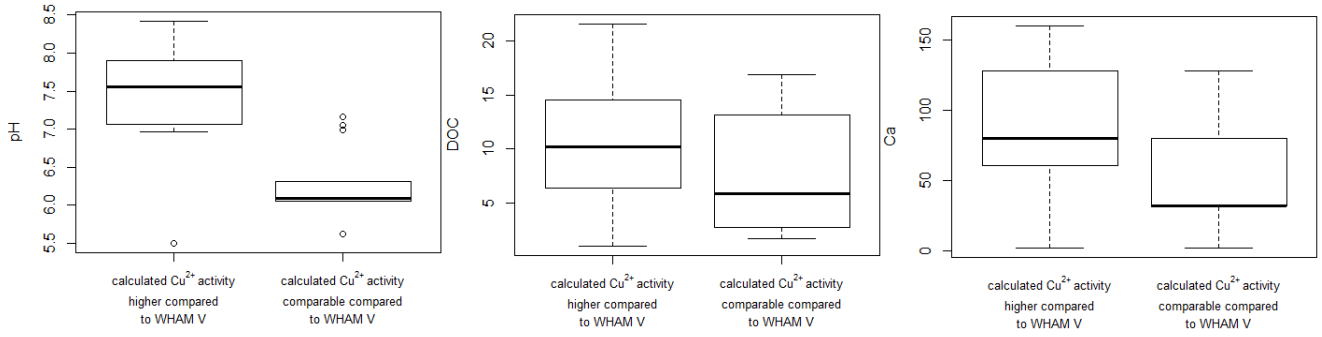

Figure 7.18. Differences in physico-chemical parameters (i.e. pH, DOC and Ca concentration) for waters for which Cu^{2+} activity is higher when calculated by WHAM VII then WHAM V (orange circle in Figure 7.17) and for waters for which the calculated Cu^{2+} activity is comparable between WHAM VII and WHAM V (green circle in Figure 7.17).

Although for *D. magna* the Cu BLM calibrated on metal speciation calculated with WHAM VII did not perform well, the Cu gBAM calibrated on WHAM VII did perform relatively well. The predictive performance in WHAM VII approached that reported in the original publication (Van Regenmortel et al. 2015; Table 7.13). However, to correctly compare the performance of the Cu BLM to that of the Cu gBAM calibrated on WHAM VII, the comparison should be based on the same data, which can be done by comparing Table 7.9 with Table 7.13. Based on these results, it is clear that the Cu gBAM is not only more accurate than the Cu BLM in predicting Cu toxicity to different clones of *D. magna* when coupled

to WHAM V (Van Regenmortel et al. 2015), but that it is also more accurate than the Cu BLM when calibrated to WHAM VII.

For freshwater green microalgae, the Cu bioavailability model performed relatively well when the model was calibrated on metal speciation calculated with WHAM VII, i.e. the majority of the data was predicted within twofold error. The prediction performance in WHAM VII approached that reported in the original publication (De Schamphelaere and Janssen, 2006; Heijerick et al. 2005 Table 7.8).

For the cross-phylum comparison (read-across) of the *D. magna* BLM and gBAM coupled to WHAM VII for *B. calyciflorus*, also here, the *D. magna* BLM did not perform well calibrated on metal speciation calculated with WHAM VII (Table 7.15). However, the Cu gBAM did perform well, i.e. 100% of the data within twofold prediction error and similar mean prediction error compared to that reported in the original publication (De Schamphelaere and Janssen, 2006c).

Lofts and Tipping (2011) reported for WHAM VII that the agreement between observation and prediction for free copper was relatively good at high free copper (> 10^{-12} M) concentrations. The free copper within the test waters considered here and of relevance for ecotoxicity was always above 10^{-12} M, which confirms the results by Lofts and Tipping (with the exception of the *D. magna* BLM), also when WHAM VII is used with adapted inorganic complexation constants (Speciation Scenario II).

For Ni, overall, the chronic bioavailability models performed well when models were calibrated on metal speciation calculated with WHAM VII. For the *D. magna*, algae and fish bioavailability models, the predictive performance in WHAM VII approached or was slightly better than those reported in the original publications (Deleebeeck et al. 2007, 2008, 2009, De Schamphelaere et al. 2006; Schlekat et al. 2010). For the *C. dubia* bioavailability model and the read-across of the *D. magna* bioavailability model to *L. stagnalis*, the performance in WHAM VII showed comparable accuracy to WHAM VI for the EC50 data. Lofts and Tipping (2011) also reported that WHAM VII (using the default inorganic complexation constants) predicted free Ni^{2+} activity in natural waters relatively accurate (i.e. 43 of 54 observations within one order of magnitude). These authors found that WHAM VII (using the default inorganic complexation constants) was a good predictor of Ni^{2+} activity at high Ni concentrations (> 10^{-8}), but overestimation of observed Ni^{2+} activity was greater at lower Ni concentrations. The free copper within our test waters was always above 10^{-12} M, which confirms the results by Lofts and Tipping), also when WHAM VII is used with adapted inorganic complexation constants (Speciation Scenario II).

For Zn, the chronic bioavailability models performed well when models were calibrated on metal speciation calculated with WHAM VII. For the *D. magna* BLM and gBAM, the algae bioavailability model and the fish BLM and gBAM, the predictive performance in WHAM VII approached or was better than those reported in the original publications (De Schamphelaere et al. 2005, De Schamphelaere et al. 2003, Van Regenmortel et al. 2017b).

Although both models are accurate in their predictive capacity based on the data for which they were developed and validated, a correct comparison between the performance of the Daphnia Zn BLM to that of the Zn gBAM calibrated on WHAM VII should be based on the same data, which can be done by comparing Table 7.29 with Table 7.34. Based on these results, it is clear that the Zn gBAM is more

accurate than the Zn BLM when calibrated to WHAM VII. When comparing the fish Zn BLM to that of the Zn gBAM (Table 7.33 and 7.37), we see that although the predictive performance is comparable, the also here Zn gBAM is more accurate than the Zn BLM.
For the read-across of the *D. magna* BLM and gBAM to *L. stagnalis* and *B. calyciflorus*, the performance in WHAM VII was also more accurate than WHAM V. Lofts and Tipping (2011) also reported that WHAM VII (using the default inorganic complexation constants) predicted free Zn^{2+} activity in natural waters relatively accurate (i.e. 72 of 84 observations within one order of magnitude). Our results confirm the results by Lofts and Tipping), also when WHAM VII is used with adapted inorganic complexation constants (Speciation Scenario II).
The identity of the inorganic complexation thermodynamic database impacted the predictive performance of the chronic Ni and Zn bioavailability models. The predictive performance of these models was in general better when the stability constants for inorganic complexation reported by NIST were applied (i.e. Speciation Scenario II). The predictive capacity of the Cu bioavailability models were less impacted.

7.5. Conclusion

For Cu, the bioavailability models performed well when the models were calibrated on metal speciation with WHAM VII, with the exception of the *D. magna* BLM for Cu. However, we have shown that the *D. magna* gBAM is a valuable and in some cases even better alternative for the BLM and that it can be used in combination with WHAM VII to accurately predict Cu toxicity to *D. magna*. Therefore, in the next Chapters in this PhD, the gBAM and not the BLM coupled to WHAM VII will be used for calculations. Because we have shown that the bioavailability models for Cu are accurate in predicting Cu toxicity when coupled to WHAM VII, we can safely assume that the fish gBAM can also be used in combination with WHAM VII to accurately predict Cu toxicity.
For Ni and Zn, overall, the chronic bioavailability models performed well when models were calibrated on metal speciation calculated with WHAM VII. In addition, we have shown that Zn toxicity to *Daphnia* and fish is best predicted using the gBAMs instead of the BLMs coupled to WHAM VII. Therefore, in future Chapters in this PhD, the gBAMs and not the BLMs coupled to WHAM VII will be used for calculations.

Overall, our results show that WHAM VII with an assumption of 65% AFA can be used as a speciation model to predict metal toxicity to different species with sufficient accuracy. In addition, the stability constants for inorganic complexation reported by NIST (Speciation Scenario II) describe the metal toxicity more accurately than the default WHAM VII inorganic stability constants.

Eight

RISK ASSESSMENT OF MIXTURES OF Cu, Zn AND Ni: THE INFLUENCE OF COMPETITION FOR DOC BINDING SITES

8. RISK ASSESSMENT OF MIXTURES OF CU, ZN AND NI: THE INFLUENCE OF COMPETITION FOR DOC BINDING SITES

8.1. Introduction

In Chapter 6, four mixture risk assessment methodologies were compared for risk estimations of mixtures of copper, zinc and nickel. Instead of using the originally published bioavailability models to normalize the toxicity data, as was done in Chapter 2, the toxicity data for Cu and Zn for invertebrates and fish were normalized with the gBAMs developed in Chapter 5. We showed that this adaptation had a small influence on msPAF values and on the % of target water samples that were predicted to be affected by the mixture of Cu, Zn and Ni or by the individual metals. However, it had a considerable influence on HC5 values. Because the predictive capacity of the gBAMs is in general higher than that of the BLMs (Chapter 5), we recommended the use of the newly developed gBAMs to normalize toxicity data for Cu and Zn. Therefore, in this chapter, we will follow this recommendation and only use gBAMs when normalizing toxicity data.

The above mentioned calculations were based on bioavailability-normalized dissolved metal concentrations. As acknowledged in Chapter 7, it is important to consider that metals can compete with each other for binding sites of Dissolved Organic Carbon (DOC) when present in mixtures. Therefore, assessing risk based on dissolved concentrations not accounting for competition, may lead to some underestimation of metal mixture risks, which is why these risks should in principle be evaluated on the basis of free ion activity. However, an evaluation based on free ion activities was previously limited due to the use of different speciation programs and different speciation assumptions regarding DOC 'activity' for the different individual metals. This limitation was tackled in Chapter 7, in which we evaluated the predictive performance of the bioavailability models coupled with a single speciation software (i.e. Windermere Humic Aqueous Model (WHAM) VII) and with a single speciation assumption regarding DOC 'activity' (i.e. 65% active fulvic acid (AFA)). We concluded in Chapter 7 that the gBAMs coupled with the software WHAM VII with the assumption of 65% AFA can be used to predict single metal toxicity to different species with reasonable accuracy.

In the present chapter, our aim was to evaluate the risks of mixtures of Cu, Zn and Ni by taking into account the competition between metals for DOC binding sites. This was done by implementing the four mixture risk assessment methodologies as described in Chapter 2, in combination with the gBAMs developed in Chapter 5 and in combination with the use of a single speciation software to calculate free ion activities, as described in Chapter 7. As such, we were able to compare 2 different methodologies in which the calculations were based on free metal ion activities: (1) In Scenario C, the monitoring data (dissolved) was converted to free ion activity separately for each individual metal. As such, we take into account the speciation of the metals, but we assume there is no competition between metals for DOC binding sites. (2) In Scenario D, the monitoring data (dissolved) was converted to free ion activity simultaneously for all metals. In this case, we do account for the competition between the metals for DOC binding sites.

Our research question was the following: Is the calculated risk of metal mixtures higher with Scenario D (competition) compared to Scenario C (no competition)? We hypothesize that this would indeed be the case, as competition between metals for DOC binding sites is taken into account in Scenario D.

8.2. Material and Methods

Normalisation tools

In Chapter 6, normalizations for Zn and Cu were performed using BLM software (HydroQual 2015) that incorporates WHAM V (Tipping 1994), and normalizations for Ni were performed using the chronic Ni bioavailability and normalization tool (Nys et al. 2014), which incorporates the WHAM Model VI (Tipping 1998).

In this chapter, all normalisations were performed using WHAM Model VII (Tipping et al. 2011). For this, the chronic Ni bioavailability and normalization tool developed by Nys et al. (2016) was adapted to incorporate the WHAM VII speciation software instead of the WHAM VI speciation software. In addition, all intrinsic sensitivities of the species for which toxicity data is present in the tool were recalibrated in WHAM VII. Finally, the S_{pH} parameters of the bioavailability models that are incorporated in the tool were updated to those reported in Chapter 7, where they were recalibrated in WHAM VII.

The adapted Ni tool (an excel file) that incorporated WHAM VII was used as a template to develop similar tools for Cu and Zn. For this, the Cu and Zn toxicity databases were imported into two separate files (i.e. two separate tools). In addition, the bioavailability models for algae and gBAMs for invertebrates and fish were incorporated into the tool. All intrinsic sensitivities of the species in the Cu and Zn toxicity databases were recalibrated in WHAM VII and S_{pH} parameters of the bioavailability models for Cu and Zn were updated to those reported in Chapter 7, where they were recalibrated in WHAM VII.

Speciation calculations

An overview of the different steps is given in Figure 8.1. First, for each individual metal, the dissolved EC10 and EC50 values in the chronic toxicity databases were converted to free metal ion activities using WHAM VII. The concentrations of other metals possibly present in test media (e.g. Zn, Cd, Co, Ni) were not taken into account and were thus assumed to be zero, because no information on this is available in the toxicity databases (with the exception of a few data points in the Ni toxicity database). These EC10 and EC50 values expressed as free metal activity were then used to calculate slope values of the ‘activity”-dose-response curves using the log-logistic function (as in Chapter 2).

Second, the EC10 values in the toxicity databases were normalized to the target water samples in the monitoring databases using the adapted bioavailability and normalization tools for Cu, Zn and Ni that incorporate WHAM VII speciation software. The normalized EC10 values (dissolved) were then converted to free metal ion activities. Also here, the concentrations of other metals possibly present in test media (e.g. Zn, Cd, Co, Ni) were not taken into account. The EC10s expressed as free metal ion activity were used to fit an ‘activity-SSD’ (log-normal) and this allowed sampling 20000 hypothetical species and subsequent analysis as before (Chapter 2).

Third, the monitoring data (dissolved) for each metal was converted to the corresponding free metal ion activity. This was done in two ways: (1) the metal concentrations (dissolved) in the monitoring databases

were converted separately for each individual metal and thus competition between metals for DOC binding sites was not taken into account (i.e., “no competition calculations”; Scenario C) and (2) the metal concentrations (dissolved) in the monitoring databases were converted simultaneously for all metals, to allow for competition between the metals for DOC sites (i.e. “competition calculations”; Scenario D). To recapitulate, in Scenario A, the metal concentrations in the monitoring databases were given in dissolved concentrations and all original bioavailability models were used for the normalization procedures (Figure 8.1). In Scenario B, the metal concentrations in the monitoring databases were also given in dissolved concentrations and the newly developed gBAMs for *D. magna* and fish for Cu and Zn (Chapter 5) in combination with the original bioavailability models for Ni and for Cu and Zn for algae (i.e. gBAMs for all metals and species) were used for the normalization procedures (Figure 8.1).

Toxic pressure (msPAF) calculations

As in Chapter 6, the toxic pressure of the metal mixture for the different target water samples within the monitoring databases was calculated with 4 different methods. The R code used to apply these methods was the same as was applied in Chapter 6. The only difference was that the metal concentrations were now not given in dissolved concentrations but in free ion activities. In addition, the toxic pressure (expressed as msPAF) was calculated in two ways, specified below for the CA_{DRC} method, but applied to all methods.

Scenario C: $msPAF_{act,no\text{-}comp}$ is the fraction of species that had a $SumTU_{EC10,act}$ larger than 1 where

$$SumTU_{EC10,\mathrm{act}} = \sum \frac{[c_{i,act,no-comp}]}{EC10_{i,act}} \quad (8.1)$$

Scenario D: $msPAF_{act,comp}$ is the fraction of species that had a $SumTU_{EC10,act}$ larger than 1 where

$$SumTU_{EC10,\mathrm{act}} \sum \frac{[c_{i,act,comp}]}{EC10_{i,act}} \quad (8.2)$$

To recapitulate, for Scenario B which was evaluated in Chapter 6, the toxic pressure (expressed as $msPAF_{diss,no\text{-}comp}$) was calculated by calculating the fraction of species that had a $SumTU_{EC10,jdiss}$ larger than 1 where

$$SumTU_{EC10,\mathrm{diss}} = \sum \frac{[c_{i,diss,no-comp}]}{EC10_{i,diss}} \quad (8.3)$$

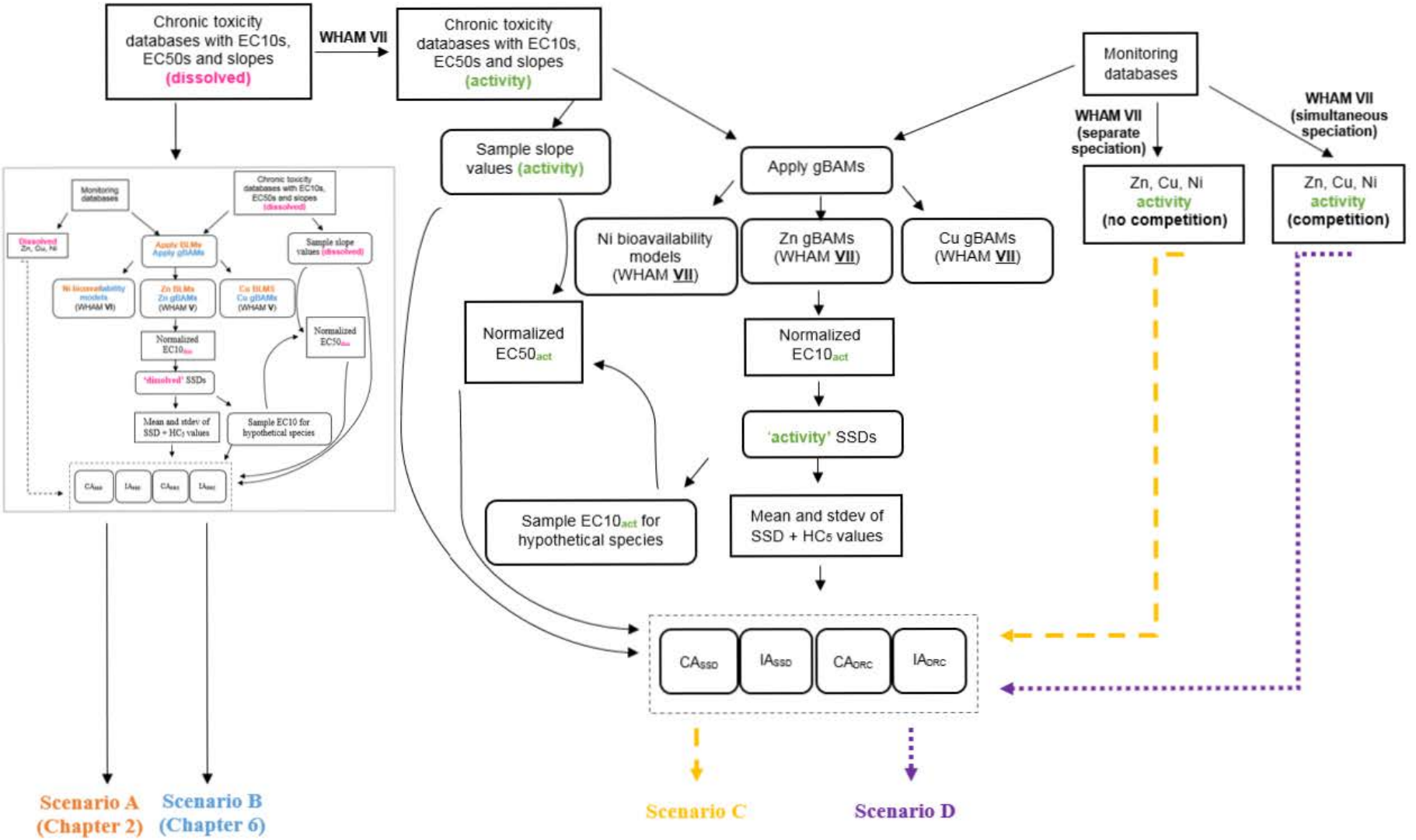

Figure 8.1 Overview of the methodology used for the calculations in (1) Scenario C, for which the monitoring data was converted to free ion activities by not taking into account competition between metals for DOC binding sites (light orange) and (2) Scenario D, for which the monitoring data was converted to free ion activities by taking into account competition between metals for DOC binding sites (purple). For both Scenario C and D the chronic toxicity data in the toxicity databases (EC10, EC50 and slope values) was converted to free ion activities. Scenario A (Chapter 2) and Scenario B (Chapter 6) are also indicated on the figure (see Figure 6.1 for more detail).

8.3. Results and Discussion

Toxic pressure calculations

Table 8.1 shows the distribution of toxic pressure (expressed as msPAF values) for all 4 methods for the different monitoring datasets, when calculations were performed with Scenario C and D.

We hypothesized that the calculated risk of metal mixtures would be higher when calculations were performed based on simultaneously calculated free metal ion activities (Scenario D) compared to calculations based on separately calculated free metal ion activities (Scenario C), as competition between metals for DOC binding sites is taken into account in the former.

However, when comparing Scenario C to Scenario D (Table 8.1), we can see that the msPAF values and the % target water samples affected are similar when metal activities in the monitoring databases are calculated accounting for competition (Scenario D) and not accounting for competition (Scenario C). This similarity is a result of the small difference in metal activity when the monitoring data is converted to activities using Scenario C and D (Figure 8.2). An average increase in metal activity (nM) for the metals in the monitoring databases between Scenario C and D of 23%, 1.8% and 1.1% for Cu, Zn and Ni was observed, respectively. At environmental relevant metal concentrations, the ratio $\{Me^{2+}_{comp}\}$ /$\{Me^{2+}_{no-comp}\}$ for Ni and Zn is approximately 1. For these metals, the amount of free ion is therefore similar when competition for DOC is not taken into account (Scenario D) and when competition is taken into account (Scenario C), which is explained by the low affinity of these metals for DOC (Tipping et al. 2011). For Cu however, the ratio $\{Me^{2+}_{comp}\}$ /$\{Me^{2+}_{no-comp}\}$ is higher than 1, which means that the amount of free ion is higher when competition between metals for DOC is taken into account (Scenario D). When Cu does not have to compete for binding to DOC, a large amount of Cu is bound to DOC due to the high affinity for Cu to DOC (Tipping et al. 2011). When Cu does have to compete for DOC, less Cu can bind to DOC due to the presence of Ni and Zn leading to a higher value of $\{Cu^{2+}_{comp}\}$ and therefore of the ratio $\{Cu^{2+}_{comp}\}$ /$\{Cu^{2+}_{no-comp}\}$ (Figure 8.3). Although the ratio $\{Cu^{2+}_{comp}\}$ /$\{Cu^{2+}_{no-comp}\}$ is above one, due to the fact that the environmental Cu concentrations are low and the contribution of Cu to the mixture is small compared to that of Ni and Zn, the increase in {Cu^{2+}} when taken into account the competition between the metals for DOC does in this case not lead to an increase of the average msPAF to above 0.05 and therefore does not lead to an increase of the % of target water samples affected.

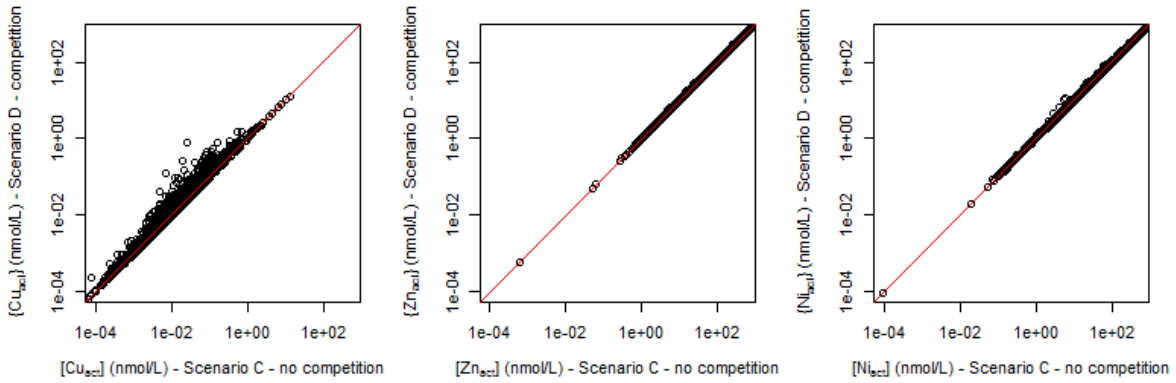

Figure 8.2 Metal concentrations in all monitoring databases expressed as free metal ion activity (nM) for the different metals when speciation is calculated not accounting for competition (Scenario C) and accounting for competition (Scenario D).

Table 8.1 Toxic pressure expressed as multisubstance potentially affected fraction of species (msPAF) for the Dommel, Flanders (VMM), Rhine, Austria, and FOREGS monitoring databases obtained with the different methods. For every result: values on the far left are a result from calculations where monitoring data is given in dissolved concentrations (Scenario B); values in the middle are a result from calculations where monitoring data were converted to activities non-simultaneously (Scenario C) and values on the far right are a result from calculations where monitoring data were converted to activities simultaneously (Scenario D)

	Dommel				VMM				Rhine			
	CA_{SSD}	CA_{DRC}	IA_{SSD}	IA_{DRC}	CA_{SSD}	CA_{DRC}	IA_{SSD}	IA_{DRC}	CA_{SSD}	CA_{DRC}	IA_{SSD}	IA_{DRC}
median msPAF	0.063/ 0.093/ 0.096	0.042/ 0.078/ 0.082	0.028/ 0.059/ 0.061	0.031/ 0.077/ 0.082	0.008/ 0.027/ 0.031	0.004/ 0.020/ 0.021	0.002/ 0.015/ 0.017	0.003/ 0.022/ 0.023	0.004/ 0.004/ 0.005	0.001/ 0.002/ 0.002	0.001/ 0.001/ 0.001	0.001/ 0.003/ 0.003
% Target water samples affected (msPAF > 0.05)	55/66/67	47/60/61	41/54/55	42/61/62	27/37/38	25/31/32	21/37/38	23/32/32	0/0/0	0/0/0	0/0/0	0/0/0
% Target water samples affected by mixture of metals and not by any individual metals	17/19/19	10/12/13	3/6/7	4/13/14	8/11/11	6/5/5	2/1/1	4/5/5	0/0/0	0/0/0	0/0/0	0/0/0
MoS provided by the CA_{SSD} approach	NA	1.23/ 1.18/ 1.18	1.53/ 1.37/ 1.37	1.45/ 1.14/ 1.14	NA	1.16/ 1.11/ 1.12	1.59/ 1.35/ 1.35	1.42/ 1.13/ 1.13	NA	1.22/ 1.20/ 1.19	1.76/ 1.46/ 1.46	1.64/ 1.12/ 1.12

	Austria				FOREGS			
	CA_{SSD}	CA_{DRC}	IA_{SSD}	IA_{DRC}	CA_{SSD}	CA_{DRC}	IA_{SSD}	IA_{DRC}
median msPAF	0.003/ 0.002/0.002	0.001/ 0.001/0.001	0.001/ 0.000/0.000	0.001/ 0.001/0.001	0.003/ 0.006/0.006	0.001/ 0.003/0.003	0.001 0.002/0.003	0.001/ 0.004/0.005
% Target water samples affected (msPAF > 0.05)	7/5/6	6/5/5	5/4/4	5/5/5	9/9/10	6/7/7	4/5/6	4/7/8
% Target water samples affected by mixture of metals and not by any individual metals	3/1/2	1/0.5/0.6	0.2/0.2/0.2	0.4/1/1	5/4/4	2/2/2	0.3/0.5/0.8	0.4/2/2
MoS provided by the CA_{SSD} approach	NA	1.20/1.19/1.19	1.55/1.39/1.39	1.48/1.12/1.12	NA	1.21/1.17/1.17	1.56/1.37/1.38	1.46/1.12/1.12

CA = Concentration Addition, IA = Independent Action, SSD = Species Sensitivity Distribution, DRC = Dose-Response Curve, msPAF = multisubstance Potentially Affected Fraction of species, MoS = Margin of Safety, NA = Not Applicable

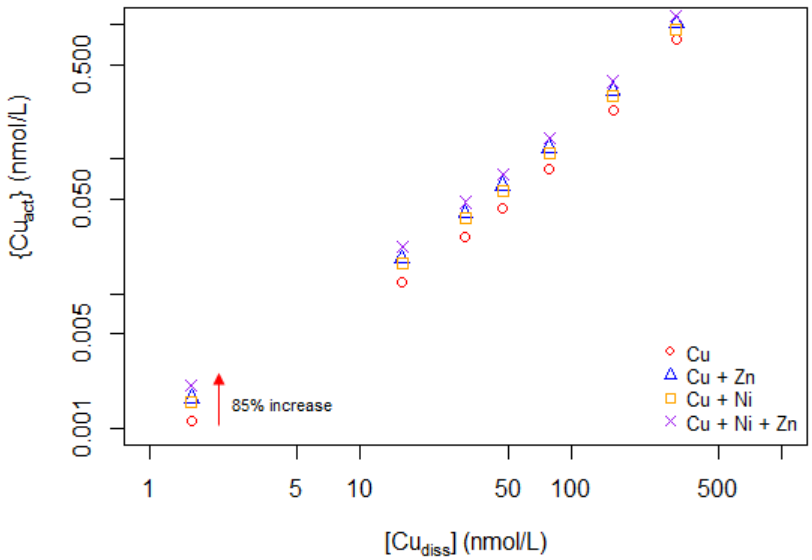

Figure 8.3 Change in free Cu activity (nmol/L) with increasing dissolved Cu concentration (nmol/L) when Cu is present alone (red circles), in a mixture with Zn (blue triangles), in a mixture with Ni (orange squares) and in a mixture with Ni and Zn (purple crosses), for an average water in the VMM database with pH 7.3, Ca concentration 43 mg/L and DOC concentration 5.5 mg/L. An increase in free Cu activity of 85% between the Cu-single and the Cu-Ni-Zn mixture is observed.

Our hypothesis concerning the influence of taking into account competition between metals for DOC binding sites is refuted, as no difference between Scenario C and D was observed. However, another unexpected observation can be made by comparing Scenario C with Scenario B, in which the metal concentrations were given as dissolved concentrations (Chapter 6). One would expect that the results of these two scenario's would be similar, as both do not take into account the competition between metals for DOC binding sites. However, when comparing Scenario B to Scenario C (Table 8.1), we can observe that there is a difference in msPAF values, which was beyond our expectation. The msPAF values calculated using Scenario C can be both higher and lower than those of Scenario B.

For the VMM database, the msPAF values and % target water samples increased when speciation of the metals was taken into account (Scenario B vs C; Table 8.1). However, this is not necessarily related to the speciation effects but more likely to the relative binding affinities of the different metals for binding to natural organic matter. To get a better insight into the matter, one should first understand the speciation chemistry of the individual metals. For this, the comparison between the normalized EC10 values in dissolved concentrations (Scenario B) and in free ion activities (Scenario C) is given in Figure 8.4. For all metals, the relation between $EC10_{diss}$ and $EC10_{act}$ is not parallel to the 1:1 line, although this is most pronounced for Cu. At low $EC10_{diss}$ concentrations, less metal is present as free ion activity relative to the dissolved concentration, compared to high $EC10_{diss}$ concentrations. Hence, the relation between $EC10_{diss}$ and $EC10_{act}$ is non-linear. The reason for the difference between Zn and Ni on the one hand and Cu on the other hand (i.e. why this non-linear relation is more pronounced for Cu) is the affinity of these metals to DOC (Tipping et al. 2011). The latter metal has the highest affinity (K_{MA}) for DOC binding sites and represents the highest heterogeneity in binding strengths (ΔLK_2) compared to the former metals. Therefore, at low Cu_{diss} concentrations, most Cu^{2+} in solution is bound to DOC which is why the free Cu activity is low (Figure 8.4). As Cu_{diss} concentrations increase, the DOC becomes

increasingly saturated and the amount of free Cu activity increases. For Zn and Ni, the same effect of DOC can be observed, although much less pronounced than for Cu. For these metals, the DOC is saturated at lower Me_{diss} concentrations than for Cu because of the low affinity of these metals for DOC.

Regarding the CA_{SSD} method, because the conversion of $EC10_{diss}$ to $EC10_{act}$ for low $EC10_{diss}$ values gives a lower free ion activity relative to high $EC10_{diss}$ values (most pronounced for Cu, but also the case for Zn and Ni), the SSD of a target water sample is also influenced. In Figure 8.5 we can see that the SSD based on $EC10_{act}$ values (i.e. 'activity'-SSD) is less steep (higher sd) than the SSD based on $EC10_{diss}$ values (i.e. 'dissolved' SSD). This is the case for all metals, although the difference is most pronounced for Cu. However, because the contribution of Cu to the mixture is in general lower than that of Ni and Zn, it is predominantly the influence on the SSD of Ni and Zn that causes the eventual change in msPAF values. A consequence of this shift in slope-steepness is that, a less steep slope of the SSD will lead to a higher value of the ratio $\frac{c_i}{HC5}$ for the given target water sample. This in turn leads to a higher chance of the community to experience risk in that target water sample due to a single metal (i.e. TU_{Me}>1) and consequently due to the mixture ($SumTU_{HC5}$ >1). The increase of the $SumTU_{HC5}$ will in turn lead to a higher $msPAF_{CA,SSD}$ in the given target water sample.

For the VMM, the 'activity'-SSD is less steep than the 'dissolved'-SSD for 100%, 98% and 100% of the target water samples for Cu, Zn and Ni, respectively (Table 8.2). As a result, for species that have an EC10 below the HC5, the ratio $\frac{c_i}{HC5}$ for Cu, Zn and Ni will increase in almost all target water samples of the VMM database. Consequently, this will result in higher $msPAF_{CA,SSD}$ values and therefore in an increase of the % target water samples affected by the mixture when calculations are performed on free ion activities (Scenario C; Table 8.1). The percentages of less steep 'activity'-SSDs for the Dommel and FOREGS database is similar to that of the VMM database (Table 8.2), which can explain the increase in $msPAF_{CA,SSD}$ values and % target water samples affected in those monitoring databases.

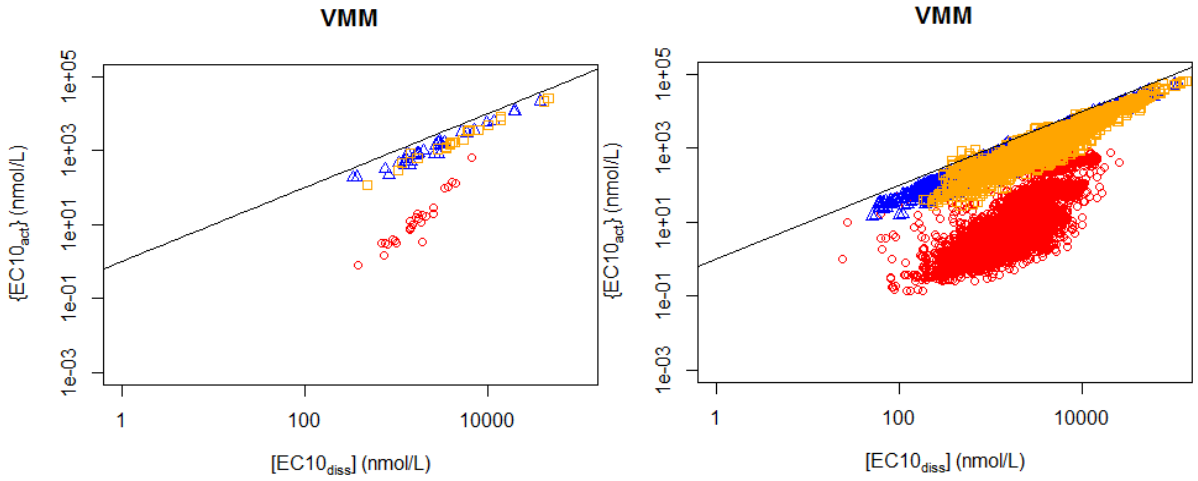

Figure 8.4 Relation between the EC10 values of Cu (red circles), nickel (blue triangles) and zinc (orange squares) when expressed as dissolved concentration and free ion activity, for the VMM database. In the left figure one target water sample of the VMM database is highlighted, in the right figure all target water samples are plotted. The 1:1 line gives a perfect match between $EC10_{diss}$ and $EC10_{act}$.

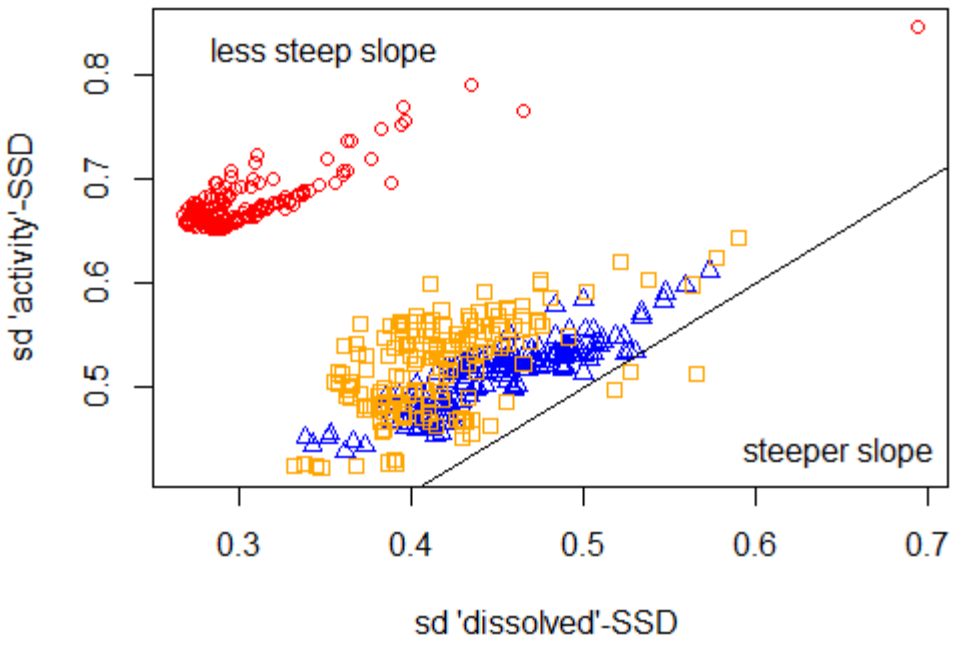

Figure 8.5 Relation between the standard deviation (sd) of the SSD based on $EC10_{diss}$ values (i.e. 'dissolved'-SSD) and on $EC10_{act}$ values (i.e. 'activity'-SSD) for Cu (red circles), Ni (orange squares) and Zn (blue triangles) for the target water samples of the VMM monitoring database. The 1:1 line gives a perfect match between the sd of the 'dissolved'-SSD and 'activity'-SSD. Values left of the 1:1 line indicate a less steep 'activity'-SSD while values on the right side of the 1:1 line indicate a steeper 'activity'-SSD

Table 8.2 Percentage of species sensitivity distributions (SSDs) for the target water samples of the Dommel, Flanders (VMM), Rhine, Austria, and FOREGS database that show a less steep slope when calculated using Scenario C compared to Scenario B.

	Dommel	VMM	Rhine	Austria	FOREGS
Ni	100	100	27	23	76
Cu	100	100	100	98	100
Zn	90	98	95	65	89

Regarding the CA_{DRC} method, because the conversion of $EC10_{diss}$ to $EC10_{act}$ for low $EC10_{diss}$ values gives a lower free ion activity relative to high $EC10_{diss}$ values, the $TU_{EC10\text{-}Me}$ of a target water sample is also influenced. This can be observed for a single target water sample of the VMM database in Figure 8.6. For Cu, the $TU_{EC10\text{-}Cu}$-distribution shifts to lower TU values when based on $\{Cu^{2+}\}$ values. However, the $TU_{EC10\text{-}Cu}$ does never exceed 1 in this case, independent of the method used, and therefore does not have a high contribution to the msPAF value. For Zn and Ni however, the $TU_{EC10\text{-}Me}$-distribution shifts to higher TU values when based on $\{Me^{2+}\}$ values, therefore a higher percentage of species is affected by the single metals ($TU_{EC10\text{-}Me}$ >1; PAF > 0.05). In turn, this will lead to a higher $SumTU_{EC10}$ and therefore to a higher $msPAF_{CA,DRC}$ and % target water samples affected.

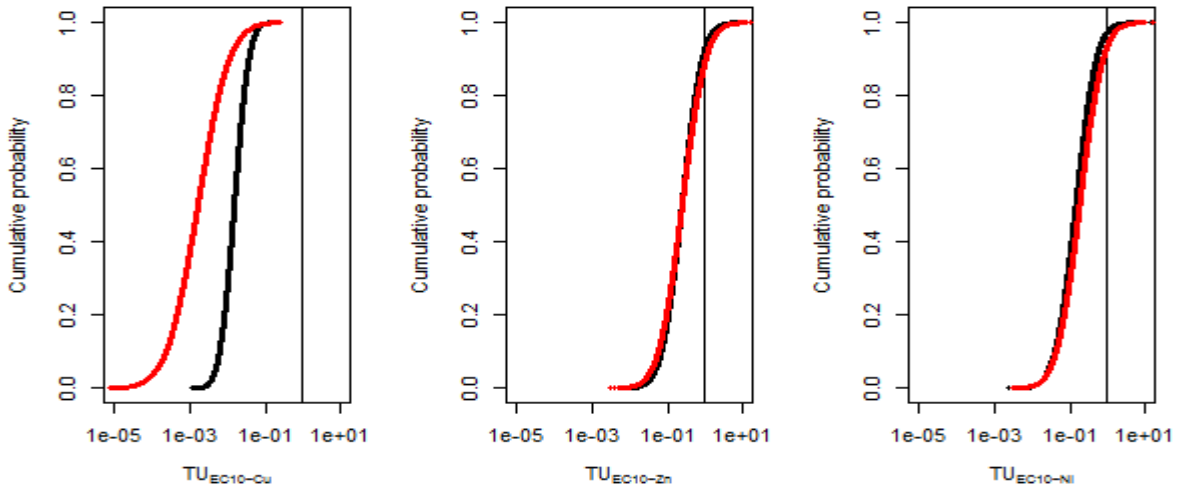

Figure 8.6 Observed cumulative distribution of $TU_{EC10\text{-}Me}$ values for a single target water sample in the VMM database when metals are given as dissolved concentrations (black distribution) and as free metal activity (red distribution). The $TU_{EC10\text{-}Me}$ is the ratio of the dissolved concentration or free ion activity of the metal in the monitoring database against the EC10 values of the 20.000 hypothetical species generated (in dissolved concentration or free ion activity). The vertical black line indicates a TU_{EC10} of 1. Above this value, the species is affected by the metal.

Regarding the IA_{SSD} method, because the SSD of a target water sample is influenced as was explained above, this also influences the PAF per metal calculated with the IA_{SSD} method. This can be observed for a single target water sample of the VMM database in Figure 8.7. For all single metals, the $PAF_{IA,SSD}$ is higher when based on free ion activities compared to dissolved concentrations. For Zn and Ni, this increase in $PAF_{IA,SSD}$ leads to an exceedance of the 0.05 value in a number of water bodies (highlighted in yellow in Figure 8.7). The $msPAF_{IA,SSD}$ values also exceed the 0.05 cut-off for a higher number of target water samples when calculations are performed on free ion activities, which explains the higher % target water samples affected.

For the IA_{DRC} method, the conversion to free metal activities does also influence the PAF per metal calculated with the IA_{DRC} method. This can be observed for a single target water sample of the VMM database in Figure 8.8. Also here, for Ni and Zn as well as for the mixture, a number of target water samples exceeds the 0.05 cut-off only when calculations are based on free metal activities (highlighted in yellow in Figure 8.8). The increase in PAF for all single metals can be explained by the use of the slope of the free ion activity dose-response-curve for the IA_{DRC} method. As can be observed in Figure 8.9, although again most pronounced for Cu but also visible for Zn and Ni, the slope of the dose-response curves are lower when based on free metal ion activities. This can again be explained by the affinity of the metals to DOC, which is larger for Cu. Hence, at low Me^{2+} activity (e.g. EC10 values), more Me^{2+} is bound to DOC resulting in lower free Me^{2+} activity and therefore a less steep dose-response curve. On average, this less steep DRC leads to a higher effect of each single metal on each species. This again results in a higher $msPAF_{IA,DRC}$ values and % affected target water samples.

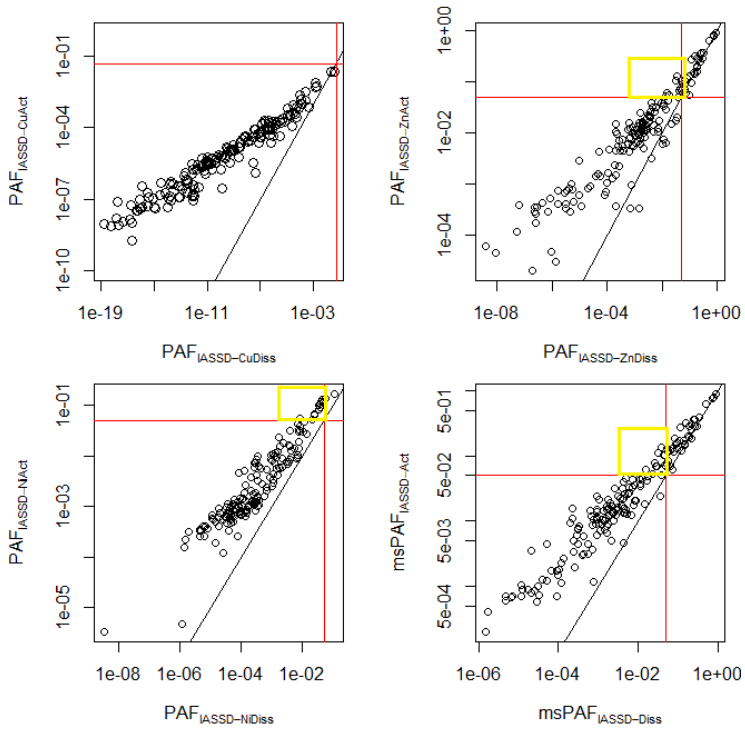

Figure 8.7 Potentially affected fraction of species (PAF) calculated with the IA_{SSD} method, due to single Cu, Zn and Ni and due to the mixture of Cu-Zn-Ni, when calculations are performed on dissolved metal concentrations and free ion activities, for the VMM monitoring database. The red lines indicates a PAF or msPAF of 0.05. Above this value, the target water sample is affected by the single metal or metal mixture. The yellow boxes indicate target water samples that are not affected when calculations are performed on dissolved metal concentrations, but are affected when performed on free ion activities.

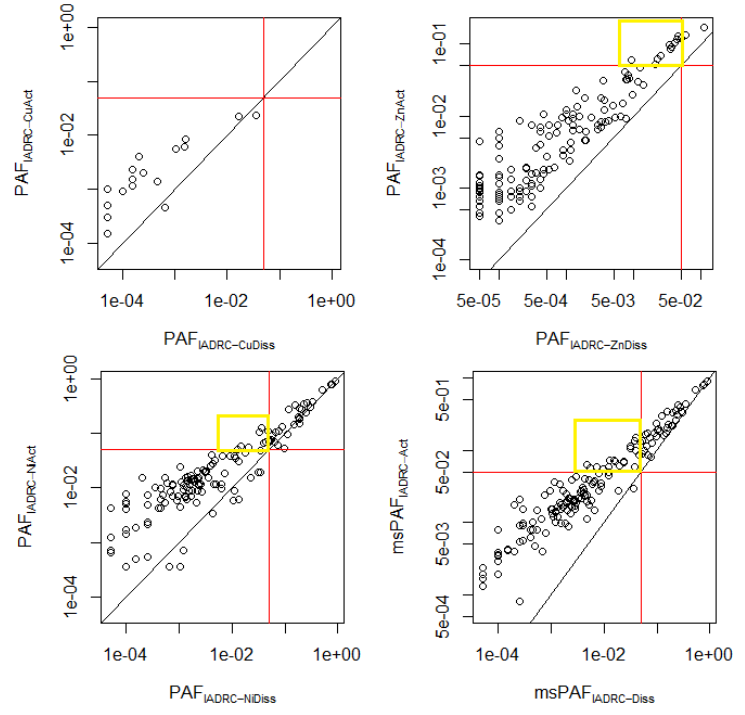

Figure 8.8 Potentially affected fraction of species (PAF) calculated with the IA_{DRC} method, due to single Cu, Zn and Ni and due to the mixture of Cu-Zn-Ni, when calculations are performed on dissolved metal concentrations and free ion activities, for the VMM monitoring database. The red lines indicates a PAF or msPAF of 0.05. Above this value, the target water sample is affected by the single metal or metal mixture. The yellow boxes indicate target water samples that are not affected when calculations are performed on dissolved metal concentrations, but are affected when performed on free ion activities.

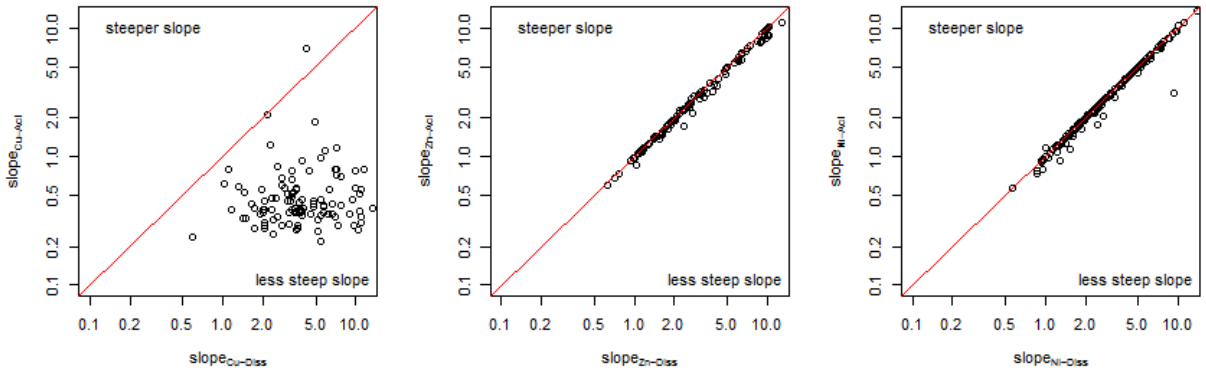

Figure 8.9. Distribution of slope values of dose-response-curves (DRC) for the Cu, Zn and Ni chronic toxicity databases when metals are given as dissolved concentrations (slope$_{Me-Diss}$) and as free ion activities (slope$_{Me-Act}$). The 1:1 line gives a perfect match between the slope of the 'dissolved'-DRC and 'activity'-DRC. Values right of the 1:1 line indicate a less steep 'activity'-DRC while values on the left side of the 1:1 line indicate a steeper 'activity'-DRC.

In contrast to the VMM, Dommel and FOREGS databases, the msPAF values and the % target water samples affected by the mixture decreases for the Austria database. Also here, this is not necessarily related to the speciation effects but more likely to the relative binding affinities of the different metals for binding to natural organic matter. The Austria database shows the lowest concentration of DOC compared to the other databases (Figure 8.10).

The comparison between the EC10 values in dissolved concentrations (Scenario B) and in free ion activities (Scenario C) for the Austria database is given in Figure 8.11. Some differences to Figure 8.4 can be observed. First of all, for Cu, the relation between EC10$_{diss}$ and EC10$_{act}$ is here more parallel to the 1:1 line compared to the VMM database (Figure 8.4). Because of the low DOC concentration in the Austria database, the DOC is saturated at lower Cu$_{diss}$ concentrations compared to a water with a higher DOC concentration, which in turn results in a higher free ion activity at lower Cu$_{diss}$ concentrations. For Zn and Ni, the relation between EC10$_{diss}$ and EC10$_{act}$ is not parallel to the 1:1 line (Figure 8.11B). This is more clear from Figure 8.11C. At high EC10$_{diss}$ concentrations, the free metal ion activity is relatively lower compared to the dissolved EC10$_{diss}$ concentrations than for low EC10$_{diss}$ concentrations. This can be explained by the complexation processes of Ni and Zn (Figure 8.12). Although the fraction of metal complexed to fulvic acid decreases with increasing metal concentration (Figure 8.12A), the concentration of metal that is bound as inorganic complexes increases (Figure 8.12B-C), which explains the low metal ion activity at high Me$_{diss}$ concentrations.

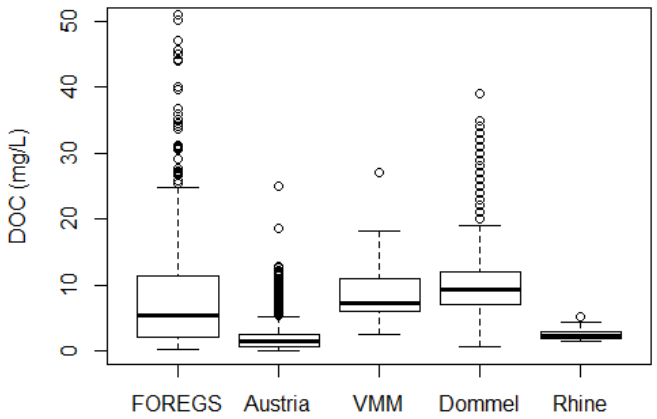

Figure 8.10 DOC concentration (mg/L) for the different monitoring databases.

Regarding the CA_{SSD} method, because the conversion of $EC10_{diss}$ to $EC10_{act}$ is not parallel to the 1:1 line, the SSD of a target water sample is also influenced. In Figure 8.13 we can see that the SSD based on $EC10_{act}$ values (i.e. 'activity'-SSD) is steeper (lower sd) than the SSD based on $EC10_{diss}$ values (i.e. 'dissolved' SSD) in a number of target water samples. This is the case for all metals, although most pronounced for Ni and Zn. The lower boundary for the Cu sd's is a result of the presence of a lower limit (i.e. the detection limit) of the DOC measurements in these target water samples. The reasoning that was followed above for the VMM database, can also be applied to the Austria database, be it reversed. A consequence of the shift in slope-steepness is that a steeper slope of the SSD will lead to a lower value of the ratio $\frac{HC5}{EC10}$ for the given target water sample. This in turn leads to a lower chance of an organism to experience risk in that target water sample due to a single metal (i.e. TU_{Me}<1) or due to the mixture ($SumTU_{EC10@HC5}$ <1). The decrease of the $SumTU_{EC10@HC5}$ will in turn lead to a lower $msPAF_{CA,SSD}$ in the given target water sample.

For the Austria database, the 'activity'-SSD is steeper than the 'dissolved'-SSD for 77% and 25% of the target water samples for Ni and Zn, respectively (Table 8.2). As a result, the ratio $\frac{HC5}{EC10}$ for Ni and Zn will decrease in almost all target water samples of the Austria database. Consequently, this will result in lower $msPAF_{CA,SSD}$ values and therefore in an decrease of the % target water samples affected by the mixture when calculations are performed on free ion activities (Scenario C; Table 8.1).

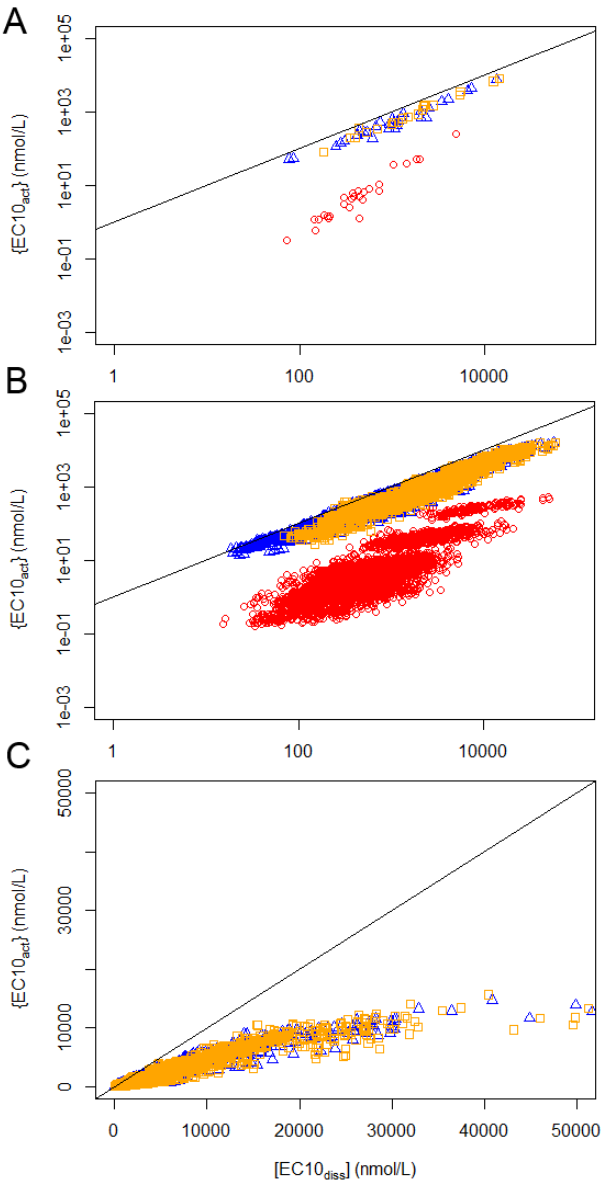

Figure 8.11 Relation between the EC10 values of Cu (red circles), nickel (blue triangles) and zinc (orange squares) when expressed as dissolved concentration and free ion activity, for the Austria database. (A) one target water sample of the Austria database is highlighted, (B) all target water samples are plotted on a log-scale, (C) all target water samples are plotted on a linear scale (for nickel and zinc). The 1:1 line gives a perfect match between $EC10_{diss}$ and $EC10_{act}$.

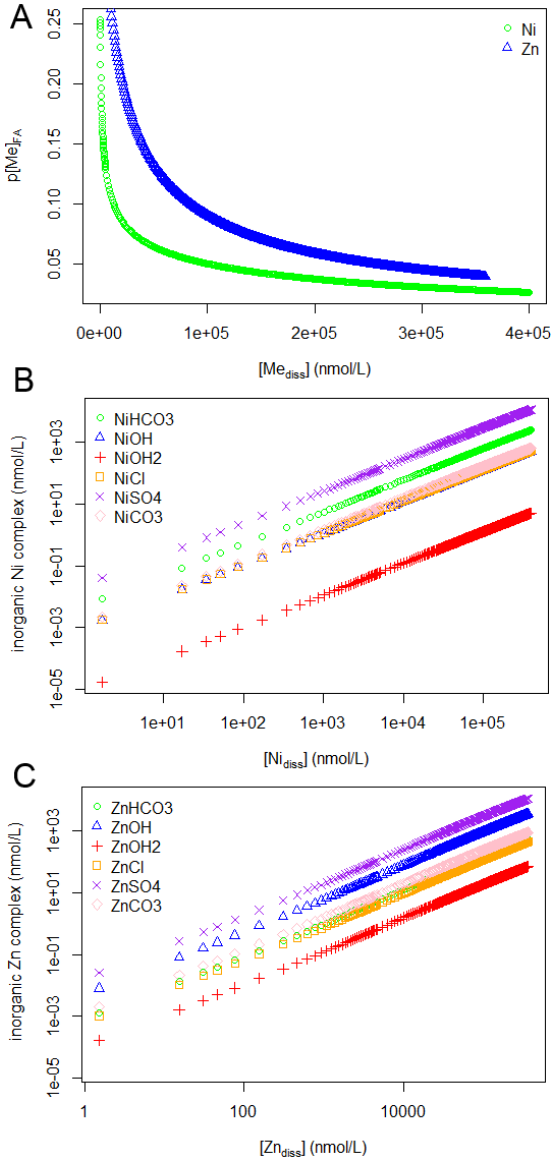

Figure 8.12 Relation between the dissolved metal concentration and (1) the fraction of metal found to FA (p[Me]FA, (B) the concentration of inorganic Ni complexes and (C) the concentration of inorganic Zn complexes.

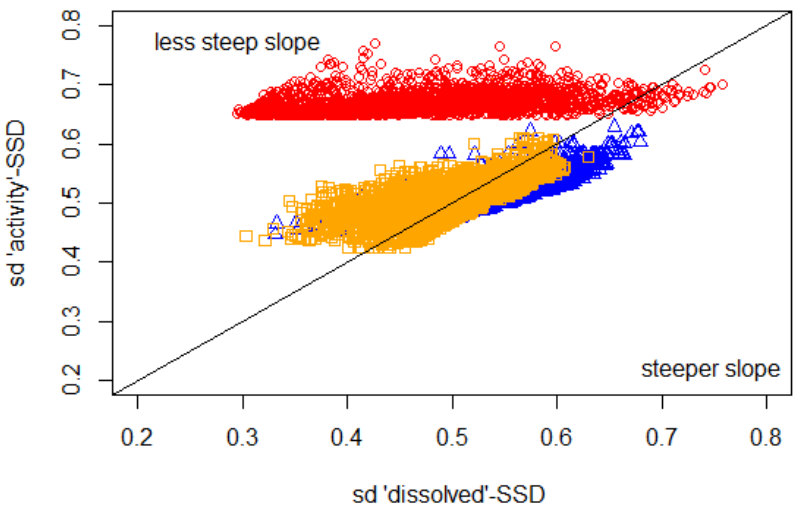

Figure 8.13 Relation between the standard deviation (sd) of the SSD based on $EC10_{diss}$ values (i.e. 'dissolved'-SSD) and on $EC10_{act}$ values (i.e. 'activity'-SSD) for Cu (red circles), Ni (orange squares) and Zn (blue triangles) for the target water samples of the Austria monitoring database. The 1:1 line gives a perfect match between the sd of the 'dissolved'-SSD and 'activity'-SSD. Values left of the 1:1 line indicate a less steep 'activity'-SSD while values on the right side of the 1:1 line indicate a steeper 'activity'-SSD

Regarding the CA_{DRC}, IA_{SSD} and IA_{DRC} methods, the same reasoning as was explained for the VMM database can be followed for the Austria database, be it reversed.

In the above paragraphs, we explained the underlying reasons for the differences between Scenario C and D. However, certain uncertainties in Scenario C calculations can be put forward, that for now hinder the use of calculated free metal ion activities as the basis for risk assessment.

First, as was explained above, at low Cu concentrations, the DOC-binding characteristics of Cu seem to be more important than potential competitive effects between metals for DOC binding sites. However, it should be noted that based on a comparison between measured $\{Cu^{2+}\}$ concentrations found in literature (Lofts and Tipping 2013) and WHAM-VII predicted $\{Cu^{2+}\}$ concentrations (Lofts and Tipping 2011), the predictive performance of the WHAM-VII speciation software to predict $\{Cu^{2+}\}$ in the low Cu concentration range is less accurate than at higher Cu concentrations. For instance, although Lofts and Tipping (2013) measured $\{Cu^{2+}\}$ as low as 10^{-16} M, WHAM VII did not predict any concentrations below 10^{-13} M. The free Cu activity in our monitoring databases predicted by WHAM VII are as low as 10^{-15} M. Thus, the speciation calculations at these low environmental Cu concentrations are associated with a certain degree of uncertainty. However, the contribution of Cu to the mixture is low in all monitoring databases, and therefore, the influence on Cu on the risk estimations is also low. Therefore, the cause for the changes in msPAF values should be sought for with Ni and Zn. Although less pronounced than for Cu, the same influence of DOC on Ni and Zn could be observed. However, it should be noted that Lofts and Tipping (2013) found that the predictive performance of WHAM VII was also less accurate at low Ni and Zn concentrations. These authors found that Zn and Ni free ion activities were well predicted when > 10^{-7} M and >10^{-8} M, respectively, but were overestimated or scattered at lower activities. The free Zn and Ni activity in our monitoring databases predicted by WHAM VII are as low as 10^{-11} M for

both metals. Thus, the speciation calculations at these low environmental Zn and Ni concentrations are associated with a certain degree of uncertainty.

Second, the SSD fit for Cu is different when EC10 values are given as dissolved Cu concentration or as free Cu activity, which is a result of the non-linear relation between Cu_{diss} and Cu_{act} (e.g. Figure 8.4). This can be observed for a fictitious Cu SSD in Figure 8.14. To create the SSD in Figure 8.14B, the dissolved Cu EC10 data underlying the SSD in Figure 8.14A was converted to free Cu activity using WHAM VII. For this, a hypothetical water with DOC concentration of 5.5 mg/L, Ca concentration of 43 mg/L and pH of 7.3 was used. Although the SSD based on the dissolved Cu concentrations (Figure 8.14A) is fitted perfectly with a log-normal distribution, the SSD based on the free Cu activity (Figure 8.14B) is not fitted perfectly with the log-normal distribution. Especially around the HC5 concentration, which is an important value in risk assessment, the difference between the actual values and the fitted distribution is large. This has consequences for the msPAF calculations. Because the HC5 value that is fitted based on the log-normal distribution is lower compared to the actual data, this will lead to an overestimation of the msPAF values. For Ni and Zn, this different fit of SSDs is not observed, because the affinity for these metals for DOC is lower than that of Cu.

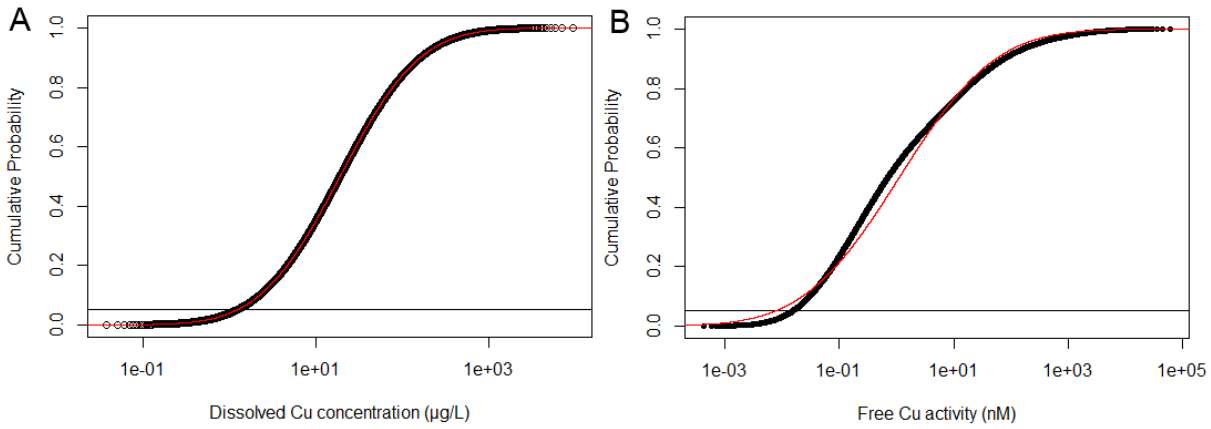

Figure 8.14 Species sensitivity distribution of Cu fitted with the log-normal distribution for dissolved Cu concentrations (A) and the same concentrations converted to free Cu activity using WHAM VII (B).

8.4. Research recommendations

The validation of WHAM VII at low environmental metal concentrations is limited (Lofts and Tipping 2013). Therefore, more research should be conducted in which measured free ion activities are compared to WHAM VII predicted free metal activities. This research should include natural waters with both high and low environmental concentrations of metals and for a large variation of water chemistry parameters and especially of DOC. In addition, we would advise to revise the DOC binding constants for the metals at low metal concentrations based on this newly generated data, if validation experiments show a need for this.

The distribution that was fitted to the 'activity' SSD was not the same as that of the 'dissolved' SSD. As such, the fit of the 'activity' SSD was not good using the log-normal distribution, which has consequences for the HC5 calculation. To overcome this issue, the distribution of the 'activity" SSD should not be fitted with a log-normal distribution but instead the option of non-parametric method to calculate the HC5 value should be further investigated.

8.5. Conclusions

A limitation of the four risk assessment methodologies for risk estimations of metal mixtures described in Chapter 6 is the fact that calculations of mixture toxicity were performed on the basis of dissolved metal concentrations, while possible interactions between metals at DOC sites were not accounted for. This limitation could result in higher predicted msPAFs. Improvement of these methodologies required the simultaneous computation of speciation for all metals with a single speciation model, in this case WHAM VII, which was tackled in Chapter 7. In the present chapter, we performed calculations for all monitoring databases described in Chapter 2, but based on free metal ion activities. For this, the dissolved metal concentrations in the monitoring databases were converted to free ion activities in two ways, one that did not take into account the competition between the metals for DOC binding sites (Scenario C) and one that did (Scenario D).

Although we had expected that taking into account the competition between metals for DOC binding sites would result in higher free metal activities, we found that, at environmental concentrations, competition between metals for DOC had relatively little effect on free metal ion activity (1.1% - 20%). As a consequence, msPAF values calculated with Scenario C were similar to those of Scenario D. Our hypothesis is therefore refuted and the main conclusion of the chapter is that competition between metals for DOC binding sites has little impact on metal mixture risk estimations.

However, another surprising observation was made. The msPAF values based on calculated free metal ion activities (Scenario C) were, depending on the monitoring database, higher or lower than those based on dissolved concentrations (Scenario B). This was not expected, as both scenarios do not take into account the competition between metals for DOC binding sites. We explained that this difference is likely related to the relative binding affinities of the different metals for binding to natural organic matter. As a consequence, the slope of the SSD curves is altered, which in turn has an influence on the msPAF values and the % target water samples calculated to be affected by the mixture.

Although the difference between Scenario B and C can be explained, certain important uncertainties in Scenario C calculations remain. First, the predictive performance of the WHAM-VII speciation software to predict $\{Me^{2+}\}$ in the low metal concentration range is less accurate than at higher metal concentrations. Thus, the speciation calculations at these low environmental metal concentrations are associated with a certain degree of uncertainty. Second, the fit of the Cu SSD is different when based on dissolved Cu concentrations compared to free Cu activities. Because the log-normal distribution is fitted to both SSDs, the HC5 value resulting from the ‘activity’-SSD is not accurate, which has consequences for the risk estimations.

Two essential points currently hinder the use of free metal ion activities instead of dissolved concentrations as the basis for risk assessment procedures. First of all, the uncertainties in the free ion activity calculations, as explained above. Second, in contrast to dissolved metal concentrations, which are commonly measured in environmental monitoring, free metal activities are rarely measured in the field (and not at all in routine monitoring programs) and we can only rely on software to calculate them, which makes calculations of free metal ion activities less robust. As a consequence, we cannot

recommend the use of calculated free ion activities in risk assessment procedures for now and advise to continue to perform metal risk assessments on the basis of measured dissolved metal concentrations. In addition, we recommend the use of the tiered metal mixture risk assessment scheme on the basis of dissolved metal concentrations (Scenario B), that was proposed in Chapter 2, in which competition between metals for DOC is assumed not to be important. The latter was confirmed in this chapter: competition between metals for DOC binding sites had little impact on metal mixture risk estimations.

Nine

General conclusions, integration and future research recommendations

9. General conclusions, integration and future research recommendations

9.1. General conclusions

The aim of ecological risk assessment is not only to protect single species but to protect entire ecosystems. For data-rich substances, such as metals, there is often enough data to construct species sensitivity distributions (SSDs), which allows the calculation of HC5 values of potentially affected fractions (PAF) of species at a given concentration. The SSD-method can also be applied to mixtures and four different methodologies have been proposed by various authors (De Zwart and Posthuma 2005; Gregorio et al. 2013). In the **second chapter** of this work, we further adapted these methods specifically for metal mixtures by combining bioavailability-normalisation based methods (the procedure for metals currently used in the EU) with the mixture reference models concentration addition (CA) and independent action (IA). Although these reference models were originally developed to predict mixture effects for individual species (Bliss 1939; Loewe and Muischnek 1926; Kortenkamp and Altenburger 2011), they have also been extended to estimate risks of mixtures for species assemblages (De Zwart and Posthuma 2005; Gregorio et al. 2013). The four following methods to evaluate mixture risks were proposed in Chapter 2: CA_{SSD} (CA applied directly to the SSD), IA_{SSD} (IA applied directly to the SSD), CA_{DRC} (CA applied to the individual Dose Response Curve) and IA_{DRC} (IA applied to the individual Dose Response Curve). All these models combine SSD-techniques with one of both mixture toxicity reference models. As such, the toxic pressure, i.e. the estimated risk of a mixture on a species-assemblage, is expressed as the 'multi-substance Potentially Affected Fraction' (msPAF), which denotes the fraction of species potentially affected by a mixture (De Zwart and Posthuma 2005). Analogously with the criteria used in the ecological risk assessment of the individual metals (e.g. Van Sprang et al. 2009; DEPI 2008), it has been assumed that risks are 'acceptable' if maximally 5% of the species are affected by the metal mixture, i.e. no risks predicted as long as the msPAF value < 0.05.

In the most simple methods, CA_{SSD} and IA_{SSD}, either CA or IA, respectively, are directly applied to the SSDs of the individual mixture components, and the msPAF value is derived by aggregation of the PAF value of each of the individual substances in the mixture (De Zwart and Posthuma 2005). The CA_{SSD} is a mathematically simple way to implement mixtures in environmental regulatory frameworks (e.g. A&NZ 2000) i.e. it evaluates mixture risks based on a risk quotient (RQ_{SSD}) that expresses mixture doses in terms of sum of toxic units (∑TU) relative to an SSD-derived environmental threshold of the different metals, such as the HC5 (Equation 9.1). In this method, for a mixture for which the RQ_{SSD} equals 1, the $msPAF_{CASSD}$ value equals exactly 5%.

$$RQ_{SSD} = \sum TU_{HC5} = \sum \frac{c_i}{HC5_i} \quad (9.1)$$

The IA_{SSD} method applies IA directly to the SSDs of the individual mixture constituents. Hence, $msPAF_{IA,SSD}$ values are estimated from the product of the fraction of species not affected by each of the individual mixture constituents (Traas et al. 2002). Although CA_{SSD} and IA_{SSD} are mathematically elegant methods, CA and IA are conceptually consistent with the assumptions of CA or IA that apply to single organisms (dose–response curves), and not to communities (SSDs) (Gregorio et al. 2013).

Theoretically more consistent, but also more complex methods apply CA or IA first to the different species in the SSD and subsequently combine the risk to all single-species to calculate risks for species assemblages (Gregorio et al. 2013). In the CA_{DRC} method, CA is applied directly to the dose-response data of each of the individual species in the SSD by calculating a ∑TU relative to the EC10 for each species ($\sum TU_{species\ j}$). If the $\sum TU_{species\ j}$ exceeds one, the species is considered to be affected by the mixture. Consequently, the $msPAF_{CADRC}$ value is estimated as the fraction of species for which $\sum TU_{species\ j} > 1$. The IA_{DRC} is the most complex method because it applies IA directly to the concentration response curves of each substance for each species in the toxicity databases (Gregorio et al. 2013). The $msPAF_{IADRC}$ value is then the estimated fraction of species for which more than 10% mixture effect is predicted.

In Chapter 2 we evaluated these four methods by using measured concentrations of Ni, Zn, and Cu of monitoring datasets of target water samples in four European regions. We demonstrated that between 0% and 52% of the target water samples were estimated to be at risk but only between 0% and 15% of the target water samples were at risk due to the mixture of metals and not due to any single metals individually. In addition, we examined the degree of conservatism of the CA_{SSD}-method relative to the other more complex methods using the margin of safety (MoS). The MoS expresses the conservatism of the CA_{SSD} method relative to the other methods for predicting equal effects (i.e. msPAF = 0.05) on communities. Based on the MoS provided by the CA_{SSD}, the following order of conservatism for the 4 mixture evaluation methods was determined CA_{SSD} > CA_{DRC} (MoS = 1.17-1.25) > IA_{DRC} (MoS = 1.38-1.60) > IA_{SSD} (MoS = 1.48-1.72). Of these four metal mixture risk prediction methods, the IA_{DRC} and CA_{DRC} are conceptually consistent with the assumptions of the CA or IA mixture reference models, while the CA_{SSD} and IA_{SSD} are not. However, to conclude which one of these two methods (IA_{DRC} or CA_{DRC}) is the most accurate one we therefore have to know which reference model (i.e. IA or CA) predicts mixture toxicity to aquatic organisms most accurately.

In chapter 3 of the present work, we therefore performed ecotoxicity experiments with microalgae, as little metal mixture literature concerning these organisms was found. In addition, it is of utmost importance to understand the effects of metal mixtures on these organisms as they are primary producers and therefore at the base of the food web. The objective was to test if interactive effects (if any) of mixtures to *Pseudokirchneriella subcapitata* were the same or different, across natural waters showing diverse water-chemistry characteristics. This was done by performing experiments with ternary Cu-Ni-Zn mixtures in 3 natural waters and with binary Cu-Ni mixtures in 5 natural waters. We showed that the ternary mixture and binary mixtures acted mostly non-interactively on algal growth. In addition, we showed that both the CA and IA model can serve as accurate models for toxicity of ternary Cu-Ni-Zn and binary Cu-Ni mixtures to *P. subcapitata* in most cases. Similar results for algae were found by Nys et al. (2017d). These authors demonstrated that IA and CA resulted in relatively similar model performances for algae (*Navicula pelliculosa* and *P. subcapitata*). On the other hand, these authors found that IA was clearly the better model for invertebrates (*Asellus aquaticus, Ceriodaphnia dubia*, and *Daphnia magna).* Overall, Nys et al. (2017d) found that chronic metal mixture toxicity was most accurately predicted with IA compared to CA. Therefore, at the single species-level, the IA reference model predicts mixture toxicity to aquatic organisms most accurately. This suggests that, at the moment,

the IA_{DRC} method is scientifically the most defensible choice to asses metal mixture risks at the community level. However, IA_{DRC} is mathematically relatively complex and requires a high data-availability. Hence, the more simple method CA_{SSD} is at the moment preferred in the regulatory arena, such as in the only actual implemented risk assessment framework for metal mixtures so far, in Australia and New Zealand (A&NZ 2000).

However, a limitation of these mathematical methods is that the degree of conservatism compared with community-level effects needs to be investigated. A literature search performed prior to the design and execution of the present study showed that no studies were appropriate for this investigation (e.g. Stockdale et al. 2010, Richardson and Kiffney 2000, Clements et al. 2013, Hickey et al. 2002; Clements 2004). One reason is the lack of Dissolved Organic Carbon (DOC) measurements, an important variable influencing metal toxicity and needed to calculate metal bioavailability. Therefore, to investigate the degree of conservatism, a multispecies microcosm experiment was performed in **Chapter 4**. In this experiment, a naturally occurring planktonic community was exposed to Cu, Ni and Zn mixture, for 8 weeks. We aimed to answer the following research questions. (1) What are the direct and indirect effects of the mixture on the community? The community-level interactions differed between the low mixture treatments and the high mixture treatments. In the low mixture treatments, the zooplankton groups were not affected. On the other hand, the Cyanobacteria were negatively affected which indirectly increased the abundances of the Chrysophyta, Diatoms and Cryptophyta. More complex community-level interactions were observed in the high mixture treatments including a decrease in Cladocera which indirectly might have resulted in an increase in Copepoda which in turn could have contributed to the decrease in Rotifera abundance. (2) When using the classic toxic unit approach, i.e. the CA_{SSD} method, from which msPAF value onward are effects observed on structural and functional community-level endpoints? We showed that many structural community endpoints (e.g. community composition, species diversity, species richness) and one functional community endpoint (i.e. DOC) did not show effects at or below an msPAF value of 0.05 (i.e. these endpoints can be considered protective). For two other functional community endpoints however (i.e. ΔDO and ΔpH), effects at this msPAF value of 0.05, which is regarded as protective in many regulatory frameworks, were observed. For these two functional community endpoints, significant community-level effects were observed at an msPAF value of 0.03 (a Ni-Zn mixture) when the SSDs contained all species (i.e. both planktonic and non-planktonic) and at an msPAF value of 0.05 when the SSDs only contained planktonic species (phytoplankton and zooplankton). A likely explanation for the effects observed at or below this cut-off value of 0.05 is the mismatch between the species in the SSD and those in the microcosm community. Especially the presence of the cyanobacteria species *Oscillatoria* sp. 1 in our community, which is not represented in the SSD, seems to have been the driver for the observed effects on community-function at these low msPAF values. Our results show that SSDs are not necessarily a good predictor of effects on all types of communities and that the presence of dominant sensitive species may result in significant effects on community functioning endpoints at an msPAF value (0.05) that is generally considered protective. In addition, our results should only be extrapolated cautiously to other systems because information whether dominant species in other systems are typically also sensitive species is usually lacking and it

is often the loss of species that are both dominant and sensitive that can result in a disproportionally large decrease in ecosystem functioning.

Both the $msPAF_{plankton}$ and the $msPAF_{AllSpecies}$ values are at the moment calculated with chronic bioavailability models for individual metals that are currently based on different software to model metal speciation: i.e. WHAM V for Zn (Van Sprang et al. 2009) and Cu (ECI 2008) and WHAM VI for Ni (DEPA 2008). Additionally, some assumptions for chemical speciation calculations differ between these metals. Therefore, in **chapters 5** these bioavailability models were re-evaluated. The first bioavailability model that was evaluated was the *D. magna* BLM for Cu. Cu BLMs have been applied to derive Water Quality Criteria in the US and PNECs in the EU. Although both frameworks use a similar approach to derive bioavailability-based WQC or PNEC values for copper, the structural formulation and parameterization of the BLMs that is used in both frameworks differ (US EPA 2007; ECI 2008). We evaluated the predictive capacity of these two BLMs for a large dataset of chronic copper toxicity data with two *Daphnia magna* clones, further denoted as K6 and ARO. We found that one BLM performed best with clone K6 data while the other performed best with clone ARO data. We also found that there is an important difference between both BLMs in how they predict bioavailability of copper as a function of pH. Finally, as fundamental differences in model structure between both BLMs made it impossible to create an 'average' BLM, we developed a generalized BioAvailability Model (gBAM). The developed gBAM was more accurate than both BLMs and can be considered a first step in further improving the accuracy of chronic toxicity predictions of copper as a function of water chemistry (to a variety of *D. magna* clones). A second and third bioavailability model that was re-evaluated were those for *D. magna* and *P. subcapitata* for Zn. These models have so far only been validated within a certain range of water chemistry. Yet, around 20% of the European surface waters fall outside this 'validation boundary' (Salminen et al. 2005). The purpose was therefore to evaluate if the Zn bioavailability models can be extrapolated outside their bioavailability ranges. Results from *D. magna* experiments suggested that the BLM is not able to reflect the pH effect over a broad pH range (5.5-8.5). In addition, due to calcium deficiency of *D. magna* in the softwater tests, we could not conclude whether the BLM is applicable below its Ca boundary. Results for *P. subcapitata* experiments showed that the bioavailability model can accurately predict Zn toxicity for Ca concentrations down to 0.8mg/L and pH values up to 8.5. Based on the *D. magna* results, we developed a generalized BioAvailability Model (gBAM) as an alternative for BLM to predict chronic effect concentrations for Zn to *D. magna*. The developed gBAM was more accurate than the original BLM over a broad pH range.

By developing the gBAMs to predict toxicity of Cu and Zn to *D. magna* the uniformisation of all bioavailability models (i.e. of Cu, Ni and Zn for invertebrates, fish and algae) to a gBAM-structure was almost complete. The models that did not yet incorporate a pH slope parameter (i.e. had the gBAM-structure) were the bioavailability models for fish for Zn and Cu. Therefore, a fourth and fifth bioavailability model that was re-evaluated were those for fish for Zn and Cu. Based on the chronic toxicity data we developed and validated a gBAM for the metals Zn and Cu for fish. These gBAMs were at least as accurate as their BLM counterparts.

In Chapter 6, the influence of these newly developed gBAMs on the msPAF values and % of target water samples affected was evaluated. Implementing the newly developed gBAMs showed a less than 2-fold difference of HC5 values compared to implementing all original bioavailability models. The largest differences were found for Cu (up to 4-fold in some monitoring databases), which was related to the experimental evidence-based incorporation of a Ca competition parameter in the *Daphnia* gBAM. Yet, despite these differences, implementing the new gBAMs only had a small influence on median msPAF values and on the % of target water samples that are predicted to be affected by the mixture of Zn, Cu and Ni. The latter is a result of the relatively low contribution of Cu to the mixture effects in the investigated monitoring databases.

Although all bioavailability models were formulated in a gBAM-structure in Chapter 5, these models were still based on different software to model metal speciation. Therefore, in **Chapter 7**, we evaluated whether these models could be updated to the WHAM VII speciation software, without loss of predictive capacity. Overall, our results showed that WHAM VII with an assumption of 65% AFA can be used as a speciation model to predict metal toxicity to different species with sufficient accuracy.
In a final chapter, **Chapter 8**, the bioavailability models integrating WHAM VII were used to perform msPAF calculations based on free metal ion activities. For this, the dissolved metal concentrations in the monitoring databases were converted to free ion activities in two ways, one that did not take into account the competition between the metals for DOC binding sites and one that did. Although we had expected that taking into account the competition between metals for DOC binding sites would result in higher free metal activities, we found that, at environmental concentrations, competition between metals for DOC had relatively little effect on free metal ion activity (1.1% - 20%). As a consequence, msPAF values calculated with both scenarios were similar. The main conclusion of the chapter is that competition between metals for DOC binding sites has little impact on metal mixture risk estimations. Additionally, due to uncertainties in the free ion activity calculations and the lack of measured free metal activities in the field we cannot recommend the use of calculated free ion activities in risk assessment procedures for now and advise to continue to perform metal risk assessments on the basis of measured dissolved metal concentrations.

9.2. Integration of the results

To integrate all the different steps that were realized in the course of this work, we performed a final analysis. In this analysis, msPAF values for the data from the microcosm experiment (Chapter 4) were calculated using the following bioavailability models: (A) for Zn and Cu: the original bioavailability models for algae (De Schamphelaere et al. 2005a and 2005b) and the newly developed gBAMs for invertebrates and fish (Chapter 5) all incorporating the WHAM VII speciation software (Chapter 7), (B) for Ni: the original bioavailability models/gBAMs for algae (Deleebeeck et al. 2009), invertebrates (Deleebeeck et al. 2008) and fish (Deleebeeck et al. 2007) all incorporating the WHAM VII speciation software (Chapter 7). We demonstrated in Chapter 5 that the newly developed gBAMs were at least as accurate or more accurate than their BLM counterparts. In addition, in Chapter 7, we demonstrated that WHAM VII with the assumption of 65% AFA can be used as a speciation model to predict metal toxicity to different

species with sufficient accuracy. Based on this, we can conclude that the new msPAF values that are calculated for the microcosm experiment are scientifically more robust than those from Chapter 4.

Table 9.1 shows an analogous table to Table 4.10 but showing the $msPAF_{plankton}$ values instead of the $msPAF_{AllSpecies}$ values. In addition, the $msPAF_{plankton}$ values were calculated with the bioavailability models listed above. These values are clearly higher than those shown in Table 4.10. This increase has multiple possible causes. A first cause can be found in the four gBAMs that were developed in Chapter 5. First, instead of a K_{HBL} parameter calculated based on data for one *D. magna* clone, the Cu *D. magna* gBAM incorporates a S_{pH} parameter that was calibrated on data for two different *D. magna* clones. Second, because recent research unambiguously showed the influence of hardness on Cu toxicity to *D. magna* (Rodriguez and Arbildua 2012), the Cu *D. magna* gBAM rightfully contains Ca and Mg competition parameters (Van Regenmortel et al. 2015), whereas the original Cu *D. magna* BLM does not (De Schamphelaere and Janssen 2004a). Third, in contrast to the Cu fish BLM, for which the pH effect was calibrated on acute *D. magna* data, the pH effect of the Cu fish gBAM was specifically calibrated on chronic fish toxicity data. Fourth, the Zn *D. magna* gBAM is applicable to a broader range of water chemistry compared to the original BLM. Finally, for all four newly developed gBAMs we showed that they were equally or more accurate than the original BLMs in predicting metal toxicity. When implementing the newly developed gBAMs in Chapter 6 we showed that up to a 2-fold and 4-fold difference in HC5 values compared to the implementation of all original bioavailability models were found. For Zn, the largest contributor to the mixture in the microcosm experiment, the ratio HC5 gBAM/BLM for the monitoring data in Chapter 7 was smaller than one (i.e. lower HC5 value when implementing the gBAMs) at the pH of the microcosm experiment (i.e. 8.07). This could possibly explain why the msPAF values are higher when implementing the gBAMs for the microcosm experiment (Table 9.1).

A second cause can be found in the difference in speciation software used. Whereas the original Cu, Ni and Zn bioavailability models incorporated WHAM V, WHAM V and WHAM VII, respectively, all with a different %AFA assumption, the models now all incorporate WHAM VII with the same %AFA assumption.

Based on these scientifically more robust calculations, we can conclude that the community structure and functioning of the planktonic community is only affected by the Cu-Ni-Zn mixture from an $msPAF_{plankton}$ value of 0.28 onwards, respectively. Based on the msPAF calculations with all original bioavailability models (Chapter 4) we concluded that effects on some functioning endpoints already occurred below the threshold of 0.05. When implementing the new gBAMs developed in Chapter 5 we now have to conclude that there is no evidence that this threshold is not protective for these endpoints as the lowest tested concentrations showed an msPAF value above this threshold.

Table 9.2 shows an analogous table to Table 4.11 but with the $msPAF_{plankton}$ values calculated with the bioavailability models listed above and gives an overview of the initial $msPAF_{plankton}$ values calculated with the CA_{DRC}, IA_{DRC} and IA_{SSD} methods. Most $msPAF_{plankton}$ values calculated using the CA_{DRC}, IA_{DRC} and IA_{SSD} methods are quite similar to those calculated using the CA_{SSD} method. At high msPAF values (>0.60), the CA_{SSD} method is no longer the most conservative method, as was seen in Chapter 2 and 4. At the Mixture treatment, the lowest treatment at which effects on the community were observed, and

which showed an initial $msPAF_{CASSD,plankton}$ value of 0.28 (Table 9.1), the most liberal method (IA_{SSD}) gives an initial $msPAF_{plankton}$ value of 0.20. This implies that based on the other methods and using the newly developed gBAMs and all models incorporating WHAM VII, we cannot conclude whether the msPAF threshold of 0.05 is protective for long-term effects on the planktonic community.

Table 9.1. Overview of the initial $msPAF_{plankton}$ value corresponding to the consistent LOEC of the structural and functional community endpoints for the single Cu, Ni and Zn treatments and the Env Ratio mixture treatment.

	Effect on	Variable	initial msPAF
Structural community endpoints	Species groups abundances	Cladocera	>0.94[a]/>0.99[b]
		Rotifera	0.72/0.95
		Copepoda	0.86/0.98
		Cyanobacteria	0.05/0.28
		Chlorophyta	>0.94/>0.99
		Chrysophyta	0.05/0.28
		Charophyta	0.86/0.98
		Diatoms	0.05/0.28
		Cryptophyta	0.05/0.28
	Community composition	Zooplankton community	0.48/0.82
		Phytoplankton community	0.15/0.60
	Species diversity	Zooplankton	>0.94/>0.99
		Phytoplankton	0.86/0.98
	Species richness	Zooplankton	0.94/0.99
		Phytoplankton	0.86/0.98
Functional community endpoints	ΔDO (community respiration)		0.05/0.28
	ΔpH (phytoplankton + bacteria abundance)		0.05/0.28
	DOC (microbial loop)		0.20/0.60

[a] For bioavailability normalizations, all original bioavailability models were used

[b] For bioavailability normalizations, the newly developed gBAMs incorporating WHAM VII (Chapter 5 and 7) were used.

LOEC = lowest observed effect concentration; Env Ratio = mixture with metal concentration ratio's based on Dommel monitoring dataset; DO = dissolved oxygen; DOC = dissolved organic carbon

Table 9.2. Average (± sd) initial msPAF values based on toxicity data of planktonic species (Supplementary C.4) calculated with the CA_{SSD}, CA_{DRC} , IA_{DRC} and IA_{SSD} methods (Van Regenmortel et al. 2017) for the different treatments. For bioavailability normalizations, the newly developed gBAMs incorporating WHAM VII (Chapter 5 and 7) were used.

	initial msPAF$CA_{SSD,plankton}$ [a]	initial msPAF$CA_{DRC,plankton}$ [a]	initial msPAF$IA_{DRC,plankton}$ [a]	initial msPAF$IA_{SSD,plankton}$ [a]
Control	0.04 ± 0.02	0.03 ± 0.01	0.02 ± 0.01	0.02 ± 0.01
Mixture 1	0.28 ± 0.12	0.28 ± 0.13	0.20 ± 0.12	0.20 ± 0.12
Mixture 2	0.60 ± 0.11	0.67 ± 0.11	0.56 ± 0.13	0.56 ± 0.13
Mixture 3	0.82 ± 0.13	0.88 ± 0.12	0.78 ± 0.20	0.78 ± 0.20
Mixture 4	0.95 ± 0.02	0.99 ± 0.01	0.96 ± 0.02	0.96 ± 0.02
Mixture 5	0.98 ± 0.00	1.00 ± 0.00	0.99 ± 0.00	0.99 ± 0.00
Mixture 6	0.99 ± 0.01	1.00 ± 0.00	0.99 ± 0.00	0.99 ± 0.00

msPAF = multi substance potentially affected fraction of species
$msPAF_{CADRC}$ = msPAF calculated using concentration addition applied to the individual dose response curves (CA_{DRC}) (Van Regenmortel et al. 2017);
$msPAF_{IADRC}$ = msPAF calculated using independent action applied to the individual dose response curves (IA_{DRC}) (Van Regenmortel et al. 2017);
$msPAF_{IASSD}$ = msPAF calculated using independent action applied to the species sensitivity distribution (IA_{SSD}) (Van Regenmortel et al. 2017);
HC5 = concentration hazardous for 5% of the species; HC50 = concentration hazardous for 50% of the species; Env Ratio = mixture with metal concentration ratio's based on Dommel monitoring dataset;
[a] msPAF values calculated based on chronic toxicity data of planktonic species, using the water chemistry measured in each microcosm separately after spiking the metals on day 1

Based on the integration of all results in the present study, we can conclude that in general the tiered metal mixture risk evaluation scheme presented in Chapter 2 has not changed. A small adaptation to the scheme is the change in bioavailability models to normalize the chronic toxicity data. Because the newly developed gBAMs for Cu and Zn for invertebrates and fish more accurately predict single metal toxicity, we recommend the implementation of the gBAMs instead of all original BLMs to normalize toxicity data for Cu and Zn prior to metal mixture risk calculations. In the metal mixture risk assessment framework (Figure 9.1) the CA_{SSD} method is incorporated as a first conservative level as the method tends to build in a relatively high conservatism (Chapter 2). The CA_{SSD} method is used to identify the monitoring sites where risks are unlikely to occur, i.e. if $\sum TU_{HC5}<1$ none of the four methods will predict risks. Hence, for these monitoring sites no further evaluation is needed. Since IA_{SSD} is generally the most liberal method, IA_{SSD} is built into the second tier. This to identify situations where risks are predicted regardless of the method used (msPAF > 0.05). In Tier 3, the more complex, but theoretically consistent methods, IA_{DRC} or CA_{DRC} can be applied, depending on the availability of the data.

For situations where at the highest tier risks are still predicted, further risk management steps are needed. These may involve direct efforts into lowering metal concentrations in affected water bodies. Alternatively, if direct prioritization would be too costly, metal mixture toxicity risks in these sites may be further evaluated on a more refined level using either targeted experiments (laboratory bioassays in natural medium and/or field bioassays) or based on field collected ecological data, or a combination of both (Gerhardt et al. 2004, 2008).

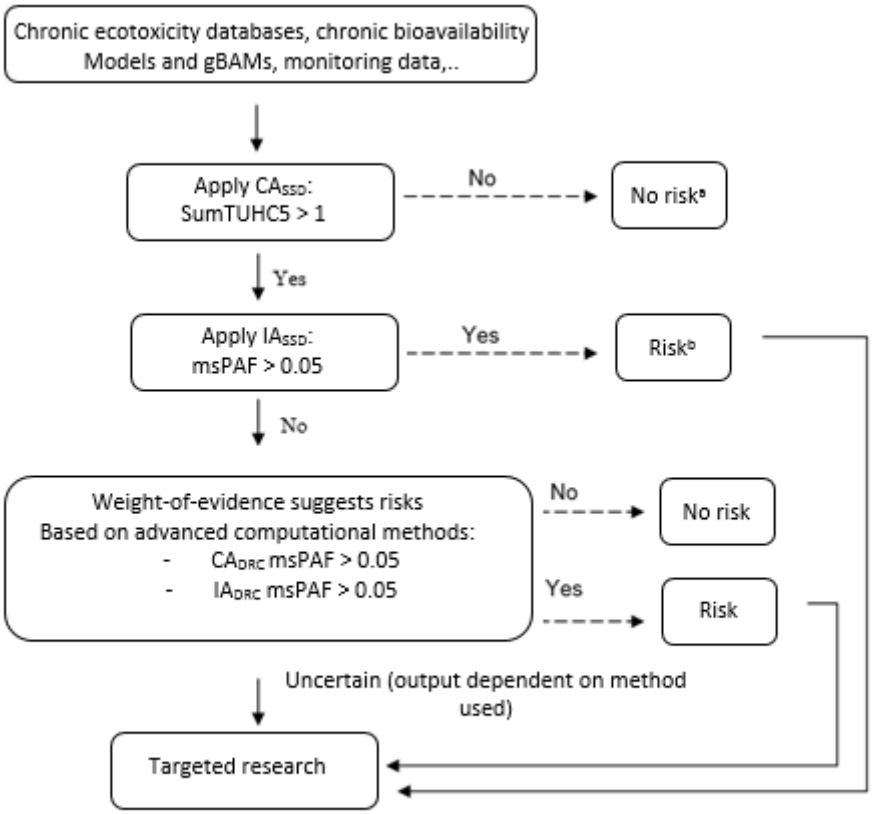

Figure 9.1. Possible tiered metal mixture risk evaluation scheme. A sample is defined to be at risk when the toxic pressure (expressed as multisubstance potentially affected fraction [msPAF]) was higher than 0.05 (or the sum toxic unit expressed relative to the hazardous concentrations affecting 5% of species within a community [SumTU$_{HC5}$] >1), which is equivalent to the typical protection goal for single substances, that is, a maximum of 5% affected species at the HC5 concentration. The msPAF values reported are on the basis of EC10 values. gBAMs = generalized bioavailability models; CA$_{SSD}$ = concentration addition applied directly to the species sensitivity distribution; IA$_{SSD}$ = independent action applied directly to the species sensitivity distribution; CA$_{DRC}$ = concentration addition applied to individual dose-response curves; IA$_{DRC}$ = independent action applied to individual dose-response curves. [a] Unless very strong synergisms at low effect levels. [b] Unless very strong antagonisms at low effect levels.

9.3. Future research recommendations

Although the recent focus on chronic metal mixture studies has increased the knowledge on metal mixture toxicity in a risk assessment context, there still remains a clear need for further research on several levels.

First, reliable chronic toxicity metal mixture toxicity data is at the moment only found for aquatic species belonging to the following two trophic levels: algae (Chapter 3 and Nys et al. 2017d), and invertebrates (Nys et al. 2017d). Hence, the mixture reference models, IA and CA, remain to be tested for the third important trophic level in environmental risk assessments, i.e. fish. Depending on results, it could be confirmed (or refuted) whether the IA$_{DRC}$ method is also the most accurate method for this trophi level. Furthermore, this trophic level should preferably also be added in a multi-species microcosm experiment. Effects on community composition or diversity were only observed at msPAF values above 0.05. However, effects on community functioning (notably community respiration and phytoplankton

metabolism) were observed at msPAF values of 0.05 or lower, i.e. in the Ni-Zn mixture, most likely because of the presence of one single dominant and very Zn and/or Ni sensitive species. This indicates that the cut-off msPAF value of 0.05 is not necessarily protective for all community level endpoints against metal mixture exposure. This should also be examined for a more complex community including fish species.

Second, the lack of chronic metal mixture data for other environmental compartments (soil, sediment and marine environments) hinders the extension of our analysis to these compartments.

Third, to further improve the relevance of metal mixture studies, we recommend to design future metal mixture studies by taking into account the following guidelines; i.e. measure dissolved metal concentrations and key water chemistry parameters, conduct single metal exposure and mixture exposure simultaneously and focus on chronic endpoints during prolonged exposures.

Fourth, despite the considerable research available, we do not yet fully understand how metals interact in mixtures. This is partly due to the fact that mechanistic studies are still largely lacking (but see below). Investigations into the mechanistic basis of these mixture interactions (e.g. at the bioaccumulation level) may lead to a better understanding of the observed interactive effects as well as the differences in observed interactive mixture effects between species.

Fifth, application of the tiered risk assessment scheme can be hampered by several issues. For instance, in reality, environmental monitoring datasets often contain a considerable number of data for which environmental concentrations are below the analytical detection limit, so called 'non-detect' data. This non-detect data increases the uncertainty of the risk predictions, because actual environmental concentrations can be any value between the detection limit and zero. In cases with $\sum \frac{DL}{HC5} > 1$, water quality managers might be advised to revisit these sampling locations and measure the metal concentrations with more precise equipment.

Sixth, although we recognize that efforts are taken to monitor the concentrations of metals and water chemistry variables throughout the year (e.g. FEA 2013), it is of utmost importance that these variables include pH, DOC concentration and Ca concentration as these three variables influence metal toxicity the most. In addition, we recommend to measure dissolved metal concentrations and not only total concentrations.

Finally, monitoring datasets may contain metals for which an SSD-based threshold derivation method is not available, because reliable toxicity data is limited (so-called 'data-poor' metals). For these metals, such as for instance tin (Sn) and antimony (Sb), the risk assessment methods explained in Chapter 2 are not applicable as these rely on SSD-based statistical extrapolation techniques. For these elements often only the so-called "base set" of toxicity data (i.e. x% effect concentration for algae, crustacean and fish) is used in environmental risk assessment processes. Hence, risks of metal mixtures containing these so-called 'data-poor' metals cannot be evaluated using the SSD-approach presented in the tiered risk assessment scheme (Figure 9.1). Currently, risks for these metals are estimated in metal-by-metal risk assessment approaches by calculating an environmental threshold value (ETV), such as the Predicted No-Effect Concentration (PNEC) or Environmental quality standard (EQS), based on the lowest ECx and applying an assessment factor which depends on the type of data (EC 2003). How risks of metal mixtures of data-rich and data-poor metals is addressed is discussed by Nys et al. (2017d). In

short, these authors combine the CA_{SSD} and CA_{DRC} methods from Chapter 2 with the calculations of the $RQ_{PEC/PNEC}$ and RQ_{STU} as described by Backhaus and Faust (2013) (see Chapter 1 and 2). As such, a tiered risk assessment scheme for mixtures combining SSD-metals and 'data-poor' metals is presented in Nys et al. (2017b).

9.4 Overall contribution of this study to risk assessment

Overall, several outcomes of the present work may contribute to risk assessment.

1. Four methods were combined to evaluate risk due to metal mixtures. These methods were extended in the present study to evaluate risks for data-rich metals. The methods combine chronic toxicity data, bioavailability modeling, SSDs, and CA or IA for ecological risk assessment by calculating the toxic pressure (expressed as msPAF values) based on measured concentrations of metals. Furthermore, we proposed a metal mixture risk evaluation scheme that may guide the incorporation of metal mixture into future risk assessment frameworks. The CA_{SSD} method could serve as a first (conservative) tier to identify situations with likely no potential risk at all, regardless of the method used ($SumTU_{HC5} < 1$) and the IA_{SSD} method could be used to identify situations of potential risk, also regardless of the method used ($msPAF_{IA,SSD} > 0.05$). The CA_{DRC} and IA_{DRC} methods could be used for site-specific assessment for situations that fall in between ($SumTU_{HC5} > 1$ and $msPAF_{IA,SSD} < 0.05$).This framework allows to pinpoint the sites that are at risk and to target the sites for which further research is necessary.
2. The chronic metal mixture toxicity data generated in this study increases our overall understanding of chronic metal mixture toxicity effects.
3. We found that metal mixture toxicity in communities is very complex and we argue that a mismatch between the species in the SSD and those in natural communities could explain why community-level effects can be observed below the cut-off value of 0.05 (msPAF) when these are not expected.
4. Four gBAM models were developed that can accurately predict chronic Cu and Zn toxicity to *D. magna* and *O. mykiss*. In addition, a metal mixture bioavailability model (MMBM) was developed that could accurately predict Cu-Ni-Zn and Cu-Ni toxicity to algae in diverse water characteristics. These models could be integrated into risk assessment frameworks to allow an ecologically more relevant and more accurate effects assessment of metals and/or metal mixtures. For instance, the chronic Zn gBAM for *D. magna* has recently been integrated in Bio-met, a tool to assess Environmental Quality Standard compliance of metals under the EU Water Framework Directive.
5. In this study, all bioavailability models were adapted to the "gBAM-structure" and all models were calibrated in WHAM VII. This ensures the uniformisation of all models to the same structure, the same speciation software and the same assumptions for binding to DOC, which can lead to an improvemed risk assessment for these metals.

References

Alstad NEW, Skardal L, Hessen DO. 1999. The effect of calcium concentration on the calcification of *Daphnia magna.* Limnology and Oceanography 44(8): 2011-2017

Anderson TD. Lydy MJ. 2002. Increased toxicity to invertebrates associated with a mixture of atrazine and organophosphate isecticides. Environmental Toxicology 21(7): 1507-1514

Arnold WR, Diamond RL, Smith DS. 2011. Acute and chronic toxicity of copper to the euryhaline rofiter, *Brachionus plicatilis* ("L" Strain). Archives of Environmental Contamination and Toxicology 60(2): 250-260

Australian and New Zealand Environment and Conservation Council and Agriculture and Resource Management Council of Australia and New Zealand. *2000*. Australian and New Zealand Guidelines for Fresh and Marine Water Quality, Vol 2: Aquatic Ecosystems—Rationale and Background Information. Australian Water Association, Artarmon, New South Wales, Australia; and the New Zealand Water & Wastes Association, Onehunga, Auckland, New Zealand.

Ay Ö, Kalay M, Tamer L, Canli M. 1999. Copper and lead accumulation in tissues of a freshwater fish *Tilapia zillii* and its effects on the branchial Na,K-ATPase activity. Bulletin of Environmental Contamination and Toxicology 62(2): 160-168

Baccouch S, Chaoui A, El Ferjani E. 1998. Nickel-induced oxidative damage and antioxidant responses in Zea mays shoots. Plant Physiology and Biochemistry 36(9), 689–694.

Backhaus T, Faust M. 2012. Predictive environmental risk assessment of chemical mixtures: a conceptual framework. Environmental Science and Technology 46: 2564-2573.

Backhaus T, Cedergreen N, Hutchinson T. *2011*. 3rd SETAC Europe Special Science Symposium, "Prospective and retrospective environmental risk assessment of mixtures: Moving from research to regulation." SETAC Globe 12 (April 14)

Baird DJ, Barber I, Bradley M, Soares AMVM, Calow P. 1991. A comparative study of genotype sensitivity to acute toxic stress using clones of *Daphnia magna* Straus. Ecotoxicology and Environmental Safety 21: 257-265

Baird DJ, Barata C. 1997. Variability in the response of Daphnia clones to toxic substances: Are safety margins being compromised? Archives of Toxicology Supplement 20:399–406.

Balistrieri LS, Mebane CA, Schmidt TS, Kelle WB. 2015. Expanding metal mixture toxicity models to natural stream and lake invertebrate communities. Environmental Toxicology and Chemistry 34:761–776.

Barata C, Baird DJ, Markich SJ. 1998. Influence of genetic and environmental factors on the tolerance of *Daphnia magn*a Straus to essential and non-essential metals. Aquatic Toxicology 42: 115-137

Besser JM, Mebane CA, Mount DR, Ivey CD, Kunz JL, Greer IE, May TW, Ingersoll CG. 2007. Sensitivity of mottled sculpins (*Cottus bairdi*) and rainbow trout (*Onchorhynchus mykiss*) to acute and chronic toxicity of cadmium, copper, and zinc. Environmental Toxicology and Chemistry 26: 1657–1665

Bio-met. Bioavailability of metals and the Water Framework Directive. http://bio-met.net/ [cited 2016 November 17]

Bliss CI. 1939. The toxicity of poisons applied jointly. Annals of Applied Biology 26:585–615.

Biesinger KE, Christensen GM. 1972. Effects of various metals on survival, growth, reproduction, and metabolism of *Daphnia magna*. Journal of the Fisheries Research Board Canada 29:1691–1700.

Bold HC, Wynne M J.1978. Introduction to the algae. Structure and reproduction. New Jersey, Prentice-Hall.

Bossuyt BTA, Janssen CR. 2005. Copper toxicity to different field-collected cladoceran species: intra- and inter-species sensitivity. Environmental Pollution 136: 145-154

Bræk GS, Jensen A, Mohus A. 1976. Heavy metal tolerance of marine phytoplankton. III. Combined effects of copper and zinc ions on cultures of four common species. Journal of Experimental Marine Biology and Ecology 25(1): 37-50

Bræk GS, Malnes D, Jensen A. 1980. Heavy metal tolerance of marine phytoplankton. IV. Combined effect of zinc and cadmium on growth and uptake in some marine diatoms. Journal of Experimental Marine Biology and Ecology 42(1): 39-54

Broderius SJ, Smith LL. 1979. Lethal and sublethal effects of binary mixtures of cyanide and hexavalent chromium, zinc or ammonia to the fathead minnow (*Pimephales promelas*) and rainbow trout (*Salmo gairdneri*). Journal of the Fisheries Research Board of Canada 36: 164-172

Brock TCM, Hammers-Wirtz M, Hommen U, Preuss TG, Ratte HT, Roessink I, Strauss T, Van den Brink PJ. 2014. The minimum detectable difference (MDD) and the interpretation of treatment-related effects of pesticides in experimental ecosystems. Environmental Science and Pollustion Research 22:1160–1174

Brönmark C, Hansson L. 2005. Biology of Lakes and Ponds. Oxford University Press, Oxford, UK.

Brown PH, Welch RM, Cary EE. 1987. Nickel: a micronutrient essential for higher plants. Plant Physiology 85(3): 801-803

Cairns Jr., J., Hart, K.M., Henebry, M.S., 1980. The effects of a sub-lethal dose of copper sulfate on the colonization rate of freshwater protozoan communities. The American Midland Naturalist 104: 93-101.

Campbell PGC, Stokes PM. 1985. Acidification and toxicity of metals to aquatic biota. Canadian Journal of Fisheries and Aquatic Sciences 42: 2034-2049.

Campbell PGC. 1995. Interactions between trace metals and aquatic organisms: a critique of the free-ion activity model. In: Tessier A, Turner DR (eds.). Metal Speciation and Bioavailability in Aquatic Systems. John Wiley & Sons Ltd., Chichester, UK. pp 45-102.

Carlisle DM, Clements WH. 1999. Sensitivity and variability of metrics used in biological assessments of running waters. Environmental Toxicology and Chemistry 18(2): 185-291

Cedergreen N, Christensen AM, Kamper A, Kudsk P, Mahiassen SK, Streibig J. 2008. A review of independent action compared to concentration addition as reference models for mixtures of compounds with different molecular target sites. Environmental Toxicology and Chemistry 27(7): 1621-1632

Chau YK, Kulikovsky-Cordeiro OTR. 1995. Occurrence of nickel in the Canadian environment. Environmental Reviews 3: 95-120.

Chen C, Huang D, Liu, J. 2009. Functions and toxicity of nickel in plants: Recent advances and future prospects. Clean - Soil, Air, Water 37(4-5): 304–313

Clements WH. 2004. Small-scale experiments support causal relationships between metal contamination and macroinvertebrate community responses. Ecological Applications 14:954–967.

Clements WH, Cadmus P, Brinkman S. 2013. Responses of aquatic insects to Cu and Zn in stream microcosms: understanding differences between single species tests and field responses. Environmental Science and Technology 47(13): 7506-7513

Colbourne, J. K., Crease, T. J., Weider, L. J., Hebert, P. D. N., Duferesne, F. and Hobæk, A. (1998), Phylogenetics and evolution of a circumarctic species complex (Cladocera: *Daphnia pulex*). Biological Journal of the Linnean Society, 65: 347–365.

Cooper NL, Bidwell JR, Kumar A. 2009. Toxicity of copper, lead, and zinc mixtures to *Ceriodaphnia dubia* and *Daphnia carinata*, Ecotoxicology and Environmental Safety 27(5): 1523-1528

Council of the European Union. 2009. Council conclusions on the Combination effects of chemicals: 17820/09. Brussels, Belgium.

Danish Environmental Protection Agency. 2008. European Union Risk Assessment Report (EU RAR) of nickel and nickel compounds prepared by the Danish Environmental Protection Agency (DEPA). Available on: http://echa.europa.eu/documents/10162/cefda8bc-2952-4c11-885f-342aacf769b3. Last accessed: 4/03/2017.

Davies DJA, Bennett BG. 1985. Exposure of man to environmental copper — An exposure commitment assessment. Science of The Total Environment 46(1): 215-227

DeForest DK, Meyer JS. 2015. Critical review: Toxicity of dietborne metals to aquatic organisms. Critical Reviews in Environmental Science and Technology 45: 1176-1241

Deleebeeck NME, De Schamphelaere KAC, Janssen CR. 2007a. A bioavailability model predicting the toxicity of nickel to rainbow trout (*Oncorhynchus mykiss*) and fathead minnow (*Pimephales promelas*) in synthetic and natural waters. Ecotoxicology and Environmental Safety 67, 1–13

Deleebeeck NME, Muyssen BTA, De Laender F, Janssen CR, De Schamphelaere KAC. 2007b. Comparison of nickel toxicity to cladocerans in soft versus hard surface waters. Aquatic Toxicology 84: 223-235.

Deleebeeck NME, De Schamphelaere KAC, Janssen CR. 2008. A novel method for predicting chronic nickel bioavailability and toxicity to *Daphnia magna* in artificial and natural waters. Environmental Toxicology and Chemistry 27: 2097–2107.

Deleebeeck NME, De Schamphelaere KAC, Janssen CR. 2009. Effects of Mg^{2+} and H^{+} on the toxicity of Ni^{2+} to the unicellular green alga *Pseudokirchneriella subcapitata*: model development and validation with surface waters. Science of the Total Environment 407: 1901–1914.

De Coninck DIM, Asselman J, Glaholt S, Janssen CR. 2014. Genome-wide transcription profiles reveal genotype-dependent responses of biological pathways and gene-families in Daphnia exposed to single and mixed stressors. Environmental Science and technology 48: 3513-3522

De Laender F, De Schamphelaere KAC, Vanrolleghem PA, Janssen CR. 2008. Do we have to incorporate ecological interactions in the sensitivity assessment of ecosystems? An examination of a theoretical assumption underlying species sensitivity distribution models. Environment International 34: 390-396

De Laender F, Janssen CR, De Schamphelaere KAC. 2009. Non-simultaneous ecotoxicity testing of single chemicals and their mixture results in erroneous conclusions about the joint action of the mixture. Chemosphere 76:428–432.

De Schamphelaere KAC, Janssen CR. 2002. A biotic ligand model predicting acute copper toxicity for *Daphnia magna*: the effects of calcium, magnesium, sodium, potassium, and pH. Environmental Science and Technology 36: 48-54.

De Schamphelaere KAC, Heijerick DG, Janssen CR. 2002. Refinement and field validation of a biotic ligand model predicting acute copper toxicity to *Daphnia magna*. Comparative Biochemistry and Physiology Part C: Toxicology & Pharmacology 133(1-2): 243-258

De Schamphelaere KAC, Vasconcelos FM, Heijerick DG, Tack FMG, Delbeke K, Allen HE, Janssen CR. 2003. Development and field validation of a predictive copper toxicity model for the green alga *Pseudokirchneriella subcapitata*. Environmental Toxicology and Chemistry 22: 2454-2465.

De Schamphelaere KAC, Janssen CR. 2004a. Development and field validation of a biotic ligand model predicting chronic copper toxicity to *Daphnia magna*. Environmental Toxicology and Chemistry 23: 1365-1375.

De Schamphelaere KAC, Janssen C. 2004b. Bioavailability of chronic toxicity of zinc to juvenile Rainbow Trout (*Oncorhynchus myskiss*) : comparison with other fish species and development of a biotic ligand model. Environmental Science and Technology 38: 6201-6209

De Schamphelaere KAC, Janssen CR. 2004c. Effects of dissolved carbon concentration and source, pH, and water hardness on chronic toxicity of copper to *Daphnia magna*. Environmental Toxicology and Chemistry 23(5): 1115-1122

De Schamphelaere KAC, Heijerick DG, Janssen CR. 2004. Comparison of different pH buffering techniques on the toxicity of copper and zinc to *Daphnia magna* and *Pseudokirchneriella subcapitata*. Ecotoxicology 13: 679-705

De Schamphelaere KAC, Lofts S, Janssen C. 2005. Bioavailability models for predicting acute and chronic toxicity of zinc to algae, daphnids, and fish in natural surface waters. Environmental Toxicology and Chemistry 24: 1190-1197.

De Schamphelaere KAC, Janssen CR. 2006. Bioavailability models for predicting copper toxicity to freshwater green microalgae as a function of water chemistry. Environmental Science and Technology 40: 4515-4522

De Schamphelaere KAC, Van Laer L, Deleebeeck NME, Muyssen BTA, Degryse F, Smolders E, Janssen CR. 2006a. Nickel speciation and ecotoxicity in European natural surface waters: development, refinement and validation of bioavailability models. Report prepared for the Nickel Producers Environmental Research Association

(NiPERA), Durham, NC, USA, Gent University, Laboratory of Environmental Toxicology and Aquatic Ecology, Gent, Belgium. Available online on: https://biblio.ugent.be/publication/5785290. Last accessed: 20/04/2017

De Schamphelaere KAC, Heijerick DG, Janssen CR. 2006b. Cross-phylum comparison of a chronic biotic ligand model to predict chronic toxicity of copper to a freshwater rotifer; *Brachionus calyciflorus* (Pallas*).* Ecotoxicology and Environmental Safety 63(2): 189-195

De Schamphelaere KAC, Janssen CR. 2008. Voluntary Risk Assessment of Copper, Copper II Sulphate Pentahydrate, Copper(I)Oxide, Copper(II)Oxide, Dicopper Chloride Trihydroxide – Chapter 3: Environmental Effects, Appendix U: Modelling copper bioavailability and toxicity in freshwater: uncertainty reduction for risk assessment (Chronic fish-BLM). European Copper Institute, Brussels, Belgium

De Schamphelaere KAC, Janssen C. 2010. Cross-phylum extrapolation of the *Daphnia magna* chronic biotic ligand model for zinc to the snail *Lymnaea stagnalis* and the rotifer *Brachionus calyciflorus*. Science of the Total Environment 408: 5414-5422.

De Zwart D, Posthuma L. 2005. Complex mixture toxicity for single and multiple species: proposed methodologies. Environmental Toxicology and Chemistry 24: 2665-2676.

Di Toro DM, Allen HE, Bergman HL, Meyer JS, Paquin PR, Santore RC. 2001. Biotic ligand model of the acute toxicity of metals. 1. Technical basis. Environmental Toxicology and Chemistry 20: 2383-2396

Downing AL, Leibold MA. 2002. Ecosystem consequences of species richness and composition in pond food webs. Nature 416: 837-841

Eaton JG. 1973. Chronic toxicity of a copper, cadmium and zinc mixture to the fathead minnow (*Pimephales promelas* rafinesque). Water Research 7(11): 1723-1736

Edwards BA, Jackson DA, Somers KM. 2015. Evaluating the effect of lake calcium concentration on the acquisition of carapace calcium by freshwater crayfish. Hydrobiologica 744: 91-100

Elendt BP, Bias WR. 1990. Trace nutrient deficiency in *Daphnia magna* cultured in standard medium for toxicity testing – Effects of the optimization of culture conditions on life history parameters of *Daphnia magna*. Water Research 24(9): 1157-1167

Elliot NG, Swain R, Ritz DA. 1986. Metal interaction during accumulation by the mussel *Mytilus edulis* planalatus. Marine Biology 93(3): 395

Enserink EL, Maas-Diepeveen JL, Van Leeuwen CJ. 1991.Combined effects of metals; an ecotoxicological evaluation, Water Research 25(6): 679-687

Erickson RJ, Benoit DA, Mattson VR, Leonard EN, Nelson HP. 1996. The effects of water chemistry on the toxicity of copper to fathead minnows. Environmental Toxicology and Chemistry 15: 181–193.

Esbaugh AJ, Mager EM, Brix KV, Santore R and Grosell M. 2013. Implications of pH manipulation methods for metal toxicity: not all acidic environments are created equal. Aquatic Toxicology 130-131:27-30.

European Commission. *2012*. The combination effects of chemicals: Chemical mixtures. Communication from the Commission to the Council. COM (2012) 252 Final. European Commission, Brussels Belgium.

European Commission. 2001. Decision N° 2455/2001/EC of the European Parliament and of the Council of 20 November 2001 establishing the list of priority substances in the field of water policy and amending Directive 2000/60/EC. Official Journal of the European Communities, Brussels, Belgium.

European Commission. 2003. Technical guidance document on risk assessment. Part 3 Environmental risk assessment. Available on: https://echa.europa.eu/documents/10162/16960216/tgdpart3_2ed_en.pdf . Last accessed: 01/04/2017.

European Commission. 2006. Directive 2013/39/EU of the European Parliament and of the Council of 18 December 2006 amending Council Directive 67/548/EEC on the approximation of laws, regulations and administrative provisions relating to the classification, packaging and labelling of dangerous substances in order to adapt it to Regulation (EC) No 1907/2006 concerning the Registration, Evaluation, Authorisation and Restriction of Chemicals (REACH) and establishing a European Chemicals Agency. Official Journal of the European Communities, Brussels, Belgium.

European Commission. 2008. Directive 2008/105/EC of the European Parliament and the Council on environmental quality standards in the field of water policy, amending and subsequently repealing Council Directives 82/176/EEC, 83/513/EEC, 84/156/EEC, 84/491/EEC, 86/280/EEC and amending Directive 2000/60/EC. Official Journal of the European Communities, Brussels, Belgium.

European Commission. 2011. Technical guidance document on deriving environmental quality standards. ISBN : 978-92-79-16228-2

European Commission. 2013. Directive 2013/39/EU of the European Parliament and of the Council of 12 August 2013 amending Directives 2000/60/EC and 2008/105/EC as regards priority substances in the field of water policy. Official Journal of the European Communities, Brussels, Belgium.

European Chemicals Agency. 2008. Guidance on information requirements and chemical safety assessment Appendix R.7.13-2: Environmental risk assessment for metals and metal compounds. Available online on: https://echa.europa.eu/documents/10162/13632/information_requirements_r7_13_2_en.pdf. Last accessed: 19/11/2015.

European Copper Institute, European Union. 2008. European Union Risk Assessment Report: Voluntary risk assessment of copper, copper II sulphate pentahydrate, copper(I)oxide, copper(II)oxide, dicopper chloride tri-hydroxide. Brussels, Belgium.

Farley KJ, Meyer JS, Balistrieri LS, De Schamphelaere KAC, Iwasaki Y, Janssen CR, Kamo M, Lofts S, Mebane CA, Naito W, Ryan AC, Santore RC, Tipping E. *2015*. Metal Mixture Modelling Evaluation Project: 2. Comparison of four modelling approaches. Environmental Toxicology and Chemistry 34:741–753

Fernandez-Leborans, G., Novillo, A., 1993. Changes in trophic structure of a freshwater protozoan community subjected to cadmium. Ecotoxicology and Environmental Safety 25, 271-279

Fernandez-Leborans, G., Novillo, A., 1996. Protozoan communities and contamination of several uvial systems. Water Environment Research 68, 311-319

Finlayson BJ, Verrue KM. 1982. Toxicities of copper, zinc, and cadmium mixtures to juvenile Chinook salmon. Transactions of the American Fisheries Society 111 (5): 645-650

Fleeger JW, Carman KR, Nisbet RM. 2003. Indirect effects of contaminants in aquatic ecosystems. Science of the Total Environment 317: 207–233.

Forbes VE, Calow P. 2002. Species sensitivity distributions revisited: A critical appraisal. Human and Ecological Risk Assessment 8: 473-492

Flouty R, Khalaf G. 2015. Role of Cu and Pb on Ni bioaccumulation by *Chlamydomonas reinhardtii*: validation of the biotic ligand model in binary metal mixtures. Ecotoxicology and Environmental Safety 133: 79-86

Fortunati P, Lombi E, Hamon RE, Nolan AL, McLaughlin MJ. 2005. Effect of toxic cations on copper rhizotoxicity in wheat seedlings. Environmental Toxicology and Chemistry 24: 372–378

Franklin NM, Stauber JL, Lim RP, Petocz P. 2002. Toxicity of Metal Mixtures to a Tropical Freshwater Alga (*Chlorella* sp.): The Effect of Interactions Between Copper, Cadmium, and Zinc on Metal Cell Binding and Uptake. Environmental Toxicology and Chemistry 11: 2412–2422

Gable DS, Schnitzer M. 1973. The chemistry of fulvic acid and its reactions with metal ions. In Singer PC, ed, Trace Metals and Metal Organic Interactions in Natural Waters. Ann Arbor Science, Ann Arbor, MI, USA, pp 225-302

Gajewska E, Skłodowska M. 2005. Antioxidative responses and proline level in leaves and roots of pea plants subjected to nickel stress. Acta Physiologiae Plantarum*: 27*(3), 329–340.

Galvez F, Gensemer RW, Goss GG, Hogstrand C, Janssen CR, McGeer JC, Naddy RB, Playle RC, Santore RC, Schneider U, Stubblefield WA, Wood CM, Wu KB. 2002. The biotic ligand model: a historical overview.

Gao C, De Schamphelaere KAC, Smolders E. 2016. Zinc toxicity to the alga *Pseudokirchneriella subcapitata* decreases under phosphate limiting growth conditions, Aquatic Toxicology 173: 74-82,

Gerhardt A, Janssens de Bisthoven L, Soares AMVM. 2004. Macroinvertebrate response to acid mine drainage: community metrics and on-line behavioural toxicity bioassay. *Environmental Pollution* 130: 263-274.

Gerhardt A, Janssens de Bisthoven L, Guhr K, Soares AMVM, Pereira MJ. 2008. Phytoassessment of acid mine drainage: *Lemna gibba* bioassay and diatom community structure. *Ecotoxicology* 17: 47-58.

Gopalapillai Y, Hale B. 2015. Evaluating the concentration addition approach for describing expected toxicity of a ternary metal mixture (Ni, Cu, Cd) using metal speciation and response surface regression. Environmental Chemistry 13: 447-456

Gregorio V, Chèvre N, Junghans M. 2013. Critical issues in using the common mixture toxicity models concentration addition or response addition on species sensitivity distributions: A theoretical approach. *Environmental Toxicology and Chemistry* 32: 2387–2395.

Grosell M. 2011. Copper. In Wood CM, Farell AP, Brauner CJ, Homeostasis and Toxicology of Essential Metals, Vol 31A, Academic Press, Londen, pp. 53-133

Halliwell B, Gutteridge JM. 1984. Oxygen toxicity, oxygen radicals, transition metals and disease. Biochemical Journa*l* 219(1): 1-14.

Hatano A, Shoji R. 2008. Toxicity of copper and cadmium in combinations to duckweed analyzed by the biotic ligand model. Environmental Toxicology 23:372–378.

Heijerick DG, De Schamphelaere KAC, Janssen CR. 2002a. Biotic ligand model development predicting Zn toxicity to the alga *Pseudokirchneriella subcapitata*: Possibilities and limitations. Comparative Biochemistry and Physiology - C Toxicology and Pharmacology 133(1-2): 207–218.

Heijerick D, Bossuyt B, Janssen C. 2002b. Euro-Ecole: Assessment of the Bioavailability and Potential Ecological Effects of Copper in European Surface Waters. Subproject 4: Evaluation and improvement of the ecological relevance of laboratory generated toxicity data.

Heijerick DG, Bossuyt BT, De Schamphelaere KAC, Indeherberg M, Mingazzini M, Janssen, CR. 2005a. Effect of varying physicochemistry of European surface waters on the copper toxicity to the green alga *Pseudokirchneriella subcapitata.* Ecotoxicology 14(6): 661-670

Heijerick, D.G., De Schamphelaere, K.A.C., Van Sprang, P.A., Janssen, C.R., 2005b. Development of a chronic zinc biotic ligand model for Daphnia magna. Ecotoxicology and Environmental Safety 62: 1-10

Hessen DO, Alstad NEW, Skardal L. 2000. Calcium limitation in *Daphnia magna*. Journal of Plankton Research 22(3): 553-568

Hickey CW, Golding LA. 2002. Response of macroinvertebrates to copper and zinc in a stream mesocosm. Environmental Toxicology and Chemistry 21: 1854–1863

Hoang TC, Tomasso JR, Klaine SJ. 2004. Influence of water quality and age on nickel toxicity to fathead minnows (*Pimephales promelas*). Environmental Toxicology and Chemistry 23: 86–92

Hochmuth JD, Asselman J, De Schamphelaere KAC. 2014. Are interactive effects of harmful algal blooms and copper pollution a concern for water quality management? Water Research 60: 41-53

Hogstrand C, Reid SD, Wood CM. 1995. Ca^{2+} versus Zn^{2+} transport in the gills of fresh-water rainbow-trout and the cost of adaptation to waterborne Zn^{2+}. Journal of Experimental Biology 198: 337-348

Hogstrand C. 2012. Zinc. In: Wood C, Farrell A, Brauner C (eds). Fish Physiology- Volume 31A: Homeostasis

Hommen U, Veith D, Ratte HT. 1994. A computer program to evaluate plankton data from freshwater field tests. In Hill IR, Heimbach F, Leeuwangh P, Matthiess en P, eds , Freshwater Field Tests for Hazard Assessment of Chemic als. Lewis, Boca Raton, FL, USA, pp 503–513.

Hommen U, Knopf B, Rüdel H, Schäfers C, De Schamphelaere KAC, Schlekat C, Garman ER. 2016. A microcosm study to support aquatic risk assessment of nickel: community-level effects and comparison with bioavailability-normalized species sensitivity distributions. Environmental Toxicology and Chemistry 35: 1172-1182

Hong S, Candelone J-P, Soutif M, Bouton DF. 1996. A reconstruction of changes in copper production and copper emissions to the atmosphere during the past 7000 years. Science of the Total Environment 188(2): 183-193

Hooper HL, Connon R, Callaghan A, Fryer G, Yarwood-Buchanan S, Biggs J, Maund SJ, Hutchinson TH, Sibly RM. 2008. The ecological niche of *Daphnia magna* characterized using population growth rate. Ecology 89(4): 1015-1022

HydroQual. 2005. BLM Windows Interface, Version 2.1.2. Mahwah, NJ, USA.

International Lead and Zinc Study Group. 2017. Lead and Zinc statistics. http://www.ilzsg.org/static/statistics.aspx. Last accessed: 10/04/2017.

Israr M, Jewell A, Kumar D, Sahi SV. 2011. Interactive effects of lead, copper, nickel and zinc on growth, metal uptake and antioxidative metabolism of *Sesbania drummondii*, Journal of Hazardous Materials 186(1-2): 1520-1526

Iwasaki Y, Kamo M, Naito W. 2015. Testing an application of the biotic ligand model to predict acute toxicity of metal mixtures to rainbow trout. Environmental Toxicology and Chemistry 34:754–760

Iwasaki Y, Brinkman SF. 2015. Application of a generalized linear mixed model to analyze mixture toxicity: survival of brown trout affected by copper and zinc. Environmental Toxicology and Chemistry 34: 816-820.

Jezierska B, Lugowska K, Witeska M. 2009. The effects of heavy metals on embryonic development of fish (a review). Fish Physiology and Biochemistry 35(4): 625-640

Jho EH, An J, Nam K., 2011. Extended biotic ligand model for prediction of mixture toxicity of Cd and Pb using single metal toxicity data. Environmental Toxicology and Chemistry 30:1697–1703.

Jonker MJ, Svendsen C, Bedaux JJM, Bongers M, Kammenga JE. 2005. Significance testing of synergistic/antagonistic, dose level-dependent, or dose ratio-dependent effects in mixture dose-response analysis. Environmental Toxicology and Chemistry 24:2701–2713.

Jonker MJ, Gerhardt A, Backhaus T, van Gestel CAM. 2011. Test design, mixture characterization and data evaluation. In: van Gestel CAM, Jonker MJ, Kammenga JE, Laskowski R, Svendsen C, editors. Mixtur toxicity: Linking approaches from ecological and human toxicology. CRC Press, Pensacola, FL, USA. pp 121-155.

Jumars PA, Penry DL, Baross JA, Perry MJ, Frost BW. 1989. Closing the microbial loop: dissolved carbon pathway to heterotrophic bacteria from incomplete ingestion, digestion and absorption in animals. Deep Sea Research Part A. Oceanographic Research Papers 36(4): 483-495

Kamo M, Nagai T. 2008. An application of the biotic ligand model to predict the toxic effects of metal mixtures. Environmental Toxicology and Chemistry 27:1479–1487.

Kandegedara A, Rorabacher DB. 1999. Noncomplexing tertiary amines as 'better' buffers covering the range of pH 3-11. Temperature dependence of their acid dissociation constants. Analytical Chemistry 71: 3140-3144

Kargin F, Cogun HY. 1999. Metal interactions during accumulation and elimination of zinc and cadmium in tissues of the freshwater fish *Tilapia nilotica*. Bulletin of Environmental Contamination and Toxicology 63(4): 511-519

Kayambo S, Mbwette TSA, Mayo AW, Katima JHY, Jorgensen SE. 2002. Diurnal cycles of variation of physical-chemical parameters in waste stabilization ponds. Ecological Engineering 18(3): 287-291

Knauer K, Behra R, Sigg L. 1997. Adsorption and uptake of copperb y the green alga *Scenedesmus subspicatus* (Chlorophyta) Journal of Phycology 33: 596-601

Kortenkamp A, Backhaus T, Faust M. 2009. State of the art report on mixture toxicity. The School of Pharmacy, University of London, London, UK.

Kortenkamp A, Altenburger R. 2011. Toxicity from combined exposure to chemicals. In: Van Gestel CAM, Jonker MJ, Kammenga JE, Laskowski R, Svendsen C (eds). Mixture toxicity: Linking approaches from ecological and human toxicology. SETAC Press, Pensacola, FL, USA. pp 95-119.

Laetz CA, Baldwin DH, Collier TK, Hebert V, Stark JD, Scholz NL. 2009. The Synergistic Toxicity of Pesticide Mixtures: Implications for Risk Assessment and the Conservation of Endangered Pacific Salmon. Environmental Health Perspectives 117(3):348-353.

Larsen, J., Nilsson, J.R., 1983. E€ects of nickel on the rates of endo-cytosis, motility, and terminations on the cell content of the metal. Protoplasma 118, 140-147

Lehman JL, Vasconcelos AC. 1979. Physiology of zinc and cadmium stress in the marine diatom *Cylindrotheca closterium*. Journal of Phycology 15: 19

Lifset RJ, Eckelman MJ, Harper EM, Hausfather Z, Urbina G. 2012. Metal lost and found: Dissipative uses and releases of copper in the United States 1975-2000. Science of the Total Environment 417-418: 138-147

Liu GD. 2001. A new essential mineral element – nickel. Plant Nutrition and Fertilizer Science 7(1): 101-103

Liu Y, Vijver MG, Qiu H, Baas J, Peijnenburg WJGM. 2015. Statistically significant deviations from additivity: What do they mean in assessing toxicity of mixtures?, Ecotoxicology and Environmental Safety 122: 37-44

Loewe S, Muischnek H. 1926. Effect of combinations: mathematical basis of problem. Archiv fur Experimentelle Pathologie und Pharmakologie 114: 313-326.

Lofts S, Tipping E. 2011. Assessing WHAM/Model VII against field measurements of free metal ion concentrations: model performance and the role of uncertainty in parameters and inputs. Environmental Chemistry 8: 501-516.

Luoma SN, Rainbow PS. 2008. Metal contamination in aquatic environments. University Press, Cambrigde, UK. 571 pp

Lynch NR, Hoang TC, O'Brien TE. 2016. Acute toxicity of binary-metal mixtures of copper, zinc, and nickel to Pimephales promelas: Evidence of more-than-additive effect. Environmental Toxicology and Chemistry 35: 446–457

Madoni P. 2000. The acute toxicity of nickel to freshwater ciliates. Enviornnmental Pollution 109: 53-59

Malmberg CG, Maryott AA. 1956. Dielectric constant of water from 0° to 100°C. Journal of Research of the National Bureau of Standards 56(1). Research paper 2641

Macomber L, Imlay JA. 2009. The iron-sulfur clusters of dehydratases are primary intracellular targets of copper toxicity. Proceedings of the National Academy of Sciences 106(20): 8344-8349

Mebane CA, Schmidt TS, Balistrieri LS. 2016. Larval aquatic insect responses to cadmium and zinc in experimental streams. Environmental Toxicology and Chemistry 36(3):749-762

Toxicol Chem, iMebane CA, Schmidt TS, Balistrieri LS. 2017. Larval aquatic insect responses to cadmium and zinc in experimental streams. Environmental Toxicology and Chemistry 36: 749–762.

Messiaen M, Janssen CR, De Meester C, De Schamphelaere KAC. 2013. The initial tolerance to sub-lethal Cd exposure is the same among ten naïve pond populations of *Daphnia magna*, but their micro-evolutionary potential to develop resistance is very different. Aquatic Toxicology 144-145: 322-331

Mendes LF, Stevani CV, Zambotti-Villela L, Yokoya N. 2014. Toxic effect of metal cation binary mixtures to the seaweed *Gracilaria domingensis* (Gracilariales, Rhodophyta). Environmental Science and Pollution Research 21(13): 8216-8223

Mehta SK, Tripathi BN, Gaur JP. 2000. Influence of pH, temperature, culture age and cations on adsorption and uptake of Ni by *Chlorella vulgaris.* European Journal of Protistology 36(4): 443-450

Meyer JS, Santore RC, Bobbitt JP, Debrey LD, Boese CJ, Paquin PR, Allen HE, Bergman HL, Di Toro DM. 1999. Binding of nickel and copper to fish gills predicts toxicity when water hardness varies, but free-ion activity does not. Environmental Science and Technology 33: 913-916.

Meyer JS, Farley KJ, Garman ER. 2015. Metal Mixtures Modeling Evaluation project: 1. Background. Environmental Toxicology and Chemistry 34: 726–740

Morel FMM. 1983. Principles of Aquatic Chemistry. John Wiley and Sons, New York, USA. 446 pp.

Morgan, G.B., Lackey, J.B., 1958. BOD determinations in wastes containing chelated copper and chromium. Sewage Industrial Wastes 30, 283-286

Muyssen BTA, Janssen CR. 2001. Multigeneration zinc acclimation and tolerance in *Daphnia magna*: implications for water-quality guidelines and ecological risk assessment. Environmental Toxicology and Chemistry 20(9): 2053-2060

Muyssen BTA, Janssen CR, Bossuyt BTA. 2002. Tolerance and acclimation to zinc of field-collected *Daphnia magna* populations. Aquatic Toxicology 56: 69-79

Muyssen BTA, De Schamphelaere KAC, Janssen CR. 2006. Mechanisms of chronic waterborne Zn toxicity in *Daphnia magna*. Aquatic Toxicology 77: 393-401

Muyssen BTA, De Schamphelaere KAC, Janssen CR. 2009. Calcium accumulation and regulation in *Daphnia magna:* Links with feeding, growth and reproduction. Comparative Biochemistry and Physiology, Part A 152: 53-57

Naeem S, Li S. 1997. Biodiversity enhances ecosystem reliability. Nature, 390(6659), 507-509

Naddy RB, Cohen AS, Stubblefield WA. 2015. The interactive toxicity of cadmium, copper and zinc *to Ceriodaphnia dubia* and rainbow trout (*Oncorhynchus mykiss*). Environmental Toxicology and Chemistry 34: 809-815

Nagai T*,* Kamo M. 2014*.* Comparative modeling of the effect of metal mixtures on algal growth using biotic ligand model, concentration additive, and independent action*.* Japanese Journal of Environmental Toxicology 17*:*57–68

Nagai T, De Schamphelaere KAC. 2016. The effect of binary mixtures of zinc, copper, cadmium, and nickel on the growth of the freshwater diatom *Navicula pelliculosa* and comparison with mixture toxicity model predictions. Environmental Toxicology and Chemistry 35: 2765–2773

Nickel Institute. 2017. http://www.nickelinstitute.org. Last accessed: 19/04/2017.

Norwood WP, Borgmann U, Dixon DG, Wallace A. *2003*. Effects of metal mixtures on aquatic biota: A review of observations and methods. Human and Ecological Risk Assess 9:795–811

Norwood WP, Borgmann U, Dixon DG. 2007. Interactive effects of metals in mixtures on bioaccumulation in the amphipod *Hyalella azteca*. Aquatic Toxicology 84(2): 255-267

Norwood WP, Borgmann U, Dixon DG, Wallace A. 2013. An effects addition model based on bioaccumulations of metals from exposure to mixtures of metals can predict chronic mortality in the aquatic invertebrate *Hyalella azteca*. Environmental Toxicology and Chemistry 32(7): 1672-1681

Nriagu JO. 1980. Nickel in the Environment. John Wiley & Sons, New York, USA. 833 pp.

Nriagu JO. 1996. A history of global metal pollution. Science 272: 223-224.

Nys C, Janssen CR, Van Sprang PA, De Schamphelaere KAC. 2012. Ni-EXTEND: extending the chronic nickel BLM from pH 8.2 to pH 8.7 and validation of the BLM-normalized HC5(50%) for Ni against the ecological effects observed in a 4-month microcosm experiment. Report prepared for NiPERA.

Nys C, Asselman J, Hochmuth JD, Janssen CR, Blust R, Smolders E, De Schamphelaere KAC. 2015 Mixture toxicity of nickel and zinc to *Daphnia magna* is noninteractive at low effect sizes but becomes synergistic at high effect sizes. Environmental Toxicology and Chemistry, 34: 1091–1102

Nys C. 2016. Bioavailability and chronic toxicity of metal mixtures in freshwater: modelling and implementation in risk assessment. PhD thesis, Ghent University, Ghent, Belgium

Nys C, Janssen CR, Blust R, Smolder E, De Schamphelaere KAC. 2016a. Reproductive toxicity of binary and ternary mixture combinations of Ni, Zn and Pb to *Ceriodaphnia dubia* is best predicted with the intendent action model. Environmental Toxicology and Chemistry 35: 1796-1805

Nys C, Van Regenmortel T, Janssen CR, Blust R, Smolders E, De Schamphelaere KAC. 2016b. Comparison of chronic mixture toxicity of nickel-zinc-copper and nickel-zinc-copper-cadmium mixtures between *Ceriodaphnia dubia* and Pseudokirchneriella subcapitata. Environmental Toxicology and Chemistry 36(4): 1056-1066

Nys C, Janssen CR, De Schamphelaere KAC. 2017a. Development and validation of a metal mixture bioavailability model (MMBM) to predict chronic toxicity of Ni-Zn-Pb mixtures to *Ceriodaphnia dubia*. Environmental Pollution 220B: 1271-1281

Nys C, Van Regenmortel T, Janssen CR, Blust R, Smolders E, De Schamphelaere KAC. 2017b. Comparison of chronic mixture toxicity of nickel-zinc-copper and nickel-zinc-copper-cadmium mixtures between *Ceriodaphnia dubia* and *Pseudokirchneriella subcapitata*. Environmental Toxicology and Chemistry 36: 1056–1066

Nys C, Versieren L, Cordery KI, Blust R, Smolders E, De Schamphelaere KAC. 2017c. Systematic evaluation of chronic metal-mixture toxicity to three species and impications for risk assessment. Enviornmental Science and Technology 51(8): 4615-4623

Nys C, Van Regenmortel T, Janssen CR, Oorts K, Smolders E, De Schamphelaere KAC. 2017d. Risk assessment of metal mixtures in aquatic systems. Environmental toxicology and chemistry, submitted

Oller AR, Costa M, Oberdörster G. 1997. Carcinogenicity Assessment of Selected Nickel Compounds. Toxicology and Applied Pharmacology: 143(1), 152–166.

Organization of Economic Cooperation and Development (OECD) 201 2011. OECD guidelines for the testing of chemicals. Section 2: Effects on Biotic Systems. Test No. 201 Freshwater Alga and Cyanobacteria, Growth Inhibition Test.

Organization of Economic Cooperation and Development (OECD) 211. 2012. OECD guidelines for the testing of chemicals. Section 2: Effects on Biotic Systems. Test No. 211 *Daphnia magna* Reproduction Test.

Pagenkopf GK. 1983. Gill surface interaction model for trace-metal toxicity to fish: role of complexation, pH, and water hardness. Environmental Science and Technology 17: 342-347.

Pane EF, Smith C, McGeer JC, Wood CM. 2003. Mechanisms of acute and chronic waterborne nickel toxicity in the freshwater cladoceran, *Daphnia magna*. Environmental Science and Technology 37: 4382-4389

Paulauskis JD, Winner RW. 1988. Effects of water hardness and humic acid on zinc toxicity to *Daphnia magna* Straus, Aquatic Toxicology 12(3): 273-290

Paquin PR, Gorsuch JW, Apte S, Batley GE, Bowles KC, Campbell PGC, Delos CG, Di Toro DM, Dwyer RL, Galvez F, Gensemer RW, Goss GG, Hogstrand C, Janssen CR, McGeer JC, Naddy RB, Playle RC, Santore RC, Schneider U, Stubblefield WA, Wood CM, Wu KB. 2002. The biotic ligand model: a historical overview. Comparative Biochemistry and Physiology C 133: 3-35

Pickering Q. 1974. Chronic Toxicity of Nickel to the Fathead Minnow. Water Pollution Control Federation 46(4): 760-765

Prevot P, Soyer-Gobillard M-O. 1986. Combined action of cadmium and selenium on two marine dinoflagellates in culture, *Prorocentrum micans* Ehrbg. and *Crypthecodinium cohnii* Biecheler1. The Journal of Protozoology, 33: 42–47.

Pyle G, Couture P. 2012 Nickel. In: Wood C, Farrell A, Brauner C (eds). Fish Physiology- Volume 31A: Homeostasis and Toxicology of Essential Metals. Academic Press, Amsterdam, The Netherlands. pp 253-289.

Radivojević M, Rehren T, Pernicka E, Šljivar D, Brauns M, Borić D. 2010. On the origins of extractive metallurgy: new evidence from Europe. Journal of Archaeological Science: 37(11): 2775-2787

Reck BK, Muller DB, Rostokowski K, Greadel TE. 2008. Anthropogenic Nickel Cycle: Insights intouse, trade and recycling. Environmental Science and Technology 42: 3394-3400.

Richardson JS, Kiffney PM. 2000. Responses of a macroinvertebrate community from a pristine, southern British Columbia, Canada, stream to metals in experimental mesocosm. Environmental Toxicology and Chemistry 19:736–743.

Risk assessment zinc metal – environmental part. Final draft submitted to the European Chemicals Bureau (Ispra, Italy) by the National Institute for Public Health and the Environment (RIVM), Bilthoven, The Netherlands; 2006

Rodriguez PH, Arbildua JJ. 2012.) in the presence of 2 mg/L DOC. Report submitted to the International Copper Association (ICA).

Salminen R, Batista MJ, Bidovec M, Demetriades A, De Vivo B, De Vos W, Duris M, Gilucis A, Gregorauskiene V, Halamic J, Heitzmann P, Lima A, Jordan G, Klaver G, Klein P, Lis J, Locutura J, Marsina K, Mazreku A, O'Connor PJ, Olsson SÅ, Ottesen R-T, Petersell V, Plant JA, Reeder S, Salpeteur I, Sandström H, Siewers U, Steenfelt A, Santore RC, Di Toro DM, Paquin PR, Allen HE, Meyer JS. 2001. Biotic ligand model of the acute toxicity of metals. 2. Application to acute copper toxicity in freshwater fish and Daphnia. Environmental Toxicology and Chemistry 20: 2397-2402.

Santore RC, Ryan AC. 2015. Development and application of a multimetal multibiotic ligand model for assessing aquatic toxicity of metal mixtures. Environmental Toxicology and Chemistry 34: 777-787.

Schäfers C. 2001. Community level study with copper in aquatic microcosms. Fraunhofer Institute for Molecular Biology and Applied Ecology, Schmallenberg, Germany.

SCHER, scientific opinion on the risk assessment report on zinc, environmental part, 29 November 2007.

Schlekat CE, Van Genderen E, De Schamphelaere KAC, Antunes PMC, Rogevich EC, Stubblefield WA. 2010. Cross-species extrapolation of chronic nickel Biotic Ligand Models. Science of the Total Environment 408(24): 6148-6157

Schwartz ML, Vigneault B. 2007. Development and validation of a chronic copper biotic ligand model for *Ceriodaphnia dubia*. Aquatic Toxicology 84(2): 247-254

Scientific Committee on Health and Environmental Risks. 2009. Voluntary Risk Assessment Report on Lead and its compounds, Environmental Part. SCHER Opinion 27th plenary on 13 January 2009. 18 p. Available on: http://ec.europa.eu/health/ph_risk/committees/04_scher/docs/scher_o_111.pdf. Last accessed: 01/04/2017.

Sevin IF. 1980. Nickel. In: Waldron HA (ed). Metals in the Environment. Academic Press, London, UK. Pp 263-291.

Shannon, C. E. & Weaver, W. 1949. The mathematical theory of communication. University of Illinois Press, Urbana.

Sharma SS, Schat H, Vooijs R, Van Heerwaarden LM. 1999. Combination toxicology of copper, zinc, and cadmium in binary mixtures: Concentration-dependent antagonistic, nonadditive, and synergistic effects on root growth in *Silene vulgaris*. Environmental Toxicology and Chemistry 18: 348–355.

Shaw JR, Dempsey TD, Chen CY, Hamilton JW, Folt CL. 2006. Comparative toxicity of cadmium, zinc and mixtures of cadmium and zinc to daphnids. Environmental Toxicology and Chemistry 25: 182-189

Skidmore JF. 1964. Toxicity of zinc compounds to aquatic animals, with special reference to fish. The Quarterly review of biology 39(3)

Smith RM, Martel AE, Motekaitis RJ. 2004. NIST standard reference database46. NIST critically selected stability constans of metal complexes database. Ver 8.0 for +Windows. National Institute of Standards and Technology, Gaithersburg, MD, USA.

Sokal RR, Rohlf FJ. 1995. Biometry: the principles and practice of statistic in biological research. WH Freeman, New York.

Spehar RL, Fiandt JT. 1986. Acute and chronic effects of water quality criteria-based metal mixtures on three aquatic species. Environmental Toxicology and Chemistry 5: 917-931

Spencer DF, Greene, RW. 1981. Effects of nickel on seven species of freshwater algae. Environmental Pollution Series A, Ecological and Biological 25(4): 241–247

Spry DK, Wood CM. 1985. A kinetic method for the measurement of zinc influx in vivo in the rainbow trout, and the effects of waterborne calcium on flux rates. Journal of Experimental Biology 142: 425-466.

Stockdale A, Tipping E, Lofts S, Ormerod SJ, Clements WH, Blust R. 2010. Toxicity of proton–metal mixtures in the field: Linking stream macroinvertebrate species diversity to chemical speciation and bioavailability, Aquatic Toxicology 100(1): 112-119

Stumm W and Morgan JJ. 1996. Aquatic chemistry: Chemical equilibria and rates in natural waters: 3rd edition. John Wiley & Sons, New York, USA.

Sverdrup HU, Ragnarsdottir KV, Koca D. 2014. On modelling the global copper mining rates, market supply, copper price and the end of copper reserves. Resources, Conservation and Recycling 87: 158-174

Tarvainen T, 2005. Geochemical Atlas of Europe. Part 1: Background Information, Methodology and Maps. Espoo, Geological Survey of Finland, 526 pages, 36 figures, 362 maps

Ter Braak CJF, Smilauer P. 2002. CANOCO Reference Manual and CanoDRAW for Windows User's Guide: Software for Canocical Community Ordination, Ver 4.5. Microcomputor Power, Ithaca, NY, USA

Tipping E. 1994. WHAM – a chemical equilibrium model and computer code for waters, sediments and soils incorporating a discrete sie/electorstatic model of ion-binding by humic substances. Computational Geosciences 20, 973-1023

Tipping E. 1998. Humic ion-binding model VI: An improved description of the interactions of protons and metal ions with humic substances. Aquat Geochem 4:3–48.

Tipping E. 2002. Cation binding by humic substances. Cambridge environmental chemistry series. Cambridge University Press, New York. 448 pp.

Tipping E, Lofts S, Sonke JE. 2011. Humic Ion-Binding Model VII: a revised parameterisation of cation binding by humic substances. Environmental Chemistry 8(3): 302-325.

Tipping E, Lofts S. 2013. Metal mixture toxicity to aquatic biota in laboratory experiments: Application of the WHAM-FTOX model. Aquatic Toxicology 142: 114-122.

Tipping E, Lofts S. 2015. Testing WHAM-Ftox with laboratory toxicity data for mixtures of metals (Cu, Zn, Cd, Ag, Pb). Environmental Toxicology and Chemistry 34: 788-798.

Traas TP, van de Meent D, Posthuma L, Hamers T, Kater BJ, de Zwart D, Aldenberg T. 2002. The potentially affected fraction as a measure of ecological risk. In: Podthuma L, Suter II GW, Traas TP (Eds): Species sensitivity distributions in ecotoxicology. Lewis Publishers, Boca Raton (FL), USA.

United States Environmental Protection Agency. 1991. Technical support document for water quality-based toxics control. EPA 505/2–90/001. Washington, DC.

United States Environmental Protection Agency. 1994. Appendix L. In Water Quality Standards Handbook, 2nd ed. Washington, DC.

United States Environmental Protection Agency. 1986. Quality criteria for water. Environmental Protection Agency, Office of Water, Criteria and Standards Division, Washington, DC, USA, EPA 440-5-86-001.

United States Environmental Protection Agency 2007. Aquatic life ambient freshwater quality criteria – copper. EPA-822-R-07-001. Office of Water 4304T, Washington DC, USA.

United States Geological Survey. 1998. Copper hazards to fish, wildlife and invertebrates: a synoptic review United States Geological Survey. 2014b. Mineral yearbook (2014): zinc. Available online: http://minerals.usgs.gov/minerals/pubs/commodity/zinc/. Last accessed: 04/04/2017.

United States Geological Survey. 2013. Mineral yearbook (2014): nickel. Available online: http://minerals.usgs.gov/minerals/pubs/commodity/nickel/. Last accessed: 04/04/2017.

United States Geological Survey. 2014a. Mineral yearbook (2014): copper. Available online: http://minerals.usgs.gov/minerals/pubs/commodity/copper/. Last accessed: 04/04/2017.

Van den Brink PJ, Van Wijngaarden RPA, Lucassen WGH, Brock TCM, Leeuwang P. 1996. Effects of the insecticide Dursban 4E (active ingredient chlorpyrifos) in outdoor experimental ditches: II. Invertebrate community responses and recovery. Environmental Toxicology and Chemistry 15: 1143-1153

Van den Brink PJ, Ter Braak CJF. 1999. Principal response curves: Analysis of time-dependent multivariate responses of biological community to stress. Environ Toxicol Chem 18:138–148.

Van Den Brink PJ, Hattink J, Bransen F, Van Donk E, Brock TCM. 2000. Impact of the fungicide carbendazim in freshwater microcosms. II. Zooplankton, primary producers and final conclusions. Aquatic Toxicology 48:251–264.

Van de Perre D, Roessink I, Janssen CR, Smolders E, Van Regenmortel T, Van Wichelen J, Vyverman W, Van den Brink BJ, De Schamphealere KAC. 2016. The effects of zinc on the structure and functioning of a freshwater community: A microcosm experiment. Environmental Toxicology and Chemistry 35 (11): 1552-8618

Van Genderen E, Adams W, Dwyer R, Garman E, Gorsuch J. 2015. Modelling and interpreting biological effects of mixtures in the environment: introduction to the metal mixture modelling evaluation project. Environmental Toxicology and Chemistry 34: 721-725.

Van Regenmortel T, Janssen CR, De Schamphelaere KAC. 2014. Cu-EXTEND: extending the chronic BLM to cover a wider range of pH/hardness combinations. Report prepared for the International Copper Association.

Van Regenmortel T, Janssen CR, De Schamphelaere KAC. 2015. Comparison of the capacity of two biotic ligand models to predict chronic copper toxicity to two *Daphnia magna* clones and formulation of a generalized bioavailability model. *Environmental Toxicology and Chemistry* 34: 1597–1608

Van Regenmortel, T., Nys, C., Janssen, C. R., Lofts, S. and De Schamphelaere, K. A.C. 2017a. Comparison of four methods for bioavailability-based risk assessment of mixtures of Cu, Zn and Ni in freshwater. Environmental Toxicology and Chemistry 36(8): 2123-2138

Van Regenmortel T, Berteloot O, Janssen CR, De Schamphelaere KAC. 2017b. Analyzing the capacity of the *Daphnia magna* and *Pseudokirchneriella subcapitata* bioavailability models to predict chronic zinc toxicity at high pH and low Ca concentrations and formulation of a generalized BioAvailability Model (gBAM) for *D. magna*. Accepted Author Manuscript. doi: 10.1002/etc.3840

Van Sprang P, Vangheluwe M, Van Hyfte A, Heijerick D, Vandenbroele M, Verdonck F. 2008. Voluntary Risk Assessment of Copper, Copper II Sulphate Pentahydrate, Copper(I)Oxide, Copper(II)Oxide, Dicopper Chloride Trihydroxide – Chapter 3.2 Environmental Effects – 3.3.3. Effect to aquatic organisms from stp. European Copper Institute, Brussels, Belgium. Available from: http://echa.europa.eu/web/guest/copper-voluntary-risk-assessment-reports

Van Sprang PA, Verdonck FAM, Van Asche F, Regoli L, De Schamphelaere KAC. 2009. Environmental risk assessment of zinc in European freshwaters: A critical appraisal. Science of the Total Environment 407: 5373-5391.

Van Wijngaarden RP, Brock TCM, Douglas MT. 2005. Effects of chlorpyrifos in freshwater model ecosystems: The influence of experimental conditions on ecotoxicological thresholds. Pest Management Science 61:923–935.

Verbruggen EMJ, van den Brink PJ. 2010. Review of recent literature concerning mixture toxicity of pesticides to aquatic organisms. RIVM report / National Institute for Public Health and the Environment : 601400001/2010

Verschoor AJ, Vink JPM, de Snoo GR, Vijver MG. 2011. Spatial and temporal variation of water type-specific no-effect concentrations and risks of Cu, Ni, and Zn. Environmental Science and Technology 45: 6049–6056.

Versieren L, Smets E, De Schamphelaere KAC, Blust R, Smolders E. 2014. Mixture toxicity of copper and zinc to barley at low level effects can be described by the Biotic Ligand Model. Plant and Soil 381: 131-142.

Versieren L, Evers S, De Schamphelaere KAC, Blust R, Smolders E. 2016. Mixture toxicity and interactions of copper, nickel, cadmium, and zinc to barley at low effect levels: Something from nothing? Environmental Toxicology and Chemistry 35: 2483–2492

Vijver MG, Elliott EG, Peijenburg WJGM, De Snoo GR. 2011. Response predictions for organisms water exposed to metal mixtures: A meta-analysis. Environmental Toxicology and Chemistry 30: 1482-1487.

Villavicencio G, Urrestarazu P, Arbildua J, Rodriguez PH. 2011. Application of an acute biotic ligand model to predict chronic copper toxicity to *Daphnia magna* in natural water of Chile and reconstituted synthetic waters. Environmental Toxicology and Chemistry 999: 1-8

Vlaamse Regering. 2015. Vlaams reglement betreffende de milieuvergunning. Bijlage 2.3.1 Basis kwaliteitsnormen voor oppervlaktewater. Besluiten van de Vlaamse regering, Brussels, Belgium.

Wang, N., Mebane, C.A., Kunz, J.L., Ingersoll, C.G., May, T.W., Arnold, W.R., Santore, R.C., Augspurger, T., Dwyer, F.J., Barnhart, M.C. 2009. Evaluation of acute copper toxicity to juvenile freshwater mussels (fatmucket, *Lampsilis siliquoidea*) in natural and reconstituted waters. Environmental Toxicology and Chemistry 28(11): 2367-2377

Wang N, Ingersoll CG, Dorman RA, Brumbaugh WG, Mebane CA, Kunz JL, Hardesty DK. 2014. Chronic sensitivity of white sturgeon (*Acipenser transmontanus*) and rainbow trout (*Oncorhynchus mykiss*) to cadmium, copper, lead, or zinc in laboratory water-only exposures. Environmental Toxicology and Chemistry 33: 2246–2258.

Weeks ME. 1932. The discovery of the elements. III. Some eighteenth-century metals. Journal of Chemical Education 9: 22-29.

Wheeler MW, Park RM, Bailer AJ. 2006. Comparing median lethal concentration values using confidence interval overlap or ratio tests. Environmental Toxicology and Chemistry 25(5): 1441-1444

Wilde KL, Stauber JL, Markich SJ, Franklin NM, Brown PL. 2006. The effect of pH on the uptake and toxicity of copper and zinc in a tropical freshwater alga (*Chlorella* sp.). Archives of Environmental Contamination and Toxicology 51: 174

Williams DA. 1972. The comparison of several dose levels with a zero dose control. Biometrics 28:519–531

Wong PTS, Chau YK, Luxon PL. 1978. Toxicity of a Mixture of Metals on Freshwater Algae. Journal of the Fisheries Research Board of Canada 35(4): 479-481

Wong JPK, Wong YS, Tam NFY. 2000. Nickel biosorption by two chlorella species, *C. vulgaris* (a commercial species) and *C. miniata* (a local isolate). Bioresource Technology 73(2): 133-137

Wong CK, Pak AP. 2004. Acute and Subchronic Toxicity of the Heavy Metals Copper, Chromium, Nickel, and Zinc, Individually and in Mixture, to the Freshwater Copepod *Mesocyclops pehpeiensis*. Bulletin of Environmental Contamination and Toxicology 73(1): 190-196

Wright DA, Welbourn P. 2002. Environmental Toxicology. Cambridge University Press

Xu X, Xi Y, Huang L, Xiang X. 2015. Effects of multi-metal (Cu, Zn, Cd, Cr and Mn) mixtures on the reproduction of freshwater rotifer *Brachionus calyciflorus*. Bulletin of Environmental Contamination and Toxicology 95(6): 714-720

Yen Le TT, Vijver MG, Hendriks AJ, Peijnenburg WJGM. 2013. Modeling toxicity of binary metal mixtures (Cu^{2+}–Ag^{+}, Cu^{2+}–Zn^{2+}) to lettuce, *Lactuca sativa*, with the biotic ligand model. Environmental Toxicology and Chemistry, 32: 137–143

Appendix A:

SUPPORTING INFORMATION OF CHAPTER 2.

Appendix A1. Gathering of monitoring data

When not present in the database, estimations of Na, Mg, K, Cl and SO_4 were based on Ca concentrations. These calculations were based on regressions reported in Van Sprang et al. (2009). These linear regressions are of the form:

$$Y = intercept + slope * log\ Ca \quad \text{(A1.1)}$$

Where the units of Ca, Na, Mg, K, Cl and SO4 are equivalents/L.

Table A1.1 reports the values (intercept and slope) needed to complete the calculations.

Table A1.1: Intercepts and slopes (equation A1.1) needed to calculate Na, Mg, K, Cl and SO_4 (eq/l) from Ca (eq/l). Note that 1 eq/l of Ca, Mg and SO_4 corresponds to 0.5 mol/l and 1 eq/l of Na, K and Cl corresponds to 1 mol/l.

Y	Intercept	Slope
log10 Mg	-2.1200	0.45373
log10 Na	-1.7329	0.51924
log10 K	-2.7639	0.50036
log10 SO_4	-1.2878	0.70712
log10 Cl	-1.5126	0.60201

In addition, alkalinity was calculated based on pH (Stumm and Morgan 1996) assuming an open system in equilibrium with atmospheric CO_2 pressure at a temperature of 20°C (Equations A1.2 and A1.3).

$$Alkalinity\ (M) = 50000 \cdot \frac{1+2\cdot\frac{K_1}{10^{-pH}}}{\frac{10^{-pH}}{K_1}+1+\frac{K_2}{10^{-pH}}} * DIC \quad \text{(A1.2)}$$

where

$$DIC\ (M) = K_H \cdot pCO_2 \cdot \left(1 + \frac{K_1}{10^{-pH}} + K_1 \cdot \frac{K_2}{(10^{-pH})^2}\right) \quad \text{(A1.3)}$$

with K_H and pCO_2, the Henry's law constant (0.0316 $mol.L^{-1}.atm^{-1}$) and partial pressure of CO_2 ($3.16E^{-4}$ atm), respectively. The temperature corrected (20°C) equilibrium constants K_1= $((H^+)(HCO_3^-)/(H_2CO_3))$ and K_2= $((H^+)(CO_3^{2-})/(HCO_3^-))$ at 20°C are equal to 4.17E-07 $mol{\cdot}L^{-1}$ and 4.23E-11 $mol{\cdot}L^{-1,}$ respectively.

A1.1 Dommel database

The Dommel database represents a local industrial exposure scenario (i.e. historic pollution). Monitoring data for sampling locations in the river Meuse tributary Dommel, the Netherlands, were obtained from Verschoor et al (2011) who used the data for a previous study The data spanned a period of 5 years, between July 2006 and June 2010. When information on the field pH was not present, the reported pH retrieved from lab experiments was used. For 0.3% of the target water samples cation and/or anion concentrations were based on reported regression relations with Ca concentrations. In addition, for 100% of the target water samples, alkalinity had to be estimated based on the pH value. Samples for the measurement of concentrations of metals were filtered to 0.45 µm before analysis. Detection limits (DL) for the different metals were equal to 1.5 µg/L for Ni, 3 µg/L for Zn and 1 µg/L for Cu. When the

target water sample included at least one metal that was reported as below detection limit and the $\sum \frac{DL}{HC5}$ for the target water sample was larger than 1, the target water sample was not considered for further analysis (i.e. 0.3% of the target water samples when the HC5 was calculated using the log-normal or the best-fit distribution). For the remaining target water samples (i.e. those that were not removed by this filter), concentrations of metals that were reported in the monitoring database to be below the detection limit were divided by two. In total, 3176 target water samples were retained covering 97 sampling locations.

A1.2 VMM database

The VMM database represents a regional mixed exposure scenario (i.e. a combination of urban, industrial and agricultural pollution). Monitoring data for Flanders (from now on referred to as "VMM") for 2012 was gathered from the online database of the Flemish Environmental Agency (VMM). For 100% of the target water samples cation and/or anion concentrations were based on reported regression relations with Ca concentrations and alkalinity had to be estimated based on the pH value. Samples for the measurement of concentrations of metals were filtered to 0.45 µm before analysis. Detection limits for the different metals were equal to 2, 4, 5 µg/L for Ni, most likely depending on the measuring technique used by the VMM, 5 or 10 µg/L for Zn and 2 µg/L for Cu. When the target water sample included at least one metal that was reported as below detection limit and the $\sum \frac{DL}{HC5}$ for the target water sample was larger than 1, the target water sample was not considered for further analysis (i.e. 8% and 10% of the target water samples when the HC5 was calculated using the log-normal and the best-fit distribution, respectively). For the remaining target water samples (i.e. those that were not removed by this filter), concentrations of metals that were reported in the monitoring database to be below the detection limit were divided by two. In total, 155 target water samples were retained covering 48 sampling locations.

A1.3 Rhine database

The Rhine database represents a regional mixed exposure scenario (i.e. urban, industrial and agricultural pollution). Monitoring data for seven sampling locations in the Rhine for 2010 and 2011 was gathered from the online database of International Commision for the Protection of the Rhine (ICPR). For the data of the year 2010, information on all the major water-chemistry variables was present for every sampling date for the locations Kampen and Weil am Rhein. As not all water-chemistry variables were measured for every sampling date, data was grouped per month for the locations Maassluis, Lobith, Koblenz-Mosel, Koblenz-Rhein and Lauterbourg. For the data for the year 2011, data was grouped per month for the locations Lobith, Koblenz-Mosel, Koblenz-Rhein and Lauterbourg, but not for the locations Kampen, Weil am Rhein and Maassluis. For 5.7% of the target water samples cation and/or anion concentrations were based on reported regression relations with Ca concentrations. In addition, for 100% of the target water samples, alkalinity had to be estimated based on the pH value. Samples for the measurement of concentrations of metals, anions, cations and DOC were filtered to 0.45 µm before analysis. In total, 209 target water samples were retained covering 53 sampling locations.

A1.4 Austria database

The Austria database represents a regional mixed exposure scenario (i.e. urban, industrial and agricultural pollution). Monitoring data for Austria for 2006 was received from ARCHE (Assessing Risks of Chemicals). Hardness was reported in German hardness degrees (dH). dH was converted to $CaCO_3$ by multiplying with 17.85. Subsequently, Ca concentrations were calculated based on the combination of Equation A1.4 (Clesceri et al. 1989) and Equation A1.5 (assumed Ca:Mg ratio of ≈ 3.3, as in Europe based on United Nation Global Environmental Monitoring System (GEMS/WATER) database; see also Heijerick et al. (2003), which gives Equation A1.6. Mg concentrations were then calculated based on hardness and Ca concentrations with Equation A1.4.

$$Hardness\ \left(mg\frac{CaCO_3}{l}\right) = Ca\ (mg/l) * 2.497 + Mg(mg/l) * 4.118 \quad \text{(A1.4)}$$

$$\frac{Ca\ (\frac{mol}{L})}{Mg\ (\frac{mol}{L})} = 3. \quad \text{(A1.5)}$$

$$Ca\ \left(\frac{mg}{L}\right) = \frac{Hardness\left(mg\frac{CaCO_3}{l}\right)}{3.329} \quad \text{(A1.6)}$$

For 100% of the target water samples cation and/or anion concentrations were based on reported regression relations with Ca concentrations. Alkalinity was reported in SäureBindungsVermögen (SBV, mmol/L) and was converted to $CaCO_3$ (mg/L) by multiplying with 50. Samples for the measurement of concentrations of metals were filtered to 0.45 µm before analysis. Detection limits (DL) range between 0.02 and 1 µg/L for Ni, between 0.16 and 1 µg/L for Cu and between 0.24 and 1 µg/L for Zn, respectively (for exact DL per target water sample see Appendix A.1). When the target water sample included at least one metal that was reported as below detection limit and the $\sum \frac{DL}{HC5}$ for the target water sample was larger than 1, the target water sample was not considered for further analysis (i.e. 16% of the target water samples when the HC5 was calculated using the log-normal or the best-fit distribution). For the remaining target water samples (i.e. those that were not removed by this filter), concentrations of metals that were reported in the monitoring database to be below the detection limit were divided by two. In total, 2138 target water samples were retained covering 249 sampling locations within eight regions.

A1.4 FOREGS database

The FOREGS-EuroGeoSurveys Geochemical Baseline Database was obtained on the website of the Geological Survey of Finland [6] and can also be found in Salminen et al. (2005). The FOREGS database (Forum of European Geological Surveys) contains high quality environmental geochemical baseline data for Europe for, among other things, stream water. This baseline data set represents the natural background concentrations of metals within freshwater streams in Europe. Since this database contains information on streams with no anthropogenic enrichments, it is expected that no or negligible risk will be observed. Information on cation/anion concentrations was present for 100% of the target water samples. Alkalinity had to be estimated based on the pH value for all target water samples. Samples for the measurement of concentrations of metals, anions, cations and DOC were filtered to 0.45 µm before analysis. Detection limits for the different metals were equal to 0.005 µg/L for Ni, 0.01

µg/L for Zn and 0.005 µg/L for Cu. None of the target water samples showed metal concentrations below the detection limits. The database contains data for 26 different countries in Europe. In total, 784 target water samples were retained.

Appendix A2. Update of and improvements to the chronic ecotoxicity database of Cu

A2.1 Introduction

Here, more information is given about the adaptations made to the chronic ecotoxicity database of Cu, originally reported in the EU RAR (2008). First, those data which were not retained in the database are summarized. Then, an overview is given of the adaptations that were made to the data that were retained in the database.

A2.2 Data not retained in the final toxicity database

First, toxicity data for *Pseudokirchneriella subcapitata* reporting a NOEC of 23.1 µg/l Cu, was not retained, as it was not reported in Heijerick *et al.* (2005), and it was not clear where the data came from. However, another relevant and reliable NOEC (defined as in Van Sprang et al. 2009), obtained in natural water from the river Rhine, was available for this species. Therefore *P.subcapitata* was still represented in the toxicity database with approximately the same NOEC. The test result with the cladoceran *Ceriodaphnia dubia* (Belanger and Cherry, 1990) reported for the New River was not retained because the NOEC was obtained in test media outside the workable range of the BLM. The chronic toxicity data obtained for *C. dubia* in the natural water from Amy Bayou were also rejected, as was done in the Zn RAR (2008). The latter stated that no information could be retrieved about the DOC concentrations of the Amy Bayou River, and that this *was* available for the other natural waters tested in the same study.

A2.3 Adaptations to data included in the Cu toxicity database

When creating the Cu database for the EU RAR (2008), assumptions were made regarding the test water chemistries. Often, the physico-chemical parameters of test waters were set at "worst case scenario' levels. These levels are not only outdated, but the values at which these levels are set also have an effect on the outcome of calculations of HC_5 values. For example, Na^{2+} concentrations were frequently set at a 'worst case level' of 5.3 mg/l. However, it is known that Na^{2+} plays an important role in the Cu BLM, as it is an effective competing ion (De Schamphelaere and Janssen, 2002), and hence, more correct concentrations of Na^{2+} should be listed in the Cu database.

Where necessary, alkalinity was recalculated. This was done based on reported pH and T (°C) or based on pH, T (°C) and DIC/CO_3 when the latter was reported.

In the table below, the adaptations made to the Cu database are listed and explained.

REF	Species and citation	Adaptations
1	*Chlamydomonas reinhardtii* Schafer *et al.* (1994)	The pH was adapted to that reported in the article (pH 6.2). Concentrations of ions were calculated based on chemical data provided in the article. Alkalinity was not reported, it was recalculated for an open system based on the reported pH and T(°C).
2	*Chlamydomonas reinhardtii* De Schamphelaere *et al.* (2006)	The temperature was adjusted to that reported in the article (T 25°C). Alkalinity was recalculated based on this new temperature and the DIC concentrations. Not NOECs, but EC10s were reported. The %AFA was reported in this study (41.1%).
2	*Chlorella vulgaris* De Schamphelaere *et al.* (2006)	The temperature was adjusted to that reported in the article (T 25°C). Alkalinity was recalculated based on this new temperature and the DIC concentrations. Not NOECs, but EC10s were reported. The %AFA was reported in this study (41.1%).
3	*Pseudokirchneriella subcapitata* Heijerick *et al.* (2005)	The reference was wrongly reported. Temperature was adapted to that reported in the article (T 23°C). Test water chemistry and pH were adapted to that reported in the article: the test water chemistry was calculated as a summation of the natural surface water chemistry and the chemistry of the ISO-medium that was added; pH at the start of the test was adjusted to the field pH. Alkalinity was recalculated based on reported IC, pH and T at 23°C. IC was calculated as the sum of the IC in the natural surface water and the IC in the ISO-medium.
4	*Ceriodaphnia dubia* Jop *et al*. (1995)	Mean alkalinity of test water was adapted for 'code 39' and 'code 42': 19 mg/l (reconstituted water) and 13 mg/l (Great Works River water) $CaCO_3$. pH, hardness and alkalinity of the Great Works River and the reconstituted water were reported. DOC values for the Great Works River were retrieved from a monitoring database of the Maine Department of Environmental Protection (Maine-DEP). Average values for DOC were used, as calculated from the values reported from a monitoring site on the Great Works River. Ca and Mg were kept as in the original Cu-database (assumed Ca:Mg ratio of ≈ 3.3, as in Europe (based on GEMS/WATER database; see also Heijerick *et al*., 2003)). Na and SO_4 were estimated based on charge balance assumptions and reported electrical conductivity of test medium. K and Cl were kept at low levels (0.1 mg/l)
5	*Ceriodaphnia dubia* Spehar & Fiandt (1985)	Alkalinity of Lester River Water was adapted for 'code 38' (97 mg/L as $CaCO_3$). Ca and Mg were kept as in the original Cu-database (assumed Ca:Mg ratio of ≈ 3.3, as in Europe (based on GEMS/WATER database; see also Heijerick *et al*., 2003)). Based on charge balance considerations, missing ions (Na, K, SO_4, Cl) were probably too low to affect outcome of the calculations. They were set at low levels (0.1 mg/l).

6	*Ceriodaphnia dubia* Belanger & Cherry (1990)	Test water chemistry for the New River and the Clinch River was adapted to the chemistry used in the Zinc Risk Assessment Report (2008): "Alkalinity during the tests was recalculated by accounting for the pH manipulation (according to Stumm and Morgan, 1996). Other chemical parameters were retrieved from a monitoring database of the Virginia Department of Environmental Quality (Virginia-DEQ) for New River and Clinch River. Average values for DOC, SO_4, and Cl were used, as calculated from the values reported for the two monitoring sites closely encompassing the sampling sites described in the Belanger and Cherry study. Ca and Mg were calculated from reported hardness using average Ca:Mg ratios for Clinch River (1.6) and New River (1.2), taken from the same database. Based on charge balance considerations, missing ions (Na, K) were probably too low to affect outcome of the calculations (both <0.4 mM). They were set at low levels."
7	*Ceriodaphnia dubia* Belanger *et al*. (1998)	The reference was wrongly reported. Alkalinity was adapted for 'code 40' (69.6 mg/l $CaCO_3$). Test water chemistry for the New River and the Clinch River was adapted to the chemistry used in the Zn RAR (2008).
8	*Daphnia magna* van Leeuwen *et al.* (1988)	pH and hardness were reported. Other chemical parameters for Lake Ijssel water was taken from the Zn RAR (2008) which reported its data from the "United Nation Global Environmental Monitoring System (GEMS/WATER; www.gemswater.org); chemistry for Lake Ijssel is also summarized in Heijerick *et al*. (2003)."
9	*Daphnia magna* De Schamphelaere & Janssen (2004)	This reference was adapted (used to be reported as 'Heijerick *et al*., 2002') because the original reference was not found, and all the data was listed in De Schamphelaere and Janssen (2004). Alkalinity was recalculated based on reported CO_3 concentrations, pH and T at 20°C. The NOEC of 'code 55' was adapted to the values reported in De Schamphelaere and Janssen (2004).
10	*Daphnia pulex* Winner (1985)	SO_4 concentrations were adapted to that reported in the article: 102.1 mg/l for hard water (code 60, 61 and 64) and kept low (0.1 mg/l) for soft and medium water (code 58, 59, 62, 63, 65 and 66).
11	*Gammarus pulex* Maund *et al.* (1992)	pH was adapted to that reported in the article (pH 7.9). Ca and Mg were kept as in the original Cu-database (assumed Ca:Mg ratio of ≈ 3.3, as in Europe (based on GEMS/WATER database; see also Heijerick *et al*., 2003)). Based on charge balance considerations, missing ions (Na, K, SO_4, Cl) were probably too low to affect outcome of the calculations. They were set at low levels (0.1 mg/l). Alkalinity was recalculated for an open system based on the reported pH and T (°C).
12	*Hyalella Azteca* Deaver & Rodgers (1996)	Ca and Mg were kept as in the original Cu-database (assumed Ca:Mg ratio of ≈ 3.3, as in Europe (based on GEMS/WATER database; see also Heijerick *et al*., 2003)). Na and SO_4 were estimated based on charge balance assumptions and reported electrical conductivity of test medium. K and Cl were kept at low levels (0.1 mg/l)

13	*Salvelinus fontinalis* *Ictalurus punctatus* Sauter *et al.* (1976)	Test water chemistry was not reported in the article. Ca and Mg were kept as in the original Cu-database (assumed Ca:Mg ratio of ≈ 3.3, as in Europe (based on GEMS/WATER database; see also Heijerick *et al*., 2003)). Na, K, SO_4, and Cl were estimated from correlations with Ca found in the GEMS database (see also Heijerick *et al*., 2003).
14	*Noemacheilus barbatulus* Solbe & Cooper (1976)	Ca and Mg were kept as in the original Cu-database (assumed Ca:Mg ratio of ≈ 3.3, as in Europe (based on GEMS/WATER database; see also Heijerick *et al*., 2003)). Na, K, SO_4, and Cl were estimated from correlations with Ca found in the GEMS database (see also Heijerick *et al*., 2003). Alkalinity was recalculated for an open system based on the reported pH and T (°C).
15	*Oncorhynchus mykiss* *Oncorhynchus kisutch* Mudge *et al.* (1993)	pH was adapted to the mean values reported in the article. Test water chemistry was not reported in the article. Ca and Mg were kept as in the original Cu-database (assumed Ca:Mg ratio of ≈ 3.3, as in Europe (based on GEMS/WATER database; see also Heijerick *et al*., 2003)). Na and SO_4 were estimated based on charge balance assumptions and reported electrical conductivity of test medium. K and Cl were kept at low levels (0.1 mg/l)
16	*Oncorhynchus mykiss* Seim *et al.* (1984)	Alkalinity was adapted to that reported in the article (126 mg CaCO3/L). Ca and Mg were kept as in the original Cu-database (assumed Ca:Mg ratio of ≈ 3.3, as in Europe (based on GEMS/WATER database; see also Heijerick *et al*., 2003)). Na, K, SO_4, and Cl were estimated from correlations with Ca found in the GEMS database (see also Heijerick *et al*., 2003).
17	*Perca fluviatilis* Collvin (1985)	Alkalinity was adapted to that reported in the article (129 mg CaCO3/L). Ca and Mg were kept as in the original Cu-database (assumed Ca:Mg ratio of ≈ 3.3, as in Europe (based on GEMS/WATER database; see also Heijerick *et al*., 2003)).Based on charge balance considerations, missing ions (Na, K, SO_4, Cl) were probably too low to affect outcome of the calculations. They were set at low levels (0.1 mg/l).
18	*Perca fluviatilis* Collvin (1984)	The reference was wrongly reported. Alkalinity was adapted to that reported in the article (131 mg/L CaCO3). Ca and Mg were kept as in the original Cu-database (assumed Ca:Mg ratio of ≈ 3.3, as in Europe (based on GEMS/WATER database; see also Heijerick *et al*., 2003)).Based on charge balance considerations, missing ions (Na, K, SO_4, Cl) were probably too low to affect outcome of the calculations. They were set at low levels (0.1 mg/l).
19	*Pimephales notatus* Horning & Neiheisel (1979)	pH adapted to that reported in the article (pH 8.01). Ca and Mg were kept as in the original Cu-database (assumed Ca:Mg ratio of ≈ 3.3, as in Europe (based on GEMS/WATER database; see also Heijerick *et al*., 2003)). Na, K, SO_4, and Cl were estimated from correlations with Ca found in the GEMS database (see also Heijerick *et al*., 2003).

20	*Pimephales promelas* Spehar & Fiandt (1985)	pH, alkalinity and hardness of Lake Superior were reported. Other chemical parameters (including Ca:Mg ratio) for Lake Superior test water were assumed similar as in Biesinger and Christensen (1972) (As in Zn RAR). DOC and $S0_4$ were taken from Erickson *et al*. (1996) as was done in the Zn RAR.
21	*Pimephales promelas* Mount & Stephan (1969)	Ca and Mg were kept as in the original Cu-database (assumed Ca:Mg ratio of ≈ 3.3, as in Europe (based on GEMS/WATER database; see also Heijerick *et al*., 2003)).Based on charge balance considerations, missing ions (Na, K, SO_4, Cl) were probably too low to affect outcome of the calculations. They were set at low levels (0.1 mg/l).
22	*Pimephales promelas* Mount (1968)	Test water chemistry was adapted to the chemistry reported in the article.
23	*Pimephales promelas* Pickering *et al.* (1977)	Ca and Mg were kept as in the original Cu-database (assumed Ca:Mg ratio of ≈ 3.3, as in Europe (based on GEMS/WATER database; see also Heijerick *et al*., 2003)). Na, K, SO_4, and Cl were estimated from correlations with Ca found in the GEMS database (see also Heijerick *et al*., 2003). Alkalinity was recalculated for an open system based on the reported pH.
24	*Pimephales promelas* Scudder *et al.* (1988)	Alkalinity (211.9 mg $CaCO_3$/L), pH (8.17), Ca^{2+} (56 mg/L) and $S0_4^{2-}$ (59 mg/L) were adjusted to that reported in the article.
25	*Salvelinus fontinalis* McKim & Benoit (1971)	Alkalinity was adapted to that found in the article (41.6 mg CaCO3/L). For the dechlorinated tap water: Ca and Mg were kept as in the original Cu-database (assumed Ca:Mg ratio of ≈ 3.3, as in Europe (based on GEMS/WATER database; see also Heijerick *et al*., 2003)). Na, K, SO_4, and Cl were estimated from correlations with Ca found in the GEMS database (see also Heijerick *et al*., 2003). For the Lake Superior water: pH, alkalinity and hardness of Lake Superior were reported. Other chemical parameters (including Ca:Mg ratio) for Lake Superior test water were assumed similar as in Biesinger and Christensen (1972) (As in Zn RAR). DOC and $S0_4$ were taken from Erickson *et al*. (1996) as was done in the Zn RAR.
26	*Lemna minor* Teisseire *et al.* (1998)	Concentrations of ions were calculated based on chemical data provided in the article. Alkalinity was recalculated for an open system based on the reported pH.
27	*Chironomus riparius* Taylor *et al*. (1991)	pH was adapted to that reported in the article (pH 7). Ca and Mg were kept as in the original Cu-database (assumed Ca:Mg ratio of ≈ 3.3, as in Europe (based on GEMS/WATER database; see also Heijerick *et al*., 2003)).Based on charge balance considerations, missing ions (Na, K, SO_4, Cl) were probably too low to affect outcome of the calculations. They were set at low levels (0.1 mg/l). Alkalinity was recalculated for an open system based on the reported pH.

28	*Clistoronia magnifica* Nebeker et al. (1984)	Ca and Mg were kept as in the original Cu-database (assumed Ca:Mg ratio of ≈ 3.3, as in Europe (based on GEMS/WATER database; see also Heijerick *et al*., 2003)). Na, K, SO_4, and Cl were estimated from correlations with Ca found in the GEMS database (see also Heijerick *et al*., 2003).
29	*Paratanytarsus parthenogeneticus* Hatakeyama & Yasuno (1981)	pH was adjusted to that reported in the article (pH 7). Ca and Mg were kept as in the original Cu-database (assumed Ca:Mg ratio of ≈ 3.3, as in Europe (based on GEMS/WATER database; see also Heijerick *et al*., 2003)). Na, K, SO_4, and Cl were estimated from correlations with Ca found in the GEMS database (see also Heijerick *et al*., 2003). Alkalinity was recalculated for an open system based on the reported pH.
30	*Campeloma decisum* Arthur & Leonard (1970)	Ca and Mg were kept as in the original Cu-database (assumed Ca:Mg ratio of ≈ 3.3, as in Europe (based on GEMS/WATER database; see also Heijerick *et al*., 2003)). Na, K, SO_4, and Cl were estimated from correlations with Ca found in the GEMS database (see also Heijerick *et al*., 2003).
31	*Juga plicifera* Nebeker *et al.* (1986)	The reference was wrongly reported. Ca and Mg were kept as in the original Cu-database (assumed Ca:Mg ratio of ≈ 3.3, as in Europe (based on GEMS/WATER database; see also Heijerick *et al*., 2003)). Na, K, SO_4, and Cl were estimated from correlations with Ca found in the GEMS database (see also Heijerick *et al*., 2003).
32	*Ceriodaphnia dubia* Cerda & Olive (1993)	Alkalinity was adapted to that reported in the article (62.5 mg $CaCO_3$/L).
33	*Brachionus calyciflorus* De Schamphelaere *et al.* (2006)	DOC concentrations are 4.91; 14.5; 4.83 and 14.7 : these for ‘code 132‘ and ‘code 134‘ were adapted.
34	*Hyalella Azteca* Othman & Pascoe (2002)	Test duration (35 days) and test medium (dechlorinated tap water) were not reported in original database. Ca and Mg were kept as in the original Cu-database (assumed Ca:Mg ratio of ≈ 3.3, as in Europe (based on GEMS/WATER database; see also Heijerick *et al*., 2003)).Based on charge balance considerations, missing ions (Na, K, SO_4, Cl) were probably too low to affect outcome of the calculations. They were set at low levels (0.1 mg/l).
35	*Oncorhynchus mykiss, Catostomus commersonii, Esox Lucius* McKim *et al*. (1978)	Test durations were adapted to those found in the article (30 days). pH, alkalinity and hardness of Lake Superior were reported. Other chemical parameters (including Ca:Mg ratio) for Lake Superior test water were assumed similar as in Biesinger and Christensen (1972) (As in Zn RAR). DOC and $S0_4$ were taken from Erickson, Benoit et al. (1996) as was done in the Zn RAR.
36	*Salvelinus fontinalis* McKim *et al*. (1978)	Test duration was adapted to that found in the article (30-60 days). pH, alkalinity and hardness of Lake Superior were reported. Other chemical parameters (including Ca:Mg ratio) for Lake Superior test water were assumed

		similar as in Biesinger and Christensen (1972) (As in Zn RAR). DOC and $S0_4$ were taken from Erickson, Benoit et al. (1996) as was done in the Zn RAR.
37	*Dreissena polymorpha* Kraak et al. (1994)	NOEC was adjusted to that reported in the article (16 µg/l). Test conducted in natural water from Markermeer (NL). Only pH, temperature and water hardness were reported. DOC and other macro-ions were adopted to those reported in the Zn RAR (Kraak *et al.* 1994b): " DOC was estimated at the average DOC concentration in Markermeer reported by Van Tilborgh (2002); other macro-ions and the Ca:Mg ratio were taken from (De Schamphelaere, Lofts *et al*. 2005)."
38	*Villosa iris* Jacobson et al. (1997)	pH was adjusted to that reported in the article (pH 8.39). Ca:Mg ratio for Clinch River was assumed 1.6 as described for Belanger and Cherry (1990). Average DOC was also retrieved from the latter article. Based on charge balance considerations, missing ions (Na, K, SO_4, Cl) were probably too low to affect outcome of the calculations. They were set at low levels (0.1 mg/l).
39	*Lymnaea stagnalis* Brix *et al.* (2011)	This data point was added to the Cu database. Test chemistry was reported. SO4 was based on charge balance considerations. Alkalinity was estimated based on pH, T and C03 concentrations.

Appendix A3. Calculation of slope data of dose-response curves

In addition to the chronic toxicity data that was already present in the toxicity databases, i.e. EC10 values, there is need for additional information, i.e. the slope of the dose-response curves, to be able to apply one of the four mixture evaluations tools, i.e. the IA_{DRC} method. For this, we retrieved all literature present in the toxicity databases for all three metals. However, information on the slope of the curves was never present in the peer-reviewed papers. Therefore, other methods were used to retrieve this information. These methods were applied in the order listed below.

(1) When the EC50, LC50 or IC50 value was reported, the slope value, β_i, was calculated based on the log-logistic function (Equation A3.1 and A3.2) and the EC10 value present in the database:

$$y = \frac{1}{1+(\frac{EC_{10}}{EC_{50}})^{\beta}} \quad \text{(A3.1)}$$

$$\beta = \log_{\frac{EC10}{EC50}}\left(\frac{1}{9}\right) \quad \text{(A3.2)}$$

With *y* = the predicted effect, EC10 and EC50 the 10% and 50% effect concentration, respectively, and *β* the slope value.

(2) When the raw dose response data was reported, an EC50, LC50 or IC50 value was calculated with the *drm* function in R (version 2.15.2, R Development Core Team, Vienna, Austria). This was done with one of the following functions, depending on which one best fitted the data (i.e. highest log likelihood): a log-logistic concentration response model with three parameters (Equation A3.3), a log-logistic concentration response model with two parameter (Equation A3.4) or a Weibull distribution with three parameters (Equation A3.5).

$$y = \frac{d}{1+exp^{(b(\ln(x)-\ln(e)))}} \quad \text{(A3.3)}$$

$$y = \frac{100}{1+exp^{(b(\ln(x)-\ln(e)))}} \quad \text{(A3.4)}$$

$$y = d \times \exp\left(-\frac{x}{k}\right)^{b} \quad \text{(A3.5)}$$

Where *y* = the predicted effect, b = a slope parameter, *x* = the dissolved metal concentration (µg/L), *e* = the EC50, LC50 or IC50 (µg dissolved metal/L), *d* = the value of the maximal response (i.e. in the control) and *k* = a scale parameter. Subsequently, the slope value was calculated with Equation A1.1.

(3) When another point effect estimate was available, e.g. the EC20, the βi value was calculation based on the log-logistic function (Equation A3.6) and the EC10 value present in the database.

$$\beta = \log_{\frac{EC10}{EC20}}\left(\frac{4}{9}\right) \quad \text{(A3.6)}$$

(4) When the paper only reported toxicity data as a figure with the effects, xyExtract software (Wilton P. Silva, 2011) was used to extract the x-values (concentrations) and the y-values (effects) from the figure. Subsequently, an EC50, LC50 or IC50 value was calculated with the *drm* function in R (based on highest log likelihood) and the slope value was calculation with Equation A3.1.

Appendix A4. Correlations between slope values and sensitivities of species

No correlation was found between slope values and the sensitivities of species, e.g. species that are sensitive to a certain metal (low EC10) can show both low or high slope values.

For copper (Figure A4.1), zinc (Figure A4.2) and nickel (Figure A4.3) Pearson correlations are low, i.e. -0.07, 0.24 and -0.4, respectively.

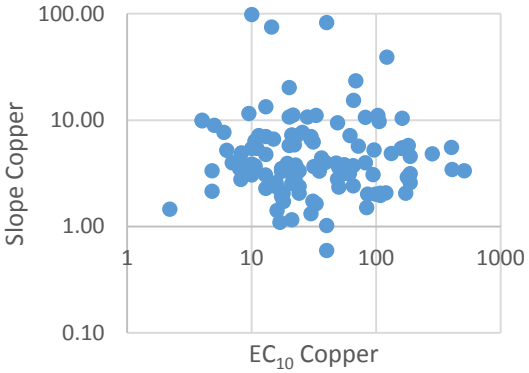

Figure A4.1 Relation between the EC10 values of the species within the chronic copper toxicity database and the slope values calculated for the dose-response of these species.

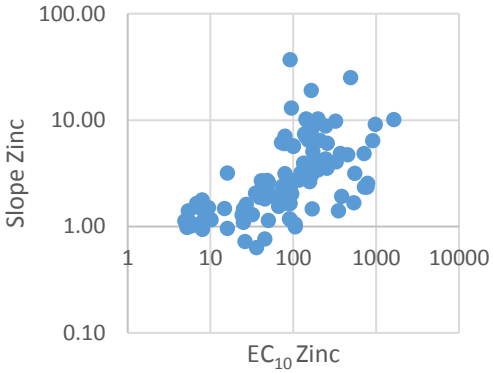

Figure A4.2 Relation between the EC10 values of the species within the chronic zinc toxicity database and the slope values calculated for the dose-response of these species.

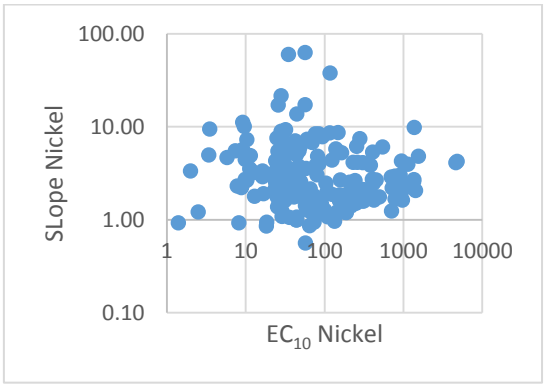

Figure A4.3 Relation between the EC10 values of the species within the chronic nickel toxicity database and the slope values calculated for the dose-response of these species.

Appendix A5. Bioavailability Models and Normalization

Bioavailability normalizations for Cu and Zn with the BLM were carried out with publicly available BLM software (HydroQual 2015). For Zn, the BLM parameters files (extension *.dat) that were modified by Van Sprang et al. (2009) were used. For Cu, the BLM parameter files were modified to reflect the adaptations that were made to the Cu toxicity database (i.e. adaptations to the physico-chemistry of the water as well as adaptations to certain EC10 values). The thermodynamic database (extension *.dbs) that was modified by Van Sprang et al. (2009) to reflect the stability constants for inorganic Cu and Zn complexes from NIST was used. For Zn and Cu the WHAM-Model V speciation software (Tipping 1994) was used. For Ni, the chronic Ni bioavailability and normalization tool (Nys el at. 2012) was used in combination with the WHAM-Model VI speciation software (Tipping 1998). Certain stability constants for inorganic complexes as well as fulvic acid binding constants in the WHAM-Model VI software were adapted to those of NIST (Smith et al. 2004), as explained in Nys et al. (2012). All analyses for calculations of msPAF were carried out with R software (version 2.15.2, R Development Core Team, Vienna, Austria).

The process of normalization will be clarified below for all three metals. This process can be divided into two subsequent parts: (1) calculation of the 'intrinsic sensitivity' of a given species and (2) calculation of the normalized dissolved EC10 in the 'target water' (Figure A5.1). These steps are explained in brief below.

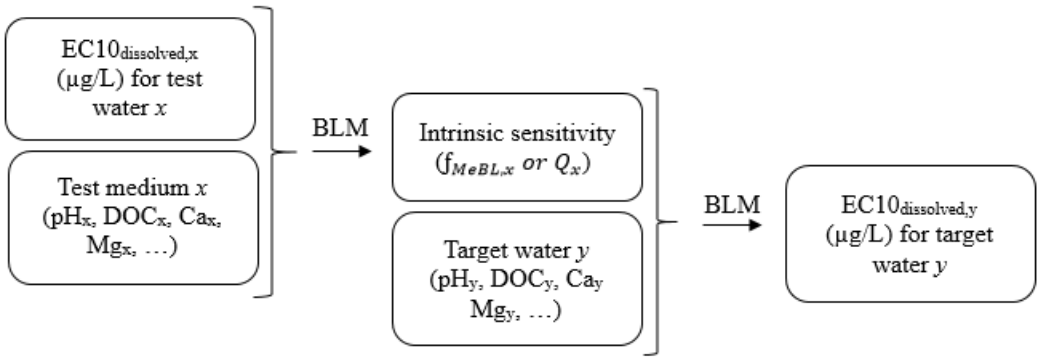

Figure A5.1. Overview of the procedure for normalization of EC10 values obtained in test media *x* to the physico-chemistry of target water *y*, using biotic ligand models (BLM). Figure adapted from Van Sprang et al. (2009)

Step 1: the 'intrinsic sensitivity' for a given species *i*, which is given by the parameter *f* or *Q*, is the fraction of the biotic ligand sites that is occupied by a metal at a concentration equal to the EC10 of that metal. Simplified equations to calculate this 'intrinsic sensitivity' are given in Equation A5.1 and A5.2.

$$f_{MeBL,i,x} = \frac{K_{MeBL} \cdot EC10_{Me^{2+},i,x}}{1 + K_{MeBL} \cdot EC10_{Me^{2+},i,x} + \sum K_{CatBL}(Cat^{2+})_{i,x}} \quad \text{(A5.1)}$$

$$Q_{i,x} = log_{10} EC10_{Me^{2+},i,x} - S_{pH} \cdot pH_{i,x} \quad \text{(A5.2)}$$

Where K_{MeBL} and K_{CatBL} are the stability constants for competitive binding of the metal Me^{2+} and other cations Cat^{2+} (e.g. Ca^{2+}, Mg^{2+}, Na^{2+}) to the biotic ligand (BL) of species *i*, respectively and $(Cat^{2+})_{i,x}$ are the chemical activities of the cations in the test medium *x*. S_{pH} is the slope of the linear regression

between the $\log_{10}$-transformed EC10 values (expressed as free metal activity) and pH. The $EC10_{Me^{2+},i,x}$, the activity of the free Me^{2+} ion at the EC_{10}, as well as the chemical activities of the competing cations are calculated from the dissolved concentrations within the test medium *x* using BLM software [1], which incorporates either WHAM-Model V (Tipping 1994) or VI (Tipping 1998) as speciation software. Assumptions for natural organic matter were different for all three metals. We assumed that natural organic matter consisted of 61% (Cheng et al. 2005), 50% (De Schamphelaere and Janssen 2004) and 40% (De Schamphelaere et al. 2006) active fulvic acid (unless specified differently) for Zn, Cu and Ni, respectively. Stability constants for inorganic complexes were taken from the National Institute of Standards and Technology (NIST) (Smith et al. 2004). An equivalent of equation 6 is used for *Daphnia magna* for Cu (De Schamphelaere et al. 2004a) and Zn (Heijerick et al. 2005) as well as for *Onchorynchus mykiss* for Cu (De Schamphelaere et al. 2008), Zn (De Schamphelaere and Janssen 2004b; De Schamphelaere and Janssen 2005) and Ni (Deleebeeck et al. 2007). An equivalent of Equation 7 is used for *Pseudokirchneriella subcapitata* for Cu (De Schamphelaere and Janssen 2006), Zn (De Schamphelaere et al. 2005) an Ni (Deleebeeck et al. 2009) as well as for *D. magna* for Ni (Deleebeeck et al. 2008). All parameters of the biotic ligand models can be found in Table A5.1 and all parameter files for Zn and Cu (extension *.dat) including the intrinsic sensitivity values can be found in the online database at doi:10.1002/etc.3746.. Intrinsic sensitivities for Ni can be consulted in the 'Ni normalisation tool' provided by Nys et al. (2012).

Step 2: The calculated 'intrinsic sensitivity' is subsequently used to calculate the Me^{2+} activity in the 'target water' *y*, which shows another physico-chemistry than the test medium *x*. Simplified equations to calculate this metal activity are given in Equation A5.3 and A5.4.

$$EC10_{Me^{2+},i,x,y} = \frac{\int_{MeBL,i,x}}{(1-\int_{MeBL,i,x})\cdot K_{MeBL}} \cdot (1 + \sum K_{CatBL}(Cat^{2+})_y) \quad \text{(A5.3)}$$

$$log_{10}EC10_{Me^{2+},i,x,y} = (Q_{i,x} - S_{pH} \cdot pH_y) \cdot \{1 + K_{CatBL}(Cat^{2+})_y\} \quad \text{(A5.4)}$$

Where $(Cat^{2+})_y$ are the chemical activities of cations (e.g. Ca^{2+}, Mg^{2+}, Na^{2+}) in the 'target water' *y* and pH_y is the pH of the target water *y*. The chemical activities of the cations are again calculated using BLM software that incorporates either WHAM-Model V or VI speciation software. Assumptions for natural organic matter were equal to those for Step 1. An equivalent of Equation A5.3 was used for *D. magna* for Cu and Zn as well as for *O. mykiss* for Cu, Zn and Ni. An equivalent of Equation A5.4 was used for *P.subcapitata* for Cu, Zn and Ni as well as for *D. magna* for Ni. For the latter, the part of Equation A5.4 in between brackets "{}" is added to include competition by other cations. For Zn and Cu, the BLM software automatically converts the obtained $EC10_{Me^{2+},i,x,y}$ to the dissolved EC_{10} of the 'target water' y, i.e. the $EC10_{dissolved,i,x,y}$, using the WHAM-Model V speciation software. For Ni, the 'chronic Ni bioavailability and normalization tool' is used together with the WHAM-Model VI speciation software to convert the Ni activities to dissolved concentrations. This step concludes the process of normalization in which a EC10 value from the ecotoxicity database is 'converted' to the physico-chemistry of the 'target water' in the monitoring database.

Toxicity data of *D. magna*, *O. mykiss* and *P.subcapitata* are normalized with the BLMs developed for these specific species, respectively. However, the chronic toxicity databases contain a numerous amount of species other than the three listed above. As it is infeasible to develop specific BLMs for each

separate species, the assumption is made that the intrinsic sensitivity (i.e. $f_{MeBL,i,x}$ or $Q_{i,x}$) between related species is different but that the interactions between the metals and other cations (e.g. Ca^{2+}, Mg^{2+}, Na^{+}, H^{+}) at the biotic ligand are equal among related species (i.e. invertebrates, fish and algae), as has been done elsewhere (Van Sprang et al. 2004). The cross-validation of the specific BLMs to related species has shown to be successful (De Schamphelaere and Janssen 2010, De Schamphelaere et al. 2006, Schlekat et al. 2010). Therefore, all invertebrate EC10 values are normalized with the *D. magna* BLMs, all vertebrate (fish) EC10 values with the *O. mykiss* BLMs and all algae EC10 values with the *P.subcapitata* BLMs.

Certain waterbodies showed a physico-chemistry outside the 'workable range' of the BLMs. These 'workable ranges' for pH and Ca differ between the different metals and are for pH equal to 6-8.4 for Cu, 5.6-8.7 for Ni and 6-8 for Zn and for Ca equal to 3-160 mg/L for Cu, 5-160 mg/L for Zn and 4-110 mg/L for Ni. For all five considered monitoring databases together, 30.8% had a chemistry outside the 'workable ranges' valid for all BLMs, i.e. pH 6-8 and Ca 3-110. 24% showed a pH>8 and 3.7% had a Ca>110 mg/L (upper boundaries), while 1.7% showed a pH<6 and 1.9% showed a Ca<3 mg/L (lower boundaries). As the physico-chemistry of these waters falls outside the validation range of the BLMs, this introduces uncertainty to the normalizations performed with the BLMs as well as to the HC_5 and msPAF calculations. Validating these BLMs outside these boundaries and therefore extending the boundaries would decrease the % of waters outside the boundaries and therefore also the uncertainty on the calculations. The largest addition to this uncertainty lies in the upper pH boundary, which is determined by the upper boundary for Zn. In relation to this, recent research at our lab has shown that the workable range of the algae BLM can be extrapolated from 8 to 8.4 (pers. communication). This implies that a considerably lower % of the waterways, i.e. 2%, shows a pH above the upper boundary of the BLMs and that now 8.9% of all the waters shows a physico-chemistry outside the 'workable range' of the BLMs. For this paper, we will assume that the BLMs can be extrapolated slightly outside their 'workable ranges' and that the uncertainty of the calculations is therefore minimal.

Table A5.1. Biotic ligand model (BLM) zinc, copper and nickel constants, competition constants and humic material assumptions for the *Daphnia magna* (De Schamphelaere et al. 2006; De Schamphelaere and Janssen 2008; De Schamphelaere and Janssen 2004b), *Oncorhynchus mykiss* (De Schamphelaere and Janssen 2004b; De Schamphelaere et al. 2005; Deleebeeck et al. 2007; De Schamphelaere and Janssen 2006) and *Pseudokirchneriella subcapitata* (Deleebeeck et al. 2007; Deleebeeck et al. 2009; Deleebeeck et al. 2008) BLMs that were used for modelling.

	Daphnia magna BLM			*Oncorhynchus mykiss* BLM			*Pseudokirchneriella subcapitata* BLM		
Parameter	Zn	Cu	Ni	Zn	Cu	Ni	Zn	Cu	Ni
Biotic ligand (BL) species									
Log K_{MeBL}	5.31[a]	8.02 [a]	NI	5.31 [a]	8.02 [a]	NI	NI	NI	NI
Log K_{MeHBL}	NI	8.02[b] (-0.5)	NI	NI	7.34[b] (0.18)	NI	NI	NI	NI
Log K_{MeCo_3BL}	NI	7.44[c] (-14.21)	NI	NI	7.01[c] (-13.78)	NI	NI	NI	NI
Log K_{CaBL}	3.22	NI	3.53	3.22	3.47	3.6	NI	NI	NI
Log K_{MgBL}	2.69	NI	3.57	2.69	3.58	3.6	NI	NI	3.3
Log K_{NaBL}	1.9	2.91	NI	1.9	3.19	NI	NI	NI	NI
Log K_{HBL}	5.77	6.67	NI	5.77	5.1	NI	NI	NI	NI
SpH	NI	NI	0.3335	NI	NI	0.324	0.754	1.354	0.143
Bioavailable species that can bind to the biotic ligand	Zn^{2+}	Cu^{2+}, $CuOH^{+}$, $CuCO3^{0}$	Ni^{2+}	Zn^{2+}	Cu^{2+}, $CuOH^{+}$, $CuCO3^{0}$	Ni^{2+}	Zn^{2+}	Cu^{2+}	Ni^{2+}
Humic material assumptions									
% of natural DOM that is composed of humic substances[d]	61%	50%	40%	61%	50%	40%	61%	50%	40%
% of humic substances that is HA (rest is FA)[e]	0%	0%	0%	0%	0%	0%	0%	0%	0%

[a] Reaction: BL-Me = Me2+ + BL

[b] First constant refers to the reaction: BL-CuOH = $CuOH^{+}$ + BL. The constant in parentheses refers to the reaction BL-CuOH + H^{+} = Cu^{2+} + H_2O + BL

[c] First constant refers to the reaction: BL-$CuCO_3$ = $CUCO_3^{0}$ + BL. The constant in parentheses refers to the reaction BL-$CuCO_3$ = Cu^{2+} + CO_3^{2-} + BL

[d] Exception: when humic acid is added to the medium, all models assume 100% of the DOM to be composed of humic substances

[e] Exception: when humic acid is added to the medium, all models assume 100% of the humic substances to be composed of humic acid

NI = Not Incorporated as constant in the BLM; DOM = Dissolved Organic Matter; HA = Humic Acid; FA = Fulvic Acid

Appendix A6. Correlations in sensitivity of species to metals

The figures below show correlations found between the sensitivity of a species for one metal and its sensitivity for a second metal, in function of main physico-chemical variables (i.e. pH, DOC (mg/L) and Ca (mg/L)).

R-values for all correlations between binary combinations of metals are given in the top graphs of each figure, while p-values of these correlations are given in the bottom graphs of each figure. Correlations are significant when p-values corresponding to the r-values are below 0.05. This is the case for 0% of the correlations between the sensitivity of a species to Ni and its sensitivity to Zn; for 6.6% of the correlations between the sensitivity of a species to Ni and its sensitivity to Cu; and for 0.6% of the correlations between the sensitivity of a species to Zn and its sensitivity to Cu.

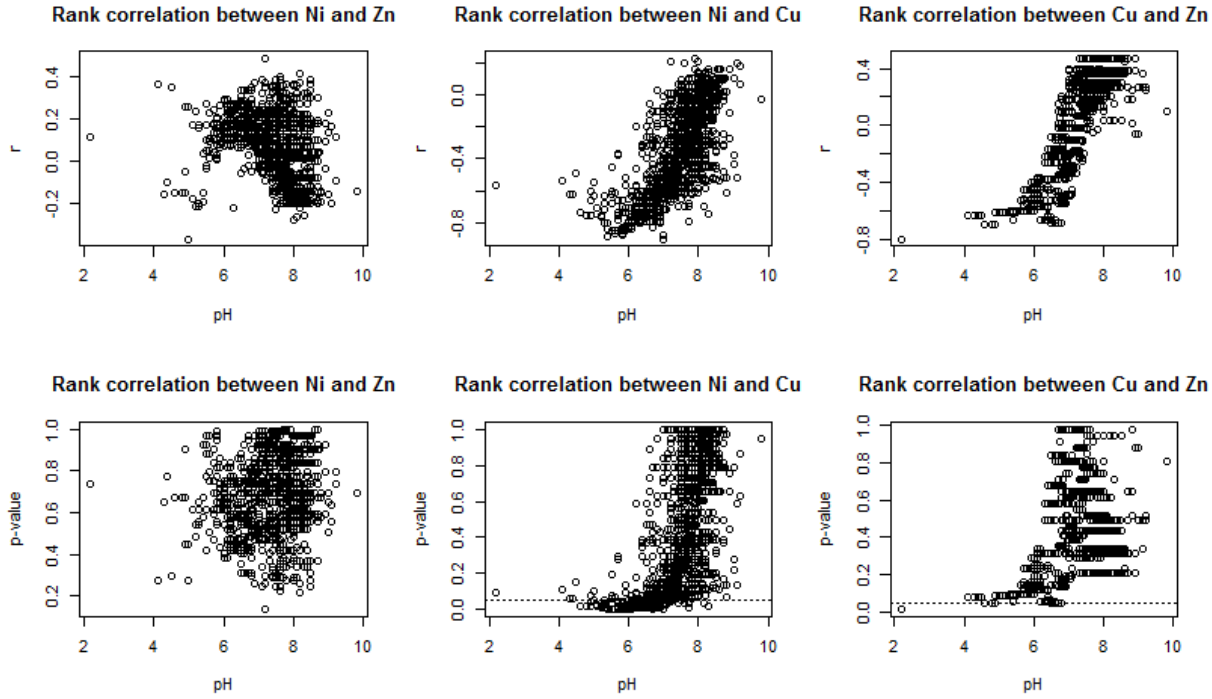

Figure A6.1. Correlations (Spearman rank) found between the sensitivity of a species for one metal and its sensitivity for a second metal, in function of pH. Top graphs give the r values corresponding to the correlations, bottom graphs give the p values corresponding to these r values. Correlations are significant when the p values are below 0.05.

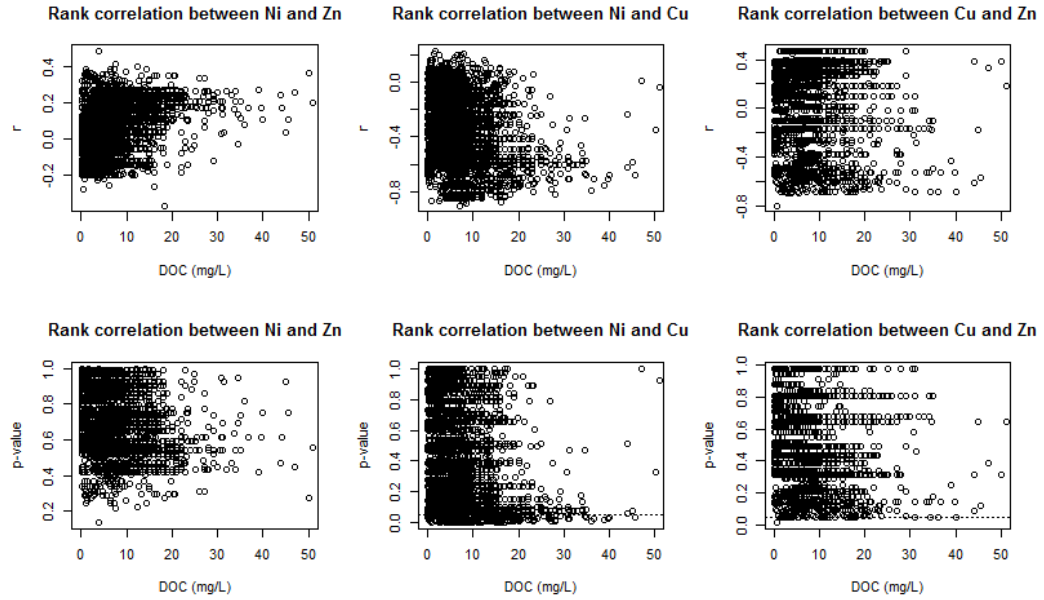

Figure A6.2. Correlations (Spearman rank) found between the sensitivity of a species for one metal and its sensitivity for a second metal, in function of Dissolved Organic Carbon (DOC) (mg/L). Top graphs give the r values corresponding to the correlations, bottom graphs give the p values corresponding to these r values. Correlations are significant when the p values are below 0.05.

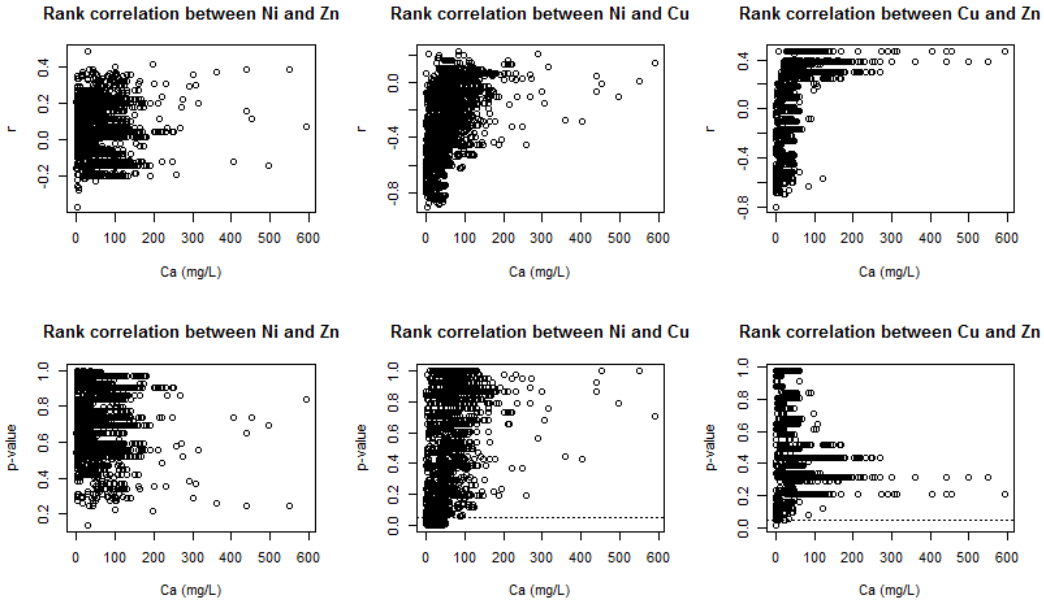

Figure A6.3. Correlations (Spearman rank) found between the sensitivity of a species for one metal and its sensitivity for a second metal, in function of Ca concentration (mg/L). Top graphs give the r values corresponding to the correlations, bottom graphs give the p values corresponding to these r values. Correlations are significant when the p values are below 0.05.

Appendix A7. Results from best-fit SSD calculations

This appendix shows the results, distribution of msPAF values for all four methods, for the different monitoring datasets using the best-fit SSD calculations.

In addition, the percentage of waterbodies that is potentially not affected and percentage that is potentially affected (msPAF > 0.05) by a mixture of Ni, Zn and/or Cu according to the CA_{SSD} method for the VMM, Rhine, Austria and FOREGS database, using a log-normal SSD distribution (analogue to Table 2.4 for the Dommel database in the main paper) is also given.

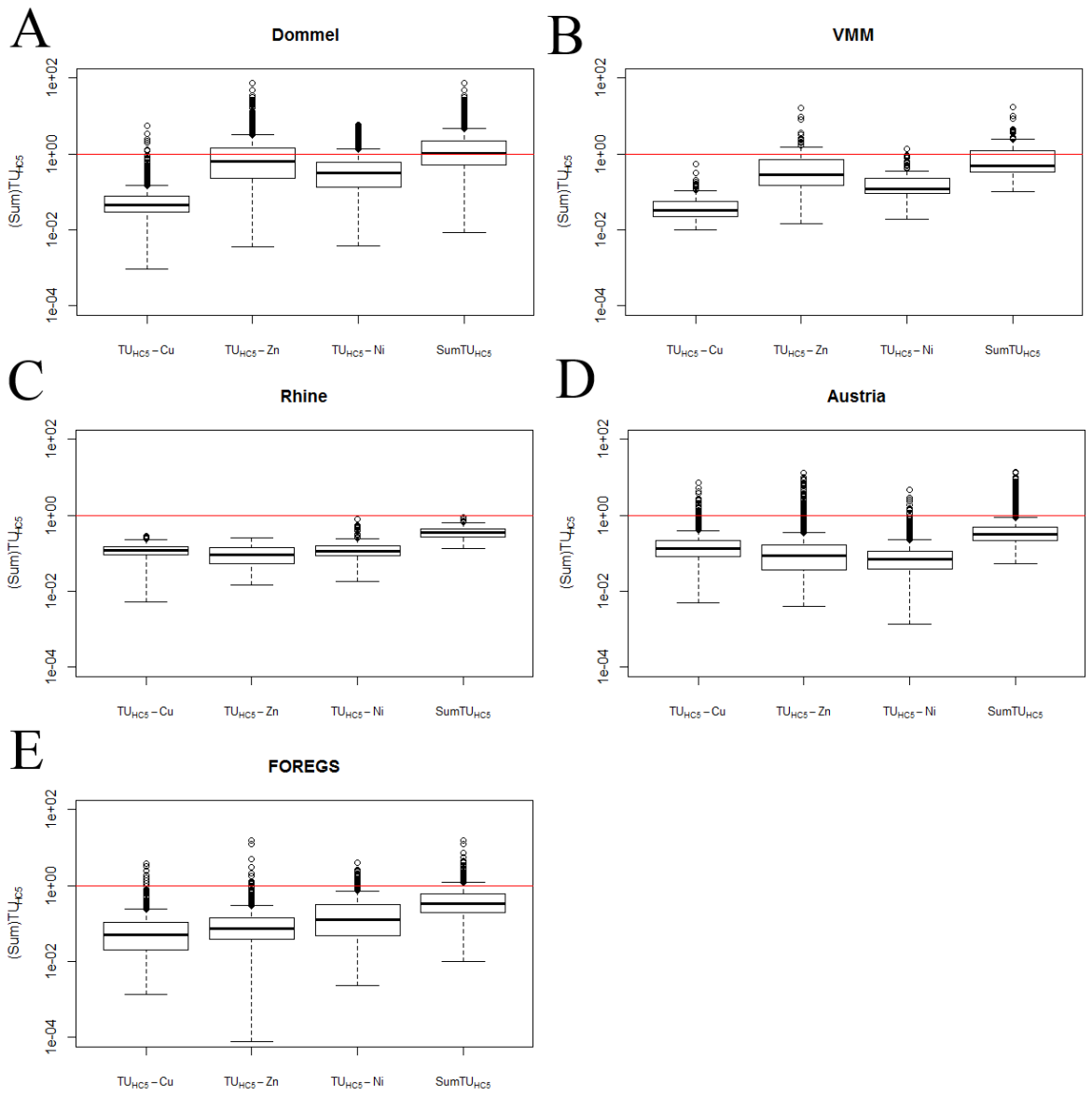

Figure A7.1 Toxic Units (TU) for Ni, Zn and Cu for the different samples of the Dommel, VMM, Rhine, Austria and FOREGS dataset. SumTU shows the summation of the TUs according to the CA_{SSD} method using the best-fit SSD distribution. The horizontal line indicates a TU or SumTU of 1. Results are represented as box plots: median values are given in bold, bottom and top of the box plots give the 25th and 75th percentile. Bottom and top of the error bars represent the 5th and 95th percentile, asterisks are outliers.

A7.1 Dommel

Table A7.1. Toxic pressure expressed as multisubstance potentially affected fraction of species (msPAF[a]) for the Dommel database obtained with the different methods (CA_{SSD}; CA_{DRC}; IA_{SSD} and IA_{DRC}) when SSDs are fitted with best-fit distributions. The percentage of affected samples is given per method. NA = not applicable, [a] the msPAF values reported are on the basis of EC_{10} values

	CA_{SSD}	CA_{DRC}	IA_{SSD}	IA_{DRC}
median msPAF	0.057	0.044	0.031	0.040
10th percentile msPAF	0.002	0.001	0.001	0.002
90th percentile msPAF	0.437	0.478	0.344	0.351
% samples affected (msPAF>0.05)	53	48	41	46
% samples affected by mixture of metals and not by any of the individual metals	15	10	4	7

A7.2 Rhine

Table A7.2. Toxic pressure expressed as multisubstance potentially affected fraction of species (msPAF[a]) for the Rhine database obtained with the different methods (CA_{SSD}; CA_{DRC}; IA_{SSD} and IA_{DRC}) when SSDs are fitted with best-fit distributions. The percentage of affected samples is given per method. NA = not applicable, [a] the msPAF values reported are on the basis of EC_{10} values

	CA_{SSD}	CA_{DRC}	IA_{SSD}	IA_{DRC}
median msPAF	0.009	0.005	0.004	0.005
10th percentile msPAF	0.003	0.002	0.001	0.002
90th percentile msPAF	0.015	0.010	0.008	0.008
% samples affected (msPAF>0.05)	0	0	0	0
% samples affected by mixture of metals and not by any of the individual metals	0	0	0	0

A7.3 VMM

Table A7.3. Toxic pressure expressed as multisubstance potentially affected fraction of species (msPAF[a]) for the VMM database obtained with the different methods (CA_{SSD}; CA_{DRC}; IA_{SSD} and IA_{DRC}) when SSDs are fitted with best-fit distributions. The percentage of affected samples is given per method. NA = not applicable, [a] the msPAF values reported are on the basis of EC_{10} values

	CA_{SSD}	CA_{DRC}	IA_{SSD}	IA_{DRC}
median msPAF	0.013	0.008	0.006	0.007
10th percentile msPAF	0.001	<0.001	<0.001	<0.001
90th percentile msPAf	0.230	0.225	0.166	0.180
% samples affected (msPAF>0.05)	27	26	26	24
% samples affected by mixture of metals and not by any of the individual metals	4	3	1	1

Table A7.4. Percentage of waterbodies that is potentially not affected and percentage that is potentially affected (msPAF > 0.05) by a mixture of Ni, Zn and/or Cu according to the CA_{SSD} method for the VMM database, using a log-normal SSD distribution.

	Percentage (%)
No effect	72.90
Effect	27.10
Individual metal effects	20.00
Only Zinc[a]	18.71
Only Nickel[a]	0.65
Only Copper[a]	0.00
Both Zinc and Nickel[b]	0.65
Mixture effects	7.10
Binary combinations[c]	6.45
Ternary combination[d]	0.65
Shows the largest TU[e]	
Zn	72.73
Ni	27.27
Cu	0

[a] The Toxic Unit of zinc, nickel or copper is above 1
[b] The Toxic Unit of all mentioned metals is above 1
[c] At least one of the possible binary combinations (i.e.Zn&Ni, Zn&Cu, Ni&Cu) shows an effect
[d] The ternary combination (but none of the 3 possible binary combinations) shows an effect
[e] For each metal the percentages of samples is given in which that metal has the largest Toxic Unit in the sample affected by a binary or ternary combination, i.e.in which that metal is the largest contributor to the toxic effect

A7.4 Austria

Table A7.5. Toxic pressure expressed as multisubstance potentially affected fraction of species ($msPAF^a$) for the Austria database obtained with the different methods (CA_{SSD}; CA_{DRC}; IA_{SSD} and IA_{DRC}) when SSDs are fitted with best-fit distributions. The percentage of affected samples is given per method. NA = not applicable, [a] the msPAF values reported are on the basis of EC_{10} values

	CA_{SSD}	CA_{DRC}	IA_{SSD}	IA_{DRC}
median msPAF	0.006	0.004	0.003	0.004
10th percentile msPAF	0.001	<0.001	<0.001	<0.001
90th percentile msPAf	0.036	0.026	0.020	0.021
% samples affected (msPAF>0.05)	7	6	5	5
% samples affected by mixture of metals and not by any of the individual metals	3	1	0.3	0.05

Table A7.6. Percentage of waterbodies that is potentially not affected and percentage that is potentially affected (msPAF > 0.05) by a mixture of Ni, Zn and/or Cu according to the CA_{SSD} method for the Austria database, using a log-normal SSD distribution.

	Percentage (%)
No effect	92.47
Effect	7.53
Individual metal effects	4.49
Only Zinc[a]	2.90
Only Nickel[a]	0.37
Only Copper[a]	0.75
Both Zinc and Nickel[b]	0.05
Both Zinc and Copper[b]	0.14
Both Nickel and Copper[b]	0.28
Both Zinc, Nickel and Copper[b]	0.05
Mixture effects	3.04
Binary combinations[c]	1.03
Ternary combination[d]	2.01
Shows the largest TU[e]	
Zn	60
Ni	14
Cu	26

[a] The Toxic Unit of zinc, nickel or copper is above 1
[b] The Toxic Unit of all mentioned metals is above 1
[c] At least one of the possible binary combinations (i.e.Zn&Ni, Zn&Cu, Ni&Cu) shows an effect
[d] The ternary combination (but none of the 3 possible binary combinations) shows an effect
[e] For each metal the percentages of samples is given in which that metal has the largest Toxic Unit in the sample affected by a binary or ternary combination, i.e.in which that metal is the largest contributor to the toxic effect

A7.5 FOREGS

Table A7.7. Toxic pressure expressed as multisubstance potentially affected fraction of species (msPAF[a]) for the FOREGS database obtained with the different methods (CA_{SSD}; CA_{DRC}; IA_{SSD} and IA_{DRC}) when SSDs are fitted with best-fit distributions. The percentage of affected samples is given per method. NA = not applicable, [a] the msPAF values reported are on the basis of EC_{10} values

	CA_{SSD}	CA_{DRC}	IA_{SSD}	IA_{DRC}
median msPAF	0.006	0.003	0.003	0.003
10th percentile msPAF	<0.001	<0.001	<0.001	<0.001
90th percentile msPAf	0.055	0.043	0.036	0.038
% samples affected (msPAF>0.05)	1	9	7	7
% samples affected by mixture of metals and not by any of the individual metals	4	2	0.6	3

Table A7.8. Percentage of waterbodies that is potentially not affected and percentage that is potentially affected (msPAF > 0.05) by a mixture of Ni, Zn and/or Cu according to the CA_{SSD} method for the FREGS database, using a log-normal SSD distribution.

	Percentage (%)
No effect	89.80
Effect	10.20
Individual metal effects	6.38
Only Zinc[a]	1.66
Only Nickel[a]	3.70
Only Copper[a]	0.64
Both Zinc and Copper[b]	0.13
Both Zinc, Nickel and Copper[b]	0.26
Mixture effects	3.83
Binary combinations[c]	2.30
Ternary combination[d]	1.53
Shows the largest TU[e]	
Zn	26.7
Ni	50.0
Cu	23.3

[a] The Toxic Unit of zinc, nickel or copper is above 1
[b] The Toxic Unit of all mentioned metals is above 1
[c] At least one of the possible binary combinations (i.e.Zn&Ni, Zn&Cu, Ni&Cu) shows an effect
[d] The ternary combination (but none of the 3 possible binary combinations) shows an effect
[e] For each metal the percentages of samples is given in which that metal has the largest Toxic Unit in the sample

Table

Appendix B:

SUPPORTING INFORMATION OF CHAPTER 3.

Appendix B1. Chemical analyses

For the ternary mixture experiment, nickel concentrations between 20-200 µg/L, copper concentrations between 25-200 µg/L and zinc concentrations below 50 µg/L were measured with inductively coupled plasma mass spectrometry (ICP-MS; Agilent 7700x, in the He mode using 72Ge as internal standard; reference material TM-27.3; limit of quantification, 0.08 µg Cu/L; 0.26 µgNi/L and 0.17 µg Zn/L; method detection limit, 0.02 µg Cu/L; 0.07 µg Ni/L and 0.05 µg Zn/L). Zinc concentrations above 50 µg/L and nickel and copper concentrations between 200-1000 µg/L were measured with flame atomic absorption spectrophotometry (FAAS, SpectrAA100, Varian, Mulgrave, Australia; reference material TMDA-70; limit of quantification, 50 µg Cu/L; 60 µgNi/L and 20 µg Zn/L; method detection limit, 15 µg Cu/L; 18 µg Ni/L and 6 µg Zn/L). Nickel and copper concentrations lower than 20 µg/L and 25 µg/L, respectively, were measured using graphite furnace atomic absorption spectrophotometry (GFAAS Furnace Autosampler, Thermo Fisher Scientific Inc. reference material TM24.3; limit of quantification, 2.5 µg Cu/L and 1 µgNi/L; method detection limit, 0.75 µg Cu/L and 0.30 µg Ni/L). Cation samples (Ca, Mg, Na, K) were measured with ICP-MS. Anion samples (SO_4, Cl) were analysed using ion chromatography (DI-ONEX2000i/SP; Dionex, Sunnyvale, CA, VS).

For the binary mixture experiment, nickel concentrations below 20 µg/L and copper concentrations below 25 µg/L concentrations were measured using GFAAS. Nickel concentrations above 200 µg/L and copper concentrations above 50 µg/L were measured using FAAS. Cations were analysed using both GFAAS and FAAS. Anion samples were analysed using spectrophotometry (Aquamate, Thermo Electron Corporation; Chloride: Merck, Spectroquant 1.14897.001; Sulphate: Merck, Spectroquant 1.14548.001).

For both the ternary and binary mixture experiment, OC and IC were measured with a Total Organic Carbon analyser following the NPOC method (TOC-5000, Shimadzu, Duisburg, Germany; Limit of Quantification 1.5 mg DOC/L; Method Detection Limit 0.5 mg DOC/L).

Appendix B2. Analyses of combined effects

The analysis of the interactive effects was made based on both the dissolved concentrations and the free ion activities, to identify possible shifts in interactions due to competitive binding of Cu, Ni and Zn onto DOC. The mean RGR for every treatment was used as input for the analysis of the combined effects, which was performed in three subsequent steps. These steps were performed in the software package R-1.0.136 (R development Core Team). A first step entailed the prediction of the RGR for the mixture combinations, which was made with the reference models CA (Equation B2.1) and IA (Equation B2.2) using the parameters of the individual dose response curves of Cu, Ni and Zn ($EC50_{Me_i}$ and b_{Me_i}).

$$\sum_{i=1}^{n} \frac{x_{Me_i}}{EC50_{Me_i} \cdot \left(\frac{100-RGR_{mix}}{RGR_{mix}}\right)^{\frac{1}{b_{Me_i}}}} = 1 \qquad \text{(Equation B2.1)}$$

$$RGR_{mix} = 100 \cdot \prod_{i=1}^{n} \left(\frac{1}{1+\left(\frac{x_{Me_i}}{EC50_{Me_i}}\right)^{b_{Me_i}}}\right) \qquad \text{(Equation B2.2)}$$

Where *n* is the number of metals in the mixture and RGR_{mix} is the predicted mixture growth rate relative to the control. These RGR_{mix} values predicted using the CA and IA reference model as well as the observed RGR_{mix} values were plotted as a function of the $\sum TU_{Me}$, a first step to visualize possible interactive mixture effects.

However, whether these observed mixture effects statistically deviated from non-interactivity had to be further investigated, which was done in the second and third step of the mixture analysis framework. In the second step, Equation B.2 and B.3 were fitted to all data (i.e. single metals and mixture data). Subsequently, in the third step, the CA and IA reference models were extended with a deviation parameter (*a*), which is a measure for the deviation of non-interactivity (*Joncker et al 2005, Hochmuth et al 2014*). To solve step 2 or 3, *x* random parameter sets (i.e. $EC50_{Me_i}$, b_{Me_i} and *a*) were sampled simultaneously from a normal distribution with the mean and standard deviation originating from the $EC50_{Me_i}$ and $b_{Me_i}$of the single metal dose-response curves, until a total of 5000 parameter sets were obtained. Five thousand parameter sets resulted in an adequate reduction of the sum of squared errors of the model. This is a small difference to the calculations done by Hochmuch et al (*2014*) and Nys et al (*2017*]),in which a fixed number of parameters sets were sampled, i.e. 5000 and 20 000 sets, respectively. We deemed it necessary to randomly sample *x* times, as the desired number of parameter sets (5000) was not necessary obtained by sampling 5000 times (i.e. not all sampling turns resulted in a fit) (see section below). Based on the lowest sum of squared errors, the best set of parameters was then selected from these 5000 parameter sets. To examine whether the deviation from non-interactivity was significant, it was checked whether the addition of the deviation parameter *a* significantly improved the predictions of the nested models from step 2 and 3 (*Hochmuth et al 2014*). This was done by performing an F-test, after checking the validity of the assumptions for this test.

Random sampling

For the interactive effects analysis, we calculated 5000 random samples of input parameter sets, because we observed that this number of samples resulted in an adequate reduction of the sum of squared errors of the model and increasing the sample numbers (up to 30000) did not change the model

fit largely (only small decreases in lowest SSE; Figure B2.1 for the CA model and Figure B2.2 for the IA model). Five thousand samples were previously also used in other metal mixture toxicity work (see Hochmuth et al. 2014).

To obtain these 5000 parameter sets, x random parameter sets (i.e. $EC50_{Me_i}$, b_{Me_i} and a) were sampled simultaneously from a normal distribution with mean and standard deviation origination from the $EC50_{Me_i}$ and $b_{Me_i}$of the single metal dose-response curves, until a total of 5000 parameter sets were obtained

This is a small difference to the calculations done by Hochmuch et al (2014) and Nys et al (2017c), in which a fixed number of parameters sets were sampled, i.e. 5000 and 20 000 sets, respectively. We deemed it necessary to randomly sample x times, as the desired number of parameter sets (5000) was not necessary obtained by sampling 5000 times (i.e. not all sampling turns resulted in a fit; Table B2.1).

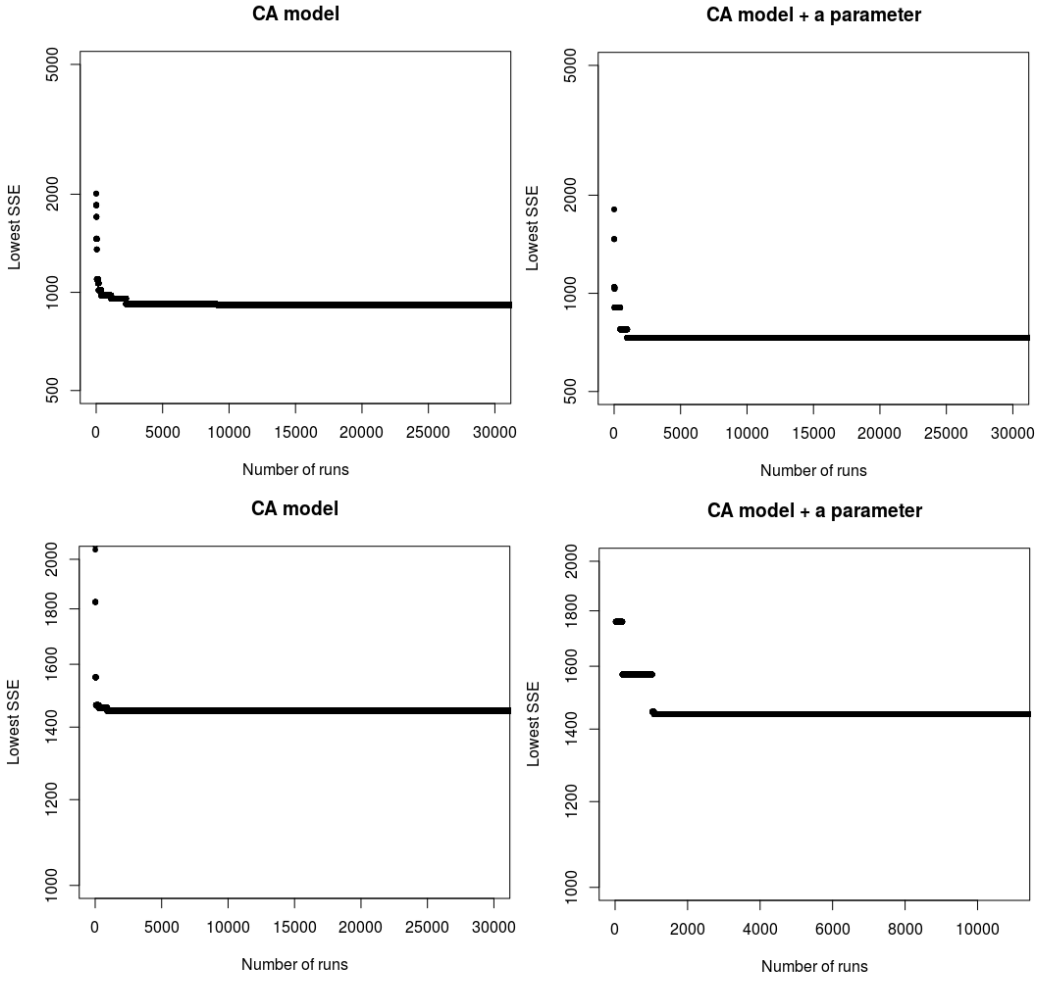

Figure B2.1: Lowest sum of squared errors (SSE) as a function of the number of runs to sample model parameters for the interactive effects analyses for the ternary mixture (Loire; top) and for the binary mixture (Bihain; bottom). The reduction in sum of squared error is shown for the CA model: for non-interaction (left graphs) and for mixture interaction (CA reference model extended with a deviation parameter (a); right graphs).

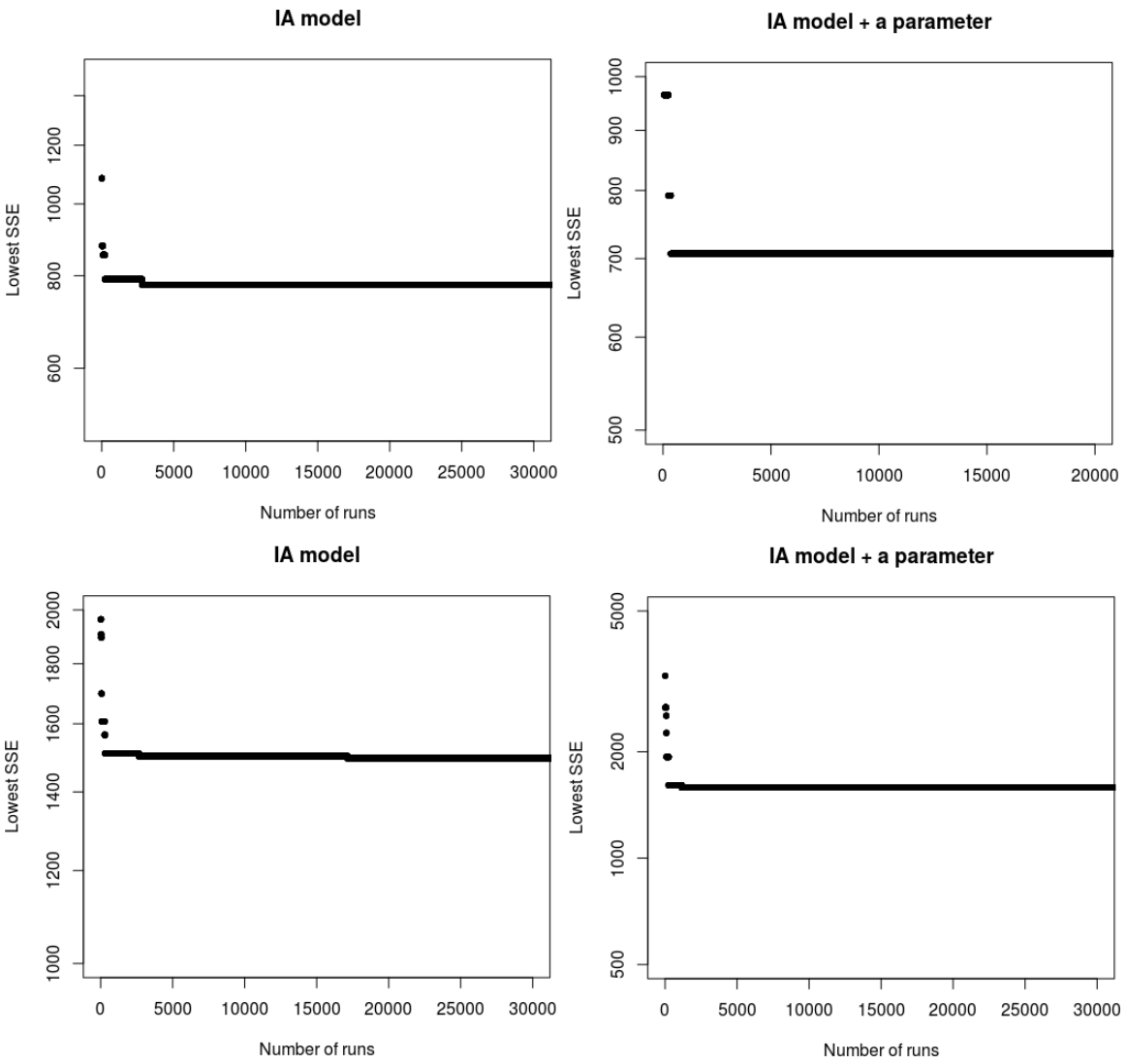

Figure B1.2: Lowest sum of squared errors (SSE) as a function of the number of runs to sample model parameters for the interactive effects analyses for the ternary mixture (Loire; top) and for the binary mixture (Bihain; bottom). The reduction in sum of squared error is shown for the IA model: for non-interaction (left graphs) and for mixture interaction (IA reference model extended with a deviation parameter (a); right graphs).

Table B1.1. A range of number of runs necessary to obtain 5000 parameter sets (i.e. $EC50_{Me_i}$, b_{Me_i} and *a)*, for ternary and binary mixtures for the mixture reference models Concentration Addition (CA; Equation 3.1) and independent Action (IA; Equation 3.2). Results are given for dissolved metal concentrations as well as free metal ion activities.

		CA non-interaction	CA mixture interaction	IA non-interaction	IA mixture interaction
Ternary	Dissolved	5000-5018	7452-9882	5000	5011-5319
	Activity	5000-5055	6107-8691	5000-5064	5009-5459
Binary	Dissolved	5018-6090	33999-60508	5000-5017	7808-8261
	Activity	5017-6680	22037-29008	5000-5107	8093-8178

Appendix B3. Test validity criteria and concentration response data of the individual metal exposures

Table B3.1 Evaluation of compliance with the validation criteria of the *Pseudokircherniella subcapitata* growth test (OECD 2002)

	Loire		Dolaison		Moselotte		Bihain		Brisy1		Voyon		Brisy2		Markermeer	
Validation criteria	72-h	48-h	72-h	48-h	72-h	48-h	72-h	48-h	72-h	48-h	72-h	48-h	72-h	48-h	72-h	48-h
Control growth rate (d^{-1})	1.56 ±0.10	1.88 ±0.10	1.68 ±0.02	1.78 ±0.03	1.65 ±0.02	1.91 ±0.04	1.44 ±0.01	1.74 ±0.01	1.60 ±0.00	1.89 ±0.01	1.50 ±0.00	1.79 ±0.01	1.52 ±0.01	1.82 ±0.01	1.55 ±0.01	1.87 ±0.01
Control biomass increase>16?[a]	104	43	172	38	108	32	77	32	125	44	91	36	97	38	98	42
$CV_{growth\ rate,\ control}$<7%?[b]	0.9%	0.7%	1.1%	1.7%	0.7%	1.2%	1.2%	1.2%	1.0%	1.6%	0.8%	1.80%	1.10%	2.0%	2.6%	1.9%
Mean $CV_{section}$≤35%?[c]	39%	14%	13%	11%	21%	9.5%	43%	28%	37%	26%	39%	26%	39%	24%	41%	13%
Pass validity criteria?	Fail	Pass	Pass	Pass	Pass	Pass	Fail	Pass	Fail	Pass	Fail	Pass	Fail	Pass	Fail	Pass

a Control biomass should have increased exponentially by a factor of at least 16 within test period.

b The coefficient of variation of average specific growth rates in the controls ($CV_{growth\ rate,\ control}$) must not exceed 7%.

c The mean coefficient of variation for section-by-section specific growth rates in the controls ($CV_{section}$) must not exceed 35%

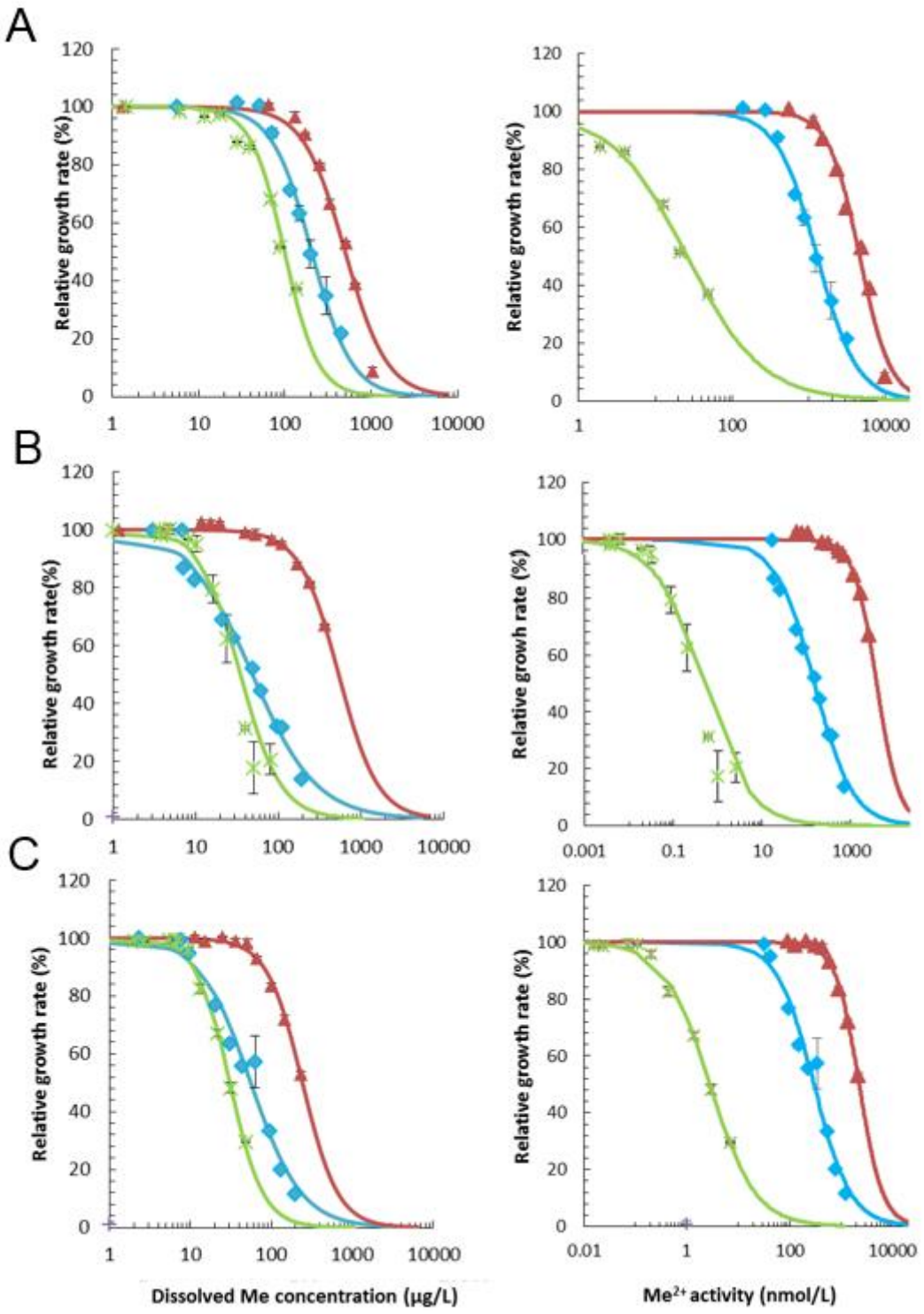

Figure B3.1 Concentration response data for relative growth rate (RGR, %) and fitted log-logistic concentration response curves of the individual Cu (crosses), Ni (triangles) and Zn (circles) exposures in the Pseudokircherniella subcapitata experiments for the waters Loire (A), Dolaizon (B), Moselotte (C). Left panels show data based on dissolved concentrations, right panels based on calculated free ion activities. Error bars represent standard errors.

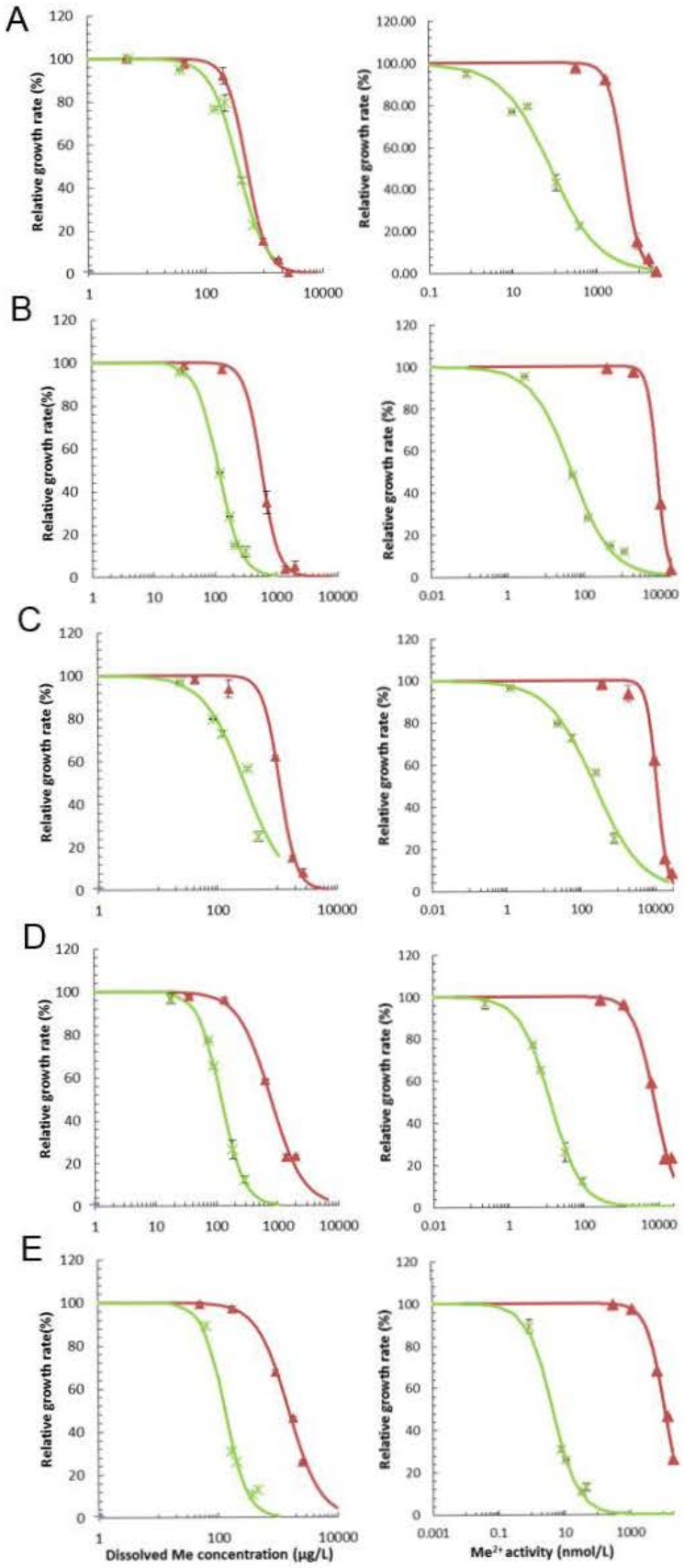

Figure B3.1 Concentration response data for relative growth rate (RGR, %) and fitted log-logistic concentration response curves of the individual Cu (crosses), Ni (triangles) and Zn (circles) exposures in the Pseudokircherniella subcapitata experiments for the waters Bihain (A), Brisy1 (B), Voyon (C), Brisy2 (D) and Markermeer (E). Left panels show data based on dissolved concentrations, right panels based on calculated free ion activities. Error bars represent standard errors.

Table B3.2 Measured metal concentrations and observed relative growth rate (RGR) in the single metal treatments during the ternary experiments with *Pseudokircherniella subcapitata*. NA = not applicable

	Loire		Dolaison		Moselotte	
	Dissolved Me concentration (µg/L; ± Stdev)	Observed RGR (%; ± Stdev)	Dissolved Me concentration (µg/L; Stdev)	Observed RGR (%; ± Stdev)	Dissolved Me concentration (µg/L; Stdev)	Observed RGR (%; ± Stdev)
Single dose Ni	6 ± 0.2	100 ± 0	1 ± 0.0	100 ± 0	0.4 ± 0.0	100 ± 0
	64 ± 2.3	101 ± 1	12 ± 0.0	103 ± 4	11 ± 0.0	101 ± 2
	130 ±0.2	97 ± 3	15 ± 0.2	105 ± 3	15 ± 0.1	98 ± 5
	172 ± 0.3	91 ± 1	19 ± 0.2	100 ± 7	25 ± 0.0	101 ± 2
	256 ± 1.0	80 ± 1	40 ± 0.3	98 ± 1	36 ± 0.1	97 ± 3
	334 ± 2.1	67 ± 1	53 ± 0.7	100 ± 2	50 ± 0.0	97 ± 4
	515 ± 0.7	53 ± 1	83 ± 0.1	99 ± 5	66 ± 0.9	92 ± 1
	657 ± 3.4	39 ± 1	110 ± 0.2	99 ± 0	100 ± 0.8	85 ± 1
	1032 ± 4.2	8 ± 2	170 ± 0.7	95 ± 3	146 ± 0.2	75 ± 2
	NA	NA	242 ± 0.4	88 ± 3	232 ± 1.4	58 ± 1
	NA	NA	365 ± 1.6	69 ± 2	NA	NA
Single dose Cu	1 ± 0.0	100 ± 0	1 ± 0.1	100 ± 0	1 ± 0.0	100 ± 0
	6 ± 0.1	98 ± 1	4 ± 0.4	102 ± 1	2 ± 0.0	97 ± 4
	12 ± 0.1	97 ± 0	4 ± 0.1	102 ± 2	3 ± 0.0	96 ± 2
	18 ± 0.1	97 ± 1	5 ± 0.0	104 ± 4	7 ± 4.3	98 ± 1
	28 ± 0.2	88 ± 1	8 ± 0.3	96 ± 5	5 ± 0.0	96 ± 2
	39 ± 0.1	86 ± 1	10 ± 0.3	94 ± 6	9 ± 0.0	89 ± 3
	68 ± 0.6	68 ± 2	16 ± 0.2	78 ± 10	13 ± 0.2	71 ± 1
	88 ± 0.8	52 ± 1	24 ± 0.1	59 ± 19	22 ± 0.6	51 ± 3
	137 ± 1.6	37 ± 1	40 ± 0.3	36 ± 20	31 ± 0.3	39 ± 2
	NA	NA	50 ± 0.6	46 ± 43	48 ± 0.4	29 ± 1
	NA	NA	80 ± 1.3	18 ± 14	NA	NA
Single dose Zn	1 ± 0.0	100 ± 0	3 ± 0.2	100 ± 0	2 ± 0.5	100 ± 0
	28 ± 0.2	101 ± 1	7 ± 0.2	103 ± 1	7 ± 0.3	100 ± 1
	51 ± 0.6	101 ± 0	7 ± 0.6	95 ± 1	9 ± 0.1	95 ± 2
	71 ± 0.4	91 ± 3	10 ± 0.2	89 ± 4	20 ± 0.6	72 ± 5
	114 ± 1.6	71 ± 2	21 ± 0.6	67 ± 1	30 ± 5.1	64 ± 1
	146 ± 1.1	63 ± 4	28 ± 0.3	63 ± 0	44 ± 0.4	57 ± 1
	198 ± 2.6	49 ± 8	49 ± 1.5	51 ± 1	63 ± 0.3	57 ± 14
	298 ± 0.9	35 ± 11	62 ± 0.3	44 ± 2	95 ± 0.4	29 ± 1
	450 ± 8.0	22 ± 0	96 ± 0.3	26 ± 2	128 ± 0.4	16 ± 0
	NA	NA	110 ± 1.2	24 ± 2	196 ± 1.8	11 ± 0
	NA	NA	188 ± 4.0	7 ± 2	NA	NA

Table B3.3 Measured metal concentrations and observed relative growth rate (RGR) in the single metal treatments during the binary experiments with *Pseudokircherniella subcapitata*.

	Bihain		Brisy1		Voyon		Brisy2		Markermeer	
	Dissolved Me concentration (µg/L; Stdev)	Observed RGR (%; Stdev)	Dissolved Me concentration (µg/L; Stdev)	Observed RGR (%; Stdev)	Dissolved Me concentration (µg/L; Stdev)	Observed RGR (%; Stdev)	Dissolved Me concentration (µg/L; Stdev)	Observed RGR (%; Stdev)	Dissolved Me concentration (µg/L; Stdev)	Observed RGR (%; Stdev)
Single dose Ni	5 ± 2.2	100 ± 0	4 ± 2.9	100 ± 0	5 ± 3.1	100 ± 0	4 ± 2.9	100 ± 0	4 ± 2.9	100 ± 0
	45 ± 0.3	98 ± 0	33 ± 4.4	99 ± 2	43 ± 0.5	98 ± 1	36 ± 3.4	98 ± 1	51 ± 2.4	99 ± 2
	208 ± 3.1	92 ± 2	135 ± 3.4	97 ± 1	159 ± 4.5	94 ± 7	138 ± 14.3	96 ± 1	180 ± 13.8	97 ± 2
	970 ± 37.1	15 ± 7	715 ± 16.6	35 ± 9	952 ± 9.7	62 ± 1	645 ± 38.0	59 ± 1	931 ± 45.6	68 ± 1
	1748 ± 0.7	6 ± 1	1381 ± 4.9	3 ± 2	1815 ± 13.4	15 ± 1	1388 ± 78.5	23 ± 2	1836 ± 83.4	46 ± 1
	2601 ± 31.8	0 ± 0	2052 ± 1.4	5 ± 4	2680 ± 21.2	8 ± 3	2015 ± 51.6	23 ± 1	2634 ± 160.5	26 ± 1
Single dose Cu	5 ± 2.6	100 ± 0	2 ± 0.5	100 ± 0	3 ± 1.3	100 ± 0	2 ± 0.7	100 ± 0	2 ± 0.2	100 ± 0
	38 ± 0.0	95 ± 1	28 ± 0.0	95 ± 1	24 ± 0.0	97 ± 1	18 ± 0.0	97 ± 4	64 ± 0.0	89 ± 6
	146 ± 8.3	77 ± 1	123 ± 6.2	49 ± 1	85 ± 3.5	80 ± 0	74 ± 8.8	77 ± 1	169 ± 16.6	31 ± 2
	223 ± 1.3	79 ± 1	176 ± 2.8	28 ±.3	122 ± 3.5	73 ± 2	92 ± 4.1	65 ± 1	204 ± 18.0	26 ± 1
	418 ± 0.6	43 ± 7	212 ± 6.9	15 ± 1	322 ± 22.1	56 ± 1	183 ± 9.0	26 ± 8	383 ± 22.8	11 ± 1
	659 ± 0.7	22 ± 2	314 ± 11.1	12 ± 4	489 ± 14.5	25 ± 4	290 ± 17.3	12 ± 3	468 ± 8.3	13 ± 3

Appendix B4. Analysis of mixture effects

Table B4.1 Metal concentrations (± st. dev.) and observed relative growth rate (RGR ± st.dev.) used for mixture response analysis for the ternary metal mixture of the *Pseudokircherniella subcapitata* in three natural waters.

Test water	Nominal $\sum TU_{EC50,Me}$	Dissolved Zn concentration (µg/L; Stdev)	Dissolved Ni concentration (µg/L; Stdev)	Dissolved Cu concentration (µg/L; Stdev)	$\sum TU_{Mediss}$	Observed RGR (%; Stdev)
Loire	0.38	26 ± 0.4	62 ± 0.2	7 ± 0.1	0.33	99 ± 1
	0.75	53 ± 0.1	133 ± 0.2	14 ± 0.0	0.63	75 ± 5
	1.00	74 ± 0.7	177 ± 1.0	23 ± 0.2	0.87	47 ± 2
	1.50	113 ± 2.5	265 ± 5.3	34 ± 0.8	1.35	31 ± 1
	2.00	155 ± 0.0	330 ± 0.9	45 ± 0.0	1.78	33 ± 1
	3.00	230 ± 1.2	531 ± 2.3	70 ± 0.6	2.69	27 ± 3
	4.00	299 ± 0.3	695 ± 2.5	88 ± 0.8	3.67	20 ± 2
	6.00	445 ± 0.9	1223 ± 3.0	131 ± 0.2	5.66	11 ± 1
Dolaizon	0.19	5 ± 0.2	11 ± 0.0	3 ± 0.0	0.27	102 ± 2
	0.25	8 ± 0.4	14 ± 0.0	4 ± 0.0	0.28	98 ± 3
	0.38	11 ± 0.3	21 ± 0.1	4 ± 0.0	0.37	94 ± 1
	0.75	21 ± 0.7	44 ± 0.1	8 ± 0.0	0.73	66 ± 5
	1.00	26 ± 0.6	56 ± 0.6	8 ± 0.1	0.97	61 ± 2
	1.50	43 ± 0.4	87 ± 0.2	16 ± 0.1	1.62	39 ± 1
	2.00	56 ± 0.5	119 ± 0.3	21 ± 0.1	2.16	27 ± 4
	3.00	95 ± 1.5	179 ± 0.0	39 ± 0.6	3.42	12± 4
	4.00	106 ± 3.8	237 ± 4.0	38 ± 0.7	4.15	9 ± 2
	6.00	183 ± 2.7	352 ± 0.1	82 ± 1.2	6.84	7 ± 1
Moselotte	0.30	8 ± 0.0	10 ± 0.2	2 ± 0.1	0.33	97 ± 2
	0.38	10 ± 0.1	13 ± 0.0	2 ± 0.0	0.28	97 ± 1
	0.75	19 ± 0.2	26 ± 0.1	3 ± 0.0	0.50	82 ± 4
	1.00	26 ± 0.1	34 ± 0.1	5 ± 0.0	0.68	73 ± 2
	1.50	42 ± 0.9	50 ± 0.6	7 ± 0.1	1.05	49 ± 1
	2.00	57 ± 0.6	65 ± 0.3	10 ± 0.1	1.48	40 ± 1
	3.00	86 ± 0.4	100 ± 0.4	17 ± 0.1	2.25	33 ± 2
	4.00	120 ± 0.3	132 ± 0.8	24 ± 0.3	3.32	26 ± 1
	6.00	176 ± 5.3	198 ± 3.2	29 ± 0.4	4.83	16 ± 2

Table B4.2 Metal concentrations (± st. dev.) and observed relative growth rate (RGR ± st.dev.) used for mixture response analysis for the binary metal mixture of the *Pseudokircherniella subcapitata* in five natural waters.

Test water	Nominal $\sum TU_{EC50,Me}$	Dissolved Ni concentration (µg/L; Stdev)	Dissolved Cu concentration (µg/L; Stdev)	$\sum TU_{Mediss}$	Observed RGR (%; Stdev)
Bihain	0.20	40 ± 0.2	13 ± 1.1	0.19	99 ± 1
	0.44	85 ± 0.6	36 ± 0.0	0.81	93 ± 1
	0.92	209 ± 3.5	52 ± 0.4	2.50	53 ± 1
	2.00	468 ± 0.7	137 ± 16.5	4.56	59 ± 3
	4.40	1004 ± 14.1	231 ± 12.4	6.88	32 ± 8
Brisy1	0.20	28 ± 0.5	6 ± 0.8	0.29	97 ± 2
	0.44	77 ± 4.7	10 ± 0.2	1.28	98 ± 2
	0.92	154 ± 3.3	19 ± 0.9	2.72	93 ± 2
	2.00	378 ± 37.3	34 ± 4.1	4.17	48 ± 2
	4.40	778 ± 9.7	173 ± 14.5	6.19	9 ± 6
Voyon	0.20	36 ± 2.8	8 ± 2.6	0.12	102 ± 7
	0.44	80 ± 2.2	14 ± 2.7	0.45	96 ± 2
	0.92	208 ± 12.1	33 ± 4.4	1.29	93 ± 1
	2.00	463 ± 0.7	63 ± 5.5	2.78	58 ± 2
	4.40	1002 ± 35.	178 ± 9.0	4.15	54 ± 1
Brisy2	0.20	36 ± 0.5	6 ± 0.0	0.20	99 ± 1
	0.44	78 ± 0.5	11 ± 2.6	0.79	98 ± 2
	0.92	156 ± 5.9	17 ± 4.1	1.58	85 ± 7
	2.00	351 ± 20.0	42 ± 7.6	3.29	64 ± 2
	4.40	741 ± 19.4	105 ± 4.1	4.97	35 ± 1
Markermeer	0.20	46 ± 3.4	10 ± 0.0	0.52	100 ± 0.4
	0.44	107 ± 9.7	24 ± 0.0	1.40	98 ± 3
	0.92	220 ± 13.2	48 ± 8.4	2.15	71 ± 1
	2.00	478 ± 15.2	134 ± 11.4	4.10	35 ± 1
	4.40	1058 ± 39.6	224 ± 16.6	5.26	14 ± 2

Figure B4.1 Observed and predicted relative reproduction in the ternary Cu-Ni-Zn and binary Cu-Ni mixture combinations as a function of the sum of toxic units based on dissolved concentrations for the *Pseudokircherniella subcapitata* experimental series for the Loire (A), Dolaizon (B), Moselotte (C), Bihain (D), Brisy1 (E), Voyon (F), Brisy2 (G) and Markermeer (H) test waters. Symbols are denoted as follows: observed reproduction (orange circles), predictions of concentration addition (CA, blue triangles), and predictions of independent action (IA, purple squares). Predictions are based on the parameters ($EC50_{Mediss,i}$ and $b_{Mediss,i}$) of the individual concentration-response curves of Cu, Ni and Zn (Table 3.4). Error bars represent standard errors.

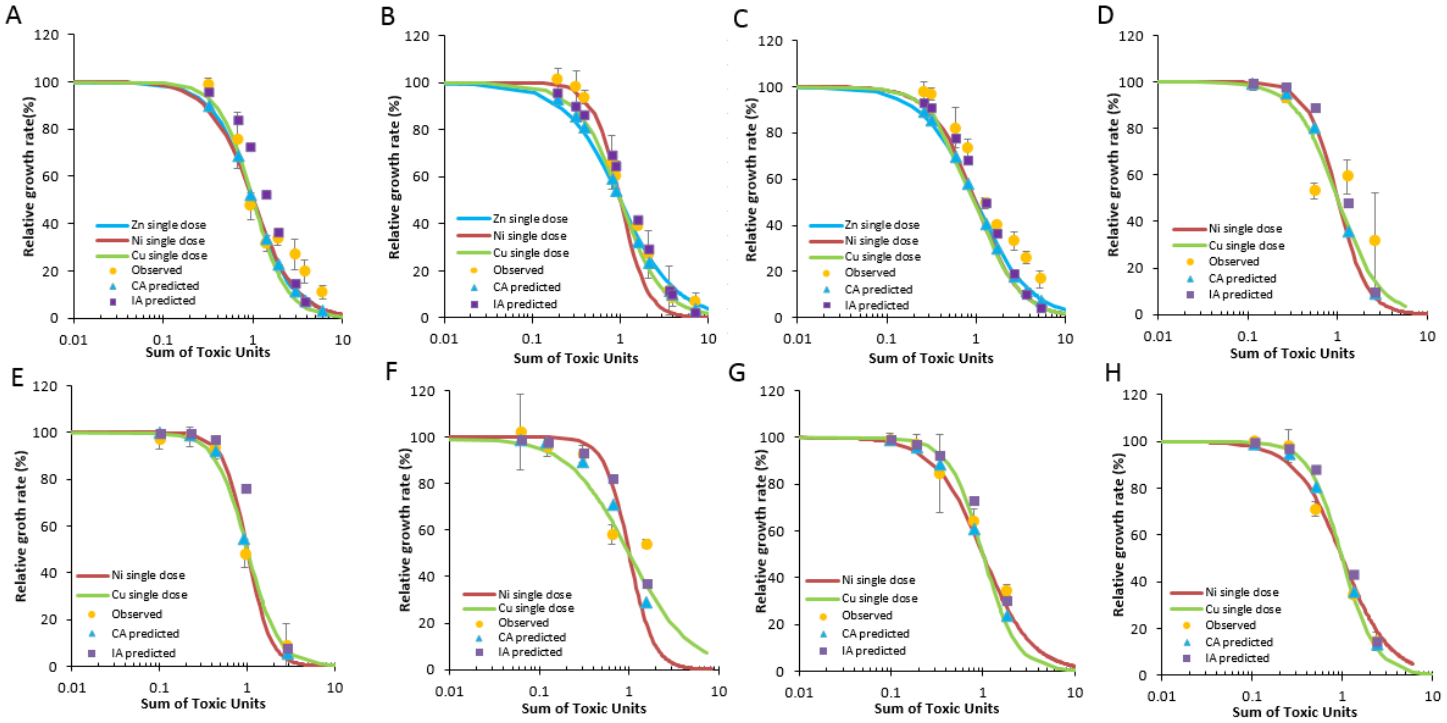

Table B4.3 Estimated model parameters for the mixture reference models Concentration Addition (CA; Equation 2) and independent Action (IA; Equation 3.3)[a] fitted to the growth data of *Pseudokircherniella subcapitata* in the ternary mixture.

		CA non-interaction			CA mixture interaction			IA non-interaction			IA mixture interaction		
		Cu	Ni	Zn	Cu	Ni	Zn	Cu	Ni	Zn	Cu	Ni	Zn
Loire	EC50Mediss (µg/L)	102	525	226	105	490	228	98	493	212	92	518	203
	bMediss	1.63	2.16	1.7	1.69	1.91	1.71	1.55	1.8	1.48	1.62	1.88	1.64
	a					1.38						-5.27	
	AIC		215			218			230			230	
	F-test	F = -1.11; p = 1						F = 1.64; p = 0.21					
	EC50Me2+ (nmol/L)	28	4809	1263	28	4210	1438	27	4713	1319	31	4740	1159
	bMe2+	0.83	1.95	1.59	0.8	1.98	1.57	0.82	2.05	1.39	0.76	1.92	1.55
	a					-1.2						3.77	
	AIC		213			221			228			232	
	F-test	F = -3.99; p = 1						F = -1.09; p = 1					
Dolaizon	EC50Mediss (µg/L)	40	518	55	38	549	56	37	558	48	36	582	49
	bMediss	1.94	3.1	1.32	2.25	2.03	1.26	1.9	1.88	1.24	1.81	1.61	1.15
	a					6.66						5.01	
	AIC		259			260			250			254	
	F-test	F = 0.85; p = 0.36						F = -1.71; p = 0.21					
	EC50Me2+ (nmol/L)	0.45	3925	167	0.58	3922	141	0.54	3779	168	0.51	4231	136
	bMe2+	0.92	1.92	1.24	0.99	1.82	1.23	0.93	1.89	1.17	0.9	1.77	1.19
	a					6.74						15.64	
	AIC		260			266			252			256	
	F-test	F = -3.41; p = 1						F = -1.68; p = 1					
Moselotte	EC50Mediss (µg/L)	34	276	72	32	239	55	31	235	65	33	247	58
	bMediss	2.29	2.05	1.36	2.54	2.16	1.52	2.29	2.46	1.4	2.28	1.97	1.32
	a					26.97						11.69	
	AIC		259			209			234			215	
	F-test	F = 90.99; p < 0.001						F = 21.73; p < 0.001					
	EC50Me2+ (nmol/L)	3.53	2563	394	3	2257	315	4	2237	396	3	2410	326
	bMe2+	1.04	1.78	1.33	1.03	2.25	1.39	1.1	2.3	1.25	0.93	1.81	1.36
	a					36.07						29.75	
	AIC		250			220			248			216	
	F-test	F = -40.82; p < 0.001						F = 46; p < 0.001					

[a] Fitted using the mixture analysis framework of Jonker et al. (2005) as described by Hochmuth et al. (2014); EC50= effective concentration causing 50% effect, a=deviation parameter to quantify mixture interactions, AIC=akaike information criterion. The F-test compares the nested models CA-non interaction with CA-mixture interaction and the IA-non-interaction with the IA-mixture interaction; $p < 0.05$ indicates significant deviation from non-interaction

[b] If a<0 the mixture components interact synergistic, if a>0 the mixture components interact antagonistic

Table B4.4 Estimated model parameters for the mixture reference models Concentration Addition (CA; Equation 2) and independent Action (IA; Equation 3)[a] fitted to the growth data of *Pseudokircheriella subcapitata* in the binary mixture.

		CA non-interaction		CA mixture interaction		IA non-interaction		IA mixture interaction	
		Cu	Ni	Cu	Ni	Cu	Ni	Cu	Ni
Bihain	$EC50_{Mediss}$ (µg/L)	364	521	331	500	364	485	420	450
	b_{Mediss}	1.51	1.84	1.63	2.11	2.18	1.57	2.85	1.7
	a^b			1.27				-0.35	
	AIC	121		123		122		126	
	F-test	F = 0.18; p = 0.68				F = -1.46; p = 1			
	$EC50_{Me2+}$ (nmol/L)	78	4350	87	3636	99	4667	83	4523
	b_{Me2+}	0.69	1.52	0.61	1.95	0.75	1.55	0.53	1.6
	a^b			5.75				3.23	
	AIC	119		118		122		120	
	F-test	F = 2.16; p = 0.17				F = 3.28; p = 0.10			
Brisy1	$EC50_{Mediss}$ (µg/L)	166	559	115	628	115	444	130	509
	b_{Mediss}	2.39	2.64	1.95	3.62	2.04	2.19	2.48	2.19
	a^b			-0.37				-1.04	
	AIC	85		89		95		98	
	F-test	F = -2.08; p = 1				F = -0.70; p = 1			
	$EC50_{Me2+}$ (nmol/L)	66	9155	54	7588	58	9284	62	8459
	b_{Me2+}	0.99	4.95	0.94	2.67	0.98	4.61	1.01	3.03
	a^b			1.26				0.66	
	AIC	99		99		88		92	
	F-test	F = 1.26; p = 0.29				F = -0.82; p = 1			
Voyon	$EC50_{Mediss}$ (µg/L)	336	1132	374	1097	293	1129	323	984
	b_{Mediss}	1.01	2.87	0.85	2.62	1.09	2.4	0.94	2.57
	a^b			1.21				0.6	
	AIC	114		116		115		119	
	F-test	F =0.38; p = 0.55				F = -1.07; p = 1			
	$EC50_{Me2+}$ (nmol/L)	250	11591	274	10653	245	12514	213	12876
	b_{Me2+}	0.57	3	0.5	3.37	0.59	3.03	0.58	3.75
	a^b			1.05				0.14	
	AIC	106		109		111		114	
	F-test	F = -0.63; p = 1				F = -0.57; p = 1			
Brisy2	$EC50_{Mediss}$ (µg/L)	125	826	122	836	121	747	122	760
	b_{Mediss}	2.29	1.59	2.52	1.4	2.3	1.41	2.17	1.22
	a^b			0.43				0.24	
	AIC	90		90		89		94	
	F-test	F = 1.29; p = 0.28				F = -2.03; p = 1			

	$EC50_{Me2+}$ (nmol/L)	14	7906	13	7534	14	8096	12	7197
	b_{Me2+}	1.06	1.42	1.09	1.3	0.99	1.4	1.06	1.25
	a[b]			0.87				1.19	
	AIC	86		88		93		93	
	F-test	F = -0.302; p = 1				F = 1.37; p = 0.27			
Markermeer	$EC50_{Mediss}$ (µg/L)	127	1507	123	1548	122	1477	131	1828
	b_{Mediss}	2.29	1.5	2.09	1.38	2.13	1.36	2.09	1.62
	a[b]			-0.75				-1.69	
	AIC	94		101		100		102	
	F-test	F = -2.61; p = 1				F = -0.06; p = 1			
	$EC50_{Me2+}$ (nmol/L)	4	11180	4	11408	4	10775	5	12432
	b_{Me2+}	1.04	1.44	0.96	1.56	0.96	1.39	1.19	1.68
	a[b]			-1.58				-1.86	
	AIC	93		92		94		97	
	F-test	F = 2.37; p = 0.15				F = -0.48; p = 1			

[a] Fitted using the mixture analysis framework of Jonker et al. (2005) as described by Hochmuth et al. (2014); EC50= effective concentration causing 50% effect, a=deviation parameter to quantify mixture interactions, AIC=akaike information criterion. The F-test compares the nested models CA-non interaction with CA-mixture interaction and the IA-non-interaction with the IA-mixture interaction; $p < 0.05$ indicates significant deviation from non-interaction

[b] If a<0 the mixture components interact synergistic, if a>0 the mixture components interact antagonistic

Figure B4.2 Observed relative growth rate (RGR; %) versus predicted or fitted RGR for the mixture reference models CA (triangles, blue) and IA (circles, red) after exposure of *Pseudokircherniella subcapitata* to the ternary Cu-Ni-Zn mixture for the Loire (A), Dolaizon (B) and Moselotte (C) test waters. Models were fitted on free ion activities. Open symbols denote RGR of single metal treatments, filled symbols denote RGR of mixture treatments. Left panel shows model predictions based on parameters estimated from the single-metal exposures alone, middle panels show models fitted to all data (single-metal and mixture treatments), right panel shows model extended with deviation parameter a fitted to all data.

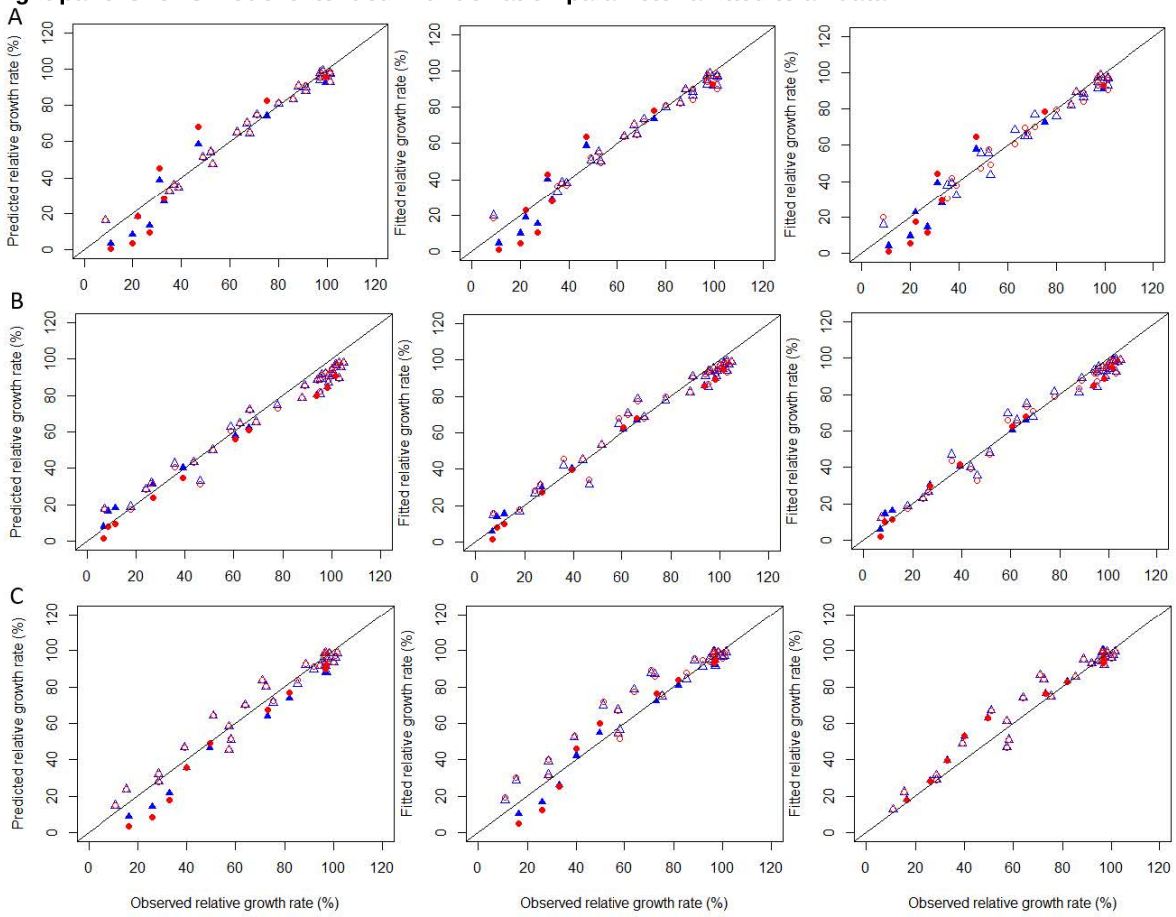

Figure B4.3. Observed relative growth rate (RGR; %) versus predicted or fitted RGR for the mixture reference models CA (triangles, blue) and IA (circles, red) after exposure of *Pseudokircherniella subcapitata* to the binary Cu-Ni mixture for the Bihain (A), Brisy1 (B), Voyon (C), Brisy2 (D) and Markermeer (E) test waters. Models were fitted on free ion activities. Open symbols denote RGR of single metal treatments, filled symbols denote RGR of mixture treatments. Left panel shows model predictions based on parameters estimated from the single-metal exposures alone, middle panels show models fitted to all data (single-metal and mixture treatments), right panel shows model extended with deviation parameter a fitted to all data.

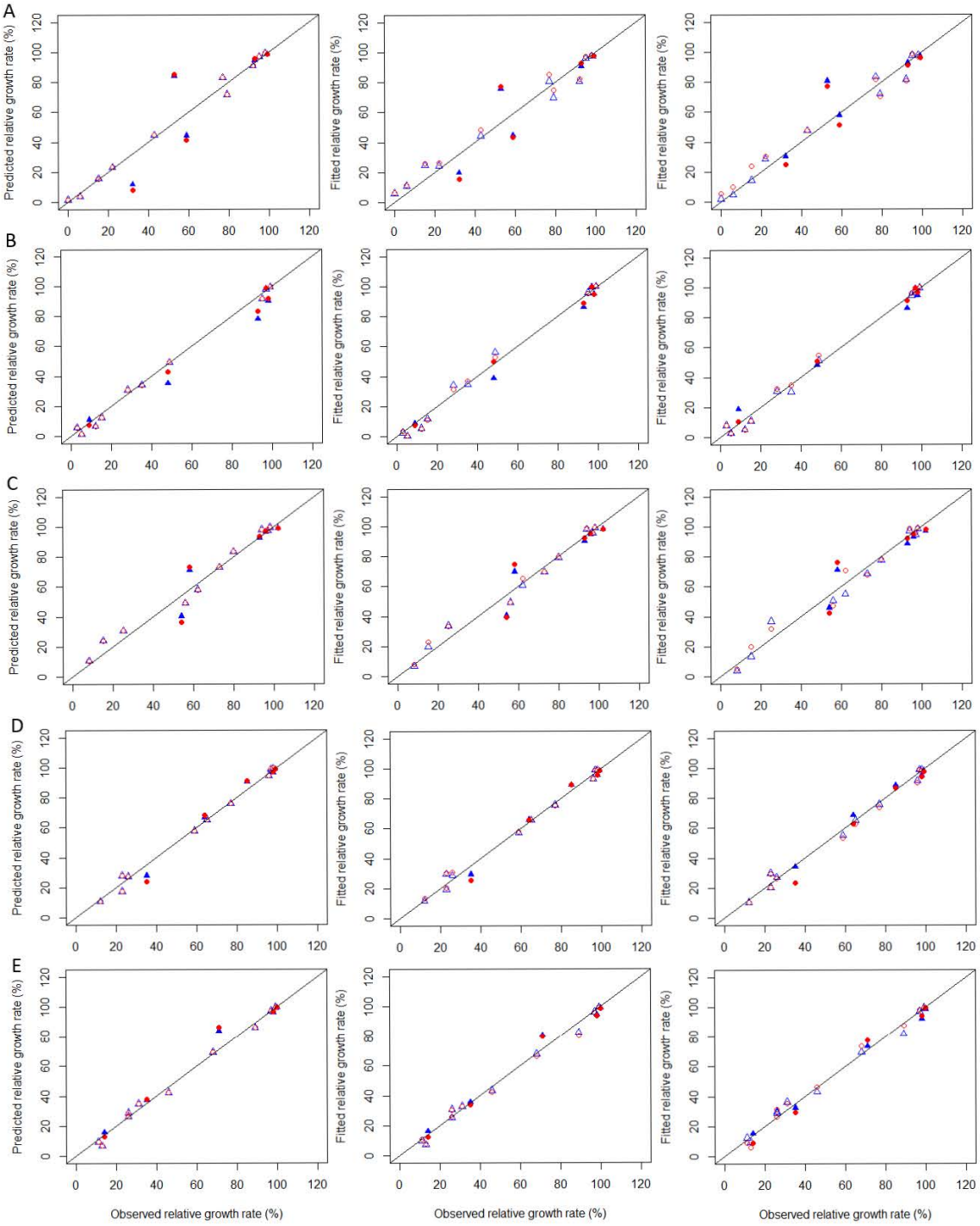

Figure B4.4. Observed relative growth rate (RGR; %) versus predicted or fitted RGR for the mixture reference models CA (triangles) and IA (circles) after exposure of *Pseudokircherniella subcapitata* to the ternary Cu-Ni-Zn mixture for the Loire (A), Dolaizon (B) and Moselotte (C) test waters. Models were fitted on dissolved concentrations. Open symbols denote RGR of single metal treatments, filled symbols denote RGR of mixture treatments. Left panel shows model predictions based on parameters estimated from the single-metal exposures alone, middle panels show models fitted to all data (single-metal and mixture treatments), right panel shows model extended with deviation parameter a fitted to all data.

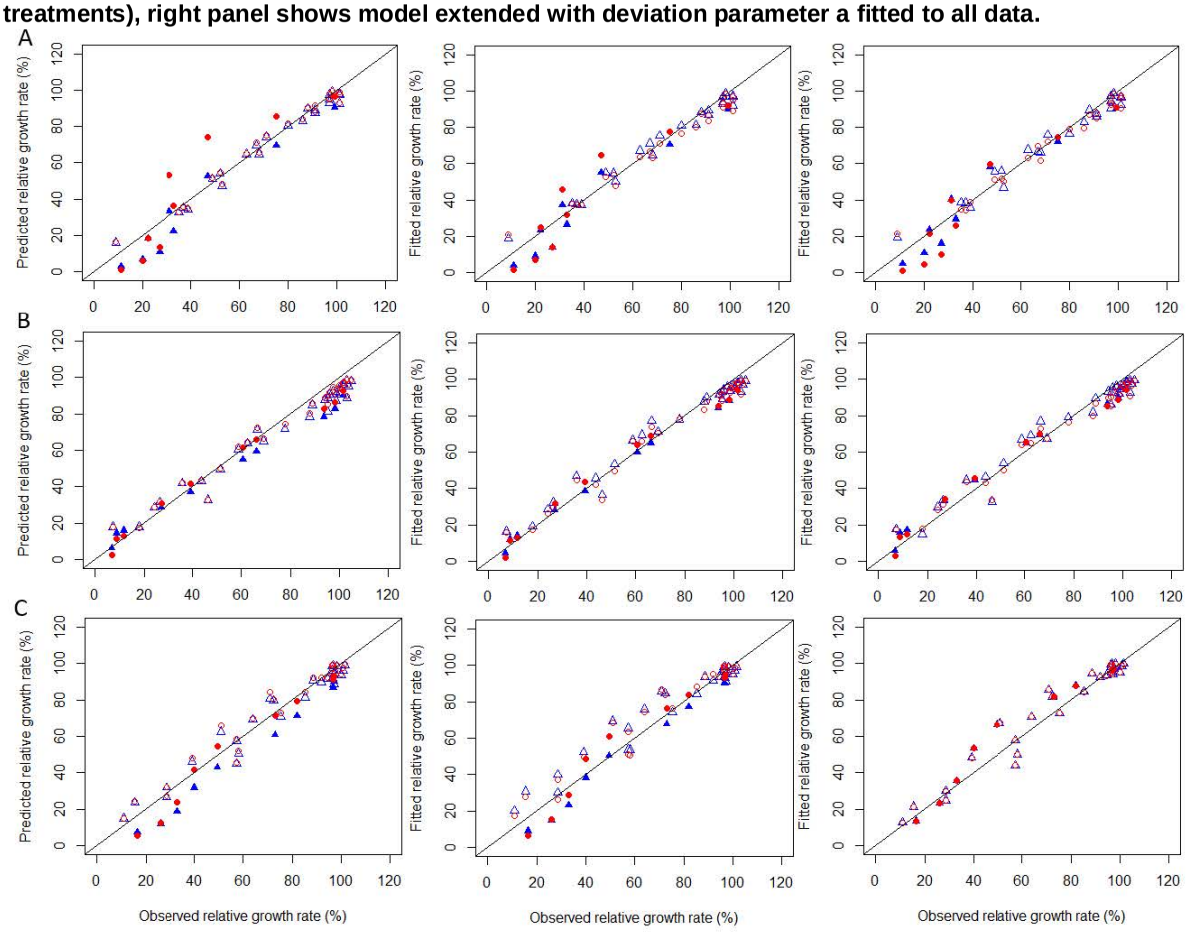

Figure B4.5. Observed relative growth rate (RGR; %) versus predicted or fitted RGR for the mixture reference models CA (triangles, blue) and IA (circles, red) after exposure of *Pseudokircherniella subcapitata* to the binary Cu-Ni mixture for the Bihain (A), Brisy1 (B), Voyon (C), Brisy2 (D) and Markermeer (E) test waters. Models were fitted on dissolved concentrations. Open symbols denote RGR of single metal treatments, filled symbols denote RGR of mixture treatments. Left panel shows model predictions based on parameters estimated from the single-metal exposures alone, middle panels show models fitted to all data (single-metal and mixture treatments), right panel shows model extended with deviation parameter a fitted to all data.

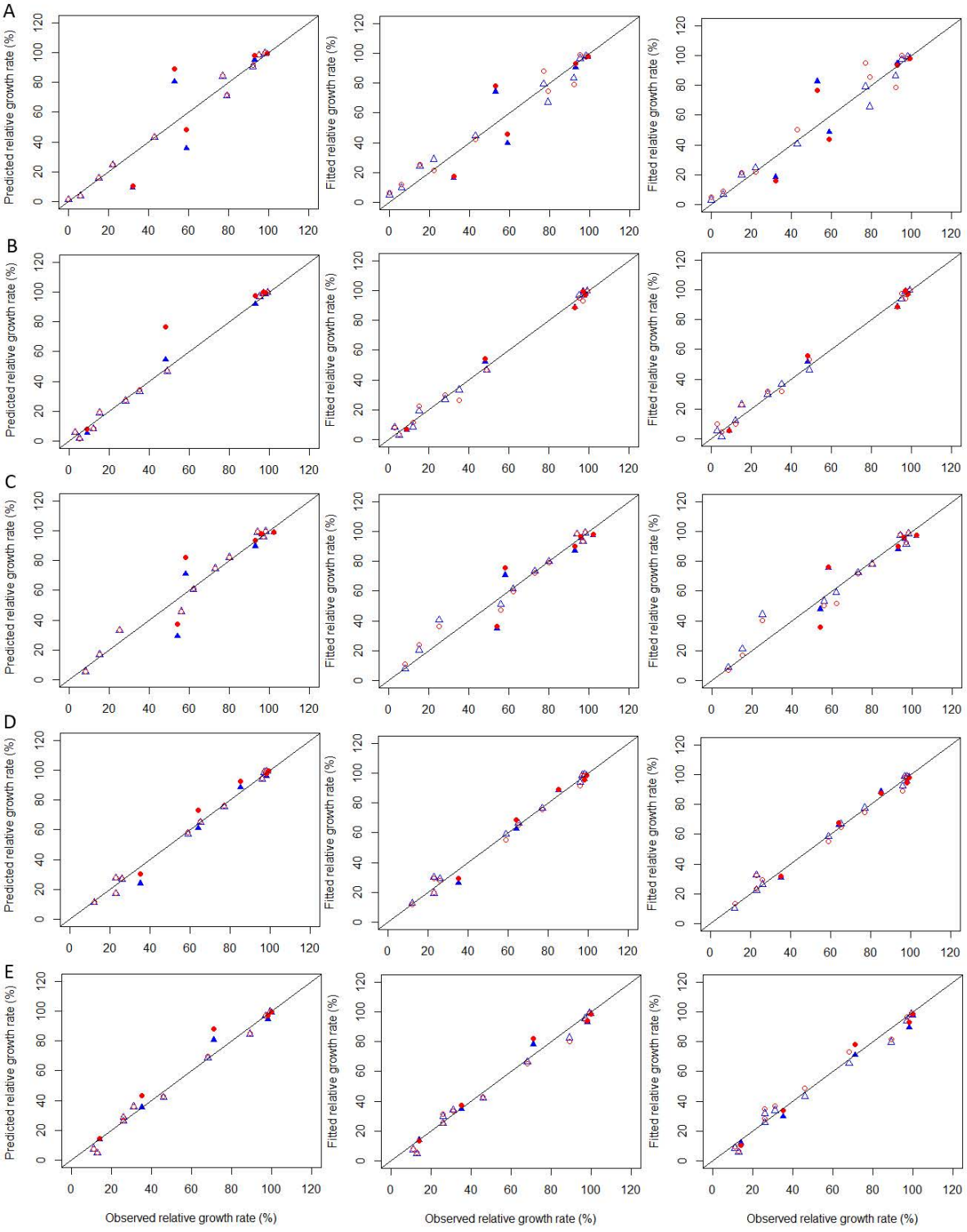

Table B4.5 Root-mean-squared-errors (RMSE) as indicators of best model fit, for the concentration addition and independent action reference models, for the ternary Cu-Ni-Zn and binary Cu-Ni mixtures within different waters bodies. RMSE is given for model fits based on dissolved concentrations and free ion activities.

		Dissolved concentrations		Free ion activities	
		Concentration Addition	Independent Action	Concentration Addition	Independent Action
Ternary	Loire	9.49	14.14	8.91	13.21
	Dolaizon	8.26	1.95	8.36	6.69
	Moselotte	11.95	9.12	9.69	12.44
Binary	Bihain	19.16	19.53	17.86	19.67
	Brisy1	3.58	12.89	9.86	6.15
	Voyon	12.71	13.28	9.59	11.95
	Brisy2	5.33	5.72	4.13	6.01
	Markermeer	4.54	8.50	5.85	6.95

Appendix C:

SUPPORTING INFORMATION OF CHAPTER 4

Appendix C1. Measured metal concentrations

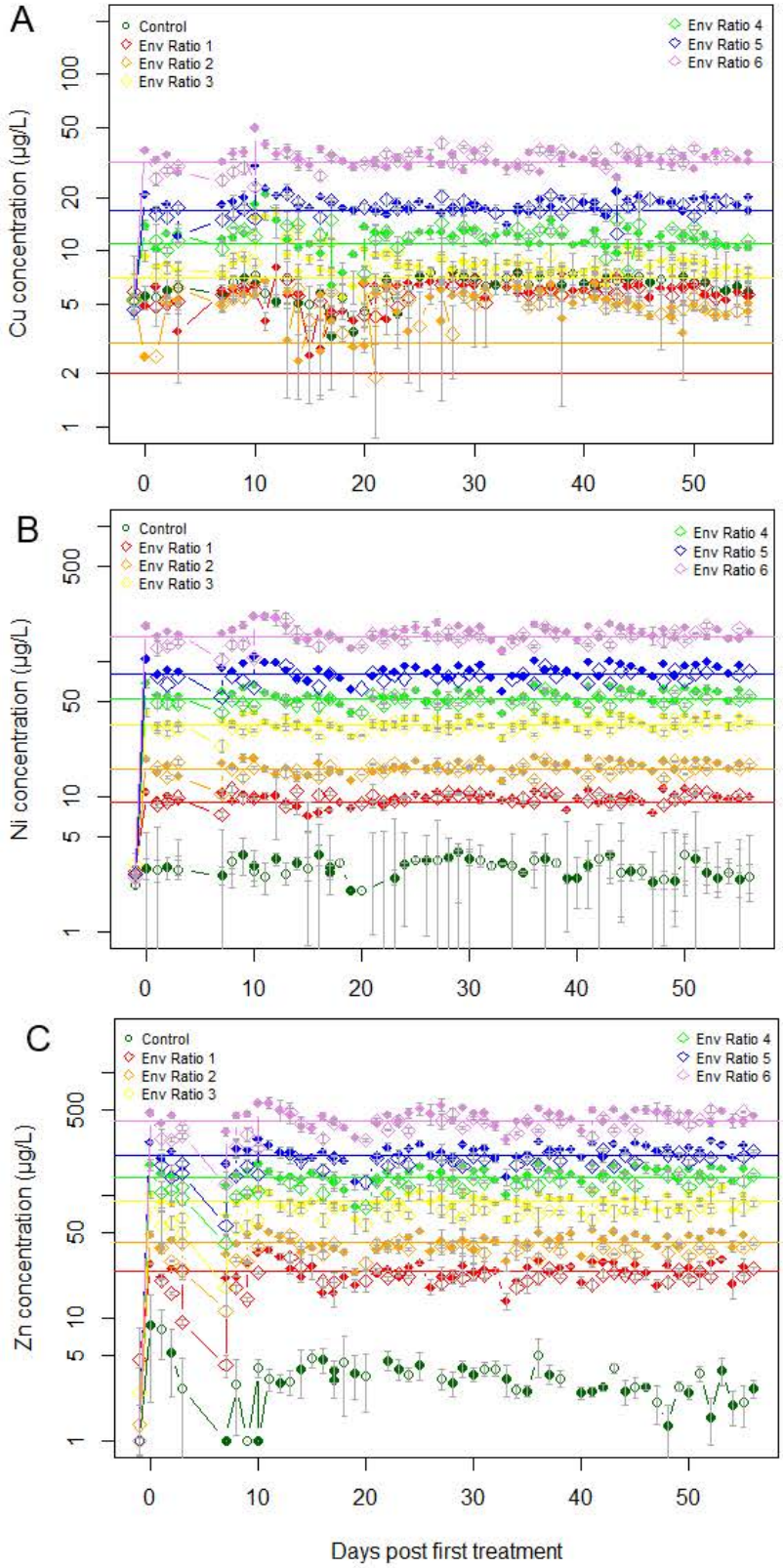

Figure B1.1. Average measured dissolved copper (A), nickel (B) and zinc (C) concentrations in the environmental ratio treatments before spiking (empty symbols) and after spiking (full symbols). Error bars denote standard deviations. Horizontal lines indicate nominal concentrations of the environmental ratio treatments

Appendix C2.

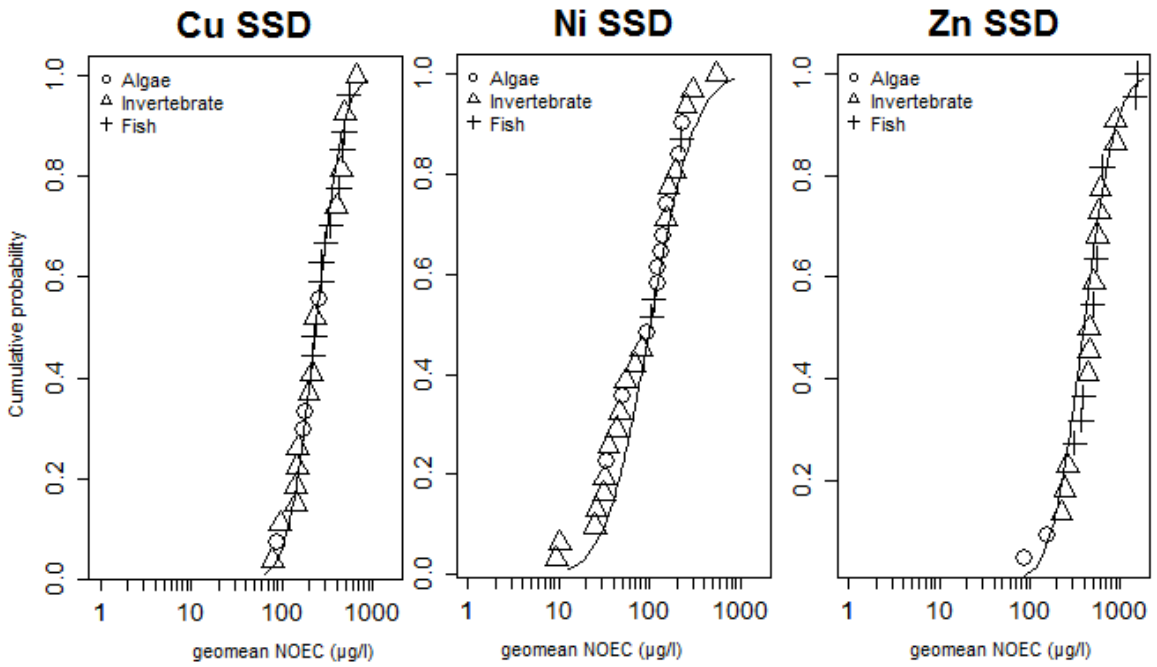

Figure B2.1 Species sensitivity distribution (SSD) of Cu, Ni and Zn including chronic toxicity data of algae, invertebrates and fish.

Appendix C3. Filamentous algae

The colonies of filamentous algae were counted as single individuals. This implies that the biomass accounted for by these filamentous algae is somewhat underestimated as is seen in Figure B3.

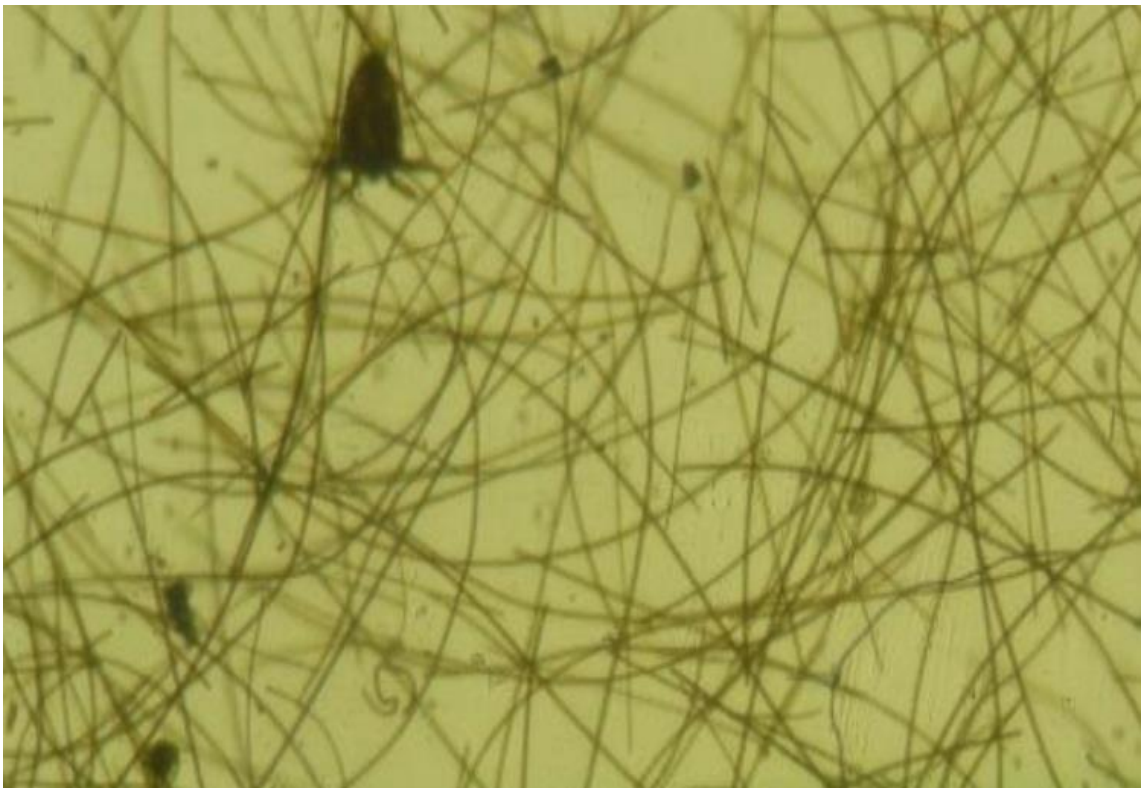

Figure B3 Image of the high abundance of filamentous algae present in the control treatments. At the top of the image, a nauplius larvae is visible.

Appendix C4. Overview of zoo- and phytoplankton present in chronic toxicity databases

Table B4.1. Zooplankton and phytoplankton species for which chronic toxicity data is present in the copper toxicity database (ECI 2008).

Species	Taxon	Group
Chlamydomonas reinhardtii	Chlorophyta	Phytoplankton
Pseudokircheneriella subcapitata	Chlorophyta	Phytoplankton
Ceriodaphnia dubia	Cladocera	Zooplankton
Daphnia magna	Cladocera	Zooplankton
Daphnia pulex	Cladocera	Zooplankton
Ceriodaphnia dubia	Cladocera	Zooplankton
Brachionus calyciflorus	Rotifera	Zooplankton

Table B4.2. Zooplankton and phytoplankton species for which chronic toxicity data is present in the nickel toxicity database (DEPI 2008, Nys et al. 2015).

Species	Taxon	Group
Pseudokircheneriella subcapitata	Chlorophyta	Phytoplankton
Daphnia magna	Cladocera	Zooplankton
Ceriodaphnia dubia	Cladocera	Zooplankton
Ceriodaphnia quadrangula	Cladocera	Zooplankton
Peracantha truncata	Cladocera	Zooplankton
Daphnia longispina	Cladocera	Zooplankton
Alona affinis	Cladocera	Zooplankton
Ceriodaphnia pulchella	Cladocera	Zooplankton
Simocephalus vetulus	Cladocera	Zooplankton
Chlamydomonas sp	Chlorophyta	Phytoplankton
Ankistodesmus falcatus	Chlorophyta	Phytoplankton
Scenedesmus accuminatus	Chlorophyta	Phytoplankton
Chlorella sp.	Chlorophyta	Phytoplankton
Desmodesmus spinosus	Chlorophyta	Phytoplankton
Pediastrum duplex	Chlorophyta	Phytoplankton
Coelastrum microporum	Chlorophyta	Phytoplankton
Brachionus calyciflorus	Rotifera	Zooplankton

Table B4.3. Zooplankton and phytoplankton species for which chronic toxicity data is present in the zinc toxicity database (Van Sprang et al. 2009).

Species	Taxon	Group
Pseudokirchneriella subcapitata	Chlorophyta	Phytoplankton
Chlorella sp.	Chlorophyta	Phytoplankton
Ceriodaphnia dubia	Cladocera	Zooplankton
Daphnia magna	Cladocera	Zooplankton
Daphnia longispina	Cladocera	Zooplankton
Anaeropsis fissa	Rotifera	Zooplankton
Brachionus rubens	Rotifera	Zooplankton
Brachionus calyciflorus	Rotifera	Zooplankton

Appendix D:

SUPPORTING INFORMATION OF CHAPTER 5

Appendix D1. Chronic Cu *Daphnia magna* bioavailability model

D1.1 Calculation of the intrinsic sensitivity, i.e. EA50, for D. magna.

To obtain toxicity predictions, the BLMs were applied in two modes. First, they were run in speciation mode to obtain an 'average' intrinsic sensitivity for *D. magna*, i.e. EA50. This 'average' intrinsic sensitivity was calculated in different steps. (1) For each test medium *i*, the $[EC50_{Cu^{2+}}]_{0,i}$ was calculated (Equation D1.1).

$$[EC50_{Cu^{2+}}]_{0,i} = \frac{\int_{CuBL}^{50\%}}{(1-\int_{CuBL}^{50\%}) \cdot K_{CuBL}} \quad \text{(D1.1)}$$

Where K_{CuBL} = the stability constant for the binding of copper to the biotic ligand ($\mathrm{L \cdot mol^{-1}}$) and $\int_{\mathrm{CuBL}}^{50\%} = \frac{[\text{Total Gill}-\text{Cu}]}{30}$. Here, [Total BL-Cu] is the 'critical gill-concentration' or 'biotic ligand concentration of copper' ($\mathrm{nmol \cdot g^{-1}}$). This is the amount of accumulation of copper to the biotic ligand that results in a well-defined effect (here: 50% reduction of reproduction relative to a control without copper). For the UGent BLM, the [Total BL-Cu] = [BL-Cu] + [BL-CuOH] + [BL-$CuCO_3$] because the BLM accounts for binding of Cu^{2+}, $CuOH^+$ and $CuCO_3$ to the biotic ligand and thus assumes that Cu^{2+}, $CuOH^+$ and $CuCO_3$ all contribute to toxicity. For the HydroQual BLM, the [Total BL-Cu] = [BL-Cu] + [BL-CuOH] because the BLM accounts for binding of Cu^{2+} and $CuOH^+$ to the biotic ligand and thus assumes that only Cu^{2+} and $CuOH^+$ and not $CuCO_3$ contribute to toxicity. Furthermore, the 30 in $\int_{\mathrm{CuBL}}^{50\%} = \frac{[\text{Total BL}-\text{Cu}]}{30}$ refers to the total copper binding capacity of the biotic ligand of 30 nmol Cu/ g wet weight. This means for example that a critical fractional biotic ligand occupancy ($\int_{\mathrm{CuBL}}^{50\%}$) of 30% would correspond to a critical accumulation of 9 nmol/g wet weight when using the BLM software. (2) In a second step, the geometric mean of all the $[EC50_{Cu^{2+}}]_{0,i}$ values (across all *n* test media) was calculated.

$$geomean([EC50_{Cu^{2+}}]_{0,i}) = \sqrt[n]{\prod_i^n [EC50_{Cu^{2+}}]_{0,i}} \quad \text{(D1.2)}$$

(3)The final 'average' $\int_{CuBL}^{50\%}$ (across all media) was calculated.

$$\int_{CuBL}^{50\%} = \left(\frac{geomean(\left[EC50_{Cu^{2+}}\right]_{0,i}) \cdot K_{CuBL}}{1+geomean(\left[EC50_{Cu^{2+}}\right]_{0,i}) \cdot K_{CuBL}} \right) \quad \text{(D1.3)}$$

(4) This value was multiplied by 30 to obtain the [Total BL-Cu], i.e. EA50, which was entered as parameter value into the BLMs.

After this, in a second phase, the BLMs were run in toxicity mode (using this parameter value) to obtain the predictions of toxicity (EC50s) as µg/L dissolved Cu.

D1.2 Calculation of Me^{2+} ion activities based on Me^{2+} ion concentrations.

Me^{2+} activities were calculated from Me^{2+} concentrations (which is one of the output variables of the BLM software) using activity constants calculated with the Davies Equation (Stumm and Morgan 1996; Malmberg and Maryott 1956). First, the dielectric constant was calculated.

$$Dielectric\ constant = 87.74 - 0.4008 \cdot T + 9.398 \cdot 10^{-4} \cdot T^2 - 1.41 \cdot 10^{-6} \cdot T^3 \quad \text{(D1.4)}$$

Where T = the temperature in °C. As the temperature was 20°C in all tests, this Dielectric constant is constant for all toxicity tests, i.e. 80.14. The Dielectric constant was then used to calculate the Davies parameter.

$$Davies\ parameter = 1.82 \cdot 10^6 (Dielectric\ constant * T')^{-\frac{3}{2}} \quad \text{(D1.5)}$$

Where T' = the temperature in Kelvin. This Davies parameter is also a constant, i.e. 0.51. The Davies parameter was in turn used to calculate the activity coefficient (γ_2).

$$\gamma_2 = 10^{\left(-Davies\ parameter \cdot 2^2 \cdot \frac{\sqrt{IS}}{1+\sqrt{IS}} - 0.2 \cdot IS\right)} \quad \text{(D1.6)}$$

Where IS = the Ionic Strength ($mol \cdot L^{-1}$) (also an output of the BLM software used). Finally the Me^{2+} activity ($mol \cdot L^{-1}$) was calculated based on the calculated free metal concentration, "Free Metal" ($mol \cdot L^{-1}$), an output from the BLM.

$$Me^{2+}activity\ (\mathrm{mol \cdot L^{-1}}) = \gamma_2 \cdot Free\ Metal \quad \text{(D1.7)}$$

The activities of Ca^{2+} $(\mathrm{mol \cdot L^{-1}})$ and Mg^{2+} $(\mathrm{mol \cdot L^{-1}})$ were calculated by multiplying $\gamma_2$with the concentration of free Ca^{2+} $(\mathrm{mol \cdot L^{-1}})$ and Mg^{2+} $(\mathrm{mol \cdot L^{-1}})$, respectively. The Na^+ activity was calculated by multiplying γ_1 with the concentration of free Na^+ $(\mathrm{mol \cdot L^{-1}})$.

$$\gamma_1 = 10^{\left(-Davies\ parameter \cdot 1^2 \cdot \frac{\sqrt{IS}}{1+\sqrt{IS}} - 0.2 \cdot IS\right)} \quad \text{(D1.8)}$$

D1.3 Intrinsic sensitivities, i.e. EA50's, for the K6 and ARO clone used in the UGent and HydroQual BLMs.

Table D1.1. Assuming an identical sensitivity for both *D. magna* clones.

	UGent BLM	HydroQual BLM
EA50 (nmol/g)	7.01	0.046

Table D1.2. Assuming a separate intrinsic sensitivity for both *D. magna* clones.

		UGent BLM	HydroQual BLM
EA50 (nmol/g)	ARO clone	6.57	0.031
	K6 clone	7.70	0.089

Table D1.3. Assuming separate intrinsic sensitivities per clone and per study.

		UGent BLM	HydroQual BLM
EA50 (nmol/g)	De Schamphelaere & Janssen (2004c) -K6 clone	5.76	0.058
	Rodriguez et al. (2012) - ARO clone	3.98	0.15
	Villavicencio et al. (2011) - ARO clone	6.81	0.027
	Heijerick et al. (2002) - K6 clone	12.10	0.16

D1.4

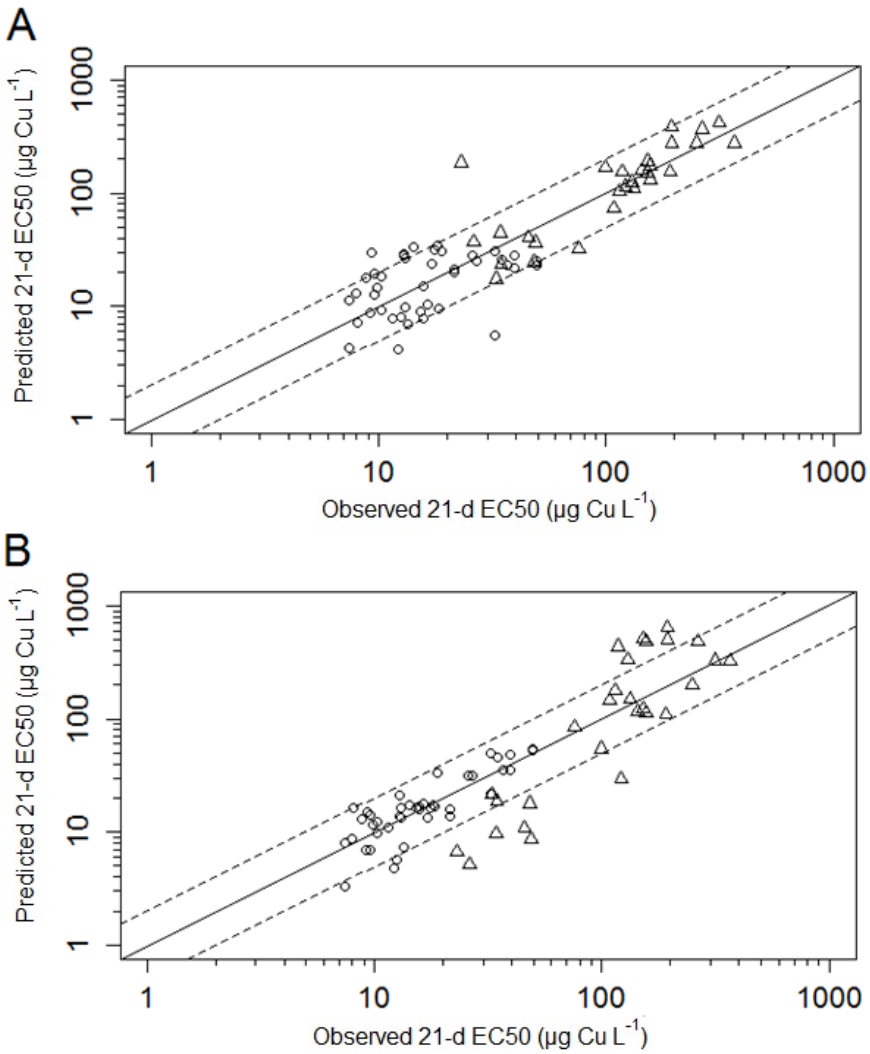

Figure D1.1 Predictive capacity of the UGent (A) and HydroQual (B) biotic ligand models (BLMs) as shown by observed versus predicted 21-day 50% effective concentrations (EC50s) of copper to *Daphnia magna*. Intrinsic sensitivities of the BLMs were calculated from data grouped by *D. magna* clone (i.e. K6 clone (Δ) and ARO clone (○)) and by study. The solid line is the 1:1 reference line indicating a perfect match between observed and predicted values; the dashed lines indicate an error of a factor of two between observed and predicted values. UGent BLM = the chronic *D. magna* BLM (De Schamphelaere and Janssen 2006); HydroQual BLM = the acute BLM (Santore et al. 2001; HydroQual 2005).

Appendix D2. Chronic Zn Daphnia magna bioavailability model

D2.1 Concentration response data and fitted dose response curves for the *Daphnia magna* and *Pseudokirchneriella subcapitata* experiments

Table D2.1. Zinc concentrations, number of replicates, reproduction and mortality of *D. magna* during the ecotoxicity tests in seven natural and two synthetic waters.

Site ID	Zn[a] (µg/L)	n[b]	Reproduction (# offspring)[c]	σ[d]	Mortality (# deaths)[e]	vc[f]
La Seille	6.13	9	85.22	19.25	2	p
	189.42	10	58.10	32.65	2	
	313.37	10	52.50	20.12	1	
	466.83	10	22.80	19.06	2	
	690.67	10	2.10	5.38	1	
	909.37	10	0.00	0.00	2	
	1377.33	10	0.00	0.00	10	
	1794.17	10	0.00	0.00	10	
Le Madon	3.90	10	85.50	26.34	1	p
	275.47	8	56.00	23.95	0	
	447.30	9	10.00	11.5	2	
	580.77	9	6.00	10.19	3	
	908.50	10	0.00	0.00	10	
	1346.50	10	0.00	0.00	10	
	1910.67	10	0.00	0.00	10	
	2598.67	10	0.00	0.00	10	
Le Dolaizon	7.03	9	87.22	22.08	0	p
	113.18	10	60.10	20.35	0	
	152.55	9	61.78	13.85	0	
	222.75	9	15.78	20.02	3	
	326.15	10	0.00	0.00	10	
	435.83	10	0.00	0.00	10	
	593.17	10	0.00	0.00	10	
	809.73	10	0.00	0.00	10	
La Moselotte	5.2	9	55.78	17.33	0	f
	42.48	10	45.80	26.75	3	
	59.28	10	43.00	20.4	1	
	82.76	10	0.00	0.00	10	
	118.55	10	0.00	0.00	10	
	166.1	10	0.00	0.00	10	
	230	10	0.00	0.00	10	
	323.65	10	0.00	0.00	10	

[a] dissolved zinc, given as the mean value of all samples taken during the test.; [b] n = the number of replicates. This is usually 10, but can be less due to accidental mortality or the organism being male; [c] number of offspring, given as the mean of the offspring of all n replicates; [d] standard deviation on the number of offspring; [e] total number of deaths (out of n replicates) in each treatment; [f] vc = validity criteria on the control treatment: p when the validity criteria are passed, f when they are failed

Table D2.1 (continued)

Le Taurion	6.6	10	31.30	11.35	6	f
	58.2	10	0.00	0.00	10	
	97.7	10	0.00	0.00	10	
	121.7	10	0.00	0.00	10	
	176.4	10	0.00	0.00	10	
	243.3	10	0.00	0.00	10	
	467.2	10	0.00	0.00	10	
	500.5	10	0.00	0.00	10	
La Maulde	6.15	10	41.20	18.56	3	f
	66.2	10	0.00	0.00	10	
	83.2	10	0.00	0.00	10	
	123.1	10	0.00	0.00	10	
	163.9	10	0.00	0.00	10	
	238.1	10	0.00	0.00	10	
	343.9	10	0.00	0.00	10	
	491.7	10	0.00	0.00	10	
La Gartempe	5.4	10	63.00	10.47	0	p
	96.5	10	0.00	0.00	10	
	148.5	10	0.00	0.00	10	
	218.7	10	0.00	0.00	10	
	290.9	10	0.00	0.00	10	
	398.7	10	0.00	0.00	10	
	597.1	10	0.00	0.00	10	
	844.8	10	0.00	0.00	10	
Synthetic water	10.2	10	69.80	28.75	1	p
	66.7	10	42.40	27.06	2	
	88.2	10	43.80	18.21	1	
	136.4	9	34.89	22.59	0	
	195.4	10	33.00	24.44	2	
	284.2	10	19.30	23.32	6	
	394.6	10	6.00	5.54	4	
	463.0	10	0.00	0.00	9	
Reference EEG	10.8	10	67.90	22.24	1	p
	89.0	10	56.90	30.39	1	
	127.5	10	79.10	16.97	0	
	213.1	9	86.67	13.20	0	
	246.3	9	52.56	32.09	4	
	350.6	10	48.40	29.45	1	
	500.4	10	0.10	0.32	10	
	721.6	10	0.10	0.32	10	

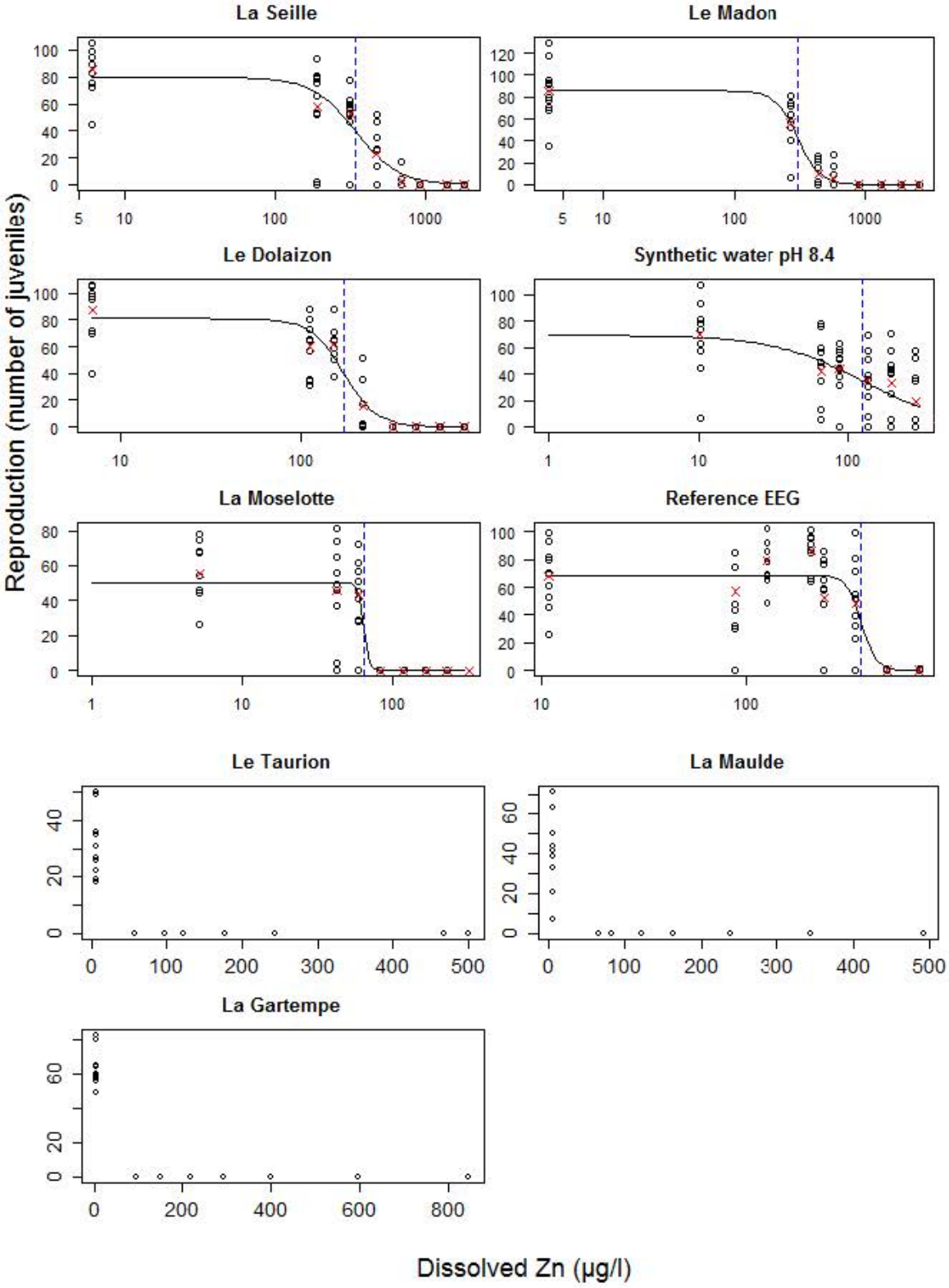

Figure D2.1. Concentration-response curves for *Daphnia magna* for seven natural waters and two synthetic waters. The mean value per treatment is indicated with an X. The EC50 concentration is indicated with a blue line. EC50 = the 50% effective concentration.

Table D2.2. Validity criteria for the 72-hours and 48-hours chronic toxicity test for *Pseudokirchneriella subcapitata*. Red values give those criteria that were not met.

Test water	72h			48h		
	Factor increase[a]	CV growth rate (%)[b]	Mean sectional CV (%)[c]	Factor increase[a]	CV growth rate (%)[b]	Mean sectional CV (%)[c]
Madon	46.0	3.2	33.9	20.5	8.4	11.6
Dolaizon	66.9	5.5	35.0	27.2	4.9	18.3
Moselotte	15.5	1.6	8.6	32.5	2.3	32.8
Taurion	41.8	1.3	36.0	21.0	0.9	6.7
Maulde	41.2	3.9	36.0	20.2	4.3	8.0
Gartempe	32.1	1.4	36.6	16	2.4	7.8
Voyon	81.0	0.6	42.7	35.0	1.6	24.8
Bihain	50.1	0.9	49.7	24.5	1.2	35.2
Brisy	102.9	1.8	36.5	38.9	4.0	21.2
Voyon	119.9	1.2	12.4	25.5	1.3	16.6
Bihain	45.3	1.1	44.8	21.6	2.8	31.4
Brisy	113.3	1.6	29.2	39.2	1.3	7.1
Loire	122.1	2.5	25.7	36.7	2.4	16.6
Loire	129.7	2.4	18.0	28.1	3.4	23.5
Brisy	79.7	1.0	22.6	22.2	2.7	26.4
Bihain	80.2	4.8	31.3	26.5	2.0	26.5
Madon	63.2	1.4	44.0	28.0	2.1	30.0
Taurion	96.7	1.7	41.0	37.2	2.7	30.4
Maulde	120.8	0.2	38.9	42.0	0.7	30.8

[a] Validity criterion 1: the biomass in the control cultures should have increased exponentially by a factor of at least 16 within the test period

[b] Validity criterion 2: the coefficient of variation (CV) of the average specific growth rates of the control replicates must not exceed 7%

c Validity criterion 3: the mean CV of the section-by-section growth rates in the controls may not exceed 35%.

Table D2.3. Zinc concentrations and growth rate (μ) of *P.subcapitata* during the ecotoxicity tests in six natural waters tested during the first time period.

Site ID	Zn[a] (μg/L)	72-h growth rate (μ)[b]	σ[c]	48-h growth rate (μ)[d]	σ[e]
Le Madon	0.75	1.29	0.04		
	11.35	0.8	0.02		
	20.00	0.75	0.08		
	44.45	0.67	0.02		
	70.35	0.50	0.05		
	184.70	0.19	0.02		
Le Dolaizon	0.86	1.40	0.08		
	23.83	0.65	0.05		
	29.03	0.58	0.08		
	47.50	0.35	0.04		
	109.90	0.12	004		
	270.15	0.05	0.04		
La Moselotte	5.15	*1.19*	*0.03*	1.37	0.02
	77.23	*1.13*	*0.02*	1.08	0.02
	139.50	*0.88*	*0.04*	0.93	0.11
	253.10	*0.33*	*0.04*	0.28	0.03
	473.47	*0.09*	*0.07*	0.15	0.01
	877.03	*0.08*	*0.02*	0.14	0.03
	1681.33	*0.05*	*0.01*	0.11	0.04
	3038.33	*0.00*	*0.00*	0.03	0.02
Le Taurion	10.50	1.28	0.02		
	68.93	0.69	0.02		
	126.70	0.32	0.04		
	225.57	0.15	0.01		
	411.87	0.05	0.03		
	724.37	0.00	0.01		
	1359.67	0.03	0.01		
	2496.00	0.05	0.03		

[a] dissolved zinc, given as the mean value of all samples taken during the test.
[b] 72-h growth rate of *P.subcapitata*, given when all validity criteria after 72-h were valid. Those given in italics did not pass validity criteria after 72-h[c] standard deviation on the 72-h growth rate
[d] 48-h growth rate of *P.subcapitata* for those water that did not pass validity criteria after 72-h
[e] standard deviation on the 48-h growth rate

Table D2.3 (continued)

La Maulde	9.80	1.25	0.05		
	73.50	0.84	0.06		
	124.20	0.32	0.01		
	228.37	0.22	0.08		
	406.33	0.05	0.06		
	728.37	0.11	0.06		
	1220.67	0.12	0.07		
	2359.33	0.11	0.09		
La Gartempe	7.63	1.18	0.02	1.36	0.03
	137.60	0.73	0.00	0.70	0.02
	264.50	0.31	0.06	0.26	0.03
	469.57	0.07	0.01	0.15	0.02
	823.80	0.14	0.07	0.12	0.02
	1560.33	0.15	0.08	0.16	0.01
	2659.33	0.07	0.05	0.04	0.04
	4584.00	0.11	0.06	0.16	0.04

Table D2.4. Measured dissolved zinc concentrations during chronic toxicity tests on *Pseudokirchneriella subcapitata* for different natural surface waters tested during the second time period.

Site ID	Treatment	Dissolved (µg/L)		72-h growth rate (µ)[c]	σ[d]	48-h growth rate (µ)[e]	σ[f]
		48h[a]	72h[b]				
Voyon	Control	14		*1.46*	*0.01*	1.78	0.03
	Zn1	37		*1.47*	*0.01*	1.79	0.02
	Zn2	51		*1.51*	*0.04*	1.77	0.02
	Zn3	87		*1.43*	*0.03*	1.63	0.03
	Zn4	344		*0.53*	*0.05*	0.45	0.04
	Zn5	702		*0.26*	*0.01*	0.23	0.02
	Zn6	1084		*0.10*	*0.04*	0.10	0.02
Brisy	Control	11		*1.54*	*0.03*	1.83	0.07
	Zn1	21		*1.53*	*0.03*	1.80	0.05
	Zn2	38		*1.51*	*0.02*	1.74	0.02
	Zn3	57		*1.26*	*0.02*	1.34	0.01
	Zn4	196		*0.33*	*0.07*	0.32	0.04
	Zn5	395		*0.10*	*0.07*	0.16	0.01
	Zn6	603		*0.07*	*0.03*	0.19	0.04
Bihain	Control	21		*1.29*	*0.01*	1.60	0.02
	Zn1	80		*1.30*	*0.00*	1.57	0.01
	Zn2	126		*1.28*	*0.01*	1.40	0.04
	Zn3	215		*1.07*	*0.04*	1.19	0.04
	Zn4	821		*0.31*	*0.03*	0.33	0.10
	Zn5	1629		*0.15*	*0.05*	0.11	0.09
	Zn6	2818		*0.17*	*0.01*	0.10	0.06

[a] Average concentration between the start of the test and 48 hours.
[b] Average concentration between the start of the test and 72 hours.
[c] 72-h growth rate of *P.subcapitata*, given when all validity criteria after 72-h were valid. Those given in italics did not pass validity criteria after 72-h
[d] standard deviation on the 72-h growth rate
[e] 48-h growth rate of *P.subcapitata* for those water that did not pass validity criteria after 72-h
[f] standard deviation on the 48-h growth rate

Table D2.4 (continued)

Site ID	Treatment	Dissolved (µg/L)		72-h growth rate (µ)[c]	σ[d]	48-h growth rate (µ)[e]	σ[f]
		48h[a]	72h[b]				
Voyon8.5	Control	10	10	1.58	0.02	1.62	0.02
	Zn1	22	18	1.27	0.03	0.36	0.04
	Zn2	40	39	1.04	0.04	1.12	0.03
	Zn3	61	63	0.70	0.01	0.82	0.01
	Zn4	185	194	0.18	0.01	0.20	0.03
	Zn5	373	393	0.04	0.03	0.11	0.04
	Zn6	569	597	0.04	0.08	0.06	0.00
Bihain	Control	24		*1.26*	*0.01*	1.53	0.04
	Zn1	95		*1.28*	*0.01*	1.42	0.02
	Zn2	163		*1.21*	*0.00*	1.25	0.01
	Zn3	285		*0.95*	*0.01*	0.99	0.01
	Zn4	524		*0.46*	*0.02*	0.43	0.03
	Zn5	1048		*0.24*	*0.02*	0.35	0.04
	Zn6	2059		*0.15*	*0.05*	0.31	0.10
Brisy	Control	18	13	1.59	0.03	1.83	0.02
	Zn1	33	29	1.57	0.02	1.75	0.04
	Zn2	53	54	1.46	0.01	1.59	0.01
	Zn3	83	85	1.18	0.02	1.25	0.02
	Zn4	144	150	0.74	0.06	0.67	0.09
	Zn5	224	244	0.32	0.04	0.7	0.06
	Zn6	495	539	0.00	0.00	0.00	0.00
Loire	Control	5	5	1.60	0.04	1.80	0.04
	Zn1	9	9	1.50	0.02	1.64	0.01
	Zn2	26	17	1.29	0.03	1.47	0.03
	Zn3	32	32	0.90	0.01	0.94	0.03
	Zn4	97	98	0.44	0.03	0.48	0.08
	Zn5	209	213	0.09	0.07	0.00	0.00
	Zn6	366	359	0.00	0.00	0.00	0.00
Loire8.6	Control	7	7	1.60	0.04	1.67	0.06
	Zn1	15	11	1.51	0.04	0.59	0.04
	Zn2	22	19	1.39	0.00	1.46	0.05
	Zn3	27	28	0.97	0.02	1.01	0.04
	Zn4	81	52	0.35	0.02	0.27	0.03
	Zn5	194	208	0.09	0.01	0.12	0.01
	Zn6	325	346	0.01	0.01	0.02	0.01

[a] Average concentration between the start of the test and 48 hours.
[b] Average concentration between the start of the test and 72 hours.
[c] 72-h growth rate of *P.subcapitata*, given when all validity criteria after 72-h were valid. Those given in italics did not pass validity criteria after 72-h
[d] standard deviation on the 72-h growth rate
[e] 48-h growth rate of *P.subcapitata* for those water that did not pass validity criteria after 72-h
[f] standard deviation on the 48-h growth rate

Table D2.4 (continued)

Site ID	Treatment	Dissolved (µg/L) 48h[a]		72-h growth rate (µ)[c]	σ[d]	48-h growth rate (µ)[e]	σ[f]
	Control	41	43	1.44	0.07	1.64	0.03
	Zn1	100	101	1.40	0.07	1.41	0.02
	Zn2	169	164	1.16	0.01	1.17	0.01
Bihain	Zn3	283	284	0.84	0.02	0.87	0.02
	Zn4	528	539	0.24	0.02	0.30	0.02
	Zn5	1025	1035	0.09	0.02	0.20	0.01
	Zn6	2027	2041	0.05	0.02	0.23	0.03
	Control	12		*1.37*	*0.02*	1.67	0.03
	Zn1	18		*1.31*	*0.01*	1.62	0.02
	Zn2	17		*1.29*	*0.01*	1.53	0.01
Madon	Zn3	44		*1.23*	*0.02*	1.42	0.03
	Zn4	137		*0.66*	*0.02*	0.79	0.03
	Zn5	248		*0.28*	*0.02*	0.35	0.02
	Zn6	375		*0.11*	*0.02*	0.19	0.01
	Control	9		*1.51*	*0.03*	1.81	0.05
	Zn1	43		*1.49*	*0.01*	1.74	0.01
	Zn2	67		*1.47*	*0.01*	1.63	0.03
Taurion	Zn3	132		*1.17*	*0.04*	1.22	0.09
	Zn4	209		*0.48*	*0.03*	0.43	0.01
	Zn5	422		*0.21*	*0.01*	0.36	0.06
	Zn6	855		*0.05*	*0.01*	0.16	0.01
	Control	15		*1.58*	*0.00*	1.87	0.01
	Zn1	48		*1.56*	*0.01*	1.86	0.01
	Zn2	70		*1.49*	*0.00*	1.71	0.01
Maulde	Zn3	106		*1.33*	*0.02*	1.33	0.02
	Zn4	230		*0.54*	*0.01*	0.44	0.01
	Zn5	430		*0.22*	*0.01*	0.20	0.01
	Zn6	813		*0.13*	*0.01*	0.18	0.03

[a] Average concentration between the start of the test and 48 hours.
[b] Average concentration between the start of the test and 72 hours.
[c] 72-h growth rate of *P.subcapitata*, given when all validity criteria after 72-h were valid. Those given in italics did not pass validity criteria after 72-h
[d] standard deviation on the 72-h growth rate
[e] 48-h growth rate of *P.subcapitata* for those water that did not pass validity criteria after 72-h
[f] standard deviation on the 48-h growth rate

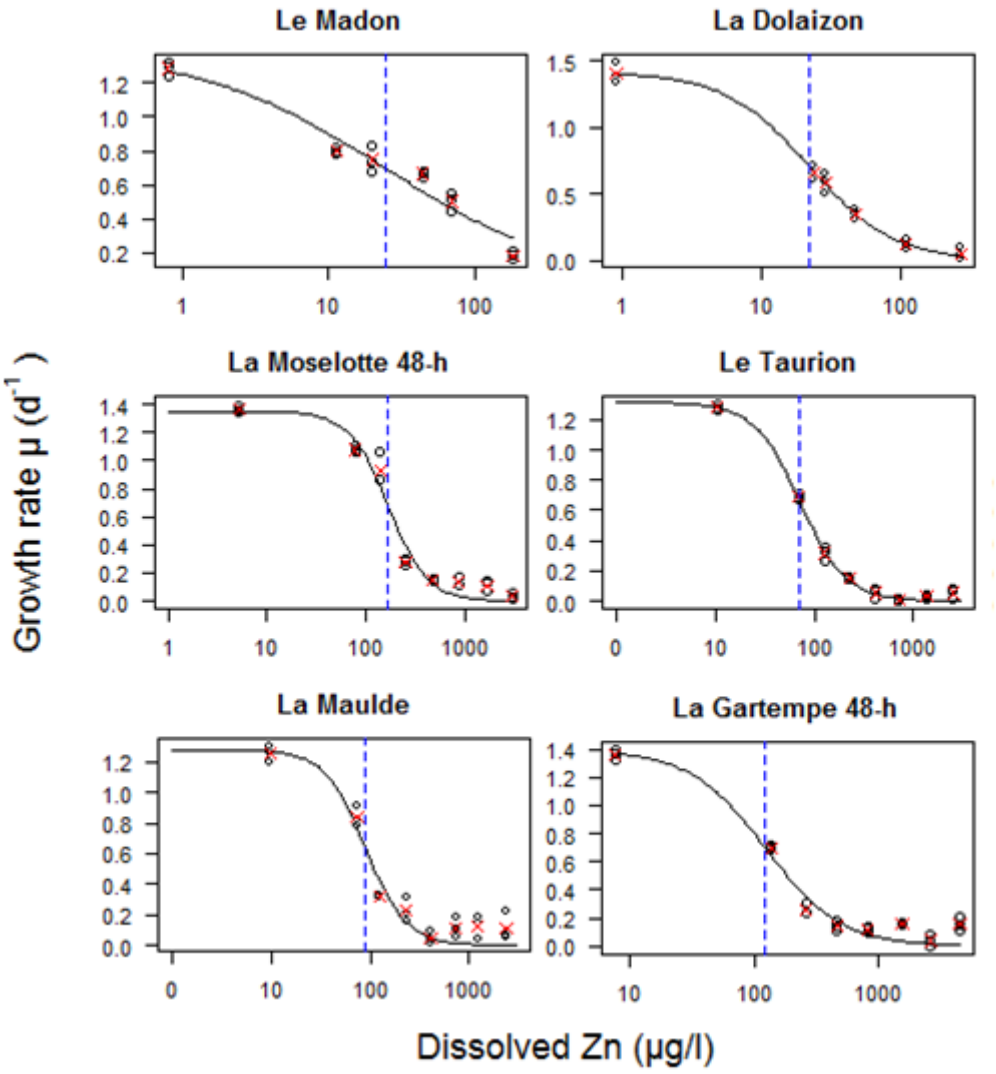

Figure D2.2 Concentration-response curves for *Pseudokirchneriella subcapitata* for five natural waters tested during the first time period. The mean value per treatment is indicated with an X. The EC50 concentration is indicated with a blue line. EC50 = the 50% effective concentration.

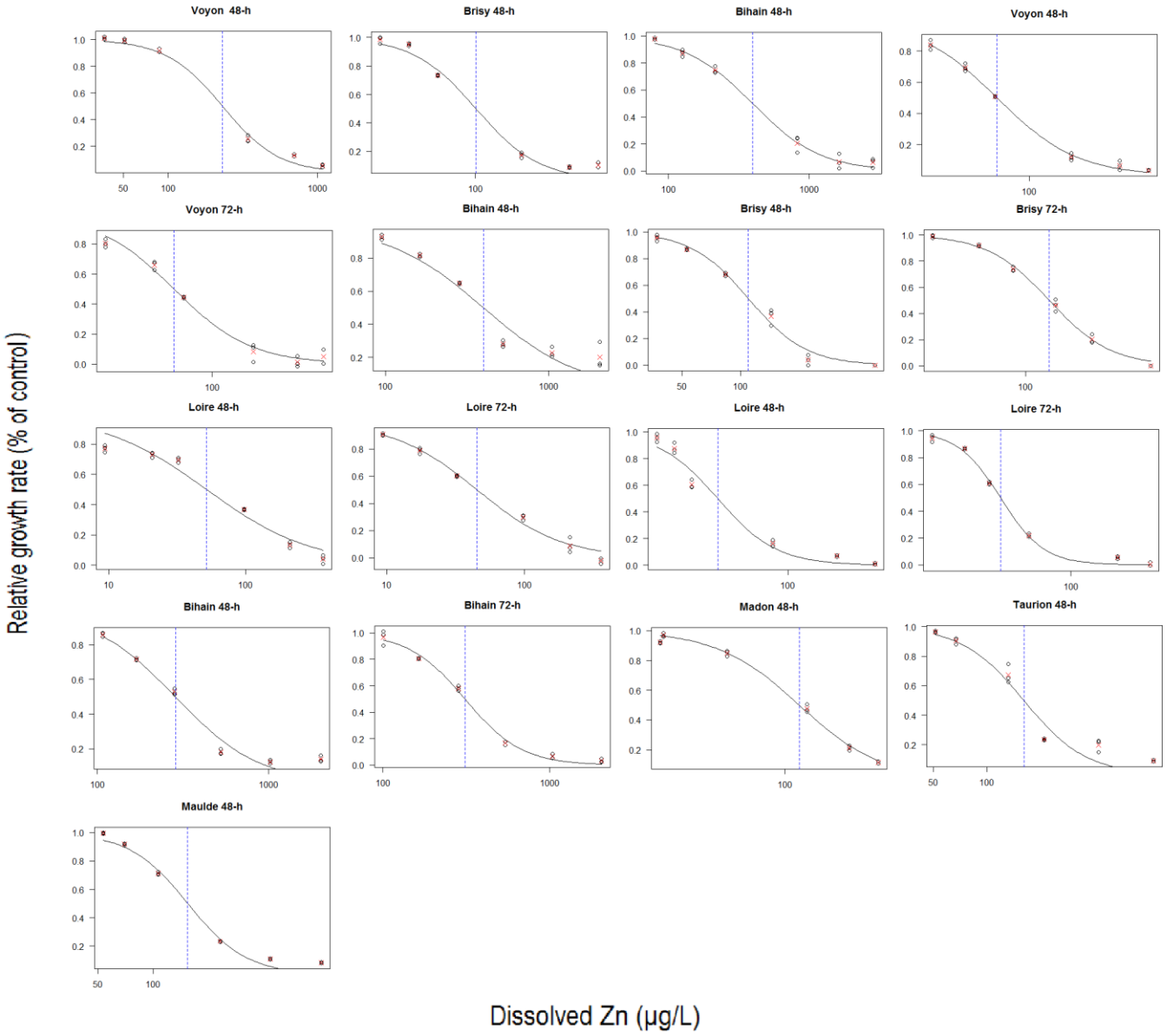

Figure D2.3. Concentration-response curves for *Pseudokirchneriella subcapitata* for nine different natural waters tested during the second time period. The order of the graphs from left to right and from top to bottom corresponds with the order of the waters in Table 5.5. The mean value per treatment is indicated with an X. The EC50 concentration is indicated with a dashed line. EC50 = the 50% effective concentration.

D2.2 Recalibration of the Pseudokirchneriella subcapitata bioavailability model for EC10 predictions

Recalibration of the *P.subcapitata* bioavailability model was performed for the EC10 data. Figure D2.4 shows the correlation (r^2) between O/P and pH, DOC (mg/l), Na^+ activity, Ca^{2+} activity and Mg^{2+} activity. No significant correlation between O/P and pH, DOC, Na^+ activity, Ca^{2+} activity and Mg^{2+} activity ($p > 0.05$) were observed.

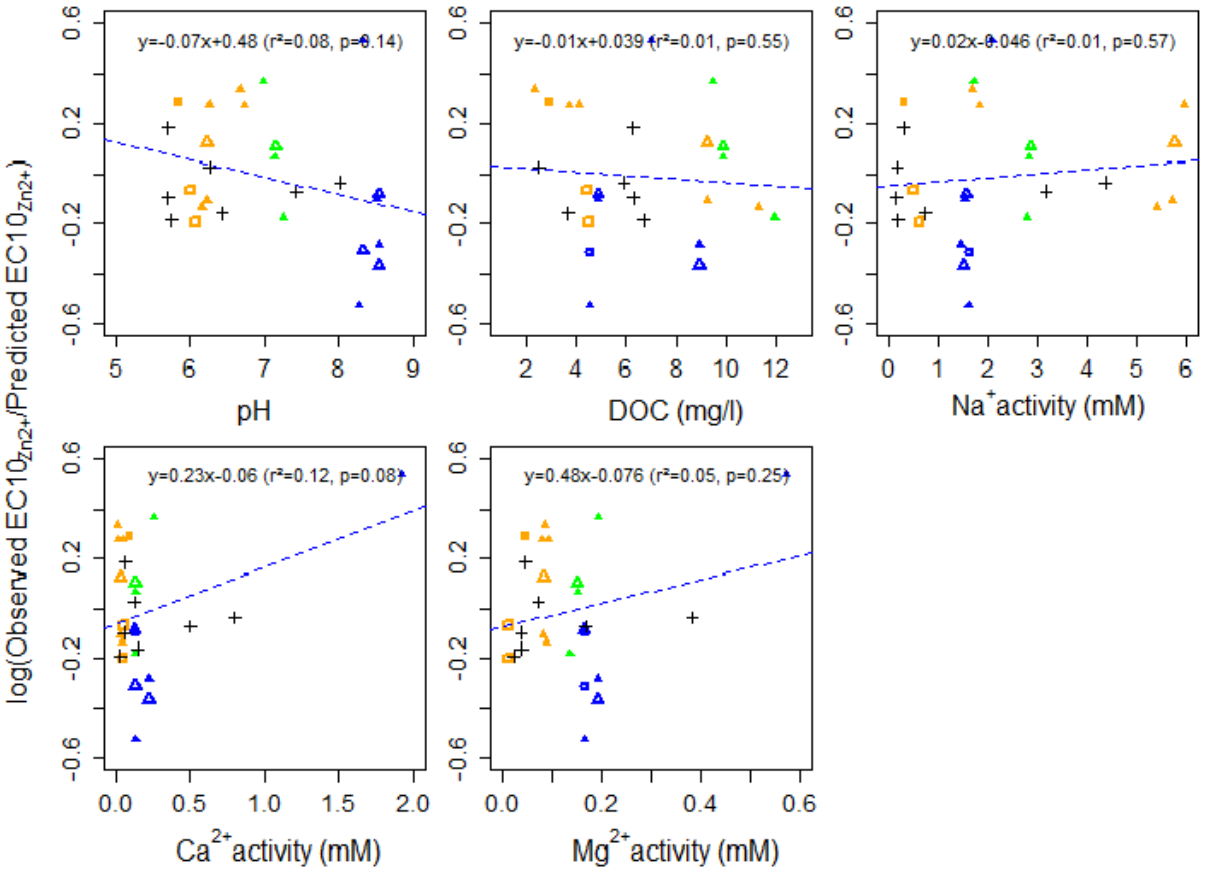

Figure D2.4. Logarithmic differences (i.e. log Observed Zn^{2+} activity – log Predicted Zn^{2+} activity) against different chemical parameters (pH, DOC (mg/L), Na^+ activity (mM), Ca^{2+} activity (mM) and Mg^{2+} activity (mM)). Squares indicate toxicity data generated in the first time period, circles indicate data generated in the second time period, crosses indicate toxicity data generated in De Schamphelaere et al. (2005). Filled symbols indicate 72-h EC10 for *Pseudokirchneriella subcapitata*, open symbols indicate 48-h EC10 for *Pseudokirchneriella subcapitata.* Symbols in green indicate waters with water chemistry that fall within the BLM boundaries (pH and calcium), blue symbols indicate waters with high pH values, orange symbols indicate waters with low calcium concentrations.

When the observed Zn^{2+} activities were used to perform a correlation analysis with pH, the relation between $\log(EC10)_{Zn^{2+}}$ and pH was significant (r^2=0.87, p<0.001) (Figure D2.5). The slope value was used as new S_{pH} value (-0.816) for recalibration of the bioavailability model. Intrinsic sensitivities were recalibrated based on this S_{pH} value and were equal to 1.769 for the data from the first time period, 1.186 for the data from the second time period and 0.943 for the data from De Schamphelaere et al. (2005).

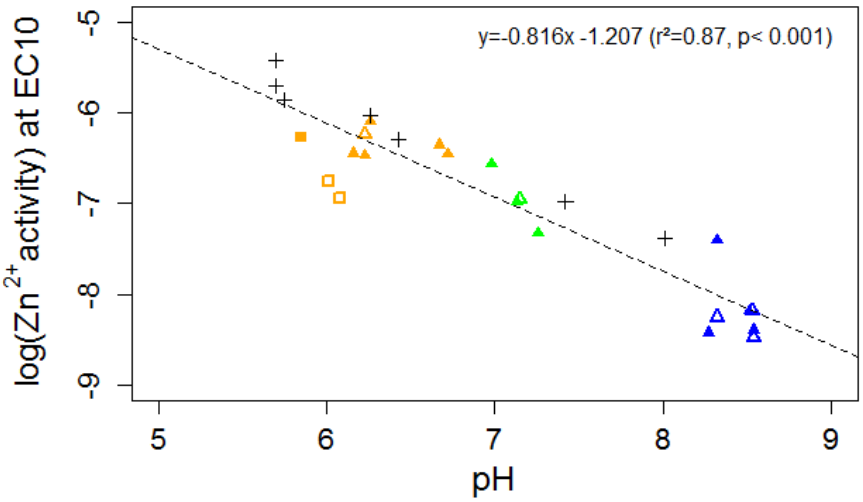

Figure D2.5. Zinc activity at the 72-h and 48-h 10% effective concentration (EC10) as a function of pH. Zinc activity was calculated with Equation A1.4. Squares indicate toxicity data generated in the first time period, circles indicate data generated in the second time period, crosses indicate toxicity data generated in De Schamphelaere et al. (2005). Filled symbols indicate 72-h EC10 for *Pseudokirchneriella subcapitata*, open symbols indicate 48-h EC10 for *Pseudokirchneriella subcapitata.* Symbols in green indicate waters with water chemistry that fall within the BLM boundaries (pH and calcium), blue symbols indicate waters with high pH values, orange symbols indicate waters with low calcium concentrations.

Figure D2.6 shows the performance of the bioavailability model in predicting Zn toxicity for EC10 data. For all EC10 data, the bioavailability model now predicts 89% within twofold error (mean prediction error of 1.6-fold) which is only 8% better than the original bioavailability model (De Schamphelaere et al. 2005) Also here, the chronic zinc toxicity for the data point from the Madon water is overpredicted.

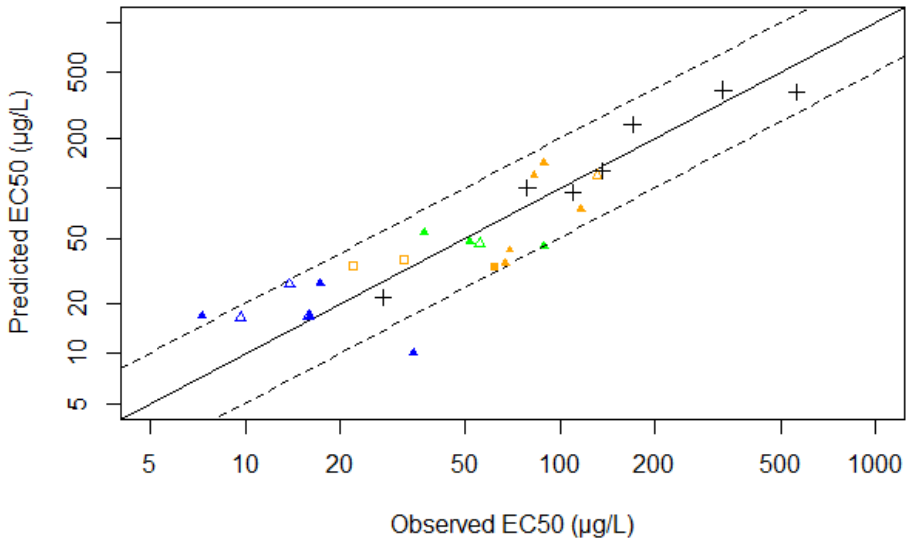

Figure D2.6. Observed versus predicted 10% effect concentrations (EC10) of zinc (as dissolved Zn). Predictions were made with the recalibrated BLM with new S_{pH} value and intrinsic sensitivities. Squares indicate toxicity data generated in the first time period, circles indicate data generated in the second time period, crosses indicate toxicity data generated in De Schamphelaere et al. (2005). Filled symbols indicate 72-h EC10 for *Pseudokirchneriella subcapitata*, open symbols indicate 48-h EC10 for *Pseudokirchneriella subcapitata.* Symbols in green indicate waters with water chemistry that fall within the BLM boundaries (pH and calcium), blue symbols indicate waters with high pH values, orange symbols indicate waters with low calcium concentrations. The full line and dashed lines indicate a perfect match and a factor two difference between the observed and predicted EC10.

D2.3 Read-across of the gBAM to Lymnaea stagnalis and Brachionus calyciflorus

We investigated if the chronic zinc generalized BioAvailiabity Model version D (gBAM-D) developed for *Daphnia magna* could be extrapolated to predict chronic toxicity of zinc as a function of water chemistry to two species from other phyla, i.e. the mollusc *Lymnaea stagnalis* and the rotifer *Brachionus calyciflorus*.

Table D2.5 shows the constants and intrinsic sensitivities that were used for modelling with gBAM-D.

Table D2.5. pH slope constants, competition constants, thermodynamic parameters and humic material assumptions of the generalized BioAvailability Model-D (gBAM-D) that were used for modelling. Intercepts (Q-values) indicating the intrinsic sensitivity of *Lymnaea stagnalis* and *Brachionus calyciflorus* are given for the 50% (i.e. Q_{50}) and 10% (i.e. Q_{10}) effective concentrations.

Parameter	gBAM-D *L. stagnalis*	gBAM-D *B. calyciflorus*
Biotic Ligand (BL) Species		
Log K_{CaBL}	3.22	3.22
Log K_{MgBL}	2.69	2.69
Log K_{NaBL}	1.90	1.90
S_{pH}	0.13	0.13
Q_{50}	4.61	4.90
Q_{10}	4.84	5.23
Bioavailable species that can bind to the biotic ligand	NA	NA
Thermodynamic Database		
pK_{MHA} Zn-HA	2.3	2.3
Humic Material Assumptions		
% of natural DOM composed of active humic substances (the rest is inactive)	50%	50%
% of the humic substances that is HA (rest is FA)	0%	0%

Figure D2.7 shows the performance of gBAM-D in predicting chronic Zn toxicity to both species. All predictions of EC_{10}s and EC_{50}s were within 1.5-fold difference from observations for *L. stagnalis*. Average prediction errors for EC_{10} and EC_{50} values were 1.24 and 1.16-fold, respectively (Table D2.6). These predictions are slightly better than the predictions made with the chronic *D. magna* BLM (Figure D2.8), which showed an average prediction error of 1.31 and 1.19-fold for EC_{10} and EC_{50} values, respectively (De Schamphelaere and Janssen 2010). All predictions for *B. calyciflorus* were also within 1.3-fold prediction error (Table D2.6). Average prediction error for EC_{10} and EC_{50} values were 1.22 and 1.18-fold, respectively (Table D2.6). These predictions are also slightly better than the predictions made

with the chronic *D. magna* BLM (Figure D2.8), i.e. average prediction error of 1.29 and 1.33-fold for EC_{10} and EC_{50} values, respectively (De Schamphelaere and Janssen 2010).

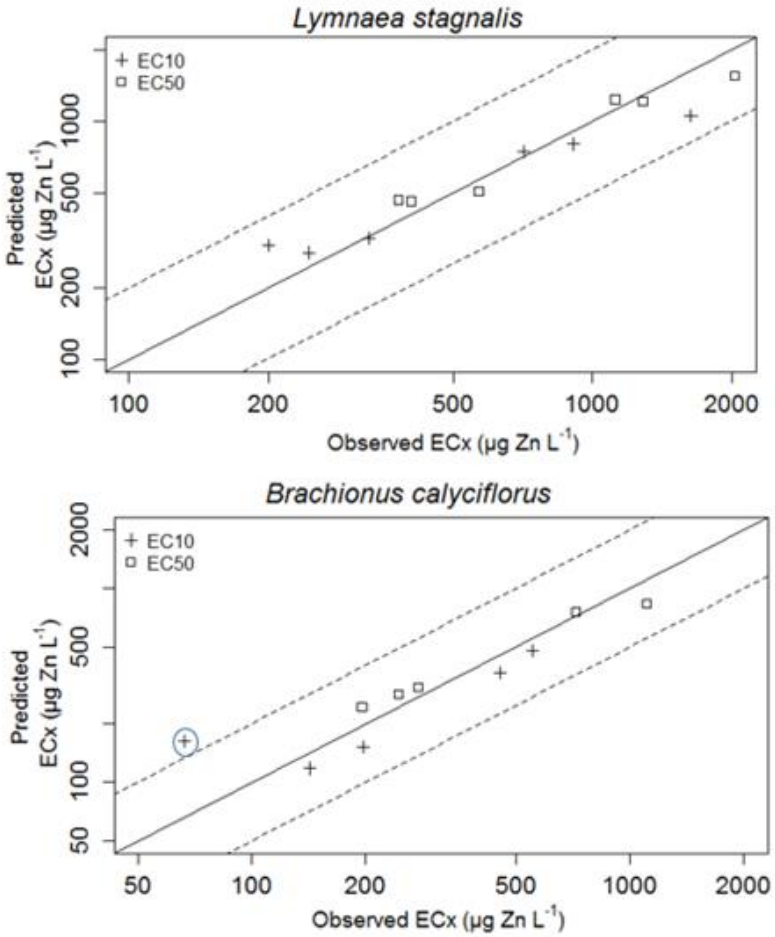

Figure D2.7. Observed and predicted 10% (EC10) and 50% effective concentrations (EC50) of dissolved Zn for *Lymaea stagnalis* and *Brachionus calyciflorus*. The predicted values were calculated using gBAM-D. The full line indicates a 1:1 ratio between observation and prediction; the dotted lines indicate the range of two-fold difference between observation and prediction. For *B. calyciflorus*, the encircled EC_{10} was considered unreliable because its 95% confidence interval spanned a larger range than the other EC10 values derived (see [1]), and was therefore not used to calculate prediction statistics.

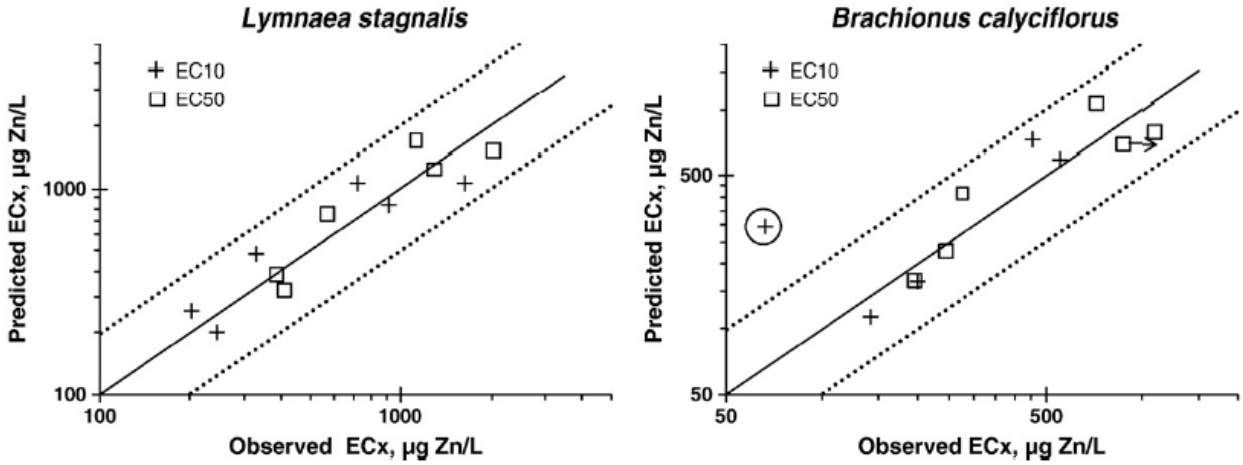

Figure D2.8. Figure taken from De Schamphelaere and Janssen (2010). Observed and Biotic Ligand Model predicted 10% (EC10) and 50% effective concentrations (EC50) of dissolved Zn for two species. The full line indicates a 1:1 ratio between observation and prediction; the dotted lines indicate the range of two-fold difference between observation and prediction. For *B. calyciflorus*, the encircled EC_{10} was considered unreliable because its 95% confidence interval spanned a larger range than the other EC10 values derived (see De Schamphelaere and Janssen 2010), and was therefore not used to calculate prediction statistics. The true EC50 of the square marked with an arrow (→) is higher than the depicted square (see De Schamphelaere and Janssen 2010), and was therefore also not used to calculate prediction statistics.

Table D2.6. Prediction statistics (fold prediction error) of the gBAM-D and the chronic *D. magna* BLM for *Lymnaea stagnalis* and *Brachionus calyciflorus*.

	gBAM-D				BLM			
	L. stagnalis		*B. calyciflorus*		*L. stagnalis*		*B. calyciflorus*	
	EC10[a] (n=6)	EC50[a] (n=6)	EC10[a] (n=4)	EC50[a] (n=5)	EC10[a] (n=6)	EC50[a] (n=6)	EC10[a] (n=4)	EC50[a] (n=5)
Mean prediction error	1.24	1.16	1.22	1.18	1.31	1.19	1.29	1.33
Median prediction error	1.14	1.13	1.22	1.16	1.37	1.30	1.23	1.38
75th percentile error	1.42	1.20	1.24	1.26	1.47	1.32	1.34	1.49
90th percentile error	1.53	1.27	1.27	1.30	1.50	1.43	1.50	1.50
Predicted within 2-fold error (%)	100	100	100	100	100	100	100	100

[a] EC_{10} = 10% effective concentration, EC_{50} = 50% effective concentration

Appendix E:

SUPPORTING INFORMATION OF CHAPTER 6.

Appendix E1 Cross-validation of the Cu D. magna gBAM

To see whether the chronic toxicity models (gBAMs) developed in Chapter 5 also work for other species, a cross-species exercise was done. This was done for five species, *Brachionus calyciflorus*, *Ceriodaphnia dubia* and *Lampsilis siliquoidea* with data from the following datasets:

a. De Schamphelaere and Janssen (2006) reported on chronic toxicity of copper to *B. calyciflorus*. Physico-chemistry and NOEC and LOEC data for modeling was taken from their Table 1.
b. Schwartz and Vigneault (2007) reported on the chronic, 7d-toxicity of copper to *C. dubia* in surface waters from Canada and in synthetic waters. Physico-chemistry and IC25 data for the natural waters was taken from their Table 1 and that for the synthetic waters was received from M. Schwartz (pers. comm.)

The cross-species predictive capacity of the developed models gBAM-A_{uni}, gBAM-B_{uni} and gBAM-C_{uni} was compared to that of the validated models (UGent and HydroQual BLM). Table E1.1 shows the constants and intrinsic sensitivities that were used for the different toxicity models. Intrinsic sensitivities for the different species for the UGent BLM and HydroQual BLM were calculated in the same way as was done for *D. magna* and those for the $gBAM_{uni}$ models were adapted in the same way as was done for *D. magna*.

Furthermore, the HydroQual BLM, UGent BLM and $gBAM_{uni}$ model predictions were compared for a pH-range between 5.5 and 8.5. This was done for *B. calyciflorus* (De Schamphelaere et al., 2006) and *C. dubia* (Schwartz and Vigneault, 2007). For every dataset the critical accumulation value was calculated based on a test with a pH larger than 7 (Table E1.2). Toxicity predictions were then made for the other pH values from the pH range (5.5 to 8.5), with the same critical accumulation value and the same physico-chemical parameters (DOC, cations, anions) as the test but with a different alkalinity value. This alkalinity value was calculated by first calculating the total carbonate concentration from the pH assuming a closed system and then using this total carbonate concentration in combination with the pH value to calculate the alkalinity (Stumm and Morgan 1996).

Table E1.1. Summary of constants and intrinsic sensitivities for the different toxicity models and BLMs used to predict toxicity for *B. calyciflorus, C. dubia and L. siliquoidea*.

		gBAM-A_{uni}	gBAM-B_{uni}	gBAM-C_{uni}	UGent BLM	HydroQual BLM
SpH		0.56	0.61	0.62	NA	NA
Q_x or $\int_{CuBL}^{50\%}$ [a]	$NOEC_{B.calyciflorus}$	-5.02	-5.09	-5.24	0.045	0.001
	$LOEC_{B.calyciflorus}$	-4.76	-4.83	-4.98	0.079	0.002
	$IC25_{C.dubia}$	-7.62	-7.26	-7.57	0.267	0.002
$logK_{CuBL}$		NI	NI	NI	8.02	7.4
$logK_{CuOHBL}$		NI	NI	NI	8.02	6.2
$logK_{CuCO3BL}$		NI	NI	NI	7.44	NI
$logK_{NaBL}$		NI	2.67	2.67	2.91	3
$logK_{CaBL}$		NI	NI	3.53	NI	3.6
$logK_{MgBL}$		NI	NI	3.53	NI	3.6
$logK_{HBL}$		NA	NA	NA	6.67	5.4
Humic material assumptions						
- % of natural DOM composed of humic substances[b]		50%	50%	50%	50%	100%
- % of the humic substances that is HA (rest is FA)[c]		0%	0%	0%	0%	10%

[a] Q_x value used in the gBAMs, $\int_{CuBL}^{50\%}$ value used in the BLMs

[b] Exception: When humic acid is added to the medium, all models assume 100% of the DOM to be composed of humic substances.

[c] Exception: When humic acid is added to the medium, all models assume 100% of the humic substances to be composed of humic acid.

NA = not applicable; NI = not included in the model DOM = dissolved organic matter; HA = humic acid; FA = fulvic acid.

Table E1.2. Water chemistry parameters used to calculate critical accumulation values to compare HydroQual BLM, UGent BLM and $gBAM_{uni}$ model predicitions for a pH-range between 5.5 and 8.5.

Parameter	De Schamphelaere et al. (2006)	Schwartz and Vigneault (2007)
species	*B. calyciflorus*	*C. dubia*
T (°C)	25.0	24.5
pH	7.80	7.63
DOC (mg/L)	4.84	0.4
Ca (mg/L)	32.0	6.6
Mg (mg/L)	4.9	1.7
Na (mg/L)	93.0	13.9
K (mg/L)	3.0	0.6
SO4 (mg/L)	120.0	22
Cl (mg/L)	64.0	5
Alkalinity[a] (mg/L)	15.0	20.4
NOEC/IC25/EC50 (µg/L)	47.8	10.9

[a] for other pH values, water chemistry data was held constant except for alkalinity. First, total carbonate was calculated from the pH and alkalinity assuming a closed system. This total corbanate was then used to calculate the alkalinity at different pH values.

E1.1 Read-across for B. calyciflorus

Figure E1.1 shows the performance of the different models in predicting Cu toxicity for the rotifer *B. calyciflorus*. Overall, the models developed in Chapter 5, gBAM-A_{uni} and gBAM-B_{uni} and gBAM-C_{uni}, perform the best (Table E1.3). They show 100 % of the data within twofold error and the lowest mean prediction errors. The UGent BLM also predicts 100% of the data within twofold error, but shows higher mean prediction errors. The HydroQual predicts only 28% within twofold error for *B. calyciflorus* data.

Table E1.3. Prediction statistics (fold prediction error) of the read across for *B. calyciflorus* (n=8).

	gBAM-A_{uni}	gBAM-B_{uni}	gBAM-C_{uni}	UGent BLM	HydroQual BLM
Mean prediction error	1.14	1.21	1.13	1.28	2.50
Median prediction error	1.14	1.22	1.13	1.27	2.66
75th percentile error	1.17	1.27	1.21	1.35	2.82
90th percentile error	1.18	1.32	1.23	1.46	3.0
Predicted within 2-fold error (%)	100	100	100	100	28
Predicted within 3-fold error (%)	100	100	100	100	88

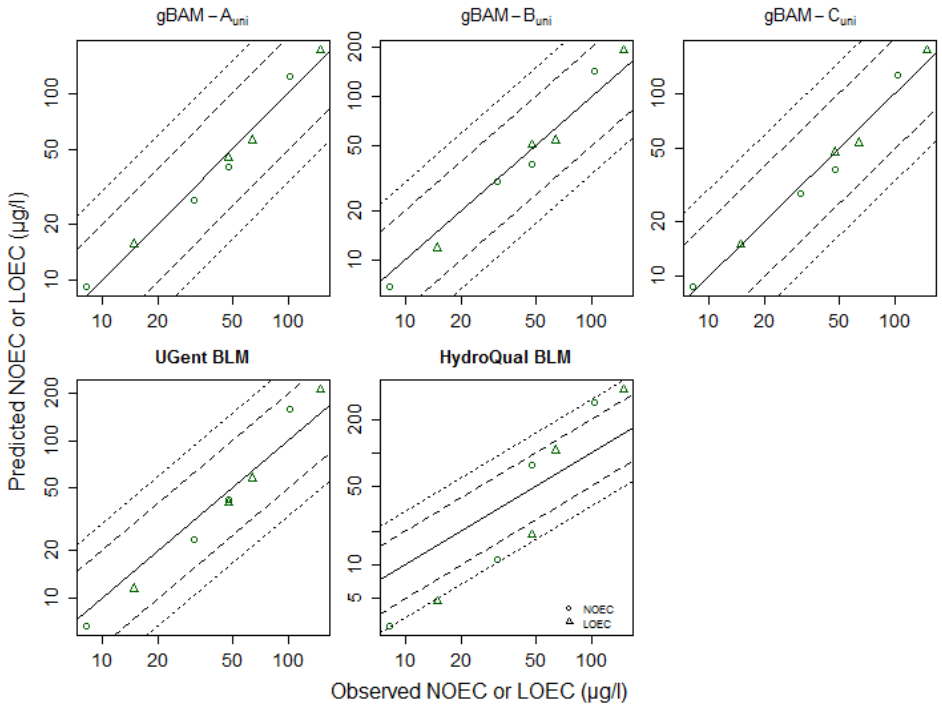

Figure E1.1. Observed versus predicted NOEC (○) and LOEC (∆) data *for B. calyciflorus* according to the different models (see Table E.1) for the endpoint 'intrinsic rate of increase'. Data from De Schamphelaere and Janssen (2006).

Figure E1.2 shows the predictive capacity of all models for a pH range between 5 and 8.5. The observed change in NOEC is approximately a factor of 5.8. The UGent and gBAM$_{uni}$ models clearly predict the changes in toxicity with pH more accurately than the HydroQual BLM.

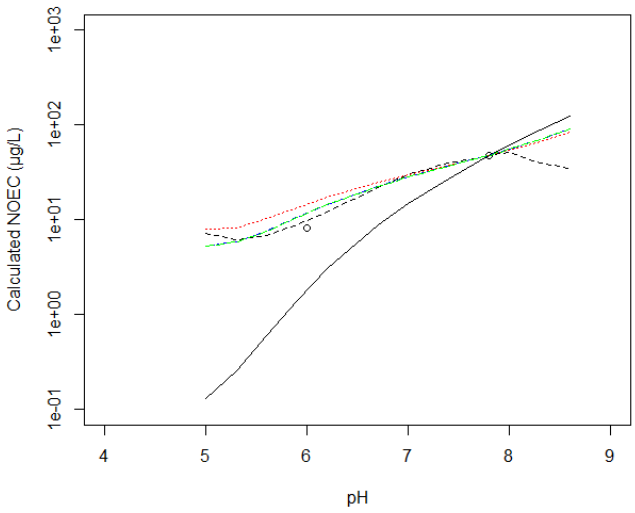

Figure E1.2. Predicted copper chronic effects and experimental observations (○) for *B. calyciflorus* (De Schamphelaere & Janssen,2006). The solid line indicates predictions by the HydroQual BLM, the dashed line indicates predictions by the UGent BLM, dotted lines indicate predictions by the gBAM$_{uni}$ models (green = gBAM-A$_{uni}$, blue = gBAM-B$_{uni}$, red = gBAM-C$_{uni}$.

E1.2 Read-across for C. dubia

Toxicity predictions for *C. dubia* were made with all available models. We would like to remark that DOC concentrations reported for the tap waters are very low (0.4 mg/L). As *C. dubia* were fed with algae and YCT during the test, which increase the amount of DOC in the medium, it is likely that *C. dubia* were tested at on average higher DOC concentrations than reported (De Schamphelaere et al. 2006b). To evaluate the effect of a higher DOC level on the toxicity predictions, the DOC concentration of all waters was increased with 0.8 mg/L. This value was chosen because it is the estimate of DOC addition due to YCT (Keithly et al. 2004). Figure E.3 shows the performance of the different models in predicting Cu toxicity for the *C. dubia*. Error bars show the influence of an increased DOC concentration (a new critical value was calculated).

Overall, the gBAM-C$_{uni}$ performs the best (Table E1.4). Increasing the DOC concentration of the waters with 0.8 mg/L has a large influence on the toxicity predictions. This higher, and probably more accurate DOC value increased the predictive capacity of the models (Table E15).

When examining Figure E1.3 we see a bias between predictions made for natural waters (at the top of the figures) and for synthetic waters (at the bottom of the figures). This is most likely due to a shift in sensitivity between both test-series. Therefore, toxicity predictions were also made when two separate critical accumulation values were calculated for the synthetic and natural waters (Figure E1.4). Now, toxicity predictions are better (Table E1.6 and Table E1.7).

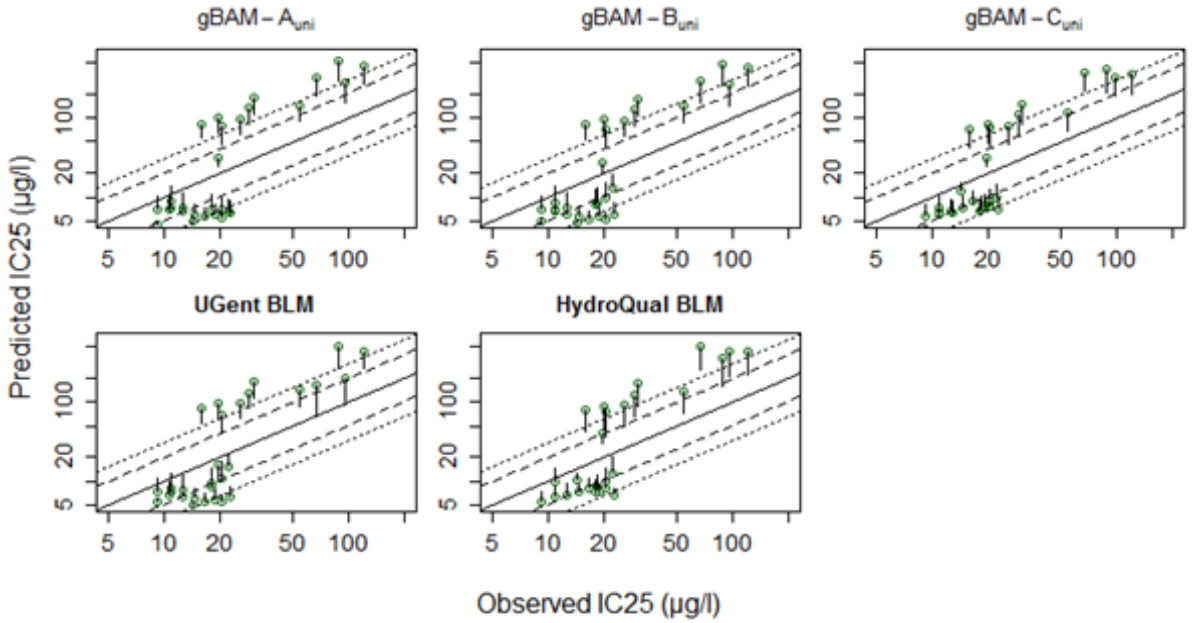

Figure E1.3. Observed versus predicted IC25 (○) data for *C. dubia* according to the different models (see Table E.1) for the endpoint 'reproduction'. Vertical error bars show the influence of adding 0.8 mg/L DOC (due to YCT addition) to all waters on the BLM and gBAM predictions. Data from Schwartz & Vigneault (2007).

Table E1.4. Prediction statistics (fold prediction error) of the read across for *C. dubia* (n=7).

	gBAM-A_{uni}	gBAM-B_{uni}	gBAM-C_{uni}	UGent BLM	HydroQual BLM
Mean factor prediction error	3.14	2.95	2.77	2.83	3.09
Median factor prediction error	2.94	2.72	2.47	2.42	2.49
75th percentile factor error	3.67	3.71	3.34	3.63	3.99
90th percentile factor error	5.11	4.78	4.42	4.93	4.08
Predicted within 2-fold error (%)	24	28	31	38	34
Predicted within 3-fold error (%)	55	52	66	62	59

Table E1.5. Prediction statistics (fold prediction error) of the read across for *C. dubia* (n=7) when adding 0.8 mg/L DOC to the waters due to YCT addition during testing.

	gBAM-A_{uni}	gBAM-B_{uni}	gBAM-C_{uni}	UGent BLM	HydroQual BLM
Mean factor prediction error	2.14	1.98	1.78	1.93	1.98
Median factor prediction error	2.21	1.90	1.77	1.83	1.71
75th percentile factor error	2.54	2.70	2.17	2.57	2.19
90th percentile factor error	3.29	2.98	2.46	3.07	2.75
Predicted within 2-fold error (%)	45	52	69	59	66
Predicted within 3-fold error (%)	86	90	97	83	93

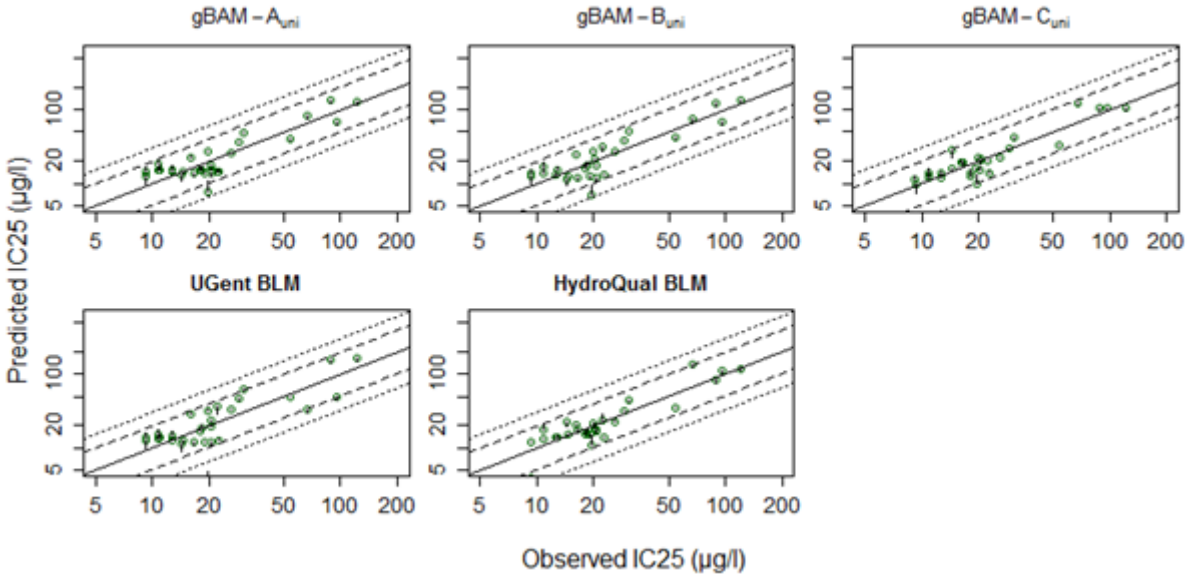

Figure E1.4. Observed versus predicted IC25 (○) data for *C. dubia* according to the different models (see Table E.1) for the endpoint 'reproduction' when a separate critical accumulation value is calculated for the natural and synthetic waters. Vertical error bars show the influence of adding 0.8 mg/L DOC (due to YCT addition) to all waters on the BLM and gBAM predictions. Data from Schwartz and Vigneault (2007).

Table E1.6. Prediction statistics of the read across for *C. dubia* (n=7) when a critical accumulation value is calculated for the natural and synthetic waters separately.

	gBAM-A_{uni}	gBAM-B_{uni}	gBAM-C_{uni}	UGent BLM	HydroQual BLM
Mean factor prediction error	1.37	1.37	1.28	1.58	1.31
Median factor prediction error	1.36	1.31	1.17	1.39	1.19
75th percentile factor error	1.50	1.49	1.34	1.74	1.44
90th percentile factor error	1.60	1.69	1.66	2.00	1.68
Predicted within 2-fold error (%)	97	97	93	90	97
Predicted within 3-fold error (%)	100	100	100	97	100

Table E1.7. Prediction statistics of the read across for *C. dubia* (n=7) when adding 0.8 mg/L DOC to the waters due to YCT addition during testing. A critical accumulation value is calculated for the natural and synthetic waters separately.

	gBAM-A_{uni}	gBAM-B_{uni}	gBAM-C_{uni}	UGent BLM	HydroQual BLM
Mean factor prediction error	1.37	1.37	1.25	1.57	1.34
Median factor prediction error	1.38	1.33	1.21	1.52	1.22
75th percentile factor error	1.52	1.54	1.30	1.70	1.35
90th percentile factor error	1.66	1.72	1.53	2.00	1.71
Predicted within 2-fold error (%)	100	97	100	90	97
Predicted within 3-fold error (%)	100	100	100	97	97

Figure E1.5 shows the predictive capacity of all models for a pH range between 5 and 8.5. The observed effect concentrations are relatively invariable with pH. The UGent BLM and $gBAM_{uni}$ models clearly predict this nearly constant toxicity with pH most accurately.

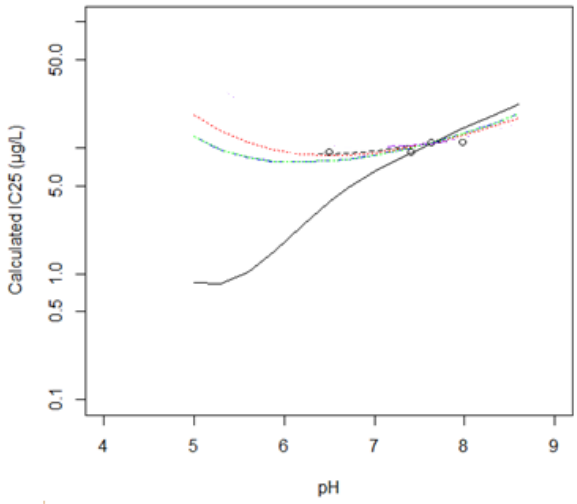

Figure E1.5. Predicted copper chronic effects and experimental observations (○) for *C. dubia* (Schwartz and Vigneault, 2007). The solid line indicates predictions by the HydroQual BLM, the dashed line indicated predictions by the UGent BLM, dotted lines indicate predictions by the gBAM$_{uni}$ models (green = gBAM-A$_{uni}$, blue = gBAM-B$_{uni}$, red = gBAM-C$_{uni}$

E.1.3 Conclusions

For the rotifer *Brachionus calyciflorus*, the three models developed in Chapter 5 (gBAM-A$_{uni}$ and gBAM-B$_{uni}$ and gBAM-C$_{uni}$) predict Cu toxicity best. They predict all data within twofold error and show the lowest mean prediction errors. The UGent BLM also predicts all data within twofold error, but shows higher mean prediction errors. The HydroQual BLM does not predict the *B. calyciflorus* data well.
Cu toxicity to the water flea *Ceriodaphnia dubia* was best predicted with the gBAM-C$_{uni}$ model.
We also remark that the influence of the uncertainty of DOC on all model predictions was important, especially at low DOC concentrations. Therefore, we would like to recommend the use of higher DOC values during tests with synthetic waters to ensure that BLM and gBAM predictions are accurate.

Overall we can conclude that the gBAM$_{uni}$ models developed in Chapter 5 perform equally well or even better than the UGent BLM during chronic toxicity read-across. The HydroQual BLM performs less well on chronic toxicity data. This trend is also seen when comparing model predictions for a pH-range. Here, the UGent BLM and gBAM$_{uni}$ models could most accurately predict the changes in toxicity with pH for chronic toxicity data.

Appendix E2. Output of Scenario B

Table E2.1 Toxic pressure expressed as multisubstance potentially affected fraction of species (msPAF) for the Dommel, Flanders (VMM), Rhine, Austria, and FOREGS database obtained with the different methods. Normalisation of the toxicity data was performed with Scenario A, i.e. the toxicity data for invertebrates, fish and algae were normalized with the original bioavailability models and the refined Ni normalization tool was implemented (Nys et al. 2016). The values between parentheses indicate the absolute difference in results between Scenario A and the same calculations but when implementing the 'old' Ni normalization tool (Nys et al. 2014; Chapter 2).

	Dommel				VMM				Rhine			
	CA_{SSD}	CA_{DRC}	IA_{SSD}	IA_{DRC}	CA_{SSD}	CA_{DRC}	IA_{SSD}	IA_{DRC}	CA_{SSD}	CA_{DRC}	IA_{SSD}	IA_{DRC}
median msPAF	0.054 (0.000)	0.035 (-0.003)	0.024 (0.000)	0.028 (-0.007)	0.009 (0.000)	0.003 (0.000)	0.003 (0.000)	0.003 (0.000)	0.004 (-0.002)	0.00 (-0.001)	0.00 (-0.001)	0.00 (-0.001)
% Samples affected (msPAF > 0.05)	52 (0.1)	45 (-1.0)	39 (-0.1)	41 (-2.6)	27 (0.0)	25 (0.0)	23 (0.0)	24 (0.7)	0 (0.0)	0 (0.0)	0 (0.0)	0 (0.0)
% Samples affected by mixture of metals and not by any individual metals	15 (0.1)	9 (-1.0)	2 (-0.1)	5 (-0.6)	7 (0.0)	4 (-0.3)	3 (0.2)	3 (-0.4)	0 (0.0)	0 (0.0)	0 (0.0)	0 (0.0)
MoS provided by the CA_{SSD} approach	NA	1.21 (0.034)	1.48 (0.031)	1.38 (0.001)	NA	1.18 (-0.001)	1.57 (0.004)	1.46 (-0.004)	NA	1.25 (-0.002)	1.72 (0.000)	1.61 (0.003)

	Austria				FOREGS			
	CA_{SSD}	CA_{DRC}	IA_{SSD}	IA_{DRC}	CA_{SSD}	CA_{DRC}	IA_{SSD}	IA_{DRC}
median msPAF	0.004 0.000)	0.001 (0.000)	0.001 (0.000)	0.001 (0.000)	0.003 (-0.001)	0.001 (0.000)	0.001 (0.000)	0.001 (0.000)
% Samples affected (msPAF > 0.05)	8 (0.0)	6 (0.1)	5 (0.0)	5 (0.0)	8 (2.0)	6 (-1.7)	4 (-2.7)	4 (-2.7)
% Samples affected by mixture of metals and not by any individual metals	3 (0.0)	1 (0.3)	0.2 (0.0)	0.6 (-0.2)	4 (0.7)	3 (1.0)	0.3 (0.1)	0.4 (0.0)
MoS provided by the CA_{SSD} approach	NA	1.21 (0.000)	1.52 (0.000)	1.45 (0.003)	NA	1.23 (0.011)	1.56 (0.034)	1.46 (0.028)

CA = Concentration Addition, IA = Independent Action, SSD = Species Sensitivity Distribution, DRC = Dose-Response Curve, msPAF = multisubstance Potentially Affected Fraction of species, MoS = Margin of Safety, NA = Not Applicable

Curriculum Vitae

TINAVANREGENMORTEL@GMAIL.COM www.linkedin.com/in/tinavanregenmortel/

17-07-1989 – MBABANE, SWAZILAND MAARTEN LAUKENS (2013)

ELISE LAUKENS (14/05/2016)

CURRICULUM VITAE

TINA VAN REGENMORTEL

RELEVANT WORKEXPERIENCE

- October 2012 – September 2017: PhD in Applied Biological Sciences: Ecotoxicity and risk assessment of metal mixtures in the freshwater environment. Promotors: Prof. Dr. Ir. Karel De Schamphelaere; Prof. Dr. Colin Janssen. Faculty of Bioscience Engineering, Ghent University, Belgium
- 2011: Internship at the Research Institute for agriculture, fisheries and food (ILVO), Ostend, Belgium
- 2008-2012: Various student jobs during the summer holiday

EDUCATION

- September 2007 – June 2012: Graduated as *Master in Biology.* Subject of Master-Thesis: '*The spatial and temporal distribution of Mnemiopsis leidyi in the Belgian part of the North Sea*'.
- September 2001 - June 2007: 6 years ASO at the Onze Lieve Vrouwencollege in Assebroek, Bruges. First four years Modern Sciences, last two years Sciences-Maths.

PUBLICATIONS (NEWEST TO OLDEST)

- **Van Regenmortel T**, Van de Perre D, Janssen CR, De Schamphelaere KAC. The effects of a Cu-Ni-Zn mixture on the structure, diversity and function of a freshwater planktonic community. Environmental Toxicology and Chemistry, submitted
- Nys C, **Van Regenmortel T**, Janssen CR, Oorts K, Smolders E, De Schamphelaere KAC. A framework for ecological risk assessment of metal mixtures in aquatic systems. Environmental Toxicology and Chemistry, accepted
- **Van Regenmortel T**, Janssen CR, De Schamphelaere KAC. Mixtures of Cu, Ni and Zn act mostly non-interactively on *Pseudokirchneriella subcapitata* growth in natural waters. Environmental Toxicology and Chemistry, accepted
- **Van Regenmortel T**, Berteloot O, Janssen CR, De Schamphelaere KAC. Analyzing the capacity of the *Daphnia magna* and *Pseudokirchneriella subcapitata* bioavailability models to predict chronic zinc toxicity at high pH and low Ca concentrations and formulation of a generalized BioAvailability model (gBAM) for *D. magna*. Environmental Toxicology and Chemistry, accepted. DOI: 10.1002/etc.3840
- **Van Regenmortel T**, Nys C, Janssen CR, Lofts S, De Schamphelaere KAC. 2017. Comparison of four methods for bioavailability-based risk assessment of mixtures of Cu, Zn and Ni in freshwater. Environmental Toxicology and Chemistry 36(8): 2123-2138
- Nys C, **Van Regenmortel T**, Janssen CR, Blust R, Smolders E, De Schamphelaere KAC. 2017. Comparison of chronic mixture toxicity of nickel-zinc-copper and nickel-zinc-copper-cadmium mixtures between *Ceriodaphnia dubia* and *Pseudokirchneriella subcapitata*. Environmental Toxicology and Chemistry 36(4): 1056-1066
- Van de Perre D, Roessink I, Janssen CR, Smolders E, **Van Regenmortel T**, Van Wichelen J, Vyverman V, Van den Brink PJ, De Schamphelaere KAC. 2016. The effects of zinc on the structure and functioning of a freshwater community: A microcosm experiment. Environmental Toxicology and Chemistry 35(11): 2698-2712

- **Van Regenmortel T**, Janssen CR, De Schamphelaere KAC. 2015. Comparison of the capacity of two biotic ligand models to predict chronic copper toxicity to two *Daphnia magna* clones and formulation of a generalized BioAvailability Model. Environmental Toxicology and Chemistry 34(7): 1597-1608

PRESENTATIONS (NEWEST TO OLDEST)

- Nys C, **Van Regenmortel T**, Janssen C, Blust R, Smolders E, De Schamphelaere KAC. Modelling the chronic effects of metal mixtures to aquatic organisms: a meta-analyse. 27th Annual Meeting of SETAC Europe, May 8-11, 2017, Brussels, Belgium.
- Nys C, Deruytter D, **Van Regenmortel T**, De Schamphelaere KAC. Chronic metal mixture toxicity: does metal concentration ratio matter? 27th Annual Meeting of SETAC Europe, May 8-11, 2017, Brussels, Belgium.
- **Van Regenmortel T**, Four methods to estimate potential risks of metal mixtures: a case study for Flemish waterways. 25th Annual Meeting of SETAC Europe, May 3-7, 2015, Barcelona, Spain.

Y

- Nagai T, **Van Regenmortel T**, De Schamphelaere KAC. Assessments of bioavailability and mixture toxicity of zinc, copper and nickel in Japanese surface waters using modeling approaches. 27th Annual Meeting of SETAC Europe, May 8-11, 2017, Brussels, Belgium.
- **Van Regenmortel T**, Nys C, Janssen CR, De Schamphelaere KAC. Effects of metal mixture contamination on a freshwater community: can predictive mixture toxicity models be validated experimentally? 26th Annual Meeting of SETAC Europe, May 22-26, 2016, Nantes, France.
- **Van Regenmortel T**, De Schamphelaere KAC. A comparison of copper Biotic Ligand Models and the first steps towards a generic BioAvailability model (gBAM). 24th Annual Meeting of SETAC Europe, May 11-15, 2014, Basel, Switzerland.

  Van Regenmortel T, De Laender F, Janssen CR, De Schamphelaere KAC. Mixture toxicity of metals as predicted by Concentration Addition. 23rd Annual Meeting of SETAC Europe, May 12-16, 2013, Glasgow, UK.

EDUCATIONAL ACTIVITIES

- Tutoring master thesis students
  - Lowie Moerman. 2015-2016. Chemische cocktails in het milieu: experimentele validatie van methodes voor realistische risico-evaluatie van gemengde vervuiling door zware metalen. Master of Science in Bioscience Engineering, Faculty of Bioscience Engineering, Ghent University. Promotor: prof. dr. ir. Karel De Schamphelaere; prof. dr. Colin Janssen. Tutor: Tina Van Regenmortel
  - Niels Verdoodt. 2014-2015. Experimentele validatie van biotisch ligand model voorspellingen voor mengseltoxiciteit van metalen. Master of Science in Bioscience Engineering, Faculty of Bioscience Engineering, Ghent University. Promotor: prof. dr. ir. Karel De Schamphelaere; prof. dr. Colin Janssen. Tutors: Tina Van Regenmortel and Charlotte Nys
  - Jenne Dierckx. 2013-2014. Toxicity predictions and ecological risk assessment of mixted heavy metal pollution in European surface waters. Master of Science in Environmental Sanitation, Faculty of Bioscience Engineering, Ghent University. Promotor: prof. dr. ir. Karel De Schamphelaere; prof. dr. Colin Janssen. Tutor: Tina Van Regenmortel
  - Tom De Turck. 2012-2014. Experimentele validatie van de toxiciteit van ternaire metaalmengsels van Ni, Cu en Zn zoals voorspeld met het concentratie additie en respons additive model. Master of Science Environmental Sanitation, Faculty of Bioscience Engineering, Ghent University. Promotor: prof. dr. ir. Karel De Schamphelaere; prof. dr. Colin Janssen. Tutor: Tina Van Regenmortel

- Teaching activities: Guidance of practical courses and technical lectures for the course Ecological Risk Assessment